

UNCLASSIFIED

AD NUMBER

AD781814

LIMITATION CHANGES

TO:

Approved for public release; distribution is unlimited.

FROM:

Distribution authorized to U.S. Gov't. agencies only; Test and Evaluation; JUN 1973. Other requests shall be referred to Air Force Flight Dynamics Laboratory, ATTN: FBA, Wright-Patterson AFB, OH 45433.

AUTHORITY

AFFDL ltr dtd 13 Oct 1975

THIS PAGE IS UNCLASSIFIED

AD 078 1814

AFFDL-TR-73-53

**ADVANCED METALLIC STRUCTURE:
CARGO FUSELAGE
DESIGN FOR IMPROVED COST, WEIGHT, AND INTEGRITY**

J. E. McCarty
et al.
Boeing Commercial Airplane Company

TECHNICAL REPORT AFFDL-TR-73-53

June 1973

APPROVED FOR PUBLIC RELEASE;
DISTRIBUTION UNLIMITED

Air Force Flight Dynamics Laboratory
Air Force Systems Command
Wright-Patterson Air Force Base, Ohio

20080815 289

NOTICE

When Government drawings, specifications, or other data are used for any purpose other than in connection with a definitely related Government procurement operation, the United States Government thereby incurs no responsibility nor any obligation whatsoever; and the fact that the Government may have formulated, furnished, or in any way supplied the said drawings, specifications, or other data is not to be regarded by implication or otherwise as in any manner licensing the holder or any other person or corporation, or conveying any rights or permission to manufacture, use, or sell any patented invention that may in any way be related thereto.

Copies of this report should not be returned unless return is required by security considerations, contractual obligations, or notice on a specific document.

**ADVANCED METALLIC STRUCTURE:
CARGO FUSELAGE
DESIGN FOR IMPROVED COST, WEIGHT, AND INTEGRITY**

J. E. McCarty
et al.

Boeing Commercial Airplane Company

AD781814

Distribution limited to U. S. Government agencies only; test and evaluation; statement applied June 1973. Other requests for this document must be referred to AF Flight Dynamics Laboratory (FBA), Wright-Patterson AFB, Ohio 45433.

FOREWORD

This report presents the results of preliminary design studies and materials testing performed by the Boeing Commercial Airplane Company, P. O. Box 3707, Seattle, Washington, under U.S. Air Force contract F33615-72-C-1893, Project 486U, Preliminary Design for a Critical Cargo/Tanker Component.

This Advanced Development Program was sponsored by the Air Force Flight Dynamics Laboratory (AFFDL) and was under joint management and technical direction of AFFDL and the Air Force Materials Laboratory, Wright-Patterson Air Force Base, Ohio. Dr. Lynn C. Rogers was the Air Force project engineer.

Mr. J. E. McCarty was the Boeing program manager. The principal participants in this program were:

J. R. Bender
L. L. Bryson
A. A. Field
D. D. Froerer
J. V. Hajari
Dr. R. R. June
W. C. Larson

B. D. Parashar
R. T. Shultz
J. O. Trent
H. N. Wantiez
R. B. Wentz
T. L. Wile
J. T. Wozumi

This work was performed in the period from June 1, 1972, to April 1, 1973. The report was submitted to the Air Force in June 1973.

This report has been reviewed and approved.



John C. Frishett, Major, USAF
Program Manager
AMS Program Office
Structures Division

ABSTRACT

This preliminary design study was conducted to identify, evaluate, and select advanced concepts for cargo aircraft fuselage structure. The goals were to reduce the structural weight, maintain the baseline fatigue life (60,000 flight-hours and 20,000 flights), and reduce the acquisition cost. All three selected fuselage shell concepts provide a reduction in both total unit cost (2% to 7%) and participating weight (17% to 19%). Fleet (50 to 89 aircraft) life cycle cost savings of \$120 to \$320 million over a 10-year period can be accrued from the projected aircraft weight savings. Screening of a broad base of structural concepts was conducted through three levels of design iteration. Three adhesive-bonded fuselage shell concepts are recommended for further study, development, and test evaluation. Adhesive-bonded construction was chosen as the primary assembly method to reduce structural weight because it allows a significant improvement in fatigue quality of the structure. The improved fatigue quality allowed effective utilization of the new aluminum alloys, which provide a combination of improved fracture toughness and strength. Fracture mechanics and fatigue life characteristics of new aluminum alloys were investigated in an exploratory testing program. Sensitivity studies were conducted to evaluate the impact of the application of the USAF Damage Tolerance Criteria, Revision D, on the baseline structure. The result of this study and the effect of implementing both a fracture control program and an NDI demonstration program are reported. A recommended follow-on program plan and schedule are included, with brief discussion of the key features of each follow-on program phase.

CONTENTS

Section	Page
I INTRODUCTION AND SUMMARY	1
II BASELINE STUDY SECTION	7
1. Baseline Airplane Selection	7
2. Selection of Fuselage Component	7
3. Fuselage Section Chosen for Study	15
4. Baseline Physical Description	16
5. Design Requirements	19
III NEW STRUCTURAL CONCEPTS AND PAYOFF	35
1. Development of New Structural Concepts	35
2. Concept Selection—Shell	38
a. Design Features of the Four Final Level 3 Shell Concepts	38
(1) Internal Stringer Concept (Fig. 29)	41
(2) Honeycomb Shell Concept (Fig. 30)	41
(3) External Stringer Concept (Fig. 31)	44
(4) Continuous-Bead Concept (Fig. 32)	46
b. Concepts for Components Other Than Shell	46
3. Program Payoff	46
a. Mission and Performance Payoff	48
(1) Missions Analysis	48
(2) Estimated 10-Year Life Cycle Savings and Program Leverage	50
(3) Application to AMST	56
b. Opportunities for Technical Advancement	65
(1) Strength Analysis	65
(2) Fatigue and Damage Tolerance	65
(3) Weight Estimating	67
(4) Manufacturing Opportunities for Technology Advancement	67
(5) Quality Control	68
IV TECHNICAL DISCIPLINE ACCOMPLISHMENTS	69
1. Introduction	69
2. Materials and Processes	71
a. Material Candidates	71
(1) Metals	71
(2) Honeycomb Core	80
(3) Nonmetals	81
b. Material Assessment and Selection	84
(1) Metals	84
(2) Nonmetals	88
(3) Honeycomb Core	89
(4) Fasteners	89

CONTENTS—Continued

Section	Page
IV	
2. c. Processes	92
(1) Adhesive Bonding	92
(2) Finishes	97
3. Design	100
a. Preliminary Design Approach	100
b. Structural Concept Development	102
(1) Level 1 Concept Studies	102
(2) Level 2 Shell Concept Studies	125
(3) Level 3 Shell Concept Studies	133
(4) Components Other Than the Shell	165
4. Structural Analysis	174
a. Stress	174
(1) Shell Analysis	174
(2) Analysis Approach	179
(3) Structural Sizing Analysis of Shell Concepts	179
(4) Final Shell Sizing	191
(5) Analysis of Other Structural Components	191
b. Fatigue	193
(1) Introduction	193
(2) Fatigue Life Requirements	195
(3) Fatigue Analysis	195
(4) Fatigue Analysis Locations	200
(5) Fatigue Data Transfer	200
(6) FQR Requirement for No Constraint on Ultimate Design	201
(7) Stringer/Frame Intersection Study	201
(8) Materials and Processes Trade Study	204
(9) Fatigue Testing	206
c. Damage Tolerance	209
(1) Introduction	209
(2) Damage Tolerance Criteria	209
(3) Damage Tolerance Analysis	211
(4) Analysis Locations	214
(5) Damage Tolerance Data Transfer	214
(6) Damage Tolerance Trade Studies	217
(7) Material Testing	223
5. Weight Estimating	225
a. Data Base	225
(1) Study Section	225
(2) Baseline Weights	225
b. Estimating Method	227
(1) Skin/Stringer Concepts	227
(2) Honeycomb Concept	229

CONTENTS—Continued

Section		Page
IV	5. c. Weight Summary—Level 2 Concepts	229
	d. Final Concept Weights	230
	(1) Geometry and Material Change Effects	233
	e. Weight Savings—Results	234
	(1) Weight Reduction—Study Section	234
	(2) Weight Reduction—Total Fuselage	234
	6. Manufacturing	235
	a. Manufacturing Requirements	235
	b. Manufacturing Planning	236
	c. Tooling Requirements	243
	d. Assembly Requirements	244
	e. Manufacturing Considerations	244
	(1) Adhesive Bonding	244
	(2) Mechanical Fastening	255
	(3) Summary	255
	f. Technology Development Required	255
	g. Manufacturing Cost Assessments	256
	(1) Standard Hours	257
	(2) Complexity Factors	257
	(3) Learning Curves	257
	7. Quality Assurance/Nondestructive Inspection (NDI)	258
	a. Quality Assurance Tasks	258
	b. Concept Review Tasks	258
	c. Quality Assurance—Concept Tasks	258
	(1) Design and Development Controls	258
	(2) Procurement Control	263
	(3) Fabrication and Assembly Control	263
	(4) Process Control	263
	d. NDI Requirements	263
	(1) Facility Requirements	264
	(2) Capability Requirements	264
	e. Fracture Control Plan—Quality Control Requirements	266
	(1) Fabrication Control	266
	(2) Material Control	266
	(3) In-Service Inspection	267
	(4) NDI Demonstration	267
	(5) Traceability of Material	267
	f. Technology Development	267
	8. Cost Estimating	271
	a. Introduction	271
	b. Background	271
	c. Cost Estimating Method	271
	d. Concept Cost Estimates	272

CONTENTS—Concluded

Section	Page
V	RECOMMENDED FOLLOW-ON PROGRAM 279
1.	Introduction 279
2.	Phase 1B—Preliminary Design 279
3.	Phase 2—Detail Design and Analysis 284
4.	Phase 3—Fabrication 285
5.	Phase 4—Test 285
6.	Phase 5—Information Transfer 287
VI	RELATED STUDIES, CONTRACT ADDITION 289
1.	Investigation of Impact of Variations in Damage Tolerance Requirements on Structural Weight or Crack Growth Life 289
a.	Introduction 289
b.	Basic Data 291
	(1) Loads 291
	(2) Material Data 291
	(3) Analysis Methodology 309
c.	Analytical Results 324
	(1) Baseline Period of Unrepaired Usage 324
	(2) Effects of Varying Material Crack Growth Rates 328
	(3) Effects of Varying Usage 330
	(4) Effects of Varying Initial Damage Size 330
	(5) Effects of Varying Inspection Intervals 332
	(6) Effects of Varying Initial In-Service Damage Size 338
	(7) Effects of Varying Period of Safe Crack Growth After Failure of a Single Principal Element 343
	(8) Effects of Multiple Defects 343
	(9) Effects of Varying Residual Load Requirement 349
d.	Concluding Remarks 349
2.	Survey of 747-100 Service Experience 353
a.	Introduction 353
b.	Exterior Environment 353
c.	Interior Environment 356
d.	Maintenance Requirements and Observed Structural Deficiencies 356
3.	Assessment of NDI Demonstration Program 357
a.	Introduction 357
b.	General Approach 357
c.	Specimen Fabrication 358
d.	Inspection Procedures 359
	(1) Penetrant Inspection 365
	(2) Eddy Current Inspection 366
e.	Flaw Characterizations 366
f.	Records 366

CONTENTS—Concluded

Section	Page
VI	
3. g. Statistical Evaluation	366
h. Estimated Man-Hours for Demonstration Programs	368
4. Study of Fracture Control Program Implementation— Incremental Cost	369
5. Study of Advisability of Proof Testing in Lieu of NDT	371
APPENDIX A—USAF Damage Tolerance Criteria	375
APPENDIX B—Material Testing	407
REFERENCES	441

LIST OF ILLUSTRATIONS

No.	Page
1 Honeycomb Shell Concept	4
2 External Stringer Shell Concept	5
3 Internal Stringer Shell Concept	6
4 Fatigue and Fail-Safe Test Setup for the 747	8
5 Typical Baseline Stresses (N_X/\bar{t})—Wing/Fuselage	9
6 Wing/Fuselage Weight History	10
7 Centerline Payload-Weight Effect	11
8 Fuselage Cyclic Stress Due to Pressurization ($\Delta P = 9$ psi)	12
9 Distribution of Jet Transport Fatigue Problems by Component (Includes Both Major Fatigue Test and Service Data)	13
10 Component Cost Comparison	14
11 Baseline 747-100 Fuselage Section	15
12 Boeing IR&D Bonded Honeycomb Panel	17
13 747 Cargo Fuselage Study Section	18
14 Shell, Top Quadrant—Baseline	20
15 Shell, Side Quadrant—Baseline	21
16 Shell, Bottom Quadrant—Baseline	22
17 Typical Frame—Baseline	23
18 Pressure Deck—Baseline	25
19 Bulkhead, Body Station 1480—Baseline	26
20 Keel Beam—Baseline	27
21 Typical Trunnion Fitting—Baseline	28
22 Actuator Support Fitting, Body Station 1480—Baseline	29
23 747 Fuselage Sign Convention	30
24 Ultimate Vertical Shear Loads	31
25 Ultimate Vertical Bending Moments	32
26 Ultimate Lateral Loads—Shear, Bending, and Torsion	33
27 Baseline Weight Distribution	37
28 Level 3 Shell Screening	39
29 Internal Stringer	42
30 Honeycomb	43
31 External Stringer	45
32 Continuous Bead	47
33 Importance of Cargo/Tanker to USAF Mission	49
34 Tanker Mission: Payoff in Increased Fuel Transfer per Airplane	51
35 Cargo Mission: Payoff in Increased Payload per Airplane	52
36 Surveillance Mission: Payoff in Increased Time on Station	53
37 AMST Applicability	57
38 General Arrangement—Boeing AMST	58
39 Fuselage Structure	59
40 Performance Sensitivity: Effect of Structural Weight Reduction on Payload and Mission Radius	61
41 Performance Sensitivity: Effect of Structural Weight Reduction on Field Length	62

LIST OF ILLUSTRATIONS—Continued

No.	Page
42	Ten-Year AMST Life Cycle Costs as a Function of Fleet Size 63
43	Boeing AMST Payoff 64
44	Concept Development Plan 70
45	Insulation and Aerodynamic Fairing 83
46	Advanced Cargo Fuselage Material Normalized Properties 85
47	Fastener Head Configurations 90
48	Split-Sleeve Cold Expansion Process 91
49	Double Cantilever Beam (DCB) Test Specimen Configuration 93
50	Mechanism of Bond Delamination and Corrosion 94
51	Surface Preparation Effect on Strain Energy Release Rates 96
52	Protective Finish System 99
53	Shell—Skin/Stringer Bonded (Concept 1-1) 105
54	Shell—Skin/Stringer Bonded, Alternate Frame Outer Chord (Concept 1-1) 106
55	Shell—Skin/Stringer Bonded, Waffled Doubler (Concept 1-1) 107
56	Shell—Skin/Stringer Integrally Stiffened (Concept 1-2) 108
57	Shell—Skin/Stringer Wide-Spaced Longerons (Concept 1-3) 109
58	Shell—Laminated Continuous Beads (Concept 1-4) 110
59	Shell—Laminated Continuous Beads, Concept Variations (Concept 1-4) 111
60	Shell—Laminated Discontinuous Beads (Concept 1-5) 112
61	Shell—Laminated Staggered Discontinuous Beads (Concept 1-5) 113
62	Shell—Laminated Discontinuous Zee Stringers (Concept 1-5) 114
63	Shell—Laminated Discontinuous Hat Stringers (Concept 1-5) 115
64	Shell—Extruded, Laminated Integrally Stiffened (Concept 1-6) 116
65	Shell—Machined, Laminated Integrally Stiffened (Concept 1-6) 117
66	Shell—Laminated Composite Sandwich (Concept 1-7) 118
67	Shell—Hat Stiffened Honeycomb (Concept 1-8) 119
68	Shell—J-Stiffened Honeycomb (Concept 1-9) 120
69	Shell—Sandwich Honeycomb (Concept 1-10) 121
70	Shell—Sandwich Honeycomb, Wide-Spaced Longerons (Concept 1-11) 122
71	Shell—External Stringers (Concept 1-12) 123
72	Shell—Barrel Body 60-in. Frame Spacing (Concept 1-13) 124
73	Baseline—Typical Crown Structure 127
74	Shell Configuration 2-1—Inverted Hat Stiffeners 128
75	Shell Configuration 2-4—Continuous Beads 129
76	Shell Configuration 2-9—Stiffened Honeycomb 130
77	Shell Configuration 2-10—Honeycomb 131
78	Shell Configuration 2-12—External Hat Stringers 132
79	Level 2 Shell Screening 134
80	Internal Stringer Shell (Concept 3-1) 135
81	Continuous-Bead Shell (Concept 3-4) 143
82	Honeycomb Shell (Concept 3-10) 150
83	External Stringer Shell (Concept 3-12) 157
84	Level 3 Shell Screening 166

LIST OF ILLUSTRATIONS—Continued

No.	Page
85 Fuselage Frame	167
86 Pressure Bulkhead, Body Station 1480	169
87 Keel Beam	170
88 Pressure Deck	172
89 Main Floor Beam	173
90 Shear Flow Distribution for Vertical Bending Plus 1.5 Factors Pressure	176
91 Bending Stress Distribution for Vertical Bending Plus 1.5 Factors Pressure	177
92 Structural Breakdown—747-100 Aft Fuselage	178
93 Fuselage Shell Analysis Locations By Quadrant	180
94 Structural Sizing Worksheet Format	181
95 Worksheet for Structural Sizing of Internal Hat Stiffened Shell Concept	182
96 Stiffened Shell Concept Component Structural Optimization for Compression as a Function of Skin Gage	185
97 Compression Stability of Aluminum (7075-T6) Honeycomb Sandwich Panels	187
98 Shear Stability of Aluminum (7075-T6) Honeycomb Panels	188
99 Combined Compression and Shear Interaction Curves for Skin/Stringer Structural Concepts	189
100 Interaction Curves—Honeycomb Sandwich Panels Under Edgewise Compression and Shear	190
101 Pressure Bulkhead, Body Station 1480	192
102 747 Keel Beam Structure	194
103 Load Environment—Maneuver	196
104 Standardized Aluminum S-N Data—FQR = 18 ksi, R = 0.06	198
105 Fatigue Analysis Locations	201
106 Fatigue Analysis Design Data	202
107 FQR Requirements for No Constraint on Ultimate Design—Crown	203
108 Material and Process Trade Study	205
109 Allowable Tension Stresses—Crown Structure	207
110 Fatigue Test Data	208
111 Potential Blade Impact Areas	211
112 Damage Tolerance Analysis Locations	215
113 Fatigue Crack Growth Life—Hoop Loading	216
114 Residual Strength—Hoop Loading	218
115 Crack Growth From Initial Flaw—Bonded/Riveted Structure, Crown Location	219
116 Fatigue Crack Growth Rates: Sheet versus Honeycomb Sandwich	220
117 Crack Growth From Initial Flaw—2024-T3/7475-T761, Side-of-Body Location	222
118 Residual Strength—Hoop Loading	224
119 Baseline Study Section	226
120 \bar{t} Locations	227
121 Typical Panel Weight Calculation	228

LIST OF ILLUSTRATIONS—Continued

No.	Page
122 Primary Fabrication of Details for Any Concept	237
123 Honeycomb Sandwich Shell Concept	239
124 Skin/Stringer Concept—External	241
125 Internal Shell Stringer Concept	245
126 Quadrant Assembly, Inspection, and Shipping	247
127 Test Section Assembly	249
128 Header-and-Skin-Type Bonding Assembly Jig for Simple Contours (Headers Ready for Application of Jig Skins)	251
129 Header-and-Skin-Type Bonding Assembly Jig Skins Being Installed	252
130 Three-Piece Cast Aluminum, Compound Contoured Bonding Assembly Jig (Machined on Five-Axis Mill)	253
131 Completed Cast Aluminum, Compound Contoured Bonding Assembly Jig	254
132 AMS/ADP Cargo Fuselage—Quality Assurance Plan	260
133 Quality Control-NDI Flow Chart for Adhesive Bonding Process and Assembly	261
134 Prototype Multilevel Recorder	265
135 Prototype—Electromagnetic Proof Testing Facility	268
136 Production Model of Bond Proof Testing Unit	269
137 Ultrasonic Through-Transmission Inspection Facility	270
138 Follow-on Program Flow Chart	281
139 Follow-On Program Schedule	283
140 Major Test Article and Fixture	286
141 Frame Construction	290
142 Crown Stress Exceedances (1-Hr Flight)	292
143 Crown Stress Exceedances (3-Hr Flight)	293
144 Crown Stress Exceedances (7-Hr Flight)	294
145 Side-of-Body Stress Exceedances (1-Hr Flight)	295
146 Side-of-Body Stress Exceedances (3-Hr Flight)	296
147 Side-of-Body Stress Exceednaces (7-Hr Flight)	297
148 Maximum Stress Exceedances (3-Hr Flight)	298
149 Critical Stress Intensity Factor (2024-T3, L-T)	300
150 Critical Stress Intensity Factor (2024-T3, T-L)	301
151 Critical Stress Intensity Factor (7075-T6, L-T)	302
152 Fatigue Crack Growth Rates (2024-T3, L-T)	303
153 Fatigue Crack Growth Rates (2024-T3, T-L)	304
154 Fatigue Crack Growth Rates (7075-T6, L-T)	305
155 Panel Test Spectrum	306
156 Test Versus Analysis	307
157 Effect of Stress Spectra Truncation—Crown	308
158 3-Hr Spectrum Crack Growth Rates—Crown (2024-T3, L-T)	310
159 Spectrum Crack Growth Rates—Crown (2024-T3, L-T)	311
160 3-Hr Spectrum Crack Growth Rates—Crown (7075-T6, L-T)	312
161 Spectrum Crack Growth Rates—Crown (7075-T6, L-T)	313

LIST OF ILLUSTRATIONS—Continued

No.	Page
162	314
163	315
164	316
165	317
166	320
167	321
168	322
169	323
170	326
171	327
172	331
173	333
174	334
175	336
176	339
177	340
178	341
179	342
180	345
181	346
182	347
183	348
184	351
185	360
186	361
187	362
188	363
189	364
190	367
191	370
192	372
193	374
II-1	410
II-2	411
II-3	412
II-4	413
II-5	414
II-6	415
II-7	416

LIST OF ILLUSTRATIONS—Concluded

No.	Page
II-8 Fatigue Crack Propagation Data (7475-T61, L-T, 3½% NaCl Solution)	417
II-9 Fatigue Crack Propagation Data (7475-T61, T-L, 3½% NaCl Solution)	418
II-10 Fatigue Crack Propagation Data (7475-T761, 90% RH Air)	419
II-11 Fatigue Crack Propagation Data (7475-T61, 90% RH Air)	420
II-12 Fatigue Crack Propagation Data (7475-T761 and 2024-T3, 90% RH Air) . . .	421
II-13 Plane Stress Fracture Toughness (W = 24 In.)	422
II-14 Plane Stress Fracture Toughness (W = 36 In.)	423
II-15 Plane Stress Fracture Toughness (t = 0.040 In.)	424
II-16 Plane Stress Fracture Toughness (t = 0.112 In.)	425
II-17 Fatigue Crack Propagation Data (7050-T736 and 7075-T76511, 90% RH Air)	426
II-18 Fatigue Crack Propagation Data (7050-T736 and 7075-T76511, Water) . . .	427
II-19 Fatigue Crack Propagation Data (7050-T736 and 7075-T76511, 3½% NaCl Solution)	428
II-20 Stress Corrosion Crack Growth	429
II-21 Stress Corrosion Crack Growth and K_{Isc}	430
II-22 Fatigue Crack Propagation Data (2024-T3 and 7475-T61)	431
II-23 Tension Test	432

LIST OF TABLES

No.		Page
I	USAF Selection Criteria Rating System—Shell Concepts	40
II	Estimated 10-Year Baseline Life Cycle Costs (1500 Hours/Year Utilization)	54
III	System Life Cycle Cost Savings Due to AMS-ADP Cargo Fuselage	54
IV	Payoff and Leverage on System Life Cycle Costs Due to AMS-ADP Cargo Fuselage	55
V	AMST Baseline Cost/Weight	60
VI	Material Selection Parameters	71
VII	Aluminum Preliminary Allowables	73
VIII	Material Fatigue Crack Growth Rate, $R = 0.05$	75
IX	Environmental Effect on Fatigue Crack Growth Rates of 7475 Material	77
X	Plane Stress Fracture Toughness Data	77
XI	Titanium Preliminary Allowables	79
XII	Steel Preliminary Allowables	80
XIII	Honeycomb Core Room Temperature Mechanical Properties	81
XIV	Adhesive Bonding Materials	97
XV	Concept Brainstorm Matrix—747 Cargo Fuselage Design Consideration	103
XVI	Design Concepts, Level 1 Study List	104
XVII	Level 1 Shell Concepts Selected for Level 2 Study	125
XVIII	Level 2 Shell Concepts Studied	126
XIX	Level 3 Weight and Cost Summary by Quadrant, Cargo Fuselage Study (Average of 201 Airplanes), Station 1420-1800—All Concepts	164
XX	General Component Analysis Considerations	175
XXI	Fatigue Life Requirements	195
XXII	Detail Design Impact on Fatigue Life	199
XXIII	Criteria for Damage Tolerance	210
XXIV	Criteria for the Identification of Fracture-Critical Parts	212
XXV	Level 2 Weight Analysis Results, 2024 and 7075 Material	230
XXVI	Level 3 Weight Analysis Results, 2024 and 7075 Material	231
XXVII	Level 3 Weight Analysis Results, 7475 Material	232
XXVIII	Component Weights Considered Constant for Level 3 Shell Studies	233
XXIX	Source of Weight Savings, Level 3 Shell Studies (Body Stations 1420 to 1800)	233
XXX	Weight Savings as a Percent of Total Body Structure	234
XXXI	Boeing Current NDI Status	259
XXXII	Sensitivity of NDI Techniques	266
XXXIII	Level 3 Weight and Cost Summary by Quadrant (Average of 201 Airplanes), Station 1420-1800—Baseline	273
XXXIV	Level 3 Weight and Cost Summary by Quadrant (Average of 201 Airplanes), Station 1420-1800—Internal Stringer Concept	274
XXXV	Level 3 Weight and Cost Summary by Quadrant (Average of 201 Airplanes), Station 1420-1800—Continuous-Bead Concept	275

LIST OF TABLES—Concluded

No.		Page
XXXVI	Level 3 Weight and Cost Summary by Quadrant (Average of 201 Airplanes), Station 1420-1800—Honeycomb Concept	276
XXXVII	Level 3 Weight and Cost Summary by Quadrant (Average of 201 Airplanes), Station 1420-1800—External Stringer Concept	277
XXXVIII	Relative Concept Cost Estimates	278
XXXIX	Spectrum Crack Growth Rate Data	318
XL	Impact of Material Property and Usage Spectra Variability for Lifetime Period of Unrepaired Service Usage	329
XLI	Impact of Variability in Initial Damage Assumption and Period of Unrepaired Service Usage on Stress and Weight	335
XLII	Impact of Variability of Damage Detectability Limits and Inspection Interval	344
XLIII	Residual Load Requirement for Crown Location	350
XLIV	Effect of Varying Residual Load Requirements	350
XLV	Baseline Capability Compared to Typical Requirements	352
XLVI	Scheduled 747 Flights	354
XLVII	Exposure Hours Per Week For Various Routes (January and July)	355
XLVIII	Penetrant Facilities	365
XLIX	Specimen Requirements	368
II-I	Material Characterization Test Specimens	433
II-II	Fatigue Specimen Definition	433
II-III	Center Crack Tension Specimens (da/dn in 90% RH Air)	434
II-IV	Center Crack Tension Specimens (da/dn in 3½% NaCl Solution)	434
II-V	“High” ΔK Crack Growth Tests (da/dn in 90% RH Air)	435
II-VI	Additional Crack Growth Panels (da/dn in 90% RH Air)	435
II-VII	Fracture Toughness (K _C) Test Validity	436
II-VIII	Compact Tension Specimens (da/dn in 90% RH Air, H ₂ O, and 3½% NaCl)	436
II-IX	Plane Strain Crack Growth/Environment (R = 0.05)	437
II-X	Plane Strain Fracture Toughness	437
II-XI	Stress Corrosion Crack Growth Tests (da/dt in 3½% NaCl Solution)	437
II-XII	Double Cantilever Beam (DCB) Specimens	438
II-XIII	Stress Corrosion Crack Growth and K _{ISCC} Data (da/dt in 3½% NaCl Solution)	438
II-XIV	Spectrum Loaded Panels (da/dS in 90% RH Air)	438
II-XV	Static Properties (F _{ty} , T _{tu} , E)	439

SECTION I

INTRODUCTION AND SUMMARY

This first phase of a multiphase program was designed to explore the application of new structural concepts to cargo aircraft fuselage structure. The goals of this first iteration preliminary design study are to reduce both weight and acquisition cost while maintaining the fatigue life. The goals are met through synergistic exploitation of advanced structural concepts, new materials applications, and improved manufacturing methods. The tasks that have been accomplished during this study phase are:

- Baseline and Component Selection
- Concepts Formulation
- Preliminary Design/Analysis
- Material Testing
- Concept Evaluation and Selection
- Assessment of Potential Aircraft System Payoff
- Follow-on Program Planning
- Damage Tolerance Criteria Sensitivity Study

The baseline structure selected for this study is a 32-foot-long aft fuselage section of the Boeing 747-100 aircraft. The 747 satisfied all of the USAF requirements for the selection of a baseline aircraft structure. The study section encompasses most of the design complexities found in a modern cargo aircraft fuselage.

The design effort devoted to the various fuselage components was in proportion to their potential weight payoff. Since approximately 72% of the fuselage weight is in the shell (skin/stringer/frames), the greatest potential for weight reduction is in these elements. Therefore, a considerable amount of the total effort was devoted to the shell structural panels and joints. The remaining design effort was devoted to improvements in the keel beam, floor beams, bulkheads, and various attachments.

Structural weight can be reduced by achieving a more efficient structural configuration or by increasing the constraining design stress level. In this study both approaches were taken. Structural efficiency is affected by structural geometric arrangement and the ability of that arrangement to act effectively under multiple loading conditions. During this study, the percentage of the total weight savings which were attributed to more efficient structural configurations varied from 65% to 95%. Design stress level is affected by material properties, damage tolerance sensitivity, and detail fatigue quality of the structure. All of the selected designs used the new high-strength aluminum alloys with improved fracture toughness. The

combination of damage-tolerant structural arrangement and the properties of the new alloys eliminated damage tolerance requirements as a stress level constraint. These new alloys, however, do not offer improved fatigue properties over current materials. This implies that the use of the higher design stress levels available from the new aluminum alloys could be limited by the goal to maintain the fatigue life equal to the baseline. Therefore, all three selected final designs use adhesive bonding as the primary joining method. With attention to design details, adhesive bonding can provide a significant improvement in the detail fatigue quality of the structure, thus allowing the design stress level to be established by material properties and design ultimate load requirement. The increased design ultimate stress level accounted for 5% to 35% of the weight savings obtained.

The fuselage shell concepts selected for the follow-on phases of this program are shown in figures 1, 2, and 3. These designs produced participating weight savings of 17% to 19% and acquisition cost savings of 2% to 7% of the study section average total unit cost for 201 airplanes.

The USAF cargo aircraft which could allow the earliest application of these concepts is the Advanced Medium STOL Transport (AMST). The performance of a STOL aircraft is more sensitive to its structural weight than that of a CTOL aircraft by a factor of approximately 2.5. The application of these concepts to AMST could produce a potential 10-year life cycle cost savings of \$325 million.

The planning and scheduling of all the required phases and tasks of the follow-on program have been summarized in section V of this report. The key output of the follow-on program will be the "across-the-board" technical information developed and verified by full-scale test article fabrication and test.

In addition to the basic phase 1A first iteration preliminary design, a study was also completed in which the USAF Damage Tolerance Criteria, Revision D,* was applied to the baseline structure. The study developed the sensitivity of the baseline to the material properties variability, inspection frequency, and inspection capabilities required by the criteria. This study of the baseline covered the following:

- Assessed the impact on the baseline structure of the application of the Air Force's new Damage Tolerance Criteria and MIL-STD-1530 (USAF), in terms of allowable stresses and life.
- Accumulated environmental and background data and assessed service experience for the baseline.
- Assessed the role of proof testing as a supplement to, or substitute for, conventional NDT.

*Structural concepts developed under this contract were designed to meet damage tolerance requirements as established by USAF Damage Tolerance Criteria, Revision, D, 18 August 1972. For convenience, a copy of these criteria have been reproduced as appendix I.

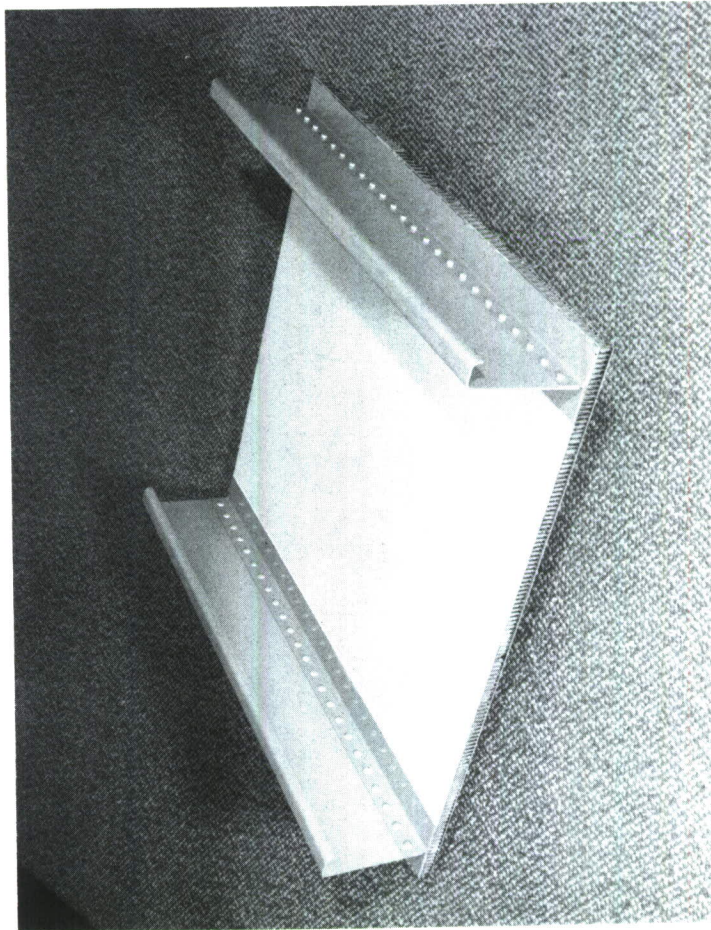
- Assessed methods and need for conducting NDT demonstration to determine sensitivity limits and effectivity of NDT as applied to the baseline.
- Assessed the impact on the baseline, in terms of incremental cost, of the application of the fracture control plan required by MIL-STD-1530 (USAF).

The results of the phase 1A cargo fuselage study are:

- The application of advanced fuselage structural concepts to future cargo aircraft systems is shown to provide a significant systems payoff.
- Four advanced cargo fuselage structural concepts have been developed; of these, three were selected and are recommended for the follow-on development program.
- The planning and scheduling required to further study the three selected concepts, and the fabrication and testing of one, have been completed.
- The impact of the application of the new USAF Damage Tolerance Criteria, and the sensitivity of its requirements as applied to a cargo fuselage, have been thoroughly evaluated.

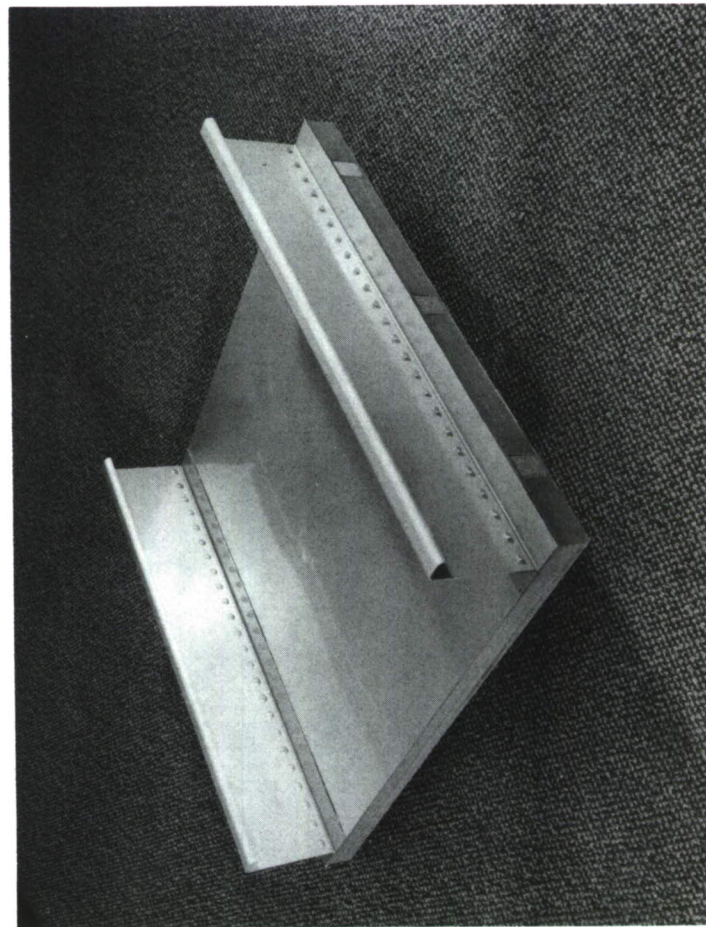
Concept 1: Honeycomb

- Shell material 7475-T761
- Bonded panel subassembly
- Improved fracture characteristics
- Improved combined load capability
- Reduced part count



Design	Total section cost savings (%)	Participating structure weight savings (%)
Current	1.8	17
Goal*	10	20
* Follow-on program goal		

Figure 1.—Honeycomb Shell Concept

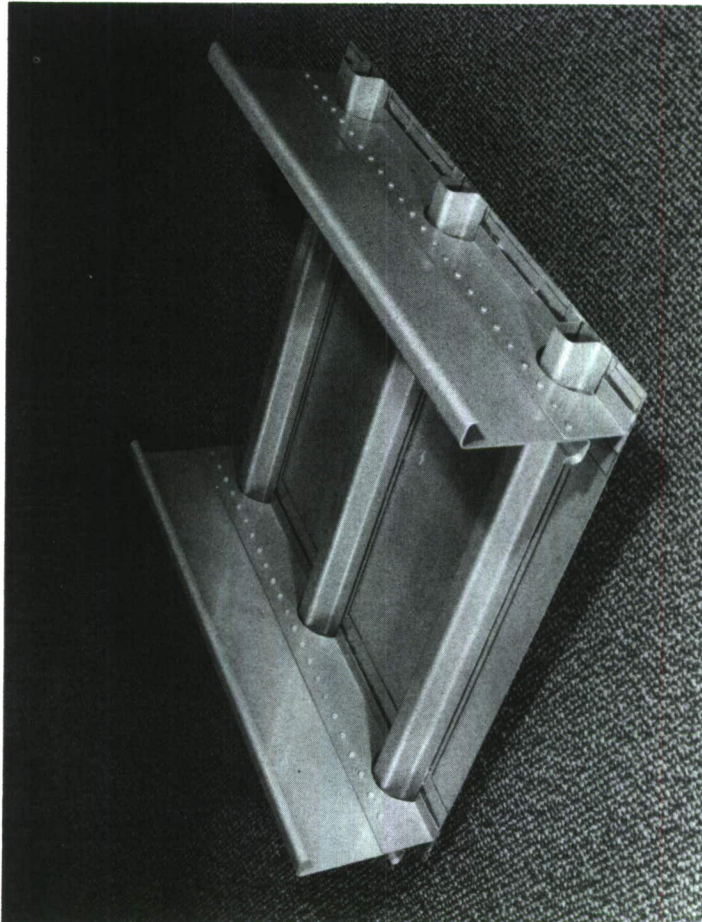


Concept 2: External Hat Stiffened

- Shell material 7475-T761
- Bonded panel subassembly
- Combined frame T/fail-safe strap
- Improved general stability
- No stringer/frame intersection
- External fairing required

Design	Total section cost savings (%)	Participating structure weight savings (%)
Current	7	19
Goal*	8	20
* Follow-on program goal		

Figure 2.—External Stringer Shell Concept



Concept 3: Internal Stringer

- Shell material 7475-T761
- Bonded panel subassembly
- Waffle doubler fail-safe strap
- Inverted hat stringers

Design	Total section cost savings (%)	Participating structure weight savings (%)
Current	4	17
Goal*	6	19
* Follow-on program goal		

Figure 3.—Internal Stringer Shell Concept

SECTION II

BASELINE STUDY SECTION

1. BASELINE AIRPLANE SELECTION

The selection of the Boeing 747-100 as an Advanced Metallic Structure—Advanced Development Program (AMS-ADP) cargo baseline airplane recognizes the fact that the increased capability of current and future large jet transports can make a significant contribution to the Air Force's ability to carry out its role in national defense. The Boeing 747-100, the largest and most efficient of the current family of wide-body commercial jets, provides an excellent baseline for this study. Exhaustive structural testing (static, fatigue, fail safety; see fig. 4), coupled with in-service use throughout the world, has established the validity of the baseline structure.

This aircraft selection satisfies the following USAF selection criteria:

- It represents 1972 state-of-the-art structures technology.
- It has, and is presently accumulating, service experience.
- It has a high potential for demonstrating significant advancement in technology.
- The component is critical to the safety of the aircraft.
- It is not a candidate for the forthcoming "prototype" programs.

2. SELECTION OF FUSELAGE COMPONENT

Boeing has selected a fuselage section as the study component most amenable to technology demonstration for the following reasons:

- Large-diameter pressurized cargo fuselages are designed largely by fatigue requirements.
- No significant advancement in fuselage structural design has occurred in the past 20 years.
- This is the only major planned development program that may develop new concepts for large fuselages.
- Pressurized fuselage design is a unique design problem for the cargo aircraft portion of the AMS-ADP.

Fuselage structure offers unique opportunities for structural improvement. Figure 5 shows design stresses for wing upper and lower surfaces, and fuselage upper, lower, and side

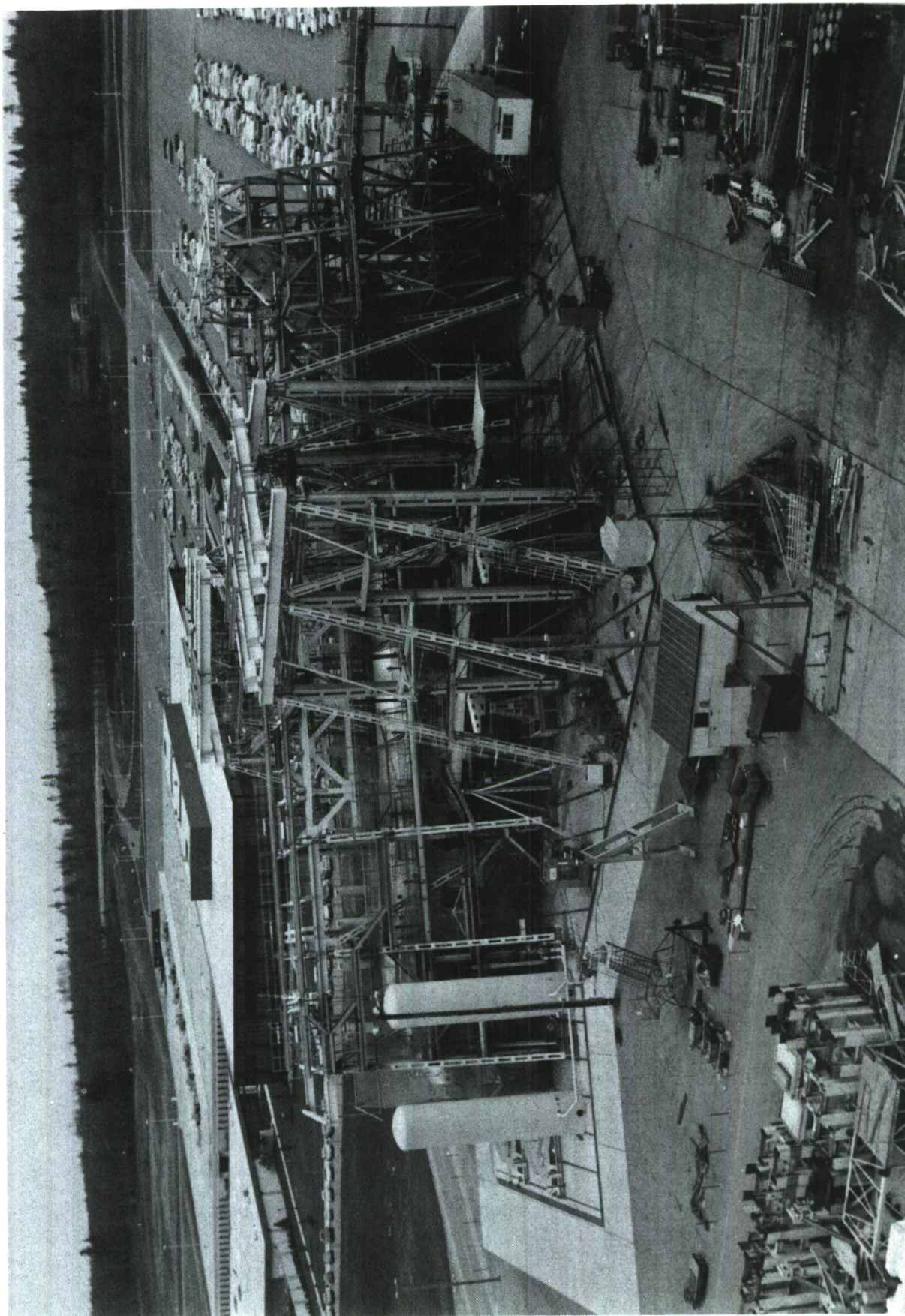


Figure 4.—Fatigue and Fail-Safe Test Setup for the 747

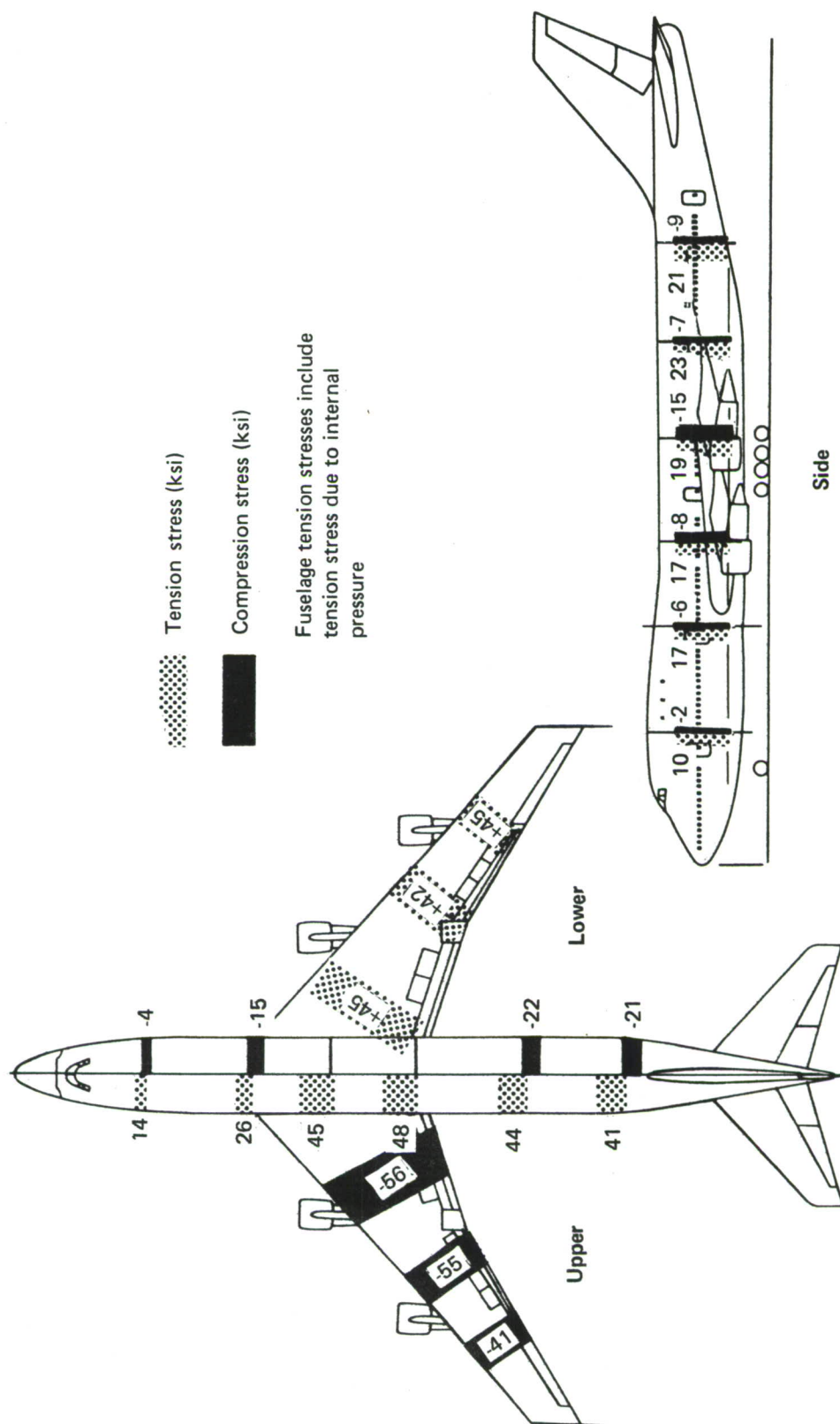


Figure 5.—Typical Baseline Stresses (N_x/t)—Wing/Fuselage

quadrants. The fuselage stresses shown include combined effects of bending and pressurization. In general, the wing is working at a higher stress level than the fuselage, resulting in a greater overall structural efficiency. Therefore, a greater opportunity exists for structural efficiency improvement in the fuselage, and this was a factor in choosing the fuselage for the study.

Historical weight trends for transport fuselage and wings are shown in figure 6. While there is considerable scatter in this plot, the trend has been for fuselage weight (as a percentage of airplane gross weight) to increase faster than wing weight, suggesting opportunities for improvement in fuselage structure.

Because of wing bending moment relief due to weight in the wing, greater payload improvement is achieved for fuselage weight reduction than for wing weight reduction. This concept, called the centerline weight effect, indicates that a higher potential payoff is available for reduced weight fuselages than for wings. Note in figure 7 that the ratio of increased payload to decreased wing structural weight is zero at a semispan of about 0.8 and is negative outboard of semispan 0.8, indicating that wing weight reduction in this region reduces payload.

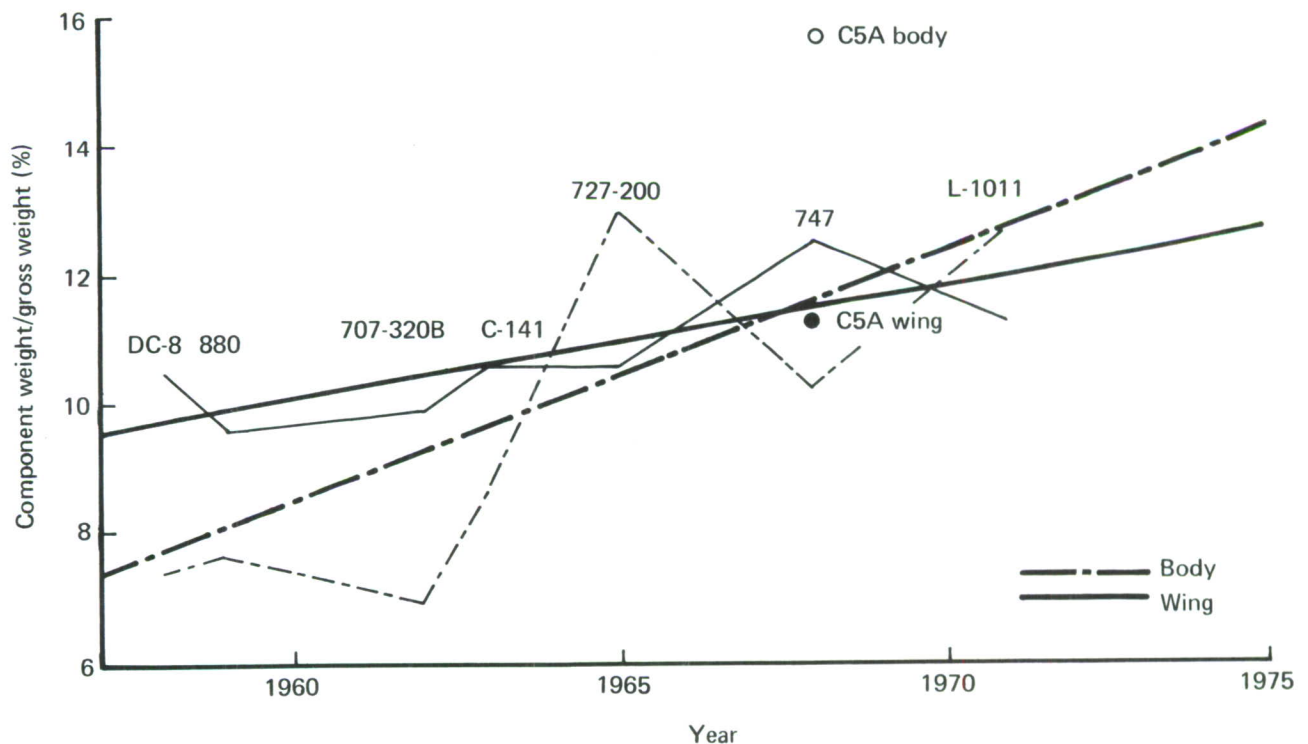


Figure 6.—Wing/Fuselage Weight History

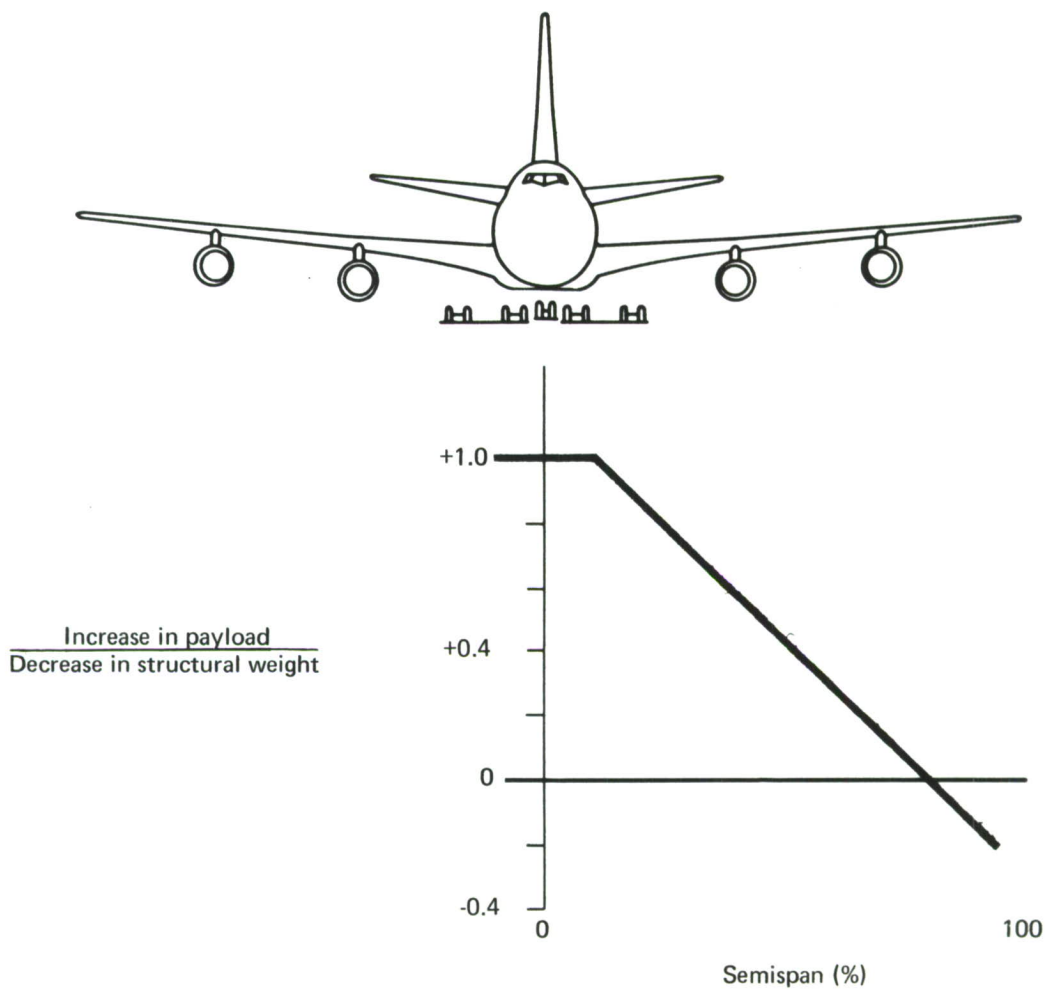


Figure 7.—Centerline Payload-Weight Effect

Fuselage structure provides a unique opportunity for the study and application of fracture mechanics because of the predictable cyclic loading due to fuselage pressurization (fig. 8). No other major structural component affords this advantage for verifying concepts and applications of fracture mechanics. The fuselage is also unique in having a strong biaxial stress field, a high degree of curvature, and significant out-of-plane loading and deformation.

Distribution of fatigue problems by major airframe component for commercial transports is shown in figure 9. Corresponding military data (ref. 1) show similar trends, with wing and fuselage percentages of 38% and 41%, respectively. This indicates that a significant opportunity for fuselage fatigue improvement exists.

Figure 10 shows that fabricated cost per pound of baseline fuselage structure is 25% higher than the airframe average. Since the fuselage constitutes approximately 37% of the baseline airframe structure weight, high leverage in reducing airframe cost is available from

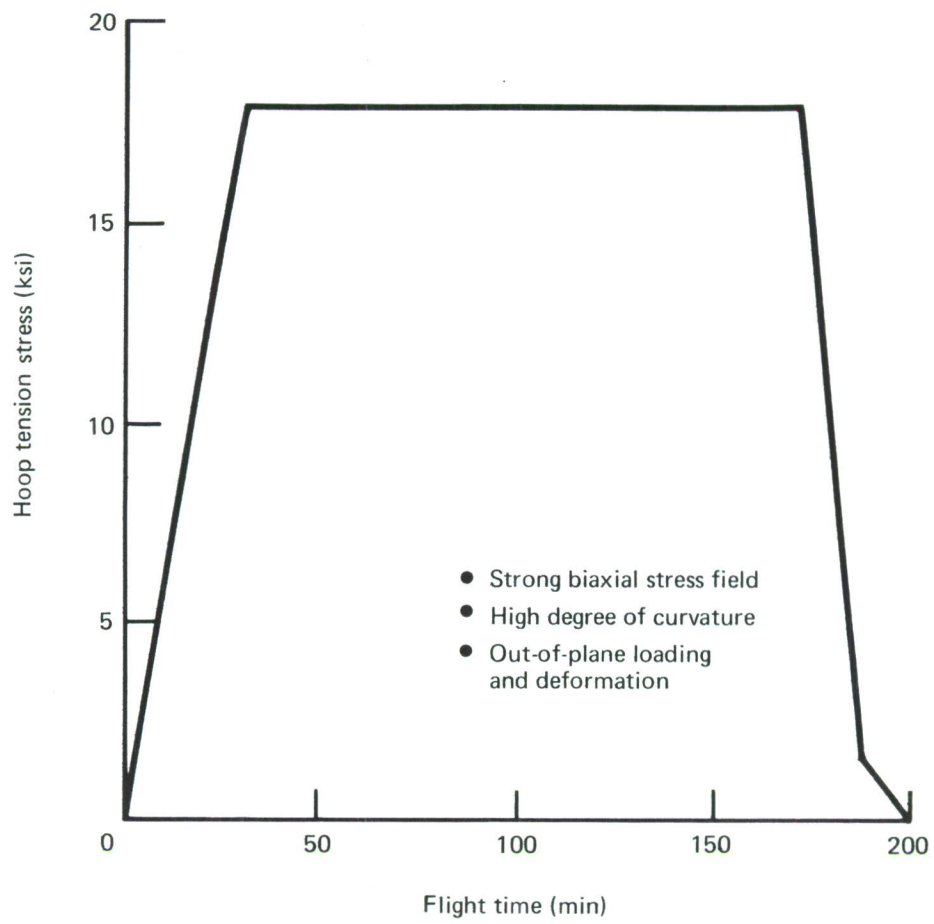
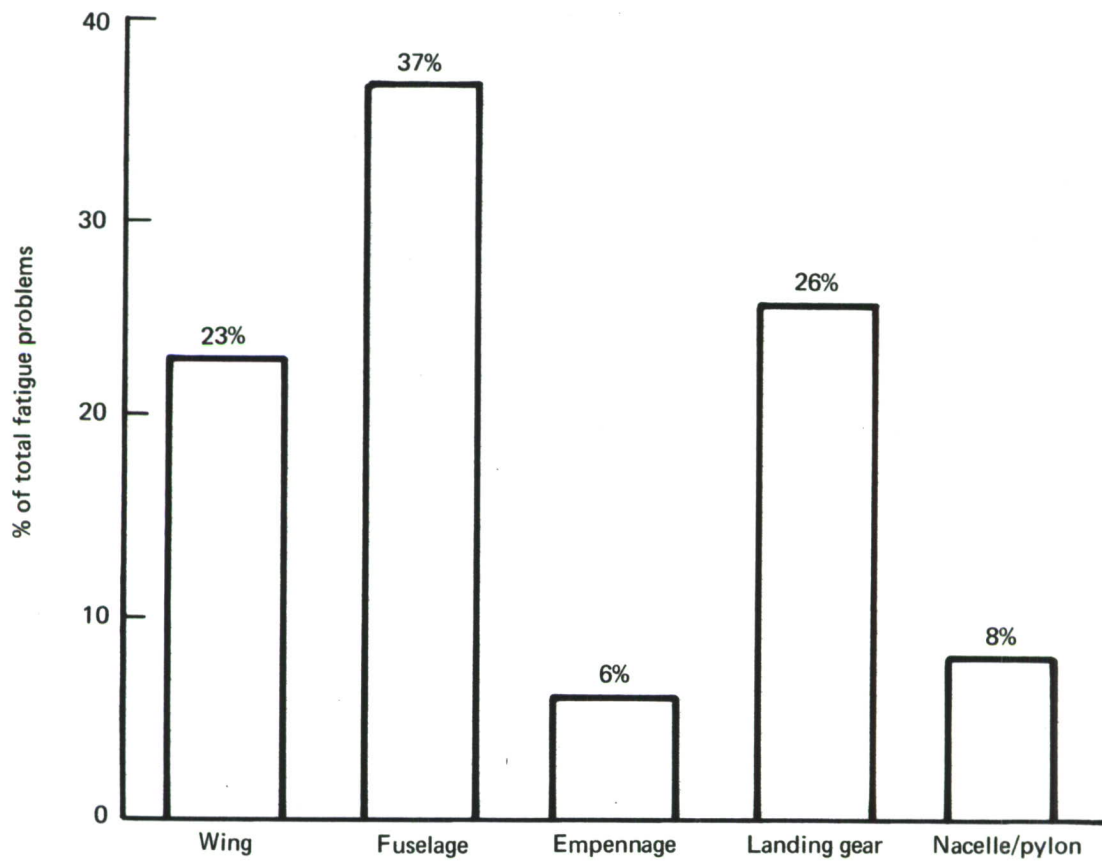


Figure 8.—Fuselage Cyclic Stress Due to Pressurization ($\Delta P = 9$ psi)



*Figure 9.—Distribution of Jet Transport Fatigue Problems by Component
(Includes Both Major Fatigue Test and Service Data)*

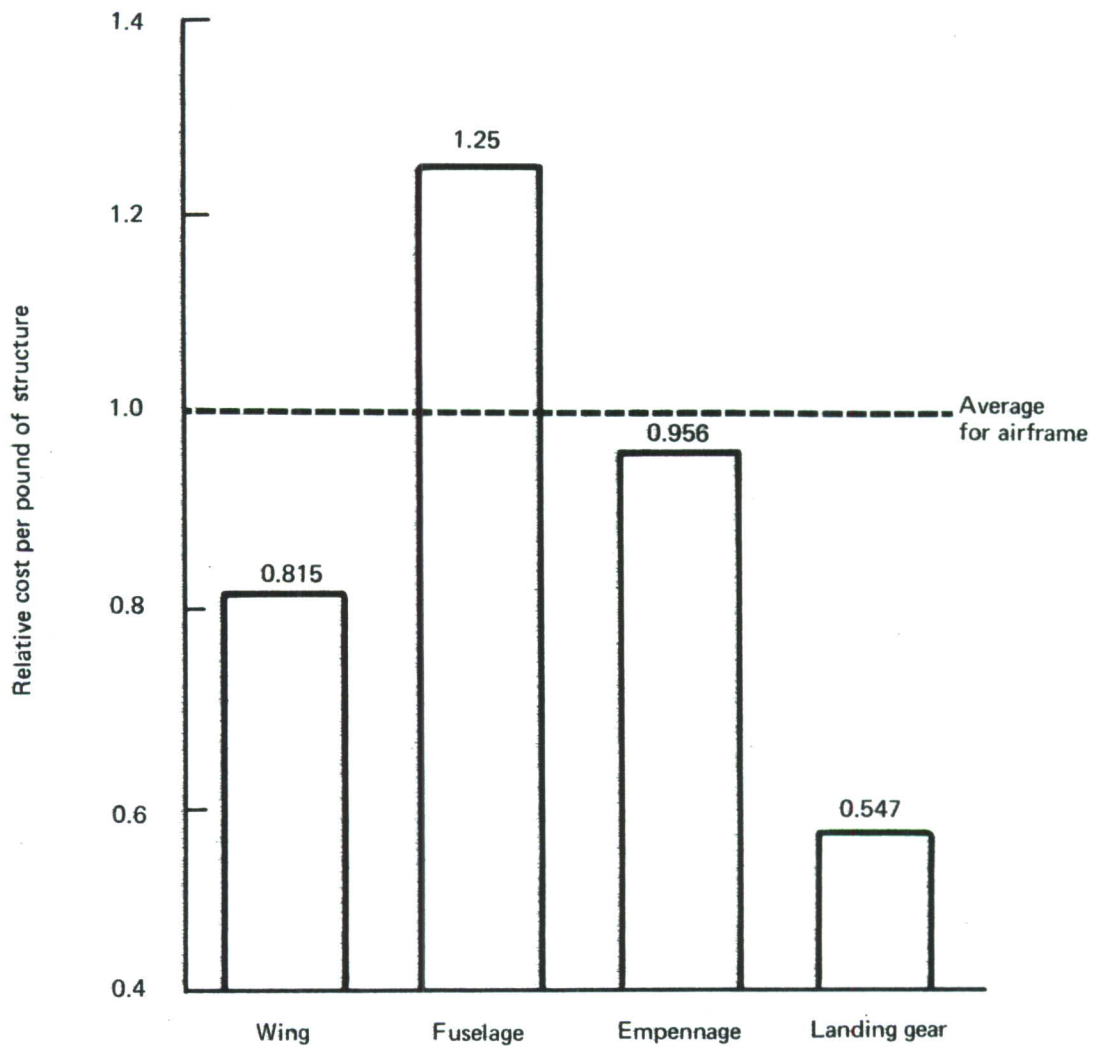


Figure 10.—Component Cost Comparison

two sources: (1) reduction in weight of fabricated fuselage structure through improved structural efficiency, and (2) development of fuselage structural concepts with improved manufacturability, resulting in lower fabricated structural cost per pound.

3. FUSELAGE SECTION CHOSEN FOR STUDY

The section of the 747-100 airplane fuselage chosen as the baseline for this study is shown in figure 11. It is a section of proven structure that has a wide variety of load conditions and load intensities and includes most of the design problems of an entire cargo fuselage. It is therefore an appropriate section for use in design evaluation of new structural concepts.

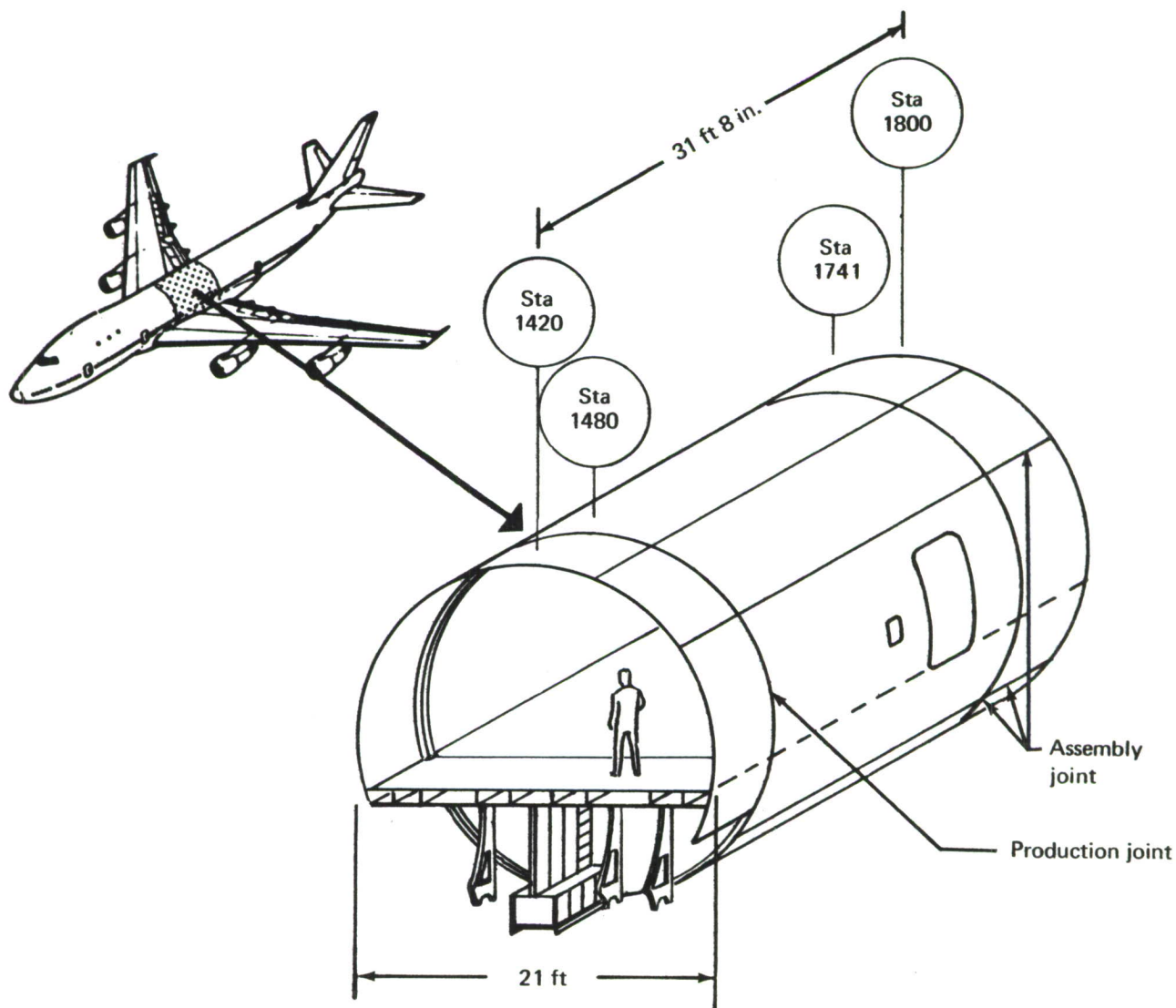


Figure 11.—Baseline 747-100 Fuselage Section

This study section encompasses most of the typical large aircraft fuselage design requirements:

- High concentrated loads due to keel beam and backup of landing gear fittings
- Both assembly splices and a major production joint
- Large and small cutouts (windows and doors)
- Major discontinuity and load redistribution at wheel well
- Bulkhead for load redistribution, which also carries fuselage pressure and supports the body-mounted landing gear
- Pressure deck over wheel well
- Wide range of shell end load intensities from 2000 to 10,000 pounds per inch
- High potential for development of various new concepts due to the different primary design requirements
 - Crown quadrant—tension, fatigue
 - Side quadrant—shear, pressure, and combined shear and compression
 - Lower quadrant—compression

Large wide-body designs are an extrapolation beyond available test data and, thus, are subject to shell stability problems. (This is important since any new subsonic jet cargo aircraft will have a wide body.)

Since the baseline study section is a section of a commercially competitive airframe, its cost and weight make extremely challenging targets for the new concept design development.

In addition, Boeing selected this particular study section because it was the subject of an extensive in-house research and development honeycomb bonding program. Full-size feasibility panels have been designed and manufactured. Figure 12 shows one of the major panels built during the IR&D program. A full-size test fixture has been designed for static testing.

4. BASELINE PHYSICAL DESCRIPTION

The baseline structural study section is a portion of the 747-100 airplane fuselage from body station 1420 to body station 1800. Figures 11 and 13 locate and show the general arrangement.

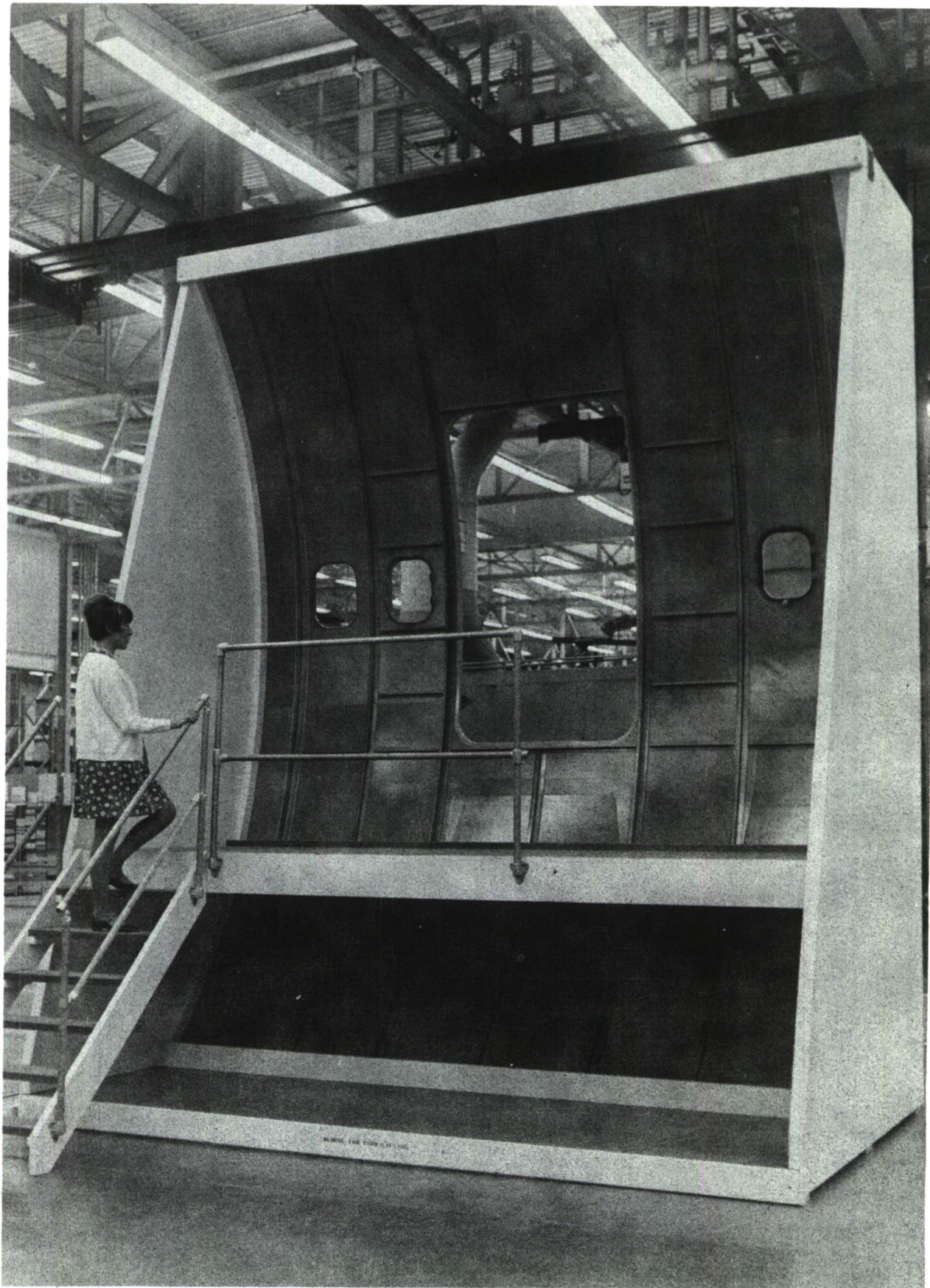


Figure 12.—Boeing IR&D Bonded Honeycomb Panel

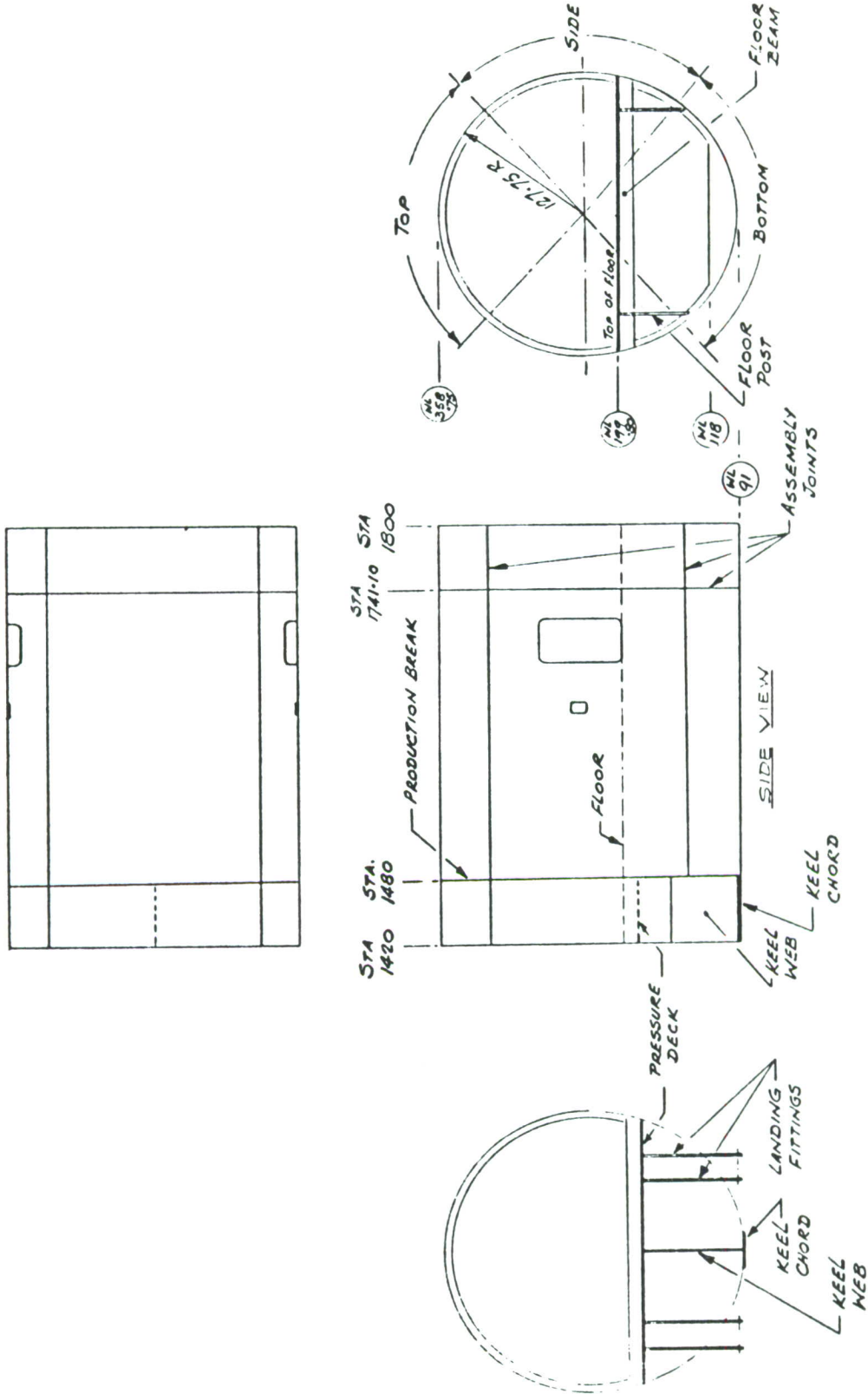


Figure 13.-747 Cargo Fuselage Study Section

The baseline structure is an all-aluminum, hat-section stiffened shell of riveted construction with machine tapered skins, bonded doublers and fail-safe straps, and frames at 20-inch spacing. The baseline contains the complexities of the keel beam to monocoque joint and a bulkhead at body station 1480, which carries pressure loads and landing gear loads and redistributes the monocoque loads. For evaluation, the shell has been broken up into three panels—crown, side, and lower—since each is critical for different basic loading conditions. One door and one window are included in the side panels of the baseline section because a review of in-service cargo aircraft fuselages showed that they contain cutouts for windows and doors. Their inclusion is desirable since window and door cutouts are a source of potential design and fatigue problems.

The present 747 fuselage structure uses 2024-T3 clad skins, 2024-T3 tear straps, 7075-T6 stringers, and 7075-T6 frames. Window and bulkhead forgings are 7075-T73.

In the baseline, alloy 2024-T3 was selected for the tension-critical areas because of its demonstrated superior fatigue behavior and high fracture toughness; 7075-T6 is used in compression-critical areas because of its high compression yield properties. Both alloys in sheet and thin plate form have demonstrated generally acceptable stress corrosion and exfoliation corrosion resistance. All internal fuselage surfaces are painted with a Skydrol-resistant epoxy finish system.

Aluminum 2017 driven rivets and titanium Hi-Lok fasteners in transition fit holes are both used in the fuselage structure.

Figures 14 through 22 contain simplified structural arrangement drawings of the baseline study section details.

5. DESIGN REQUIREMENTS

The 747-100 baseline loads used in this study equal or exceed the requirements of FAR 25. The certification loads, fatigue spectrum, and basic design criteria for the 747-100 airplane applicable to the study section (ref. 2) were used throughout the study. The basic design criteria were modified to be in agreement with MIL-STD-1530 (USAF) and the Air Force's Damage Tolerance Criteria (app. I).

The fatigue and damage tolerance requirements can be found in sections IV-4b and c of this document.

Figure 23 shows the sign convention indicating positive and negative directions for shear, moment, and torsion loads.

Lateral, vertical, and torsional design ultimate loads have been calculated for the aft fuselage for various flight, landing, and ground conditions. The effects of inertia, body airloads, empennage loads, landing gear loads, and wing loads have been considered in the basic load calculations. Critical loads have been determined by analyzing each load condition for various combinations of gross weight, center-of-gravity location, and payload distribution. These critical loads have been combined to form a design load envelope and are shown in figures 24 through 26.

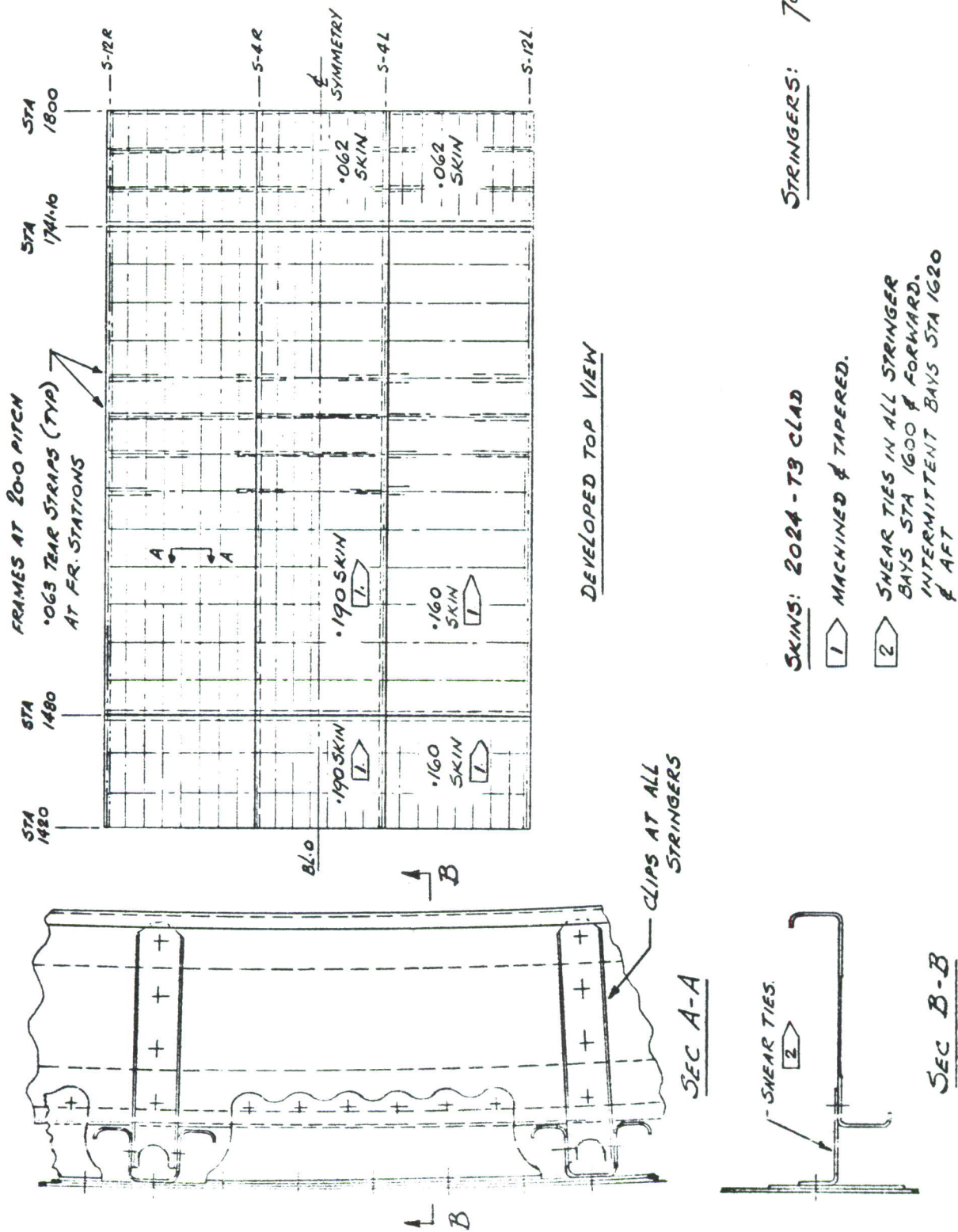


Figure 14. --Shell, Top Quadrant--Baseline

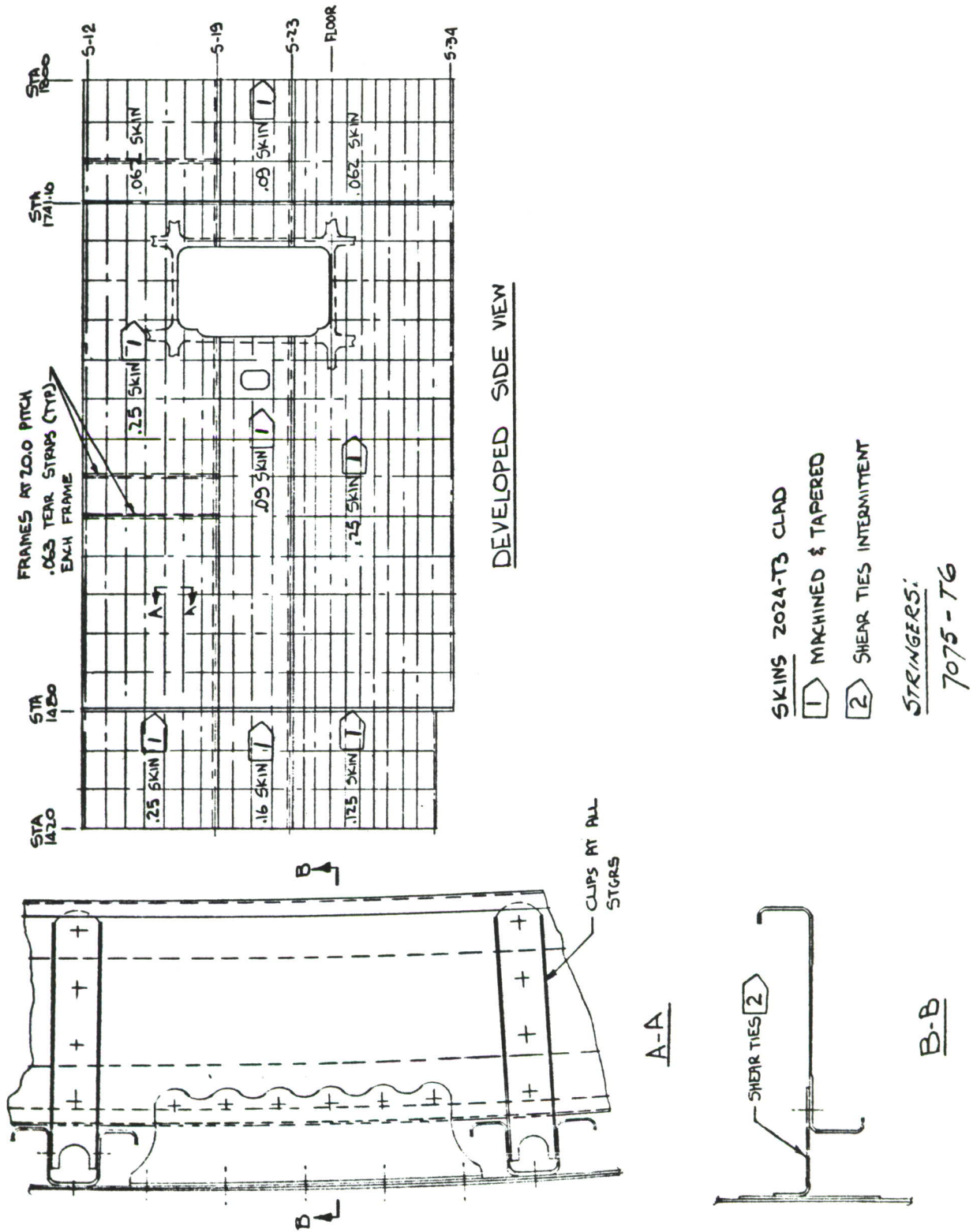
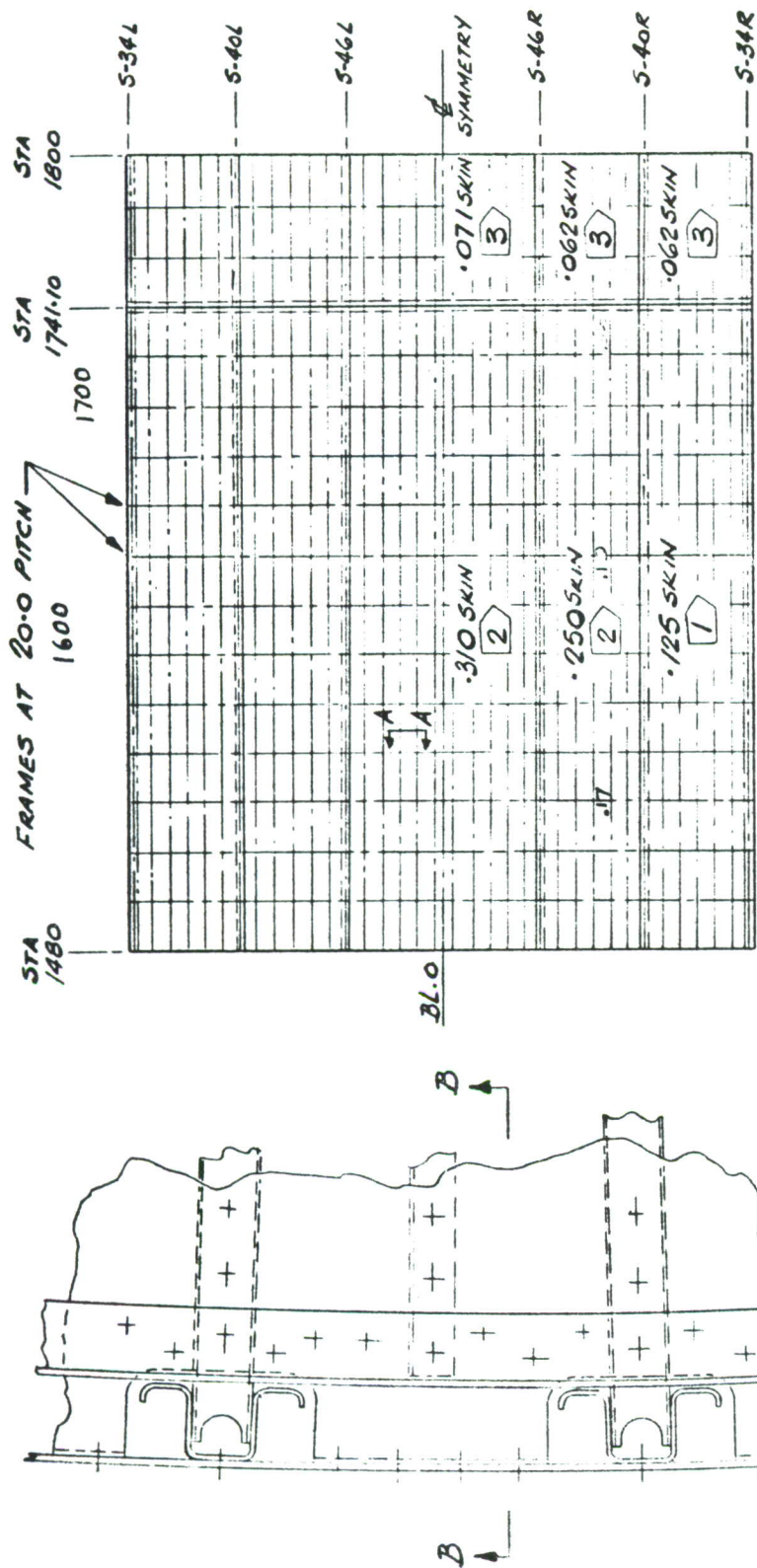


Figure 15.—Shell, Side Quadrant—Baseline



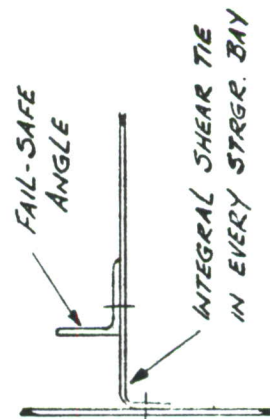
DEVELOPED BOTTOM VIEW

SKINS:-

- 1 2024-T3 CLAD. MACHINED & TAPERED
- 2 2024-T351 CLAD. MACHINED & TAPERED
- 3 2024-T3 CLAD

STRINGERS:-

7075-T6



B-B

Figure 16.-Shell, Bottom Quadrant - Baseline

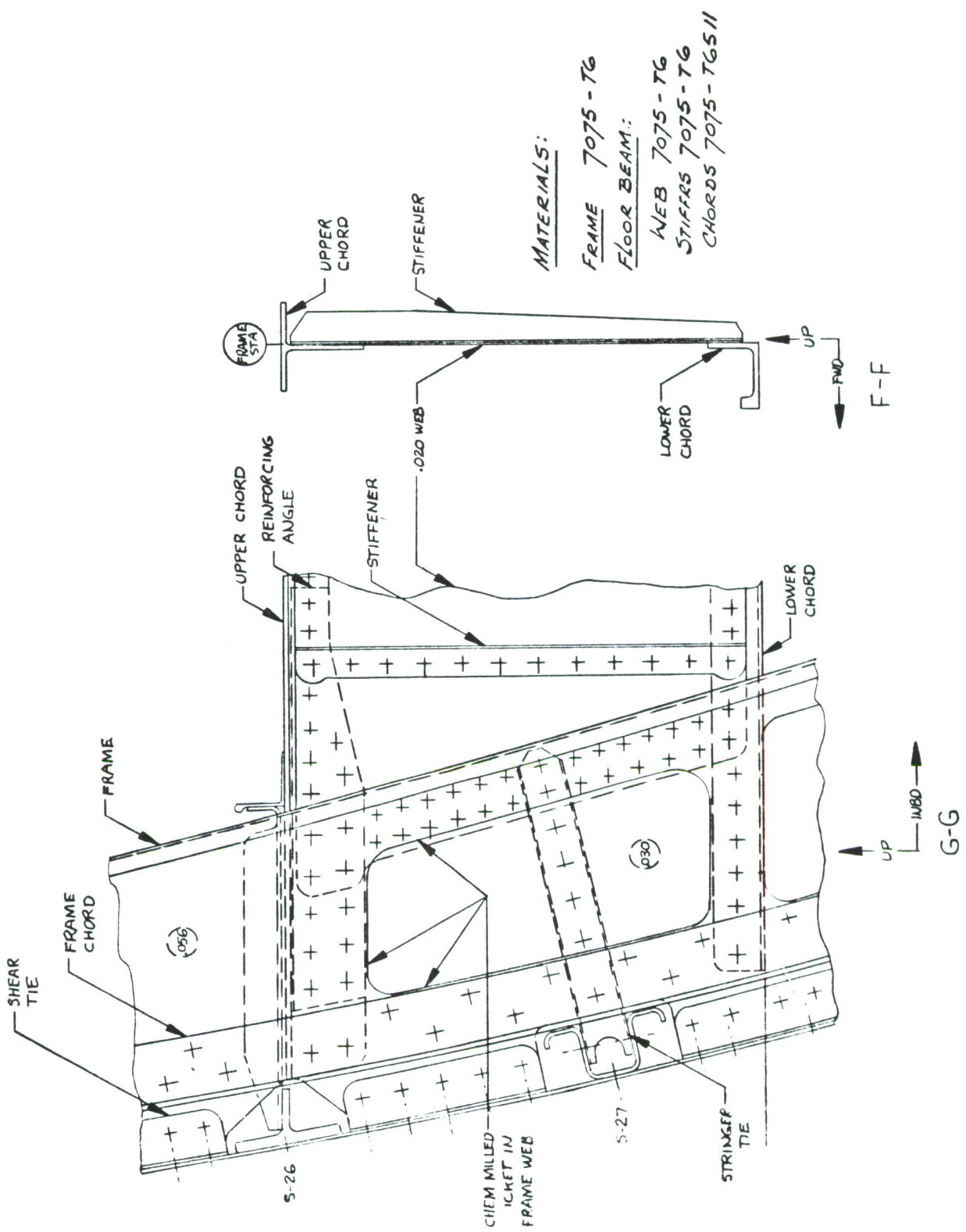


Figure 17.—Concluded

STIFFERS 7075-76511



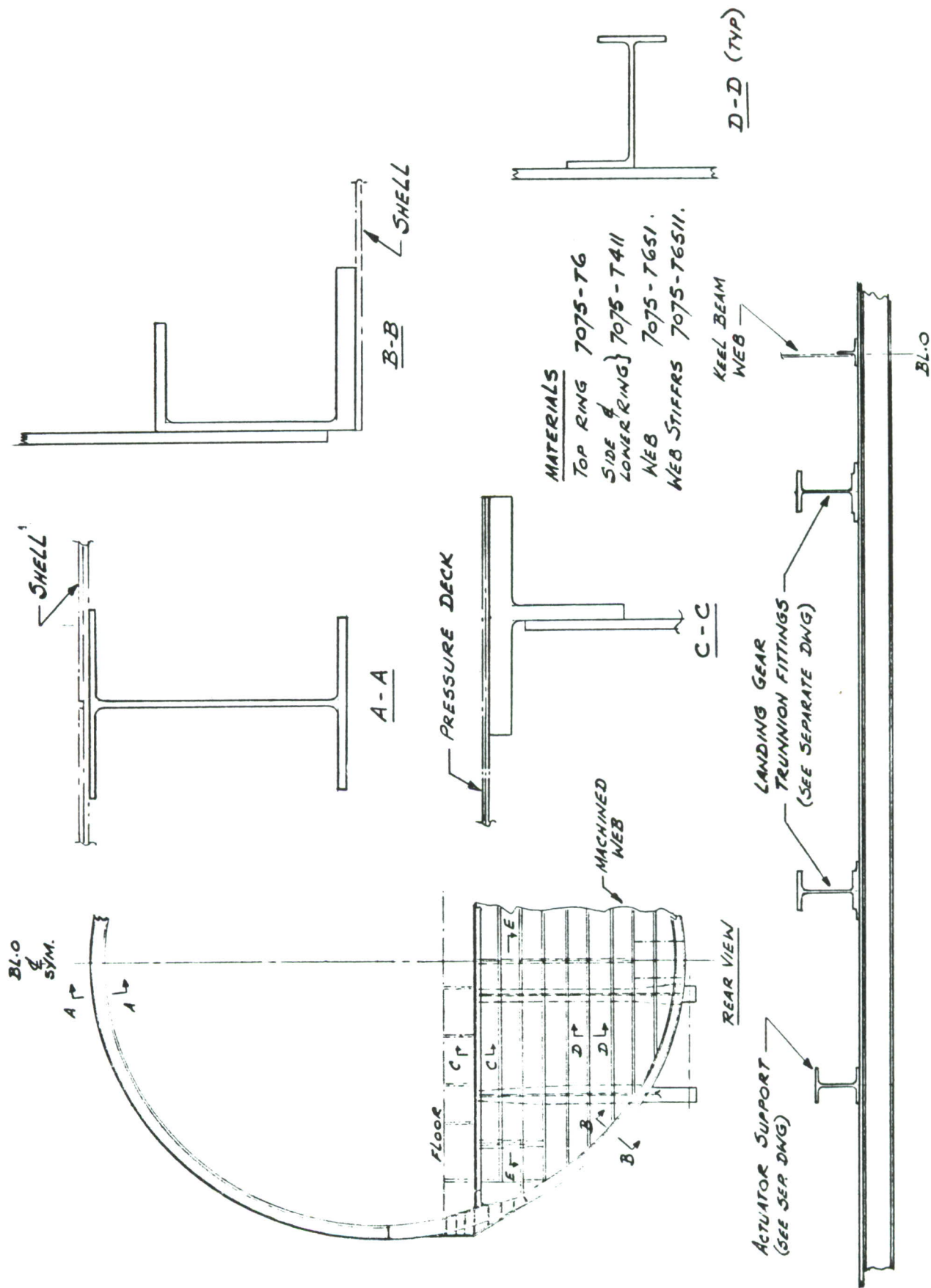
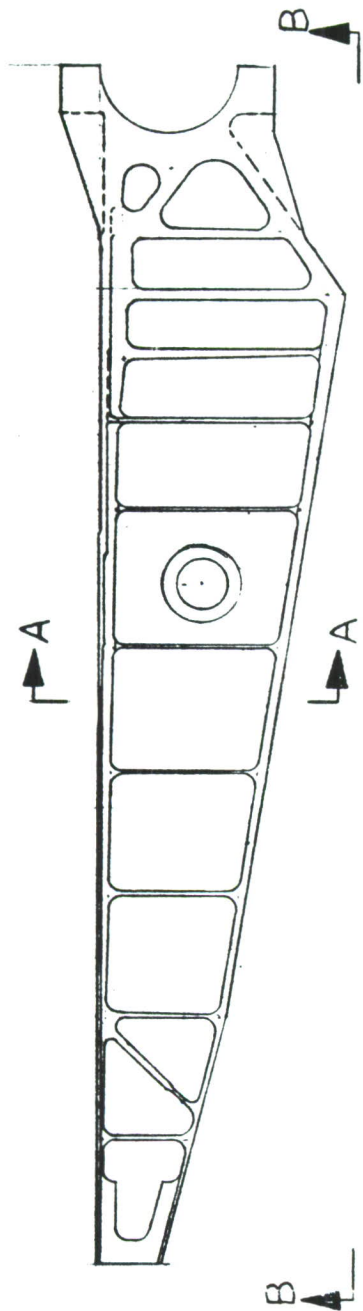
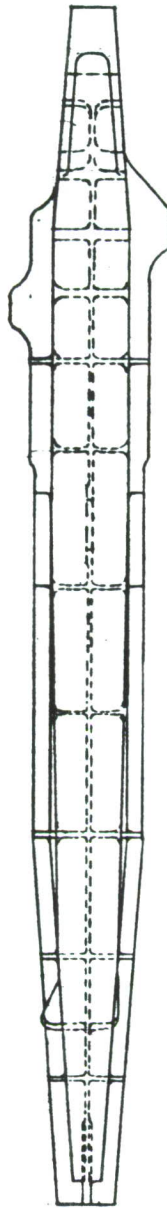


Figure 19.—Bulkhead, Body Station 1480—Baseline



PLAN VIEW



B-B

FITTING IS MADE FROM FORGING
 MATERIAL: 7075-T73
 SEE BULKHEAD STA 1480
 FOR LOCATION

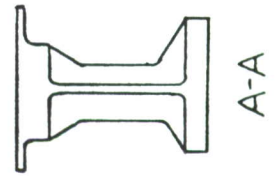
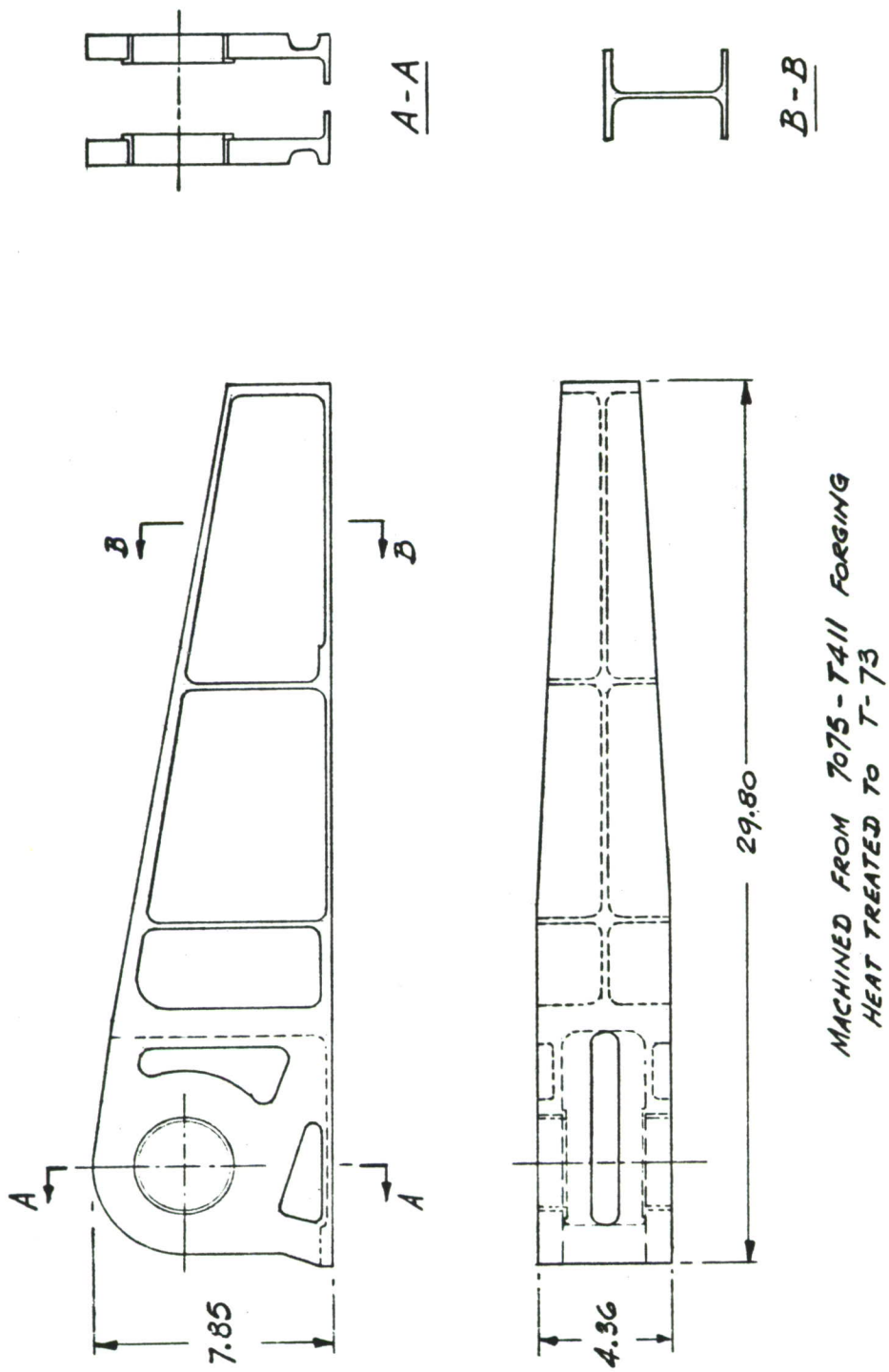


Figure 21.—Typical Trunnion Fitting—Baseline



SEE BULKHEAD STA 1480 FOR LOCATION.

Figure 22. —Actuator Support Fitting, Body Station 1480—Baseline

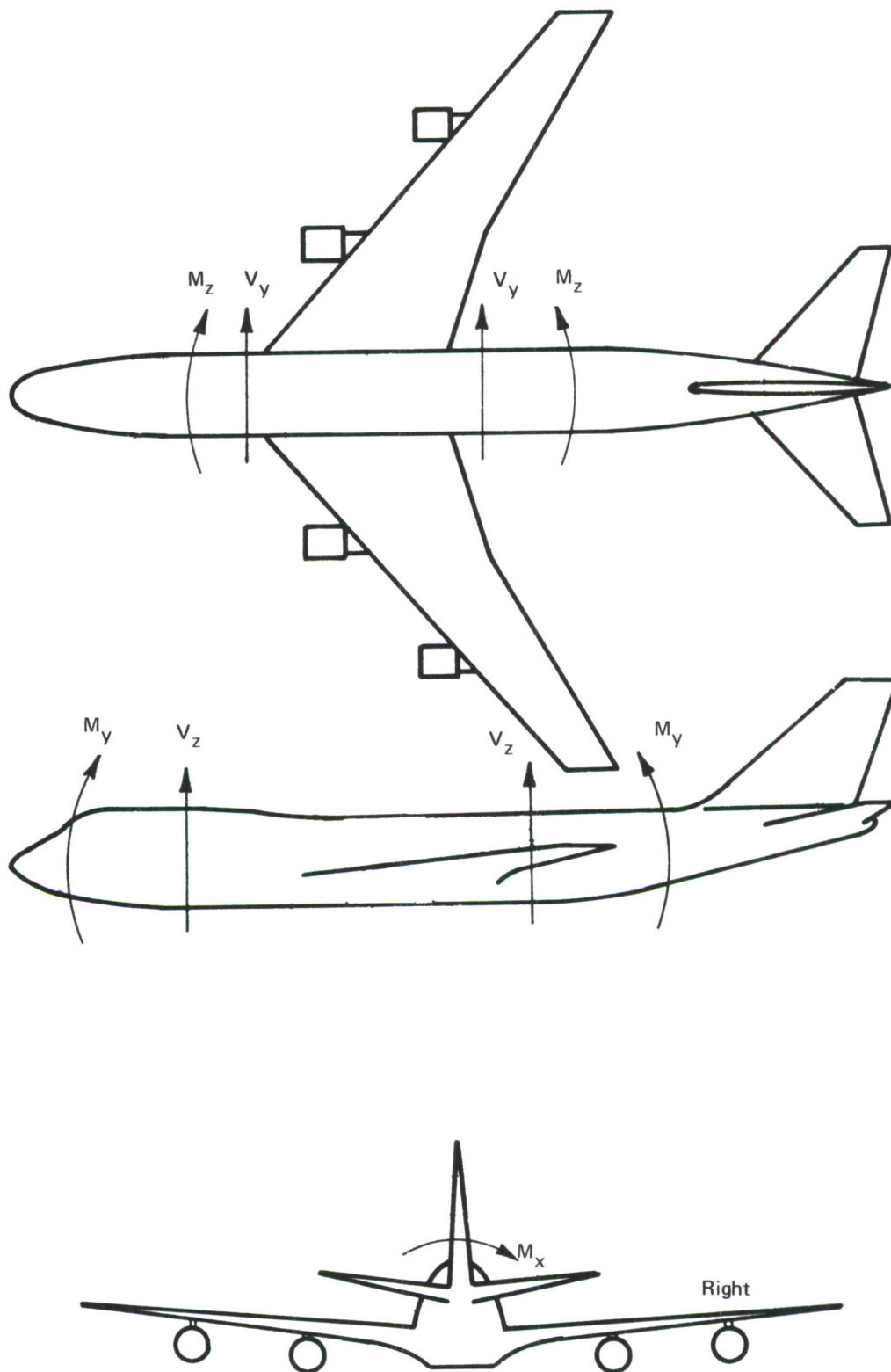


Figure 23.—747 Fuselage Sign Convention

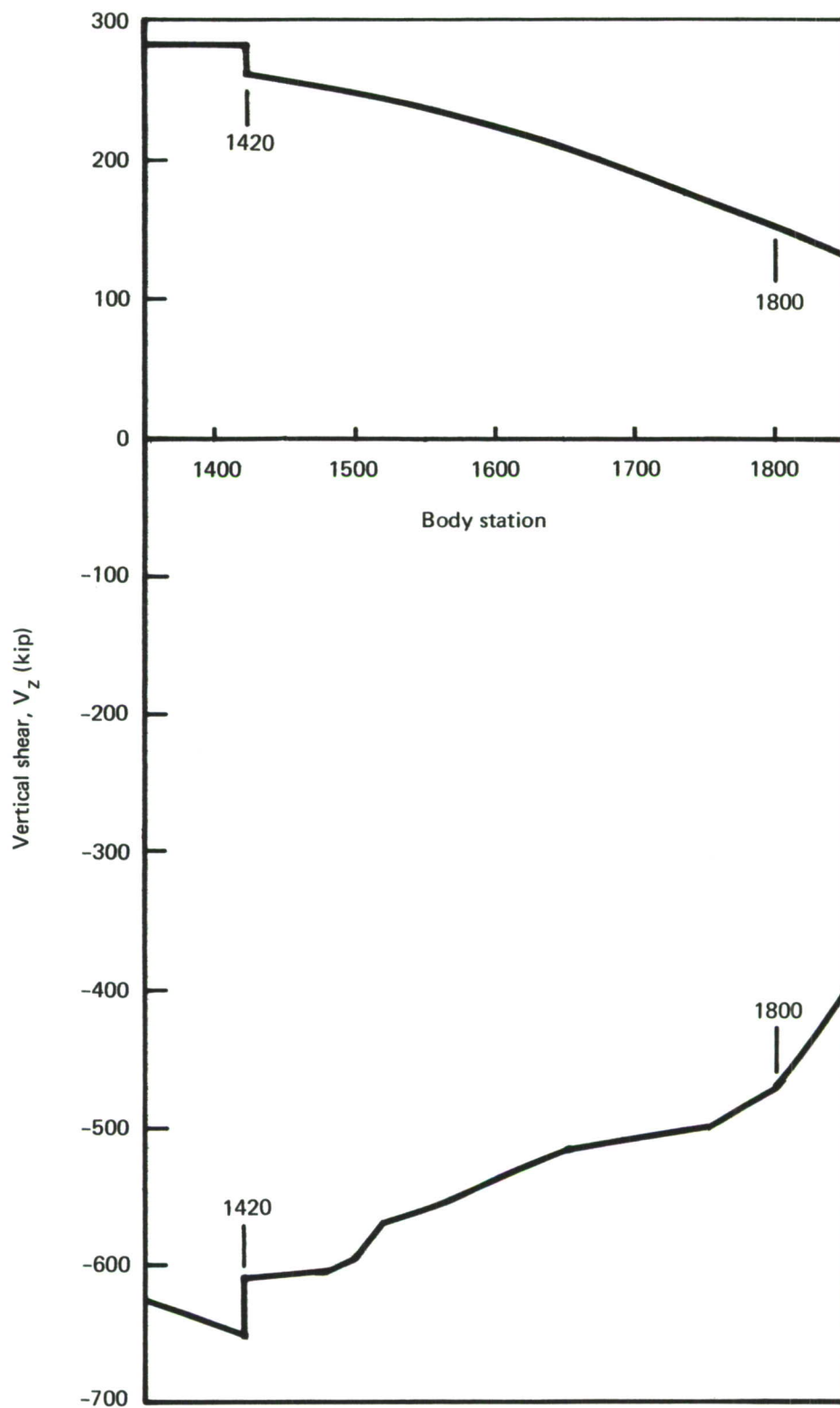


Figure 24.—Ultimate Vertical Shear Loads

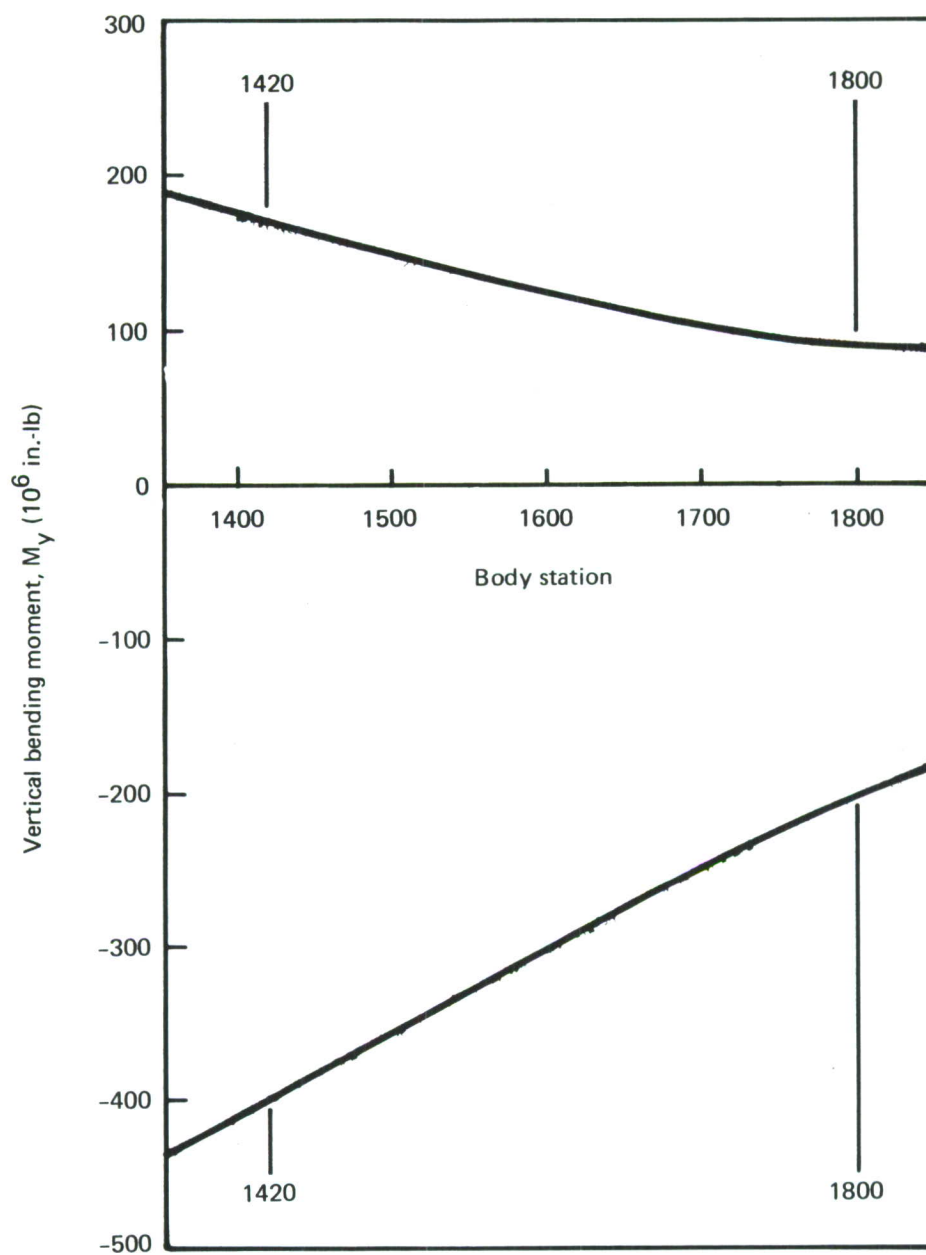


Figure 25.—Ultimate Vertical Bending Moments

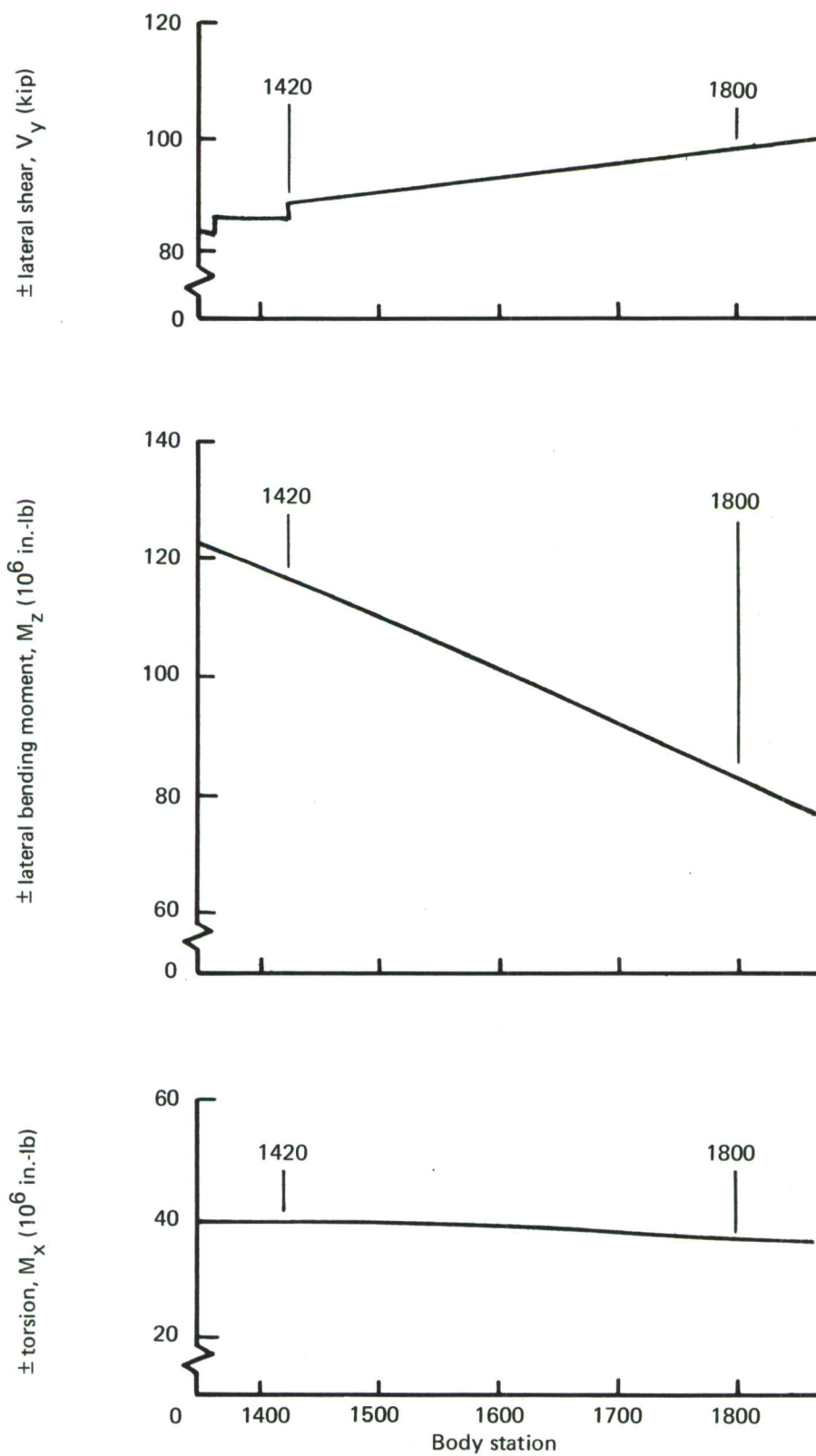


Figure 26.—Ultimate Lateral Loads—Shear, Bending, and Torsion

SECTION III

NEW STRUCTURAL CONCEPTS AND PAYOFF

The new structural concepts developed in this study and selected for the follow-on program apply concepts, materials, and manufacturing methods that can provide both significant structural improvement and substantial system performance payoff. These new concepts not only improve structural efficiency in terms of weight and cost but also provide a high degree of structural durability and safety. The materials and manufacturing methods employed in these new concepts offer a real opportunity to adequately develop new technologies for system application.

The 747-100, as the baseline for this study, has provided a challenging point of departure for establishing the study goals. The baseline airplane fatigue life exceeds the MIL-STD-1530 (USAF) fatigue life requirements for a cargo airplane. The baseline study section is a portion of a commercially competitive airplane fuselage that presents an extremely difficult cost target to match with new design concepts.

Since the study objectives of fatigue life and cost are at or near their real hardware optimum, the payoff potential is in weight reduction. Therefore, to obtain an improved performance payoff, the specific objective of this study was to reduce structural weight while maintaining the baseline fatigue life and costs.

1. DEVELOPMENT OF NEW STRUCTURAL CONCEPTS

To make the new concept evaluation effective, specific design goals were established. This cargo fuselage study identified three structural design parameters—fatigue life, structural weight, and structural hardware cost. The goals were to reduce the participating structural weight while maintaining the baseline fatigue life and unit cost, as noted below:

- Fatigue Life—The fatigue life of the advanced structural component design shall be equal to the baseline life (60,000 flight-hours and 20,000 flights), with no fatigue design constraint on ultimate strength design.
- Weight—The weight saving of the advanced structural component design shall be 25% of the participating structural weight of the baseline.
- Cost—The estimated cost of the advanced structural component design, in production, shall be equal to or less than the production cost of the participating structure of the baseline.

These study goals fit the real aircraft design situation because:

- Aircraft are purchased to perform a specified mission, and a defined mission or use fixes the fatigue life requirements.

- Weight is a parameter that appears directly in most performance equations and therefore provides a direct measure of improvement in aircraft performance.
- Weight is the parameter on which cost relationships have been developed. Cost of producing an airframe is expressed in dollars per pound of fabricated structural weight. The value of weight saving is most often expressed in dollars per pound of weight saved.
- Operating stress changes can be directly related to ultimate strength, crack growth, and damage tolerance so that trades for various stress levels can be made.

Weight is the key parameter. The success of new concepts in improving structural efficiency is best demonstrated by weight-related factors.

For a given load intensity, a reduction in the structural weight results in an increase in stress levels, both ultimate and fatigue. Geometric material rearrangement can improve the ultimate allowable stress, particularly when it is designed by shear and/or compression. Newer materials with higher ultimate strength can also be used. But to maintain the baseline fatigue life at higher fatigue stress levels, the fatigue quality of the details must be improved.

Fatigue quality can be increased most readily by eliminating the rivets and their holes, which are stress concentrations. Because of its improved fatigue quality and reduced costs, adhesive bonding is the primary candidate for a construction method that can best meet study goals.

A subsonic airplane fuselage environment does not require the use of steels and titaniums. For the study section structure, neither steel nor titanium was competitive with aluminum in cost or structural efficiency. Therefore, as will be seen in the discussion of concept development (sec. IV-3), the study narrowed down to adhesive-bonded aluminum structures for the final design concepts.

In developing and applying any new structural concept, the payoff must be significant enough to warrant the associated development cost. If weight is used as the payoff or improvement indicator of new concept potential, then the weight of all functional parts must be known. In this case, the key items contributing to the greatest percentage of the total can be identified by reviewing the percentage weight breakdown of the study section (fig. 27), which is typical of the total fuselage distribution. The major design effort must obviously be directed at the fuselage shell. For example, a weight saving of 20% on the shell, which makes up approximately 70% of the study section weight, would produce a 14% reduction in total section weight. The same 20% saving on a component that is 5% of the section weight would reduce total section weight by only 1%. If the technology to obtain both weight savings is the same, then that technology would be applied to the other component once it is developed for the shell. There is an exception to this in that each component application must stand on its own in terms of weight-saving cost effectiveness in that application. This approach of working in areas of large potential payoff was available for effective screening of materials, processes, and manufacturing methods.

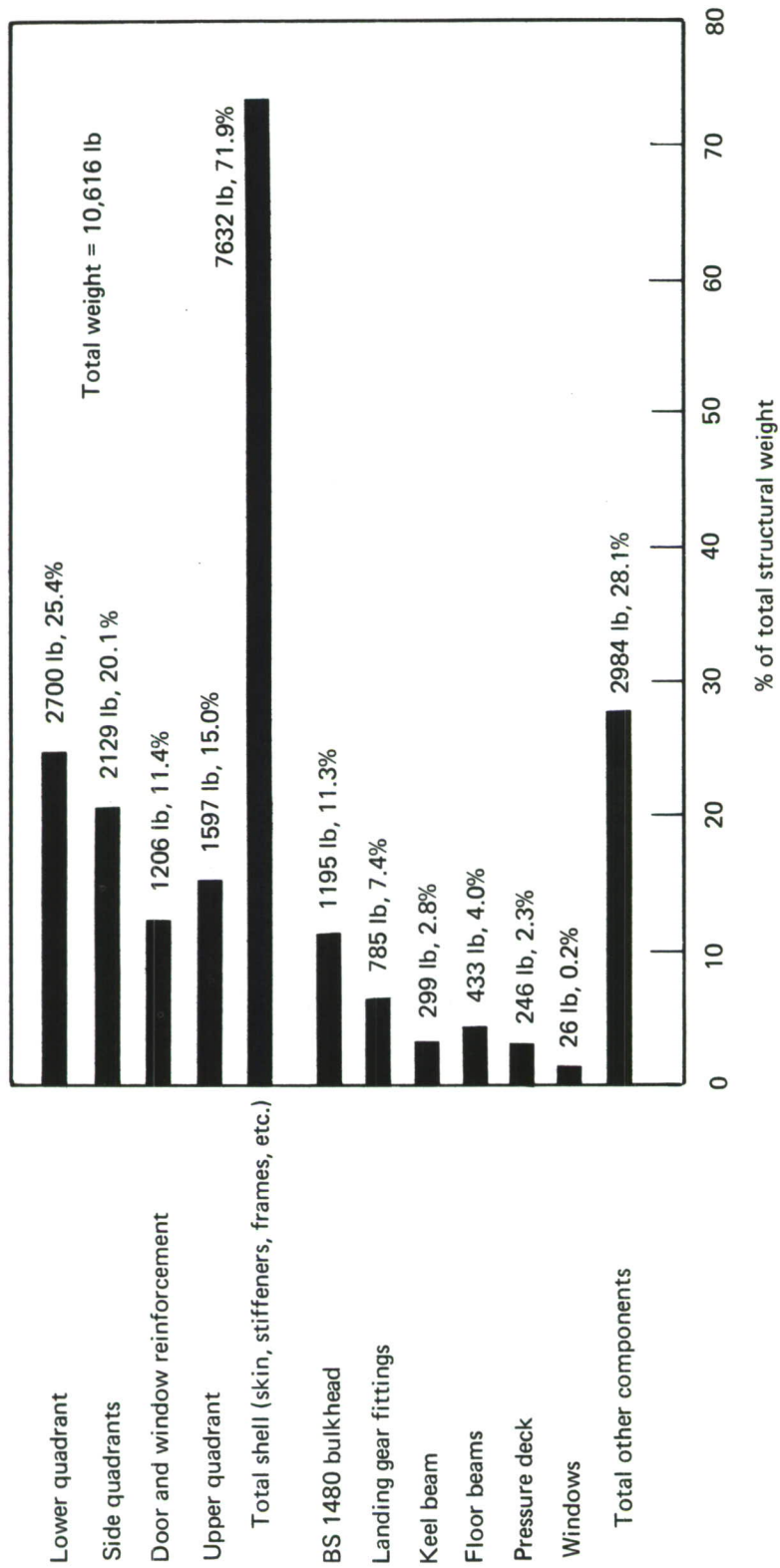


Figure 27.—Baseline Weight Distribution

2. CONCEPT SELECTION—SHELL

The three shell concepts selected for further study during the follow-on program were chosen as the three concepts that most nearly meet the preliminary design study goals.

All of these concepts use 7475-T761 advanced technology aluminum alloy, which has fracture toughness and fatigue characteristics comparable to 2024-T3 and strength nearly as good as 7075-T6. They are all adhesive-bonded designs that take advantage of the improved strength of 7475-T761. Bonded designs differ from the baseline in:

- Reduced assembly cost (equal subassembly cost)
- Higher subassembly tooling cost
- Reduced number of parts
- Reduced number of potential crack growth sites
- Closer tolerance control required for bonding fitup
- More process control and NDI required for bonding

Figure 28 compares the total study section cost and participating structure weight of the baseline with the four final level 3 shell design concepts. For comparison purposes, the baseline values of weight and cost are used as unity. The results of the design team evaluation of the four final shell concepts using the Air Force selection criteria are shown in table I.

In selecting the final three concepts, the study team was asked to apply the Air Force selection criteria rating system both objectively and subjectively to the four level 3 concepts. The objective evaluation was to be based on cost, weight, strength, fatigue, fracture, manufacturing, and quality assurance information generated during this study. The subjective evaluation was to bring in the many years of technical and practical experience background of each team member, covering all categories listed. Table I shows the final team-selected individual category values along with the totals. The baseline rating was set at a value of 5 so that on a scale of 1 through 10, the concepts could be rated better than, equal to, or less than the baseline. This approach was used on all categories except predictability, where the concepts were rated against each other.

Using the results from these two evaluations, the internal stringer, honeycomb, and external stringer shell concepts have been selected as the concepts to be studied more thoroughly during the follow-on program.

a. Design Features of the Four Final Level 3 Shell Concepts

The four final level 3 shell concepts are described in this section. The first three are the ones recommended for further study. The fourth has been eliminated from further consideration.

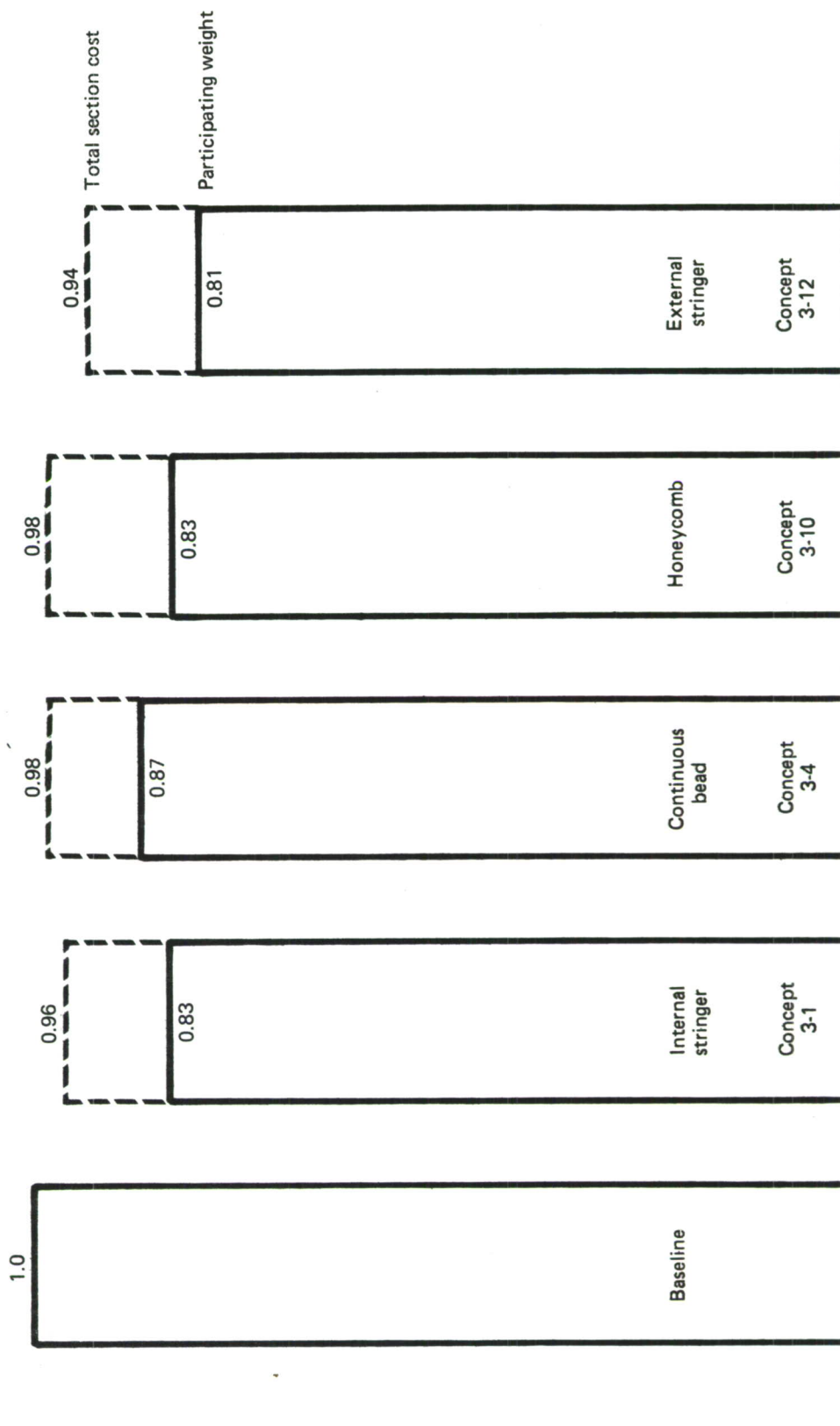


Figure 28.—Level 3 Shell Screening

Table I.—USAF Selection Criteria Rating System—Shell Concepts

N is a rating number from 1 to 10

Items	Factor (f)	f x N _{max}	Baseline		Internal stringer		Continuous bead		Honeycomb		External stringer	
			N	f x N	N	f x N	N	f x N	N	f x N	N	f x N
Weight efficiency												
Weight	0.15	1.50	5	0.75	8	1.20	7	1.05	8	1.20	9	1.35
Cost	0.12	1.20	5	0.60	9	1.08	8	0.96	7	0.84	10	1.20
Life	0.03	0.30	5	0.15	7	0.21	6	0.18	10	0.30	8	0.24
Total		3.00		1.50		2.49		2.19		2.34		2.79
Technical advancement												
Concepts	0.09	0.90	5	0.45	7	0.63	8	0.72	10	0.90	9	0.81
Manufacturing	0.09	0.90	5	0.45	6	0.54	7	0.63	9	0.81	8	0.72
Material	0.09	0.90	5	0.45	8	0.72	8	0.72	8	0.72	8	0.72
Damage tolerance	0.03	0.30	5	0.15	5	0.15	5	0.15	8	0.24	7	0.21
Total		3.00		1.50		2.04		2.22		2.67		2.46
Integrity and reliability												
Static strength	0.03	0.30	5	0.15	6	0.18	7	0.21	8	0.24	8	0.24
Fatigue quality	0.09	0.90	5	0.45	7	0.63	7	0.63	10	0.90	8	0.72
Slow crack	0.06	0.60	5	0.30	7	0.42	7	0.42	10	0.60	7	0.42
Multiple load path	0.12	1.20	5	0.60	7	0.84	6	0.72	9	1.08	8	0.96
Total		3.00		1.50		2.07		1.98		2.82		2.34
"Illities"												
Inspectability	0.05	0.50	5	0.25	4	0.20	4	0.20	3	0.15	4	0.20
Manufacturability	0.02	0.20	5	0.10	8	0.16	9	0.18	6	0.12	8	0.16
Maintainability	0.01	0.10	5	0.05	4	0.04	4	0.04	3	0.03	2	0.02
Repairability	0.01	0.10	5	0.05	4	0.04	4	0.04	3	0.03	3	0.03
Predictability	0.01	0.10	5	0.05	9	0.09	7	0.07	8	0.08	6	0.06
Total		1.00		0.50		0.53		0.53		0.41		0.47
Concept rating		10.00		5.00		7.13		6.92		8.24		8.06

(1) Internal Stringer Concept (Fig. 29)

The internal hat stringer panel design consists of closed hat-section stringers adhesively bonded to the skin. The frame-to-skin ties are cut out to clear the stringers. Due to this cutout discontinuity of the frame-to-skin ties, circumferential tear straps are required for fail safety in the blade penetration areas or to act as crack arresters for a damage tolerance requirement of a one-bay skin crack. Additional hoopwise straps are required between the frames to meet this damage tolerance requirement when the skin gages are designed by hoop tension.

Because of the fitup and bonding problems associated with joggling the stringers over these hoopwise straps, the fail-safe straps are made with interconnecting longitudinal straps under each stringer to provide a flat surface for ease of bonding. This interconnecting grid of fail-safe straps and longitudinal straps is called a waffle doubler. The doubler sheet stock is bonded to the skin panels. After bonding it is masked and the centers of the bays are removed by chem milling. The bond layer between the skin and doubler sheet acts as a chem-mill stop surface.

This type of wide area bonding and pocket chem milling is a proven production process that has been used on aircraft fuselage skin panels.

The closed hat-section stringer has high torsional compression stability and improves the effective width of skin for compression loading. The two bonded flanges give the stringer good peel resistance and good local load transfer capability, yet the flanges are sufficiently flexible to resist peel due to local skin buckling. The hat-section rolled stringer is easily rolled and tapered during the automatic stringer rolling operation, is easy to splice with its flat sides, and has a flat, stable surface for ease of bonding composite reinforcement, if desired. Corrosion of the closed section is a potential problem that must be considered in selecting the proper process controls and protective finish.

The internal stringer concept has a total unit cost 4% less than the average baseline section cost and a participating structure weight reduction of 17%.

(2) Honeycomb Shell Concept (Fig. 30)

The honeycomb shell concept consists of two equal face gage skins adhesively bonded to aluminum honeycomb core. The frame outer chord is a tee section bonded to the inner skin of the honeycomb panel. The tee section is continuous from quadrant splice to quadrant splice.

The quadrants are made with hot bonded subassembly joints. The four shell quadrants are joined by mechanical fasteners.

The honeycomb shell gives improved fracture characteristics, as listed below:

- Effect of curvature is reduced.

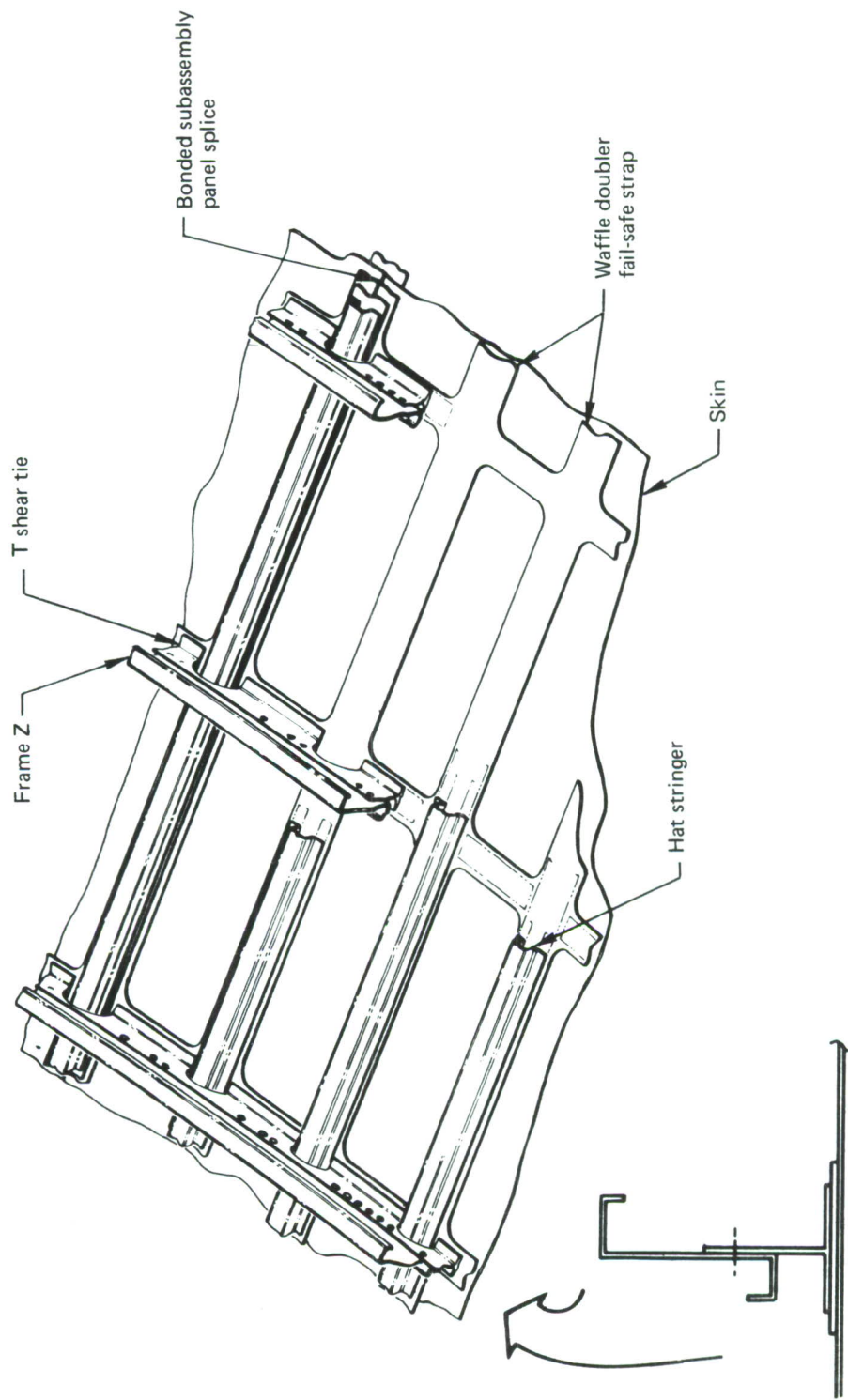


Figure 29.—Internal Stringer

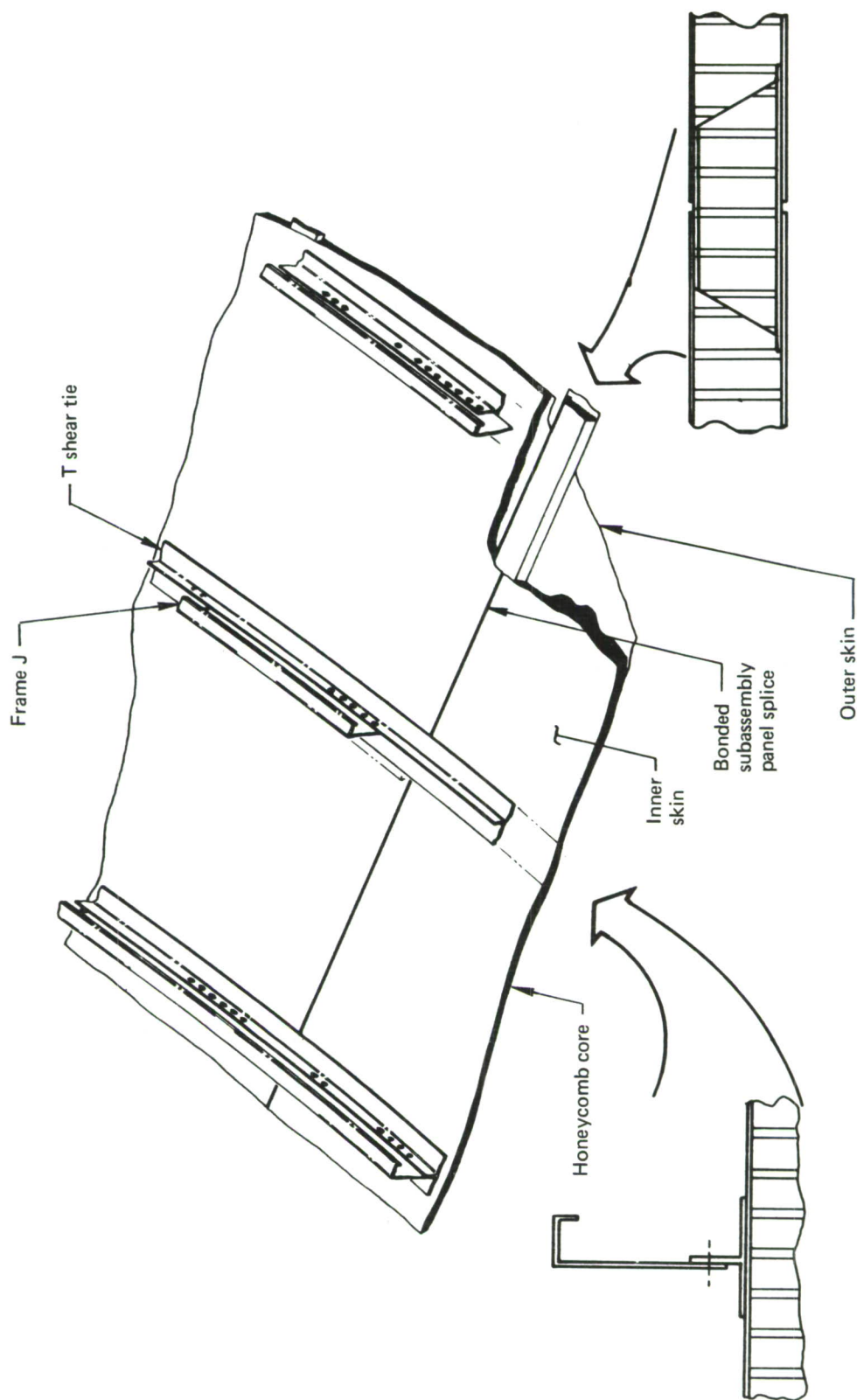


Figure 30.—Honeycomb

- Honeycomb stabilizes crack tip and area on each side of crack. (Buckling on either side of crack and out-of-plane action at crack tip reduces effective fracture toughness.)
- Two skins provide dual load path in tension, reduced probability of crack in both faces at same location, and reduced crack growth rate.

The honeycomb shell skin is fully effective in all directions, and it has better interaction characteristics for combined shear and compression than skin/stringer designs. Also, the stringers of a skin/stringer design do not contribute to hoop tension capability and only indirectly contribute to the skin shear-carrying capability by breaking up the panel sizes.

As shown in the concepts weight statement (sec. IV-5), the splices and joints of the honeycomb concept are much heavier than the skin/stringer concept splices. This has historically been a problem in efficient use of honeycomb construction. Innovative design and development of joints with better weight efficiency will be a major goal for this concept during the follow-on studies.

The honeycomb shell design shows a total section cost 2% less than the average baseline section cost and a participating structure weight reduction of 17%.

(3) External Stringer Concept (Fig. 31)

This structural arrangement has the closed hat-section stringers bonded on the outside of the skin with the frames on the inside. The frame outer tee chords can be continuous and are bonded directly to the skin, eliminating the requirement for fail-safe hoop straps at the frames. When required, midbay fail-safe straps can be added internally between frames without interfering with the stringers. By eliminating the waffle doubler required on the internal stringer concept and because the frames are less complex, the side and upper quadrant weights are slightly lower than those of the internal stringer concept. The external stringer concept has all the advantages listed for the internal stringer design discussed in section III-3a1.

Even though this concept is structurally very efficient, it has a rough exterior surface that must be covered with a smooth aerodynamic surface. An exterior insulation material, which has a resin-reinforced, urethane-coated surface, must be attached on the outside of the external stringers. A preliminary design study shows that this exterior insulation cost and weight can be partially offset by removing the interior insulation batts required on the baseline and the other three configurations.

Of the three concepts selected for follow-on evaluation, the exterior insulation aerodynamic surface panels are the area of highest technical risk. The problems to be investigated during further concept studies include:

- Buckling strain caused by induced deformation
- Environmental stability, water absorption

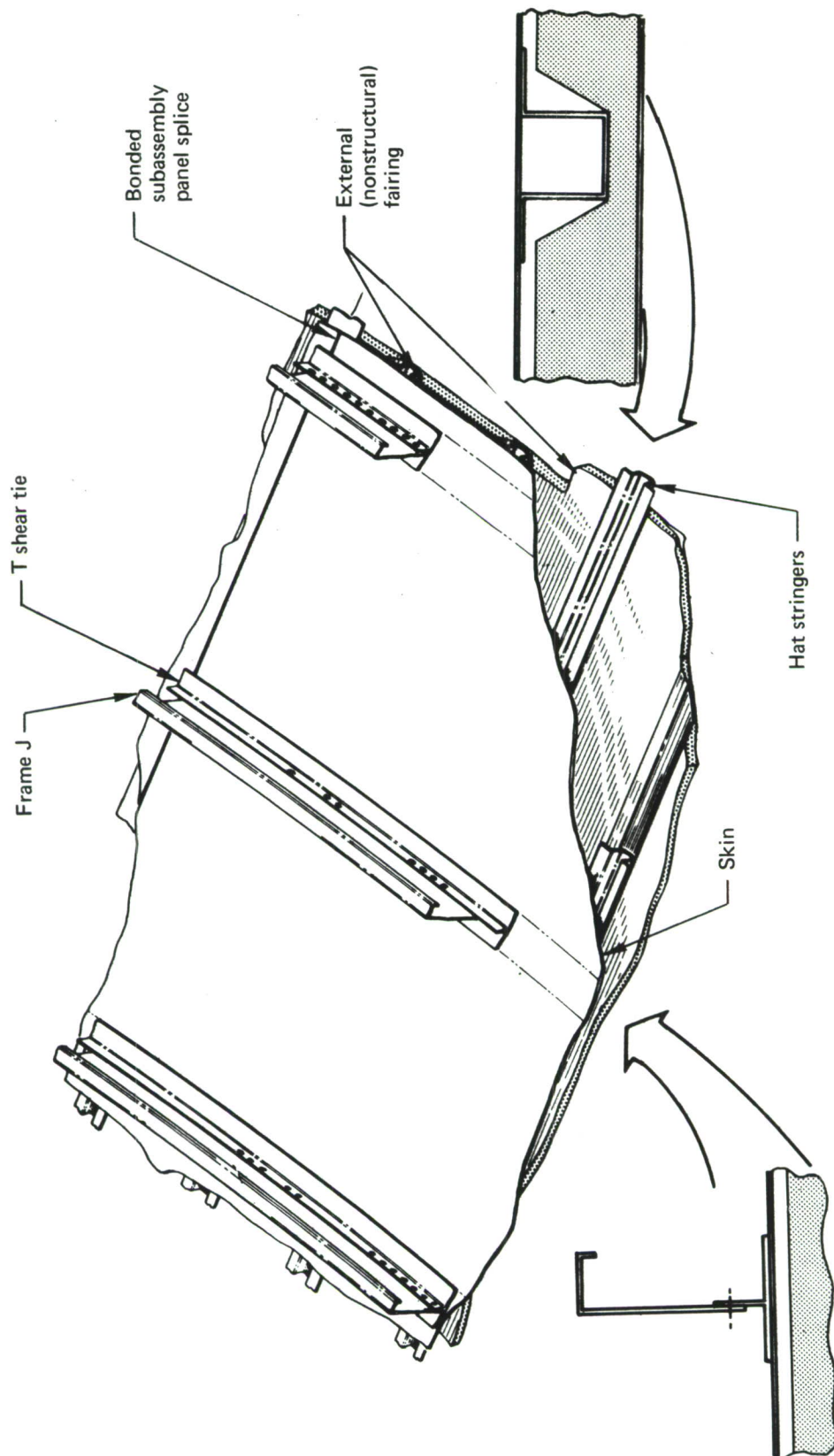


Figure 31.—External Stringer

- Cavity venting
- Aerodynamic pressure load-carrying capability

(4) Continuous-Bead Concept (Fig. 32)

The continuous-bead shell concept consists of an inner skin that is corrugated into continuous beads and adhesively bonded to the primary exterior skin. The resulting laminated skin/stringer panel requires less extensive jigging than the individually formed stringers, but it has the increased complexity of fabricating tapered, corrugated sheets.

The frame-to-skin tie members are bonded to the panel between the beads and are similar to the members used on the internal stringer concept. Since this shell concept does not lend itself to the incorporation of continuous circumferential fail-safe straps, a separate fail-safe outer chord, similar to the baseline lower quadrant frame segment, is included in the frame design. The rolled, stretch-formed frames and fail-safe chords are riveted to the skin ties during final panel assembly.

This continuous-bead concept shows a total study section cost that is 2% less than the average baseline section cost and a 13% reduction in weight of the participating structure.

b. Concepts for Components Other Than Shell

The design concept studies for components other than the shell are discussed in section IV-3b4. The only two component designs that were shown to be both weight and cost effective were the following:

- Honeycomb keel beam web concept (component weight reduction of 18% with a 3% cost reduction).
- Honeycomb pressure deck concept (component weight reduction of 12% with a 20% cost reduction).

Although their weight and cost savings appear significant, these components make up such a small portion of the baseline structure that, when combined, they would contribute to a baseline weight reduction of only 0.34% and a cost reduction of only 0.31%.

3. PROGRAM PAYOFF

The AMS-ADP program payoff may be measured in terms of improved aircraft performance and by an increase in fundamental structural information. The improvement in aircraft performance is reflected by a reduction in fleet O&M costs and increased mission capability. Opportunities for development of additional structural information will be exposed in all of the involved technologies as a result of the design, fabrication, and testing carried out during this program. A review of potential payoff from the AMS-ADP program is presented.

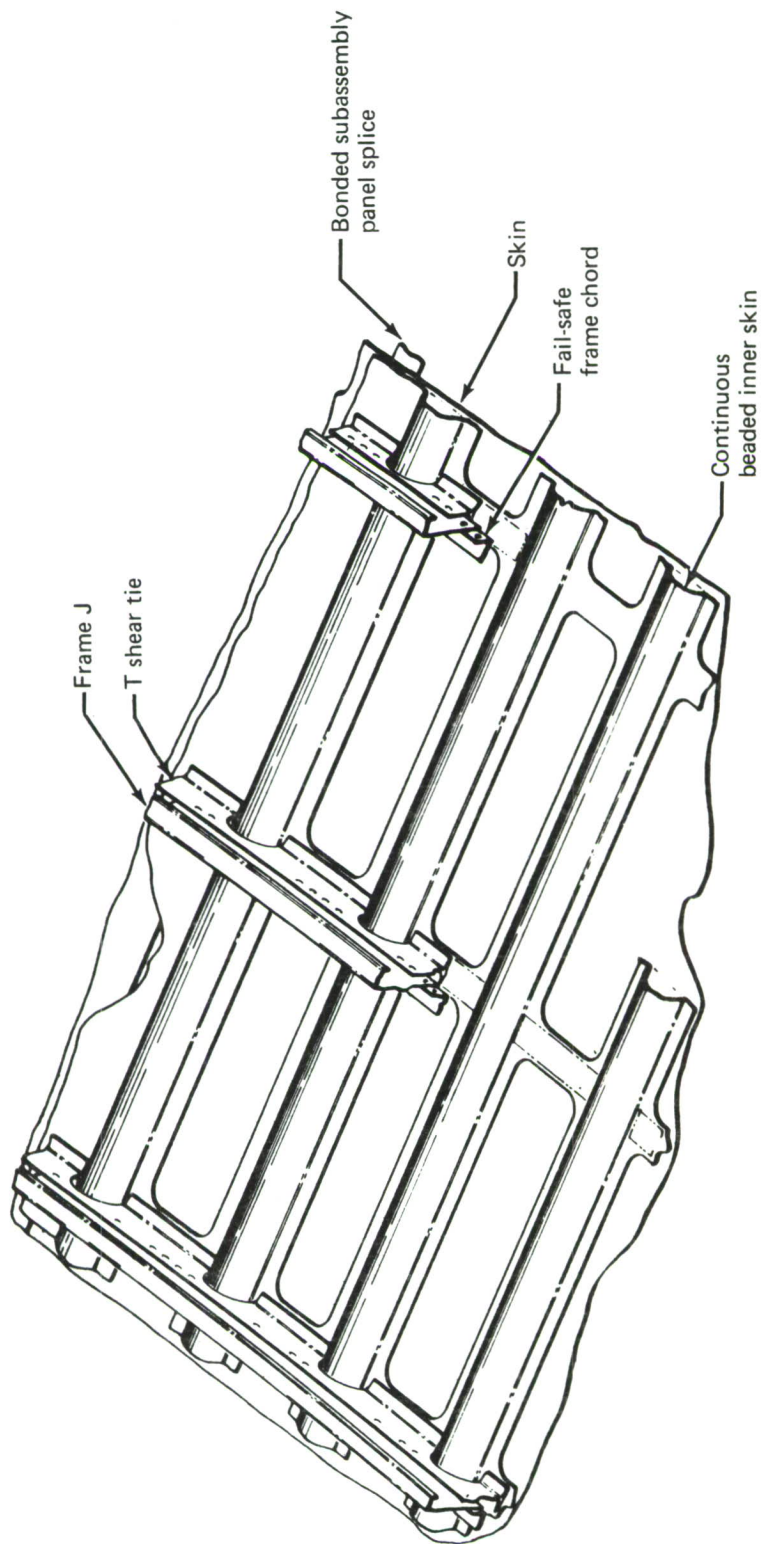


Figure 32.—Continuous Bead

a. **Mission and Performance Payoff**

System capability and cost improvements are the prime drivers for this Advanced Development Program. These improvements must be measured from a reliable and established base. The baseline for the cargo fuselage AMS-ADP is described in section II. The system capability and cost improvements from this base are discussed in the following paragraphs. Answers are provided to a couple of pertinent questions:

- Why have an ADP for the cargo category of aircraft?
- What is the payoff for the Air Force in terms of mission capability increase and life cycle cost reduction?

Figure 33 shows that 25% of the Air Force active aircraft inventory is in the cargo category. Since cargo aircraft are essential to the total Air Force defense mission (TAC is 50% tanker supported, SAC 100% tanker supported), emphasis must be given to advanced technology directed at improvements to this class of aircraft. Geopolitical developments could result in the loss of forward bases in Europe and Asia, which would place increased demands for added capability on the cargo family for POL and airlift missions, for example. Advanced structures technology can contribute to this added capability.

(1) Missions Analysis

Some of the typical missions being considered for military derivatives of the 747 are:

- Advanced tanker
- Advanced strategic airlift (cargo) system
- POL resupply to Europe
- Advanced airborne command post
- Advanced all-weather surveillance system
- AMST (Advanced Military STOL Transport)

Potential payoff from the AMS-ADP has been applied to the first four items.

Payoff resulting from reduced structural weight can be taken several ways:

- Increased capability per airplane—total fleet capability constant
 - Payoff in reduced fleet size and operational cost
 - Resized and fixed size airplane

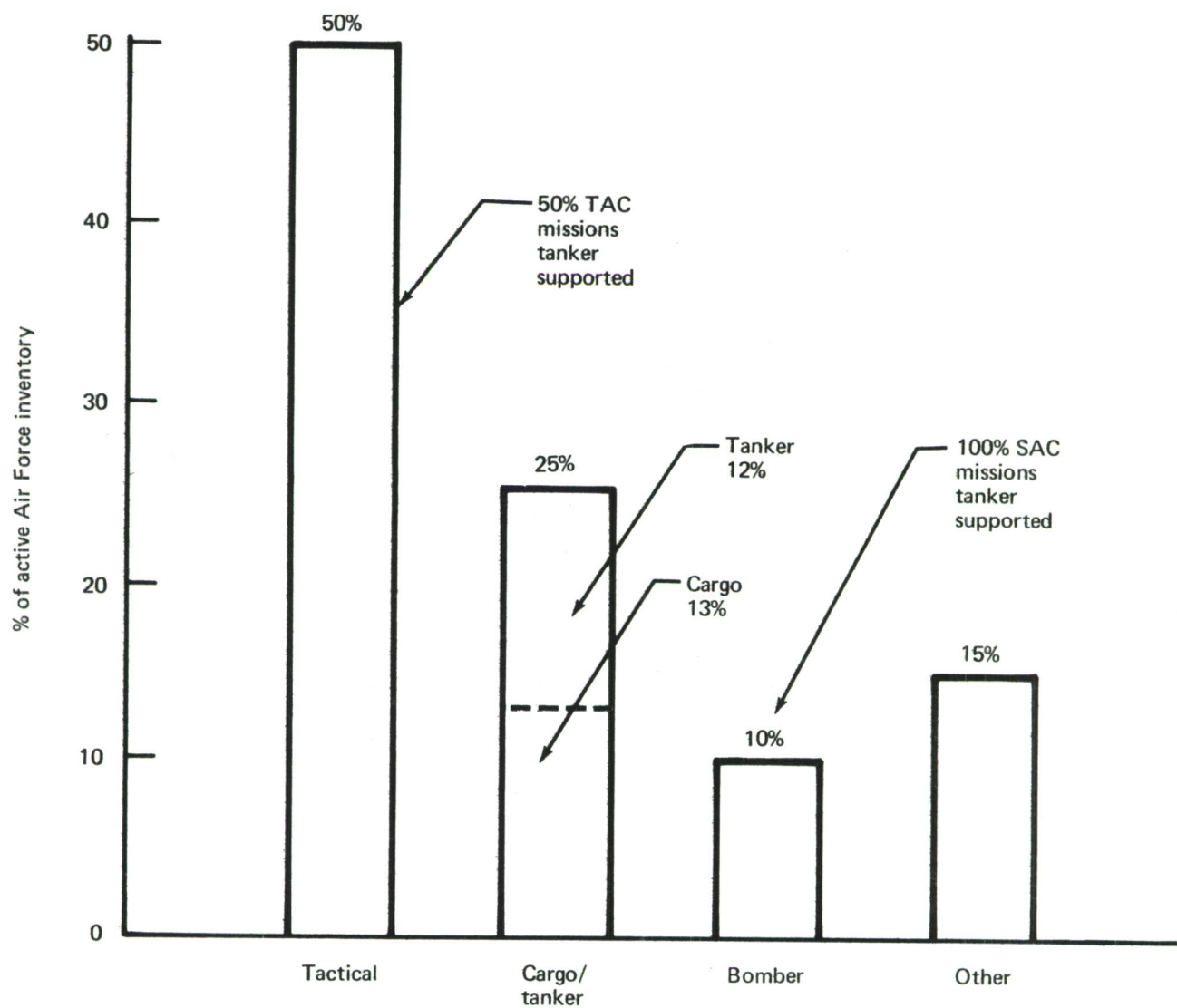


Figure 33.—Importance of Cargo/Tanker to USAF Mission

- Increased capability per airplane—number of airplanes in fleet constant
 - Payoff in increased mission capability and reduced operational cost per unit of mission parameter
 - Resized and fixed size airplane
- Constant capability per airplane—number of airplanes in fleet constant
 - Payoff in reduced operational cost
 - Resized and fixed size airplane

The maximum leverage payoff takes advantage of a reduced fleet size, and elimination of the associated O&M costs for airplanes is not required. Payoff analyses are based on this approach.

Tanker Mission: Increased fuel transfer per airplane is the payoff parameter selected for the tanker mission. An assumed baseline fleet of 50 airplanes could be reduced to 46 resized airplanes and 48 fixed size airplanes for the fuselage weight savings projected as a result of the AMS-ADP, based on the data shown in figure 34.

Cargo Mission: The cargo mission covers both the MAC 5 Army Division 30-day move, and the European POL resupply mission. The payoff shown in figure 35 is for the MAC mission, based on an 89-baseline airplane fleet. The payoff is relatively small for this mission, due to a high percentage of low-density cargo. A fleet reduction of one fixed size airplane and two resized airplanes is estimated.

Surveillance Mission: Time-on-station is the critical parameter of the surveillance mission. As shown in figure 36, fuselage weight reduction of 10% (7500 pounds) leads to resized and fixed size improvements of 7.92% and 3.75%, respectively. An assumed 50-airplane fleet for this mission can be reduced to 46 and 48 airplanes (resized and fixed size, respectively) for nearly equivalent fleet time on station.

(2) Estimated 10-Year Life Cycle Savings and Program Leverage

Ten-year life cycle cost estimates per baseline airplane are shown in table II based on 1500 hours utilization per year per airplane at \$2000 per flight-hour for the tanker and cargo missions. Ten-year life cycle was chosen as being an accepted standard for systems comparisons. It is recognized that the baseline airplane has a much longer useful life. Additional increments for acquisition and O&M costs for the surveillance mission are due to electronic equipment.

Shown in table III are estimated system life cycle cost savings for the missions indicated, consistent with the assumptions noted, for both the fixed size and resized airplane cases. The totals are \$340 million and \$680 million, respectively.

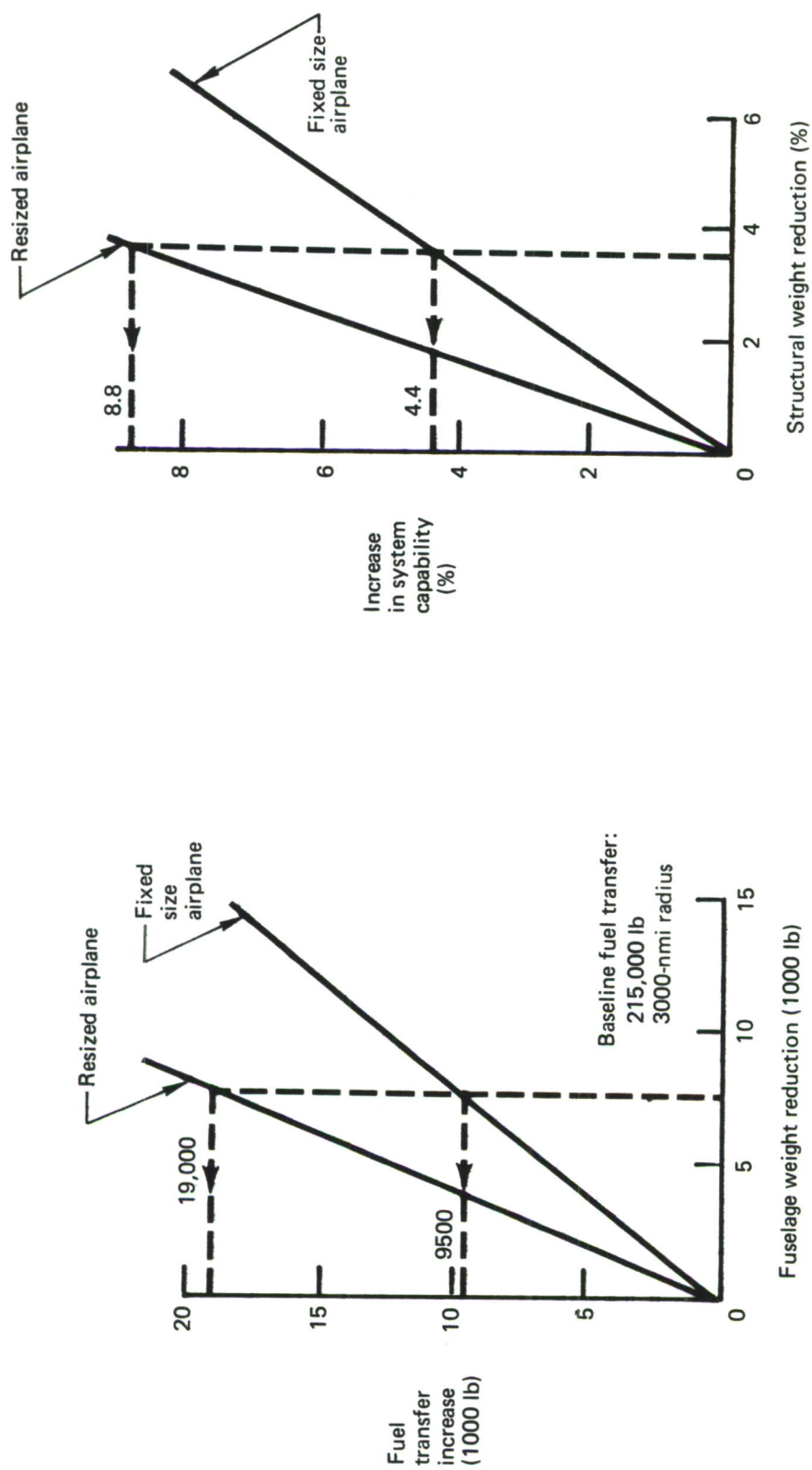


Figure 34.—Tanker Mission: Payoff in Increased Fuel Transfer per Airplane

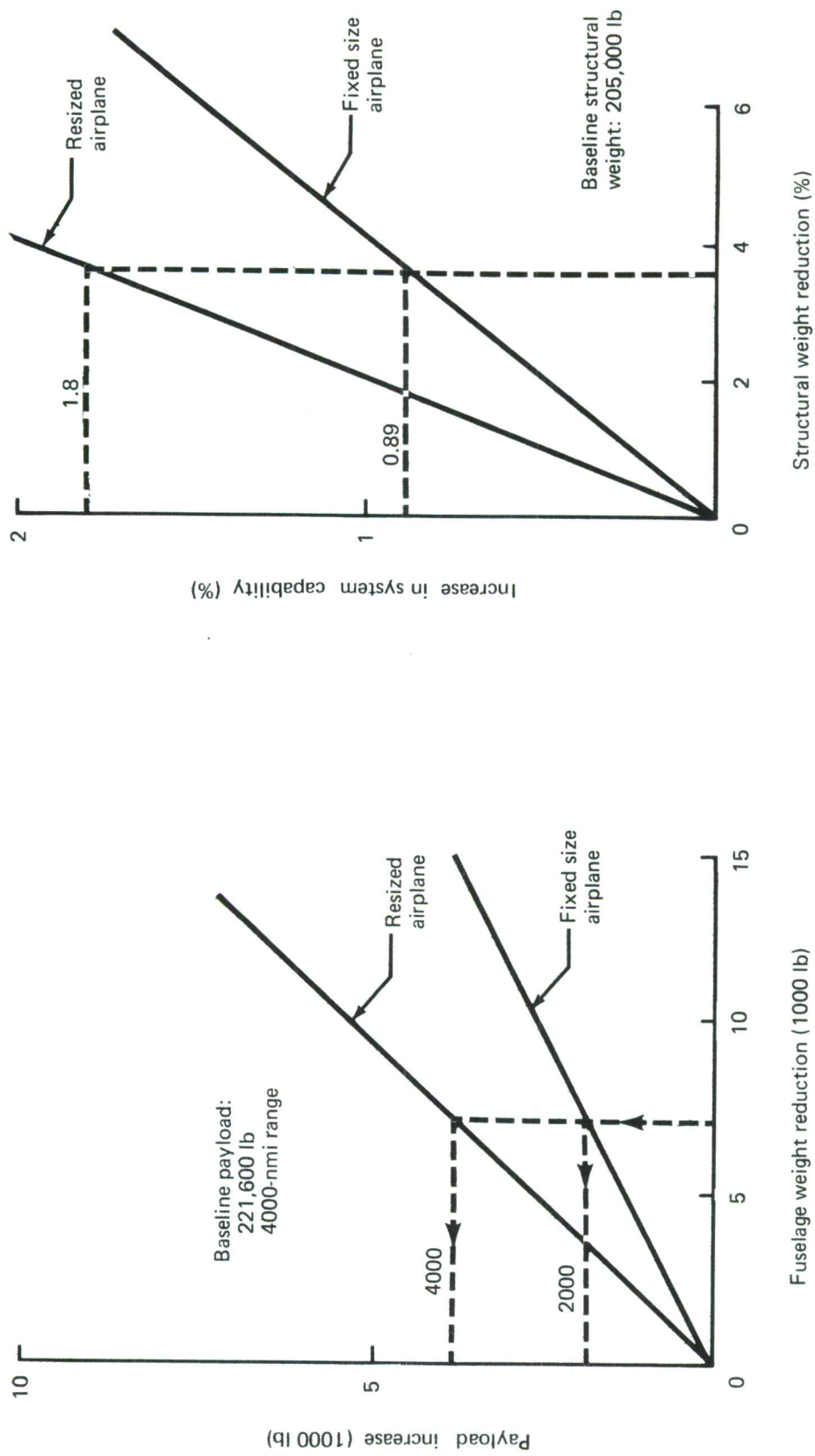


Figure 35.—Cargo Mission: Payoff in Increased Payload per Airplane

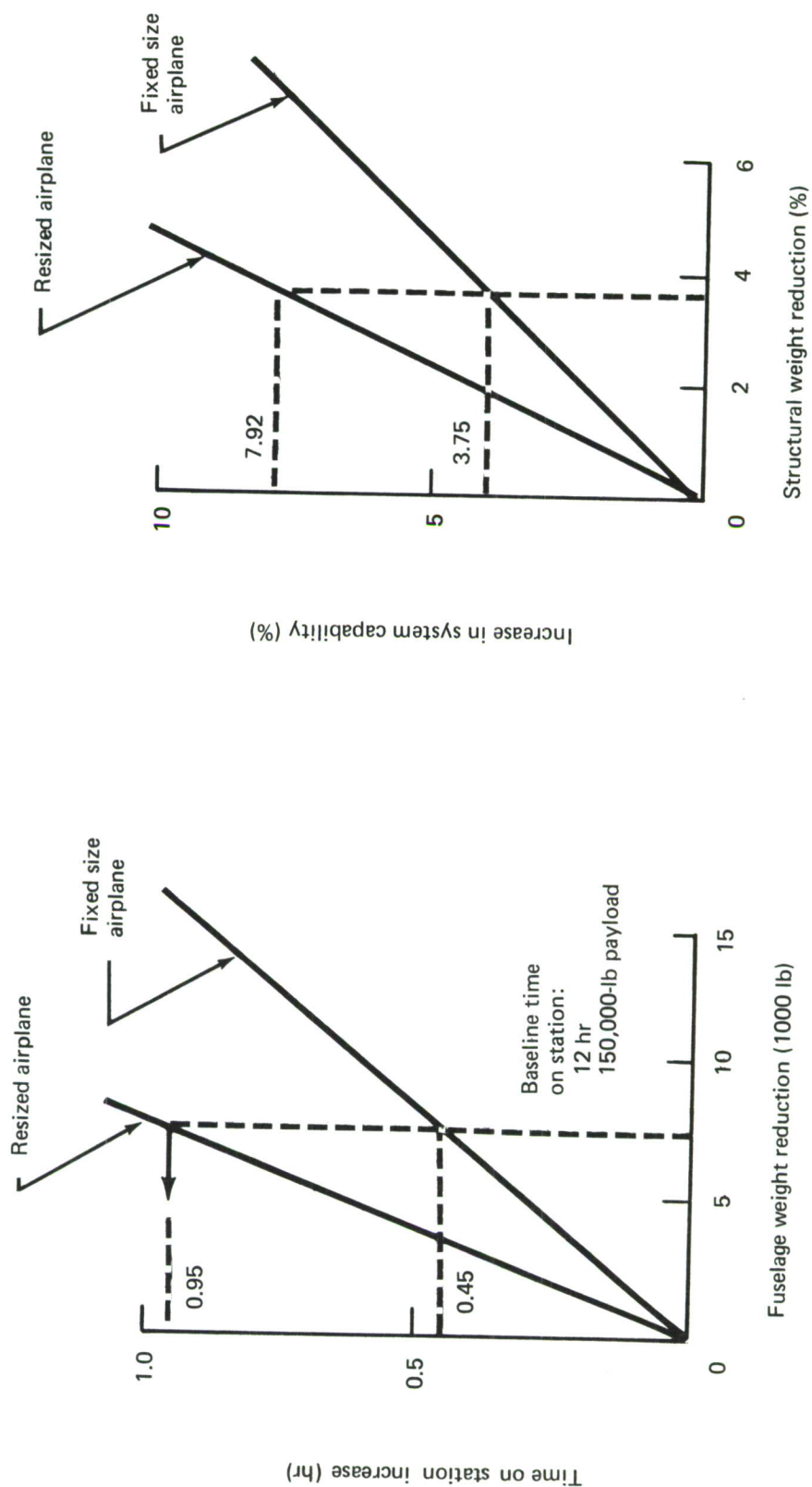


Figure 36. —Surveillance Mission: Payoff in Increased Time on Station

*Table II.—Estimated 10-Year Baseline Life Cycle Costs
(1500 Hours/Year Utilization)*

	Dollars in Millions		
	Tanker	Cargo	Surveillance
Initial airplane acquisition	\$30	\$30	\$30
Electronic equipment acquisition	—	—	\$15
O&M	\$30	\$30	\$35
Totals	\$60	\$60	\$80

*Table III.—System Life Cycle Cost Savings Due To
AMS-ADP Cargo Fuselage*

	Fixed size airplane	Resized airplane
Tanker mission	2 airplanes at \$60 million = \$120 million	4 airplanes at \$60 million = \$240 million
Cargo mission	1 airplane at \$60 million = \$60 million	2 airplanes at \$60 million = \$120 million
Surveillance mission	2 airplanes at \$80 million = \$160 million	4 airplanes at \$80 million = \$320 million

Assumptions:

- 50 baseline airplane fleet each for tanker and surveillance missions
- 89 baseline airplane fleet for cargo mission
- 7500-lb fuselage weight saving
- Same structural cost per pound and fatigue life as for baseline
- 1500 flight hours per airplane per year
- \$80 million 10-year life cycle cost per airplane for surveillance mission
- \$60 million 10-year life cycle cost per airplane for cargo and tanker missions

The program payoff, in terms of life cycle cost saved per pound of weight saved, is shown in table IV for both the fixed size and resized airplanes. The leverage of this program, in terms of life cycle cost saving per dollar cost of the ADP, is more than 28 for the fixed size airplane and 56 for the resized airplane. Leverage of this magnitude indicates a high degree of effectiveness per dollar cost for the cargo fuselage AMS-ADP.

*Table IV.—Payoff and Leverage on System Life Cycle Costs
Due to AMS-ADP Cargo Fuselage*

	Fixed size airplane	Resized airplane
Total dollars saved per pound of weight saved	$\frac{\$340 \text{ million}}{7500} = \$45,000/\text{lb}$	$\frac{\$680 \text{ million}}{7500} = \$90,000/\text{lb}$
Total dollars saved per dollar cost of AMS-ADP	$\frac{\$340 \text{ million}}{\$ 12 \text{ million}} = \$28 +$	$\frac{\$680 \text{ million}}{\$ 12 \text{ million}} = \$56 +$

Assumptions:

- 50 baseline airplane fleet each for tanker and surveillance missions
- 89 baseline airplane fleet for cargo mission
- 7500-lb fuselage weight saving
- Same structural cost per pound and fatigue life as for baseline
- 1500 flight hours per airplane per year
- \$80 million 10-year life cycle cost per airplane for surveillance mission
- \$60 million 10-year life cycle cost per airplane for cargo and tanker missions
- \$12 million cost for AMS-ADP cargo fuselage

(3) Application to AMST

The results of this ADP are directly applicable to STOL transports. In fact, the greatest payoff can be achieved for STOL aircraft such as the AMST. Shown in figure 37 are the impacts on OEW of configuration resizing improvements due to structural weight reduction.

Boeing AMST Baseline Description: Figure 38 shows the general arrangement of the Boeing AMST. Fuselage arrangement is shown in figure 39.

The fuselage is designed with a conventional aluminum stiffened sheet metal shell and frames. The pressurized cabin extends from the forward bulkhead over the nosewheel well, under the wing and aft to the fin rear spar bulkhead. The cab structure has frames at 10-inch spacing continuously attached to the skin. The cargo compartment monocoque structure is of skin/stringer construction, stabilized by frames. Frames forward of the constant section are locally attached to the skin to resist bending in the flat area due to cabin pressure. Cargo compartment frames are basically at 20-inch spacing to obtain minimum weight in monocoque and cargo floor and are attached to the skin only at the floor level. The aft body monocoque structure is of skin/stringer construction, stabilized by upper frames at approximately 20-inch spacing, with box section longerons above the cutout for the ramp and cargo door. The tail cone is of nonpressurized fiberglass construction with full ring frames at 40-inch spacing.

Three overhead hatches and two overhead lift raft doors are located in the cargo compartment. Entry doors at the forward end of the cargo compartment are overhead-opening, plug-type doors and are opposite installations. Troop jump doors at the aft end of the cargo compartment are identical overhead-opening, plug-type doors positioned at floor level. A portion of the main landing gear fairing articulates to provide jump clearance. A hinged cargo loading ramp and an inward-opening cargo door with actuating and latching systems are installed in the aft body. The cargo floor includes cargo tiedowns and cargo pallet/airdrop pallet handling provisions. Some of the major features of this fuselage are:

- Constant circular cross section in major portion of body minimizes weight of pressure vessel and minimizes cost of parts and tooling.
- Maximum use is made of common skin/stringer/frame details.
- Circular aft body cross section above ramp and door longeron minimizes pressure-induced bending.
- Twenty-five-foot-long conical section in aft body eliminates forming of skin and stringers.
- Single bulkhead is used for attaching wing rear spar and supporting aft main landing gear.
- Main landing gear does not penetrate fuselage pressure shell.

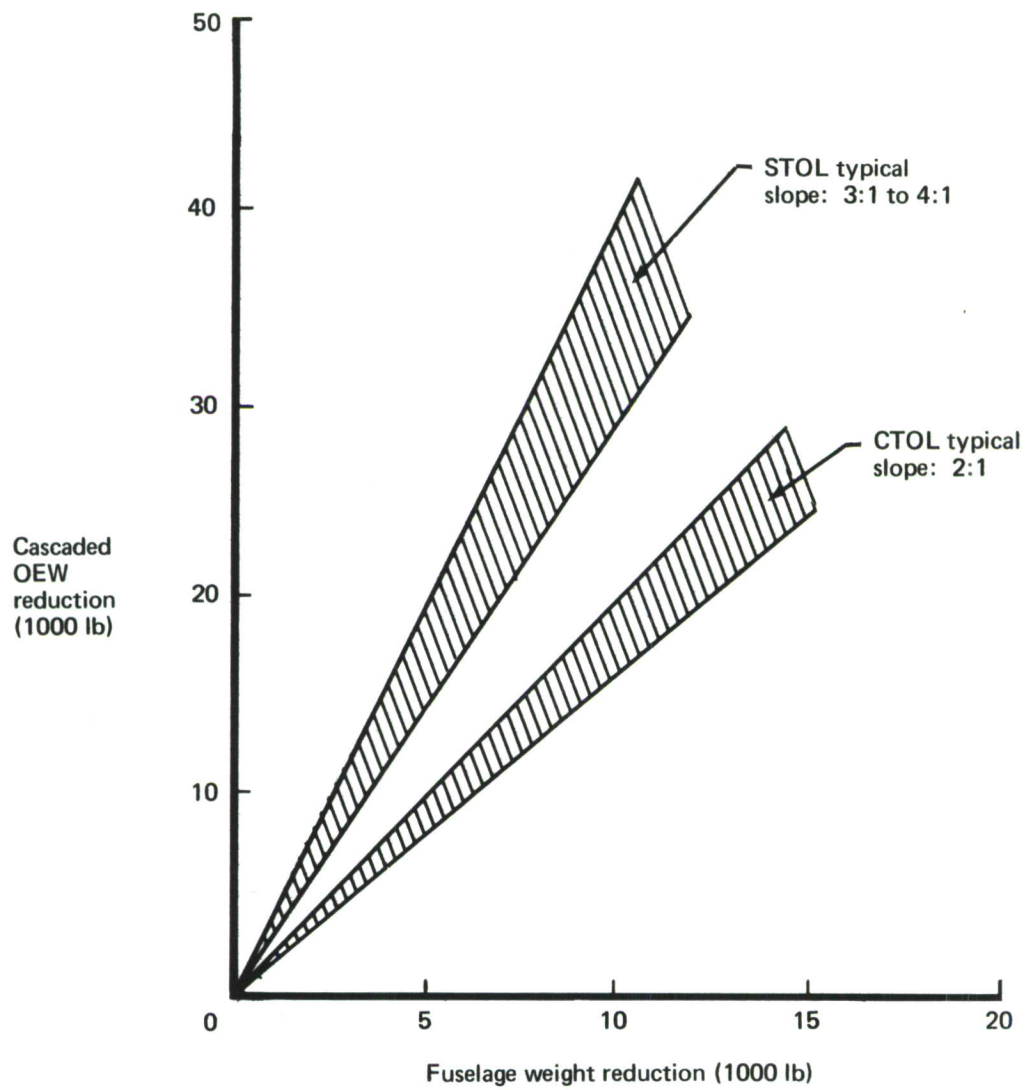


Figure 37.—AMST Applicability

● Aerodynamic data

Area	sq ft	Wing	Horiz tail	Vert tail
Span	ft	1761.5	437.17	499.14
Aspect ratio		130.16	42.83	22.33
Sweep C/4	deg	9.44	4.0	1.0
Dihedral	deg	5.35	10	35
Incidence	deg	0	-4	-
Taper ratio		3	0.5	1.0
t/c: body side to		0.273 b/2	0.12	0.14
		0.50 b/2	0.12	0.14
MAC	in.	Tip	0.12	0.14
Volume coefficient		177.7	130.09	268.09
			1.35	0.15

- Powerplant
(2) GE CF6-50D, rated 50,300 lb SLST each

- Landing gear
Main (8) 40 x 18-17 tires
Nose (2) 40 x 18-17 tires

- Cargo compartment
140/144 in. wide 140/146 in. high 564-in. long (excl ramp)
734-in. long (incl ramp)

- Weights
STOL mission gross weight lb 171,000 (N = 3)
Maximum design weight lb 225,000 (N = 2)

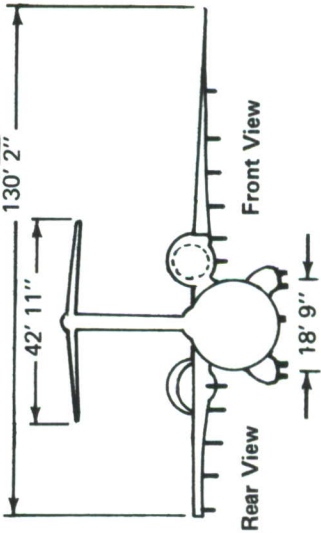
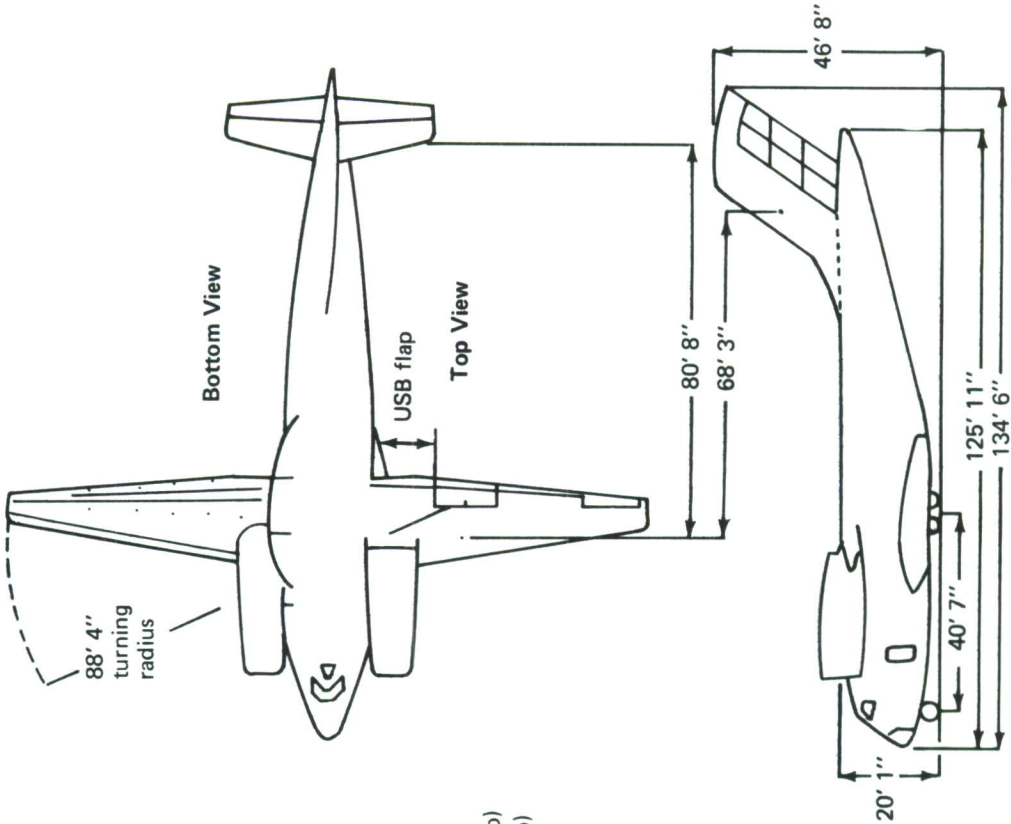


Figure 38. – General Arrangement –Boeing AMST

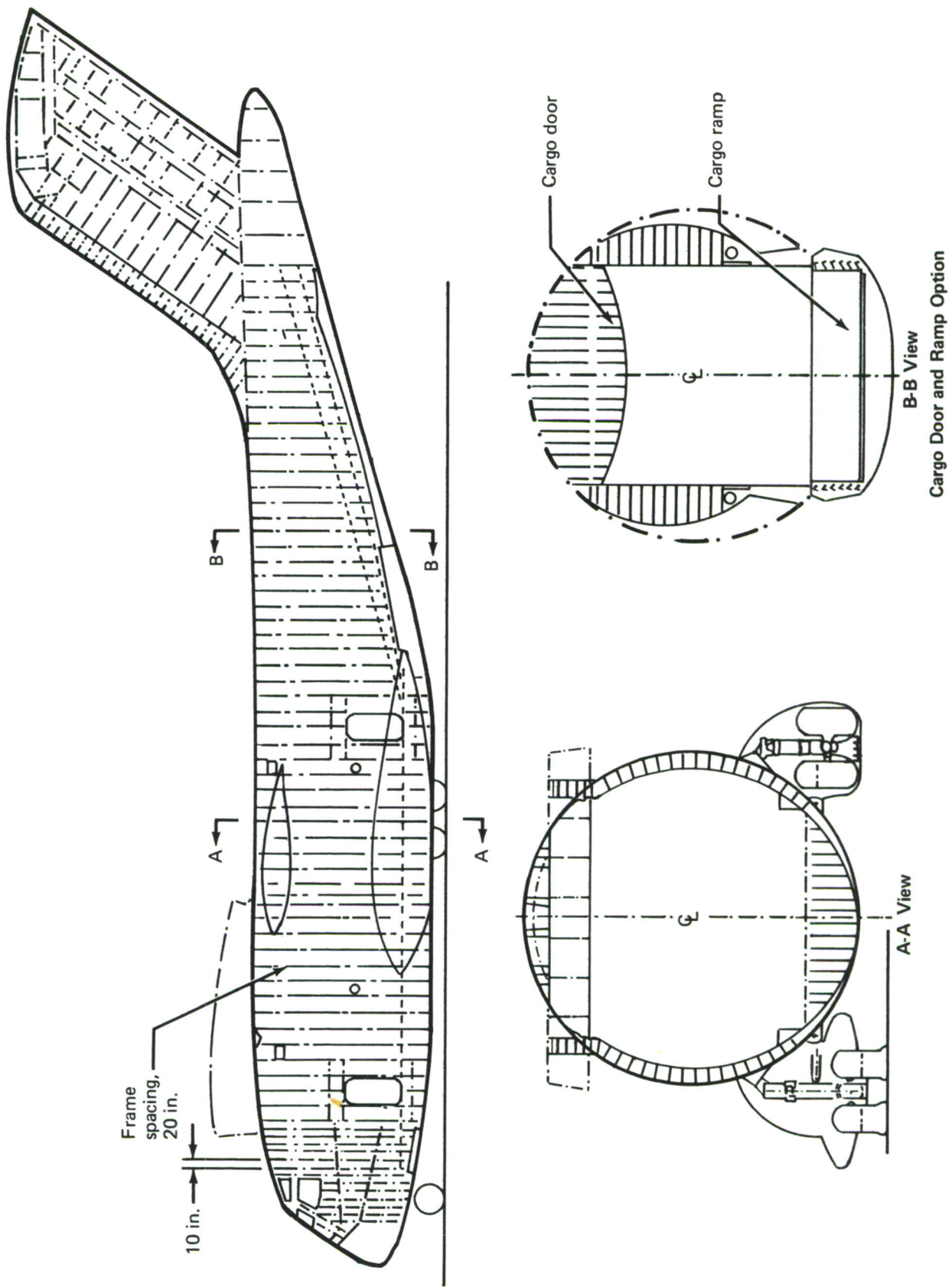


Figure 39.—Fuselage Structure

Table V lists Boeing AMST baseline component estimated weight and relative costs. Note that the fuselage component is the heaviest and, with the exception of nacelle structure, costs most on a per-pound basis. These facts provide incentive for seeking fuselage structure improvement.

Table V.—AMST Baseline Cost/Weight

Component	Structural weight (lb)	% of total weight	% of total structural cost	$\frac{\text{Component cost (\$/lb)}}{\text{Wing cost (\$/lb)}}$
Wing	21,800	29.0	24.0	1.0
Fuselage	29,490	39.0	41.3	1.27
Empennage	6,350	8.4	7.4	1.08
Landing gear	8,750	11.6	3.3	0.35
Nacelle	9,060	12.0	24.0	2.45

Sensitivity of payload, mission radius, and field length performance parameters to structural weight reduction is shown in figures 40 and 41.

Relative 10-year life cycle costs for various unit equipment/buy (UE/buy) quantities are shown in figure 42.

AMST Payoff Potential: Figure 43 shows potential payoff for the AMST. Figures 40 and 41, with the structure weight savings shown in figure 43, reveal that modest improvements in field length and significant increases in payload or mission radius can be achieved with the projected fuselage weight savings shown.

Translating a 6% fuselage weight savings and corresponding 5.8% payload increase to fleet size reduction shows that a UE/buy ratio of 288/339 airplanes can be reduced to 271/319. Ten-year life cycle system cost savings are estimated to be \$325 million. Assuming a \$12 million cost for the cargo AMS-ADP, the leverage, or payoff/cost ratio, is 27+ for the ADP.

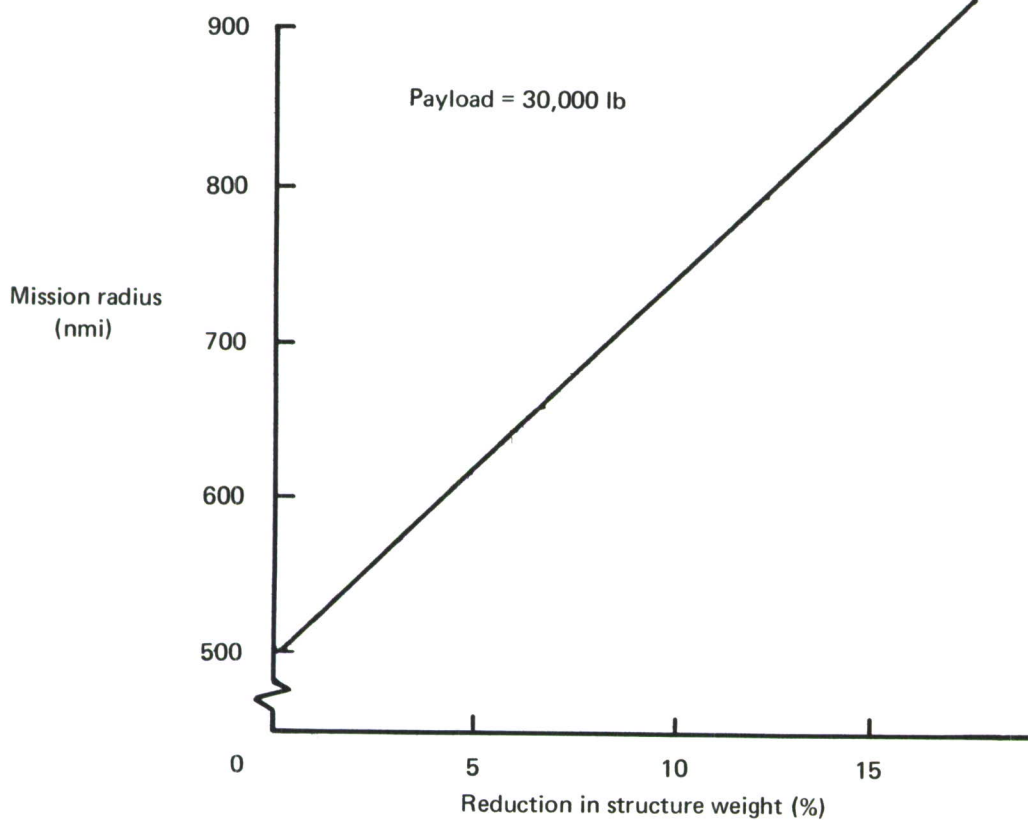
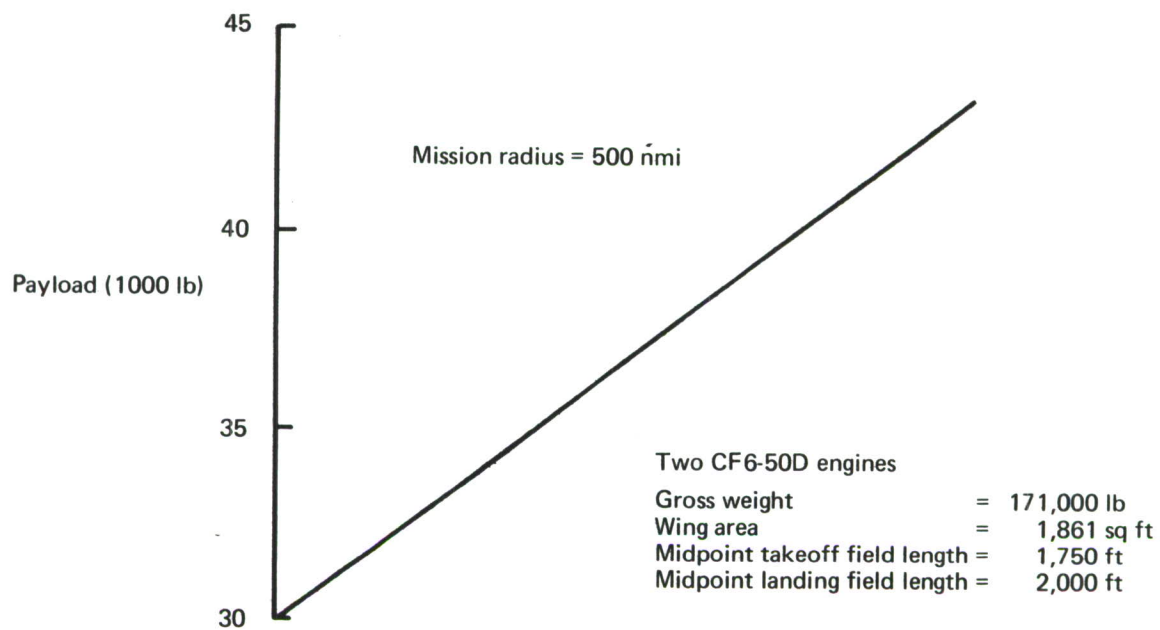


Figure 40.—Performance Sensitivity: Effect of Structural Weight Reduction on Payload and Mission Radius

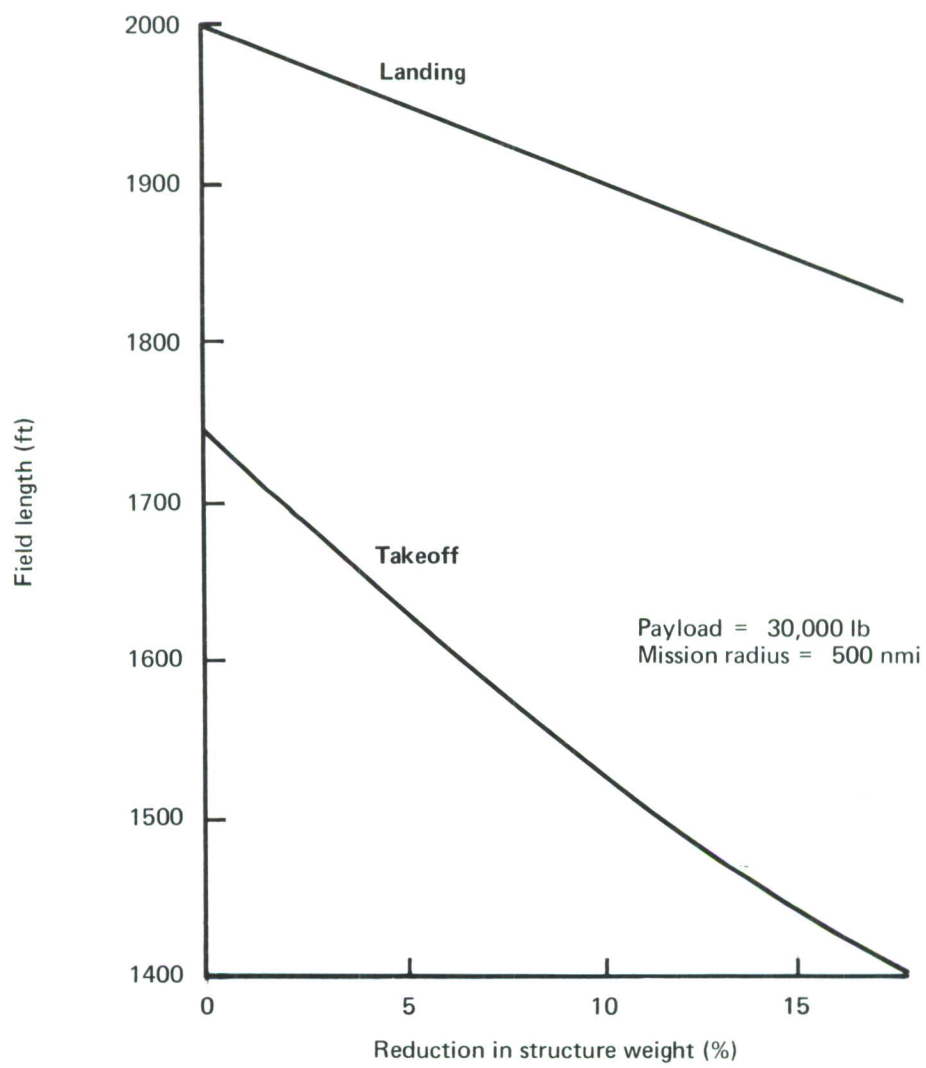


Figure 41.—Performance Sensitivity: Effect of Structural Weight Reduction on Field Length

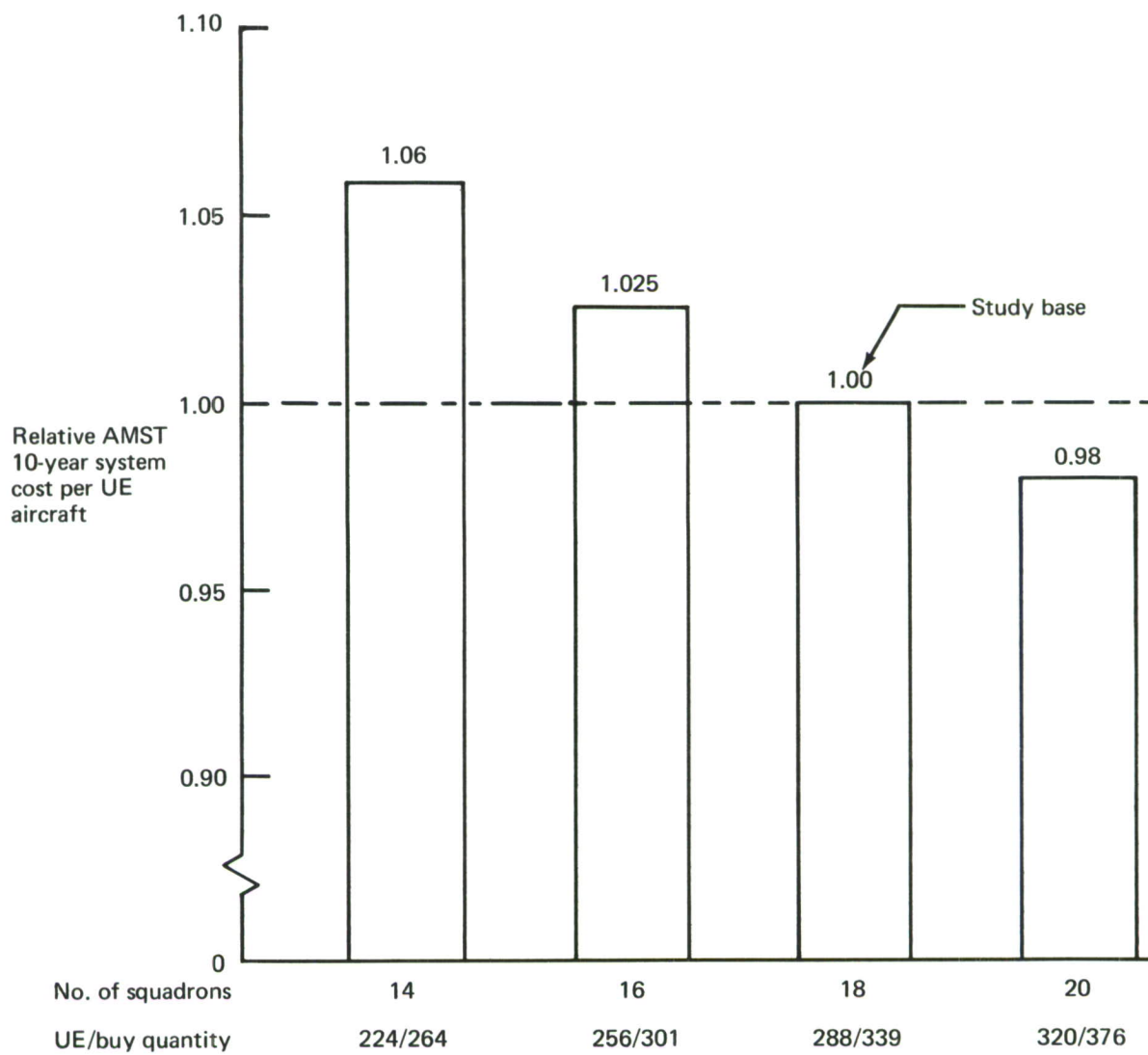
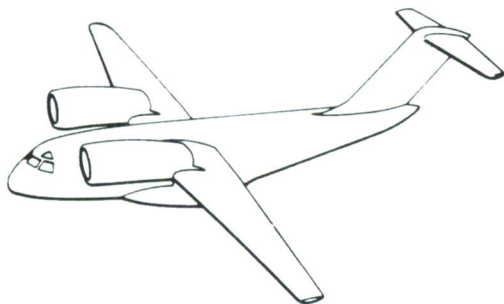


Figure 42.—Ten-Year AMST Life Cycle Costs as a Function of Fleet Size



Baseline structure
 Conventional skin/stringer
 Body structural weight: 29,490 lb
 Payload: 30,000 lb
 Mission radius: 500 nmi
 UE/buy 288/339 airplanes

Projected AMST weight saving due to cargo fuselage AMS-ADP: 1769 lb

Payoff in:

- Reduced field length requirements and a lower approach speed
- Reduced vulnerability to enemy gunfire
- Increased range
- Increased payload

Weight reduction permits:

- Payload increase of 1740 lb (5.8%), which enables fleet size reduction to 271/319 (UE/buy) airplanes for same total mission capability

Estimated 10-year life cycle cost saving: \$325 million

Leverage: Life cycle cost saving/AMS-ADP cost = \$325 million/\$12 million = 27+

Figure 43.—Boeing AMST Payoff

b. Opportunities for Technical Advancement

The continuation of this Advanced Development Program offers opportunities for advancement in several technological areas that not only meet the requirements of this program but also have general application. Some of the items listed below may have applications broad enough to justify additional development in separate programs.

(1) Strength Analysis

During more detailed design studies, further development and more extensive application of structural element weight optimization computer programs will help to optimize material distribution and utilization. This is particularly true in the case of combined-load conditions such as shear and compression.

A verification panel test program will verify the strength analysis methods, particularly the effective width of skin working with the stringers of an adhesive-bonded structure loaded in compression.

(2) Fatigue and Damage Tolerance

Areas of development remain in the detail design and analysis of fatigue-resistant and damage-tolerant structure. The follow-on program recommended in section V and a continuing Boeing-funded durability R&D program are intended to supply some of those elements required to effect a final design. Four areas considered to require additional depth of investigation are discussed.

Fatigue Performance of Bonded Joints Under Environmental Exposure: As observed from in-service experience, the fatigue performance of bonded joints exposed to a moist environment has ranged between the extremes of good to poor. Materials and processing studies are proceeding in an effort to develop bonding processes that exhibit immunity to environmental degradation (sec. IV-2).

Further development of the adhesive bonding process must be accomplished before a completely reliable process may be committed to a production program. Some understanding of the mechanism of environmental degradation of bonded joints has been obtained through in-house research and development programs. These investigations indicate that adequate protection of the substrate is the key to obtaining bonds that exhibit stability under adverse environmental conditions. The anodic surface preparation process shows potential for achieving the required degree of protection. However, additional effort to fully define its performance under actual service conditions is required.

More effort is needed in developing the adhesives and primers themselves to improve their tolerance to processing variability.

Additional long-term fatigue testing of bonds fabricated from advanced bonding materials and processes is required to provide firm design data and a verification of the bonding techniques intended for use on the advanced cargo fuselage structure.

Fatigue Performance Under Spectrum Loading: The Boeing fatigue analysis methodology uses the Palmgren-Miner cumulative damage rule to determine fatigue performance. Spectrum loading effects are accommodated by suitably adjusted S-N curves to reflect observed in-service fatigue behavior.

The Design Methodology Group, Design Criteria Branch, Structures Division (AFFDL/FBEB) has conducted interesting test and analytical work on fatigue design methodology concerning fatigue crack initiation under conditions of spectrum loading. In general, the results are reasonably consistent with those obtained through use of Boeing fatigue analysis methodology. The work reported to date by the AFFDL/FBEB promises improvement in fatigue performance prediction capability; however, before this method can be used, several important questions must be resolved:

- More complex stress histories typical of airframe structure should be tested. Mean stress variation occurring throughout all segments of flight play a significant role in fatigue crack initiation.
- Testing to investigate the effects of spectrum truncation should include joints with varying degrees of complexity. The conclusions reached as a result of simple specimen fatigue testing have proved disappointing in Boeing experience.
- Spectrum test techniques must be simplified to the maximum extent practical if costs are to be kept reasonable.

Further development of the AFFDL/FBEB fatigue design methodology is required before it may be applied to aircraft fatigue analysis; however, this methodology gives promise to fatigue analysis improvement.

Fracture Mechanics Data for Honeycomb Core Sandwich Panels: The limited fracture mechanics testing conducted on honeycomb core sandwich panels (ref. 3) indicates the beneficial effects of the core material in reducing fatigue crack and crack growth rates for the condition of a fatigue crack propagating in one face of a sandwich panel (ref. sec. IV-4c). Analytical techniques have been developed to determine the load transfer characteristics of the core material and the resulting reduced crack tip stress intensity, K_{red} , and thereby enable prediction of the apparent reduced fatigue crack growth rate. Further development of the existing analytical technique is required, coupled with additional testing to determine the exact influence of each core and bond line parameter (core density, core depth, bond line yielding, etc.) that affect the reduced crack tip stress intensity, K_{red} .

Fracture mechanics testing conducted at Boeing indicates that the critical stress intensity level, K_{IC} , of thin ($t \leq 0.063$) sheet is enhanced by the stabilizing influence of the core. Further testing is required to adequately define this phenomenon and to arrive at firm design allowables.

Dynamic Crack Arrest Requirements: The advanced cargo fuselage concepts were sized to exhibit adequate unrepaired service use capability under conditions of stable crack growth. Dynamic crack growth was not allowed since it is felt that fracture mechanics technology is not sufficiently developed to define the conditions under which a dynamically propagating crack will be arrested.

USAF Damage Tolerance Criteria (app. I) requires that a dynamic factor (DF) of 1.15 be used to reflect the energy release due to load path failure. This requirement seems reasonable and conservative; however, until improved analytical techniques are developed and sufficient verification testing is accomplished to fully define the conditions required to ensure dynamic crack arrest, working stresses will be limited to achieve subcritical fatigue crack growth.

(3) Weight Estimating

The follow-on contract will provide the opportunity to check the weight-estimating methods used in evaluating advanced technology structure with actual hardware weights. The methods will be refined as required and will provide a needed tool for future preliminary design work. In addition, the definition of many specific items, such as cutout reinforcement and splice details, can be used to more accurately assess weight trends as applied to the remainder of the body or to other aircraft of similar construction.

(4) Manufacturing Opportunities for Technology Advancement

There are several opportunities for advancing current technology in manufacturing that are related to adhesive bonding of primary aircraft structure.

Process Development: The development of an automated, continuous process line for metal preparation and application of corrosion-inhibiting primer constitutes a major step in improving the costs and reliability of adhesive-bonded primary structure.

Proven economic processes for the repair of damaged bonded primary aircraft structure must be developed if bonding is to succeed as an airframe construction method.

Fabrication/Assembly: The development of a production (as opposed to laboratory) process for verifying the strengths of adhesive-bonded joints in primary aircraft structure would be of great benefit. During fabrication, the joint quality of subassemblies and major bonded assemblies would be ensured. After airplane delivery, customer personnel would have a reliable check on continued joint integrity.

In bonded honeycomb structure, the adhesive is usually applied in a uniform thickness to the face sheets; upon curing, only 40% of the applied adhesive wets and bonds the honeycomb. Preliminary efforts with a reticulating adhesive have indicated the possibility of developing a process that applies the adhesive to the honeycomb in a thin sheet; the adhesive is then caused to melt and cling (reticulate) to just the periphery of the honeycomb cell ends. The face sheets are then positioned and the assembly is cured in an autoclave.

For panels fabricated in this way, the honeycomb-to-panel adhesive weight can be cut by 60%. Achievement of this attractive weight savings requires process development.

(5) Quality Control

In addition to the state-of-the-art NDT techniques used on current production programs, development of advanced and improved technology applicable to cargo fuselage fabrication is required. Some of the significant quality control techniques currently lacking in the industry are being developed.

Bond Proof-Test Equipment: Void detection capability has been successfully developed and implemented on adhesive-bonded structures. However, there is a need to determine the bond strength of the bonded parts. A Boeing in-house IR&D program developed an electromagnetic proof-testing technique, and a prototype unit is currently under evaluation. Further development of this test method and the design and construction of a production model are required.

Automated Eddy Current Inspection: Eddy current inspection, when used manually, is successful in detecting cracks in drilled holes. Automated eddy current inspection has been used in various production applications throughout the industry. The integration of the automated eddy current inspection with the numerically controlled riveter is required. No serious technical problems are anticipated.

SECTION IV

TECHNICAL DISCIPLINE ACCOMPLISHMENTS

1. INTRODUCTION

In the performance of a first-iteration preliminary design study, all technologies that could impact the validity of the study require careful attention. The Boeing design team for this study consisted of representatives from all of the technologies listed below.

- Design
- Stress analysis
- Fatigue analysis
- Material
- Fracture analysis
- Weights
- Manufacturing
- Quality assurance
- Cost analysis

Because team inputs were required at all levels (1 through 3) of the advanced design development and screening, the final three designs selected are ones for which a high level of confidence has been established.

The design procedure was to isolate the key details and maximum payoff potential components. This approach was followed throughout the design and analysis steps shown in figure 44. This stepwise screening and component isolation identified those changes, such as structural geometry, material, and detail design quality improvement, which have the greatest effect on the program weight reduction goal.

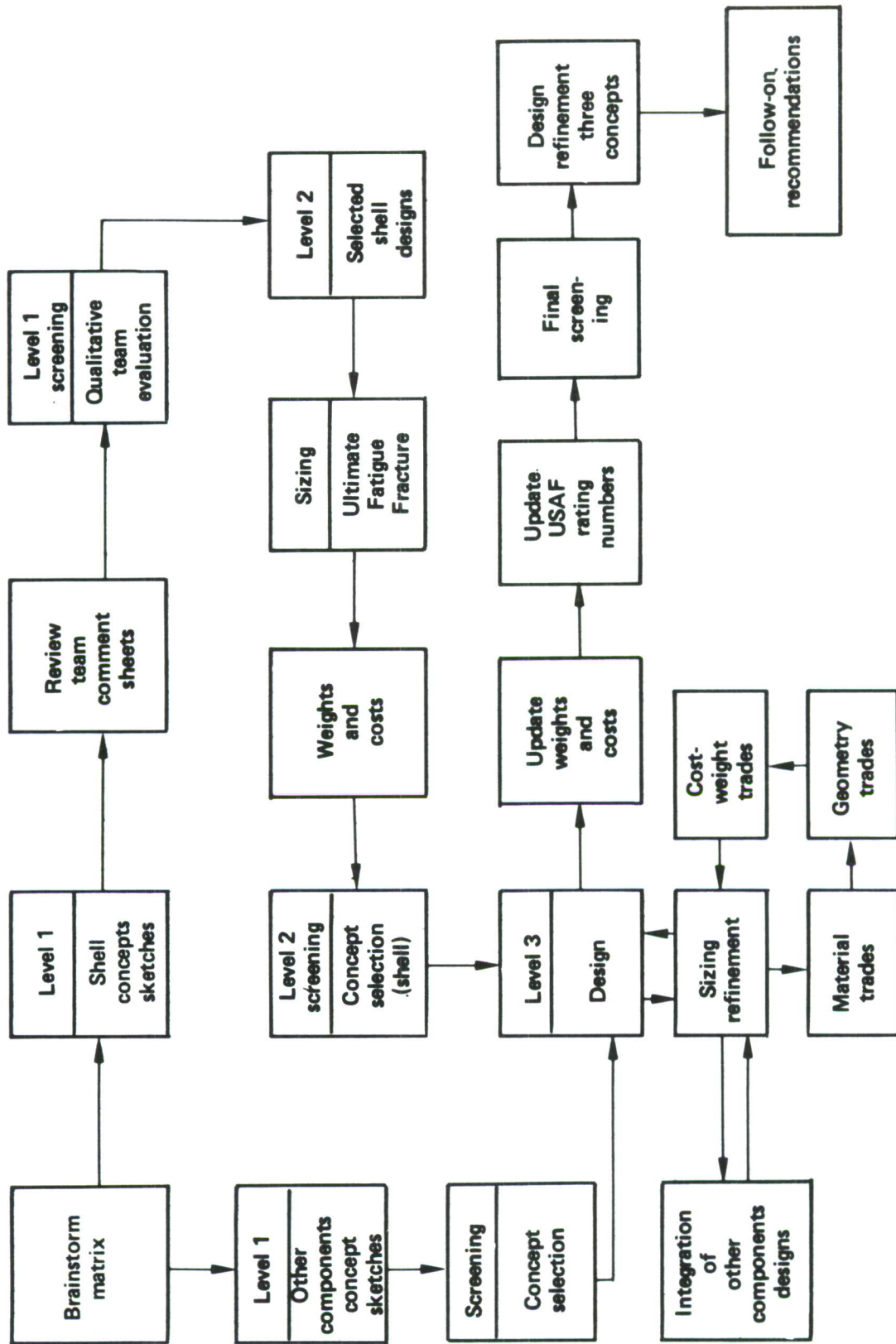


Figure 44. --Concept Development Plan

2. MATERIALS AND PROCESSES

To achieve the stated program goals (see sec. III-1), those advanced materials and processes which are through the exploratory development stage (or nearly so) were considered as candidates for concept application.

a. Material Candidates

Commensurate with the objectives of the advanced metallic structures development program, the decision was made to fabricate the primary load-bearing elements of the fuselage component from metallic materials, limiting the use of nonmetallic materials (advanced composites, adhesives, primers, etc.) to local reinforcement, bonding, or finishing applications.

(1) Metals

Metals considered for structural applications included aluminums, titaniums, and steels. No single metal has all the attributes necessary to produce the optimum structure. Depending on the intended structural application of a metallic material, one, or more than one, of the parameters describing the capability of that material may be emphasized. In order to achieve a lightweight, cost-effective structure, consideration must be given to all the parameters shown in table VI.

Table VI.—Material Selection Parameters

Material characteristics
Mechanical properties (F_{tu} , F_{ty} , F_{cy} , F_{su} , etc.)
Physical properties (ρ_{wt} , α_{temp})
Fracture toughness (K_{Ic} , K_{Isc})
Fatigue properties
Life (S vs N)
Notch sensitivity (K_t vs N)
Crack growth (da/dn)
Specific properties (F_{tu}/ρ_{wt} , F_{ty}/ρ_{wt} , K_{Ic}/ρ_{wt} , G_m/ρ_{wt} , etc.)
Corrosion resistance
Environmental sensitivity
Protection requirements
Application considerations
Structural consideration (configuration, end load, etc.)
Manufacturing consideration (machinability, weldability, formability, etc.)
Cost consideration (material cost and manufacturing cost)

Aluminum: The high-strength aluminums considered for use on this program are shown in table VII. Those aluminum alloys which are sufficiently developed to meet the criteria established for candidate materials (sec. IV-2a) were assessed and incorporated into the program. Both baseline materials and advanced materials which exhibit potential improvement in any of the important structural parameters were considered in the program.

For monocoque skin and formed stringers, bare aluminum sheet or plate will be used. Bare aluminum is lightweight and cost effective for this application. Its structural and fatigue allowables are approximately 7% higher than those of clad aluminum. Bare sheet is cheaper than clad for equal surface finish. In addition, organic finishing (sec. IV-2c2) offers enhanced corrosion protection; this will be demonstrated during phase IB testing.

Alloy 2024 was considered for use in the sheet, plate, and wide extrusion forms. In the appropriate heat treatments, this alloy possesses excellent fatigue and fracture characteristics with relatively low static properties and must be considered for use in areas of high damage tolerance requirements. The exfoliation corrosion resistance of 2024 is considered adequate for the intended applications. This material has almost universal acceptance for use in fuselage skins and is the standard against which all alternate materials must be measured.

Alloy 2219 exhibits the lowest static properties of the sheet and plate alloys considered for this program. While its poor static properties militated against its extensive use on this program, 2219 was considered for use in welded assemblies. Other aluminum alloys are weldable; however, 2219 was judged to possess the best combination of strength, toughness, and stress corrosion resistance in both the parent metal and the weld nugget.

Alloy 7075 was considered for use in the sheet, plate, extrusion, and forging forms. This material possesses excellent static properties with relatively low fatigue and fracture characteristics, and was considered for use in areas of moderate damage tolerance requirements.

Various heat treatments have been developed for 7075 ranging from T6, which has the highest static properties with poorest stress corrosion resistance, to the overaged T73 temper, which has the lowest static properties with highest resistance to stress corrosion.

The 7075-T6 sheet material is used extensively as stock for formed fuselage stringers and frames on all Boeing commercial airframes. The 7075-T651 plate is used for the upper surface in-spar skins on the 747 wing. The 7075-T6 sheet and 7075-T651 plate are used as the skin material in the in-spar area of the 707 and 747 stabilizer and vertical fin. Service experience accumulated on 7075 material used on such external surfaces as wing and empennage skins has proved the corrosion resistance of this material, in the appropriate heat treatments, to be adequate for use in exposed locations.

Alloy 7178 was considered for use in the extruded form for those unique applications where fatigue and damage tolerance requirements are low. This material is used

Table VII.—Aluminum Preliminary Allowables ^a

Form	Alloy	Gage	Heat treatment	Grain dir.	ρ (lb/in. ³)	F_{tu} (ksi)	F_{tu}/ρ (in. x 10 ³)	F_{ty} (ksi)	F_{cy} (ksi)	F_{su} (ksi)	F_{brv} e/D=2.0 (ksi)	E (ksi x 10 ³)	E/p (in. x 10 ⁵)	E_c (ksi x 10 ³)	$K_{C'}$ K_{Ic} (ksi $\sqrt{in.}$)	Short transverse smooth specimen threshold (ksi)
Sheet	2024 Bare	.010-.249	T3	L	.100	66	660	49	41	41	80	10.5	1050	10.7	110	
				T	.100	65	650	44	41	41	80	10.5	1050	10.7		
	2219 Bare	.040-.249	T87	L	.102	61	598	50	50	36	80	10.5	1029	10.8	100	
				T	.102	62	608	50	53	36	80	10.5	1029	10.8		
Plate	7075 Bare	.040-.249	T37+ Weld+Age To T87	(b)	.102	33	324	25	25	19		10.5	1029	10.8		
			T6	L	.101	80	792	72	71	48	106	10.3	1020	10.5	69	
				T	.101	80	792	70	74	48	106	10.3	1020	10.5		
	7475 Bare	.040-.249	T761	L	.101	70	693	61	60	44	91	10.3	1020	10.5	100	
				T	.101	71	703	60	63	44	91	10.3	1020	10.5		
		.040-.249	T61	L	.101	75	743	66	65	46	98	10.3	1020	10.5	90	
				T	.101	75	743	64	68	46	98	10.3	1020	10.5		
	2024	.25-2.00	T351	L	.100	64	640	49	40	38	77	10.7	1070	10.9	55	8
				T	.100	64	640	44	46	38	77	10.7	1070	10.9		
		.25-2.00	T651	L	.101	78	771	71	68	45	105	10.3	1020	10.6	26	8
				T	.101	79	781	69	73	45	105	10.3	1020	10.6		
	7475	.25-2.00	T76151	L	.101	70	691	59	59	39	80	10.3	1020	10.6	44	25
				T	.101	70	691	59	61	39	80	10.3	1020	10.6		
		.25-2.00	T73651	L	.102	74	725	66	64	42	98	10.3	1020	10.6	36	35
				T	.102	74	725	64	67	42	98	10.3	1020	10.6		
Extrusion	2024	.25-2.99	T3511	L	.100	62	620	47	39	31	71	10.8	1080	11.0	46	8
				T	.100	56	560	39	43	31	71	10.8	1080	11.0		
	7075	.25-2.99	T6511	L	.101	85	841	76	76	43	105	10.4	1030	10.7	28	7
				T	.101	74	732	65	71	43	105	10.4	1030	10.7		
	7049	.25-2.99	T73511	L	.102	75	735	67	67	40	92	10.4	1020	10.7	34	35
				T	.102	71	696	62	66	40	92	10.4	1020	10.7		
		.25-2.99	T76511	L	.102	77	755	70	70	41	97	10.4	1020	10.7	32	25
				T	.102	72	706	64	69	41	97	10.4	1020	10.7		
	7178	1.50-2.50	T6511	L	.102	86	843	77	76	43	106	10.4	1020	10.7	25	7
				T	.102	74	725	64	72	43	106	10.4	1020	10.7		

^a Varies with thickness; representative values shown for comparative purposes^b Through weld bead

Table VII.—Concluded

Form	Alloy	Gage	Heat treatment	Grain dir.	ρ (lb/in. ³)	F_{tu} (ksi)	F_{tu}/ρ (in. x 10 ³)	F_{ty} (ksi)	F_{cy} (ksi)	F_{su} (ksi)	F_{brv} e/D=2.0 (ksi)	E (ksi x 10 ³)	E/ρ (in. x 10 ⁵)	E_c (ksi x 10 ³)	$K_{c'}$ K_{Ic} (ksi√in.)	Short transverse smooth specimen threshold (ksi)
Extrusion	7050	.25-2.99	T73511	L T	.102 .102 .102 .102	75 71 77 72	735 696 755 706	67 62 70 64	67 66 70 69	40 40 41 41	92 92 97 97	10.4 10.4 10.4 10.4	1020 1020 1020 1020	10.7 10.7 10.7 10.7	34 22 32 20	35 35 25 25
Die forging	7075	3.00	T73	L T	.101 .101	68 66	673 653	58 55	60 57	40 40	81 81	10.0 10.0	990 990	10.4 10.4	31 25	43 43
	7175	3.00	T736	L T	.101 .101	78 73	772 723	68 64	70 67	44 44	91 91	10.0	990	10.4	34	35 35
	7050	3.00	T736	L T	.102 .102	74 72	725 706	64 63	66 65	40 40	86 86	10.2 10.2	1000 1000	10.6 10.6	33	35 35
	7049	3.00	T73	L T	.102 .102	74 72	725 706	64 63	66 65	40 40	86 86	10.2 10.2	1000 1000	10.6 10.6	33	35 35

for the keel beam chords on the baseline, where its extremely high static properties are utilized. Although this material possesses very poor resistance to exfoliation corrosion and stress corrosion cracking, no service problems have appeared in this particular application.

Alloy 7475, a recently developed alloy, was considered for use as sheet and plate in the appropriate heat treatments. This material possesses good static properties and excellent fatigue and fracture characteristics, comparable to those of 2024-T3 sheet. It is considered a replacement material for the 2024-T3 sheet or 7075-T651 plate material presently used in the baseline structure.

Alloy 7475 is available as sheet and plate with a maximum thickness of 4.0 inches. Its chemical composition is similar to that of 7075, except that iron and silicon content are lowered to increase toughness. A small reduction in magnesium content slightly lowers the strength but also increases fracture toughness. Special mill processing controls the metallurgical structure and is another factor responsible for increased toughness.

Table VIII compares fatigue crack growth rate data for 7475-T761, 7475-T61, 2024-T3, and 7075-T6 sheet when tested in humid air. It may be observed that 7475-T761 exhibits fatigue crack growth rates comparable to those of 2024-T3 sheet, slower at $\Delta K > 20 \text{ ksi}\sqrt{\text{in.}}$ and faster at $\Delta K \leq 20 \text{ ksi}\sqrt{\text{in.}}$. The T61 temper of this alloy exhibits crack growth rates that are faster than those of T761 at all ΔK values but slower than those of 7075-T6.

Table VIII.—Material Fatigue Crack Growth Rate, $R = 0.05$

Material	Data source	Grain direction	Fatigue crack growth rates, $da/dn \times 10^6 \text{ in./cycle}$						
			$\Delta K = 10 \text{ ksi}\sqrt{\text{in.}}$	15	20	25	30	40	50
2024-T3 Clad	1	L T	3.3 15.0	12.8 70.0	33.0 210.0	70 500	125 1000	330 3500	620 8000
7075-T6 Clad	1	L T	5.5 8.8	2.2 37.2	62.0 117.0	140 370	290 767	1100 2430	5000 —
7475-T761	2	L T	6.6 4.5	17.0 14.0	33.0 31.5	59 62	100 110	300 460	— —
	3	L T	3.7 —	11.6 —	21.0 —	33 —	50 —	— —	— —
7475-T61	2	L T	6.6 8.1	22.0 24.2	50.0 44.0	98 71.5	180 114	555 440	— —
	4	L T	6.0 —	17.0 —	34.0 —	52 —	87 —	260 —	640 —

Data source: 1 Boeing data (room air)
2 Boeing Advanced Cargo Fuselage material test program; humid air ($RH \geq 90\%$) (ref. app. II)
3 Interim Material Test Data Interchange program; $R = 0.10$, dry air
4 Dickson, J.A., "Alcoa 467 Process X7475 Alloy," Alcoa Green Letter, May 1970; environment and grain direction not noted (ref. 9)

Of particular interest is the almost orthotropic fatigue crack growth properties of both 7475 tempers. The 7475-T761 and 7475-T61 actually exhibit slower crack growth rates in the transverse grain direction than the 2024-T3, making them particularly suitable for fuselage skins which are characterized by a high degree of load biaxiality.

Table IX shows fatigue crack growth rates observed for 7475-T761 and -T61 as tested in a salt solution. The 7475 exhibits considerable acceleration of growth rates under the influence of an aggressive environment which, while significant, is not considered of sufficient magnitude to eliminate this material from consideration. Table X summarizes plane stress fracture toughness values of the various candidate sheet materials as reported in appendix II, and as extracted from an interim material test data interchange program. The interim data interchange covered the testing accomplished through the middle of phase IA of the fighter and cargo contracts of the AMS-ADP. The complete results of material testing conducted on these contracts are reported in:

AFFDL-TR-73-50 "Advanced Metallic Structure:

(Air Superiority Fighter Wing) Design for Improved Cost, Weight, and Integrity" (ref. 4)

AFFDL-TR-73-51 "Advanced Metallic Structure:

(Cargo Wing) Design For Improved Cost, Weight, and Integrity" (ref. 5)

AFFDL-TR-73-52 "Advanced Metallic Structure:

(Air Superiority Fighter Wing) Design For Improved Cost, Weight, and Integrity" (ref. 6)

The majority of these data are considered invalid under the requirements of reference 7 ($2a_{CR} \leq W/S$ and $f_c \leq 0.67 f_{ty}$). The validity of fracture data obtained through material testing conducted under this program is summarized in table II-VII. Fracture mechanics considerations indicate that specimens which do not meet the validity requirements of reference 7 yield critical plane stress intensity factors (K_c) less than those which would be associated with valid panels; therefore, the invalid data are considered to be significant in that a lower bound value of K_c is defined.

Alloy 7050, a recently developed material, provides increased strength over 7075-T73, with comparable toughness and immunity to stress corrosion cracking.

The alloy contains less manganese and chromium to reduce quench sensitivity. The iron and silicon were lowered to increase fracture toughness. The increase in alloying elements zinc and copper maintains high strength in the alloy in the overaged conditions, which are resistant to stress corrosion cracking and exfoliation.

Alloy 7049 was considered for use in the extruded and forged forms. In general, it offers equal static strengths and lower fracture properties than the newer 7050 alloy. Its only advantage over 7050 is that it is further into the hardware application stage than 7050. This material was evaluated as an alternative to 7050 since both alloys have similar properties.

Table IX.—Environmental Effect on Fatigue Crack Growth Rates of 7475 Material

Material	Grain direction	Environment	Fatigue crack growth rates, $da/dn \times 10^6$ in./cycle			
			$\Delta K = 15 \text{ ksi}\sqrt{\text{in.}}$	20	25	30
7475-T761	L	Moist air 3-1/2% NaCl	17 62	33 100	59 160	100 230
	T	Moist air 3-1/2% NaCl	14 62	31.5 100	62 155	110 220
7475-T61	L	Moist air 3-1/2% NaCl	22 72	50 120	98 190	180 290
	T	Moist air 3-1/2% NaCl	24.2 71	44 120	71.5 190	114 290

Data source: Boeing Advanced Cargo Fuselage material test program (ref. appendix II)

Table X.—Plane Stress Fracture Toughness Data

Material	Grain direction	Data source	K_{IC} (ksi $\sqrt{\text{in.}}$)			
			t = 0.040	t = 0.063	t = 0.112	t = 0.125
2024-T3	L	1	100	164	133	
	T	1	103	125	125	
	T	2	—	138	—	
7075-T6	L	1	63	63	63	
	L	3	—	65	—	
7475-T761	L	3	—	100	—	
	L	4	116	—	136	
	T	4	114	—	117	
	T	2	—	140	—	
7475-T61	L	3	—	95	—	
	L	4	112	—	114	
	T	4	102	—	104	
7475-T76151		5				134

Data source: 1 Boeing data

- 2 Wang, D.Y., "Plane Stress Fracture Toughness and Fatigue Crack Propagation of Aluminum Alloy Wide Panels," Douglas paper 6054 (ref. 8)
- 3 Dickson, J.A., "Alcoa 467 Process X7475 Alloy," Alcoa Green Letter, May 1970 (ref. 9)
- 4 Boeing Advanced Cargo Fuselage material test program (ref. app. II)
- 5 Interim Material Test Data Interchange program; R = 0.10, dry air

Alloy 7175 was considered for use in forgings. This is a relatively recent modification of 7075 in which lower iron and silicon impurity content and improved processing controls offer better static strength than 7075-T73 with improved toughness values. The special processing control required for this material increases its cost in comparison with the competing alloys.

Titanium: Titanium alloys in all mill forms were considered for use on this program (table XI). In general, titanium exhibits excellent specific yield strengths, F_{ty}/ρ . Compared to the aluminums, titanium specific fracture properties, K_C/ρ , are relatively poorer in sheet form and better in heavy sections.

The ELI and Super ELI compositions of this material offer improved resistance to aggressive environments; however, these compositions adversely affect static properties.

The high material and fabrication costs associated with titanium militate against its extensive use in applications involving low structural loadings, typical of fuselage structure, and in the absence of an extreme thermal environment.

Appropriate heat treatments of Ti-6Al-4V were considered for use as sheet, plate, extrusion, and forging. This alloy possesses an excellent strength-to-density relationship and superior fatigue characteristics (better than those of any aluminum alloy considered for this program). In spite of the high material and manufacturing costs associated with titanium, the advantages offered by the good strength and fatigue characteristics of Ti-6Al-4V require that it be considered as a potential candidate material.

Alloy Ti-6Al-6V-2Sn in the STA 1100 temper was considered for use in forgings and extrusions. It possesses static strength properties superior even to those of Ti-6Al-4V, with reduced fracture toughness. It was considered for use only in specific areas with low damage tolerance requirements. For keel beam chord members, the use of Ti-6Al-6V-2Sn STA was considered since this particular element experiences extremely high structural loadings of a predominantly compressive nature.

Steels: Steel alloys, both iron base and corrosion resistant, were considered for use on this program (table XII).

On a specific strength basis, F_{ty}/ρ , F_{tu}/ρ , etc., it is difficult to justify the use of any of the steels on fuselage components. The low-alloy, high-strength steels do exhibit specific strengths competitive with the specific strengths of aluminum and titanium. However, these steels are generally characterized by poor resistance to aggressive environments. The precipitation-hardening stainless steels exhibit adequate corrosion resistance but are characterized by poor specific strengths.

The relatively low structural loadings experienced by fuselage structures require thin skin gages of steel which result in unacceptably low crippling and local stability capability.

Table XI.—Titanium Preliminary Allowables

Form	Alloy	Gage	Heat treatment	Grain dir	ρ (lb/cu in.)	F_{tu} (ksi)	F_{tu}/ρ (in. x 10^3)	F_{ty} (ksi)	F_{cy} (ksi)	F_{su} (ksi)	F_{bry} $e/D = 2.0$ (ksi)	E (ksi x 10^{-3})	E/ ρ (in. x 10^5)	E_c (ksi x 10^{-3})	K_c, K_{Ic} (ksi $\sqrt{\text{in.}}$) (a)	K_{sc}, K_{Isc} (ksi $\sqrt{\text{in.}}$) (a)
Sheet	6Al-4V ^b	0.070	Cont. rolled & cont annealed, 60 ft max length	L T	0.160	140	875	122	125	88	208	16.0	1000	16.4	150	100
					0.160	140	875	127	140	88	208	17.1	1069	17.1	160	105
Plate	6Al-4V ^b	0.020- 0.187	Hand milled, duplex annealed, 20 ft max	L&T	0.160	134	838	126	130	87	212	16.1	1006	16.5	150	100
					0.160	130	814	118	122	84	192	16.1	1006	16.5	95	60
Bar & Forging	6Al-4V ^b	0.187- 4.00	Beta annealed	L&T	0.160	130	814	115	121	84	189	16.3	1018	16.7	95	60
					0.160	152	960	136	141	91	214	16.3	1018	16.7	75	45
Extrusion	6Al-6V-2Sn	0.51- 1.00	STA 1000	L&T	0.160	170	1060	160	165	100	229	17.0	1036	17.5	35	25
					0.164	125	780	112	117	81	182	16.7	1044	17.0	95	60
	6Al-4V ^b	2.00	Beta annealed	L&T	0.160	155	970	140	143	96	224	16.7	1044	17.0	75	45
					0.160	170	1060	160	165	100	229	17.0	1036	17.5	35	20

^a Estimated "B" basis allowables

^b Boeing specification material

Table XII.—Steel Preliminary Allowables

Form	Alloy	Gage	Heat treatment	Grain dir	ρ (lb/cu in. ³)	F_{tu} (ksi)	F_{tu}/ρ (in. x 10 ³)	F_{ty} (ksi)	F_{cy} (ksi)	F_{su} (ksi)	F_{bry} e/D = 2.0 (ksi)	E (ksi x 10 ⁻³)	E/ ρ (in. x 10 ⁵)	E _c (ksi x 10 ⁻³)	K _c , K _{lc} (ksi√in.)	K _{sc} , K _{lsc} (ksi√in.)
Forging	9Ni-4Co-0.2C	2.00	1025°F Temper	L	0.284	194	683	172	184	117	262	28.5	1003	28.5	120	20
	18Ni-Marge	2.00		L	0.286	218	762	212	215	130	320	28.0	980	28.0	150	105
	HY-140	1.00		L	0.285	150	526	140	150	90	240	29.5	1035	29.5	210	140
	AFC-77	3.00		L	0.282	220	851	168	175	144	280	32.5	1152	32.5	110	60
	4340M	0.25	275°-300°F	L	0.283	280	989	234	252	168	363	29.0	1025	29.0	60	12
	15-5PH	2.00	180°-200°F	L	0.282	180	648	150	165	165	270	28.5	1010	28.5	80	60

The steel alloys were considered as possible candidates for the forged landing gear fittings only.

Candidate Metallic Material Properties: Tables VII through XII show the allowables for each of the metals considered for application to this program. Data shown in table X are from a number of sources (refs. 8 and 9 and app. II). Mechanical properties shown are “B” basis allowables as defined in MIL-HDBK-5B. For those materials where only limited data are available, the values are estimated from typical values and/or specification minimums. Toughness values are best estimates of the lower bound material toughness available with modest specification controls. The results of studies conducted under this contract and reported in section VI-1 demonstrate the insensitivity of the allowable period of unrepaired service usage to the material critical stress intensity factor, K_{Ic} . As a result, a conservative value for K_{Ic} has been established for use during the preliminary design phase.

(2) Honeycomb Core

Initial assessment of available design concepts indicated that honeycomb core sandwich structure offers promise of achieving the program goals. Metallic and nonmetallic core are available; however, for structural applications, nonmetallic core does not compete with aluminum core on a strength-to-weight basis. Only metallic cores were considered for use on this program.

Of the available metallic cores, only aluminums were considered, since titanium and steel cores are not cost effective for low temperature (under 350°F) structure.

Alloy 5052 and 5056 cores were considered for use on this program. Alloy 5052 core in H-38 or H-39 tempers exhibits lower strengths than the 5056; however, it is approximately 10% cheaper. Alloy 5056 core exhibits higher shear allowables than 5052 core. There are indications from the manufacturers that although the present cost of this core is higher than that of 5052, with increased production this differential will decrease.

These cores, with a corrosion-resistant treatment, are available in a multitude of cell sizes and foil thicknesses. They can be obtained from two sources, and are covered by military specifications. Design allowables for these cores are shown in table XIII (data from ref. 10).

Table XIII.—Honeycomb Core Room Temperature Mechanical Properties

Nominal core density (pcf)	Core designation MIL-C-7438F	Longitudinal shear properties		Transverse shear properties		Compression properties	
		Shear strength, F_{sL} (psi)	Shear modulus, G_L (ksi)	Shear strength, F_{sW} (psi)	Shear modulus, G_W (ksi)	Compression strength, F_{cc} (psi)	Compression modulus, E_{cc} (ksi)
3.1	3.1-1/8 -07(5052)	155	45.0	90	22.0	215	75.0
4.5	4.5-1/8 -10(5052)	285	70.0	168	31.0	405	150.0
6.1	6.1-1/8 -15(5052)	455	98.0	272	41.0	680	240.0
8.1	8.1-1/8 -20(5052)	670	135.0	400	54.0	1100	350.0
3.1	3.1-3/16-10(5052)	155	45.0	90	22.0	215	75.0
4.4	4.4-3/16-15(5052)	280	68.0	160	30.0	385	145.0
5.7	5.7-3/16-20(5052)	410	90.0	244	38.5	600	220.0
6.9	6.9-3/16-25(5052)	540	114.0	328	46.4	800	285.0
8.1	8.1-3/16-30(5052)	670	135.0	400	54.0	1100	350.0
3.1	3.1-1/8 -07(5056)	200	45.0	110	20.0	260	97.0
4.5	4.5-1/8 -10(5056)	350	70.0	205	38.0	500	185.0
6.1	6.1-1/8 -15(5056)	525	102.0	305	38.0	825	295.0
8.1	8.1-1/8 -20(5056)	740	143.0	440	51.0	1300	435.0
3.1	3.1-3/16-10(5056)	200	45.0	110	20.0	260	97.0
4.4	4.4-3/16-15(5056)	340	68.0	198	27.5	490	180.0
5.7	5.7-3/16-20(5056)	480	94.0	280	36.0	735	270.0

Notes:

1. Properties shown for 5/8-in. core depth
2. Properties shown for stabilized core
3. Data from Hexcel TSB 120, 8/15/72 (ref. 10)

(3) Nonmetals

Nonmetallic materials were considered for local reinforcement of primary structural elements, fairings, and insulation.

Advanced composites and fiberglass were considered for local reinforcement of conventional structure where their high specific strengths may be exploited to the greatest advantage and for application as fuselage tear straps on this program.

Molded fiberglass batting was considered for use as the aerodynamic skin surface of the externally stiffened shell concept. In this application it serves the multiple purpose of fairing, thermal insulation, and acoustic insulation.

Advanced Composites: The primary objective of the AMS-ADP program is to develop a metallic structure which would satisfy the goals stated in section III-1. However, the use of local reinforcement to increase structural efficiency and stiffness was studied. The use of graphite- and boron-filament-reinforced epoxies was also studied.

Graphite filaments (HTS) offer the advantage of high strength-density and stiffness-density characteristics as compared with boron, with the added advantage of reduced material costs

Graphite exhibits a greater mismatch in coefficient of thermal expansion with aluminum as compared with boron; however, the lower tensile modulus of the graphite results in thermally induced residual stresses, due to hot-bonding, which are approximately equal to those caused by boron.

It is not immediately obvious which of the composite systems offers the greater advantage; therefore, both systems were retained until further studies indicated a clear superiority for either. The allowables for either composite system will be extracted from the AFML "Advanced Composites Design Guide" (ref. 11).

Fiberglass: For primary structural applications, fiberglass has proven neither cost nor weight effective as compared with metals or the advanced composites. Studies conducted at Boeing indicate that fiberglass fail-safe straps should exhibit excellent crack arresting capability due to the high strength of the glass fibers.

E-, D-, and M-glass were immediately eliminated from consideration. The low strength and modulus of E- and D-glass made them noncompetitive, whereas M-glass, which displays excellent strength and modulus, is no longer available. The production of M-glass has been discontinued due to the health hazard imposed by the beryllium in its constituency.

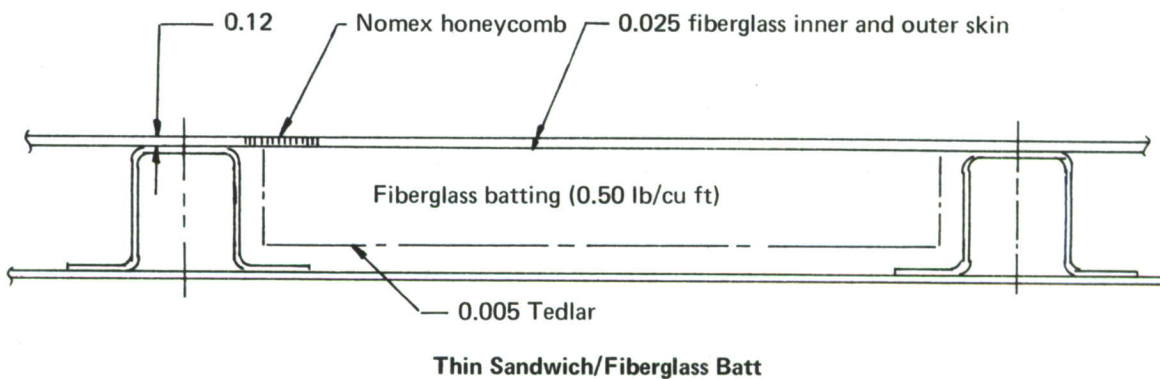
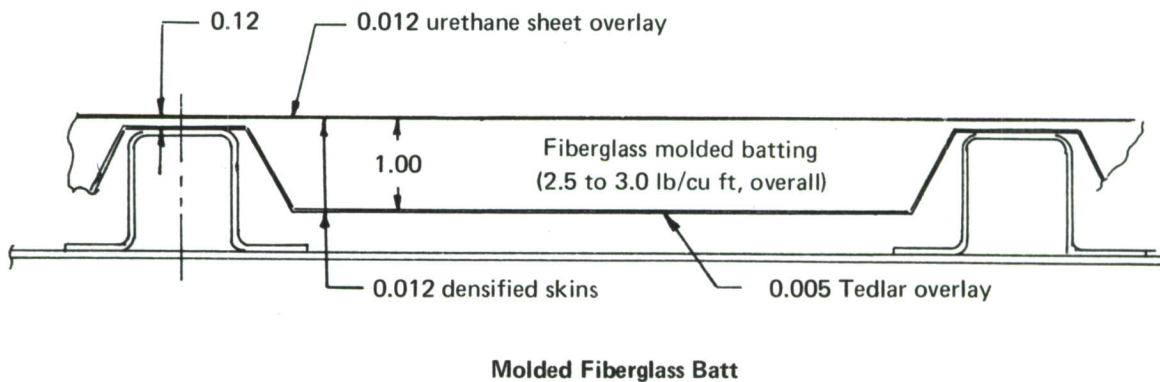
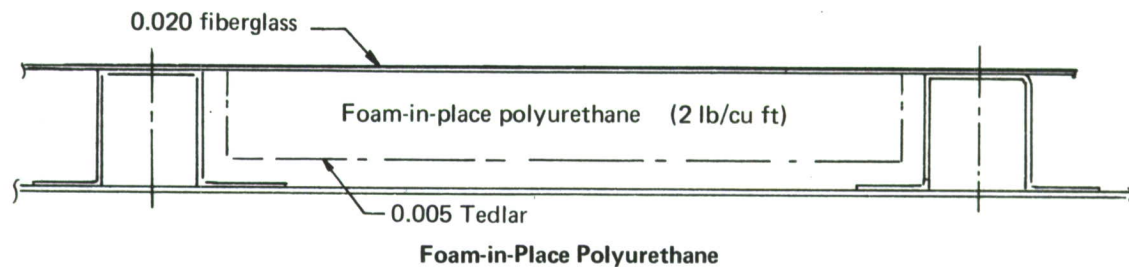
Fail-safe straps fabricated from unidirectional S-glass-reinforced epoxy were considered for this program. Among the available glasses, S-glass exhibits the highest strength and modulus.

Insulation and Aerodynamic Fairing: The externally stiffened shell concept developed during this program utilizes stringer elements bonded to the external surface of the structure. To reduce the surface drag caused by the exposed stringers, an aerodynamic fairing is required, and to reduce the weight penalty associated with this aerodynamic fairing, it is designed to act as a combination fairing and thermal and acoustic insulation.

Three material systems were considered for the aerodynamic fairing.

Foam-in-Place Polyurethane. A low-density polyurethane foam was considered for this application. This low-density ($\rho = 2$ pounds per cubic foot) foam has fair thermal insulation properties; however, it will absorb moisture during freeze-thaw cycling, unless adequately sealed. This foam was considered for use with an outer shell of 0.020-inch fiberglass and an inner vapor barrier of 0.005-inch (fig. 45).

Molded Fiberglass Batt. A low-density ($\rho = 1.5$ pounds per cubic foot), resin-impregnated fiberglass batt with densified skins ($\rho = 30$ pounds per cubic foot) was considered for this application (fig. 45). The fiberglass batt, together with the densified



Note: Dimensions in inches

Figure 45. —Insulation and Aerodynamic Fairing

skins, acts as a sandwich structure to provide sufficient stiffness to support the induced and direct loads on the fairing. To provide moisture resistance, the external densified surface will receive an overlay skin of 0.012-inch urethane sheet and the interior surface will receive a 0.005-inch Tedlar overlay.

Thin Sandwich With Fiberglass Batt. A Nomex core sandwich with 0.025-inch fiberglass faces was considered for use as the fairing. The fiberglass batt with a Tedlar vapor barrier is bonded to the sandwich to provide thermal and acoustic insulation (fig. 45).

b. Material Assessment and Selection

As a result of the continuing assessment of the candidate materials, for each specific application the material which offers the highest potential for weight or cost effective structure was selected. The reasons for the selection of various candidate materials are discussed below.

(1) Metals

All titanium and steel alloys were eliminated from the program, for primary structure, prior to level 2 screening activities since they were shown to be neither cost nor weight competitive with the aluminums. However, use of titanium for a special application, splice plate at body station 1480, is still being considered.

Aluminum alloys which were not eliminated prior to or during level 2 screening were further analyzed to identify the optimum alloy for each application. As an aid in making this identification, a comparative bar graph of the significant properties of the most attractive aluminum alloys was prepared.

The allowables of the surviving materials are shown in figure 46, in terms of anticipated use, where such values have been normalized against those of the baseline materials. This method of display of material characteristics is a valuable aid to material selection since it is known that, depending on the anticipated use, some characteristics may be emphasized at the expense of others. Since only aluminum alloys remain, and their densities are relatively equal, direct comparisons of the listed quantities are indicative of the potential for weight savings offered by use of the advanced materials.

The properties selected for this comparison are:

- Static, F_{tu}
- Fatigue, fatigue quality rating (FQR) material constant
- Fracture, K_c or K_{Ic}

The ultimate tensile strength, F_{tu} , is felt to adequately express the static capability of a material since most other design static properties are proportional to this value.

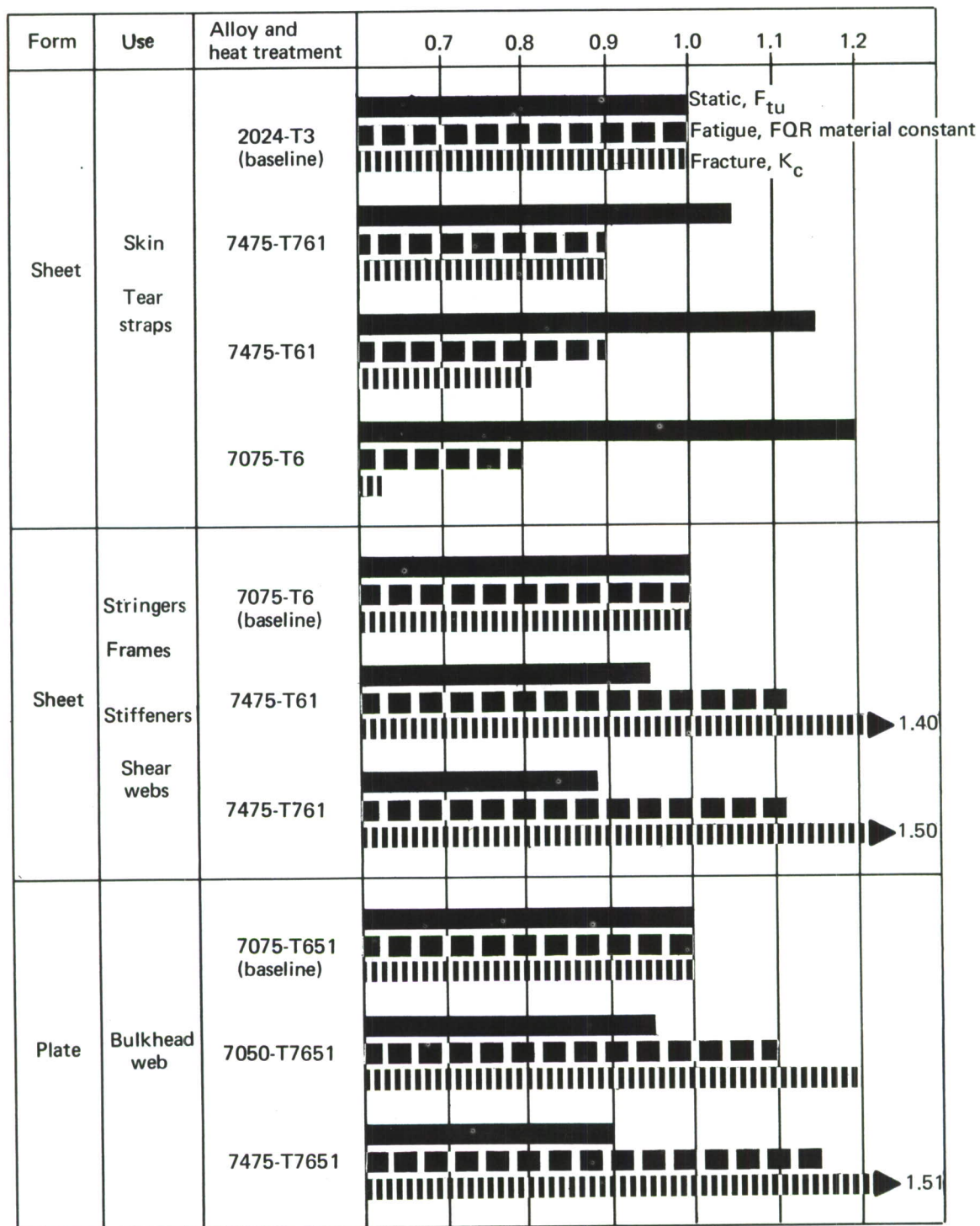


Figure 46. —Advanced Cargo Fuselage Material Normalized Properties

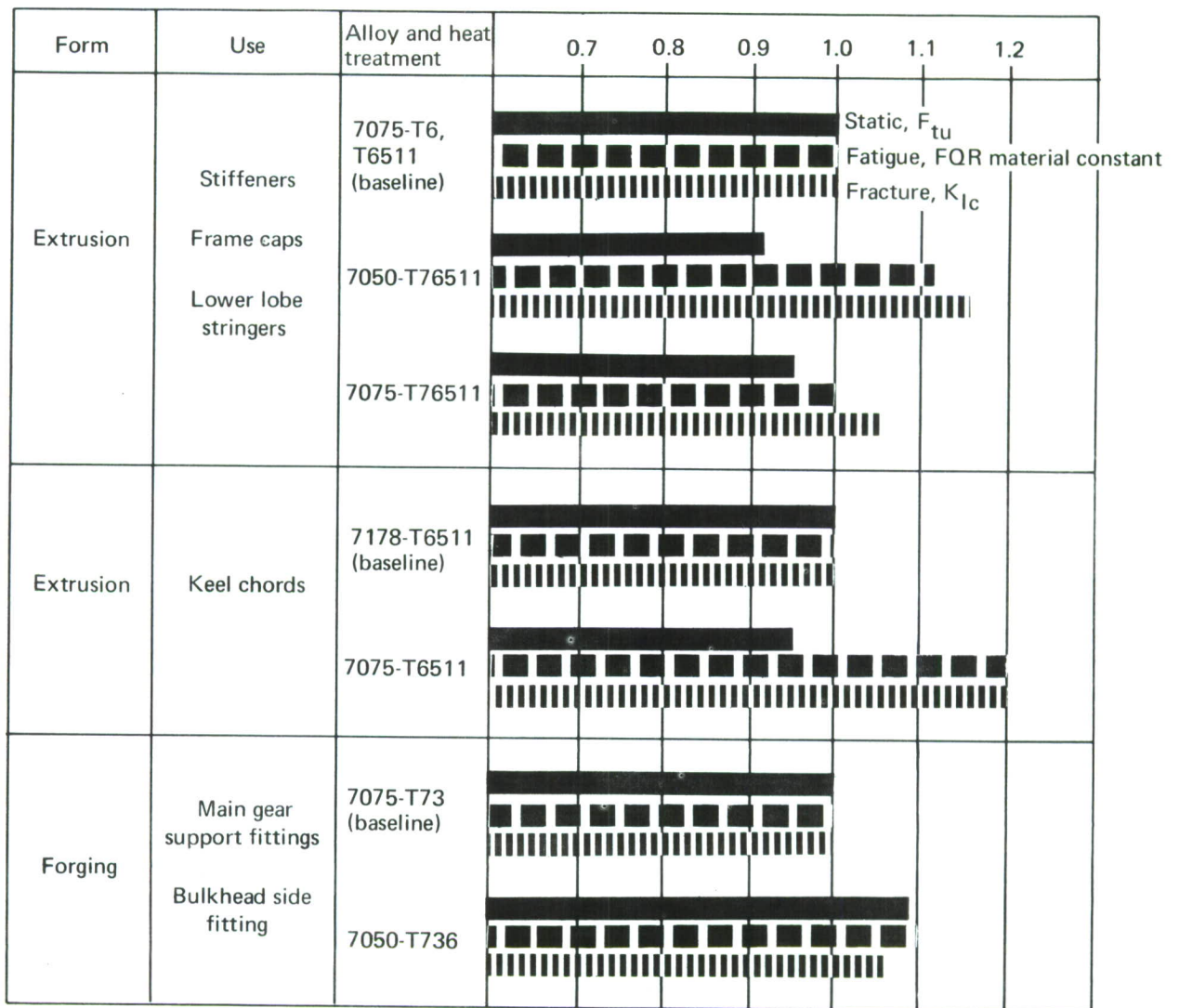


Figure 46.—Concluded

The FQR material constant is an expression of the capability of a material to withstand fatigue loading prior to crack initiation. For comparison, the FQR material constant is evaluated from simple notched-specimen fatigue testing at $K_t = 3.0$.

The critical stress intensity, K_{IC} or K_{IC} , is chosen to reflect fracture properties. These critical stress intensity factors are a direct measure of the residual strength capability of a material, and crack growth rates are roughly proportional to the critical stress intensity. While fracture properties in an aggressive environment are not necessarily proportional to the critical stress intensity factor, it is felt that the characterization of fracture properties by this parameter is adequate for the intended purpose.

Aluminum Alloys Selected for Use: Only certain of the aluminum alloys, plus one titanium alloy, remain for consideration on this program. Comments supporting their retention are given below.

7475-T761 sheet was selected for use as the monocoque covering material on all concepts, with the exception of local areas of the sandwich shell. As a result of testing conducted on this program, and from data presented in the literature, the transverse fracture properties and the fatigue properties of 7475-T761 have been assessed as equal to those of 2024-T3. In view of the superior static values of this material, it has been selected for use on the monocoque skins and formed stringers.

7475-T61 sheet was selected for use as the face sheets of the honeycomb fuselage shell in the crown and lower lobe (refer to sec. IV-3b3). Due to the enhanced fracture characteristics of sandwich face sheets stabilized by honeycomb core, the improved static properties of this heat treatment of the 7475 alloy may be used efficiently.

7475-T76151 plate was selected for use on the body station 1480 bulkhead pressure web. Test data received on the AMS-ADP data interchange program reinforce the indications, obtained from previously published fracture properties, that this material exhibits fracture properties approximately equal to those of the 2024-T351 plate used on the baseline. While the 2024-T351 exhibits a slightly slower fatigue crack growth rate at low ΔK levels, $\Delta K \leq 20 \text{ ksi}\sqrt{\text{in.}}$, studies conducted on this program indicate that the use of 7475-T76151 plate results in adequate life to satisfy the design requirements.

7075-T6511 extrusions were selected for use on lower lobe stringers of the internally and externally stiffened shells. This material will also be used for frame caps and for those web stiffeners which are to be fabricated from extrusions. Although this material exhibits lower stress corrosion properties than the more recently developed 7050-T76511 or the 7075-T76511, the enhanced static properties make its use attractive. The baseline structure presently uses this material for lower lobe stringers, loaded primarily in compression, and no service problems have been experienced to date. This material is used in airplanes such as the 707-120, 720, and 707-320 for wing lower surface stringers, and no service problems have been experienced to date.

This alloy has been selected to replace the baseline 7178-T6511 for use on keel beam chords. The 7075-T6511 exhibits a 5% lower compressive yield stress than the baseline; however, the baseline keel beam chords exhibit sufficient margin of safety to

permit the direct substitution of this material. The improved fracture properties and resistance to stress corrosion of 7075 makes this substitution desirable.

7050-T736 has been selected for use on all forgings. This material provides the best compromise of high static properties with good K_C and K_{IC} . The threshold stress for stress corrosion is superior to that exhibited by the baseline 7075-T73 material, with improved static properties.

7075-T6 sheet has been selected for use on formed frames, shear webs, and web stiffeners. The baseline makes extensive use of this material, and service experience has proven its suitability for these applications. None of the alternate materials investigated show potential for significant weight savings in these applications over the baseline 7075-T6 due to the low damage tolerance requirements imposed on these parts.

Titanium Alloy Selected for Use: Ti-6Al-4V sheet, in the ELI composition with the Boeing-developed special processing control, will remain under consideration for tear straps on the externally stiffened shell concept. The improved specific strength, F_{tu}/ρ , offered by this material over that afforded by the aluminums offers a potential for improved weight efficiency.

Ti-6Al-4V plate, in the ELI composition and special processing, has been selected for use on the outer splice plate to effect the upper-to-side-quadrant splice at body station 1480 of the honeycomb sandwich configuration. The increased static properties of this material, when compared with aluminum, minimize the thickness of the outer splice plate, hence reducing the projection out of contour.

(2) Nonmetals

The nonmetallic material candidates discussed in section IV-2a have been assessed for application to the program. The selection of those materials which exhibit the greatest potential, in terms of cost or weight effectiveness, has been made and the rationale for each selection follows.

Advanced Composites: The advanced composite has been selected for use on alternate concepts for the floor beams and keel chords (sec. IV-3b4). Although the primary concepts proposed for fabrication of these elements utilize bonded or mechanically fastened all-metal components, unidirectional reinforcement of the floor beam and keel beam chords will continue to be evaluated through phase IB.

Fiberglass: The use of unidirectional fiberglass tear straps for the externally stiffened shell concept will continue to be studied. Damage-tolerance trade studies conducted on the externally stiffened shell have indicated an increase in structural efficiency (higher hoop stresses) with 10-inch tear strap spacing. Fiberglass appears attractive for this application.

The consideration of unidirectional fiberglass for tear straps on the honeycomb shell and the internally stiffened shell has been dropped.

Insulation and Aerodynamic Fairing: The insulation and aerodynamic fairing for the externally stiffened shell concept will be fabricated from either molded fiberglass batt or thin sandwich with fiberglass batt. Studies will continue on these fairing candidates to determine the most weight- and cost-effective system.

The foam-in-place fairing has been dropped from further consideration on this program. This material has a lower thermal insulation efficiency than the other two systems considered, and the anticipated difficulties in accomplishing an effective seal against water absorption disqualified it as a candidate material.

(3) Honeycomb Core

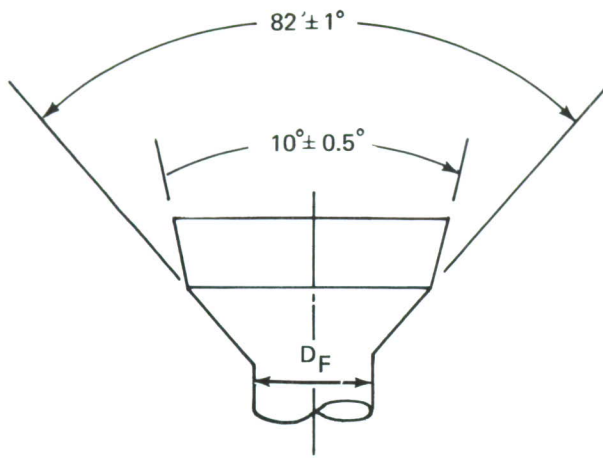
Aluminum alloy 5056 honeycomb core has been selected for the honeycomb shell concept. Structural configurations employing honeycomb sandwich construction are designed to minimize core shear due to primary load transfer. However, secondary shear loading is frequently induced in the core due to eccentric load conditions, and the higher strength aluminum alloy 5056 honeycomb core is preferable to alloy 5052 core in this application.

(4) Fasteners

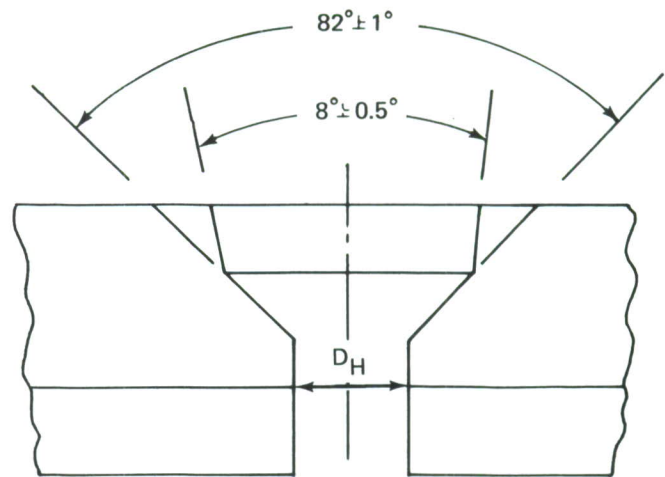
The primary joining process used on the advanced concepts is adhesive bonding; however, mechanical fastening will be used for assembly splices and manufacturing joints. Generally, mechanically fastened joints exhibit poorer fatigue performance than bonded joints. The elevated temperature and tight tolerances required to produce a satisfactory bonded joint make this process impractical for production line assembly. Fastening used in these assemblies must be carefully selected and installed to provide joint fatigue capability sufficient to attain life goals.

Design of fatigue-rated, mechanically fastened joints will be per Boeing fatigue design methodology, and static design allowables will be per MIL-HDBK-5, or as established by tests. Installation of mechanical fasteners selected for use on this program will be controlled by Boeing process specifications.

Rivets: The 2000-series aluminum alloy solid rivets are considered for this program based on static strength, ease of installation, joint fatigue performance, and cost. Four basic configurations were considered, consisting of standard 100° countersink head, protruding head, reduced 100° countersink head, and "index" head. The index head (fig. 47) rivet is a Boeing development with a head configuration matching the 82°-30° modified NACA countersink used for improved fatigue performance. This rivet configuration, when installed by automatic riveting machines, exhibits good fatigue performance. BAC R15BA and BAC R15RB (same as MS 20470 and MS 20426 except for closer dimensional tolerance controls) rivets were considered for use in both drilled holes and cold-worked holes. BAC R15CE (reduced 100° shear head) aluminum alloy 2017 and 2024 rivets will be used in thin sheet gages to minimize knife edge conditions and to provide better joint fatigue performance. The above rivet usage criteria are standard practice at Boeing and have proven adequate and reliable both in laboratory testing and airplane fleet performance.



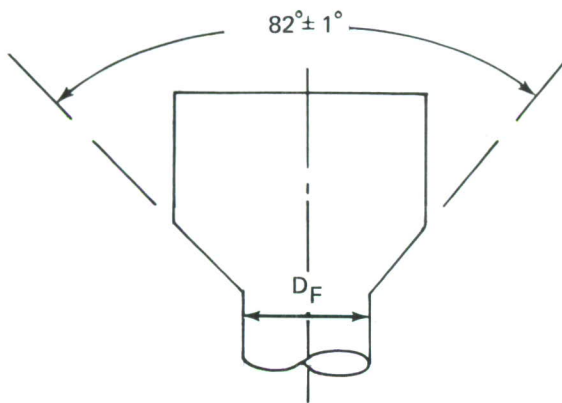
Fastener



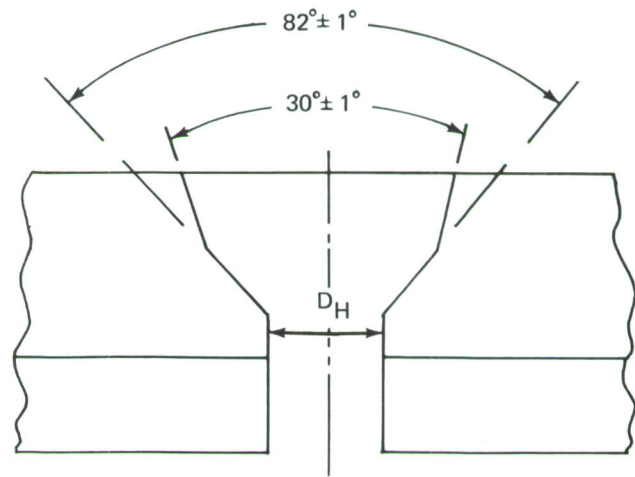
Hole

Note: $D_F = D_H + 0.0060 + 0.0025$

Wedge-Head Fastening System



Rivet



Hole

Index-Head Rivet System

Note: $D_H > D_F$

Figure 47. –Fastener Head Configurations

Bolts: For structural applications where the load transfer and clamp-up capability or accessibility considerations ruled out the use of driven rivets, threaded mechanical fasteners of the Hi-Lok type were used on the baseline. As a weight savings measure, titanium Hi-Loks were used in preference to steel Hi-Loks.

For the advanced cargo fuselage, alloy steel threaded fasteners were selected as preferable to titanium fasteners on a cost-effectiveness basis. Hi-Lok and lockbolt-type fasteners were considered over standard threaded bolts and nuts because of lower manufacturing installation costs, lower weight, better fastener-hole fit potential, and more consistent preload control. Cadmium-plated 95-ksi shear alloy steel and anodized 7075-T6 aluminum alloy fasteners were considered over other available material-finish combinations for one or more of the following reasons: (1) lower cost, (2) lower weight (aluminum fasteners), (3) better galvanic corrosion compatibility with structural materials, (4) Boeing testing and operating fleet experience, and (5) availability. Steel fasteners were considered for use where static loads and clamp-up requirements were greater than those which could be provided by aluminum fasteners. Aluminum Hi-Loks and lockbolts were considered for use where installation conditions, clamp-up, load requirements, or installation accessibility considerations eliminated solid driven rivets.

For applications requiring superior fatigue performance, close-tolerance lockbolts and Hi-Loks will be installed in the Boeing-developed high interference cold-worked holes. This hole preparation consists of cold working the material surrounding the hole by pulling a mandrel through a split sleeve placed in a starter hole (fig. 48). After cold expansion is complete, the hole is broached or reamed to final size. Tests conducted at Boeing and WPAFB (ref. 12) demonstrate the superior fatigue resistance provided by this method of hole preparation.

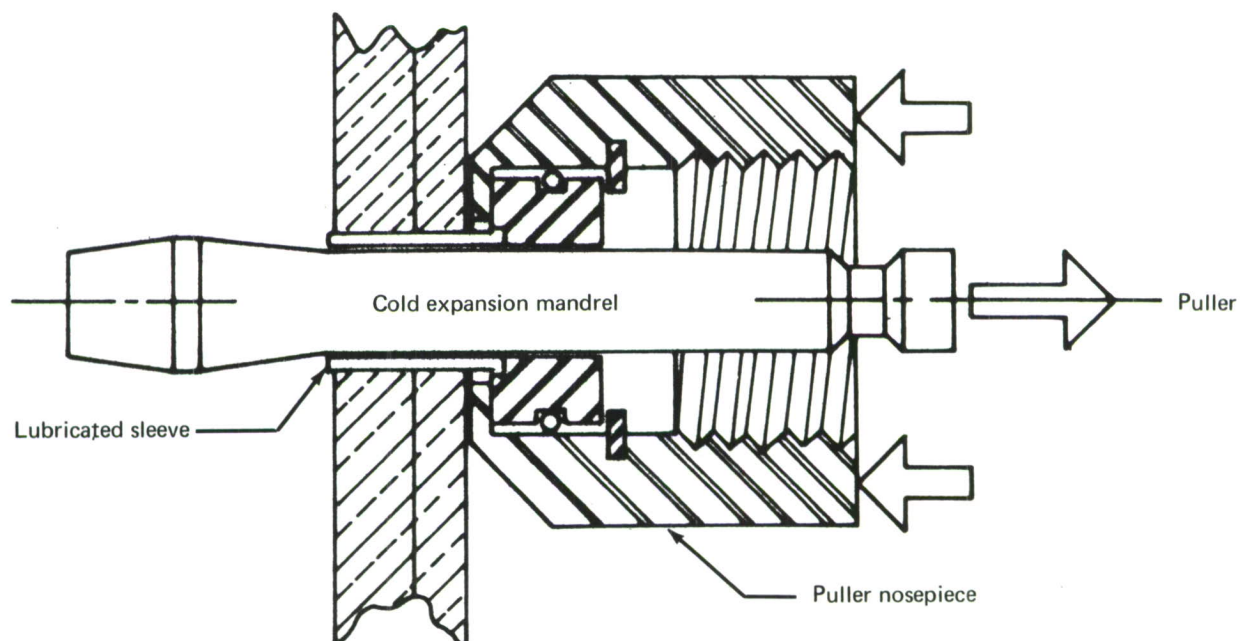


Figure 48. —Split-Sleeve Cold Expansion Process

For applications requiring a moderate increase in joint fatigue capability over that afforded by lockbolts or Hi-Loks in transition fit holes, the Boeing-developed “wedge head” lockbolt will be considered. The significant feature of this fastening system is in the controlled shank and countersink head interference (fig. 47).

c. Processes

Materials and processes for the fuselage component have been selected on the basis of structural efficiency, reliability, and cost effectiveness. Adhesive bonding has been selected as the primary joining process, and organic finishing for environmental protection.

(1) Adhesive Bonding

Adhesive bonding, because of its improved fatigue performance, has been selected over mechanical fastening as the primary joining method. Total elimination of mechanical fastening was not practical; however, the number of fasteners required has been greatly reduced. All structural bonding on the cargo fuselage program is considered to be primary structural bonding, which requires a high confidence in the ability of the bonding process to produce a strong, durable, and reliable joint. To achieve this high level of confidence, attention must be directed to the materials and processes used to effect the bond.

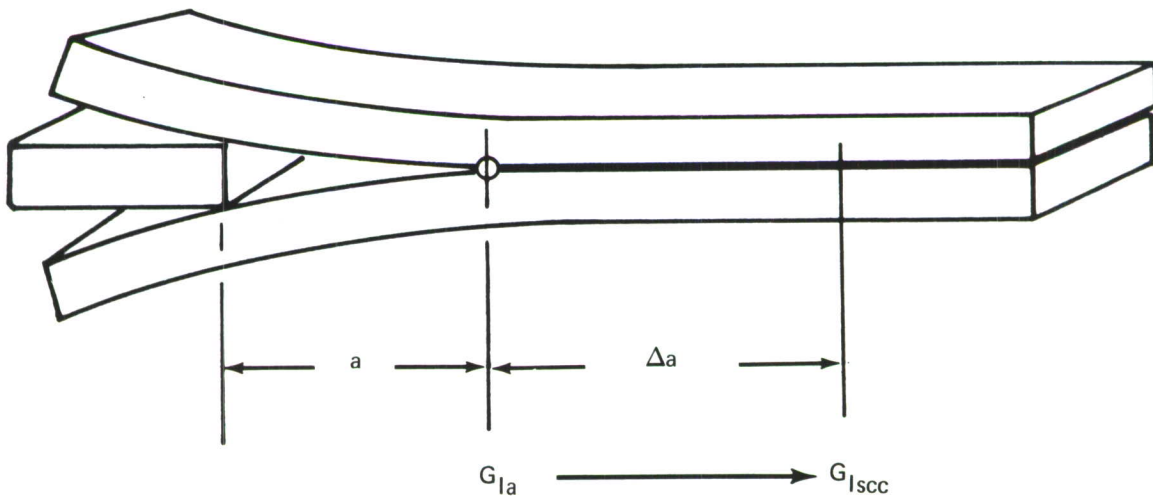
Bonded joints produced by traditional processes with traditional methods of process control have not exhibited consistently satisfactory structural durability under service conditions. In an effort to improve structural bonding, Boeing examined in-service failures and determined that a majority of bond failures were interfacial. The interfacial failure mode is characterized by:

- A free surface initiation site
- Progressive growth under low stresses

To preclude the possibility of interfacial failures in bonded joints, improved processing and process control testing techniques have been developed.

Process Control Testing: Traditional environmental exposure tests do not duplicate service experience, since they measure residual strength after unstressed exposure. Therefore, new test methods have been developed by Boeing. Developed under a Boeing in-house IR&D program, these methods correlate well with service experience by duplicating the characteristics of interfacial failure. They have been used both to control current processing and as an aid to developing new technology adhesives and processes.

- Lap shear specimens tested under sustained load while subject to temperature and humidity environmental conditions can be used to identify variations in the durability of surface preparations and adhesive systems as well as to establish environmental effects in bonded joint allowables.
- The double cantilever beam (DCB) specimen (fig. 49) tested under similar environmental conditions has been shown to be more sensitive to small variations in surface preparation and adhesive systems than the lap shear specimens. It offers a sensitive method of screening new bonding processes and can be used also for shop in-process control testing.



- Measures ability of bond system to contain a defect
- Duplicates interfacial service failures
- Is easily fabricated and exposed to environments
- Yields quantitative and qualitative data

Figure 49.—Double Cantilever Beam (DCB) Test Specimen Configuration

Surface Preparation: Surface preparation is one of the primary keys to reliable bonding, as all service failures have occurred at the adhesive/adherend interface. This type of failure occurs when moisture reaches the oxide layer at the adhesive/oxide interface by diffusion through the adhesive. A weak hydrated oxide layer forms in contact with the moisture, and the oxide then fails under stress and forms a crevice between the oxide and the adhesive. Corrosion takes place within this cavity, further accelerating the delamination and corroding the metal (see fig. 50).

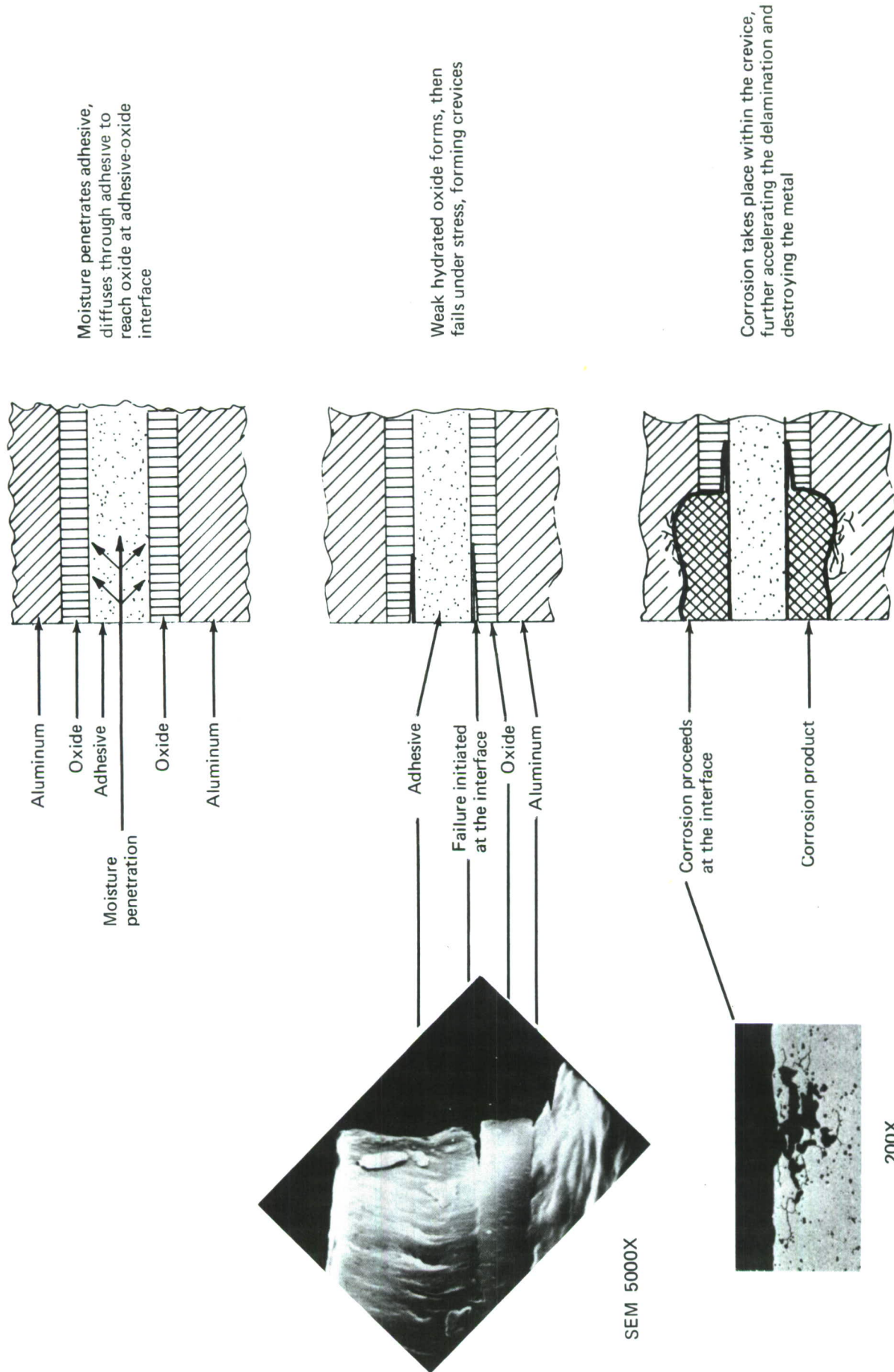


Figure 50.—Mechanism of Bond Delamination and Corrosion

Current industry standards and controls are incapable of consistently producing high-durability bonded primary structure. Bonded primary structure can be produced by Boeing using the new technology adhesives and processes with the DCB test method for production control.

FPL Etch, a sodium dichromate-sulfuric acid deoxidizer, will be considered as a surface treatment. This solution is an industry standard and is capable of producing good bonds when properly applied; however, stringent control of time, temperature, contamination, and solution is required.

Anodic surface preparation will be considered as an alternative for use on this program. This new surface treatment reliably produces stable surfaces, resulting in high-durability bonds. Tests conducted on DCB specimens have demonstrated the ability of this process to consistently produce more environmentally stable bonds than the FPL etch (see fig. 51). This figure shows the superior environmental stability of adhesive bonds on anodic surfaces. Metallurgical considerations indicate that anodic preparation of the advanced alloy 7475 in the bare condition should produce bonds with environmental stability approximately midway between that obtained on 2024 bare and 7075 clad material. The anodic surface preparation is controlled by an established Boeing process specification.

Primer: Corrosion inhibiting adhesive primer (CIAP) BR 127 will be used on bonding surfaces. This material has proven more effective in long-term environmental resistance than other standard adhesive primers. Although it was developed primarily for adhesive bonding, its superior corrosion-inhibiting properties make it an outstanding finish candidate. It is compatible with other advanced finishes, and service experience accumulated on present production models (inner surface of monocoque skins protected by CIAP finish) has proven its reliability.

Adhesives: Epoxy adhesives are being considered for use on this program. They are characterized by good strength and excellent resistance to solvent attack. Table XIV shows the important properties of the epoxy adhesives considered for this program.

AF 126, a 250°F curing modified epoxy, is widely used at present and exhibits good in-service performance in secondary structure.

EA 9628, a 250°F curing modified epoxy, is a new-generation adhesive which is qualified to Boeing material specifications and for which preliminary design allowables have been developed. The EA 9628 has greater defect containment capability and environmental stability than the AF 126 system. Using this material, existing facilities are capable of producing hardware with no major change or equipment purchase.

EC 3700, a powder adhesive, is also being considered. Its properties are similar to those of EA 9628, and it has higher toughness and greater environmental stability. Manufacturing processes require additional development for its application. At present, use of EC 3700 is limited to a critical electrostatic spray process. This material is qualified to a Boeing specification, and preliminary design allowables have been developed.

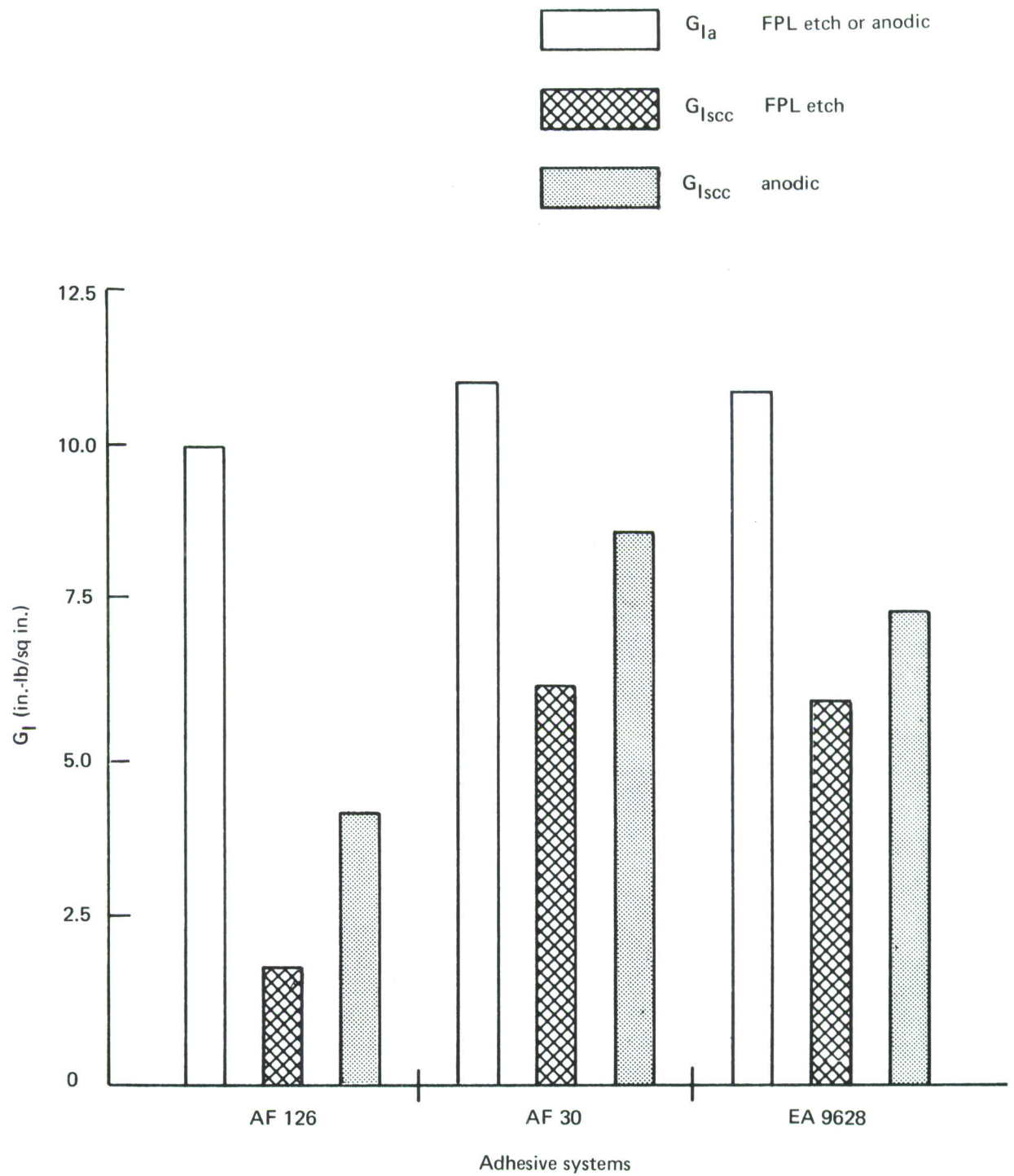


Figure 51.—Surface Preparation Effect on Strain Energy Release Rates

Table XIV.—Adhesive Bonding Materials

Choice: Hysol EA 9628, 250°F cure modified epoxy

Rationale: Qualified new generation adhesive

Possible alternates: 3M Company's EC 3700

Properties comparisons:

Adhesive	Metal-to-metal climbing drum peel—minimum individual (in.-lb/in.)	Shear minimum individual (psi)	Initial arrest, G_{Ia} (in.-lb/sq in.)	Exposure at 140° F, 100% RH	
				14-week exposure FPL etch 2024 bare G_{Isc} (in.-lb/sq in.)	16-week exposure BAC 5555 7075 clad G_{Isc} (in.-lb/sq in.)
3M Company (AF 126 BMS 5-51)	45	4000	10.0	1.1	1.9
Hysol (EA 9628)	46	4560	10.0	3.3	5.2
3M Company (EC 3700)	84	5050	13.4	—	6.6

Status: One source, Boeing material specification, preliminary design allowables

(2) Finishes

Finishes considered for use on this program were selected for their corrosion resistance properties. Cladding, plating, and organic finishing were considered. Due to the superior corrosion resistance properties of the organic finishes, and for manufacturing reasons and considerations of structural effectivity, cladding and plating have been eliminated as primary means of corrosion protection.

All structural elements were analyzed to determine both the service exposure anticipated and the degree of protection required to provide adequate corrosion resistance. The protective finish was then determined in context with the manufacturing processes used on that part. The areas determined to require prime corrosive protection are:

- Fuselage shell, skin, stringers, and frames, both exterior and interior surfaces
- Dissimilar metals contact areas, i.e., steel or titanium fasteners in aluminum structure

Fuselage Shell: The advanced concepts developed on this program utilize adhesive bonding as the primary means of structural joining. Adhesive bonding requires that certain manufacturing processes be performed, which in themselves provide a degree of corrosion protection and which, when combined with organic finishing, provide corrosion protection superior to that of clad skins, a current industry standard. The protective finish system selected for use on this program is shown in figure 52.

All surfaces will require an anodic surface treatment (sec. IV-3c1). In addition, all surfaces will receive a coat of CIAP primer. This primer (CIAP BR127), which is covered by a Boeing specification, exhibits long-term environmental resistance superior to that of standard adhesive primers. An additional advantage is that in field repair, a simple MEK (methyl-ethyl-ketone) wipe applied to the CIAP surface provides a suitable bonding surface.

Bond faying surfaces will receive the bonding adhesive (sec. IV-2c1). External surfaces will receive a coat of polyurethane compatible epoxy primer which will be overcoated with a permanently flexible polyurethane enamel. This combination of primer and enamel provides a superior degree of corrosion protection. The primers considered are De Soto Inc. 513-713 or Finch Paint and Chemical Co. 463-6-3. The enamels considered are Catillac or Super Chloropon. The primers and enamels are covered by Boeing specifications.

Fasteners: Cadmium-plated, corrosion-resistant steel or titanium fasteners will be used in lieu of low-alloy steel fasteners. The fasteners themselves exhibit satisfactory corrosion resistance; however, for dissimilar metals applications cadmium plating is required to provide galvanic protection.

All fasteners installed in honeycomb core areas of sandwich panels will be installed with a synthetic rubber sealant containing corrosion-inhibiting chromates.

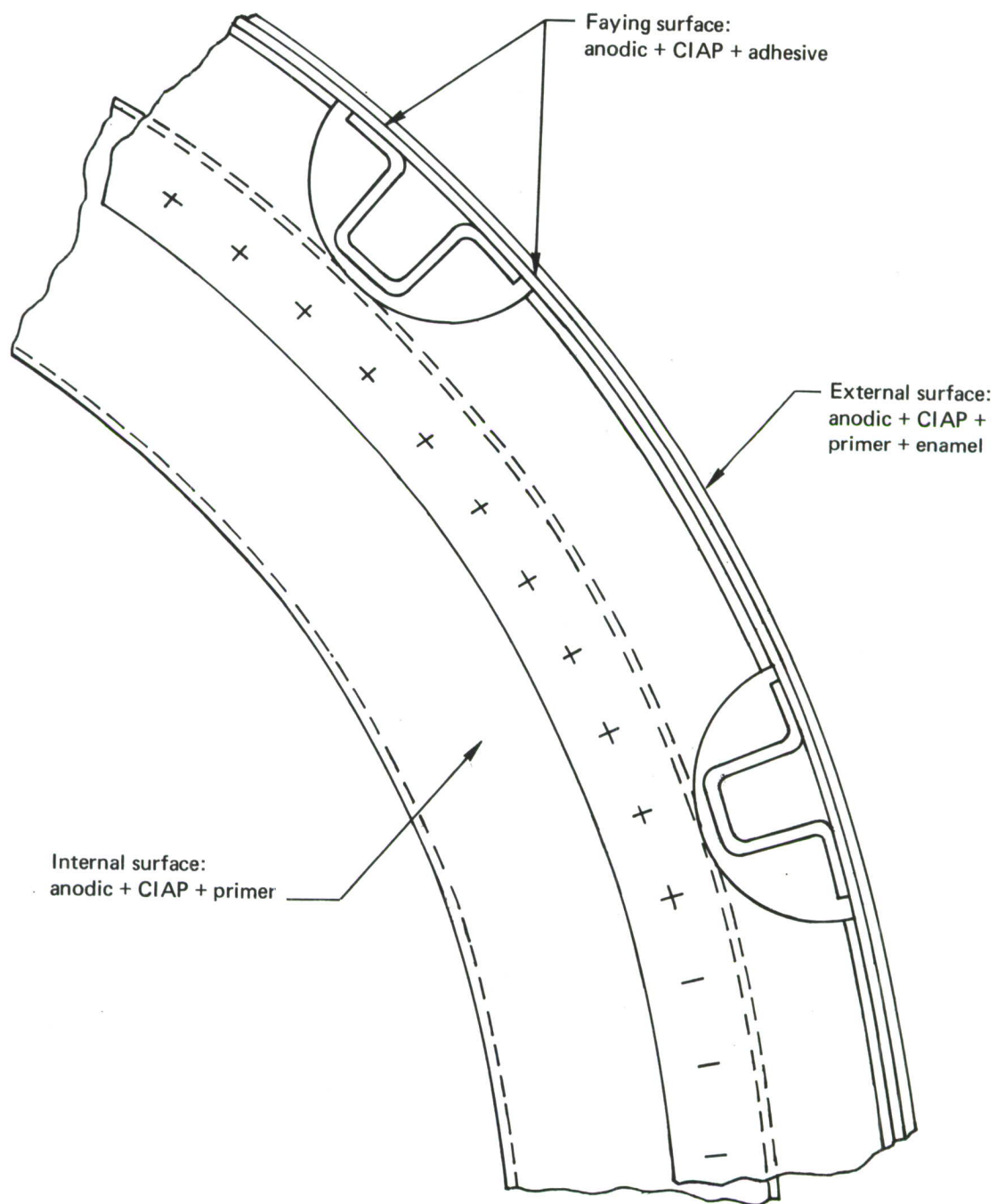


Figure 52. -Protective Finish System

3. DESIGN

a. Preliminary Design Approach

To maintain fatigue life and reduce structural weight, the design effort was concentrated on improvement in material utilization, both improved distribution and geometric variations, improvement in fatigue quality of design details, and use of advanced materials with improved properties.

For those areas designed by tension loads, the effort was centered on improving fatigue quality of details and material properties. In the case of shear and compression designed structure, variations in local element geometry were considered in order to increase allowables. The use of new materials with improved material allowables was also considered.

The major factors that affect the costs of new concept designs are the manufacturing, processing, and quality assurance requirements. Inputs from these three areas were continuously considered during the new concept design development and evaluation.

During this preliminary design study, a study approach was adopted to identify and concentrate major effort on those structural components that offered the highest potential for fulfilling the study goals. The shell and its associated frames account for 72% of the baseline section weight; thus, this portion of the structure received most of the design effort.

The following list contains the main sources of weight and cost improvement that were considered continuously during the development of new structural concepts.

- Weight reduction
 - Removal of fatigue-imposed ultimate allowable constraint (detail improvement)
 - Increased element allowables (geometry improvement)
 - Increased material allowables (material improvement)
- Cost reduction
 - Reduction in part count
 - Reduction in number of mechanical fasteners
 - Reduction in assembly time

The geometry improvement effort concentrated on improving the panel compression end load capability by increasing the effectiveness of the skin. Closer stringer spacing, changing stringer geometry to increase the number of flanges attached to the skin, and using

honeycomb to stabilize the skin are example methods of accomplishing this. The use of adhesive bonding instead of riveting eliminates the rivet hole-out; this improves fatigue quality. Improvement in the fatigue quality allows use of higher strength materials. The end result is weight reduction because the total amount of material required for static strength, fatigue life, and damage tolerance is reduced.

The following study ground rules were established for all new concept designs so that a rational comparison of weight, cost, and fatigue life could be made with the baseline section. Trade studies were not made on these items, except as noted.

- All external contours and key component geometry were maintained. The external shape of this section of the fuselage is not fully circular. Since it acts structurally as a pressure vessel, a circular section would be optimum. However, weight savings effected by changing the shape from noncircular to circular were not evaluated.
- Inside frame contours were maintained. The total shell and frame depth was not allowed to violate the internal usable volume of the baseline. Since both frame stiffness and bending stress level are a function of depth, increasing the frame depth might show weight savings that would be misleading.
- Floor beam depth was maintained. Again, depth is the significant factor in strength and stiffness. Depth is constrained by maintaining main deck and belly cargo volume.
- Frame spacing/shell stability weight trades were not included in this study. Shell weight trades have been made by NASA and USAF studies in the past. Further detailed trade studies in this area would not contribute significantly to this concept development program. Some frame spacing changes have been made where local detail design improvement contributes to improved life, reduced weight, or lower cost.
- Floor panel designs were not included in the trade studies. Floor panel design is a whole study field of its own, with the most promising weight reductions being in the field of advanced filamentary composite designs.
- Wing/body fairing and fairing support structure were maintained. This structure is a fiberglass, aerodynamic fairing that does not contribute to the structural strength of the study section.
- Location of all external attaching structure was maintained. Trades considering relocation of the landing gear, landing gear doors, wing/body fairing, etc., are not considered to be within the scope of this program.
- The size of the door cutout and the plug door structure were not included in weight/design trades. The doublers around the door cutout are part of the shell and were evaluated.

- Window size was maintained. Making the window smaller or changing its shape would obviously affect local structural weight, but this type of trade is not within the intent of this program.

The certification loads, fatigue spectrum, and basic design criteria for the 747-100 airplane were used throughout the study so that a one-to-one relationship could be maintained between the study concepts and the baseline. The basic design criteria were modified to be in agreement with the requirements of:

- MIL-STD-1530 (USAF)
- USAF Damage Tolerance Criteria, Revision D, 18 August 1972 (app. I)

b. Structural Concept Development

Concept development and evaluation was planned as a three-level operation. Level 1 was a preliminary evaluation of numerous concepts. Level 2 was a more detailed design of the most promising concepts. Level 3 was further detail design and selection of the three best candidate concepts for development and evaluation during the follow-on program.

(1) Level 1 Concept Studies



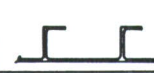
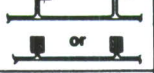


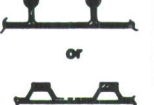
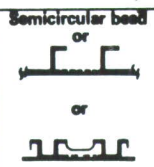














The major level 1 configuration development and screening effort was concentrated on the shell and associated frame concepts since they account for the greatest percentage of the baseline study section weight.

The first step in the level 1 concept evolution was formation of the “brainstorm list,” which considered all types of structural concepts, methods of construction, and types of materials. (See table XV.) The brainstorm list was reduced to 13 different basic shell concepts made from either aluminum or titanium, as applicable, and composite reinforced where applicable. (See table XVI.) Steel was eliminated early as a shell material because of the very thin gages that would be required to be weight competitive with the baseline. Very thin shell gages are subject to crippling at low stress levels and are easily damaged in service unless backed by honeycomb.

All brazed configurations were eliminated due to the inherent high cost of such construction, which could not be justified. The load intensities are relatively low, and there is no environmental requirement for brazed titanium or steel structure. Diffusion-bonded titanium was also eliminated for the same reasons and particularly because this type of construction is too costly.

The Structures Design group produced concept sketches of the 13 selected concepts for level 1 reviews (see figs. 53 through 72). The sketches were reviewed by a team composed of personnel from Structures Design, Stress, Fatigue/Fracture Mechanics, Materials Technology, Weights, and Manufacturing Research. Evaluation sheets for each concept were made by all review team members. These comments and recommendations were then reviewed. The most promising configurations, considering structural efficiency (strength, fail safety, and fatigue life versus weight), cost, and manufacturability, were selected for more detailed evaluation during the level 2 phase.

Table XVI.—Design Concepts, Level 1 Study List

Concept	No.	All metal	Material		No.	Composite reinforced	Material	
			Al	Ti			Al	Ti
Skin/scr	Bonded	1-1		✓ ?			✓ ?	
	Integrally stiffened	1-2		Welded or diffusion bonded Z210			✓ ?	
	Wide spaced longerons	1-3		✓				
Laminations	Beaded (continuous at frame)	1-4		✓ -			✓ -	
	Punched (discontinuous at frame)	1-5		✓ -			-	-
	Int. stiffened	1-6		✓ ✓			✓ ✓	
	Composite sandwich	1-7					✓ ✓	
Honeycomb	Stiffened honeycomb	1-8		✓ ✓			✓ ✓	
		1-9		✓ ✓			✓ ✓	
							✓ ✓	
	Sandwich honeycomb	1-10		✓ ✓			✓ ✓	
		1-11		✓ ✓			✓ ✓	
	External stringers	1-12		✓				
	Barrel body 60-in. frame	1-13		✓				

Summary

- 13 Shell concepts
- 2 Materials
Aluminum and titanium
- 3 Methods of assembly
Riveted
Bonded
Welded
- Variations in concepts
Geometric
Composite reinforced
- Sketches made for each concept

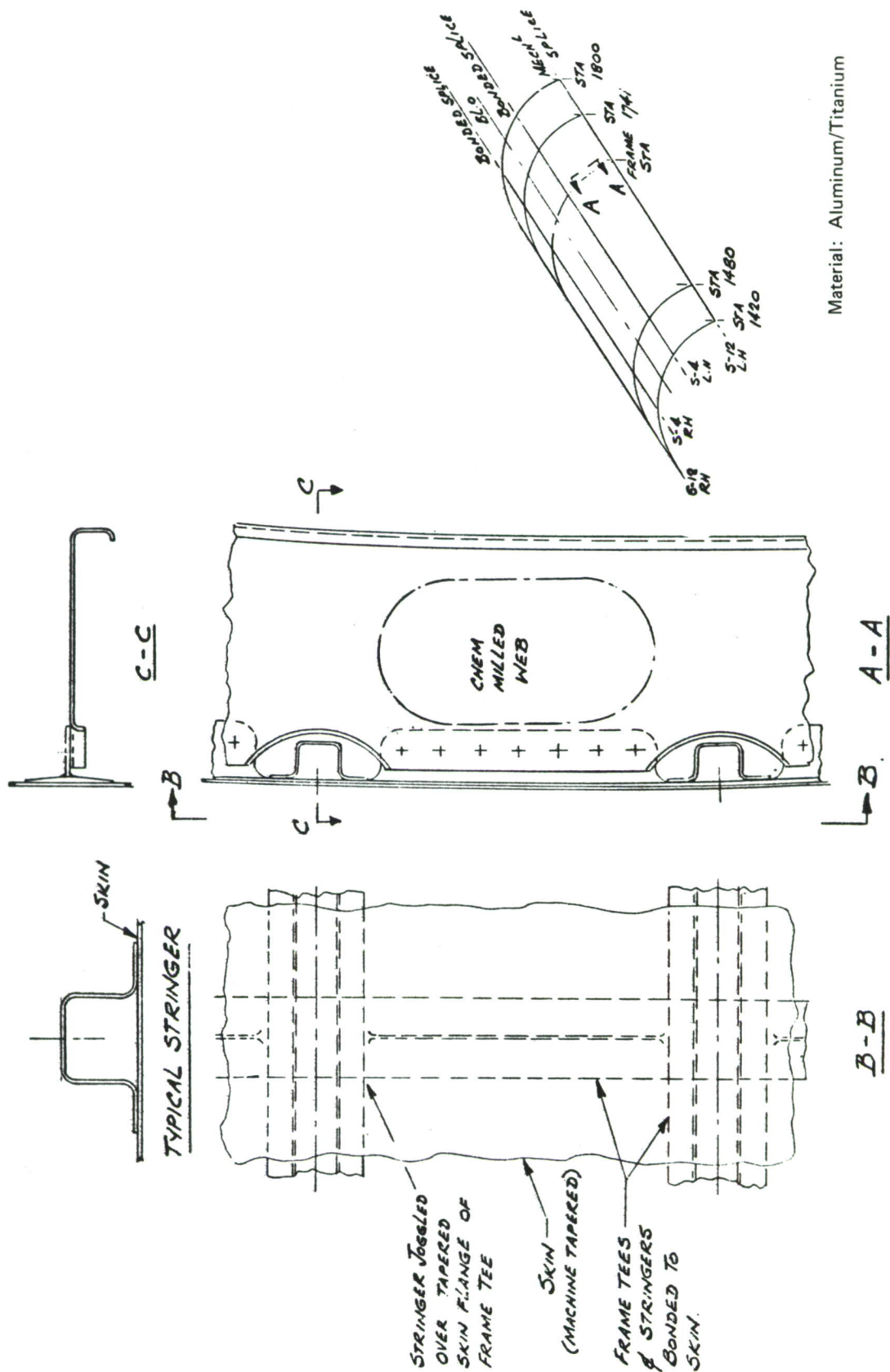


Figure 53. --Shell-Skin/Stringer Bonded (Concept 1-1)

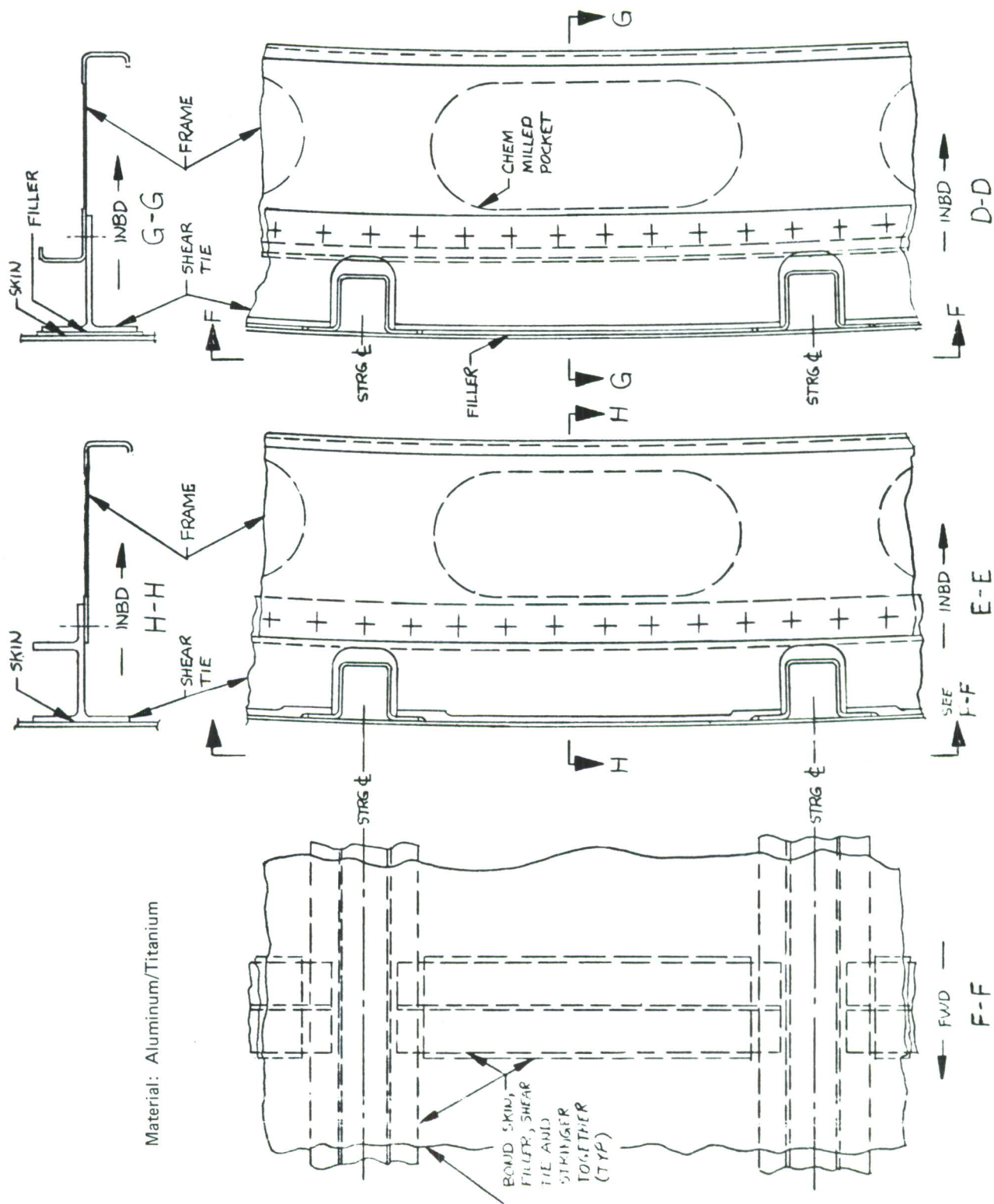


Figure 54. —Shell—Skin/Stringer Bonded, Alternate Frame Outer Chord (Concept 1-1)



The drawing consists of two views of a structural component. The top view is a plan view showing a rectangular section with a central longitudinal slot. The slot is defined by dashed lines and has a waffled (corrugated) interior surface. The outer edges of the section are also waffled. A label 'WAFFLED DOUBLER' with an arrow points to the waffled outer edge on the left. Section lines 'K-K' and 'J-J' are indicated with arrows. The bottom view is a cross-section 'K-K' showing the profile of the waffled doubler. It features a central longitudinal slot with a waffled interior. The outer edges are waffled. A label 'WAFFLED DOUBLER' with an arrow points to the waffled outer edge on the left. Section lines 'K-K' and 'J-J' are indicated with arrows.

Figure 55.—Shell—Skin/Stringer Bonded, Waffled Doubler (Concept 1-1)

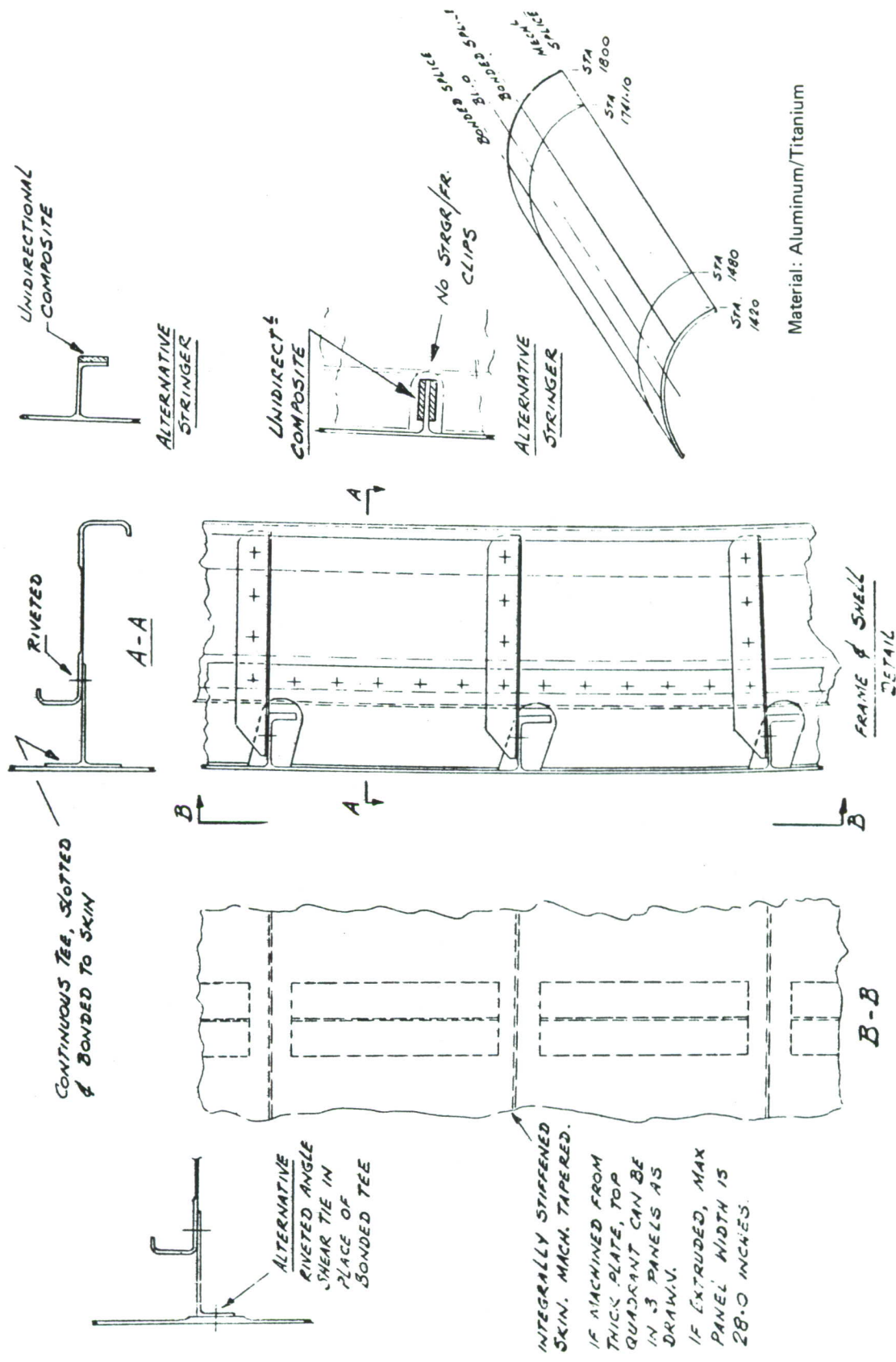


Figure 56. -Shell-Skin/Stringer Integrally Stiffened (Concept 1-2)

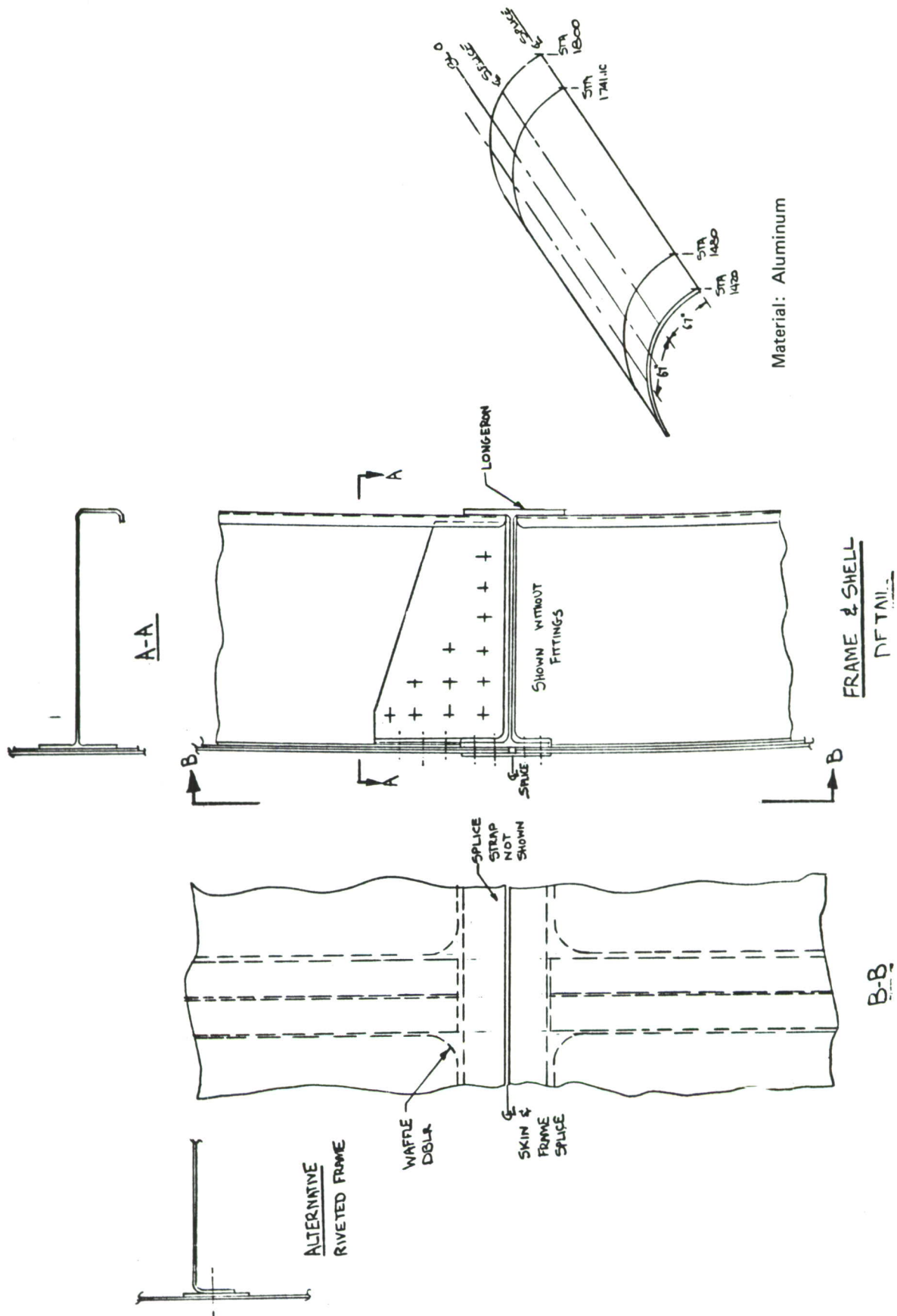


Figure 57. —Shell—Skin/Stringer Wide-Spaced Longerons (Concept 1-3)

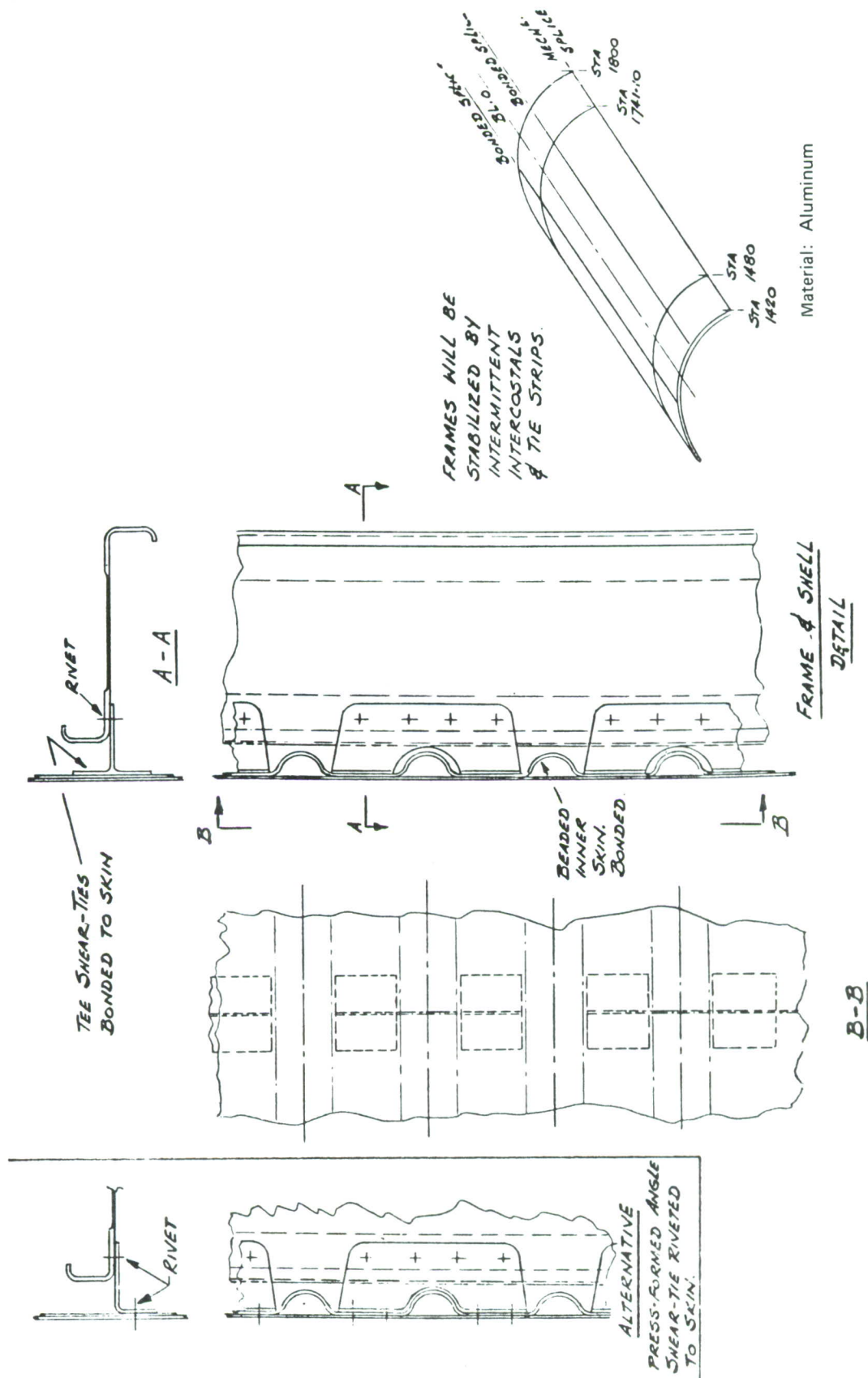


Figure 58.—Shell—Laminated Continuous Beads (Concept 14)

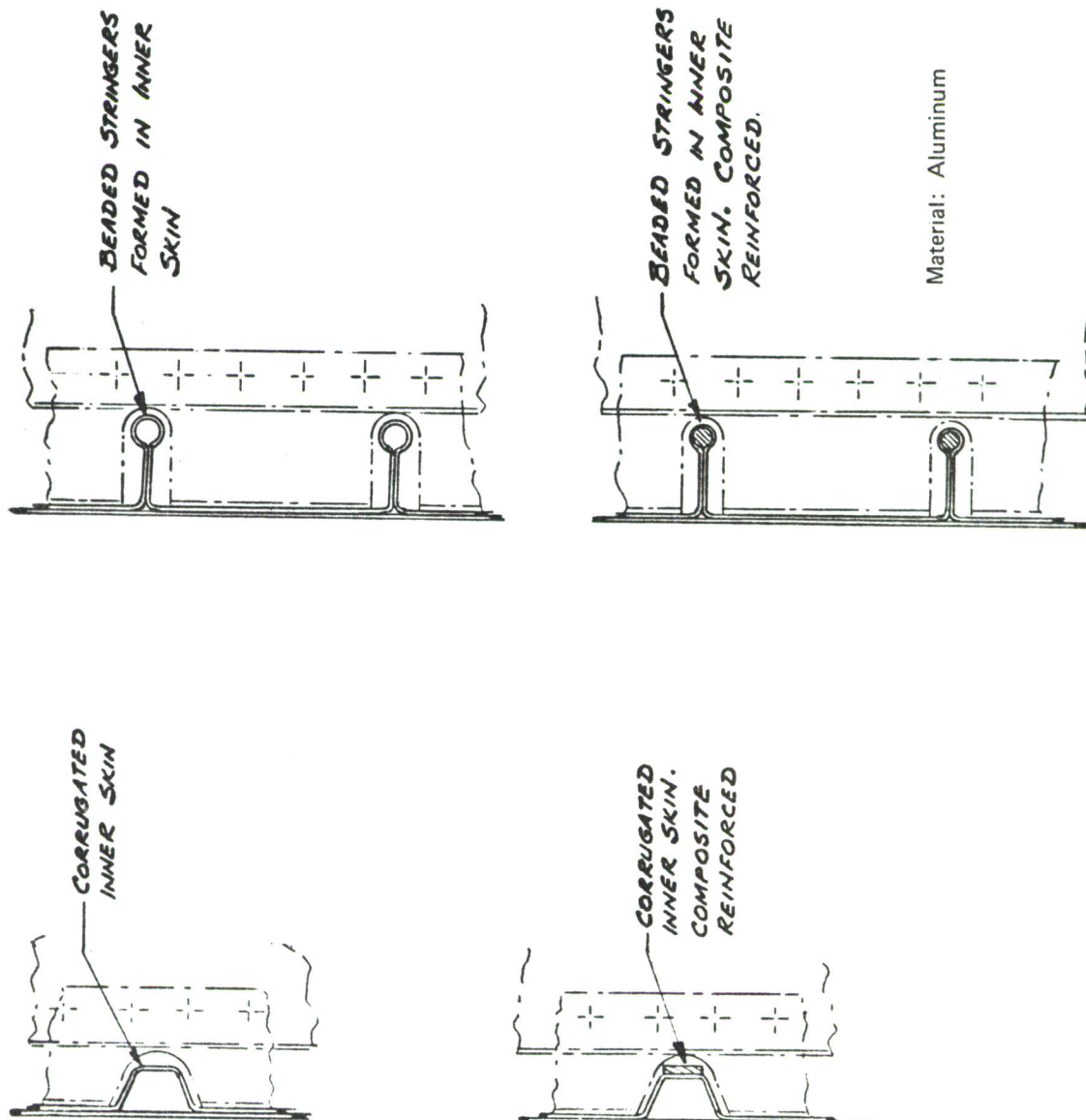


Figure 59. —Shell—Laminated Continuous Beads, Concept Variations (Concept 1-4)

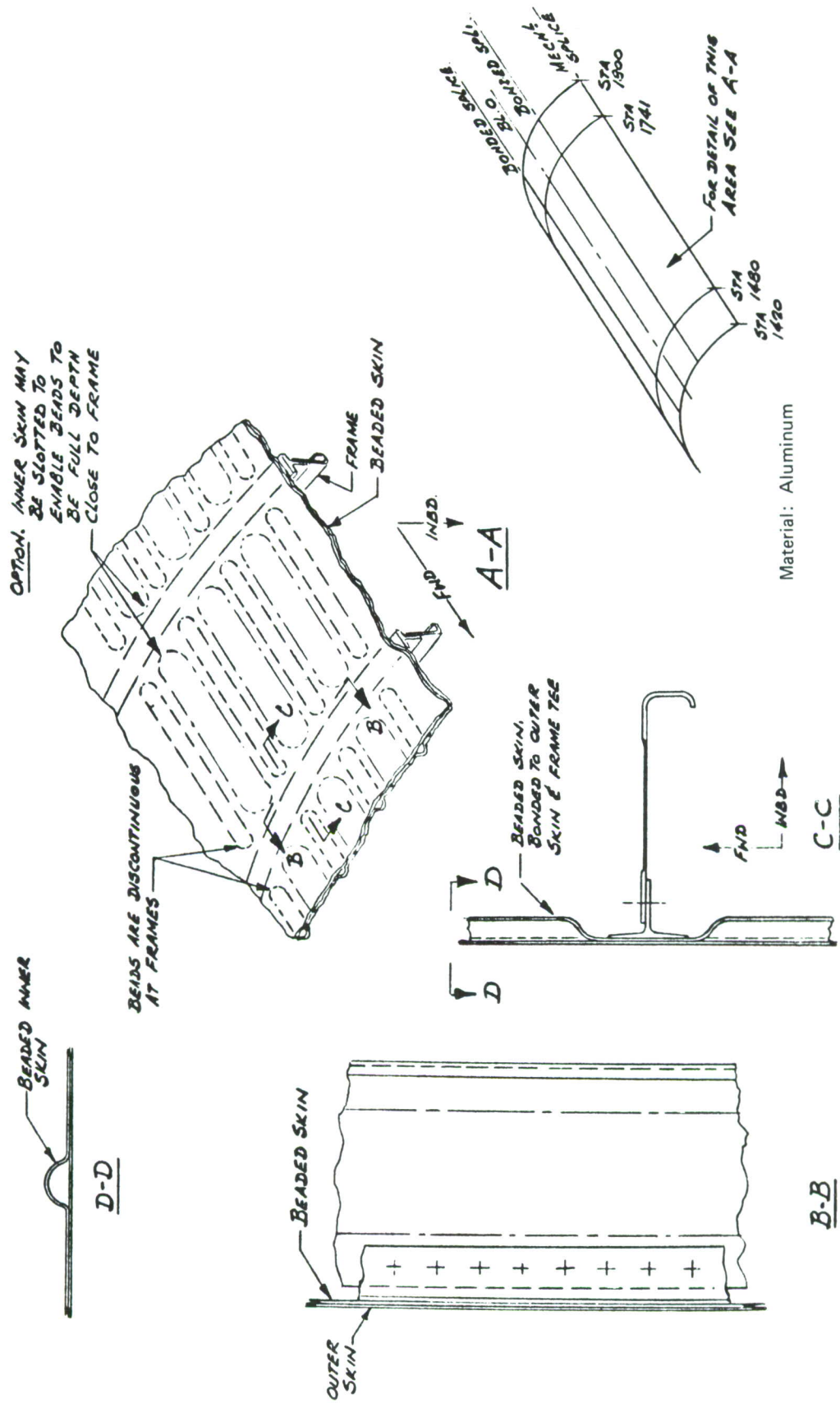


Figure 60. -Shell-Laminated Discontinuous Beads (Concept 1-5)

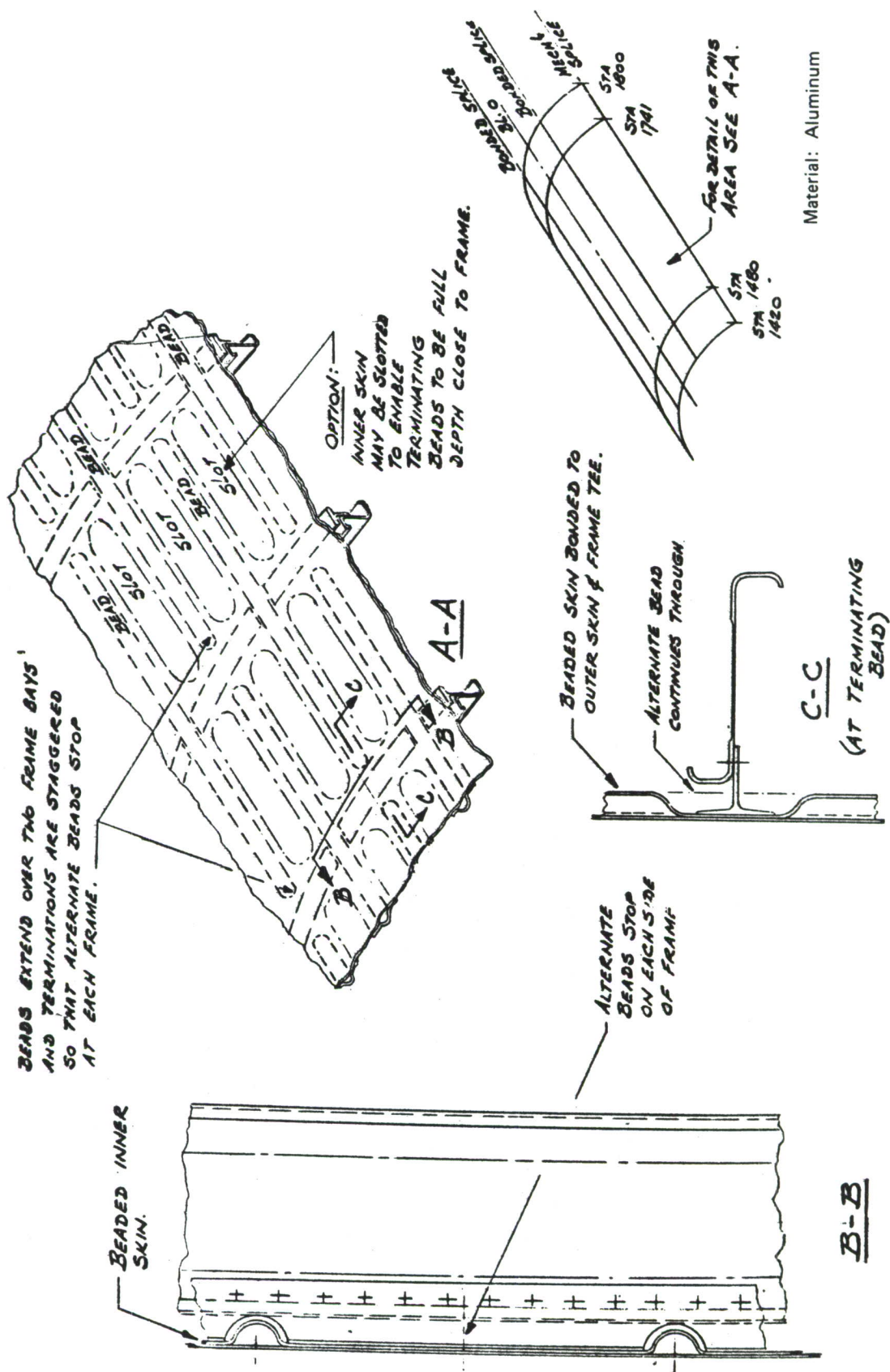


Figure 61.—Shell—Laminated Staggered Discontinuous Beads (Concept 1-5)

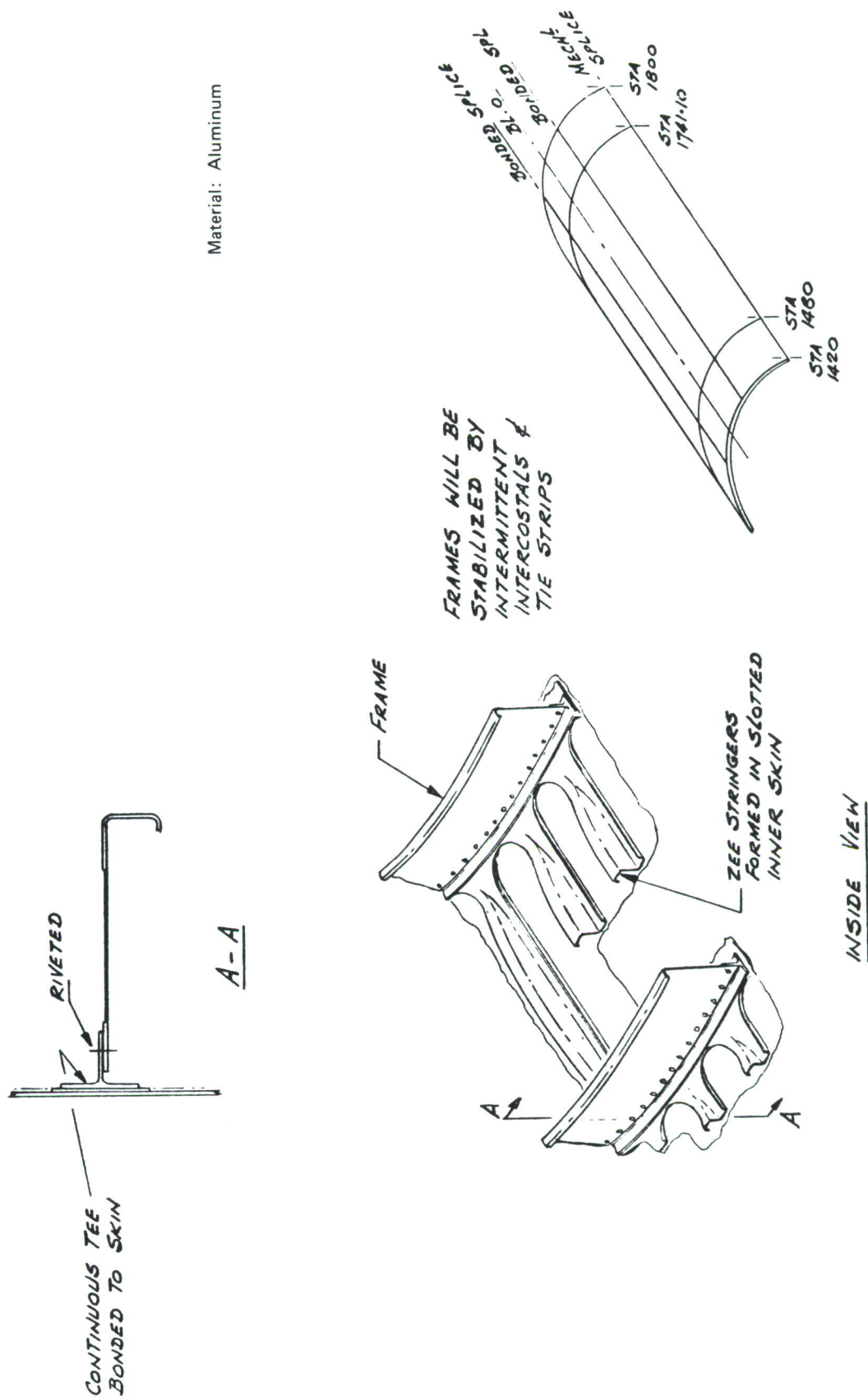
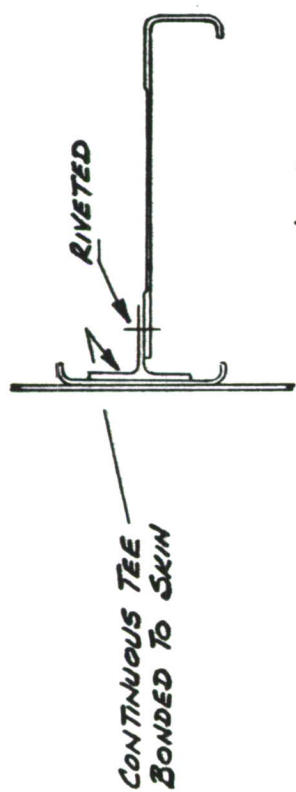
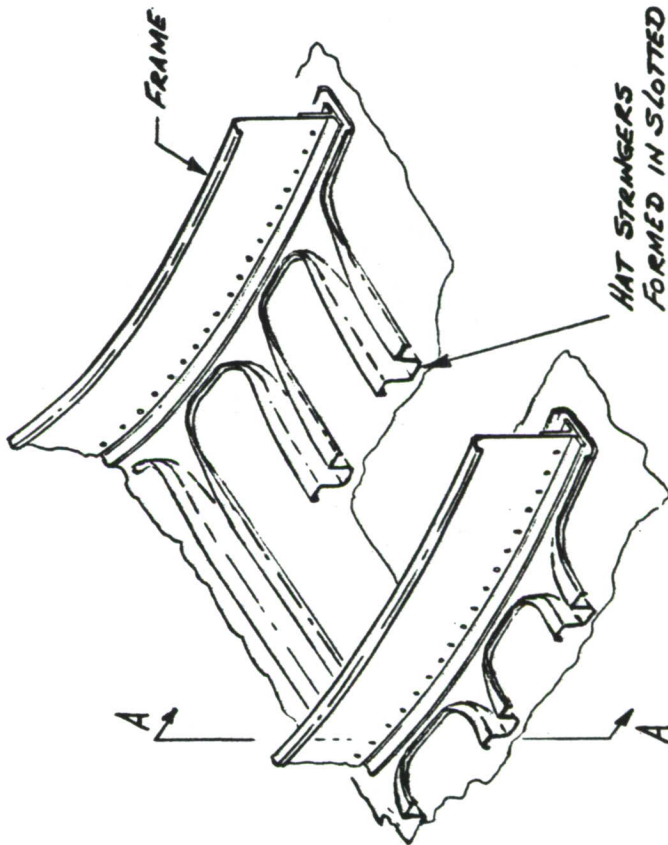


Figure 62. -Shell-Laminated Discontinuous Zee Stringers (Concept 1-5)



A-A



INSIDE VIEW

Material: Aluminum

FRAMES WILL BE
STABILIZED BY
INTERMITTENT
INTERCOSTALS &
TIE STRIPS

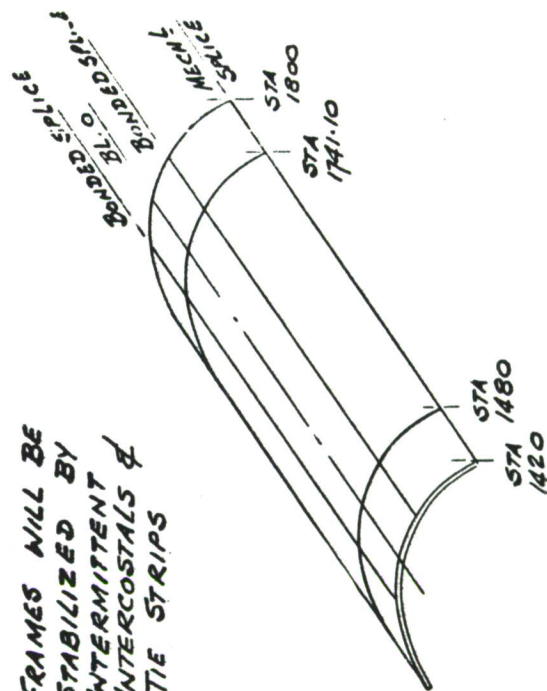


Figure 6.3. - Shell-Laminated Discontinuous Hat Stringers (Concept 1-5)

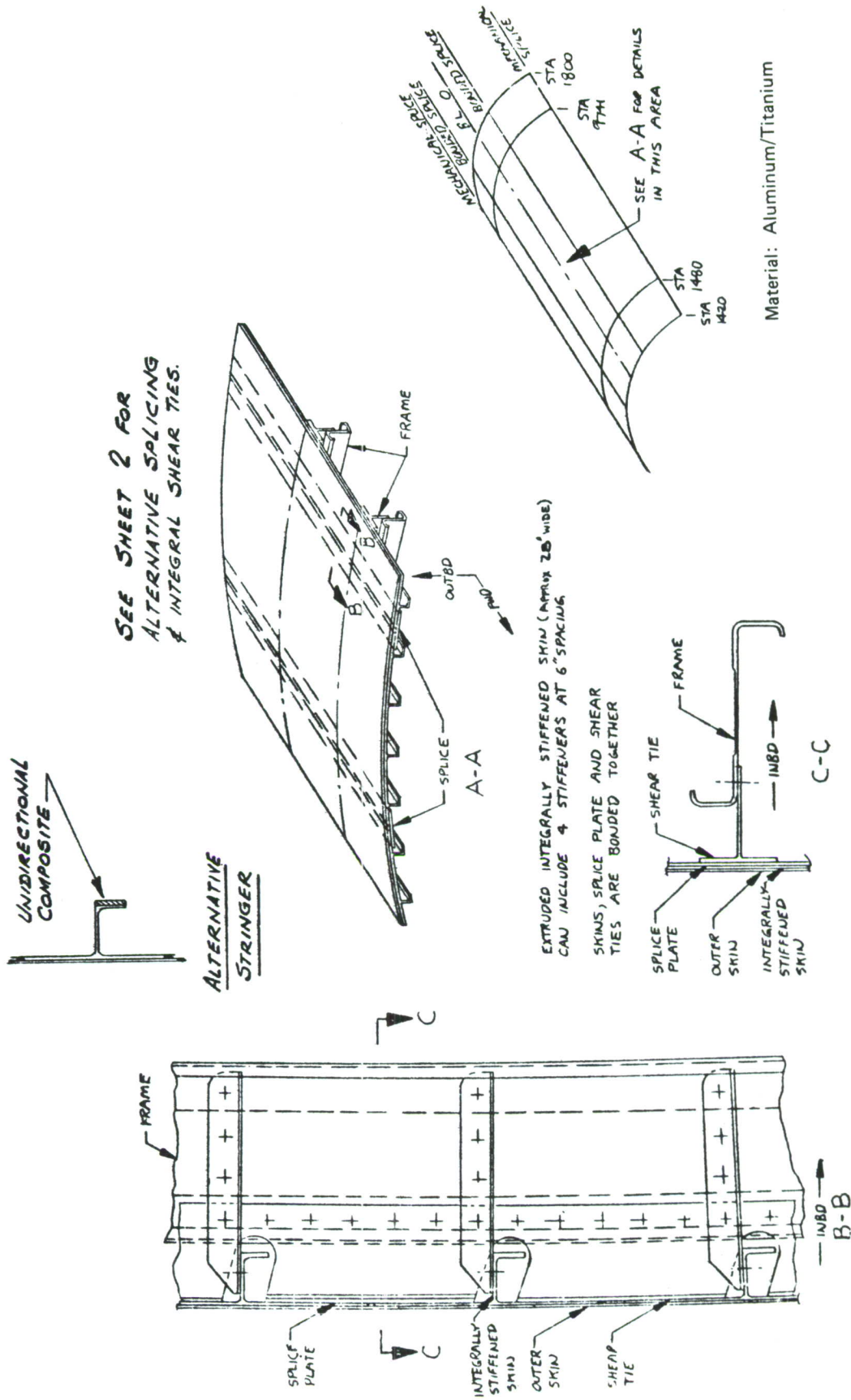


Figure 64. —Shell—Extruded, Laminated Integrally Stiffened (Concept 1-6)

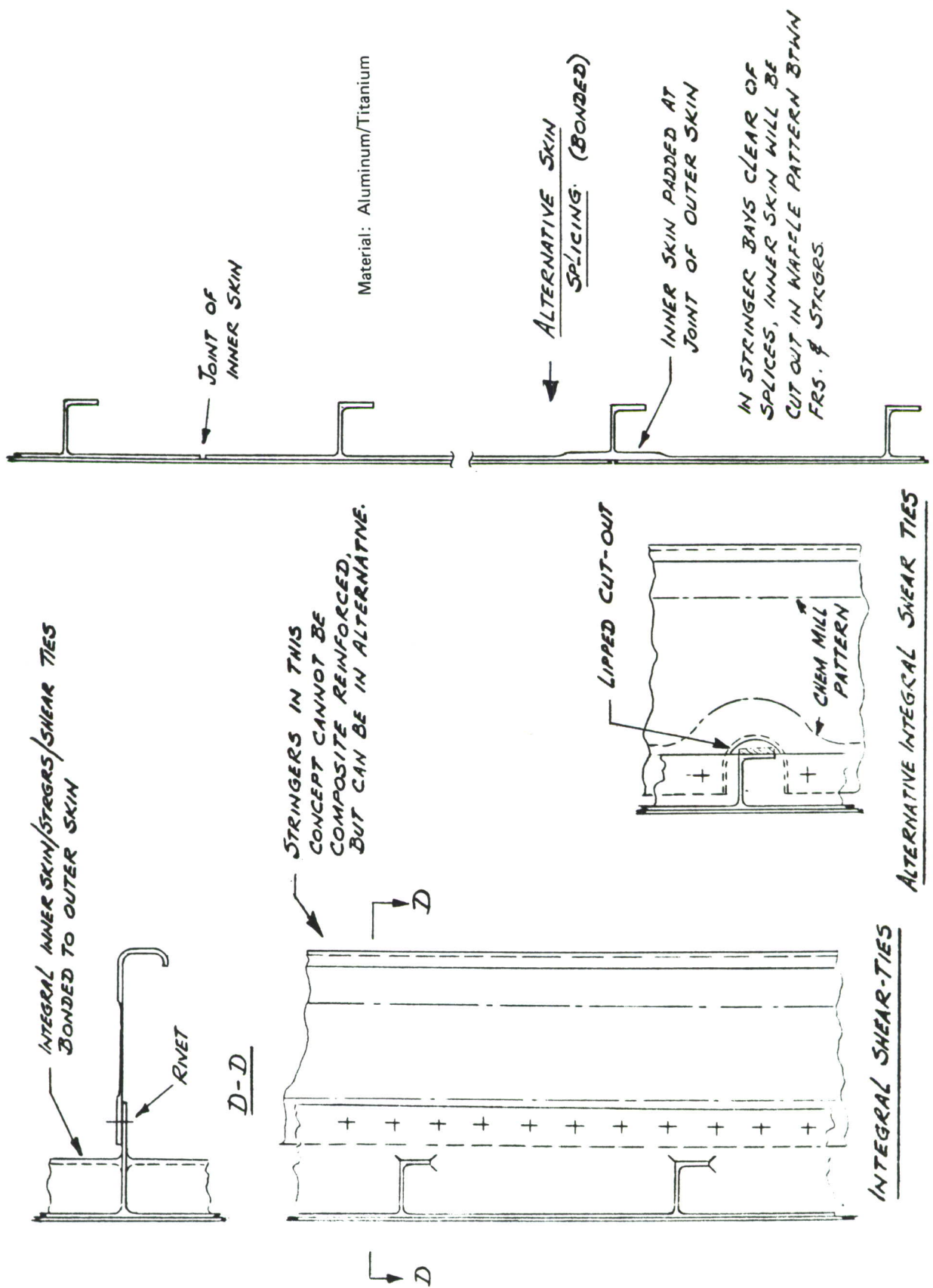


Figure 65. —Shell—Machined, Laminated Integrally Stiffened (Concept 1-6)

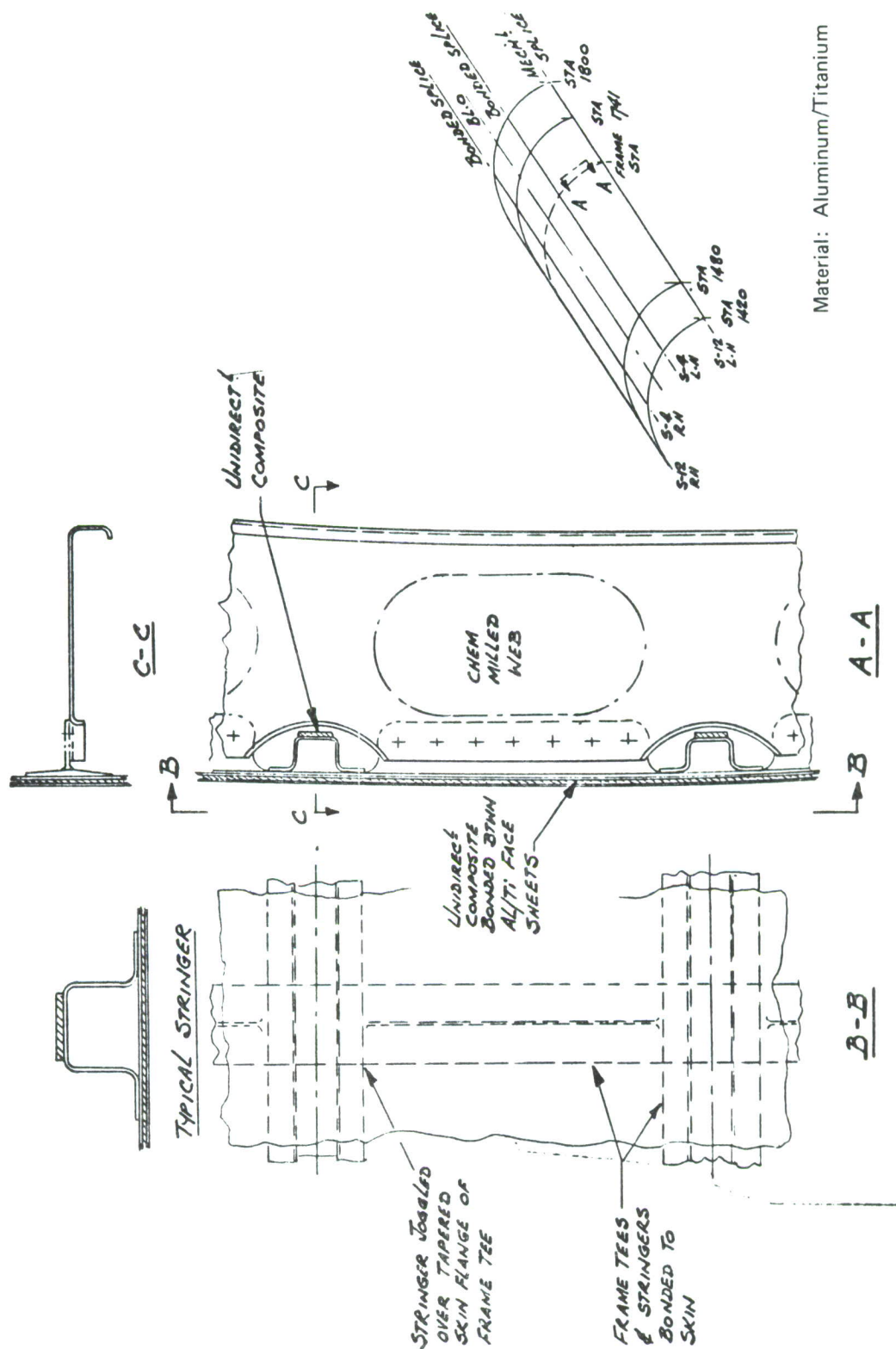


Figure 66. —Shell—Laminated Composite Sandwich (Concept 1-7)

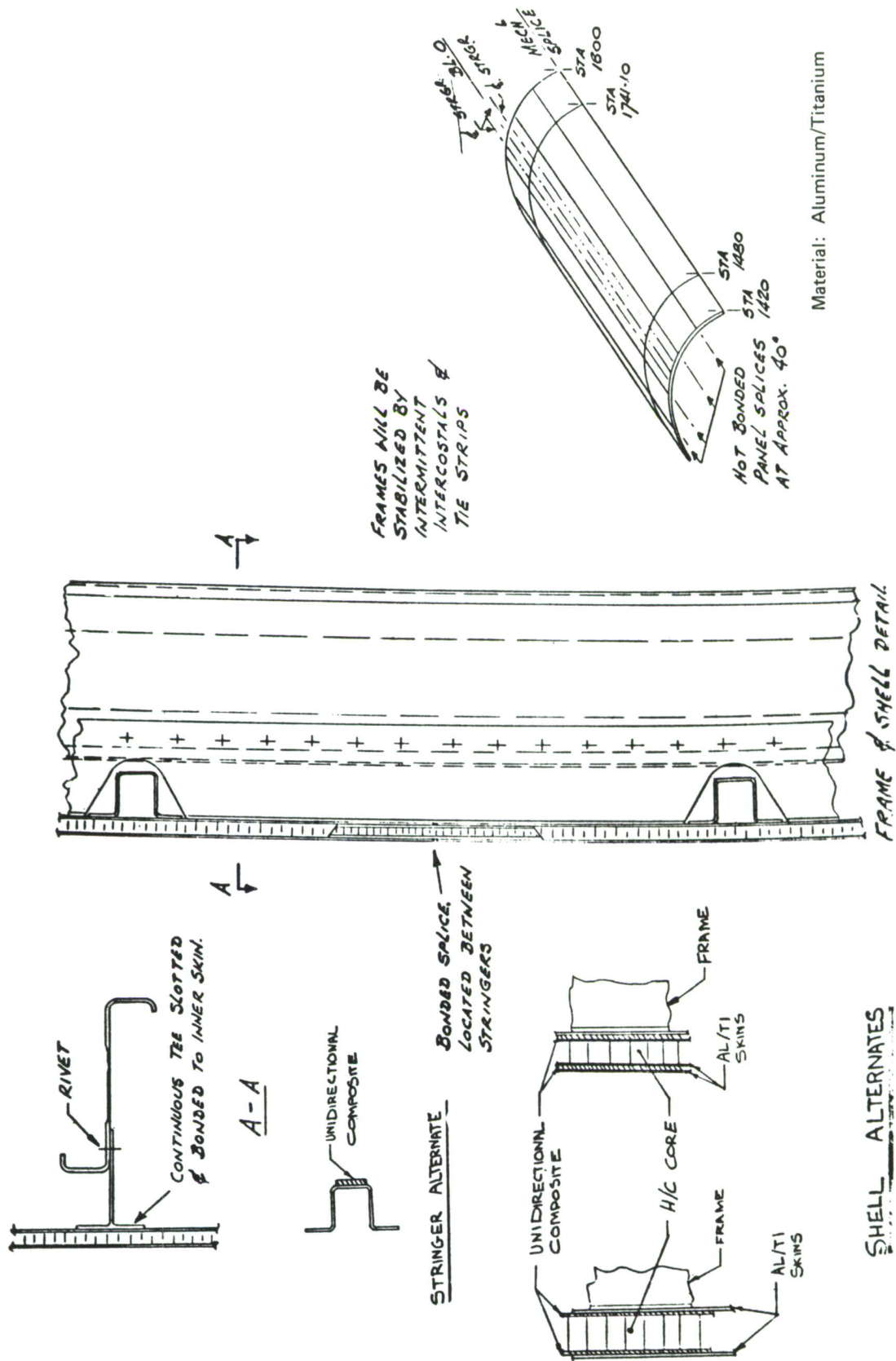


Figure 67.—Shell—Hat Stiffened Honeycomb (Concept 1-8)

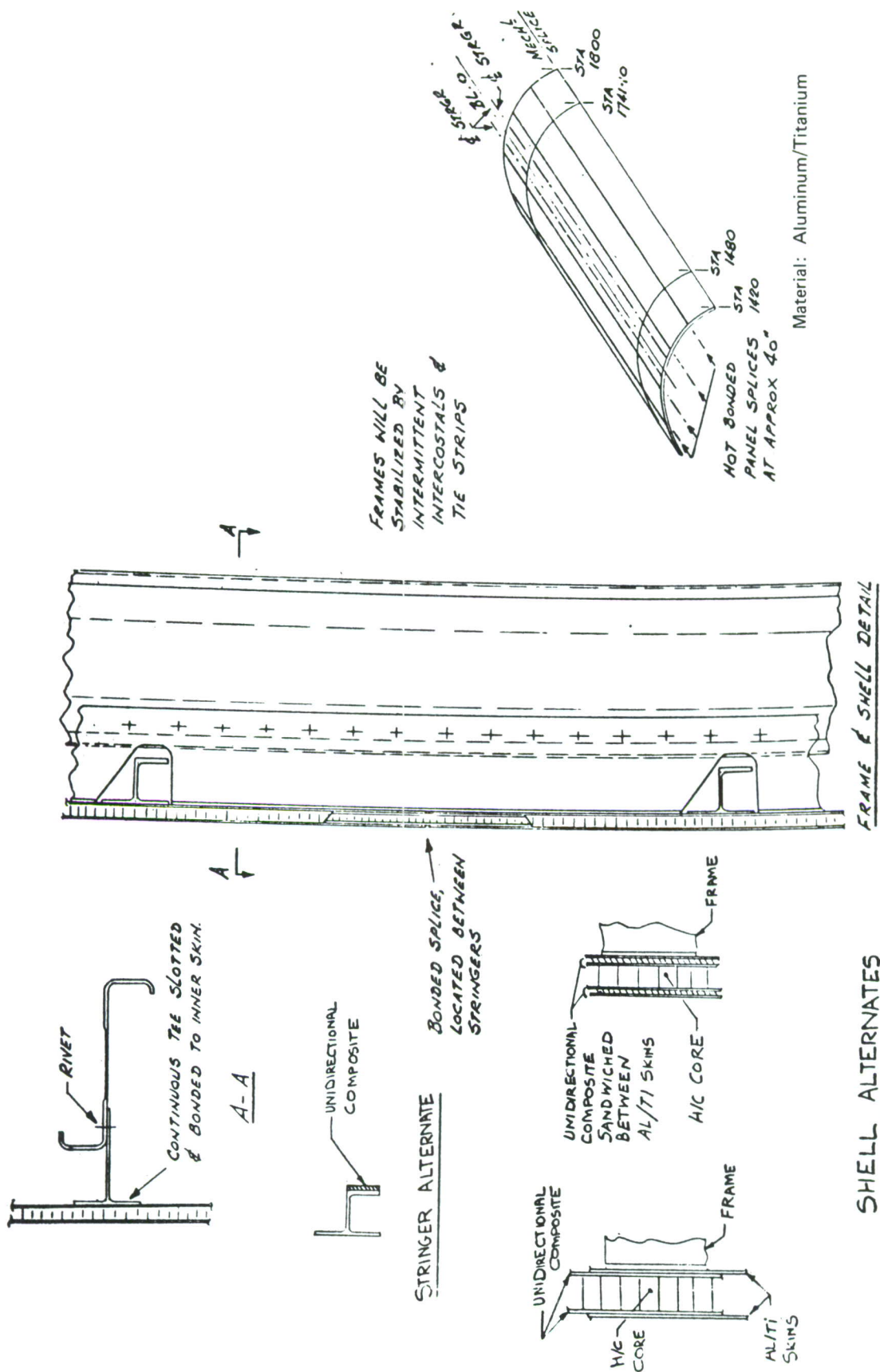
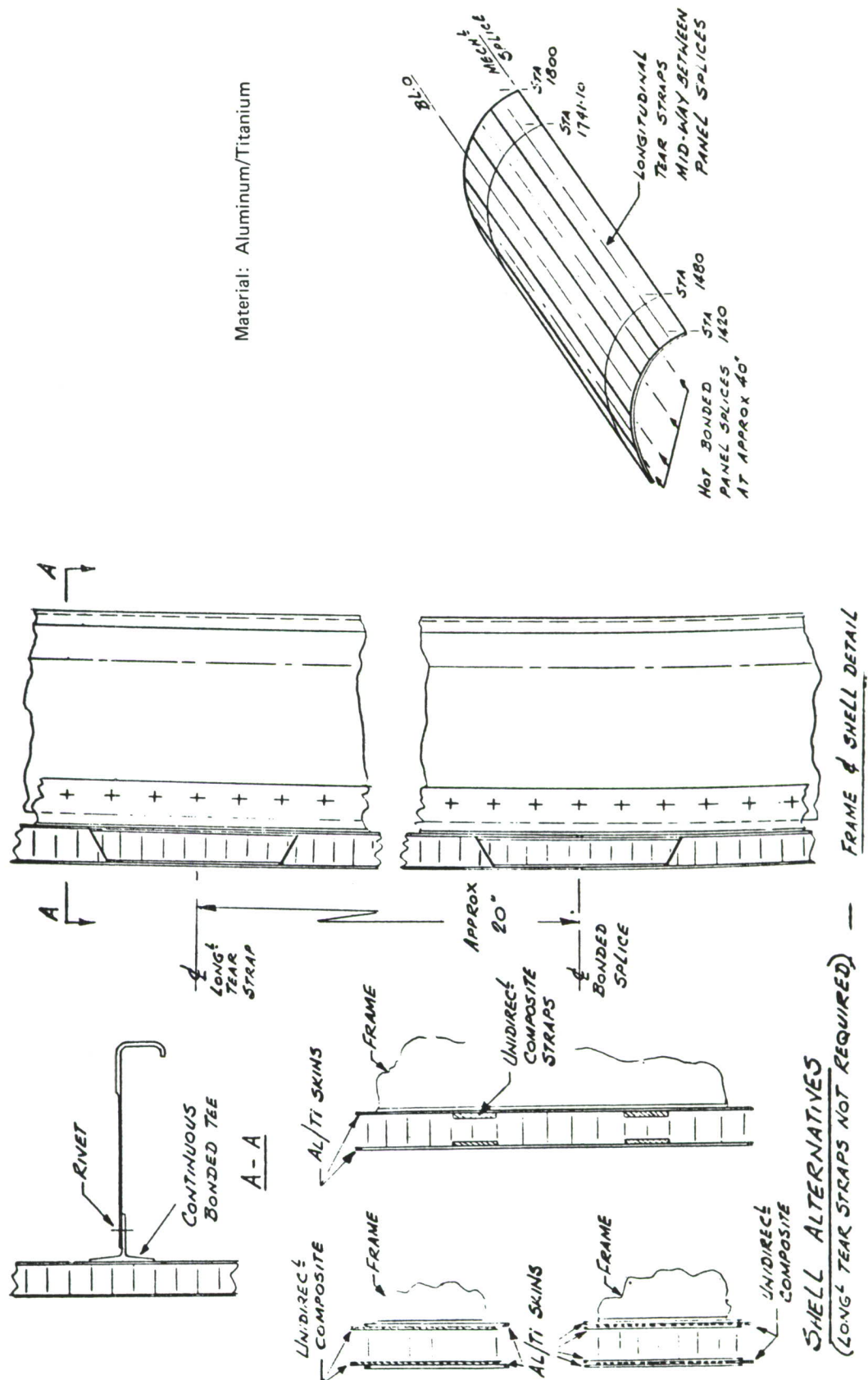


Figure 68. -Shell-J-Stiffened Honeycomb (Concept 1-9)



Material: Aluminum/Titanium

Figure 69. —Shell—Sandwich Honeycomb (Concept 1-10)

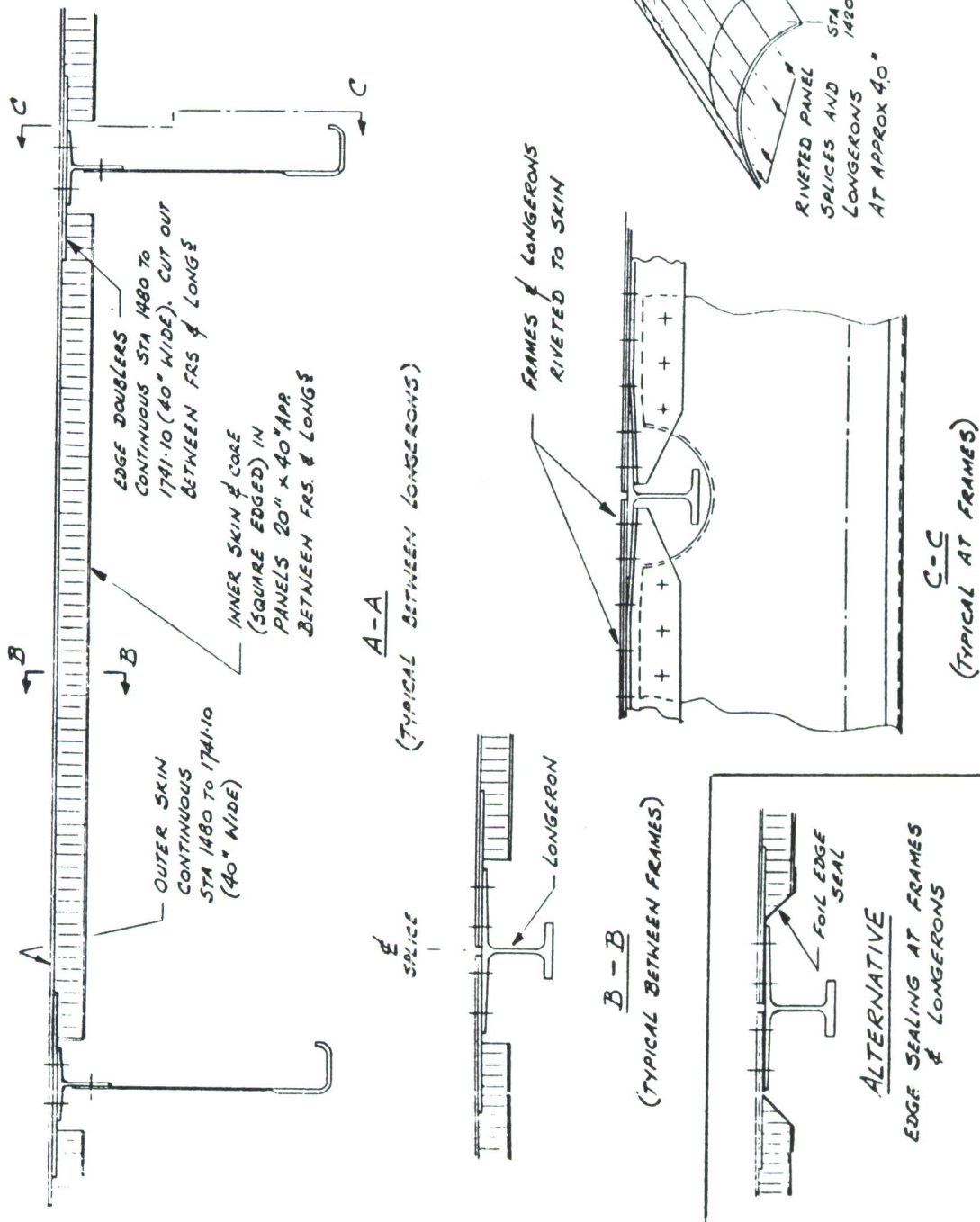
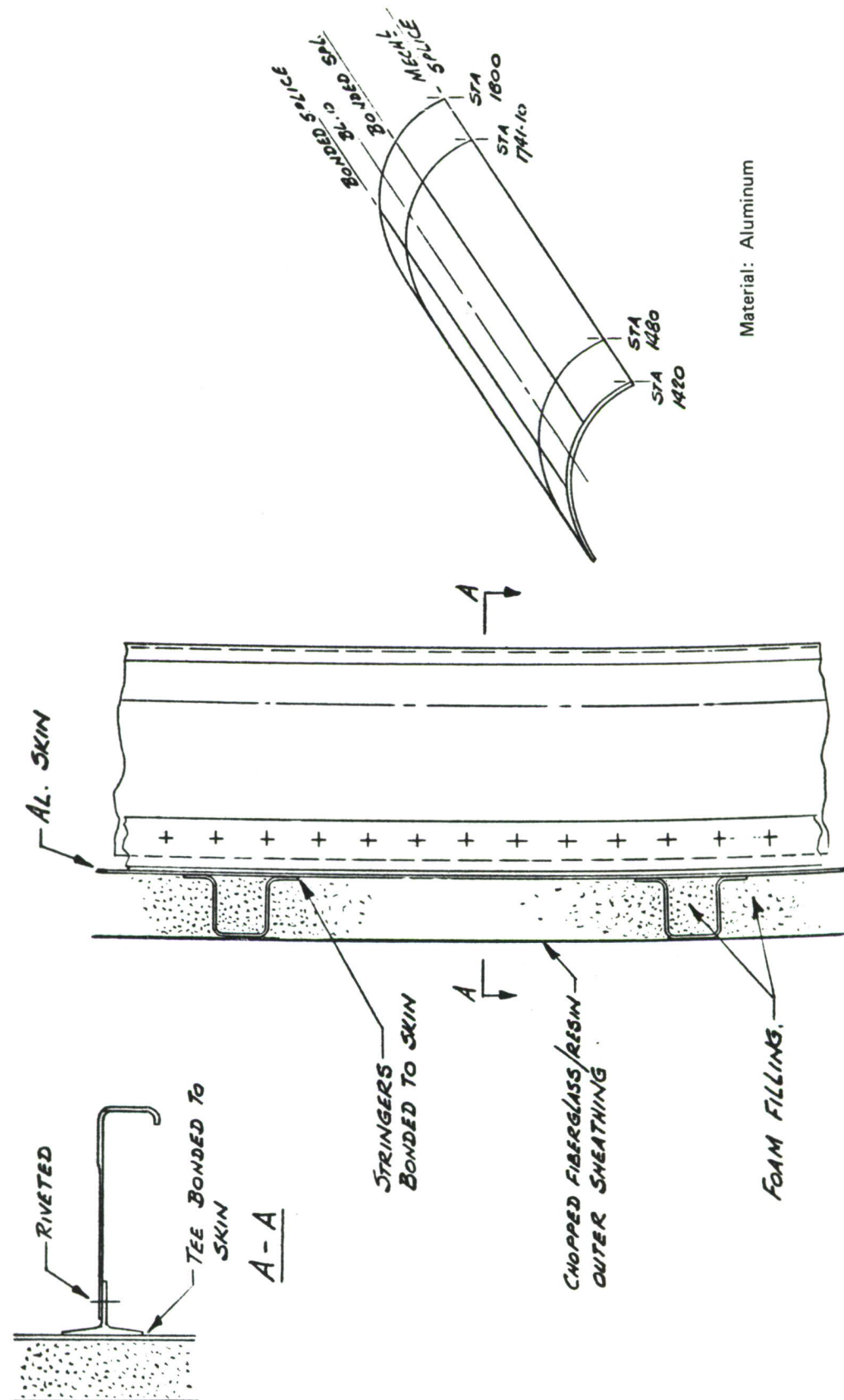


Figure 70.—Shell—Sandwich Honeycomb, Wide-Spaced Longerons (Concept 1-11)



FRAME & SHELL DETAIL

Figure 71. -Shell-External Stringers (Concept 1-12)

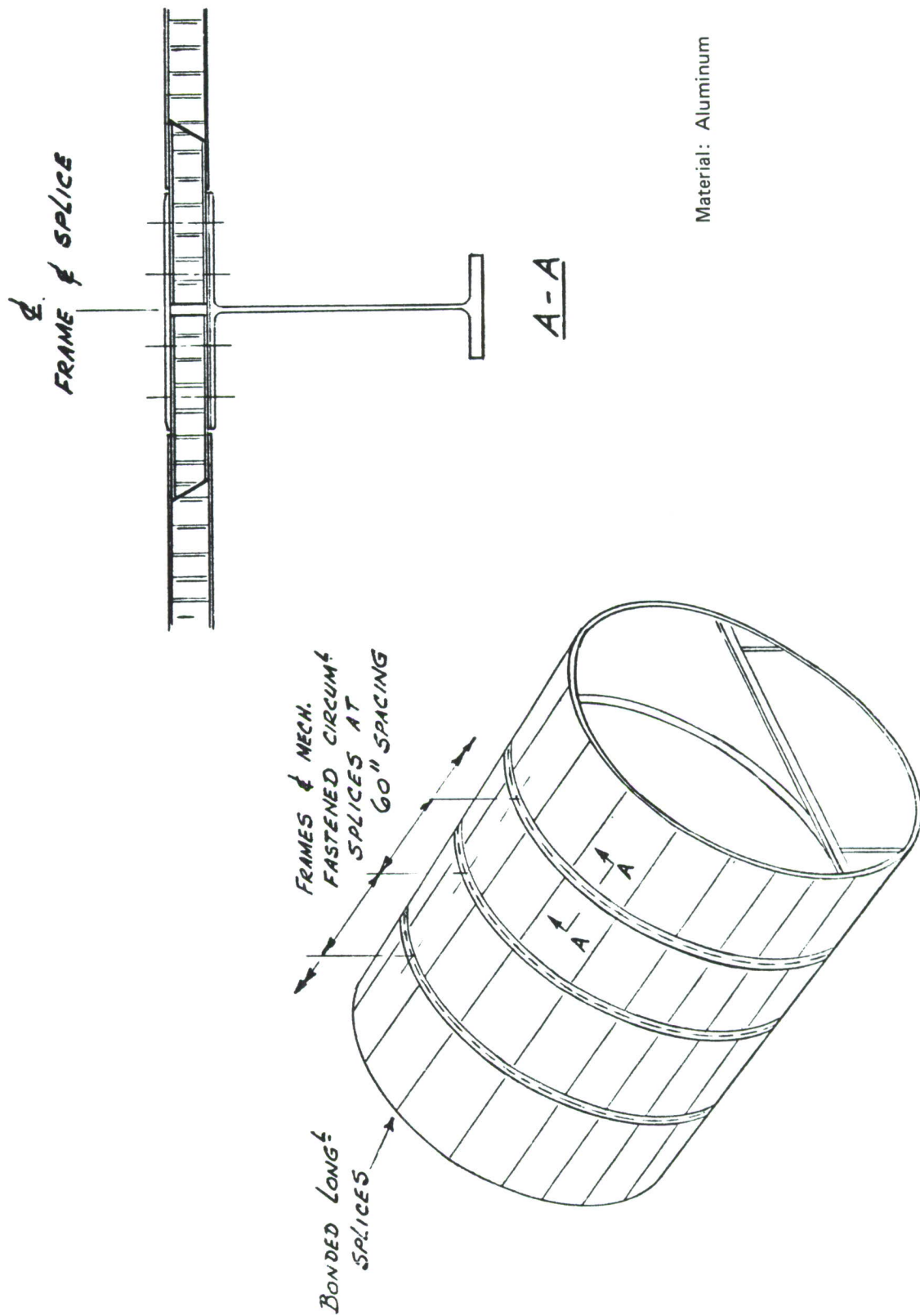










Figure 72.—Shell—Barrel Body 60-in. Frame Spacing (Concept 1-13)

The seven level 1 shell concepts selected for level 2 study are shown in table XVII.

Table XVII.—Level 1 Shell Concepts Selected for Level 2 Study

Concept			Aluminum ^a			Titanium ^a		
Name	No.	Construction	R	B	EP/B	R	B	W
Inverted hat	1-1		✓	✓				
Composite reinforcement	1-1		✓	✓				
Zee stiffener	1-2				✓			✓
Continuous bead	1-4		✓	✓				
Stiffened honeycomb	1-9			✓				
Honeycomb sandwich	1-10			✓				
Square-edge honeycomb	1-11			✓				
External stringers	1-12		✓	✓				

^a R = Riveted

EP = Extruded panel

B = Bonded or
weld-bonded

W = Welded

(2) Level 2 Shell Concept Studies

It was recognized during level 1 screening that the square-edge honeycomb design (1-11) had an inherently low end-load capability; but, because of its potential for low-cost fabrication, the design group requested that it be retained for study of alternate edge configurations. This design study was not successful, so the concept was dropped from further consideration. In a total fuselage design, however, this concept would be a candidate for use in areas of low end loading.

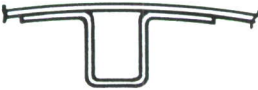

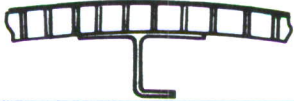


Titanium was eliminated as a candidate primary material for the study structure. Stress, fatigue/fracture, and manufacturing studies showed that it was neither cost nor weight competitive with aluminum for the loading intensities and environment of a

subsonic cargo/transport fuselage. It was considered for limited, space-critical applications such as tear straps and splice plates.

Extruded, integrally stiffened panel concept 1-2 was eliminated from further study due to poor damage-tolerance capability inherent with this type of structure. Integrally stiffened structure provides a single load path and when evaluating for damage-tolerance capability, loss of the full panel width must be assumed. This leads to designs consisting of narrow panels, thus increasing the number of longitudinal splices required and, consequently, adding weight and cost. Concept 1-2 was not competitive with the baseline or the other concepts retained in the study.

The level 2 shell concept studies were thus reduced to the use of aluminum alloys and the five configurations shown in table XVIII.

Table XVIII.—Level 2 Shell Concepts Studied

Concept			Material	Quadrant		
Name	No.	Construction		Upper	Side	Lower
Inverted hat	2-1		Al	Bonded	Bonded	Riveted (Alternate, riveted + composite reinforced)
Continuous bead	2-4		Al	Bonded	Bonded	Bonded and/or riveted
Stiffened honeycomb	2-9		Al	Bonded	Bonded	Bonded
Honeycomb sandwich	2-10		Al	Bonded	Bonded	Bonded
External stringers	2-12		Al	Bonded	Bonded	Bonded and/or riveted

To evaluate the remaining shell concepts on a common basis, each was sized using the baseline aluminums (2024-T3 sheet for skin and 7075-T6 sheet for frames and stringers). Cost and weight could then be compared on the basis of one configuration's geometric advantage over another during level 2 screening. The concepts chosen for level 3 study were evaluated for different aluminum alloy trades.

Figure 73 shows typical construction of the baseline skin, stringers, shear ties, and frames. The construction is all-riveted, with circumferential tear straps bonded to the skin at each frame location.

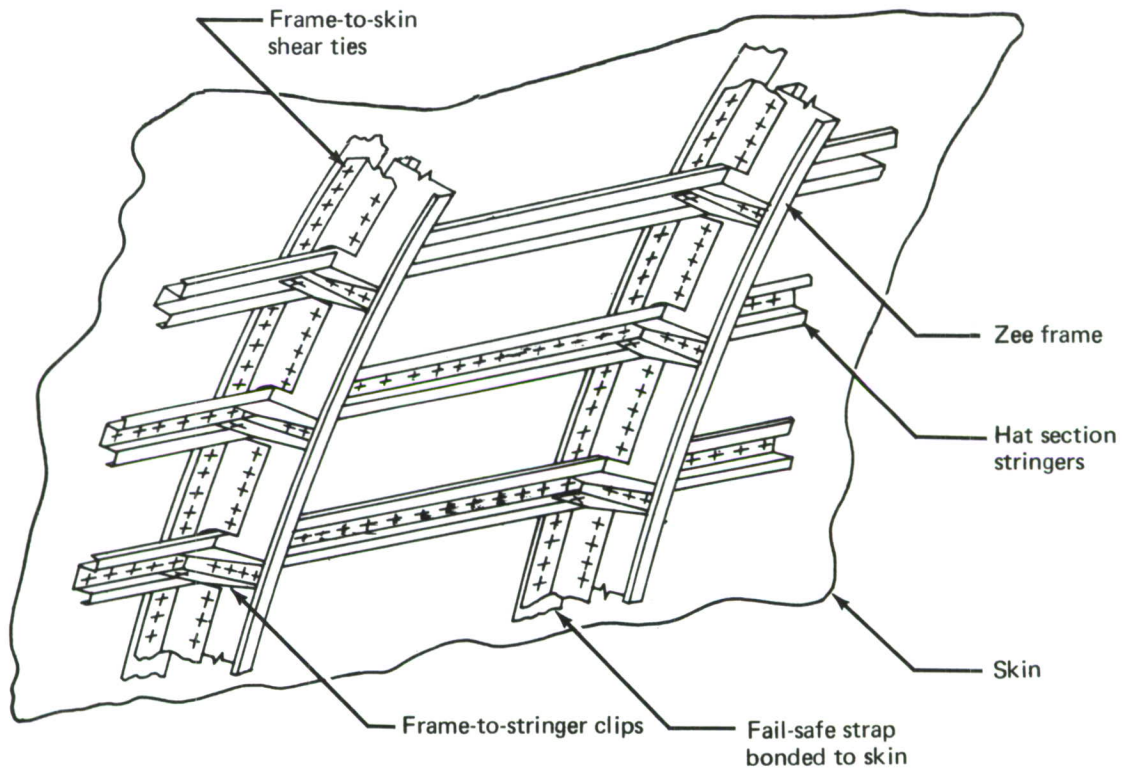


Figure 73.—Baseline—Typical Crown Structure

Figures 74 through 78 are sketches of the concepts screened in level 2. To increase the fatigue quality, all the skin panel concepts are bonded assemblies with riveting only at the joint between the frame-to-skin tie and the frame. Each concept is configured to reduce the number of parts, thus keeping down assembly costs.

Figure 74 shows the bonded waffle doubler, internal inverted hat stringer design (concept 2-1). The continuous frame-to-skin tie members with slots over the stringers are bonded to the waffle doubler. The frames are rolled, stretch formed, and riveted to the frame-to-skin tie members.

The continuous-bead concept 2-4 is shown in figure 75. The continuous beads are formed from sheet material and adhesively bonded to the primary skin, forming a laminated skin/stiffener panel. A continuous-frame tie, similar to that used in concept 2-1, is bonded to the panel, and a rolled, stretch-formed frame member is riveted in place on final assembly. This concept does not lend itself to a continuous circumferential fail-safe strap. Therefore, a separate fail-safe outer chord is included in the frame design, similar to the baseline lower quadrant frame segment.

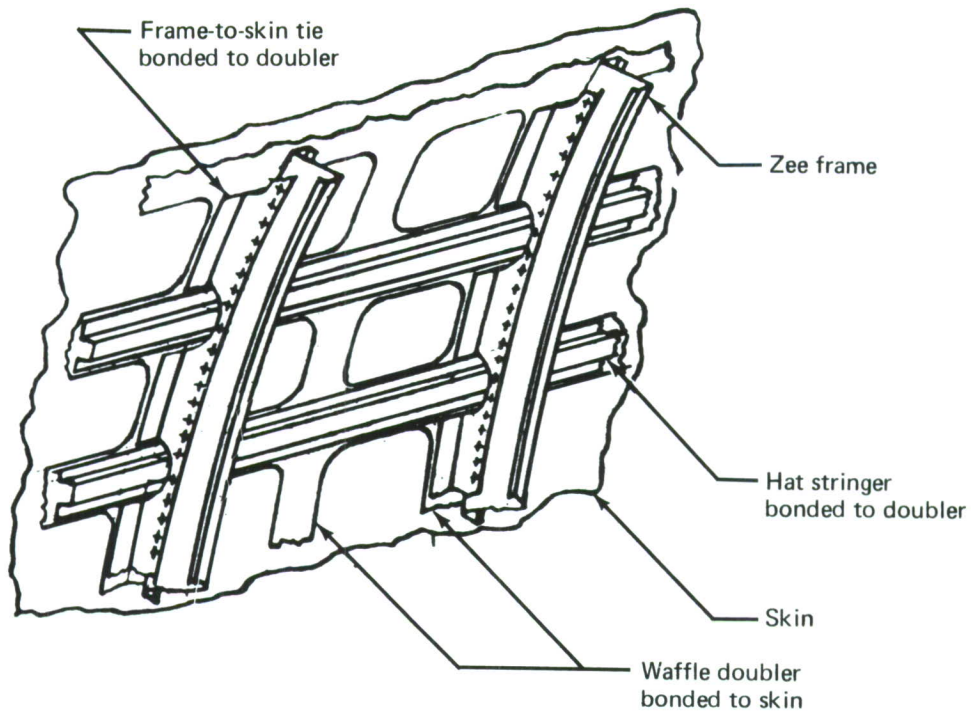


Figure 74.—Shell Configuration 2-1—Inverted Hat Stiffeners

Figure 76 shows details of the stiffened honeycomb concept 2-9. In this design, the stringers have a wider spacing and the skin is stabilized by a thin honeycomb core. The frame and fail-safe chord details are similar to those of the continuous-bead design.

Figure 77 is a sketch of the all-bonded, frame-stiffened, honeycomb shell concept 2-10. The frames are simplified by reducing their complexity. Maximum use of the skin material is possible because it is fully effective for both hoop and longitudinal loading.

Figure 78 shows the externally stiffened, skin/stringer concept 2-12. This concept uses the improved shell stability characteristics inherent in an externally stiffened skin/stringer concept. The hat-section stringers and continuous frame-tie outer chords are adhesively bonded to the contoured skin. The outer frame chord serves as frame tie and circumferential fail-safe strap. Local load redistribution in the frames (in other concepts caused by notches at the stringer locations) is eliminated in this design. A smooth aerodynamic surface is obtained by using insulation with thin, fiberglass, external, nonstructural skin. This configuration, with the insulation and fiberglass external surface, will require careful investigation of corrosion protection and inspection requirements.

The level 2 concepts were sized for ultimate strength and checked for fatigue, and the material was distributed to meet residual strength requirements using the baseline aluminum alloys. The design sketches were updated and submitted to the Weights unit and Manufacturing organization for evaluation.

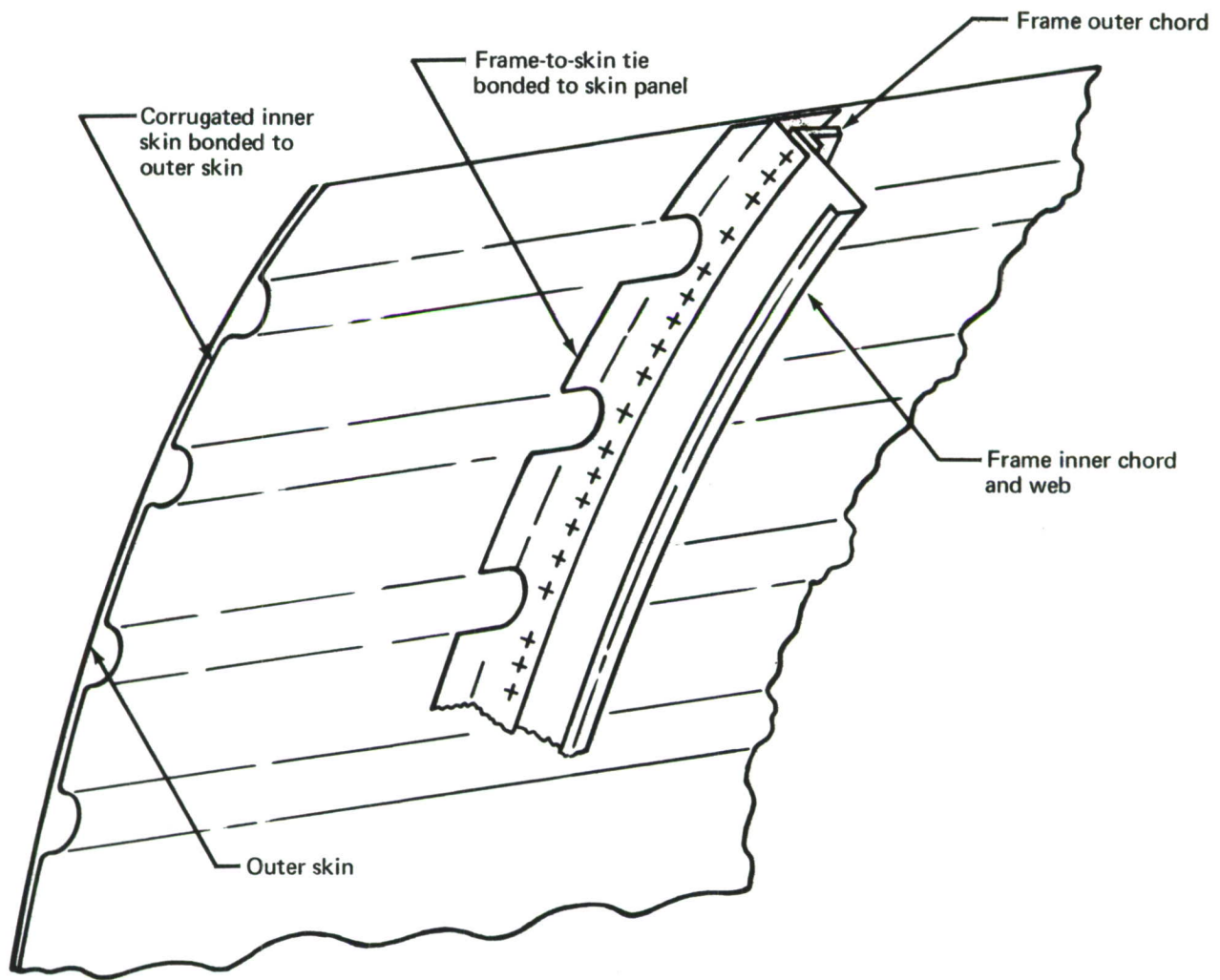


Figure 75.—Shell Configuration 2-4—Continuous Beads

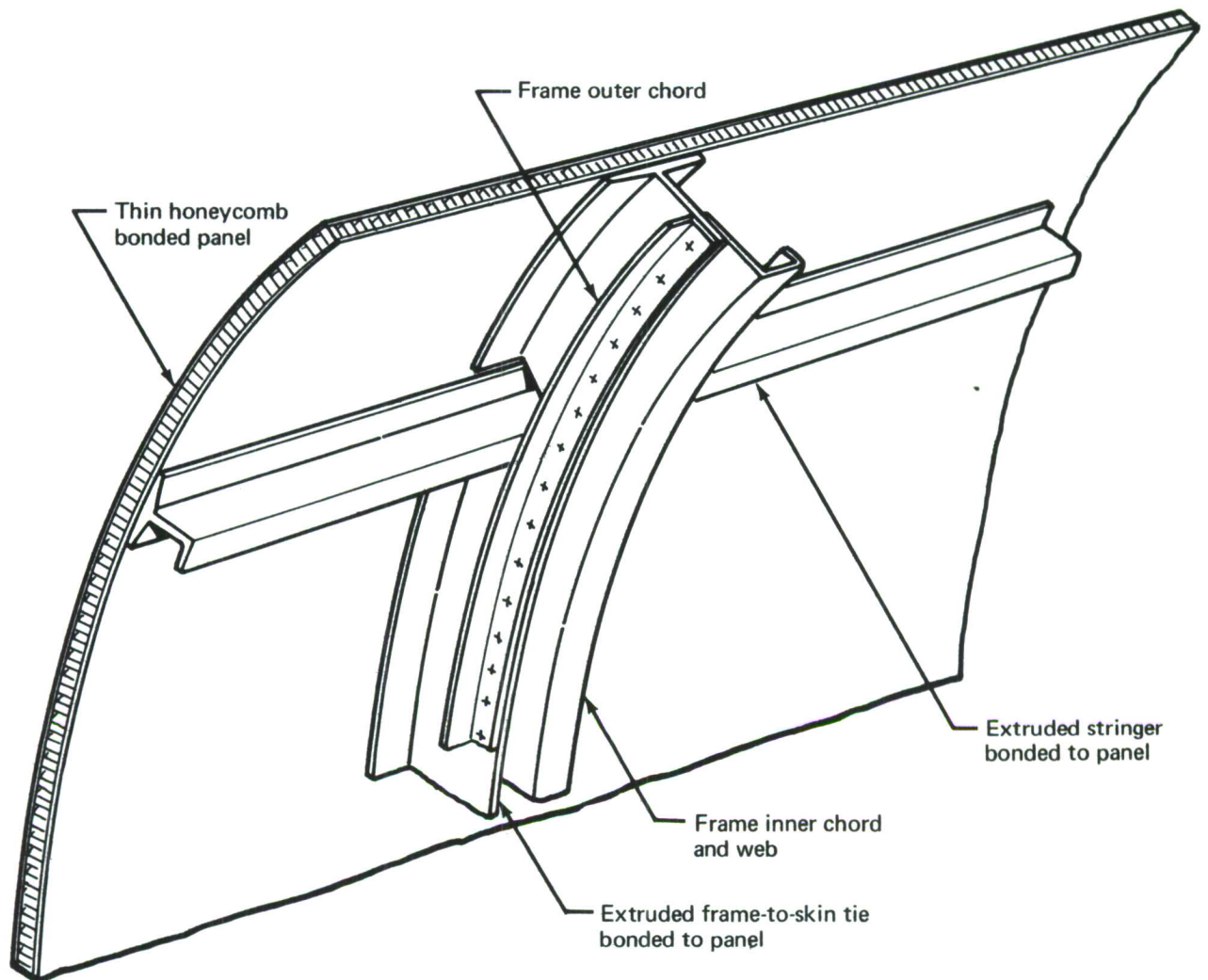


Figure 76.—Shell Configuration 2-9—Stiffened Honeycomb

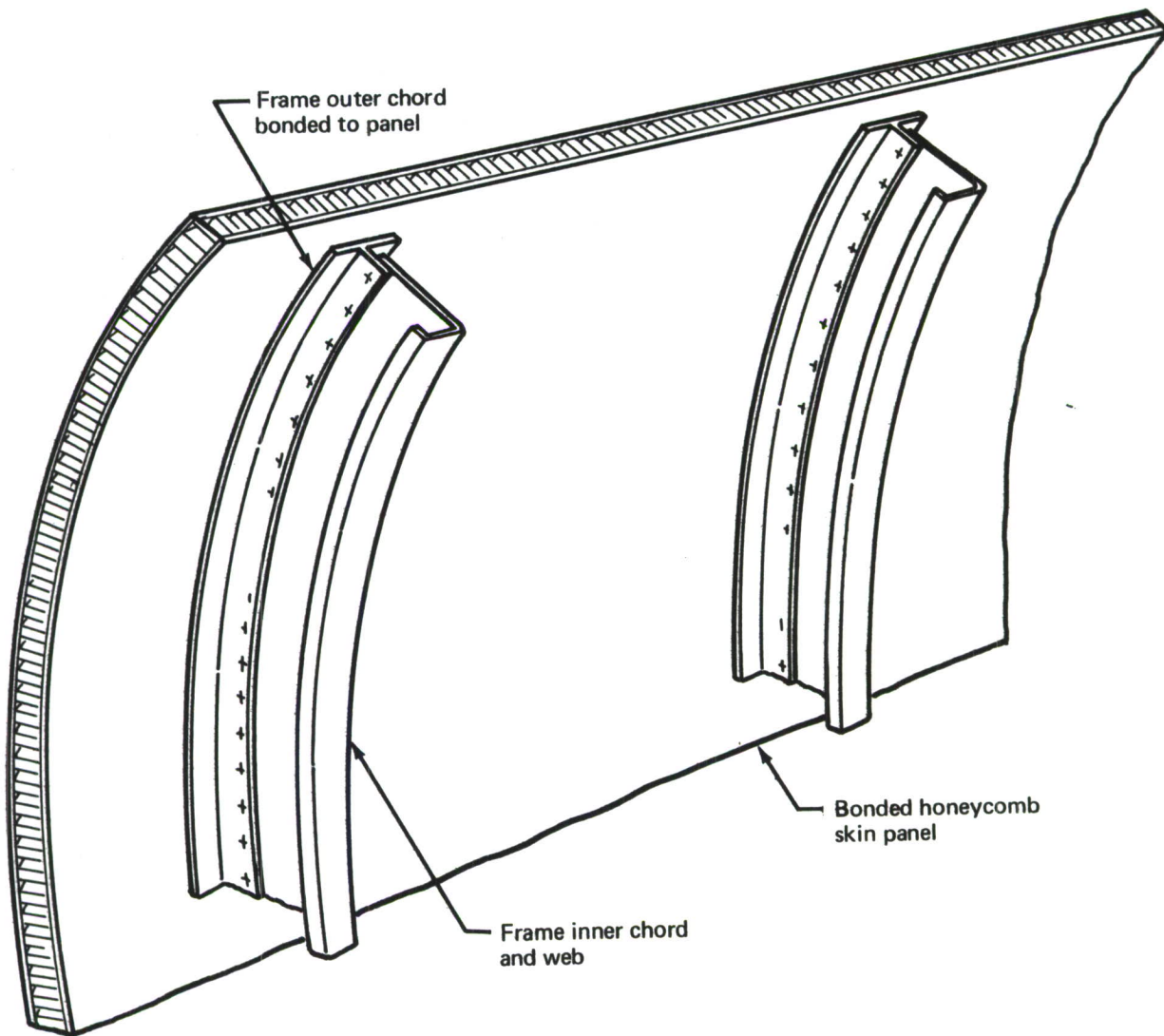


Figure 77.—Shell Configuration 2-10—Honeycomb

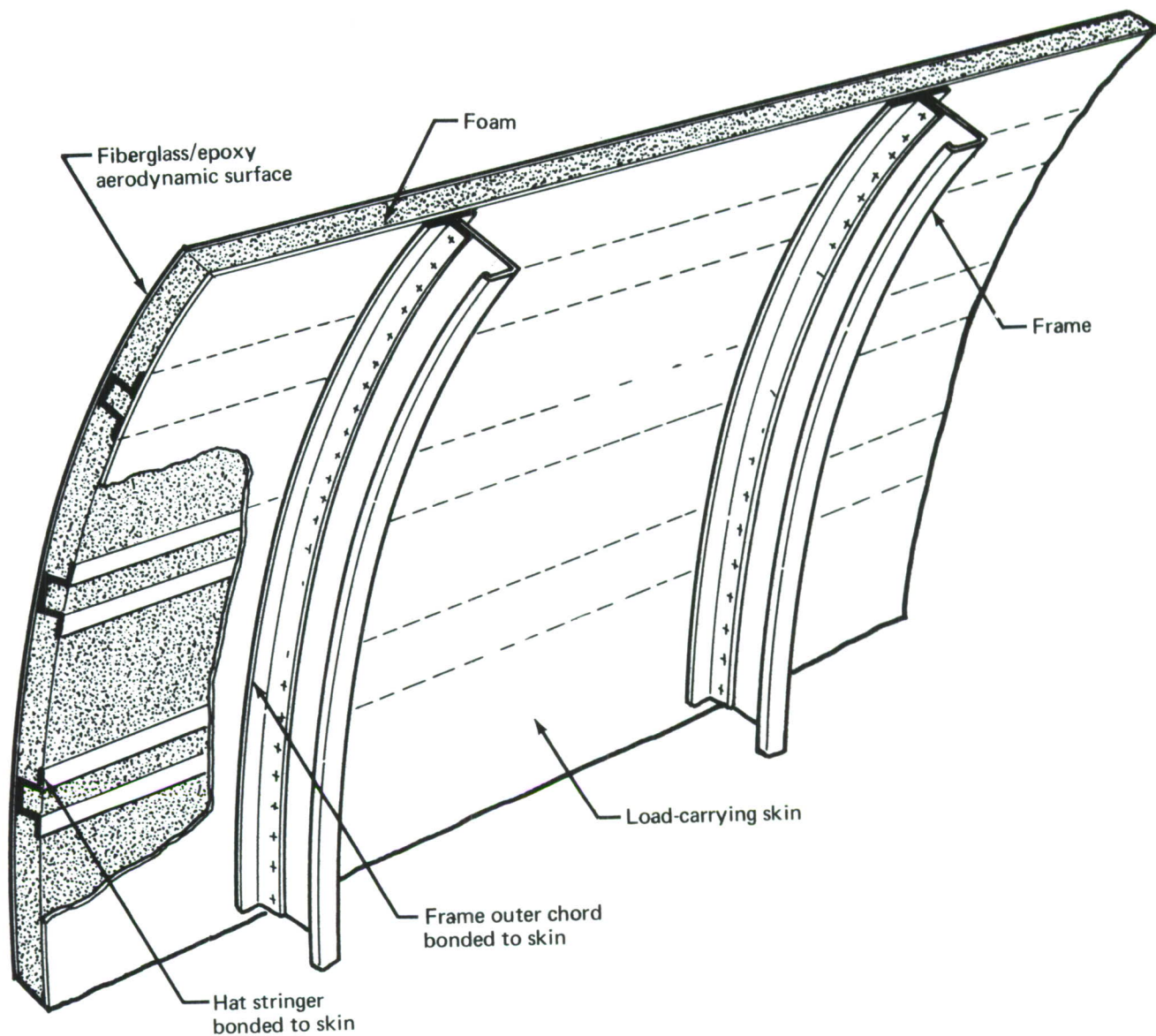


Figure 78.—Shell Configuration 2-12—External Hat Stringers

Manufacturing, in conjunction with Industrial Engineering, reviewed the shell concepts and assigned manufacturing complexity factors to each based on such criteria as tooling, part count, assembly methods, man-hours, part size, etc. The complexity factors were then transmitted to the Cost Analysis group, along with appropriate learning curves.

The Weights unit prepared a weight statement for each design; these data were transmitted to the Cost Analysis group. With the manufacturing complexity factors, structural weight, and appropriate learning curves, the Cost Analysis group established an average unit out-the-door price for 201 units of each of the five concepts.

These cost and weight numbers were based on shell variations only (skin, stringers, frames, tear straps, and skin ties, as appropriate, for each concept). The other components (body station 1480 bulkhead, keel beam, landing gear fittings, and pressure deck) were included as baseline values for weight and cost for all five shell concepts.

The relative weight and out-the-door price for each of the remaining level 2 shell concepts is graphically depicted in figure 79. All components other than the shell were given baseline weights and prices so that the merits of the different shell concepts could be evaluated. The unit price for each concept is based on the average unit out-the-door price of a 201-unit lot.

The calculated values for the weight and unit price of the level 2 shell study have changed during the more in-depth level 3 study. But these values provided a valid comparison of the relative merits of the level 2 concepts.

Based on these cost and weight comparisons, the stiffened honeycomb concept was dropped from the study. The four remaining concepts were carried on to level 3.

(3) Level 3 Shell Concept Studies

During this phase of the study, local joint design, splices, and reinforcements were investigated to greater detail than in the level 2 study. The effects of manufacturing requirements and assembly sequence were included in the design detail trade studies, and the results were incorporated into the final concept designs.

During the final level 3 structural sizing, a trade study was made on each of the final four concepts comparing the weight using the baseline 2024-T3 skin and the weight using 7475-T761 skin. The 7475-T761 skin showed a definite weight-saving advantage for all concepts because of its higher ultimate strength combined with fatigue and fracture properties comparable to 2024-T3. The final weight statements of the new concepts are based on the use of 7475-T761 skin material instead of 2024-T3.

The final level 3 concept design drawings are shown in figures 80 through 83.

Manufacturing and Industrial Engineering updated the manufacturing complexity factors for the final four shell concepts. Using the updated weight and complexity factors, the Cost Analysis group evaluated the unit costs for the level 3 shell concepts (table XIX).

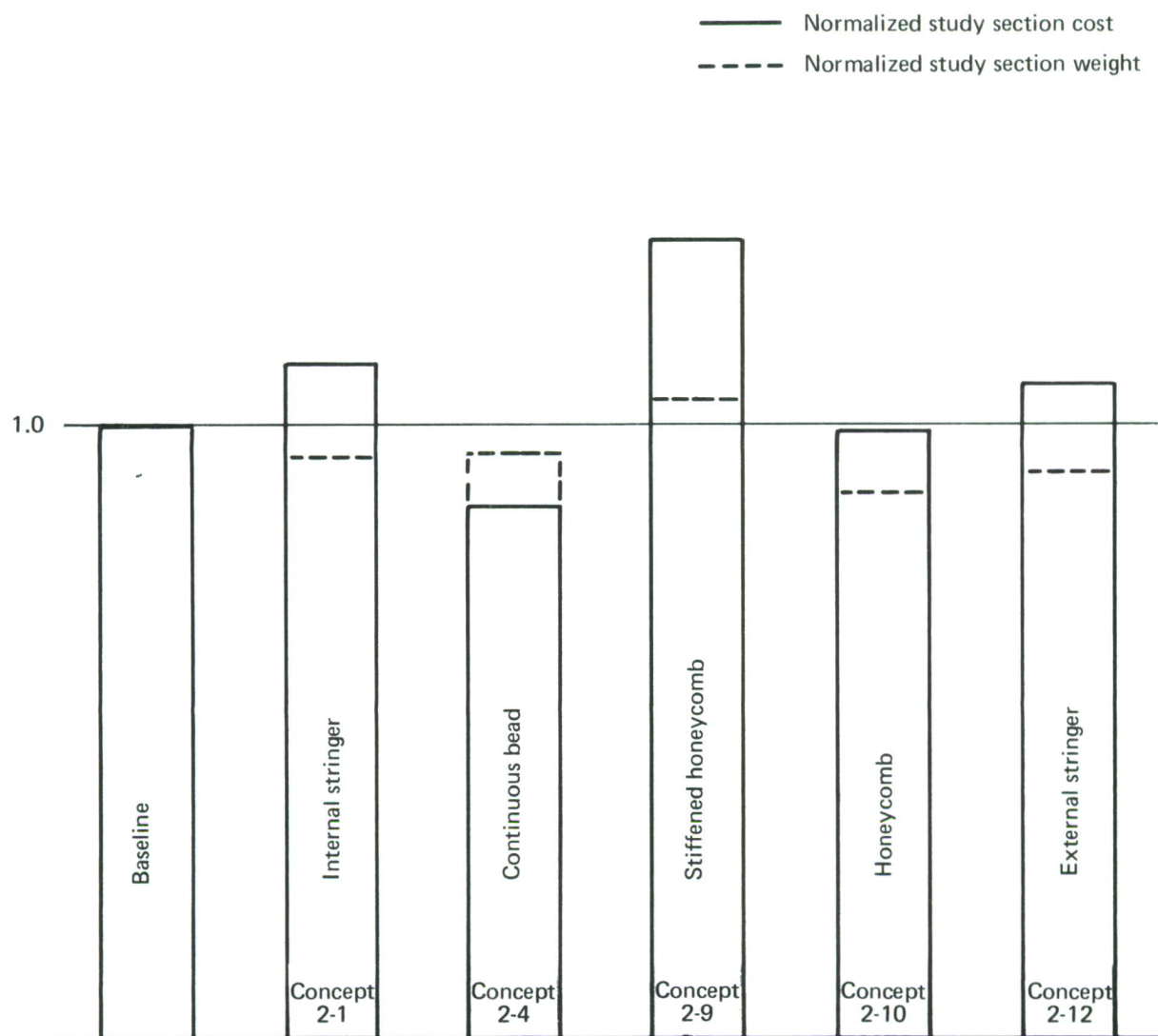
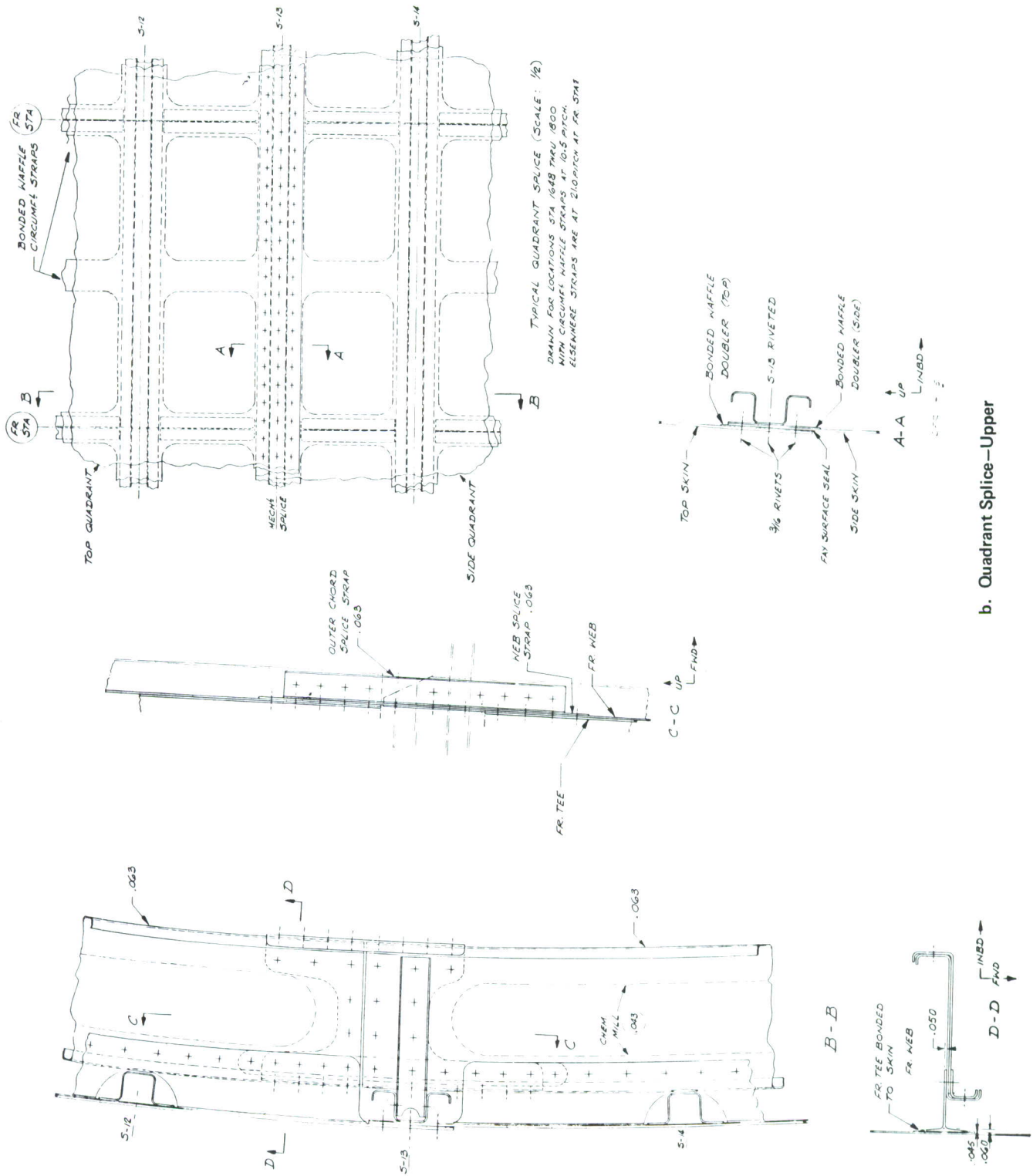


Figure 79.—Level 2 Shell Screening



135



b. Quadrant Splice—Upper

Figure 80.—Continued

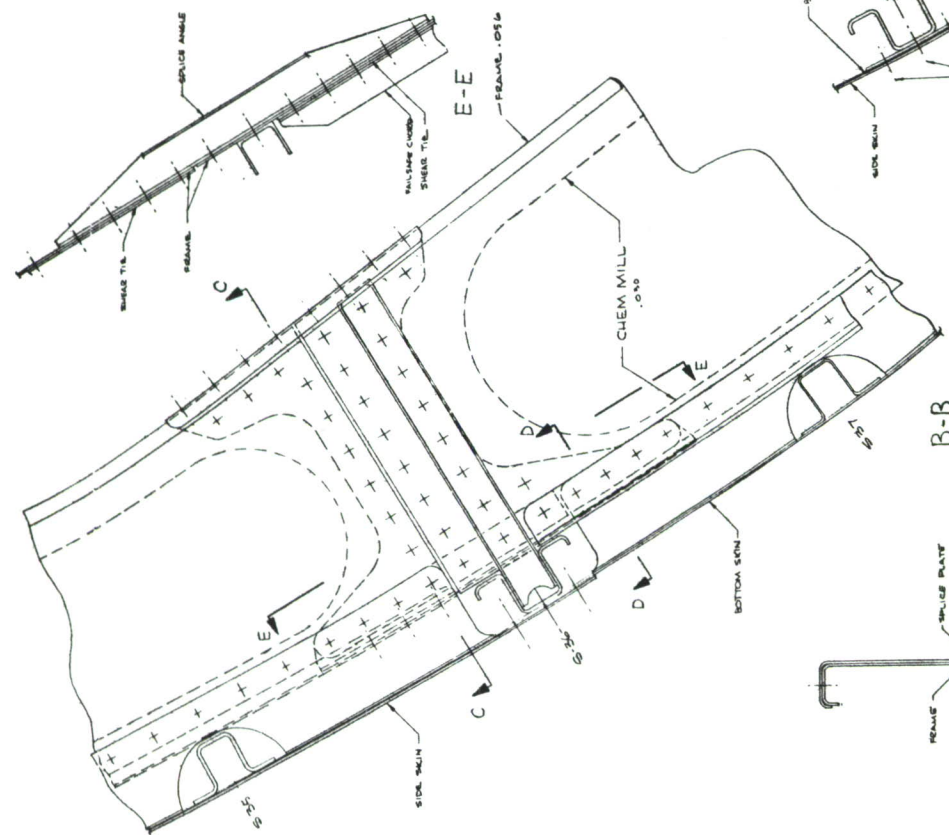
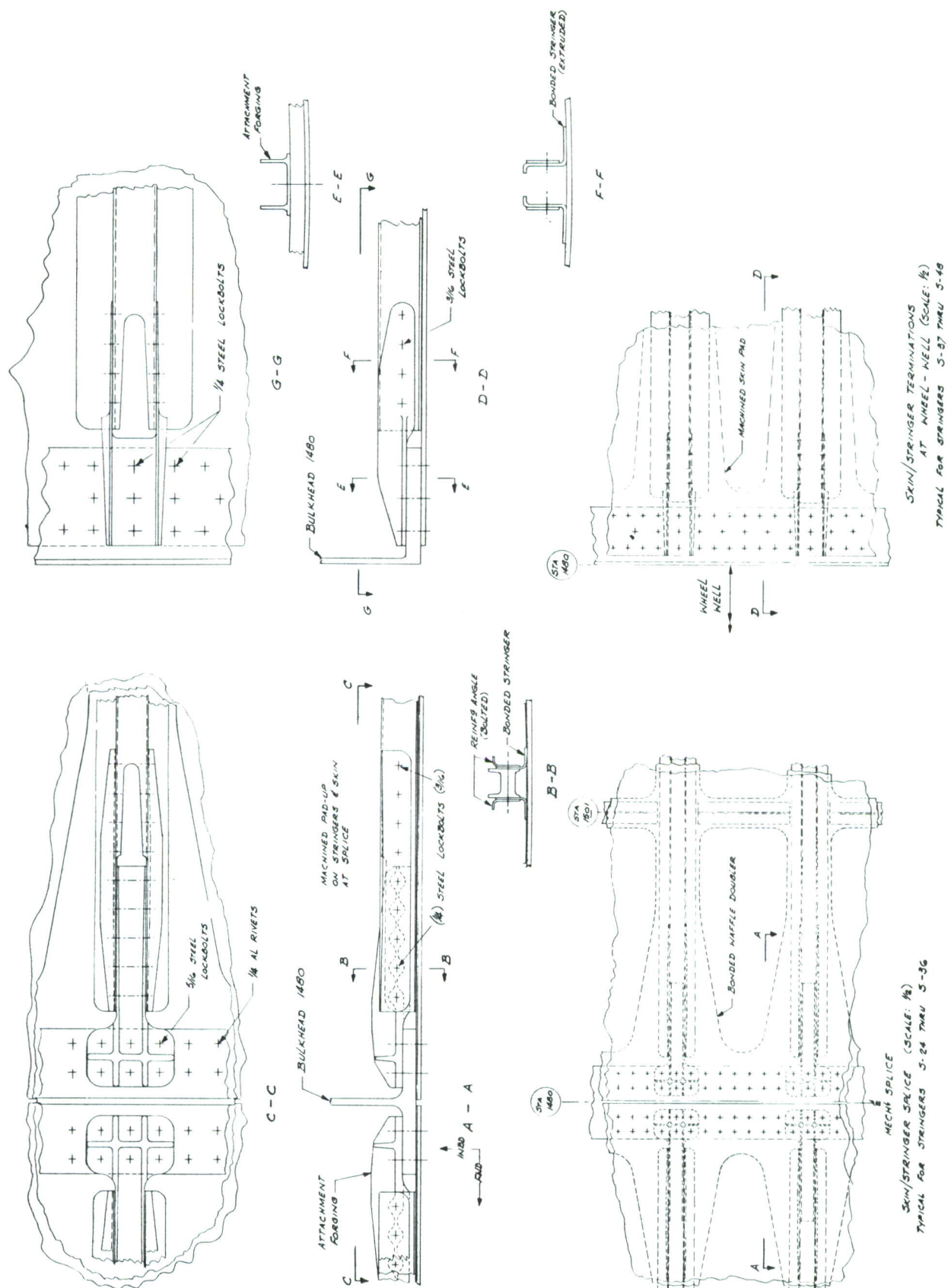


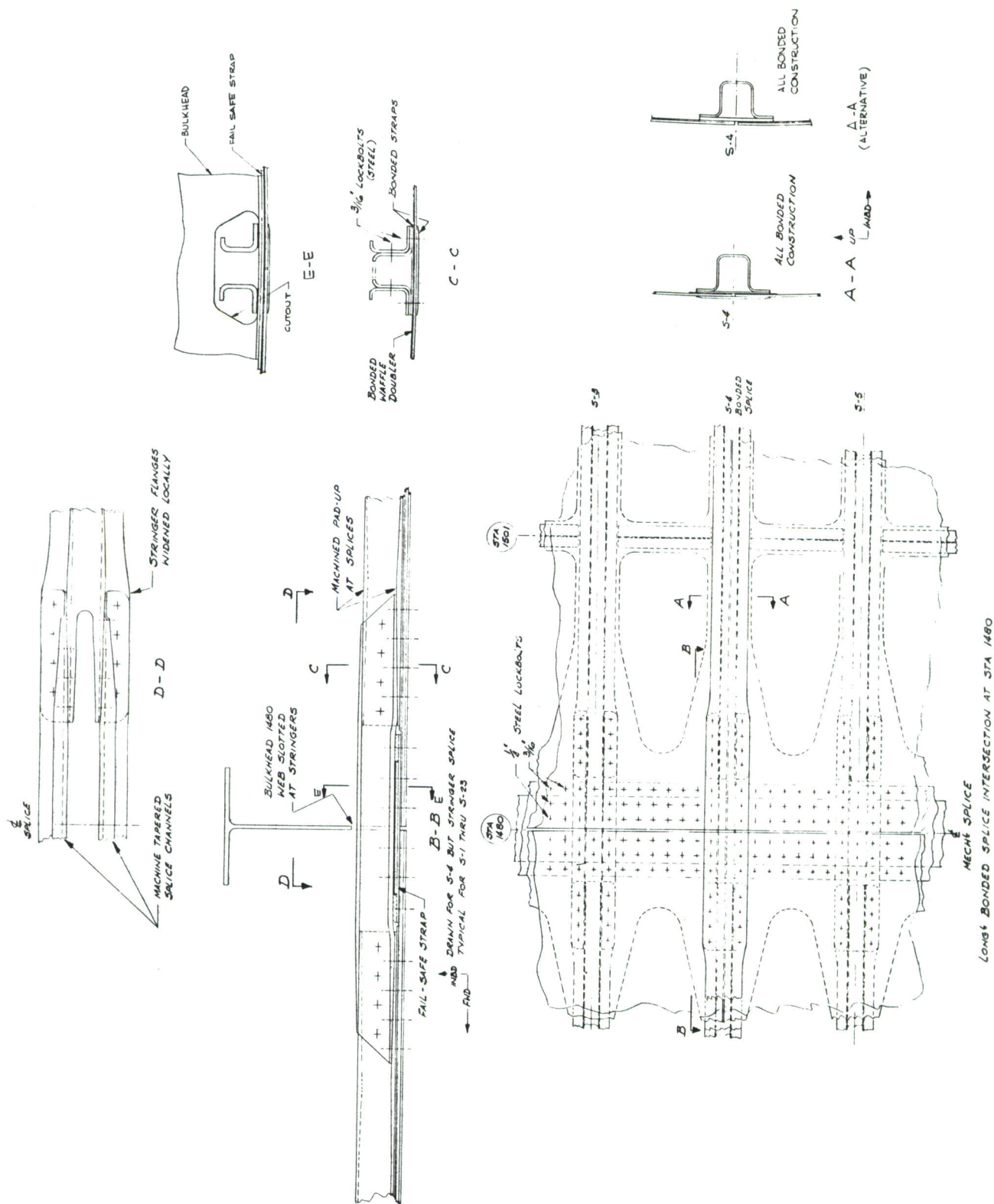
Figure 80.—Continued





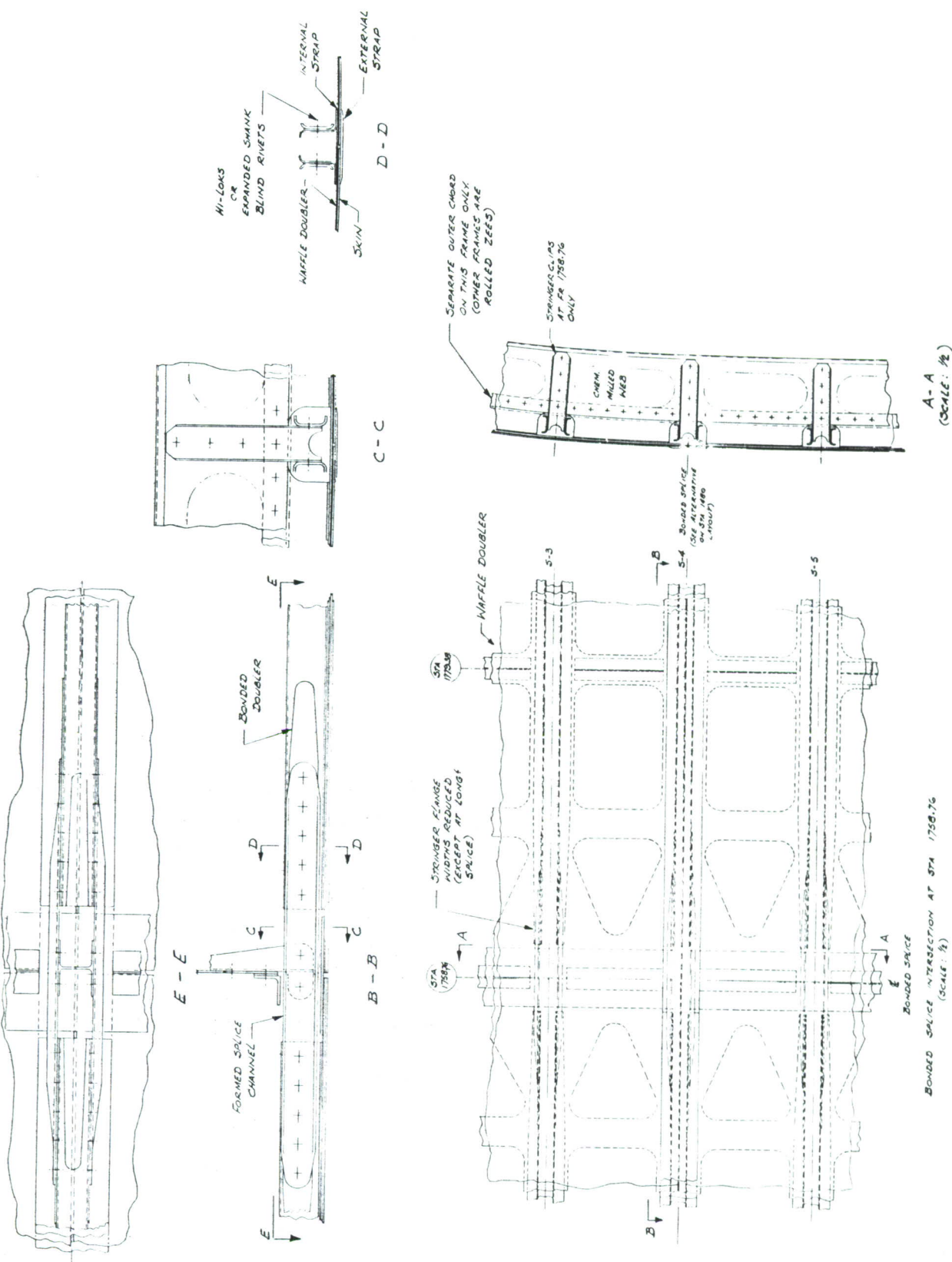
d. Stringer Joints at Body Station 1480

Figure 80.—Continued



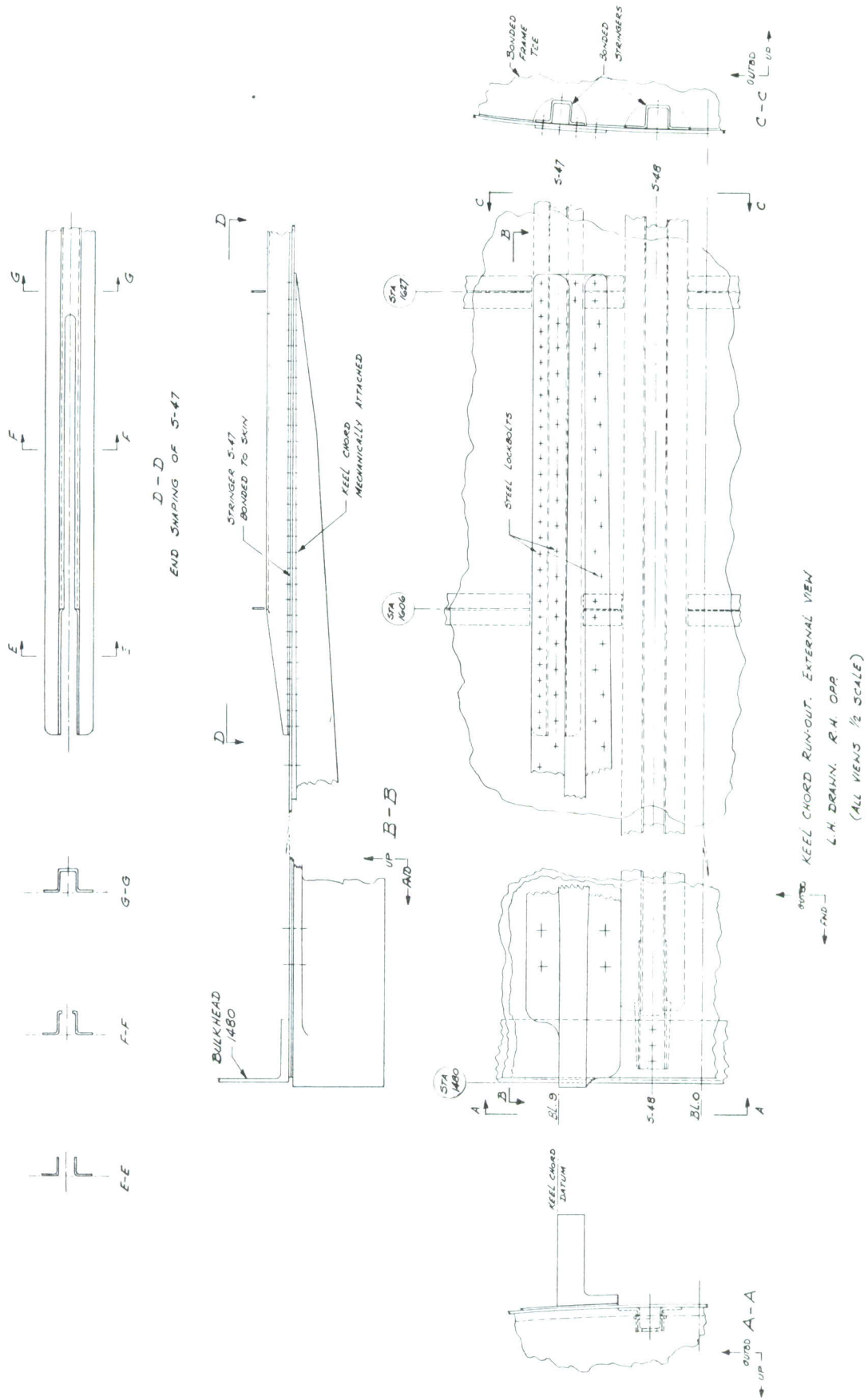
e. Bonded Splice Intersection at Body Station 1480

Figure 80.—Continued



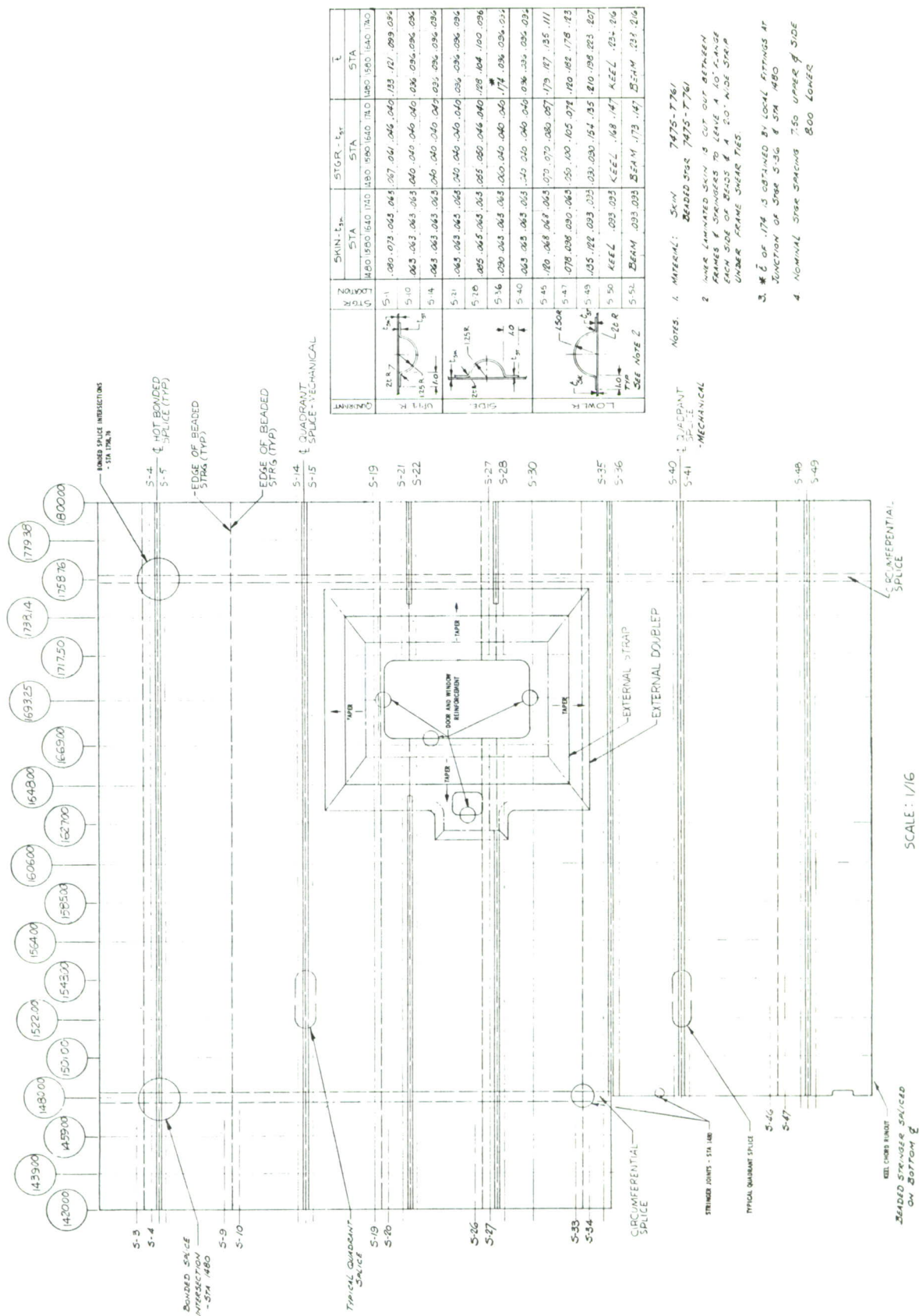
f. Bonded Splice Intersection at Body Station 1758.76

Figure 80.—Continued



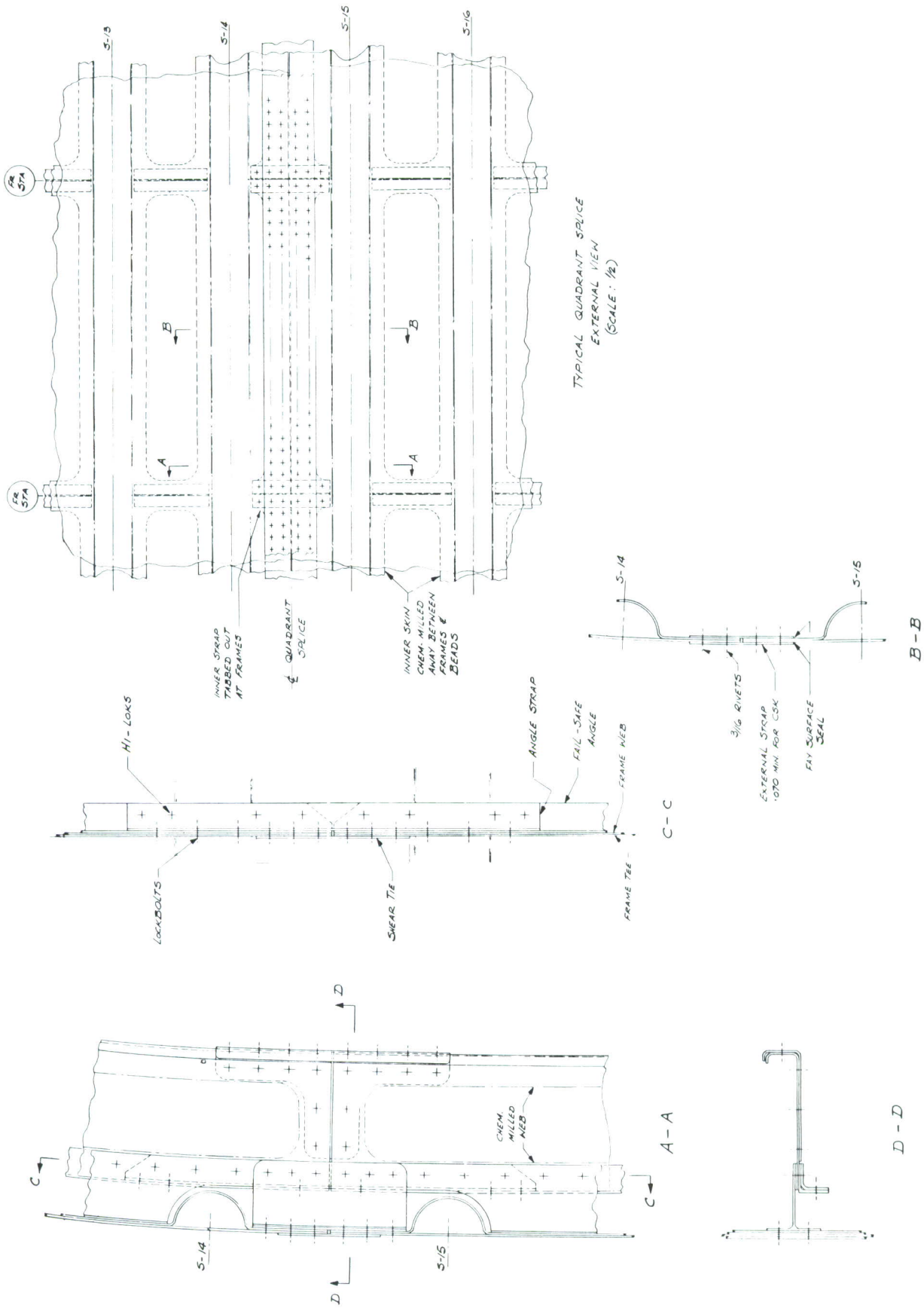
h. Keel Chord Runout

Figure 80.-Concluded



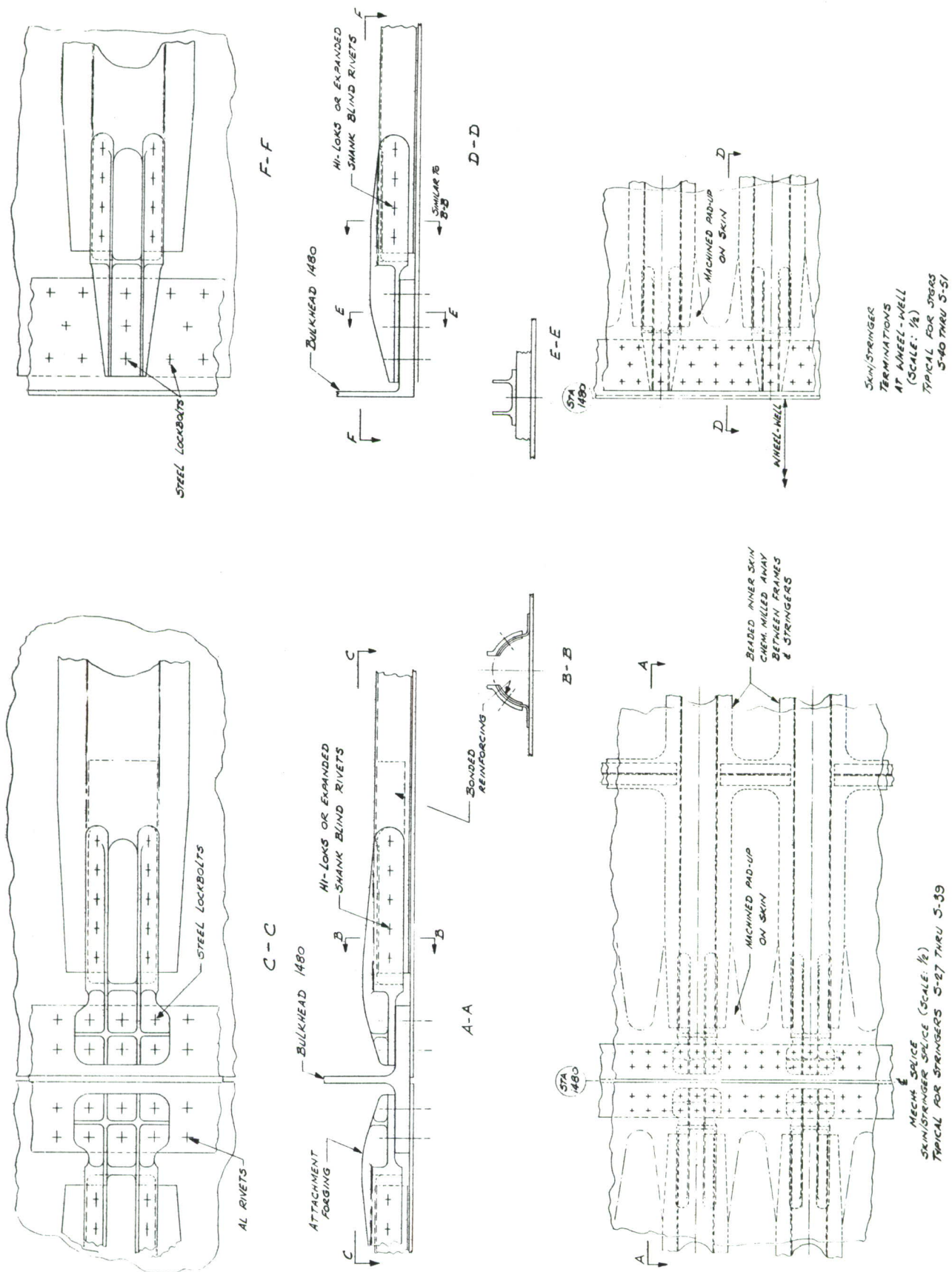
a. Developed Skin

Figure 81.—Continuous-Bead Shell (Concept 3-4)



b. Typical Quadrant Splice

Figure 81.—Continued

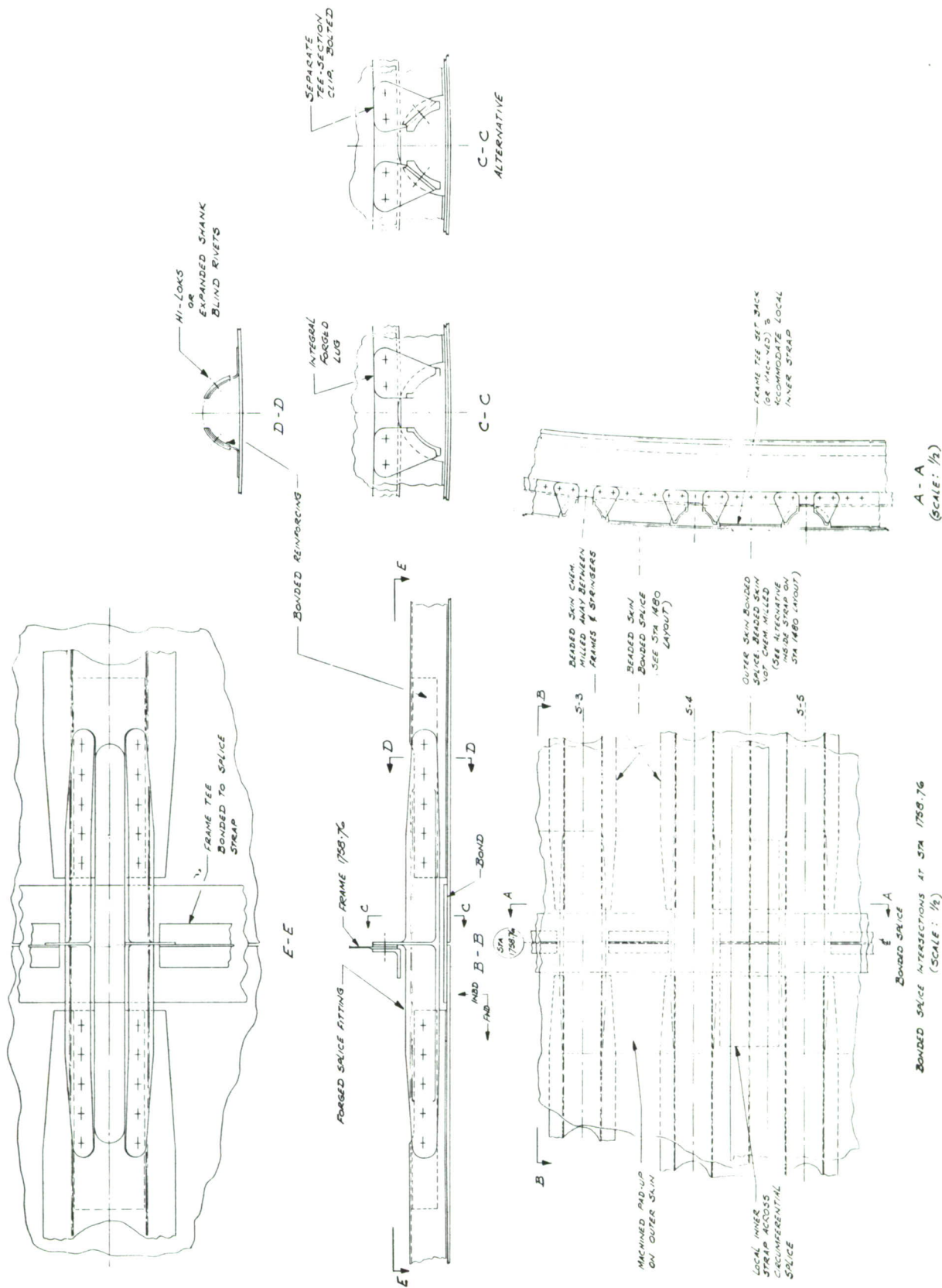


c. Stringer Joints at Body Station 1480

Figure 81.—Continued

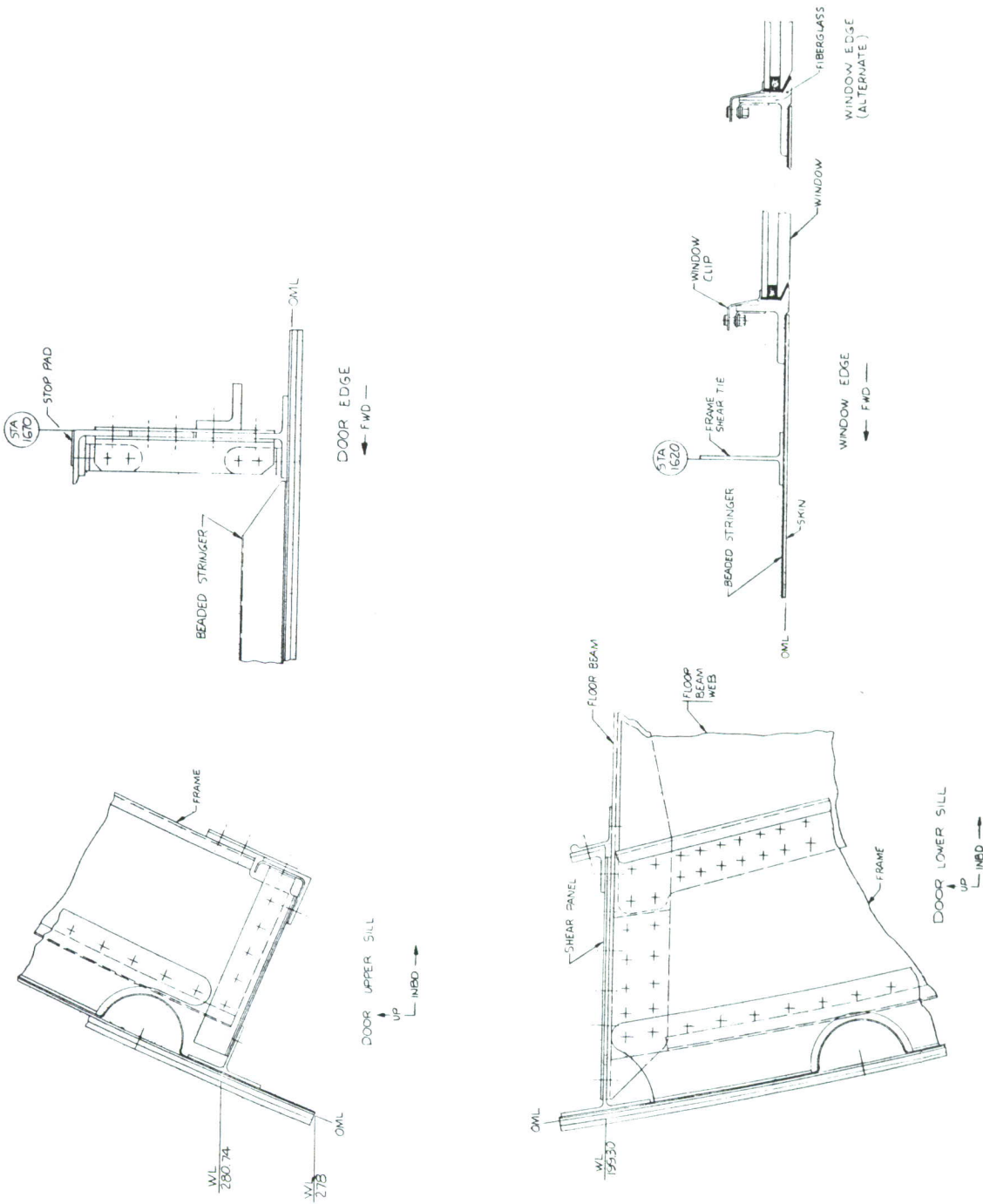


Figure 81.—Continued



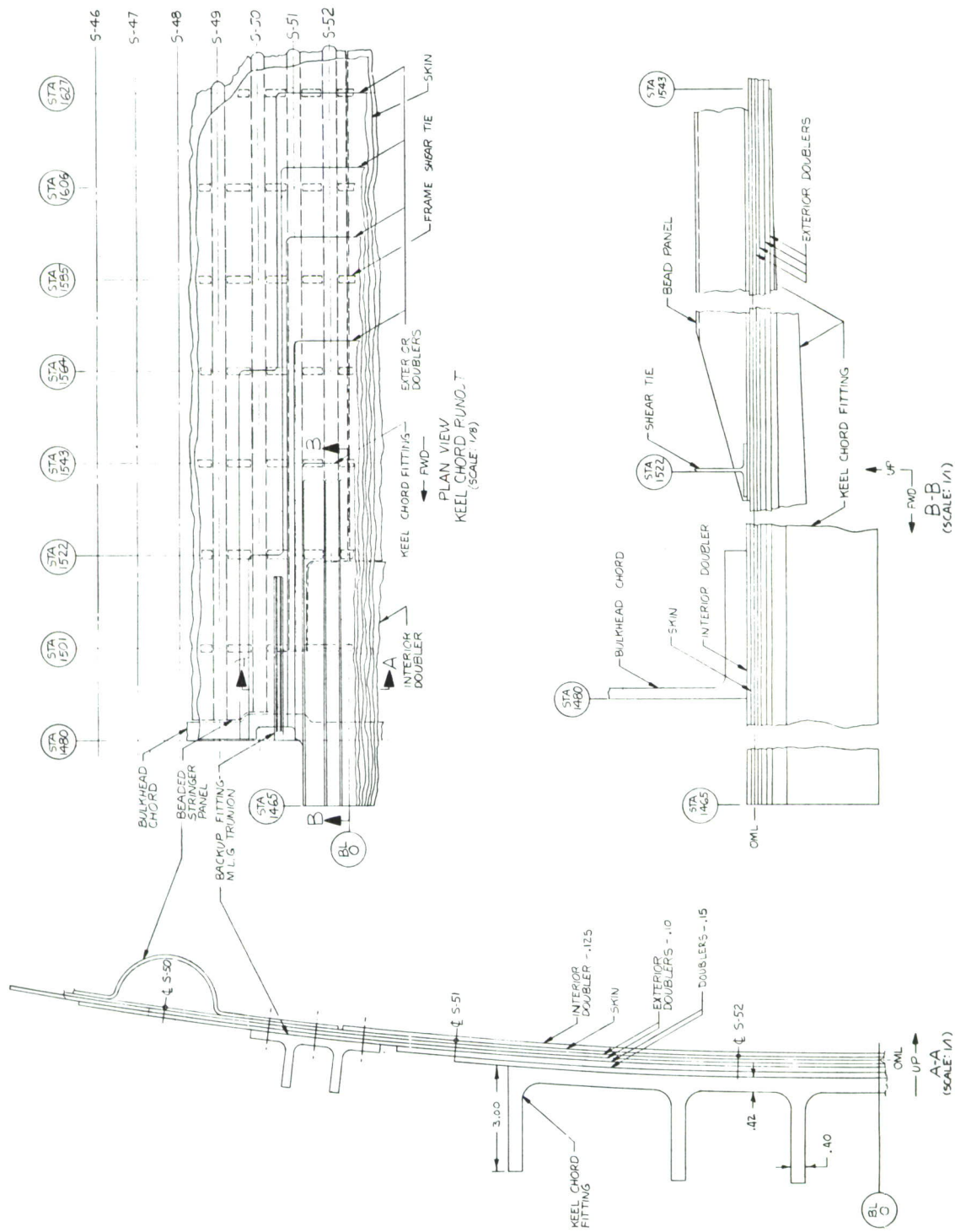
e. Bonded Splice Intersection at Body Station 1758.76

Figure 81-Continued



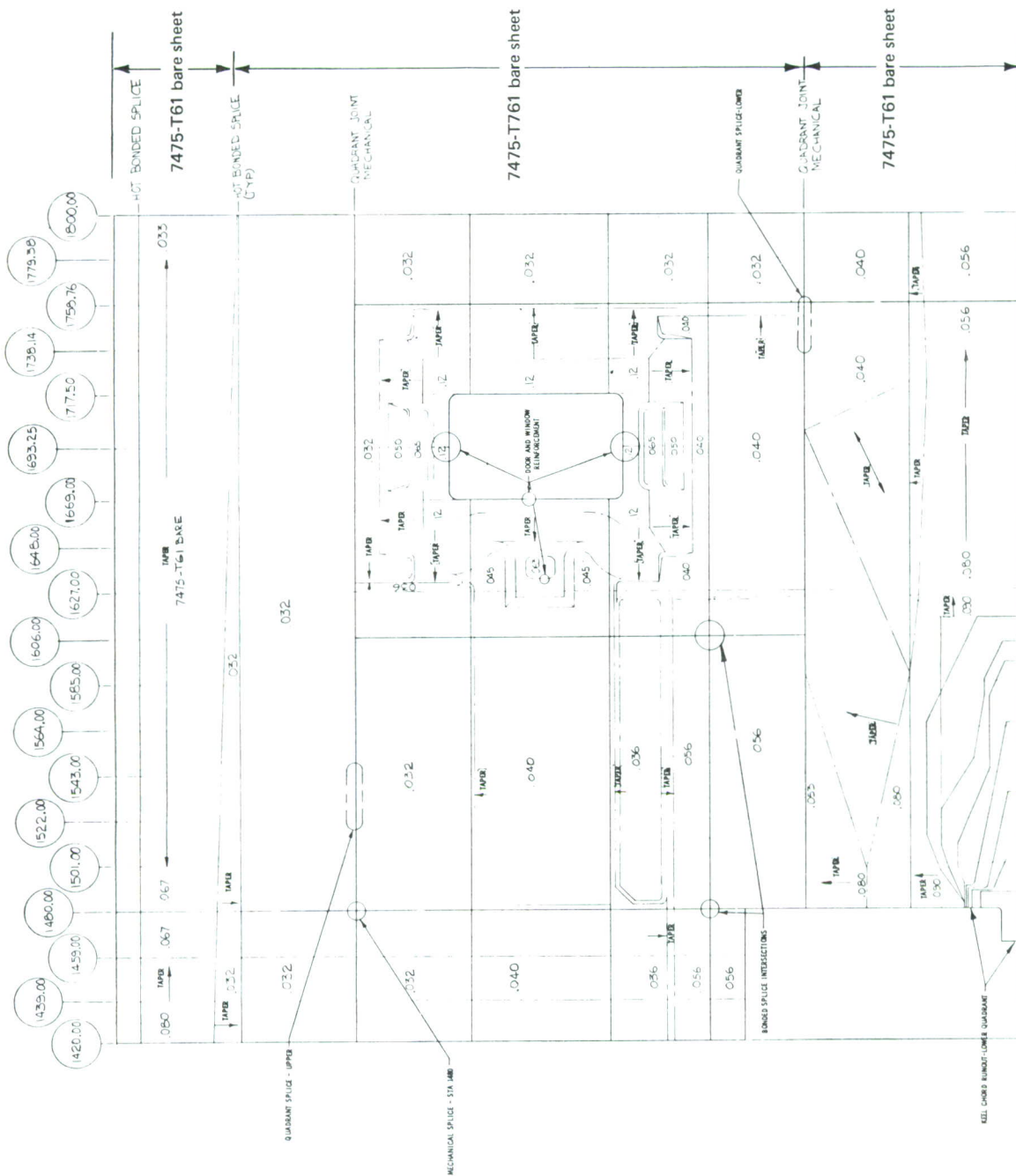
f. Door and Window Reinforcement

Figure 81.—Continued



g. Keel Chord Runout—Lower Quadrant

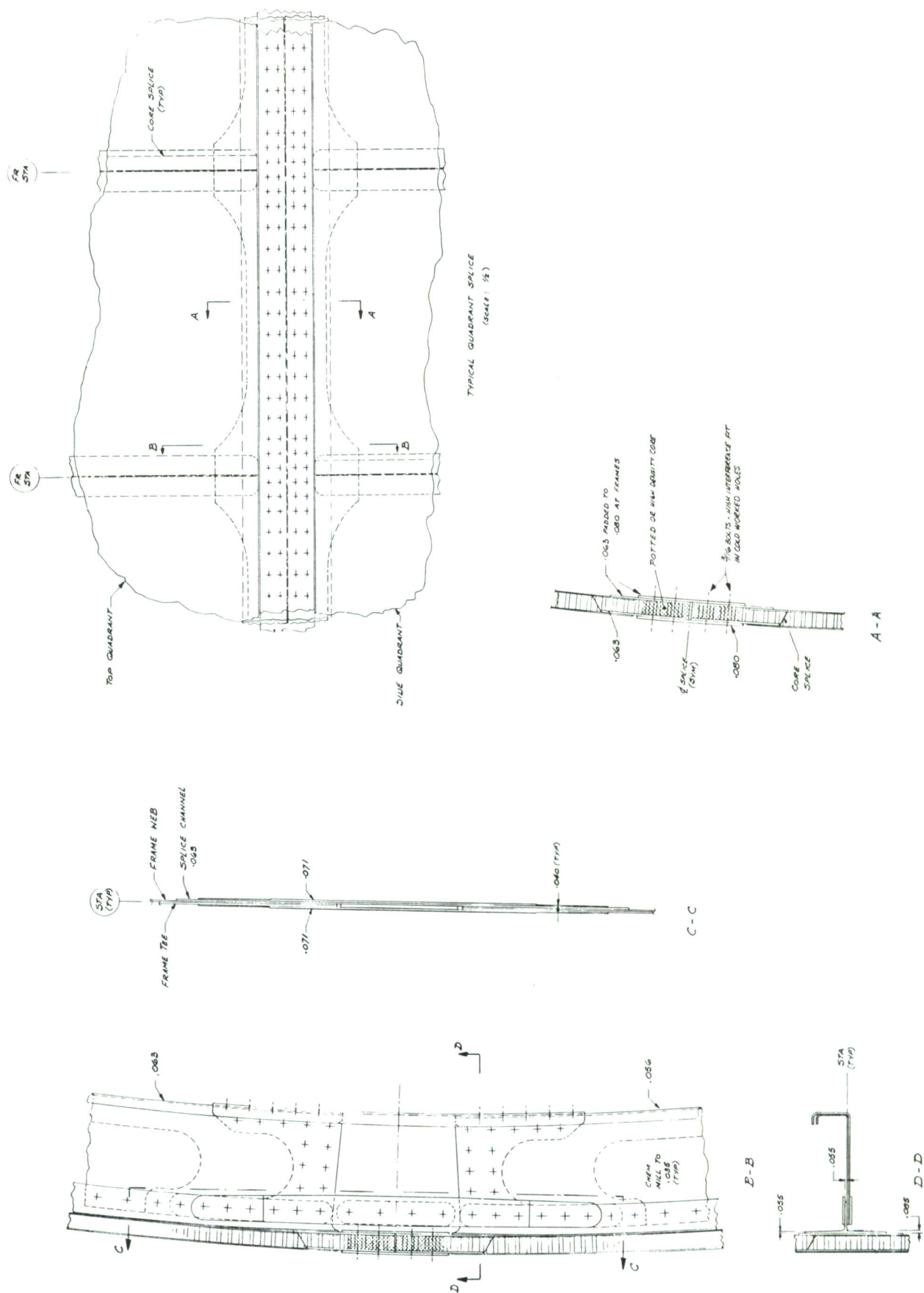
Figure 81.—Concluded



SKIN GAGE - EACH FACE
SCALE: 1/16

a. Developed Skin

Figure 82.-Honeycomb Shell (Concept 3-10)

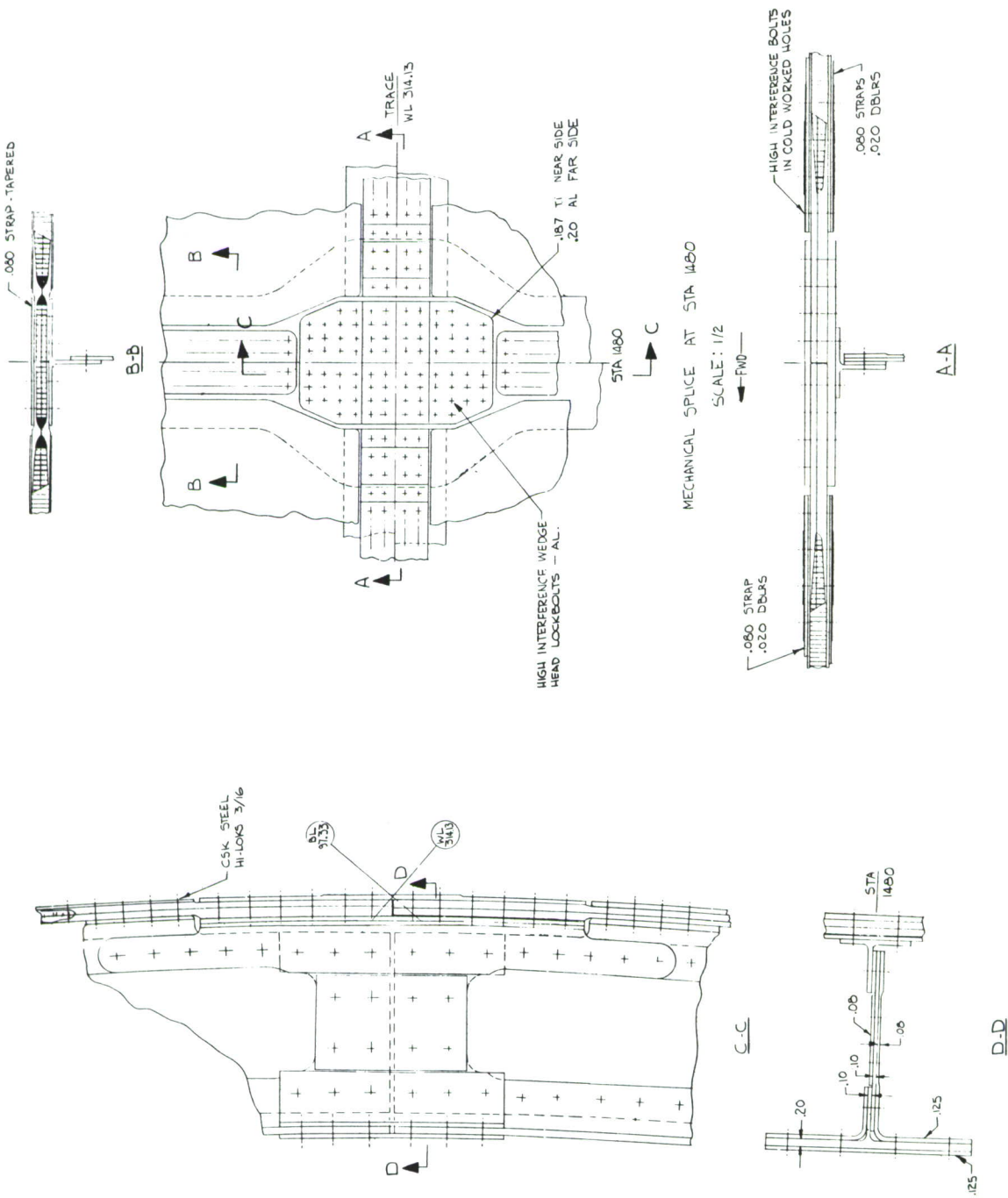


b. Quadrant Splice—Upper

Figure 82.—Continued

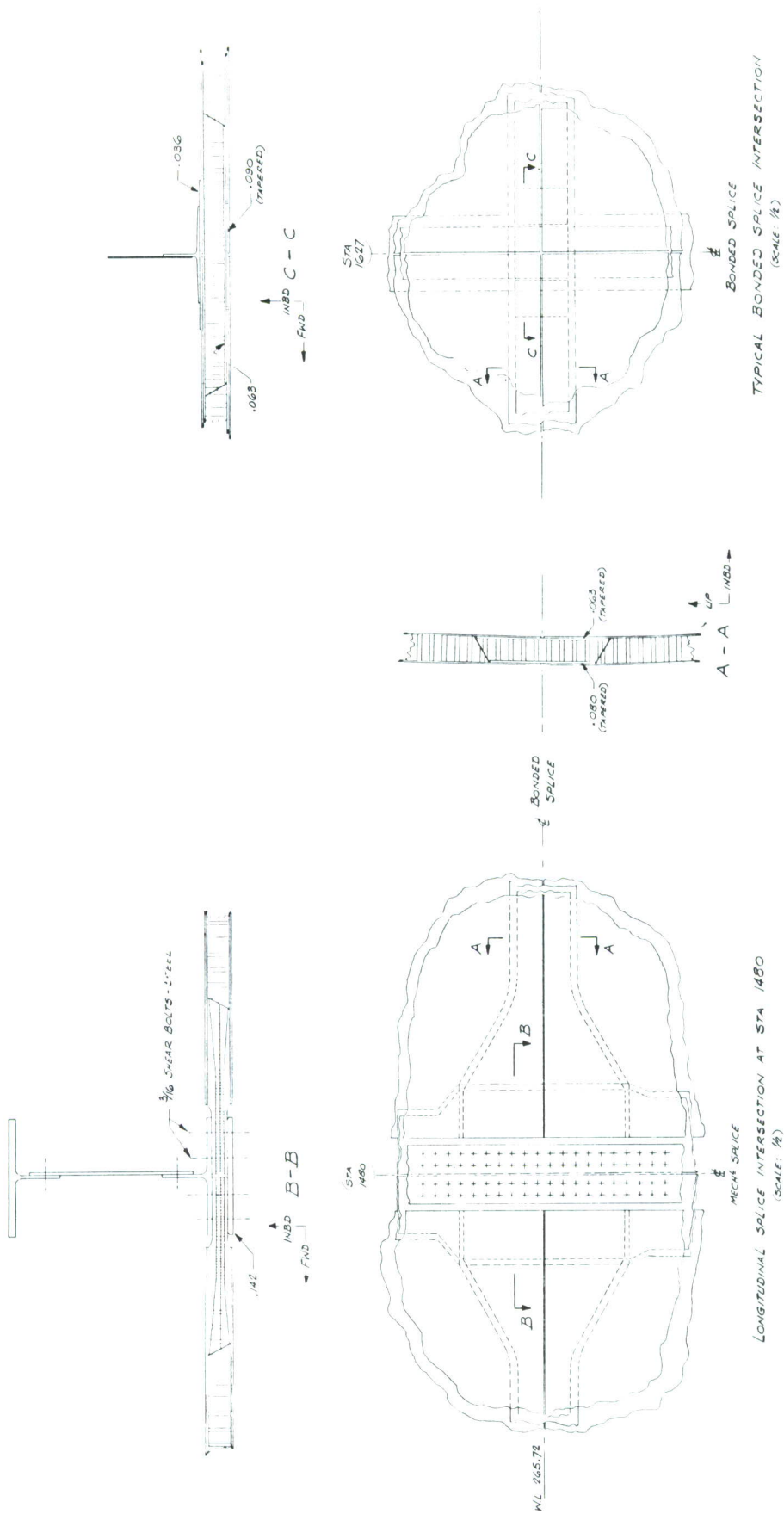
c. Quadrant Splice—Lower

Figure 82.—Continued



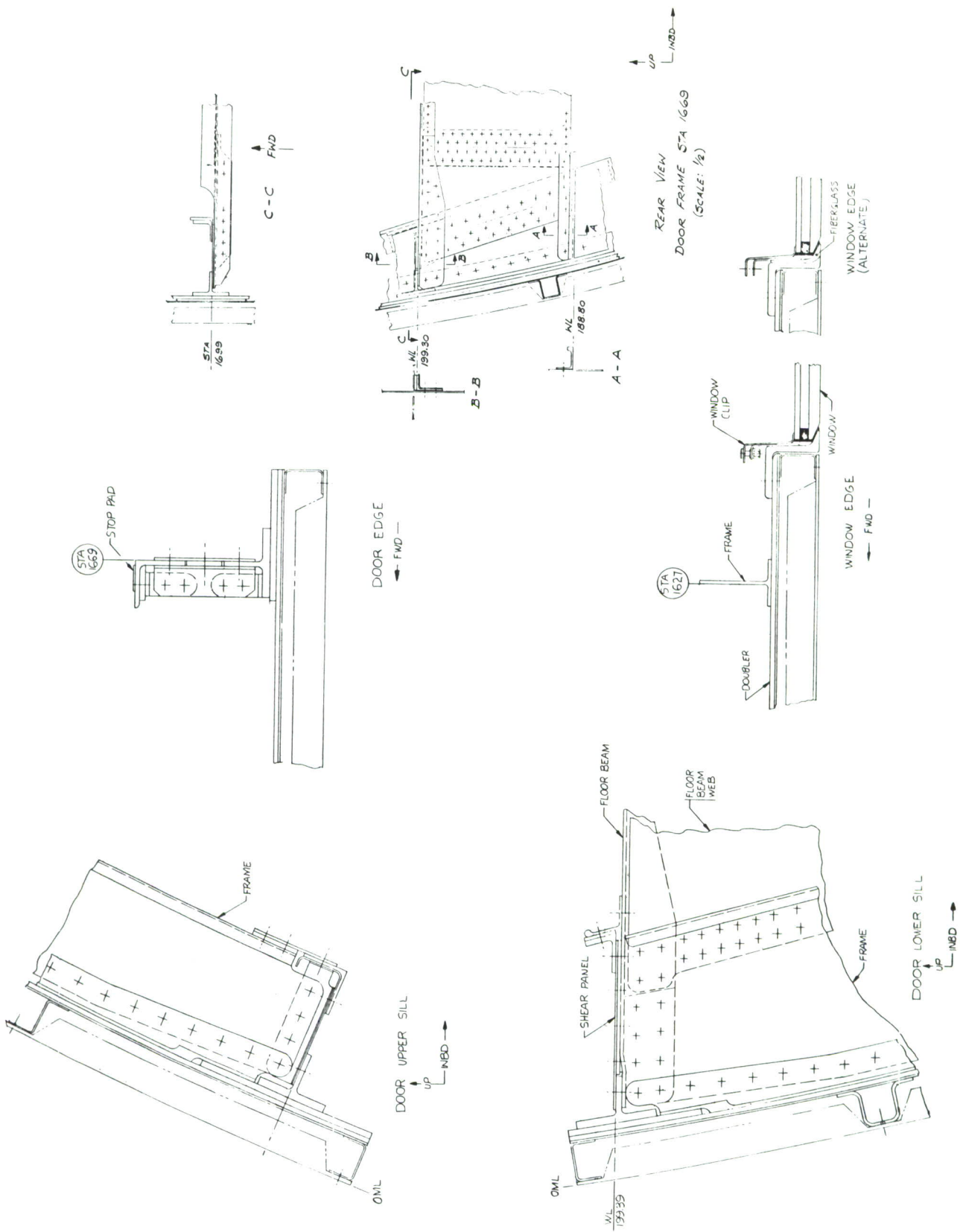
d. Mechanical Splice—Body Station 1480

Figure 82.—Continued



e. Bonded Splice Intersection

Figure 82.—Continued

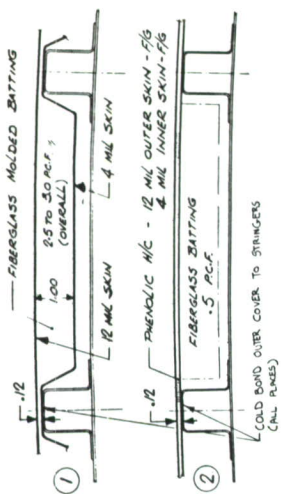


f. Door and Window Reinforcement

Figure 82.—Continued

g. Keel Chord Runout—Lower Quadrant

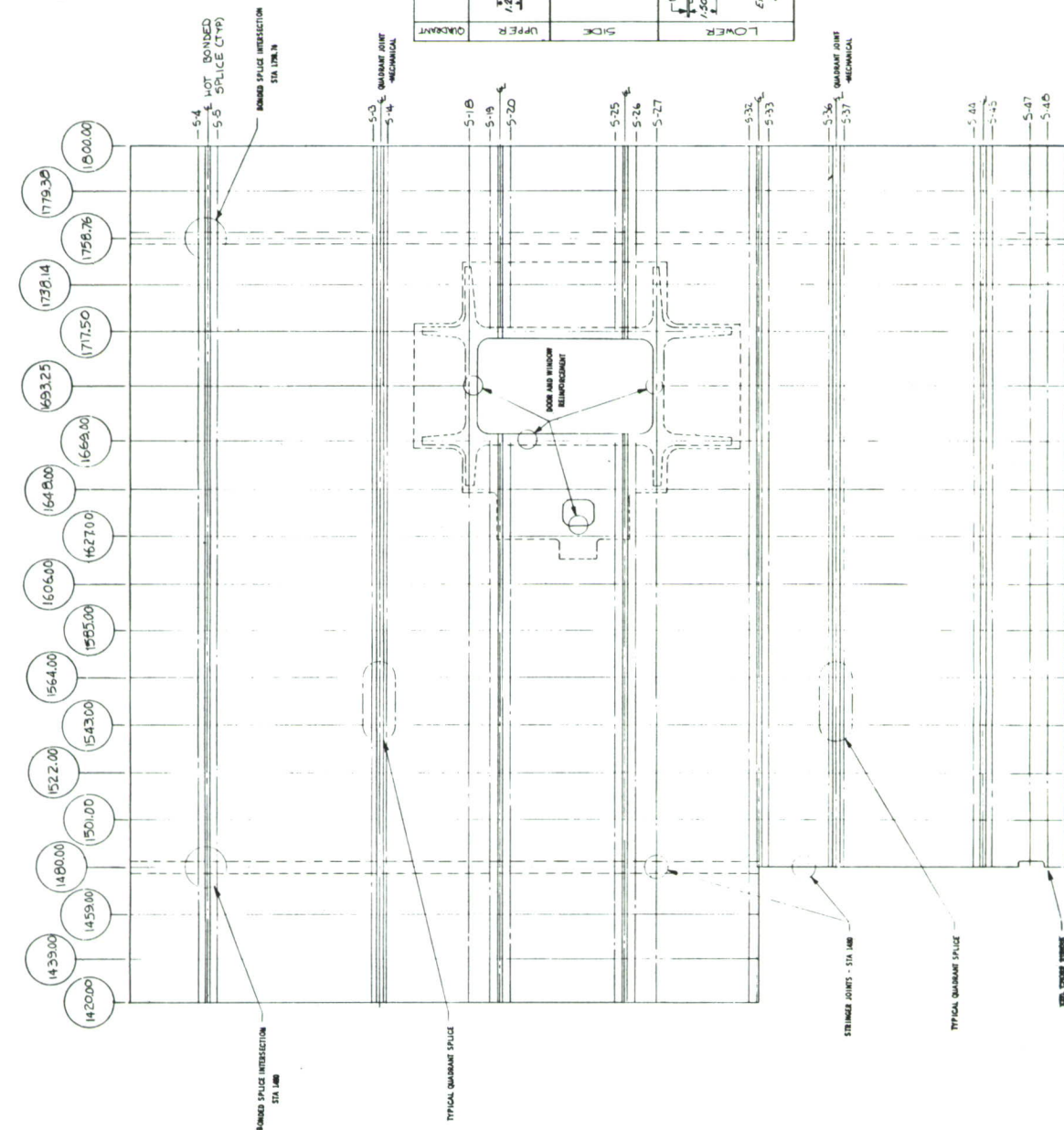
Figure 82.—Concluded



ALTERNATIVE OUTER COVERS

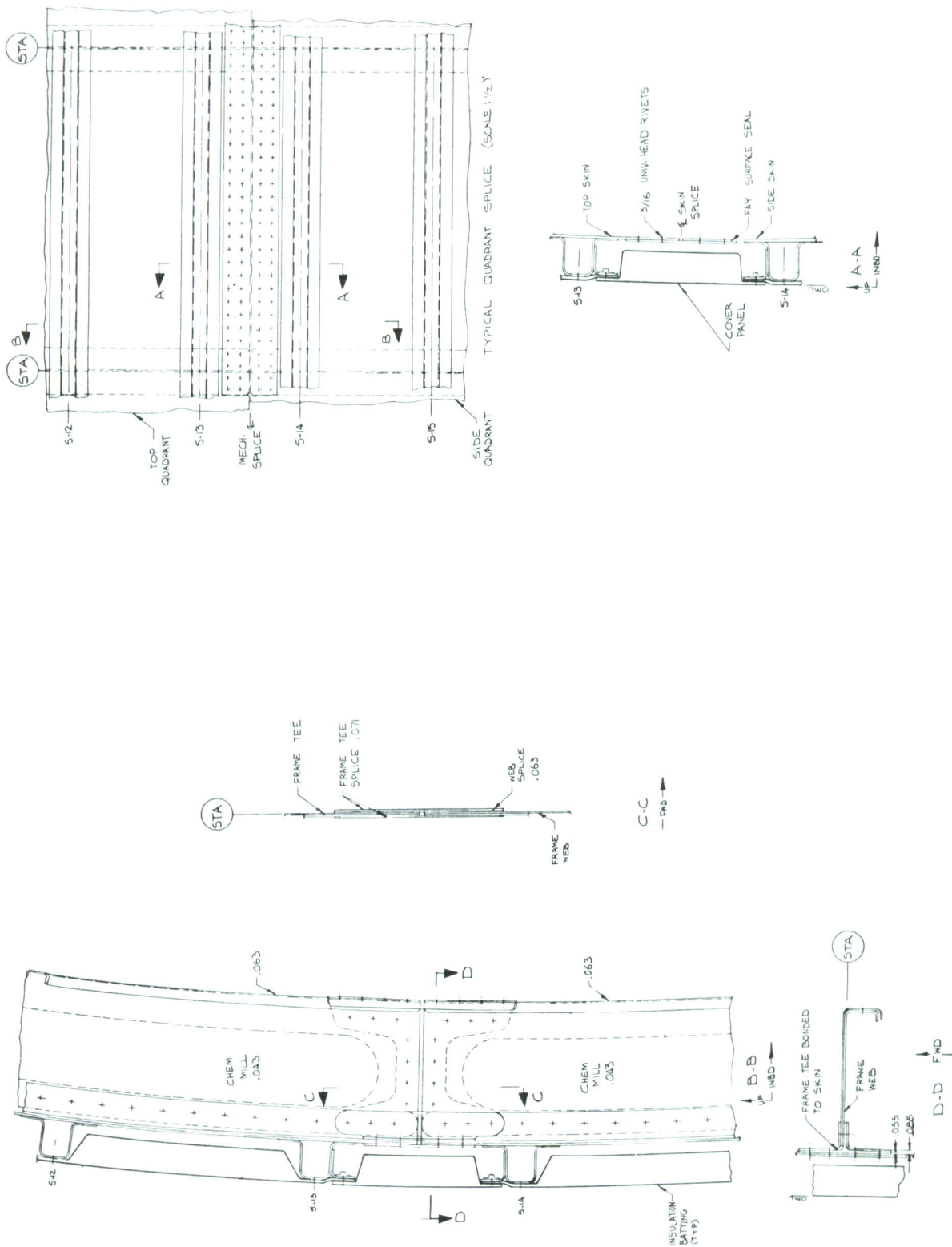
QUANT	LOTTN	SKIN - 1/4"	STR - 1/4"	STA	STA	STA
UPPER	5-1	1500 (140) 140	140 (150) 140	140	140	140
UPPER	5-2	1500 (140) 140	140 (150) 140	140	140	140
UPPER	5-3	1500 (140) 140	140 (150) 140	140	140	140
UPPER	5-4	1500 (140) 140	140 (150) 140	140	140	140
UPPER	5-5	1500 (140) 140	140 (150) 140	140	140	140
UPPER	5-6	1500 (140) 140	140 (150) 140	140	140	140
UPPER	5-7	1500 (140) 140	140 (150) 140	140	140	140
UPPER	5-8	1500 (140) 140	140 (150) 140	140	140	140
UPPER	5-9	1500 (140) 140	140 (150) 140	140	140	140
UPPER	5-10	1500 (140) 140	140 (150) 140	140	140	140
UPPER	5-11	1500 (140) 140	140 (150) 140	140	140	140
UPPER	5-12	1500 (140) 140	140 (150) 140	140	140	140
UPPER	5-13	1500 (140) 140	140 (150) 140	140	140	140
UPPER	5-14	1500 (140) 140	140 (150) 140	140	140	140
UPPER	5-15	1500 (140) 140	140 (150) 140	140	140	140
UPPER	5-16	1500 (140) 140	140 (150) 140	140	140	140
UPPER	5-17	1500 (140) 140	140 (150) 140	140	140	140
UPPER	5-18	1500 (140) 140	140 (150) 140	140	140	140
UPPER	5-19	1500 (140) 140	140 (150) 140	140	140	140
UPPER	5-20	1500 (140) 140	140 (150) 140	140	140	140
UPPER	5-21	1500 (140) 140	140 (150) 140	140	140	140
UPPER	5-22	1500 (140) 140	140 (150) 140	140	140	140
UPPER	5-23	1500 (140) 140	140 (150) 140	140	140	140
UPPER	5-24	1500 (140) 140	140 (150) 140	140	140	140
UPPER	5-25	1500 (140) 140	140 (150) 140	140	140	140
UPPER	5-26	1500 (140) 140	140 (150) 140	140	140	140
UPPER	5-27	1500 (140) 140	140 (150) 140	140	140	140
UPPER	5-28	1500 (140) 140	140 (150) 140	140	140	140
UPPER	5-29	1500 (140) 140	140 (150) 140	140	140	140
UPPER	5-30	1500 (140) 140	140 (150) 140	140	140	140
UPPER	5-31	1500 (140) 140	140 (150) 140	140	140	140
UPPER	5-32	1500 (140) 140	140 (150) 140	140	140	140
UPPER	5-33	1500 (140) 140	140 (150) 140	140	140	140
UPPER	5-34	1500 (140) 140	140 (150) 140	140	140	140
UPPER	5-35	1500 (140) 140	140 (150) 140	140	140	140
UPPER	5-36	1500 (140) 140	140 (150) 140	140	140	140
UPPER	5-37	1500 (140) 140	140 (150) 140	140	140	140
UPPER	5-38	1500 (140) 140	140 (150) 140	140	140	140
UPPER	5-39	1500 (140) 140	140 (150) 140	140	140	140
UPPER	5-40	1500 (140) 140	140 (150) 140	140	140	140
UPPER	5-41	1500 (140) 140	140 (150) 140	140	140	140
UPPER	5-42	1500 (140) 140	140 (150) 140	140	140	140
UPPER	5-43	1500 (140) 140	140 (150) 140	140	140	140
UPPER	5-44	1500 (140) 140	140 (150) 140	140	140	140
UPPER	5-45	1500 (140) 140	140 (150) 140	140	140	140
UPPER	5-46	1500 (140) 140	140 (150) 140	140	140	140
UPPER	5-47	1500 (140) 140	140 (150) 140	140	140	140
UPPER	5-48	1500 (140) 140	140 (150) 140	140	140	140
UPPER	5-49	1500 (140) 140	140 (150) 140	140	140	140
UPPER	5-50	1500 (140) 140	140 (150) 140	140	140	140
UPPER	5-51	1500 (140) 140	140 (150) 140	140	140	140
UPPER	5-52	1500 (140) 140	140 (150) 140	140	140	140
UPPER	5-53	1500 (140) 140	140 (150) 140	140	140	140
UPPER	5-54	1500 (140) 140	140 (150) 140	140	140	140
UPPER	5-55	1500 (140) 140	140 (150) 140	140	140	140
UPPER	5-56	1500 (140) 140	140 (150) 140	140	140	140
UPPER	5-57	1500 (140) 140	140 (150) 140	140	140	140
UPPER	5-58	1500 (140) 140	140 (150) 140	140	140	140
UPPER	5-59	1500 (140) 140	140 (150) 140	140	140	140
UPPER	5-60	1500 (140) 140	140 (150) 140	140	140	140
UPPER	5-61	1500 (140) 140	140 (150) 140	140	140	140
UPPER	5-62	1500 (140) 140	140 (150) 140	140	140	140
UPPER	5-63	1500 (140) 140	140 (150) 140	140	140	140
UPPER	5-64	1500 (140) 140	140 (150) 140	140	140	140
UPPER	5-65	1500 (140) 140	140 (150) 140	140	140	140
UPPER	5-66	1500 (140) 140	140 (150) 140	140	140	140
UPPER	5-67	1500 (140) 140	140 (150) 140	140	140	140
UPPER	5-68	1500 (140) 140	140 (150) 140	140	140	140
UPPER	5-69	1500 (140) 140	140 (150) 140	140	140	140
UPPER	5-70	1500 (140) 140	140 (150) 140	140	140	140
UPPER	5-71	1500 (140) 140	140 (150) 140	140	140	140
UPPER	5-72	1500 (140) 140	140 (150) 140	140	140	140
UPPER	5-73	1500 (140) 140	140 (150) 140	140	140	140
UPPER	5-74	1500 (140) 140	140 (150) 140	140	140	140
UPPER	5-75	1500 (140) 140	140 (150) 140	140	140	140
UPPER	5-76	1500 (140) 140	140 (150) 140	140	140	140
UPPER	5-77	1500 (140) 140	140 (150) 140	140	140	140
UPPER	5-78	1500 (140) 140	140 (150) 140	140	140	140
UPPER	5-79	1500 (140) 140	140 (150) 140	140	140	140
UPPER	5-80	1500 (140) 140	140 (150) 140	140	140	140
UPPER	5-81	1500 (140) 140	140 (150) 140	140	140	140
UPPER	5-82	1500 (140) 140	140 (150) 140	140	140	140
UPPER	5-83	1500 (140) 140	140 (150) 140	140	140	140
UPPER	5-84	1500 (140) 140	140 (150) 140	140	140	140
UPPER	5-85	1500 (140) 140	140 (150) 140	140	140	140
UPPER	5-86	1500 (140) 140	140 (150) 140	140	140	140
UPPER	5-87	1500 (140) 140	140 (150) 140	140	140	140
UPPER	5-88	1500 (140) 140	140 (150) 140	140	140	140
UPPER	5-89	1500 (140) 140	140 (150) 140	140	140	140
UPPER	5-90	1500 (140) 140	140 (150) 140	140	140	140
UPPER	5-91	1500 (140) 140	140 (150) 140	140	140	140
UPPER	5-92	1500 (140) 140	140 (150) 140	140	140	140
UPPER	5-93	1500 (140) 140	140 (150) 140	140	140	140
UPPER	5-94	1500 (140) 140	140 (150) 140	140	140	140
UPPER	5-95	1500 (140) 140	140 (150) 140	140	140	140
UPPER	5-96	1500 (140) 140	140 (150) 140	140	140	140
UPPER	5-97	1500 (140) 140	140 (150) 140	140	140	140
UPPER	5-98	1500 (140) 140	140 (150) 140	140	140	140
UPPER	5-99	1500 (140) 140	140 (150) 140	140	140	140
UPPER	5-100	1500 (140) 140	140 (150) 140	140	140	140

- NOTES.
1. MATERIAL: SKIN AND DOUBLES 7475 - 7761 BARE
STRIPS 5-1740 5-36 7475 - 7761 BARE
STRIPS 5-37 7475 5-49 7078-76511
 2. A. C. OF 1740 IS OBTAINED BY LOCAL FITTINGS
 3. AT JUNCTION OF STRIP 5-33 & STA 1480
2" WIDE x .025 CIRCUMFERENTIAL TEAR STRIPS
BONDED TO INSIDE OF SKIN MIDWAY BETWEEN
FRAMES AFT OF STA 1640 & EXTENDING FROM
STRIP 5-36 L TO 5-36 R
 4. NOMINAL STRIP SPACING 9.00



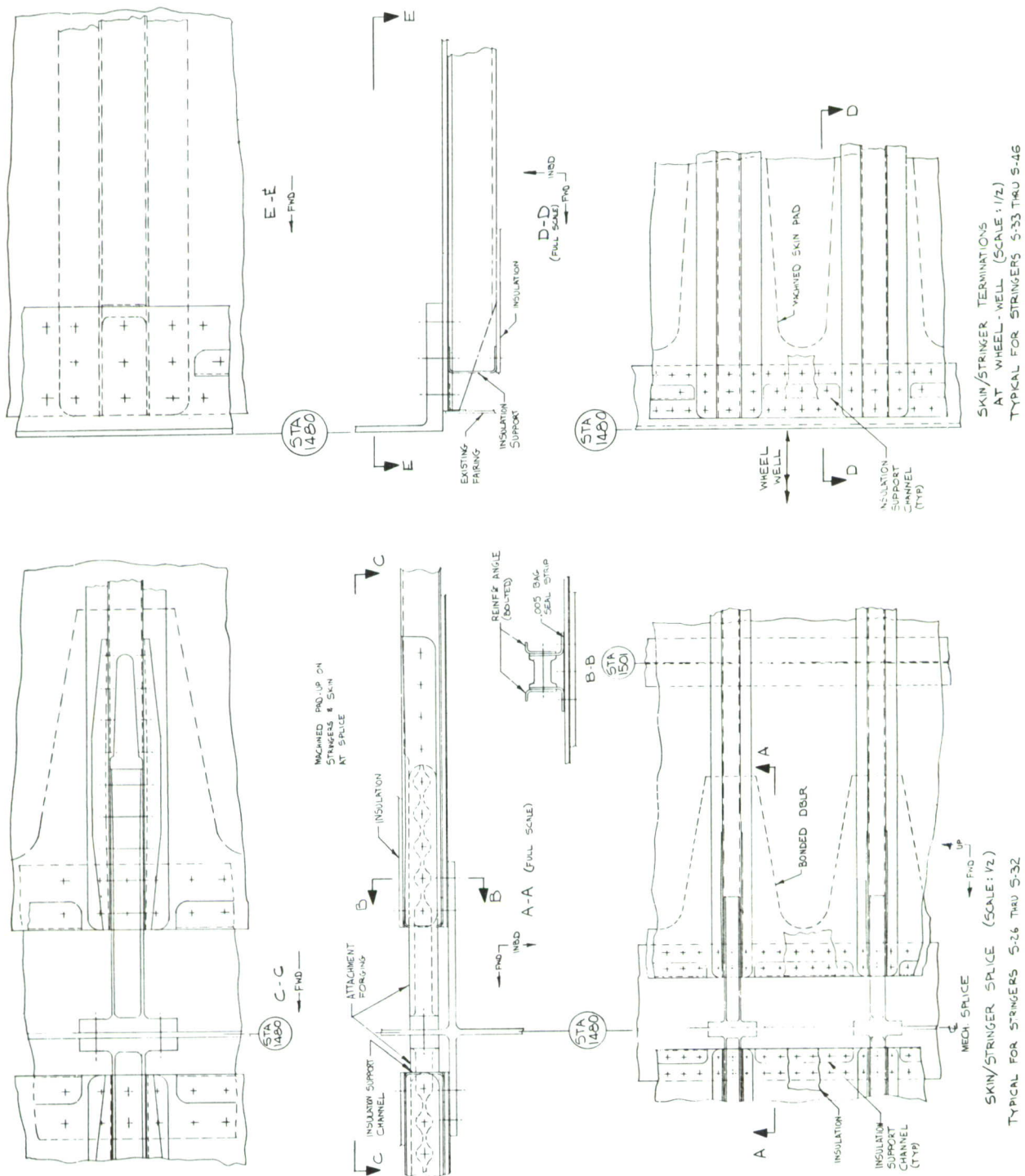
a. Developed Skin

Figure 83.—External Stringer Shell (Concept 3-12)



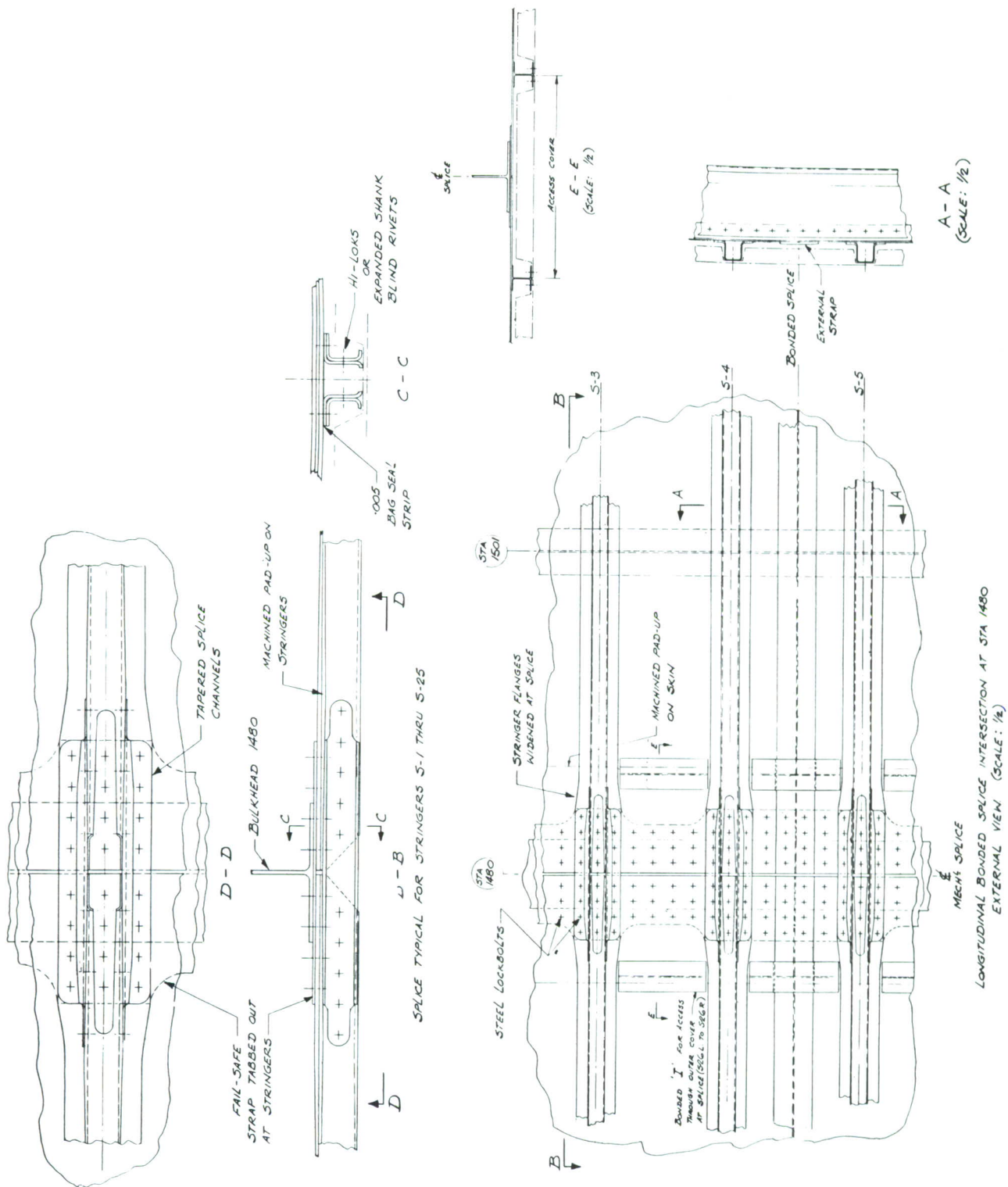
b. Typical Quadrant Splice

Figure 83.—Continued



c. Stringer Joints at Body Station 1480

Figure 83.—Continued



d. Bonded Splice Intersection at Body Station 1480



f. Door and Window Reinforcement

Figure 83.—Continued

*Table XIX. –Level 3 Weight and Cost Summary by Quadrant,
Cargo Fuselage Study
(Average of 201 Airplanes), Station 1420-1800 –All Concepts*

Item	Baseline		Internal stringer Concept 3-1		Continuous bead Concept 3-4		Honeycomb Concept 3-10		External stringer Concept 3-12	
	2024/7075 weight (lb)	Total (1973 \$)	7475 weight (lb)	Total (1973 \$)	7475 weight (lb)	Total (1973 \$)	7475 weight (lb)	Total (1973 \$)	7475 weight (lb)	Total (1973 \$)
Upper quadrant										
Skin and stringer/core	753	23,991	614	24,109	636	23,318	545	23,318	582	17,449
Frames	142	9,008	138	8,974	158	9,146	130	8,655	130	8,905
Splices, fasteners, and edges	49	1,206	45	1,200	58	1,312	263	3,051	45	1,200
Straps	28	1,081	14	961	0	0	0	0	4	874
External insulation ^a	0	0	0	0	0	0	0	0	13	1,680
Total	972	35,286	811	35,244	852	33,776	909	33,904	774	30,108
Side quadrant										
Skin and stringer/core	1,748	76,220	1,643	67,364	1,676	68,263	1,356	74,577	1,584	654
Frames	336	29,832	291	28,268	340	28,940	173	26,691	269	27,519
Splices, fasteners, and edges	84	15,228	81	16,406	104	15,008	522	19,004	81	13,886
Straps	24	1,243	23	1,234	0	0	0	0	6	1,088
External insulation ^a	0	0	0	0	0	0	0	0	24	3,049
Total	2,192	122,523	2,038	113,272	2,120	112,211	2,051	120,272	1,964	101,196
Lower quadrant										
Skin and stringer/core	1,721	56,723	1,185	35,442	1,339	38,814	1,111	52,137	1,184	35,798
Frames	484	24,444	443	23,699	443	23,979	252	21,772	443	23,419
Splices, fasteners, and edges	64	4,864	50	4,155	39	5,572	185	5,907	50	5,611
External insulation ^a	0	0	0	0	0	0	0	0	12	1,493
Total	2,269	86,031	1,678	63,296	1,821	68,365	1,548	79,816	1,689	66,321
Sized section 1480-1741 total	5,433	243,840	4,527	211,812	4,793	214,352	4,508	233,992	4,427	197,625
Shell extensions total (Sta 1420-1480 and 1741-1800)	2,199	107,995	1,829	93,242	1,881	94,558	1,858	105,056	1,766	84,654
Total of items studied	7,632	351,835	6,356	305,054	6,674	308,910	6,366	339,048	6,192	282,279
Items held constant										
Section 44 lower lobe	1,195	47,800	1,195	47,800	1,195	47,800	1,195	47,800	1,195	47,800
Sta 1480 bulkhead	299	9,568	299	9,568	299	9,568	299	9,568	299	9,568
Aft keel beam	785	39,250	785	39,250	785	39,250	785	39,250	785	39,250
Landing gear fittings	26	212	26	212	26	212	26	212	26	212
Windows	679	22,830	679	22,830	679	22,830	679	22,830	679	22,830
Pressure deck and floor beams										
Total	2,984	119,660	2,984	119,660	2,984	119,660	2,984	119,660	2,984	119,660
Total recurring cost		471,495		424,714		428,570		458,708		401,939
Total nonrecurring cost		193,726		213,070		222,768		193,726		222,768
Total cost		665,221		637,784		651,338		652,434		624,707
Profit		79,826		79,534		78,160		78,292		74,965
Unit total	10,616	745,047	9,340	714,318	9,658	729,498	9,350	730,726	9,176	699,672

^aDelta weight and cost of replacing internal insulation with external insulation

The total study section cost and weight of the four level 3 shell designs are compared in figure 84, using the baseline cost and weight as unity.

(4) Components Other Than the Shell

During the level 1 design period, design concept drawings were made for the other major components of the study section. Fuselage frames, body station 1480 bulkhead, keel beam, pressure deck, floor beams, and landing gear fittings were investigated for alternate design concepts. Since the number of variations for these items was more limited than for the shell, these structural concepts were evaluated during the level 2 screening.

In level 3, trade studies were conducted to evaluate the weight-saving potential and cost effectiveness of advanced structural concepts applied to these components. Material trades, new structural arrangements, application of honeycomb sandwich, and composite-reinforced concepts were considered. A brief description of the nature and results of these studies is presented.

Frames: The fuselage frames were considered independently from the basic shell concepts. The existing baseline frame is of variable depth, increasing in section from the window area of the fuselage down through the shell lower quadrant. A study was conducted to evaluate a constant-depth frame, with a secondary, lower cargo compartment floor beam to replace the deep, built-up frame structure presently used in the lower quadrant. The two concepts are depicted in figure 85. The principal advantage offered by a constant-section frame is a reduction in manufacturing complexities and costs associated in forming variable-depth frame sections. The trade studies indicated that design strength and stiffness requirements could be maintained with a 4-inch, constant-depth frame with varying amounts (up to 0.3 square inch) of composite reinforcement applied to both the inner and outer frame chords. Although this concept was determined to be structurally feasible, it was considered not to be weight-cost effective.

A parallel study indicated that a constant-depth frame with metal strap chords would reduce material and fabrication costs, but a weight penalty would be incurred. Additional consideration of this concept is warranted on a cost-effectiveness basis.

Minor weight saving is possible as a result of structural configurations of the shell concept. For example, the honeycomb sandwich and external stringer shell concepts permit the use of a continuous outer frame chord bonded directly to the skin. This allows additional skin material to be considered effective with the frame outer chord for strength and stiffness considerations. It also allows the removal of an equivalent area from the frame chord itself resulting in a weight reduction. In addition, the continuous chord eliminates the requirement for separate shear ties and fail-safe tear straps thus reducing frame costs.

Body Station 1480 Bulkhead: The lower lobe of the station 1480 bulkhead serves as a pressure seal between the lower aft fuselage and the wheel well cutout area as well as a support structure for the main landing gear fittings. Trade studies were conducted to determine a more efficient structure to replace the existing, stiffened, shear-resistant web. Three concepts were evaluated.

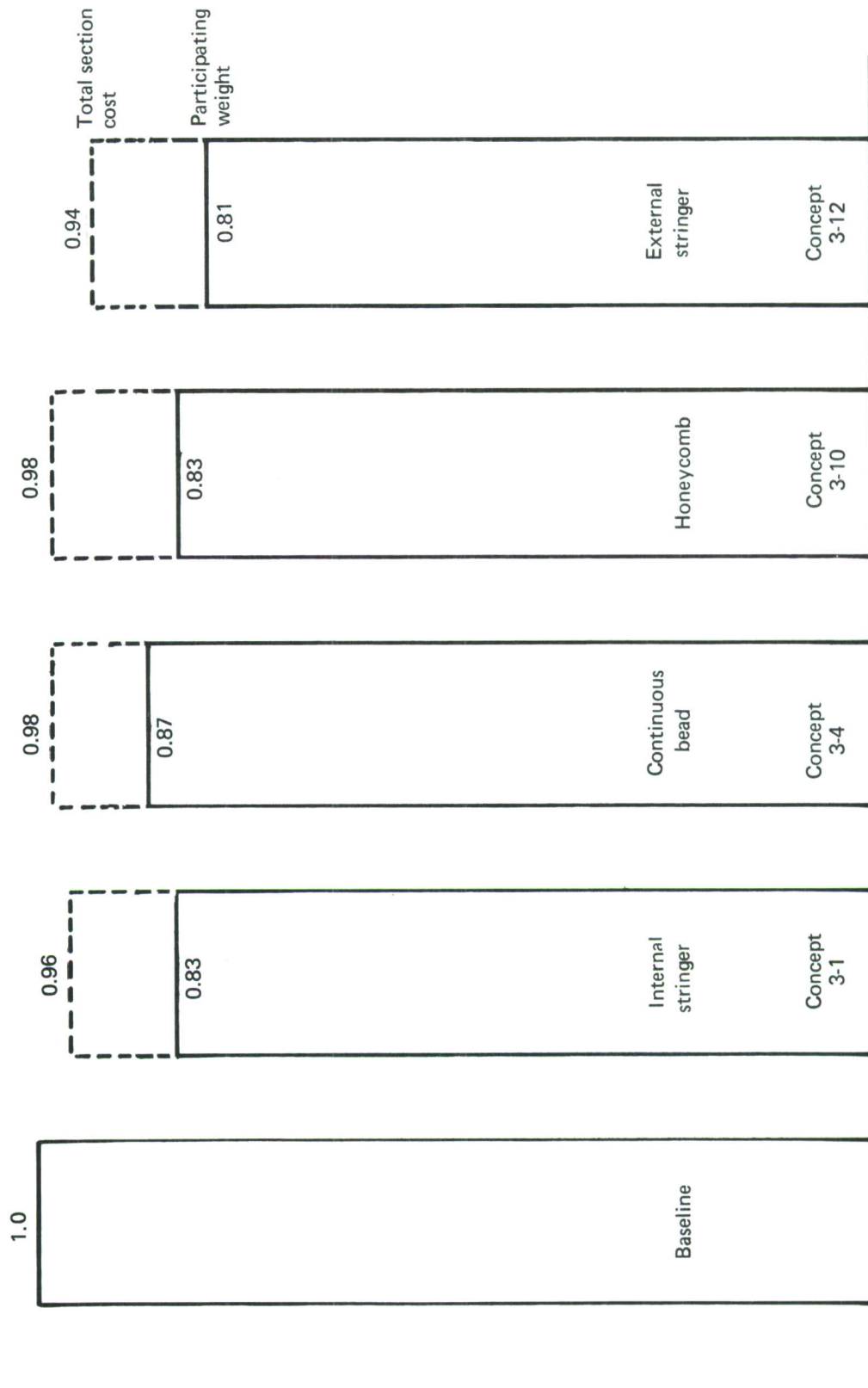


Figure 84. –Level 3 Shell Screening

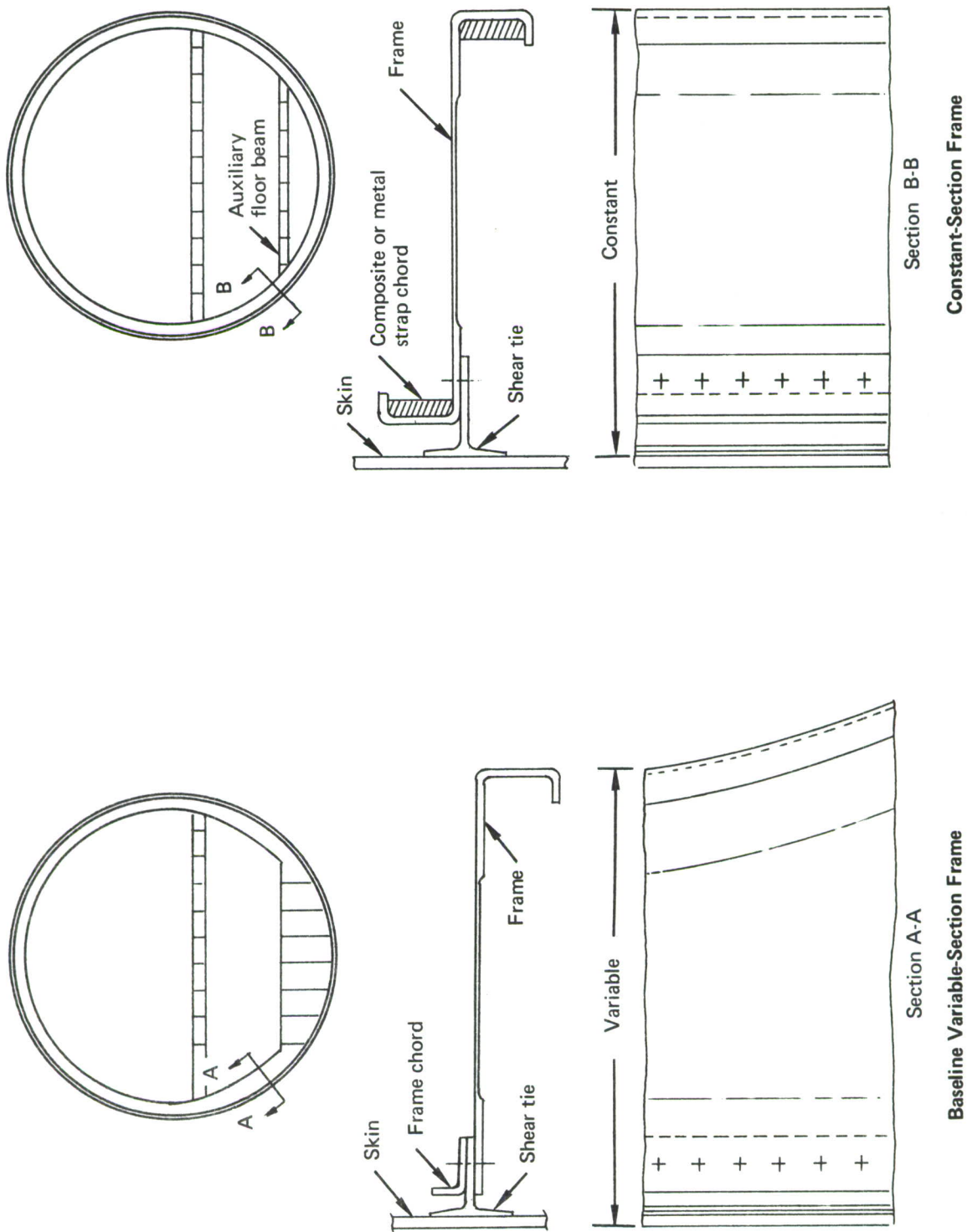


Figure 85. —Fuselage Frame

Honeycomb Sandwich. Bonded aluminum honeycomb sandwich was found to be weight effective in meeting strength and fail-safe requirements. However, stiffness and deflection criteria required excessive core thicknesses for sandwich design. Thus, the major drawback of this concept was the weight penalty incurred in providing circumferential panel closeout fittings and vertical reinforcement in the landing gear fitting attachment areas. All weight-saving potential demonstrated for the basic panel was nullified by the closeout and reinforcement requirements. The concept was considered to be neither weight nor cost effective and was dropped from further review.

Stiffened, Thin Honeycomb Sandwich. A second concept consisting of a stiffened, thin honeycomb sandwich was evaluated. This concept combined the inherent stiffness and stability of sandwich construction with the added stiffness of a stringer to meet deflection requirements. The thin sandwich also greatly reduced the weight penalty incurred for edge closeout, which penalized the thick honeycomb concept. This concept was dropped from further consideration due to marginal weight-saving potential and increased fabrication and assembly costs.

Composite-Reinforced Stiffened Web. A third concept consisted of retaining the baseline, shear-resistant web and redesigning the all-metal stiffeners to incorporate composite reinforcement. This concept is illustrated in figure 86. To fully utilize the high-modulus composite materials, the reinforcement was applied to the outstanding flange of the stiffener. Equivalent baseline strength and stiffness were maintained. A weight saving of 34 pounds, representing 2.6% of the bulkhead structural weight, was realized. This concept was considered not to be cost effective due to increased material and fabrication costs.

Keel Beam: Two components of the keel beam were considered for redesign: the main vertical web and main lower chord members.

Main Vertical Web. The main vertical web was redesigned as a bonded, honeycomb sandwich shear web (fig. 87). The upper and lower chords of the main vertical web were redesigned to form the sandwich closeout edge fittings, providing double shear connection to the sandwich faces. A weight saving of 12 pounds, representing 18% of the baseline keel beam web weight, was shown by this design. A cost saving of 3% of the baseline keel web cost was also indicated.

Main Lower Chord Members. The main lower chord fittings in the keel beam box assembly consist of heavy aluminum extrusions designed primarily for compression stability and ultimate strength. These structural members transfer large, concentrated compression loads across the wheel well cutout area. The high-strength, high-modulus composite materials are ideally suited to this type of design application. The chord members were redesigned with a boron-epoxy, laminated fiberglass central core, encapsulated in a built-up titanium outer shell (fig. 87). A weight saving of 30 pounds, representing 22% of the baseline keel beam chord weight, was realized from this design concept. A keel beam chord cost increase of 147% from baseline may be attributed to high material and fabrication costs associated with this design.

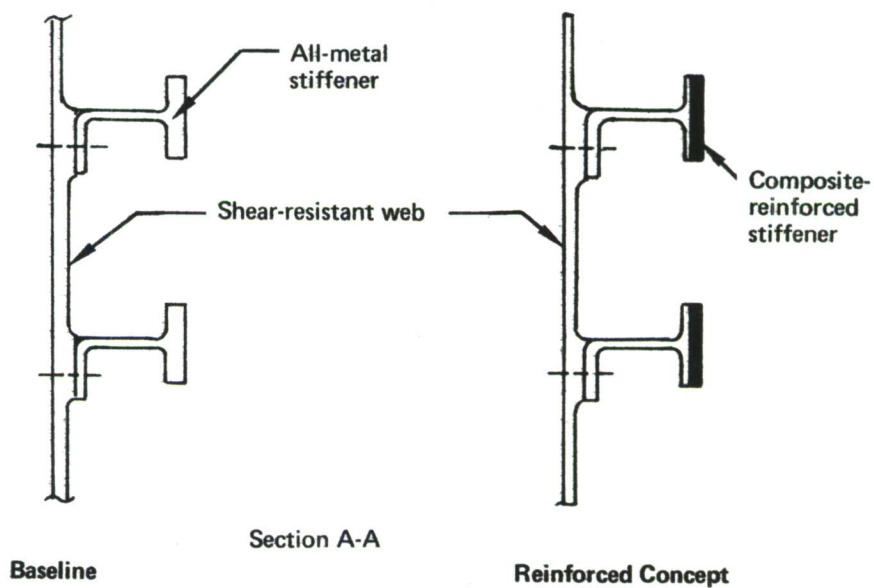
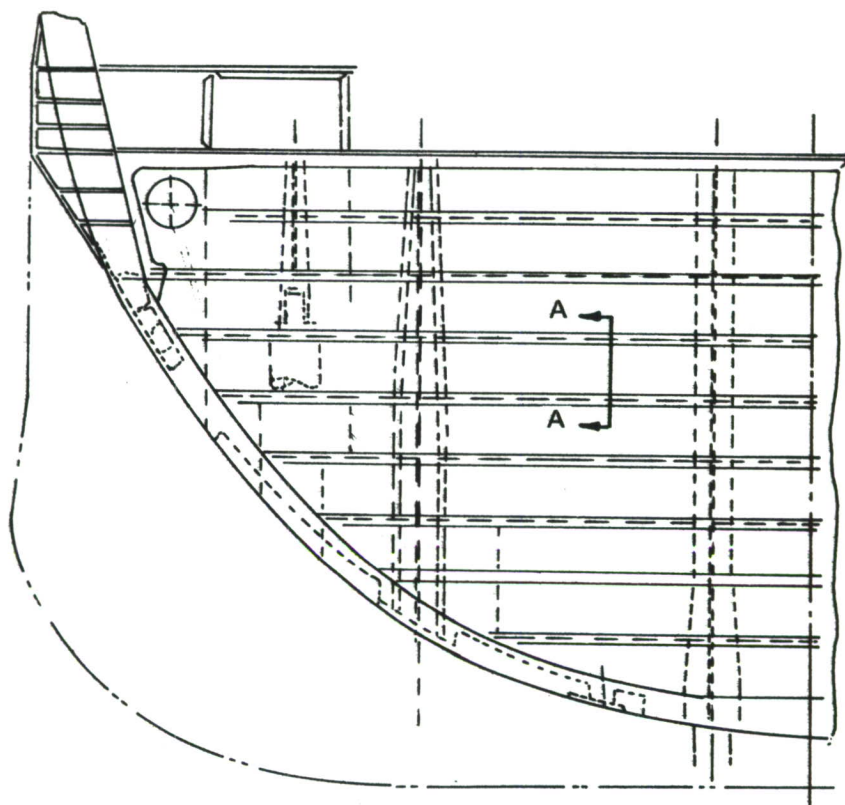


Figure 86.—Pressure Bulkhead, Body Station 1480

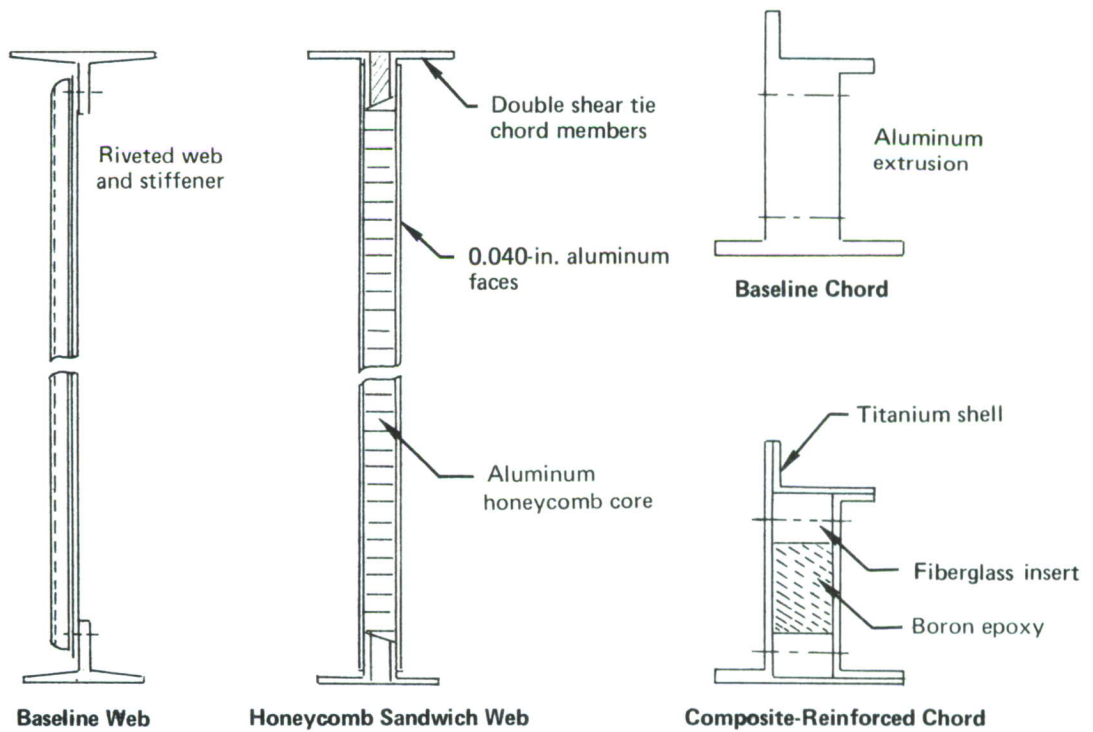
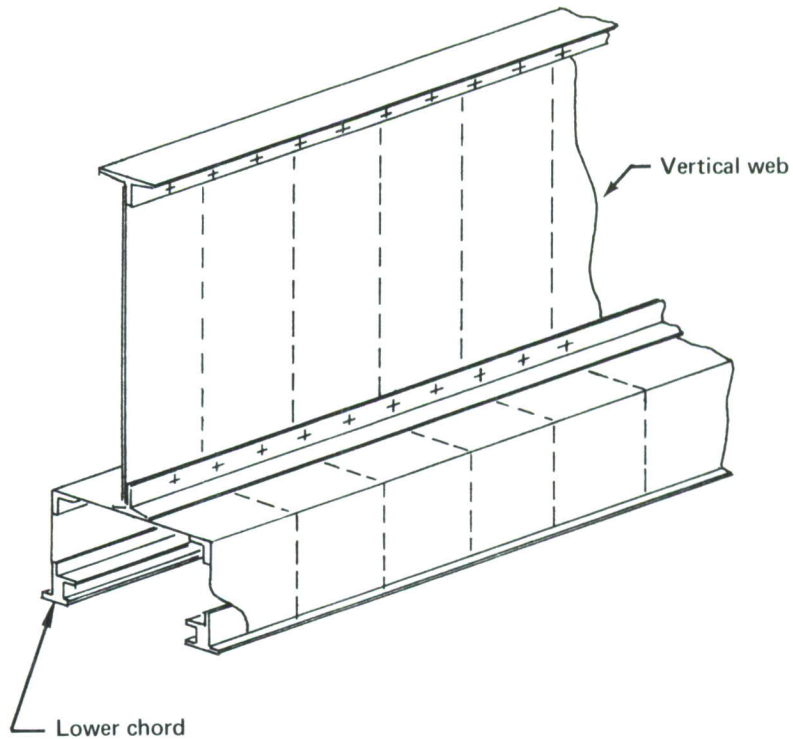


Figure 87.—Keel Beam

Pressure Deck: The pressure deck was redesigned to replace the baseline, stiffened-plate design with a bonded, honeycomb sandwich structure. The honeycomb sandwich was sized by strength considerations, maintaining an acceptable stress level in the face sheets to meet damage tolerance and crack growth requirements. The pressure deck is designed to tie in directly with the fuselage skin for an effective pressure seal; thus cutouts are required at each frame and where other structural members pass vertically through the pressure deck area. In sandwich construction, an extraordinary amount of edge closeout structure per square foot of basic panel is required, rendering this design non-weight-effective. To avoid the weight penalty associated with full sandwich closeout structure, an uneven-faced, square-edge sandwich concept was selected for this application (fig. 88). The square-edge panel design was oriented in a manner so that the thin face was in compression under pressure loading and the heavy face was sized for shear and damage tolerance capability. The edge closeout consists of high-density core for shearing loads from the thin inner face to the heavy outside face, which is locally reinforced with multiple doublers. The tie to the fuselage shell is accomplished through this reinforced outer skin in much the same manner as the baseline design. A weight saving of 30 pounds, representing 12% of the baseline pressure deck weight, was realized from this concept and it has been carried through for further study. A cost saving of 20% of the baseline pressure deck cost was indicated for this concept.

Floor Beams: The main floor beams were broken into two components for redesign consideration: webs and chords.

Floor Beam Web. The existing stiffened-sheet, floor beam webs were evaluated for application of a bonded honeycomb sandwich design. This concept was determined not be weight effective and was eliminated from further consideration.

Floor Beam Chords. The floor beam chords were redesigned to incorporate composite reinforcement (fig. 89). Equivalent baseline strength and stiffness were maintained. A potential weight saving of 41 pounds, representing 9% of baseline floor beam weight, was indicated by this study. This concept was not cost effective.

Landing Gear Fittings: Preliminary evaluation of the landing gear fittings during level 2 screening indicated that insufficient payoff potential existed to warrant an in-depth trade study for this structure.

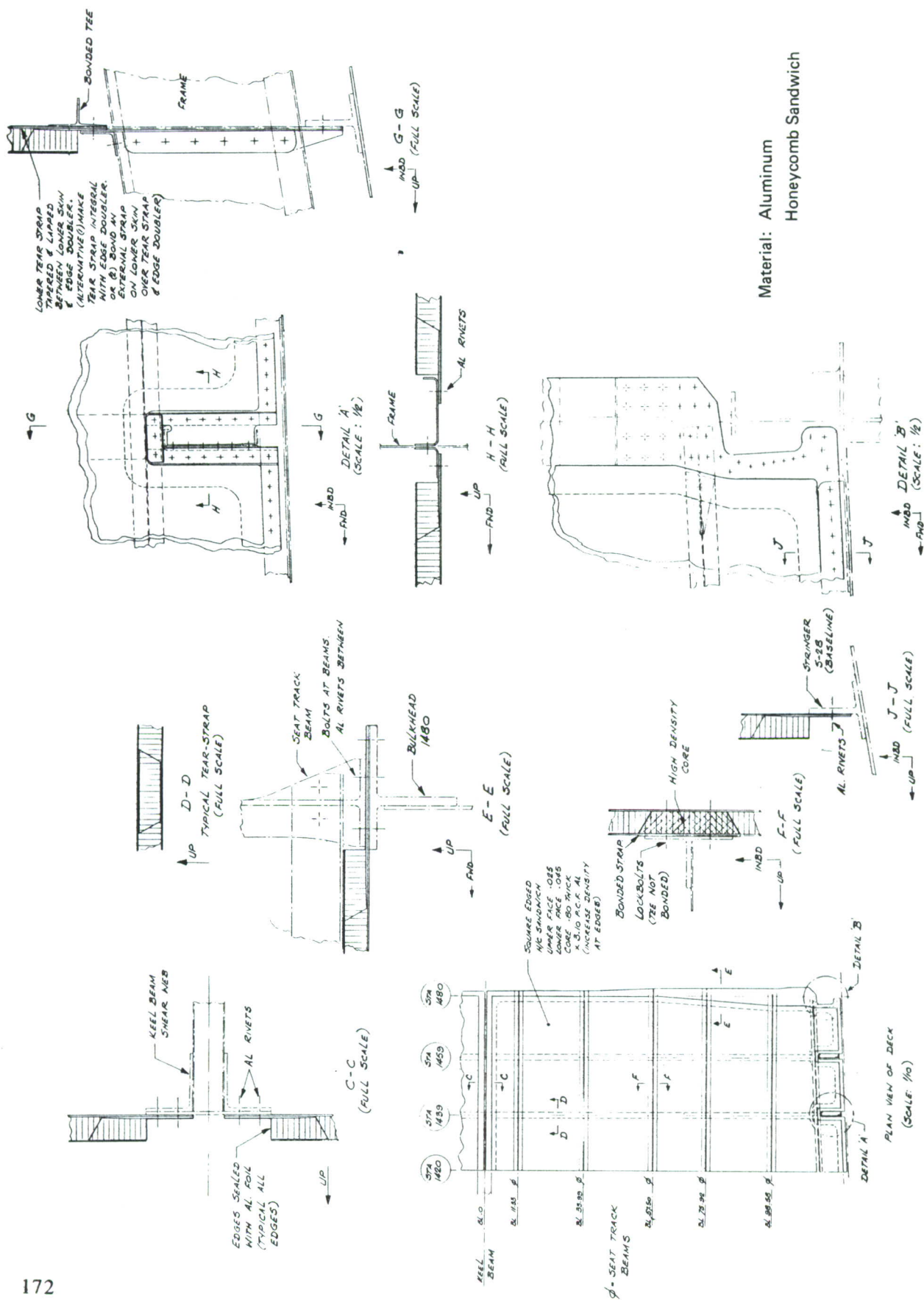


Figure 88.—Pressure Deck

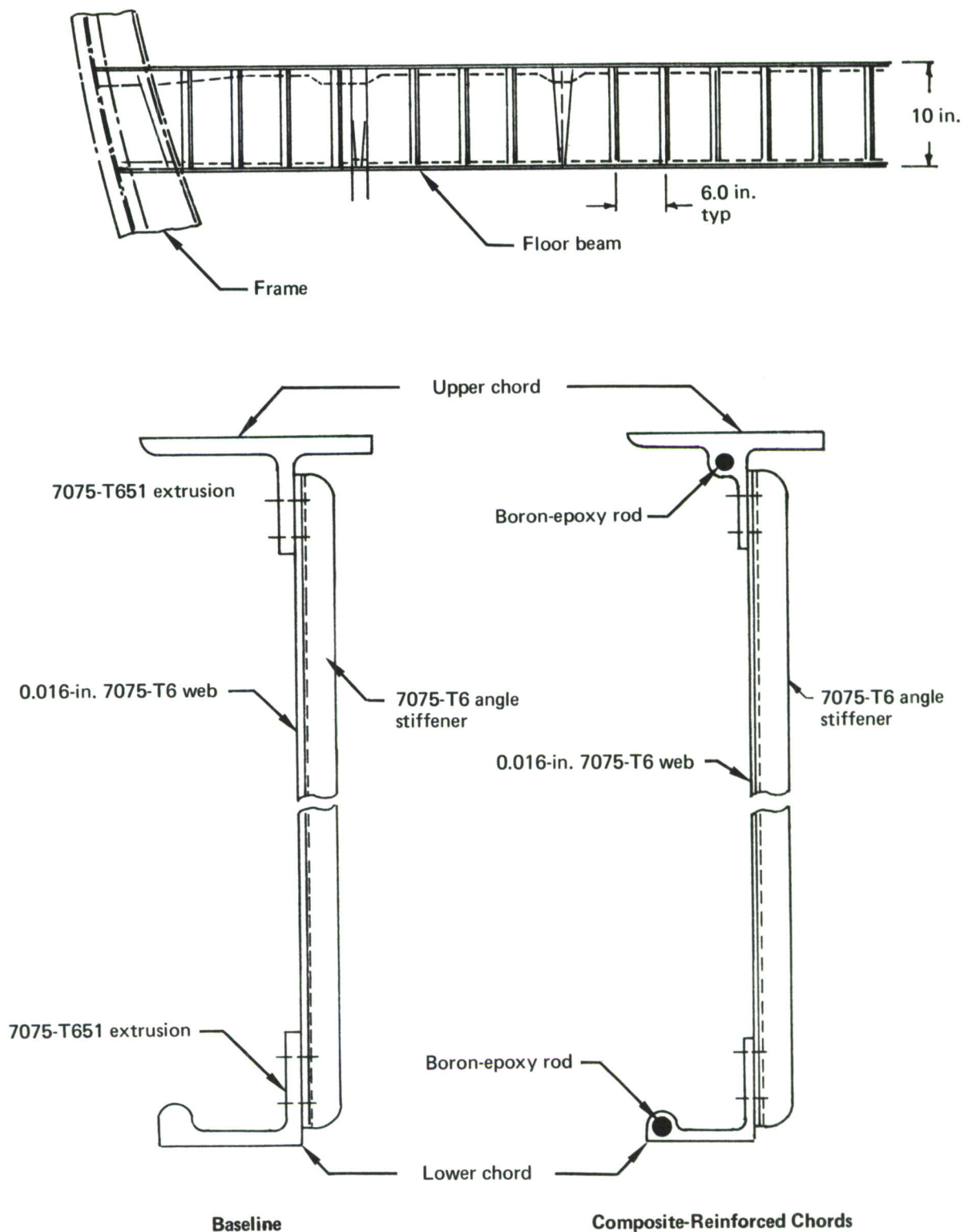


Figure 89.—Main Floor Beam

4. STRUCTURAL ANALYSIS

A balanced design of the cargo fuselage component was dependent on a systematic analysis for ultimate strength, fatigue durability, and damage tolerance. Table XX lists the various structural elements included in the design and the respective critical analytical considerations.

a. Stress

The fuselage component was analyzed for static strength capability to sustain critical flight loads. The 747-100 baseline fuselage design loads used during this study were the same as those contained in the external loads document submitted to the FAA for airplane certification.

The three bonded skin/stringer advanced concepts were sized for the same internal loads distribution as the baseline riveted skin/stringer structure. These internal loads were generated by finite element analysis and are contained in the 747-100 formal fuselage stress analysis.

The honeycomb shell concept was sized by the internal loads distribution generated by finite element analysis of the study section during the in-house IR&D honeycomb studies conducted prior to this contract study. The shear flow and bending stress distribution shown in figures 90 and 91 for vertical bending plus pressure are typical of the internal load and stress distributions determined by this method.

The preliminary design sizing was accomplished by conventional calculator and slide-rule analysis based on the established internal loads and structural element allowables data contained in the Boeing design manual. A structural element optimization computer program was used to determine optimum skin/stringer thickness and geometric relationships for various compression end-load intensities.

The fuselage component was divided into several structural subcomponents for analysis: the shell, frames, pressure bulkhead, keel beam, pressure deck, and floor beams. This breakdown of structural components is shown in figure 92.

(1) Shell Analysis

The shell was segmented into four quadrant panels, as shown in figure 92. The breakdown of the shell structure conveniently matches the structure to specific loading conditions.

Upper Quadrant: The principal design load condition in the upper quadrant results from a positive dive maneuver. The fuselage crown is placed in tension, which dictates the static strength requirement of this portion of the fuselage structure. The presence of high tension stresses and cyclic loading resulting from gust and maneuver conditions, combined with internal pressurization loads, indicates a fatigue-oriented design for structural efficiency improvement.

Table XX.—General Component Analysis Considerations

Component	Strength design					Fatigue design		Damage tolerance design	
	Tension nonpressure	Shear	Beam bending	Compression	Pressure	Tension nonpressure	Pressure	Tension nonpressure	Pressure
Frames		•	•		•		•		•
Bulkheads		•	•		•		•		•
Pressure deck		•			•		•		•
Keel beam		•		•			•		
Floor beams			•		•		•		
Shell									
Upper quad	•	•			•	•	•	•	•
Side quad		•			•		•		•
Lower quad		•		•	•		•		•

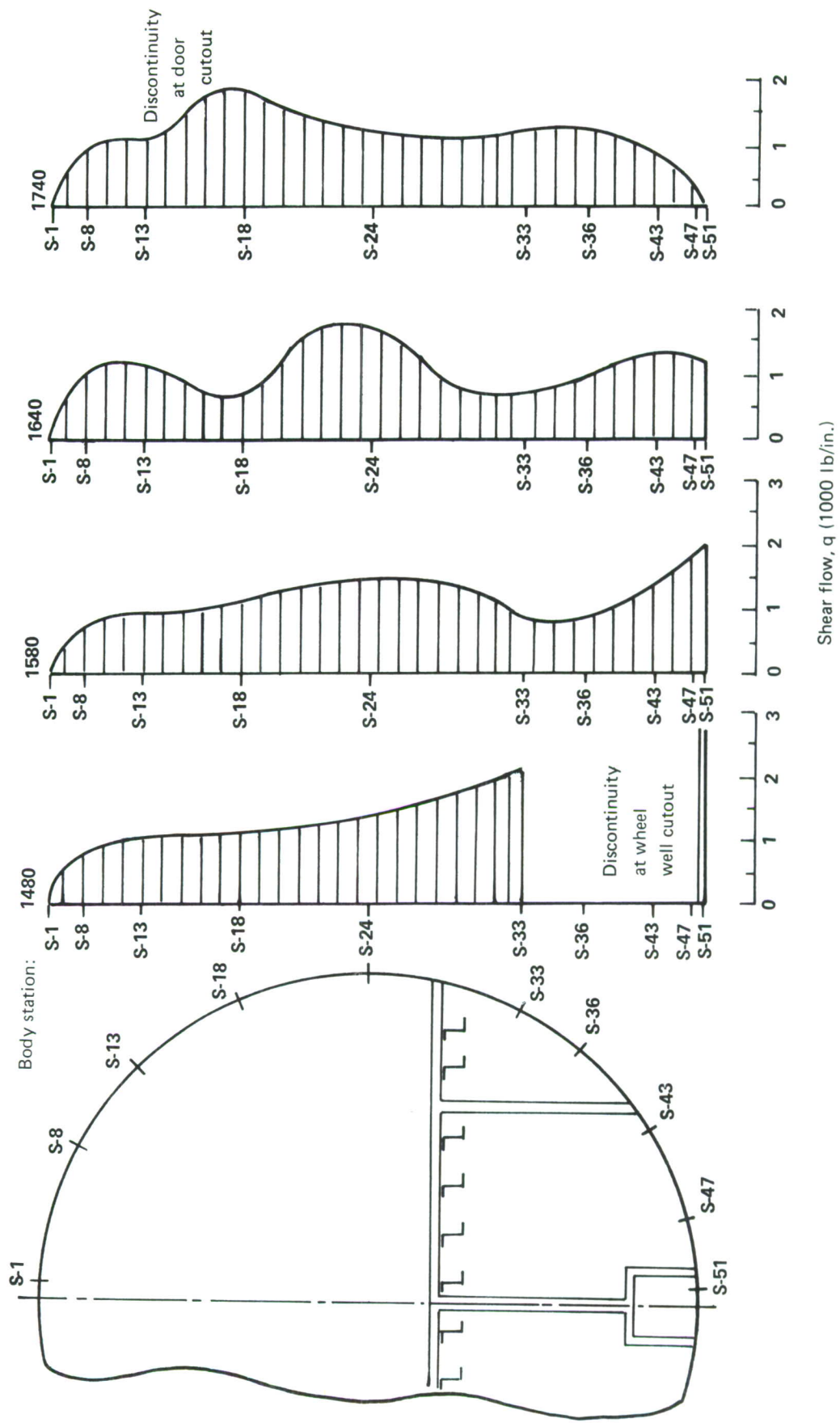


Figure 90.—Shear Flow Distribution for Vertical Bending Plus 1.5 Factors Pressure

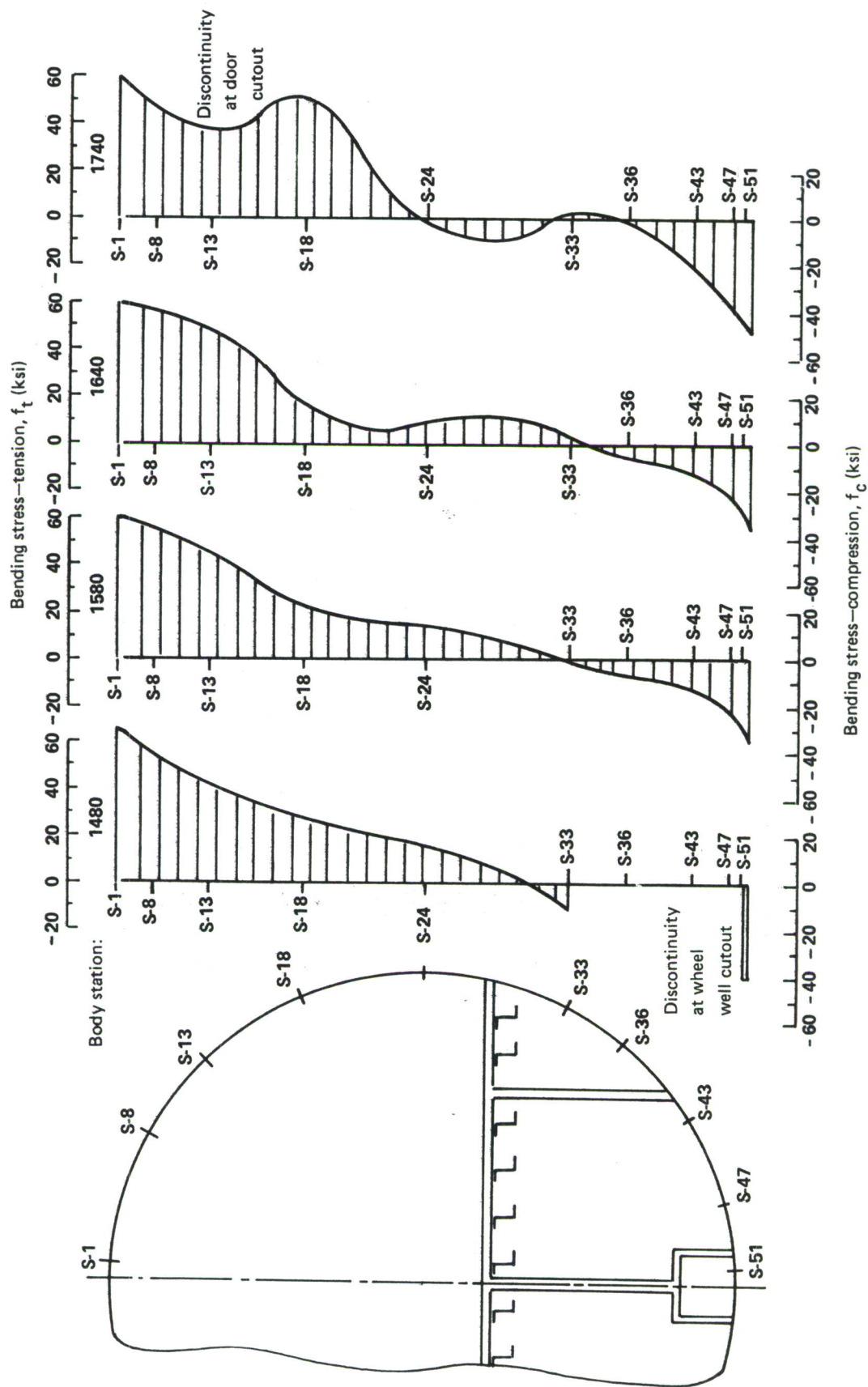


Figure 91.—Bending Stress Distribution for Vertical Bending Plus 1.5 Factors Pressure

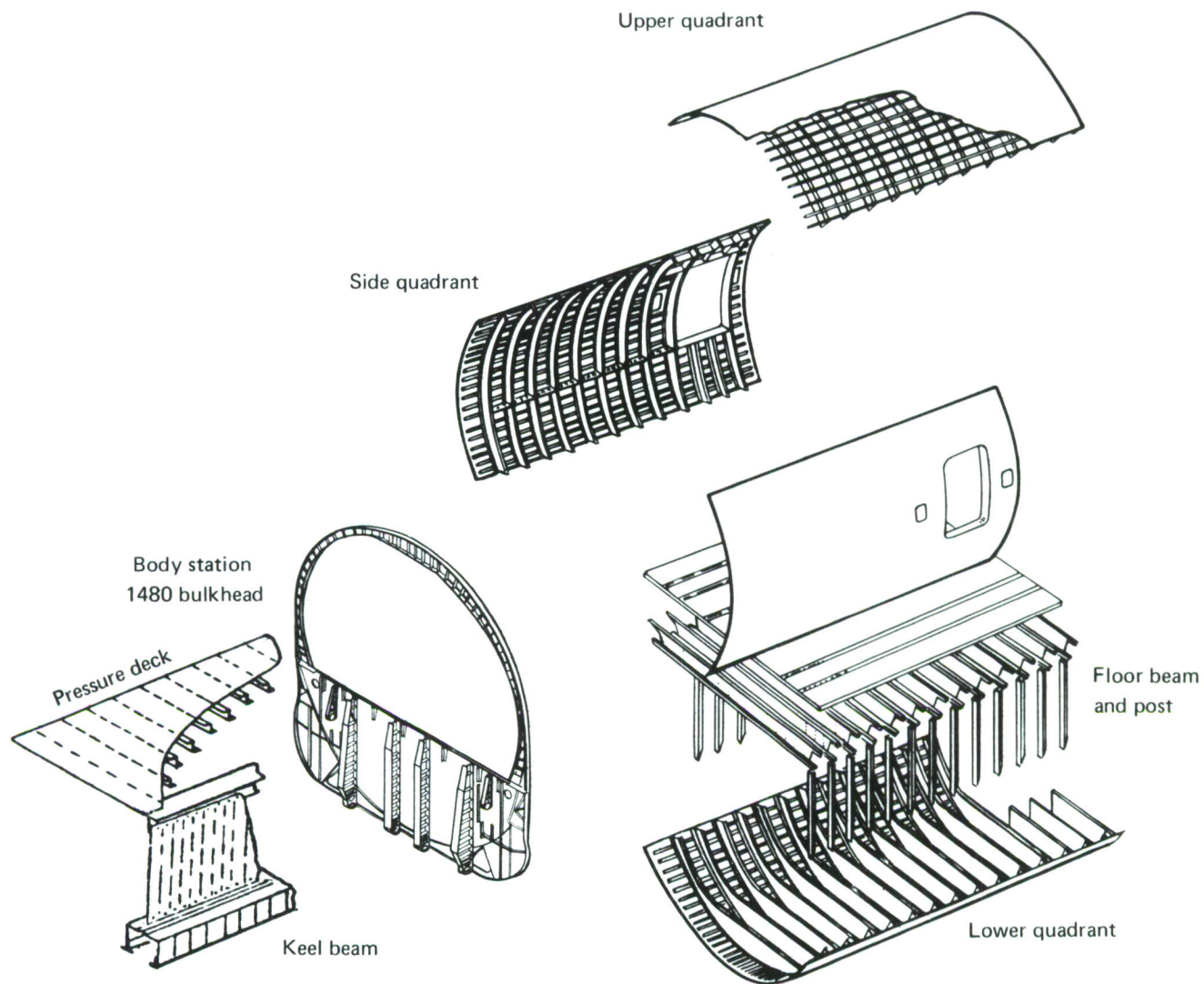


Figure 92.—Structural Breakdown—747-100 Aft Fuselage

Side Quadrant: Vertical shear, side bending, and body torsional loads resulting from positive maneuver and fin gust conditions comprise the critical design requirements for the side quadrant shell structure. Analysis of this fuselage section primarily considered panel stability under combined compression and shear loading. The resulting structure was then analyzed for its capability to sustain damage due to foreign object penetration. Efficient use of shear material in the side quadrant was a prime consideration for maximizing structural efficiency.

Lower Quadrant: The primary design load condition in the lower quadrant results from a positive dive maneuver, which induces high compression loads in the lower fuselage structure. This portion of the shell is typically critical for compression stability. The forward center section of the lower quadrant receives concentrated loads from the keel beam termination, and the structure in this area was analyzed for its ability to redistribute these concentrated loads into the surrounding shell structure.

(2) Analysis Approach

The fuselage section selected for this study is unique from an analysis consideration due to the structural discontinuities created by the wheel well and door cutouts. These discontinuities influence the internal load and stress distribution in the shell to such a degree that an M_c/I distribution does not adequately define the true stress distribution within the shell. The distributions determined by finite element structural analysis methods were therefore used for this study.

A critical design load envelope was established by selecting the maximum shear flows and end-load intensities from the load conditions analyzed. Discrete points on the fuselage shell, consisting of stringer and frame intersection points, were selected to establish a coarse analysis grid as shown in figure 93. The fuselage is symmetrical and analysis of only one half of the shell was required. Forty-eight analysis points, twelve stringer and four frame locations, were considered.

The critical loads for these analysis points were determined from the design envelope and conventional analysis methods were employed to conduct preliminary sizing of the advanced shell concepts. The standard worksheet format shown in figure 94 was used to ensure a uniform sizing procedure. Figure 95 is a typical example of a completed work sheet for one structural arrangement and one material combination. These stress work sheets, which contain the minimum gages required to meet the static strength, damage tolerance, and fatigue requirements, were transmitted to the Design group. The Design group, in conjunction with Manufacturing, incorporated these data into concept drawings with those modifications necessary to ensure manufacturable cost- and weight-effective designs. The final shell concept gages and materials are shown in figures 80 through 83.

(3) Structural Sizing Analysis of Shell Concepts

The following analysis procedures were established for structural sizing of the shell elements for specific load conditions. The same procedures were used for skin/stringer and honeycomb sandwich concepts, except as noted.

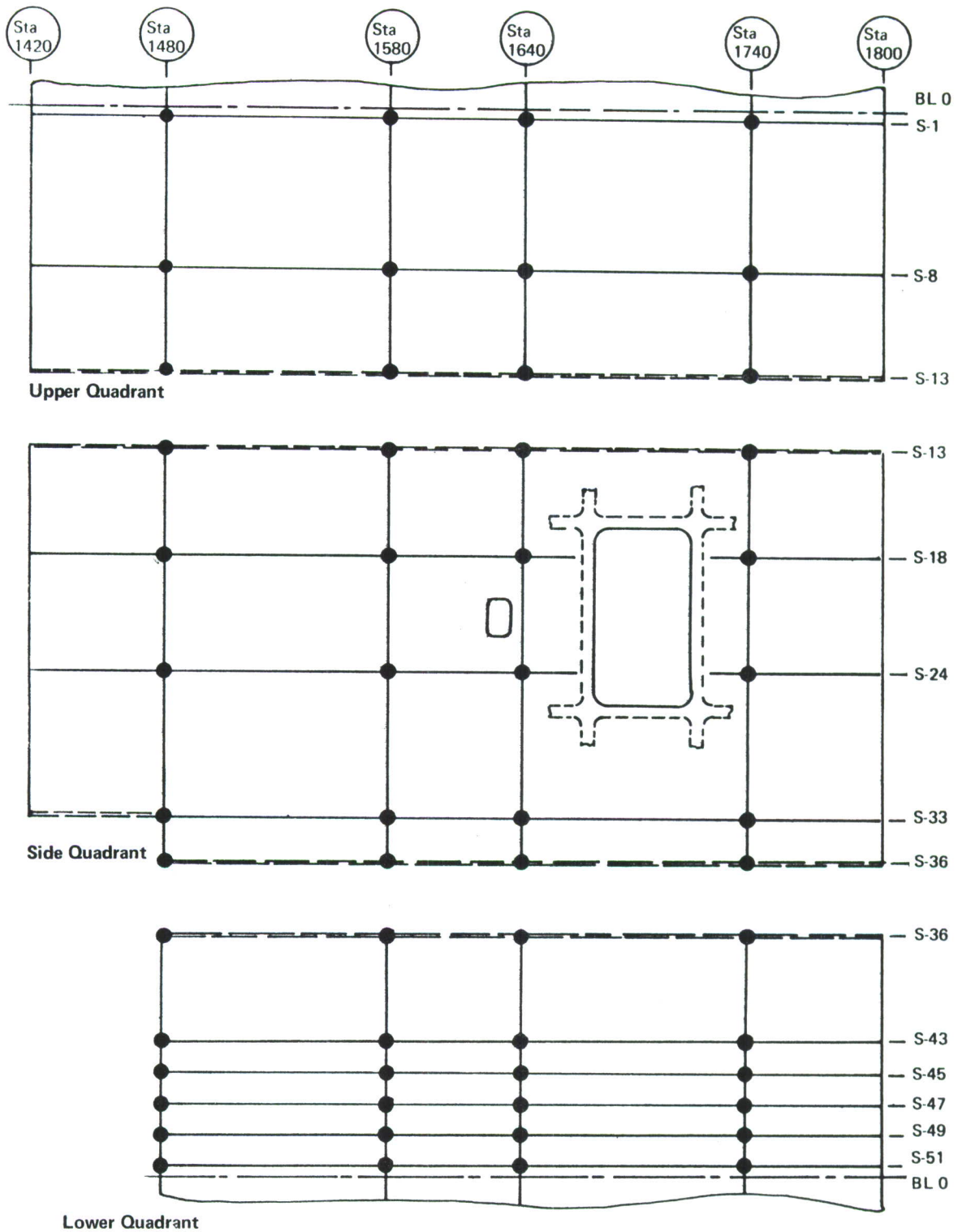


Figure 93.—Fuselage Shell Analysis Locations By Quadrant

Baseline										Concept															
	1	2	3	4	5	6	7	8	9	10	11	12	13	14	15	16	17	18	19	20	21	22	23	24	25
Body Stringer	N_{TE}	N_{TP}	N_T	N_c	q	t_B	t_B	N_{Tf} [6 x 7]	$f_{maxDFRL}$	\bar{t}_f [8/9]	F_{Tult} [3/11]	\bar{t}_T [3/11]	\bar{t}_c	\bar{t} [max of 10,12,13]	f_{maxHT} [PR/15]	t_{HT} [PR/15]	F_{sult}	$t_{s_{ult}}$ [q/17]	t_{min} [max of 16,18] (in.)	t_s [1.5x19] (in.)	\bar{t}_{cs}	t_{min} [max of 14,20,21] (in.)	t_s	Final design	
	(kip/in.)	(kip/in.)	(kip/in.)	(kip/in.)	(lb/in.)	(ksi)	(in.)	(kip/in.)	(ksi)	(in.)	(ksi)	(in.)	(in.)	(in.)	(ksi)	(in.)	(ksi)	(in.)	(in.)	(in.)	(in.)	(in.)	(sq m.)	A_{st}	A_{TS} (sq in.)
S-1																									
S-8																									
S-13																									
S-18																									

NOMENCLATURE

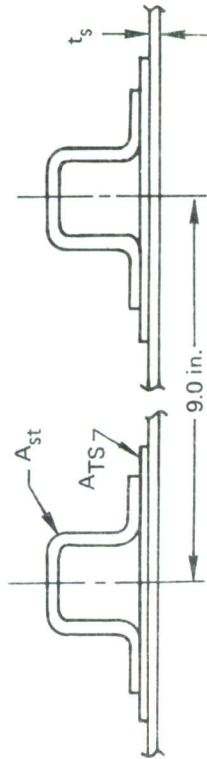
N_{TE}	Tension end load (ultimate) due to bending	$f_{maxDFRL}$	Allowable fatigue stress (longitudinal)	F_{sult}	Allowable shear stress intermediate diagonal tension web
N_{TP}	Tension end load (ultimate) due to pressure	\bar{t}_f	Smear thickness for fatigue	t_{sult}	Minimum skin gage for shear
N_T	Total tension end load (ultimate) ($N_{TE} + N_{TP}$)	F_{Tult}	Allowable tensile stress	t_{min}	Minimum skin gage
N_C	Compression end load (ultimate)	\bar{t}_T	Smear thickness for tension	\bar{t}_s	Smear thickness for shear
q	Shear flow (ultimate)	\bar{t}_c	Smear thickness for compression stability	\bar{t}_{cs}	Smear thickness for combined compression and shear
f_{fB}	Baseline fatigue stress	\bar{t}	Minimum smeared thickness, tension, compression, and fatigue	\bar{t}_{min}	Minimum smeared thickness for strength design
\bar{t}_B	Baseline smeared thickness	f_{maxHT}	Allowable hoop tension stress (damage tolerance one-factor pressure)	t_s	Design skin gage
N_{Tf}	Baseline fatigue end load	t_{sHT}	Minimum skin gage for damage tolerance	A_{st}	Design stringer area
				ATS	Design tear strap area

Notes:

- 1
- 2
- 3
- 4
- 5

Determined from optimized \bar{t} vs N_c curves
 Minimum skin gage for hoop tension $t = PR/f_{maxHT}$
 Minimum skin gage for shear
 Smear thickness for shear with 50% stiffening
 Smear thickness for combined compression and shear, from interaction curves

Figure 94. —Structural Sizing Worksheet Format



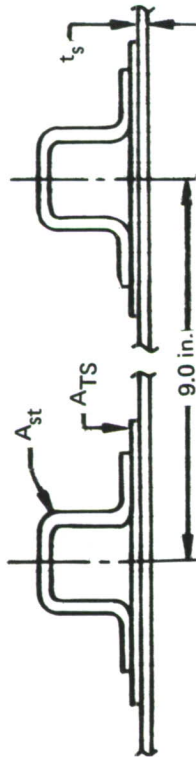
Shell Concept: Internal Hat Stringer

Materials

 Skin: 2024-T3
 Stringer: 7075-T6

		Baseline										Concept															
		1	2	3	4	5	6	7	8	9	10	11	12	13	14	15	16	17	18	19	20	21	22	23	24	25	
Stringer	Body Station	N _{TE}	N _{TP}	N _T	N _C	q	t _B	t _B	N _{Tf} [6 x 7]	f _{maxDFR_L}	t _f	F _{Tult} [3 / 11]	t _c	t̄ [max of 10,12,13]	f _{max,HT}	t _{sHT} [PR/15]	F _{sult}	t _{s_{sult}} [q/17]	t _{min} [max of 16,18]	t _s [1.5x19]	t _{c_s}	t _{min} [max of 14,20,21]	t _s	A _{st}	A _{TS}		
		(kip/in.)	(kip/in.)	(kip/in.)	(kip/in.)	(lb/in.)	(ksi)	(ksi)	(kip/in.)	(ksi)	(in.)	(ksi)	(in.)	(in.)	(in.)	(ksi)	(in.)	(ksi)	(in.)	(in.)	(in.)	(in.)	(in.)	(sq in.)	(sq in.)	(sq in.)	
1480	S-1	7.06	1.15	8.21		307	14.1	170	2.40	27.0	.089	57.5	.143	.143	23.0	.050	20.0	.015	.050	.075	.081	.143	.090	.475		.075	
	S-8	5.02	1.04	6.06		635	14.4	116	1.67	25.0	.067		.105	.105				.032	.050	.075	.081	.105	.070	.325			
	S-13	3.20	0.85	4.15	.32	1089	13.4	.094	1.26	24.0	.053		.080	.080				.055	.055	.082	.096	.096	.060	.250			
	S-18	1.42	0.41	1.83	.94	1289	10.2	.097	0.99	17.0	.059		.087	.087				.064	.064	.127	.106	.106	.070	.250			
	S-24	2.36	0.54	2.90	2.20	1691		.179					.051	.090	.090				.085	.085	.127	.127	.085	.400			
	S-33	2.06	1.65	3.71	4.42	1167		.174					.065	.160	.160				.059	.059	.080	.184	.125	.535			
	S-36	0.31	.04	0.34	.02	657		.116					.006						.033	.050	.075	.106	.070	.250		.075	
	S-43	4.00	.29	4.29	1.95	2398		.257					.075	.100	.100				.120	.120	.179	.183	.120	.569			
	S-45	1.00	.20	1.20	.70	1757		.187					.021	.085	.085				.088	.088	.132	.144	.144	.090	.450		
1580	S-47	0.90	.44	1.34	2.18	2989		.240				.024	.105	.105				.150	.150	.225	.240	.240	.150	.810			
	S-49		2.45	2.45	13.3	8825		.507				.043	.380	.380				.440	.440*		.432	.432	.240	.393			
	S-51		1.20	1.20	7.6	797		.310				.021	.235	.235				.040	.050	.075	.255	.255	.175	.810			
	S-1	6.35	1.15	7.50		172	15.0	153	2.30	27.0	.085	57.5	.130	.130	18.3	.063	20.0	.009	.063	.095	.094	.130	.080	.450		.075	
	S-8	4.22	0.88	5.10	.28	668	13.8	111	1.53	24.0	.064		.089	.089				.033	.063	.095	.094	.095	.063	.250			
	S-13	2.72	0.76	3.48	1.18	1074	12.5	.094	1.18	21.0	.056		.061	.088	.088				.054	.063	.095	.094	.095	.063	.275		
	S-18	1.74	0.55	2.29	1.14	1302	12.9	.097	1.25	19.0	.066		.040	.088	.088				.065	.065	.097	.106	.106	.070	.315		
	S-24	2.22	0.90	3.12	2.18	1291		.146					.055	.096	.096				.065	.065	.097	.112	.112	.070	.350		
	S-33	1.07	0.62	1.69	1.32	677		.140					.030	.089	.089				.034	.063	.095	.106	.106	.070	.300		.075
S-36	0.53	0.46	0.99	1.07	736		.124					.018	.087	.087				.037	.063	.095	.106	.106	.070	.300			
S-43	1.01	0.75	1.76	3.44	1358		.257					.031	.118	.118				.068	.068	.102	.148	.148	.080	.569			
S-45		.90	.90	6.05	1958		.277					.016	.184	.184				.098	.098	.147	.209	.209	.125	.720			
S-47		1.51	1.51	6.95	2422		.330					.027	.214	.214				.112	.112	.168	.227	.227	.130	.810			
S-49		1.47	1.47	9.20	1947		.370					.026	.250	.250				.097	.097	.145	.263	.263	.150	.775			
S-51		1.05	1.05	7.37	6		.310					.019	.230	.230				0	.063	.095	.230	.255	.125	.810			

Figure 95. — Worksheet for Structural Sizing of Internal Hat Stiffened Shell Concept



Shell Concept: Internal Hat Stringer

Materials

Skin: 2024-T3
Stringer: 7075-T6

Baseline										Concept																
	1	2	3	4	5	6	7	8	9	10	11	12	13	14	15	16	17	18	19	20	21	22	23	24	25	
Stringer	N_{TE}	N_{TP}	N_T	N_C	q	t_B	t_B	N_{Tf} (6 x 7)	f_{maxDFR_L}	t_f (8/9)	$F_{T_{ult}}$	\bar{t}_T (3/11)	\bar{t}_c	\bar{t} (max of 10,12,13)	$f_{max_{HT}}$	t_{HT} (PR/15)	$F_{s_{ult}}$	$t_{s_{ult}}$ (q/17)	t_{min} (max of 16,18)	t_s (1.5x19)	\bar{t}_{cs}	\bar{t}_{min} (max of 14,20,21)	Final design			
Body station																							t_s	A_{st}	A_{TS}	
1640	8-1	5.24	0.91	6.15	1.72	609	13.1	1.134	1.75	.061	57.5	.107	.092	.107	.107	.063	20.0	.031	.063	.063	.095	.105	.107	.070	.335	.075
	8-8	3.76	0.91	4.67	1.18	807	12.1	1.103	1.25	.043		.081	.087	.087				.041	.063	.063	.095	.099	.063	.250		
	8-13	2.42	0.91	3.33	0.75	888	11.6	1.094	1.09	.038		.058	.085	.085				.045	.063	.063	.095	.095	.063	.250		
	8-18	2.40	0.98	3.38	0.85	1057	9.8	1.110	1.08	.045		.059	.085	.085				.053	.063	.063	.095	.095	.063	.250		
	8-24	2.20	0.92	3.12	1.55	1171	3.6	1.127	.46	.026		.055	.090	.090				.059	.063	.063	.095	.099	.063	.300		
	8-33	1.07	0.92	1.99	1.30	1110		1.110					.035	.088	.088				.056	.063	.095	.099	.063	.300		
	8-36	0.78	0.92	1.70	1.43	1059		1.116				.030	.089	.089				.053	.063	.063	.095	.099	.070	.250	.075	
	8-43	1.84	0.92	2.76	4.06	823		1.205				.048	.127	.127				.042	.063	.063	.095	.148	.080	.569		
	8-45	2.22	0.92	3.14	6.56	702		.230				.055	.185	.185				.035	.063	.063	.095	.207	.110	.810		
	8-47	3.46	0.92	4.38	8.95	475		.323				.076	.242	.242				.023	.063	.063	.095	.245	.145	.954		
	8-49	3.60	0.92	4.92	9.65	243		.338				.079	.247	.247				.012	.063	.063	.095	.247	.125	.810		
	8-51	3.68	0.92	4.60	9.85	106		.338				.080	.255	.255				.006	.063	.063	.095	.255	.125	.810		
1740	8-1	4.14	0.92	5.06	1.35	557	13.2	1.110	1.45	.052	57.5	.088	.081	.088	23.0	.050	20.0	.028	.050	.050	.075	.082	.088	.060	.250	.075
	8-8	3.12	0.92	4.04	0.98	705	12.3	1.096	1.18	.042		.071	.080	.080				.035	.050	.050	.075	.082	.082	.050	.225	
	8-13	2.29	0.92	3.21	0.72	869	11.0	1.094	1.03	.041		.056	.078	.078				.044	.050	.050	.075	.080	.080	.050	.225	
	8-18	2.03	0.98	3.01	0.80	1037	9.2	1.110	1.01	.042		.053	.079	.079				.052	.052	.052	.078	.086	.086	.056	.225	
	8-24	1.87	0.92	2.79	1.42	1145	3.3	1.127	0.42	.024		.049	.088	.088				.058	.058	.058	.087	.092	.092	.060	.250	
	8-33	0.93	0.92	1.85	1.18	1060		1.110				.033	.087	.087				.053	.053	.053	.080	.092	.092	.060	.250	
	8-36	0.62	0.92	1.54	1.30	1001		1.108				.027	.088	.088				.051	.051	.051	.077	.101	.101	.065	.315	.075
	8-43	1.27	0.92	2.19	2.46	786		1.135				.038	.098	.098				.040	.050	.050	.075	.134	.134	.080	.450	
	8-45	1.42	0.92	2.34	3.50	712		1.148				.041	.110	.110				.036	.050	.050	.075	.144	.144	.090	.450	
	8-47	3.04	0.92	2.96	7.88	492		.288				.052	.235	.235				.025	.050	.050	.075	.237	.237	.130	.865	
	8-49	3.41	0.92	4.33	8.50	253		.314				.076	.242	.242				.013	.050	.050	.075	.242	.242	.120	.810	
	8-51	3.45	0.92	4.37	8.55	129		.314				.076	.242	.242				.007	.050	.050	.075	.242	.242	.120	.720	

Figure 95.—Concluded

Tension: Three primary conditions were considered in analyzing the shell structure for tensile loading conditions:

- Ultimate tensile strength
- Fatigue life and durability
- Damage tolerance

From this analysis a minimum “smeared” thickness \bar{t} , capable of sustaining the critical applied loads at the design allowable stress, was determined for each analysis location.

Hoop Tension: The following design requirements were considered in analyzing the shell structure for hoop tension load conditions:

- Ultimate strength, hoop direction for two-factor pressure loading
- Fatigue life and durability requirements
- Damage tolerance for one-factor pressure loading

The minimum skin gage and fail-safe member sizing for hoop tension were determined by damage tolerance requirements. The allowable hoop tension stress is material and configuration dependent. A detailed description of damage tolerance analysis is presented in section IV-4c4.

Compression Analysis: Compression analysis of the shell structure for compression loading considered the following design requirements:

- Ultimate compression strength
- General panel compression stability
- Local crippling of structural elements

A structural element optimization computer program was used to generate column stability and local crippling properties of the proposed skin/stringer shell concepts. These data were used to construct families of minimum weight design curves, representing the optimum structural arrangement of skin/stringer combinations. Figure 96 shows such a family of curves determined for a hat stiffened skin concept. Complete optimization is limited by practical considerations. In this instance the frame and stringer spacing has been held constant at 20 and 9 inches, respectively. A fixed-stringer geometry, as noted, was also considered. These plots were used to determine a minimum weight structure for design compression end-load intensities.

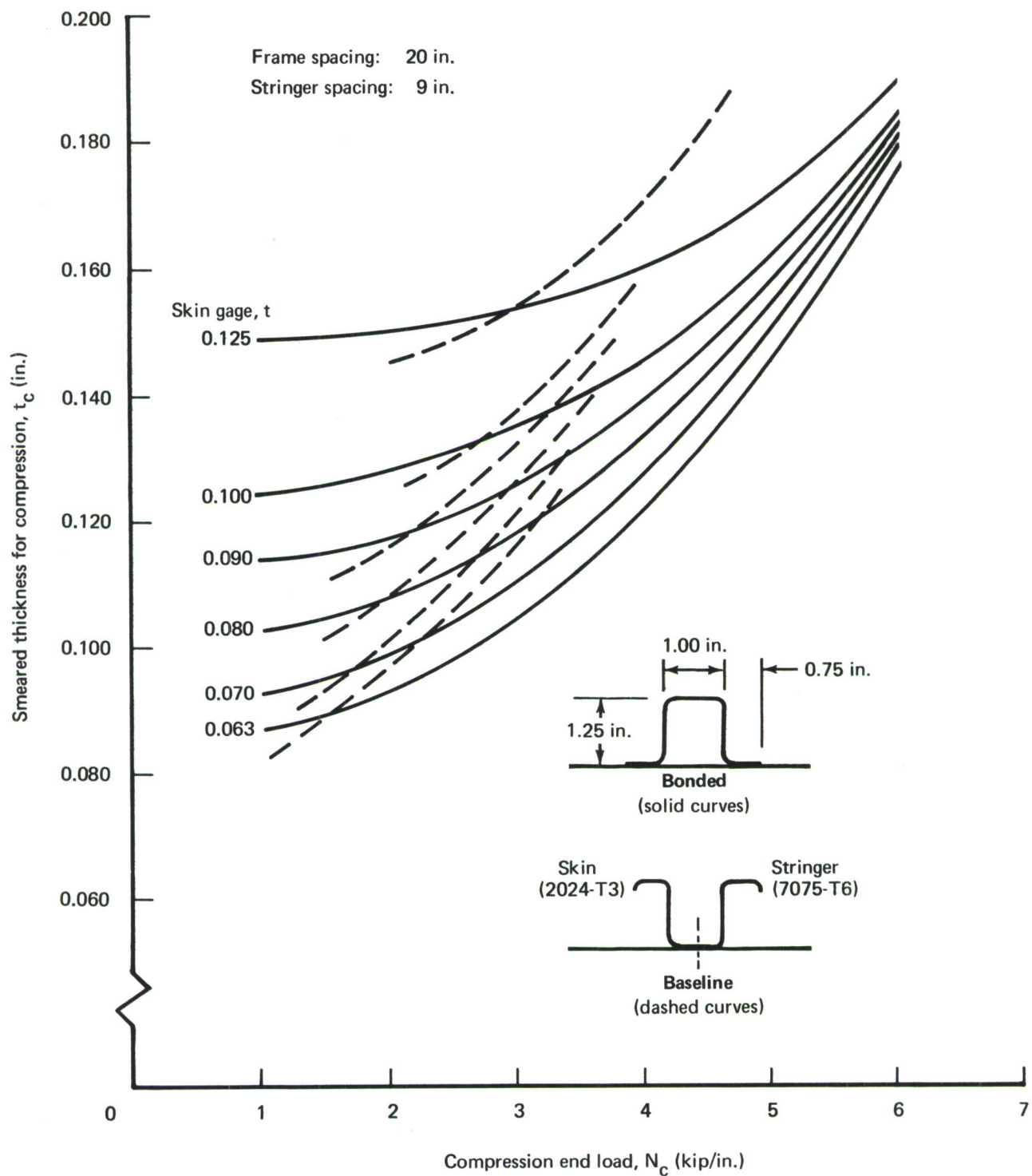


Figure 96.—Stiffened Shell Concept Component Structural Optimization for Compression as a Function of Skin Gage

A similar analysis was conducted for the honeycomb sandwich shell. Basic face sheet and core sizing for compression stability was determined from sandwich panel compression stability curves such as shown in figure 97. Secondary analysis of sandwich structure was conducted to evaluate:

- Local crippling
- Shear crimping
- Intercell buckling

Shear: Analysis of the shell structure for shear loading conditions considered the following design requirements:

- Intermediate, diagonal tension webs for skin/stringer concepts
- Shear-resistant panels in honeycomb sandwich concepts

For skin/stringer concepts, 50% stiffening ($A_{\text{stringer}}/A_{\text{skin}} = 0.50$) was maintained for shear stability considerations. Minimum skin gage for shear was determined from the expression:

$$F_S = q_{\text{max}}/t_s$$

where:

F_S = allowable shear stress

q_{max} = maximum shear flow measured in pounds per inch

t_s = skin gage (minimum for shear)

A minimum “smeared” thickness for shear, \bar{t}_s , was then calculated for 50% stiffening.

The honeycomb sandwich shell concept was designed to be shear resistant. Face gages and core requirements were determined from honeycomb sandwich, panel shear allowable curves such as shown in figure 98.

Combined Compression and Shear: The side and lower quadrant shell structure was sized primarily by combined compression and shear loading conditions. Combined compression and shear interaction curves were generated to determine the depreciation in column compression buckling allowables due to the presence of shear loading. The sample curve shown in figure 99 permits selection of the minimum weight skin/stringer combination capable of carrying the design compression end load and associated shear flow. The compression load-carrying capability of the skin is based on an effective width analysis and strain compatibility between the stringer and effective skin. The cross-plot of panel compression stress F_c indicates the effective stress level at which the stringer and effective skin are working. The remaining portion of skin is considered to have

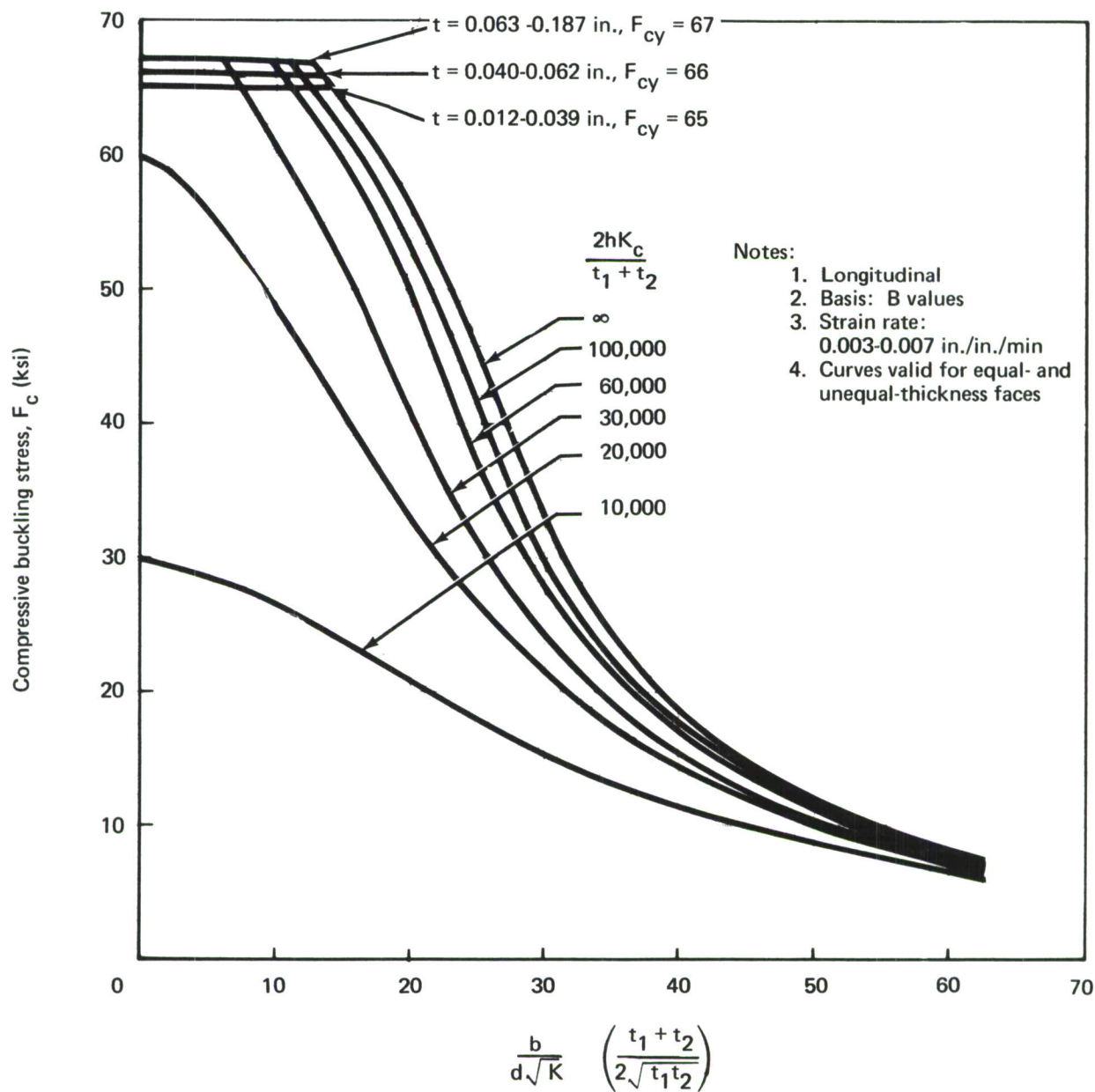


Figure 97.—Compression Stability of Aluminum (7075-T6) Honeycomb Sandwich Panels

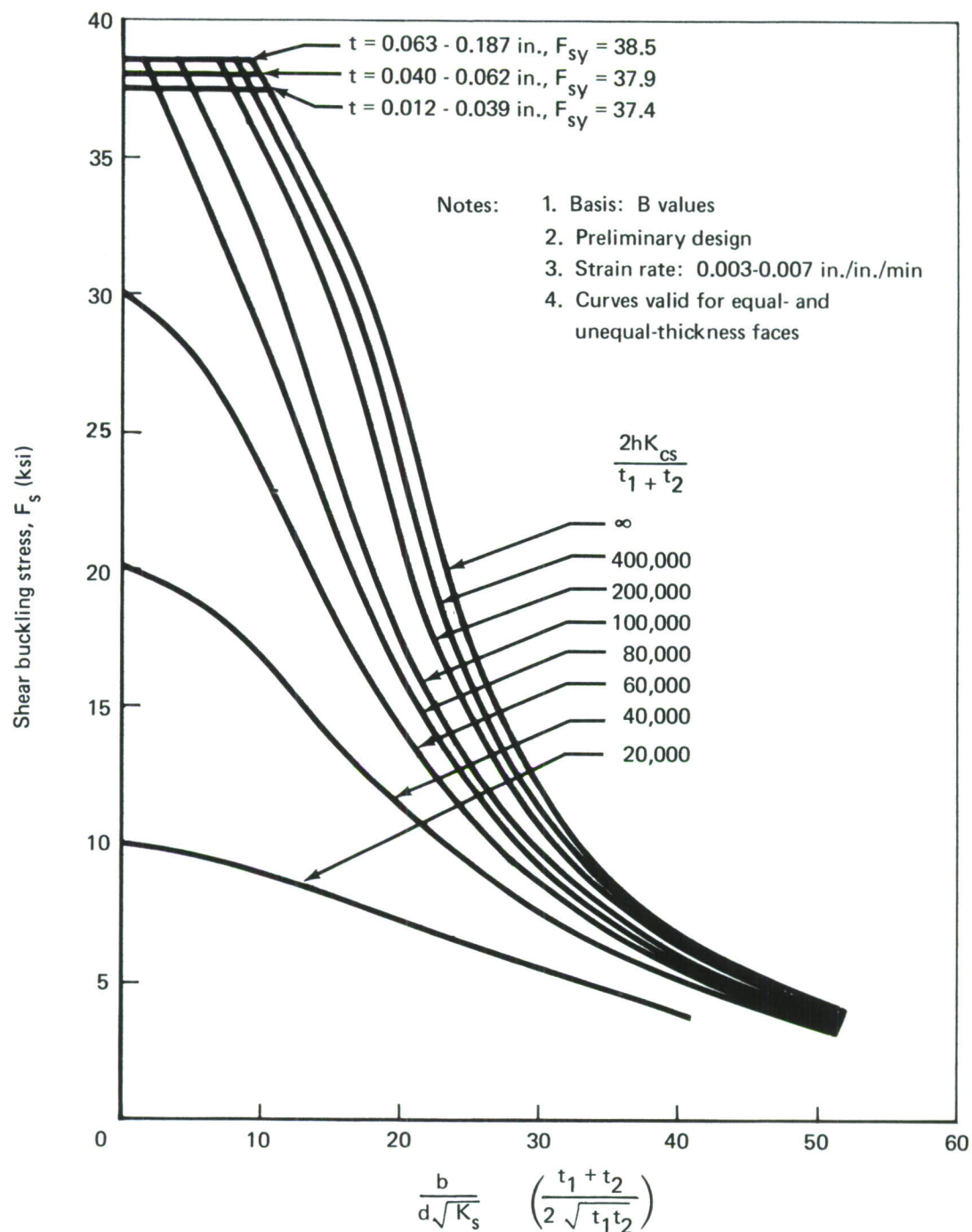


Figure 98.—Shear Stability of Aluminum (7075-T6) Honeycomb Panels

buckled at a lower stress level and is incapable of carrying additional end load. A minimum “smeared” thickness for combined loading, \bar{t}_{CS} , is determined from this analysis.

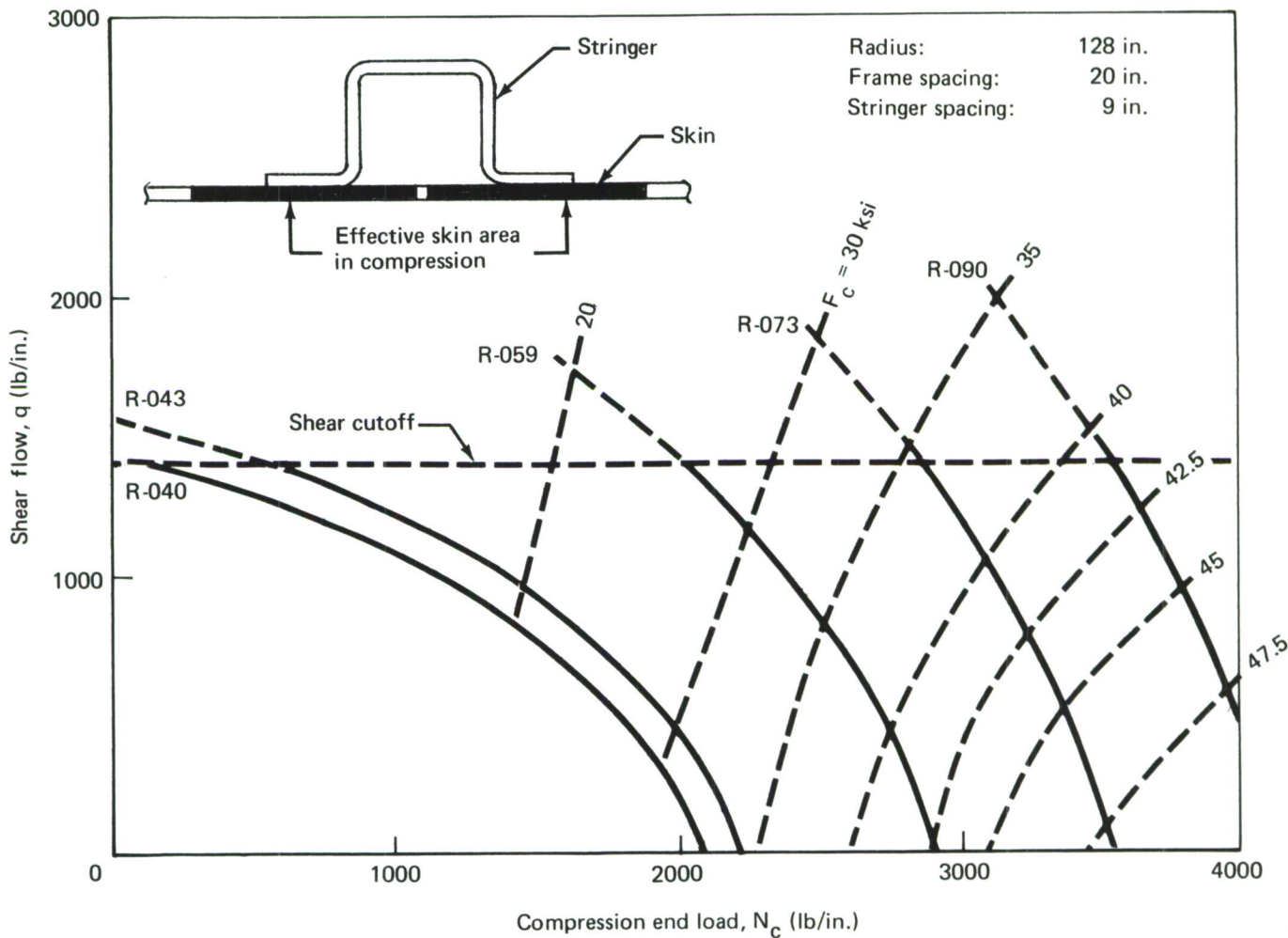


Figure 99.—Combined Compression and Shear Interaction Curves for Skin/Stringer Structural Concepts

A similar analysis procedure was followed for combined loading of honeycomb sandwich shell concepts. The interaction curves shown in figure 100 were generated for honeycomb sandwich panels under edgewise compression and shear. These curves were based on the relationship:

$$\frac{f_c}{F_{c_{cr}}} + \left(\frac{f_s}{F_{s_{cr}}} \right)^m = 1$$

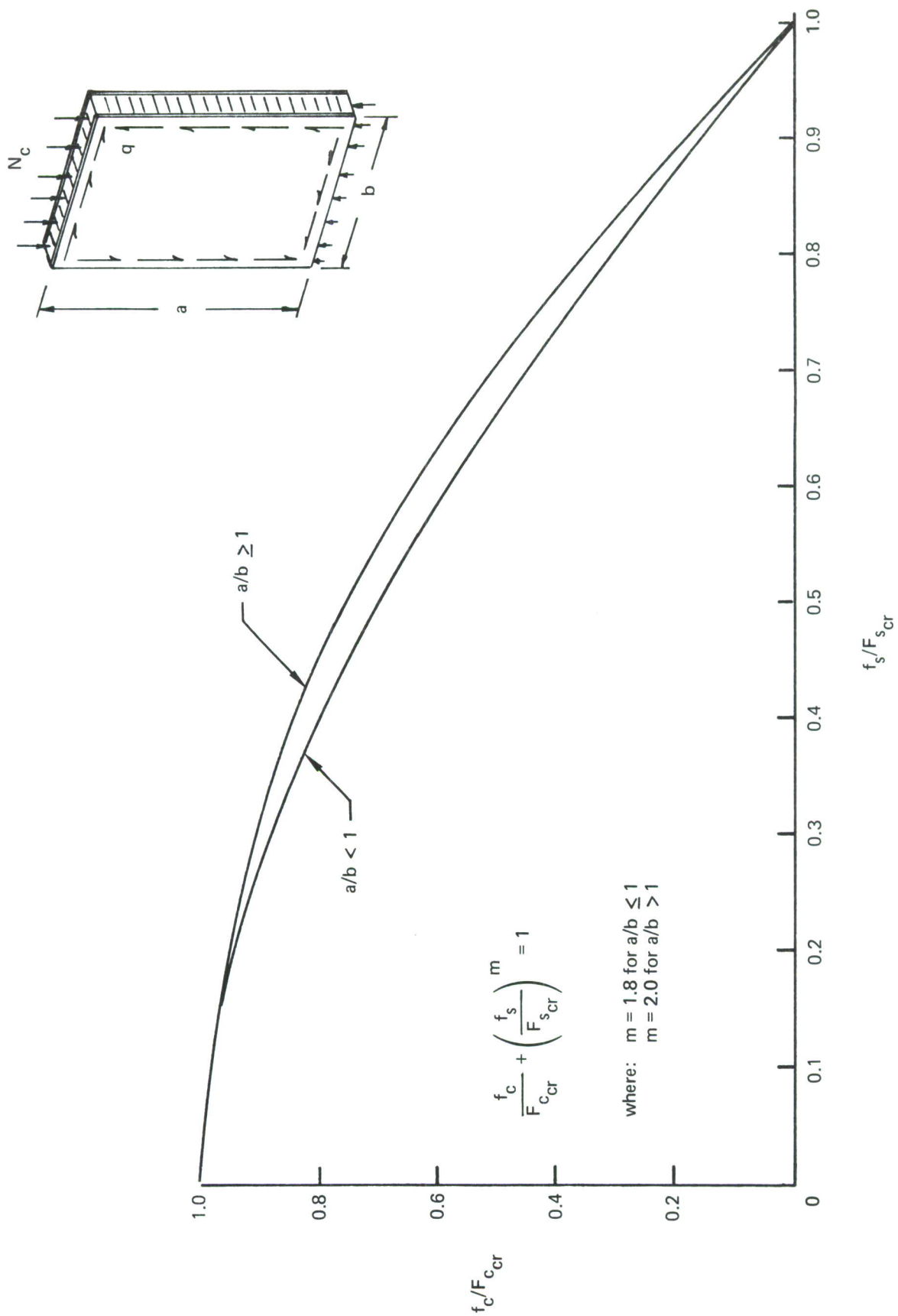


Figure 100. —Interaction Curves—Honeycomb Sandwich Panels Under Edgewise Compression and Shear

where:

- f_c = compression stress in panel
- $F_{c_{cr}}$ = critical compression buckling stress for panel
- f_s = shear stress in panel
- $F_{s_{cr}}$ = critical shear buckling stress for panel
- m = exponent, dependent on panel aspect ratio
 $m = 1.8$ for $a/b < 1$
 $m = 2.0$ for $a/b \geq 1$

The procedure used was to size independently for compression and shear and then check the resulting design for combined loading.

(4) Final Shell Sizing

The final sizing of the shell structure was determined by selecting the maximum “smeared” thickness \bar{t} resulting from the analysis for tension, compression, shear, and combined loading conditions. Care was taken to ensure that minimum skin gages met hoop tension, shear, and damage tolerance requirements. The 50% stiffening was maintained to meet shear stability criteria, and stringer-to-skin area ratios were maintained to meet fail-safe and circumferential crack growth criteria in the crown. Additional precautions were taken during final sizing exercises to ensure that stiffener geometries agreed with the configurations evaluated in the structural optimization and combined loading analysis.

(5) Analysis of Other Structural Components

Trade studies requiring strength check analysis were conducted to evaluate the potential for weight saving and improved structural efficiency of the other major components contained in the fuselage study section. As in the shell concept, these studies were based on load and stress distributions determined by formal stress analysis of the corresponding baseline structure.

Frames: In monocoque and semi-monocoque shell structures, several design requirements must be considered in the analysis and sizing of fuselage frames. Principal considerations include:

- Shell general stability
- Pressure loading
- Damage tolerance
- Floor, cargo, and equipment inertia loads

In general, frames are designed by stiffness requirements to provide shell general stability under vertical bending, side bending, and torsional loading due to flight and ground conditions. Ultimate strength analysis is required for hoop tension loads caused by internal pressurization. Inner flange elements must be analyzed for local crippling stability. Secondary bending effects determine frame-to-shell area ratios for balanced designs. Damage tolerance and fail-safe designs must also be considered.

Body Station 1480 Bulkhead: The major structural bulkhead, located at station 1480 in the forward end of the study fuselage section, is shown in figure 101. Station 1480 is the location of a major circumferential production splice of two fuselage sections, and the bulkhead must be strength analyzed to ensure efficient transfer of primary fuselage loads across the splice. The lower lobe of the bulkhead serves as a pressure seal at the wheel well cutout and as a support structure for the main body landing gear fittings. This structure was analyzed to assess the static strength, cyclic fatigue durability, damage tolerance, deflection compatibility, and concentrated load diffusion capability of the bulkhead web.

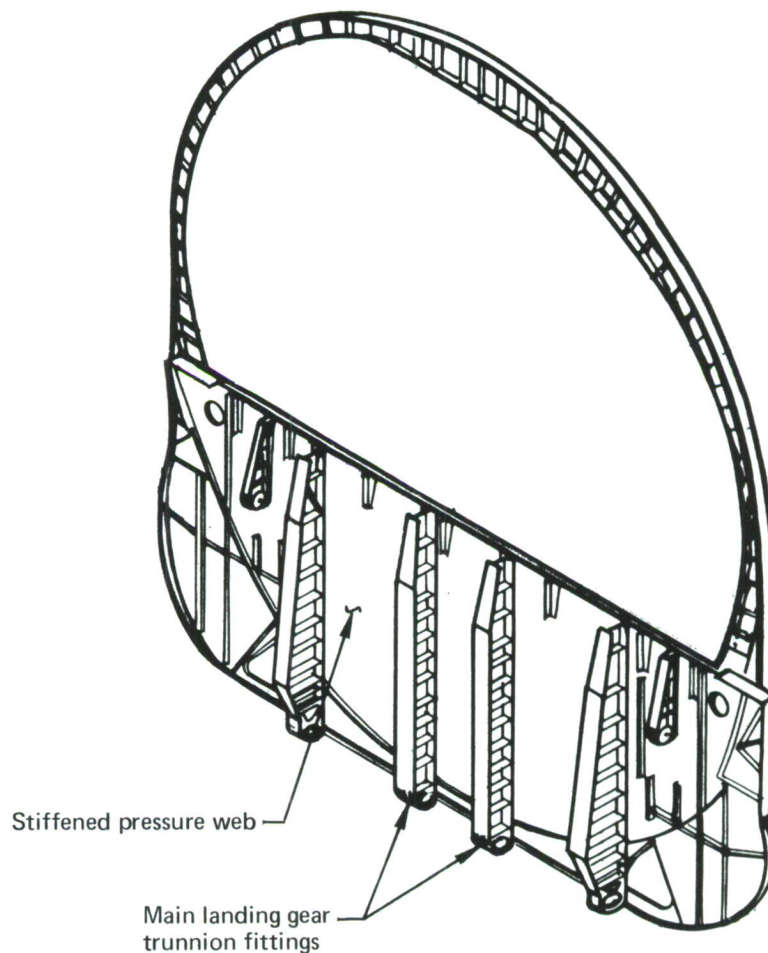


Figure 101. —Pressure Bulkhead, Body Station 1480

Keel Beam: Fuselage loads in the wheel well area are applied to the keel beam located at the centerline of the airplane. The keel beam structure (fig. 102) extends from body station 1232 through 1480, and consists of a deep, built-up beam with a vertically stiffened web. Axial loads due to fuselage bending are applied to the lower chord members, and fuselage shears are carried in the web. Critical load conditions are positive dive maneuver and four-point braked roll. The keel beam structure was analyzed for compression and shear stability and ultimate strength using classical analysis methods.

Pressure Deck: The pressure deck serves as a pressure seal between the main cabin floor and the wheel well area. The baseline structure consists of a stiffened plate suspended from the lower chord of the seat track beams. The pressure deck was analyzed as a stiffened plate on multiple supports subjected to a uniformly distributed pressure load. The structure was also assessed for damage tolerance and shear capability.

Floor Beams: The floor beams are analyzed as semi-field-tension beams with an upper cap, lower cap, and thin, vertically stiffened web. The beam distributes floor loads directly to the shell frames by means of the outboard end-to-frame rigid connection, and indirectly by two intermediate vertical posts. The beam also acts as a tension tie to resist differential pressure effects. The beam reactions and loads were obtained from a finite element analysis of the shell and frames.

b. Fatigue

(1) Introduction

To ensure satisfaction of the fatigue life goals selected for design of the advanced cargo fuselage (table XXI), high-quality structural details were required. An accurate assessment of the fatigue capability of those structural details that evolved during the design phases was required to achieve lightweight, cost-effective structure.

Recently developed “hand” and improved computer fatigue analysis methods were used to ensure the satisfaction of the fatigue life goals. These new analysis techniques were developed in an in-house IR&D program and are based on fundamental considerations as modified by actual fleet service experience.

The early identification of fatigue design problems and the application of a consistent, disciplined fatigue analysis methodology has enabled the development and selection of concepts that avoid potential fatigue problems. Application of this methodology to fuselage shell structure offers the opportunity during the design process to take account of the unique conditions that prevail in pressurized fuselage structure:

- High biaxiality of stress field
- Pillowing effects of pressurization
- Diagonal tension effects of light skins loaded in shear
- Intersection of two heavily loaded elements (stringer/frame)

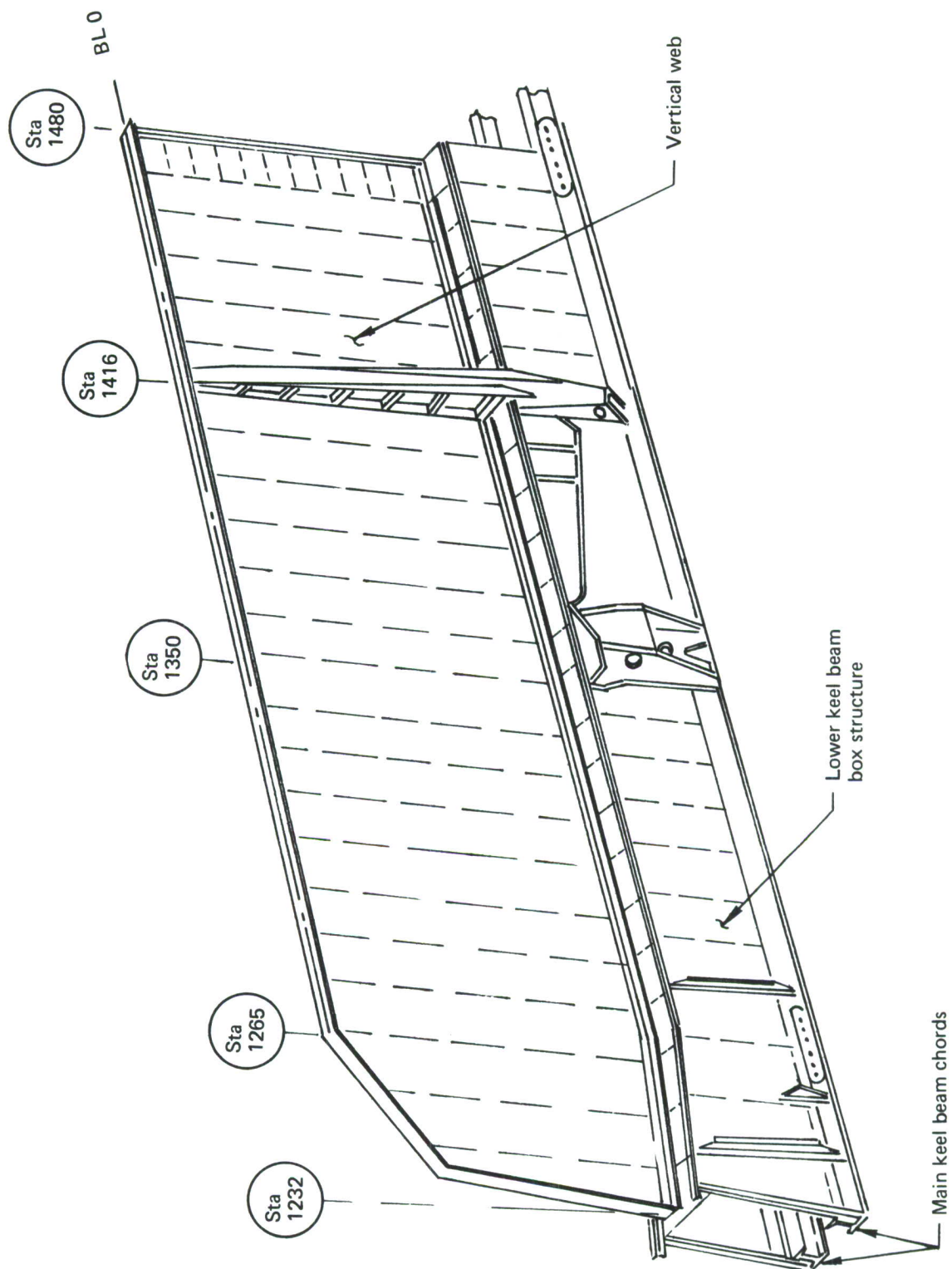


Figure 102.—747 Keel Beam Structure

Table XXI.—Fatigue Life Requirements

Baseline (747-100) advanced cargo fuselage component and ADP requirements	MIL-STD-1530 (USAF)
<ul style="list-style-type: none"> ● 60,000 flight-hours 9600 short flights 4800 medium flights 4800 long flights 600 training flights 24,600 landings ● Load environment Maneuver—Figure 103 Gust—MIL-A-8866 Taxi—MIL-A-8866 ● Four factors on life 	<ul style="list-style-type: none"> ● 50,000 flight-hours 12,500 flights 25,000 landings 15,000 fuselage pressure ● Load environment Maneuver—MIL-A-8866 (USAF) Gust—MIL-A-8861 Taxi—MIL-A-8866 (USAF) ● Four factors on log-mean life

Full-scale fatigue testing of the baseline substantiates the design of that structure and provides a good base for further refinement and modification to evolve more weight- and cost-effective structure.

(2) Fatigue Life Requirements

The fatigue life requirements for the cargo fuselage component are the same as those specified for the baseline. These requirements are compared with the fatigue life requirements of MIL-STD-1530 (USAF) in table XXI and shown graphically in figure 103. The comparison shows that the fatigue life requirements are similar, and detailed analysis has shown that the load environment is comparable.

(3) Fatigue Analysis

Three important keys are recognized in fatigue analysis:

- The *load environment* and airplane utilization influence the fatigue performance of a structural element. The designer or analyst has little control over this; however, its impact must be accurately evaluated to ensure adequate fatigue performance.
- The *stress environment* to which a structural element is exposed directly affects its fatigue performance. Adjustment of the stresses through detail resizing may significantly enhance fatigue performance, but it results in a significant weight penalty.

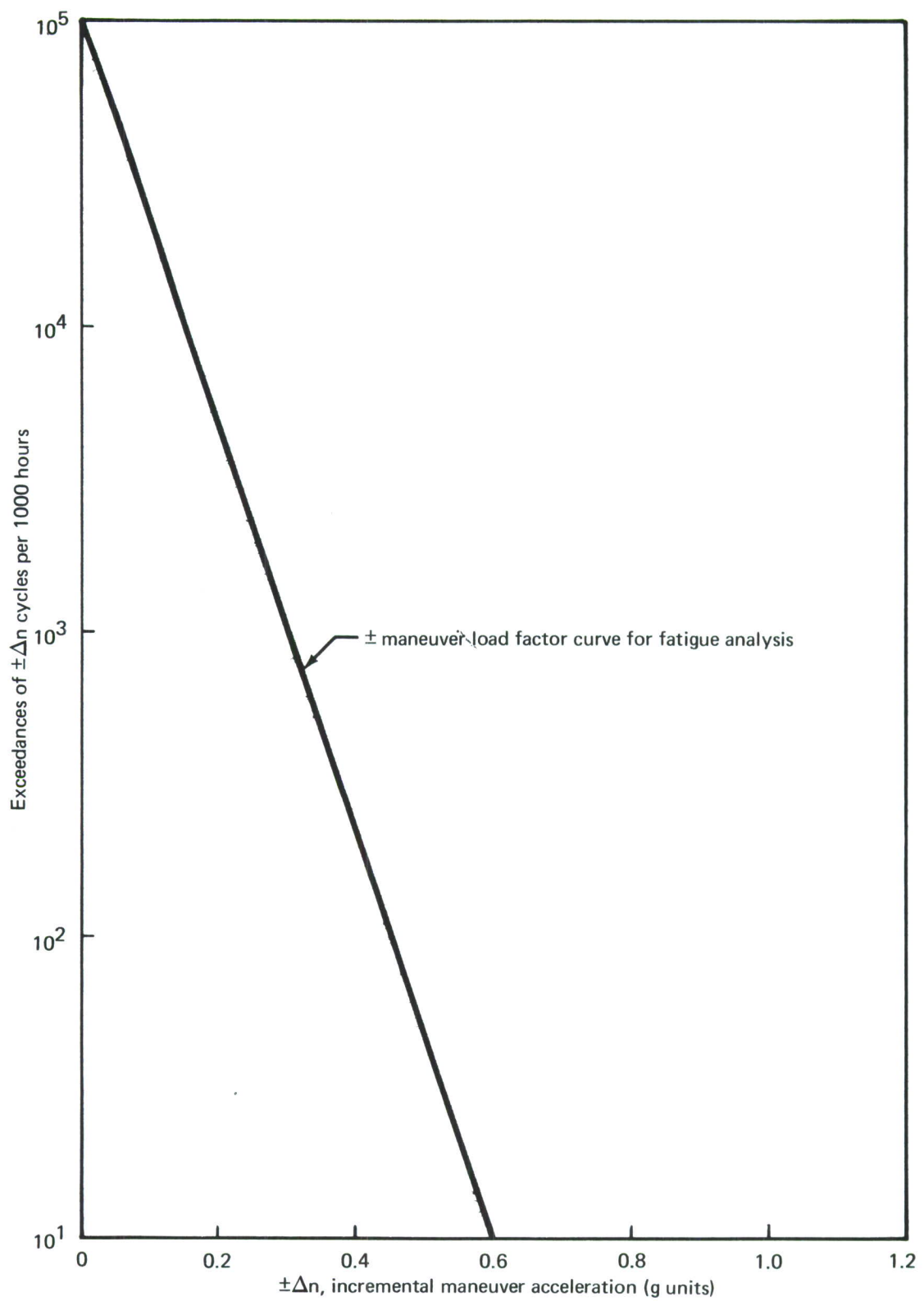


Figure 103.—Load Environment—Maneuver

- The *detail design* of a structural element directly affects its fatigue performance, and careful attention to this item results in significant weight payoff.

Following is a description of the sequence of events performed during a fatigue analysis:

- Establish airplane utilization and mission profiles
- Establish gust, taxi, and maneuver environment
- Establish airplane response to environment
- Evaluate fatigue quality rating (FQR)
- Apply supplementary fatigue factor (SFF)
- Sum damage, using the Palmgren-Miner rule
- Calculate fatigue margin based on stress

Aeroelastic response to the environment was computed by the Loads unit, and the resulting loads were transmitted to the Stress unit. Structural response in terms of $\Delta f/U_{de}$, $\Delta f/\Delta n$, etc., was then obtained by means of computer programs. The structural response to loads used on this component was the same as that used on the baseline, as reported in section VI-1b1.

Fatigue performance was then determined for a particular structural detail by means of a fatigue analysis computer program that operates on the load environment, structural response, and assigned detail fatigue quality rating. The fatigue performance is determined in terms of fatigue life capability, N , cumulative damage, $\sum n/N$, and fatigue margin of safety.

The capability of a structural detail, skin, fitting, splice, etc., to resist fatigue damage is, in Boeing nomenclature, identified by its fatigue quality rating (FQR). This is a quantitative assessment based on service experience and test data.

The fatigue quality rating of a structural detail is defined as the maximum cyclic stress at $R = 0.06$ that results in a fatigue life for that detail of 10^5 cycles with 95% confidence of 95% survival on a Weibull distribution. A typical S-N curve, as defined by an FQR of 18 ksi, is shown in figure 104. A significant feature of the fatigue quality rating S-N curve is the reduction of the endurance limit to approximately 2% to 3% of the ultimate tension stress. This modification has been found to correlate service experience with laboratory behavior and to effectively reflect spectrum loading effects. It also reflects experience gained from tests of full-size airframe components that show structure fatigue performance to be equivalent to that of the test specimens with $K_t = 2$ to 3 at moderate alternating stress levels, and to specimens with much higher K_t values at lower alternating stress levels. These modifications have the effect of using a high equivalent K_t for the range of alternating stress levels over which most of the damage is computed. Detail properties affecting the FQR are:

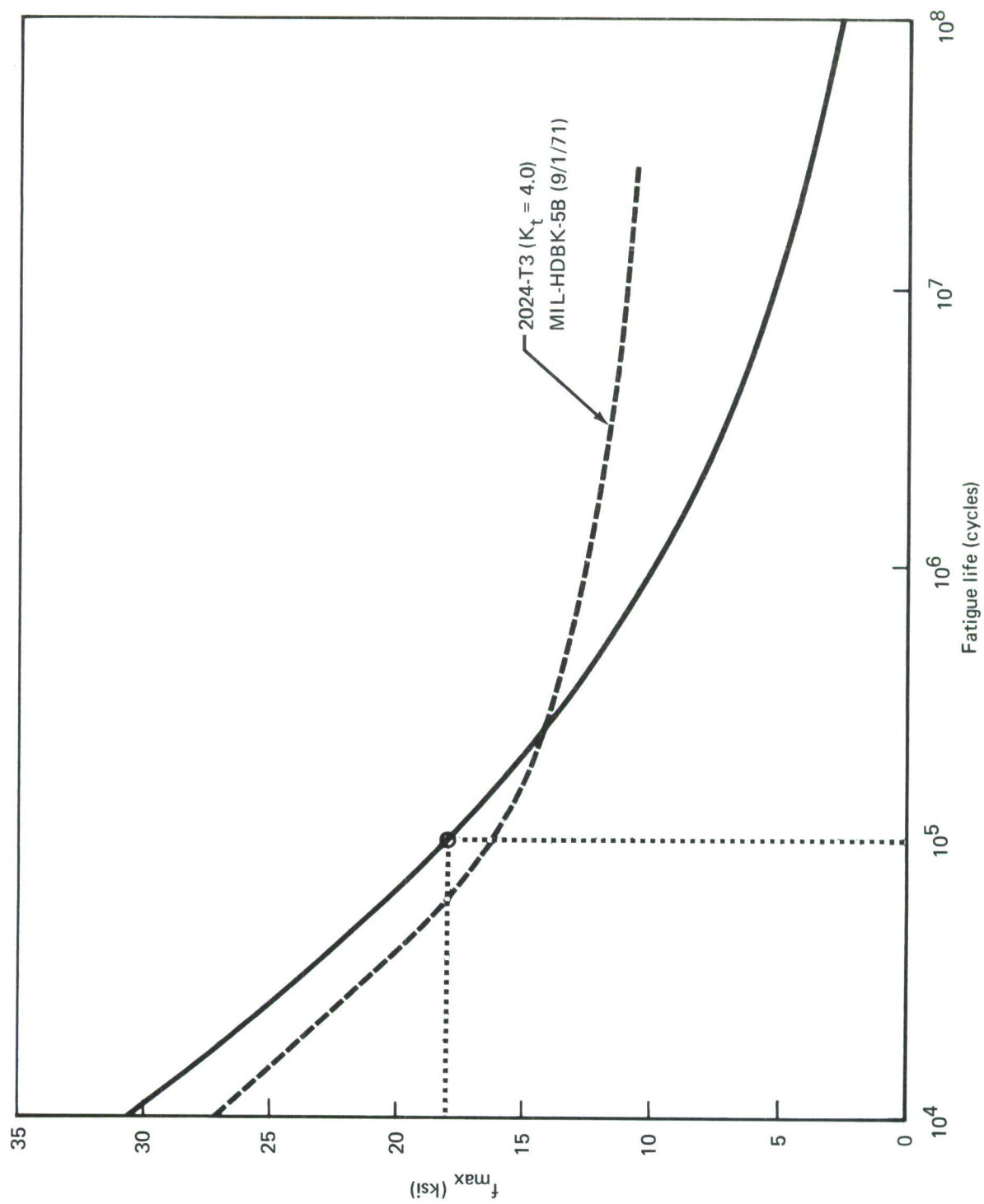
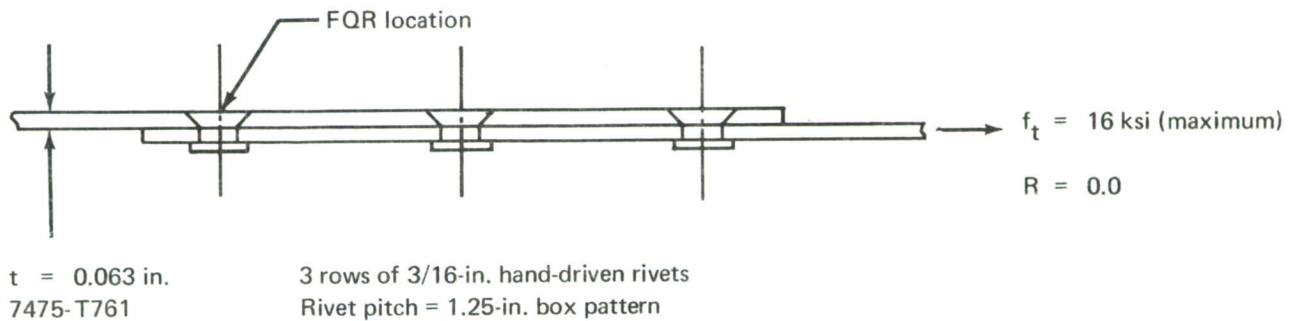


Figure 104.—Standardized Aluminum $S-N$ Data— $FQR = 18$ ksi, $R = 0.06$

- Geometric stress concentration
- Material constant
- Load transfer
- Hole filling
- Countersink depth
- Stack-up
- Fastener clamp-up
- Pad-up efficiency

An example of the impact of changes in detail properties on the fatigue performance of a particular detail (skin lap splice) is shown in table XXII. Various methods are indicated that improve fatigue performance: decreasing rivet pitch, applying fay surface sealant, and increasing the minimum driven rivet head size to 1.4d (1.4 times shank diameter), replacing the standard 1.3d.

Table XXII.—Detail Design Impact on Fatigue Life



Item	FQR	N (cycles)	N/N_1
(1) Detail as shown	10	6,550	1.0
(2) Rivet pitch 0.75 in.	12	13,100	2.0
(3) Fay surface sealant	13.5	21,800	3.3
(4) Driven rivet head 1.4 x shank diameter	16	39,000	6.0

Design and manufacturing studies indicate that mechanical fastening must be resorted to in order to effect assembly (shell quadrant) splices and production joints. Fleet service experience has indicated that mechanical joints must be carefully designed if they are to exhibit satisfactory fatigue performance. The systematic method of evaluating fatigue quality ratings allows rapid design and evaluation of structural details.

As a consequence of this investigation, quadrant assembly joints will be fabricated using fay surface sealant and rivets with minimum driven head sizes of 1.4d. Also, rivet pitch and local geometry will be adjusted as necessary to satisfy fatigue requirements.

(4) Fatigue Analysis Locations

The satisfaction of the fatigue requirements was ensured by conducting detailed fatigue analyses at the following locations:

- Stringers 1, 8, 13, 18, and 23 at body stations 1480, 1580, 1640, and 1741
- Skin (S-23) at body stations 1480, 1580, 1640, and 1741
- Keel beam web at body station 1480
- Frame chords at body station 1520
- Joints and details
- Cutout areas

The fatigue analysis locations, shown in figure 105, were selected on the basis of service experience and theoretical considerations that indicate potential fatigue problem areas. This experience was accumulated in the design of similar airframes subjected to similar load environments and use.

(5) Fatigue Data Transfer

The results of the fatigue analysis at these locations were transferred to the designers and stress analysts in terms of allowable, once-per-flight, maximum cyclic stresses, F_{gag} . Figure 106 is an example of the data transfer format used by the fatigue analysts. This example represents the result of the fatigue analysis conducted on stringers 1, 8, 13, 18, and 23 at body station 1580. It should be noted that as the quality of a detail is increased, i.e., an increase in the FQR, the allowable, maximum once-per-flight stress level is increased. Data of this type at all fatigue analysis locations were transferred to the Stress and Design units. All elements of the design team are indoctrinated to the systematic evaluation of the detail FQR; hence, these curves of allowable fatigue stress, F_{gag} , versus FQR permit rapid structural sizing and are useful in design trade studies.

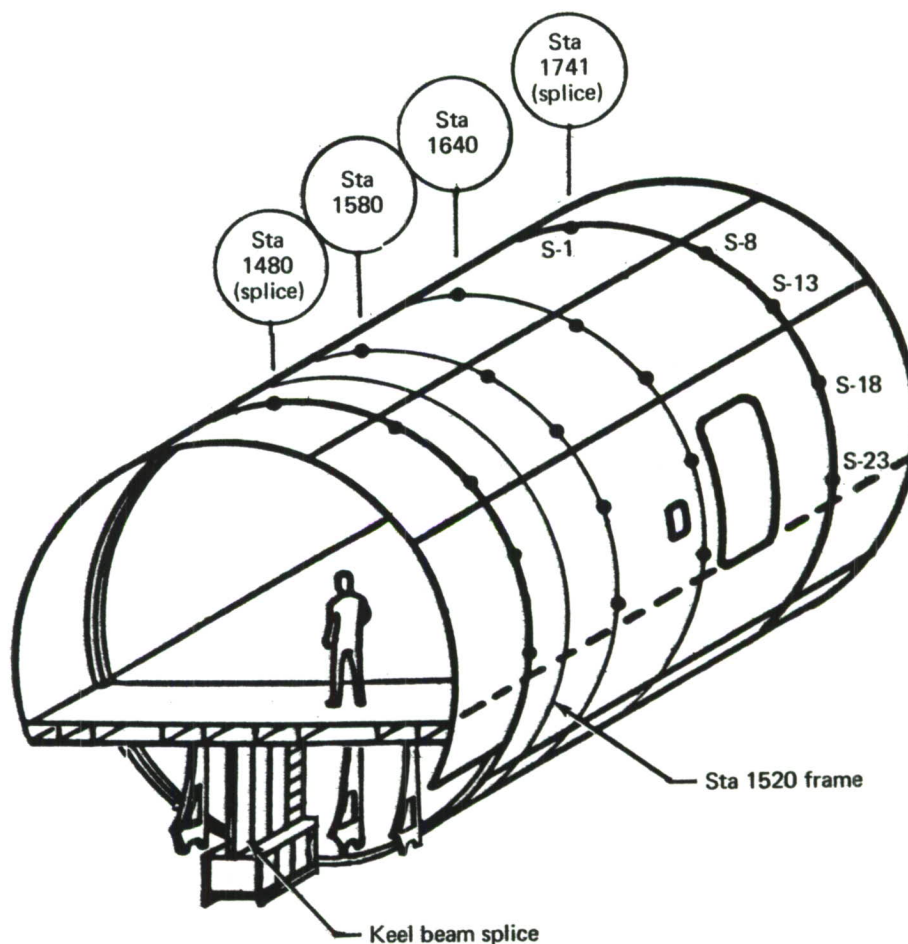


Figure 105.—Fatigue Analysis Locations

(6) FQR Requirement for No Constraint on Ultimate Design

One of the specific design goals imposed on the cargo fuselage component is that there be no fatigue design constraint on ultimate strength design, as stated in section III-1. The FQR requirements to ensure that the ultimate allowable stresses assigned to the various crown candidate materials would not be constrained by fatigue considerations are shown in figure 107. The 16 ksi FQR assessed for the baseline structure, which uses 2024-T3 skins riveted to 7075-T6 stringers, is shown for reference. It may be observed that this 16 ksi value fully exploits the static capability of the baseline structure, ultimate $F_t = 52$ ksi. It was concluded that in order to realize the enhanced static properties of the advanced materials a corresponding increase in detail fatigue quality must be attained.

(7) Stringer/Frame Intersection Study

In the cargo fuselage, approximately 30% of the fatigue problems occur at the intersection of two or more members. Most of these problems occur at stringer/frame intersections.

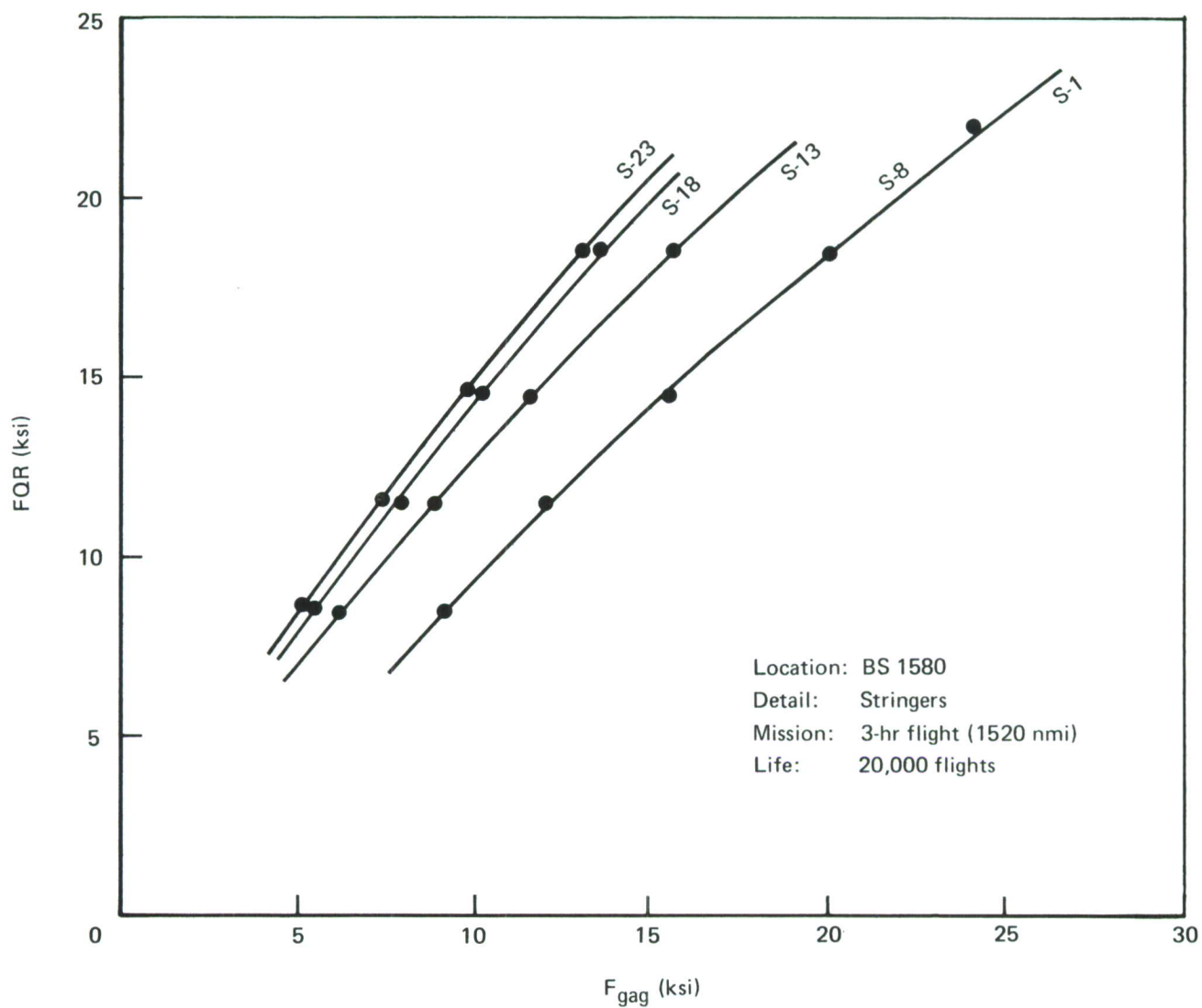


Figure 106.—Fatigue Analysis Design Data

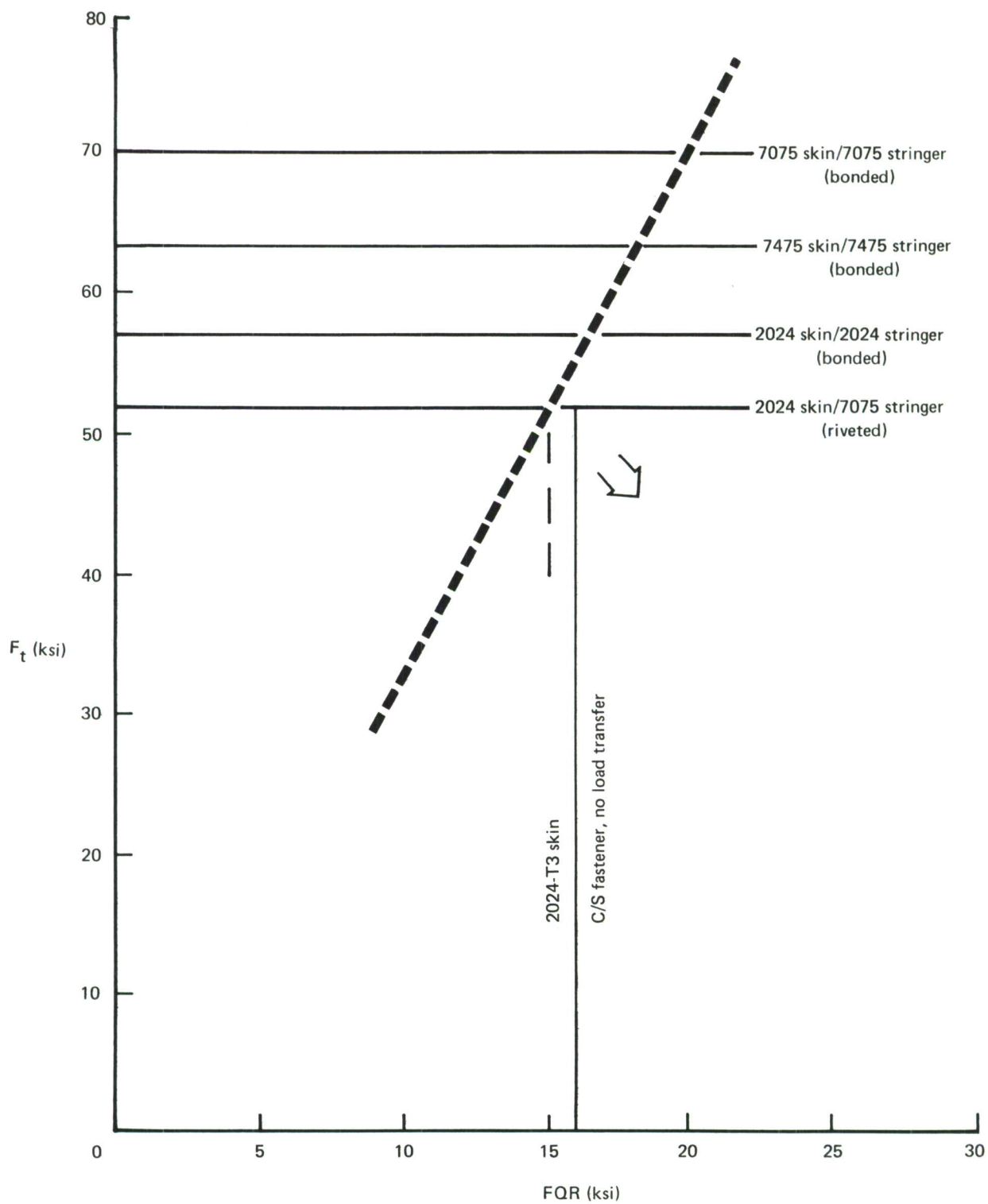


Figure 107.— FQR Requirements for No Constraint on Ultimate Design—Crown

All airframe structure requires intersection of structural elements; however, in the fuselage shell, the intersection of frames and stringers is characterized by increased fatigue severity due to:

- Transfer of the stringer shear loads, due to pressure, to the frames
- Discontinuity of frame load paths occasioned by stringer continuity requirements

Design details were developed during level 1 and 2 studies to avoid this stringer/frame intersection problem. The honeycomb sandwich shell and the externally stiffened shell eliminate the cutouts required in the frame. The other concepts developed retain the frame cutout for stringers; however, the details at these cutouts have been refined to ensure satisfactory fatigue performance.

(8) Materials and Processes Trade Study

Since the capability of baseline materials is fully exploited for the baseline fuselage structure, a materials and processes trade study was initiated to define those materials and joining techniques which can reduce structural weight while maintaining fatigue performance.

Evaluation of joining processes conducted during level 1 screening exposed the desirability of changing the skin-to-stringer joining system from the riveted construction of the baseline to adhesive bonding. The reasons for this change are as follows:

- Bonding eliminates stress concentrations around fastener holes which seriously degrade fatigue performance. Figure 108 shows the improvement in fatigue performance of the fuselage crown using bonded instead of riveted joints.
- Bonding results in higher ultimate allowables due to the elimination of “hole-out” requirements for mechanical fasteners.

Therefore, this method of joining was selected for use on the cargo fuselage component.

Other methods of upgrading the fatigue quality of the fuselage shell were considered, such as cold-working of holes, high-squeeze riveting, etc. However, these alternate joining techniques were eliminated since they exhibit reduced structural performance under damage tolerance considerations as compared with bonded construction (sec. IV-4c6).

The final selection of materials for use on this program was made during level 3 material studies. Fuselage skin and stringer materials had been narrowed to three candidates during level 1 and 2 screening.

- The baseline materials (2024-T3 skins and 7075-T6 stringers) were retained for use in evaluating the alternate materials and joining processes.

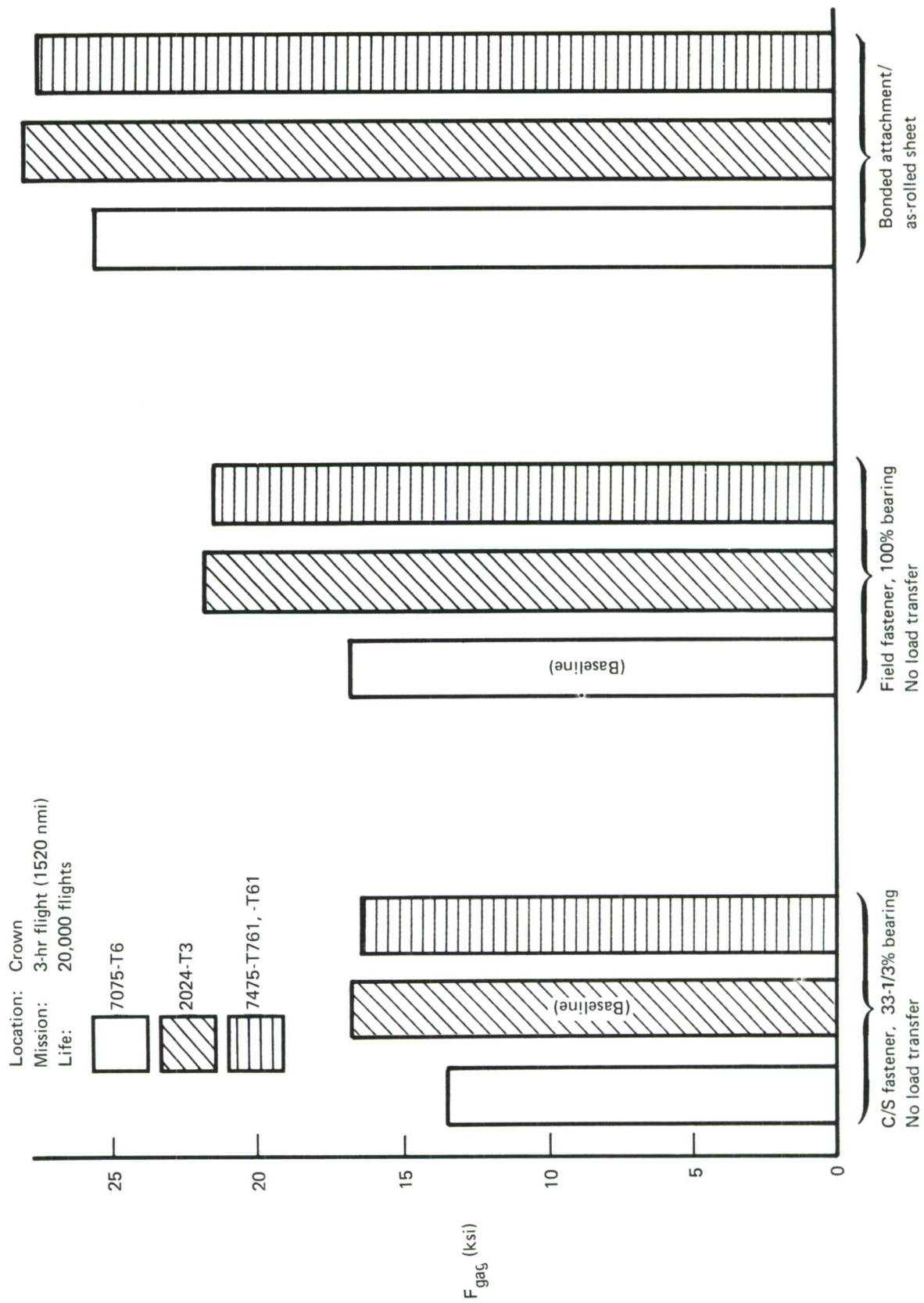


Figure 108.—Material and Process Trade Study

- The 7475-T761 and 7475-T61 were retained because of their good static and excellent fatigue properties. Results of fatigue testing conducted on this program (app. II), reported in reference 9 and received through the interim material test data interchange program described under “Aluminum” in section IV-2a1, indicate that this material exhibits fatigue performance equal to, or very nearly to, that of the baseline 2024-T3. The improved static properties of this material over those of the baseline are particularly important since the baseline fuselage shell fully exploits the static capability of the baseline materials.
- The 7075-T6 was retained because of its excellent static properties. Although this material exhibits relatively poor fatigue performance, it was felt that the enhancement in fatigue quality rating due to bonding would allow its use.

The crown allowable fatigue stresses, F_{gag} , were determined as described in section IV-4b5. They were converted to crown allowable tension stresses by means of the following relation:

$$F_t = 3.31 F_{gag}$$

and are shown in figure 109.

Figure 109 demonstrates that 7475-T761 fulfills the goal of no fatigue design constraint on ultimate strength design and shows potential for weight reduction.

The 7475-T761 was selected for use on skins and stringers because of its superior combination of fatigue and static properties. Damage tolerance studies indicate that the full potential of this material can be realized for fuselage crown skins and stringers. Use of this material and bonded construction results in a potential weight saving of 30% for fatigue-critical elements as compared with the baseline materials and joining process; however, static and damage tolerance considerations limit the weight savings that may be realized.

(9) Fatigue Testing

A survey of the material candidates, conducted early in the program, indicated the high potential of 7475-T761 and -T61 for use as the fuselage shell material; thus, it was decided that fatigue data would be obtained for this material. The assessment of existing fatigue and fracture data for these materials (ref. 9) indicated that only a minimum of fatigue test data was required to effect an adequate fatigue analysis and design.

The results of fatigue testing conducted on this program are shown in appendix II.

The allowable fatigue S-N curves developed through testing for use on this program, from data presented in reference 9 and received through the interim material test data interchange program described under “Aluminum” in section IV-2a1, are shown in figure 110.

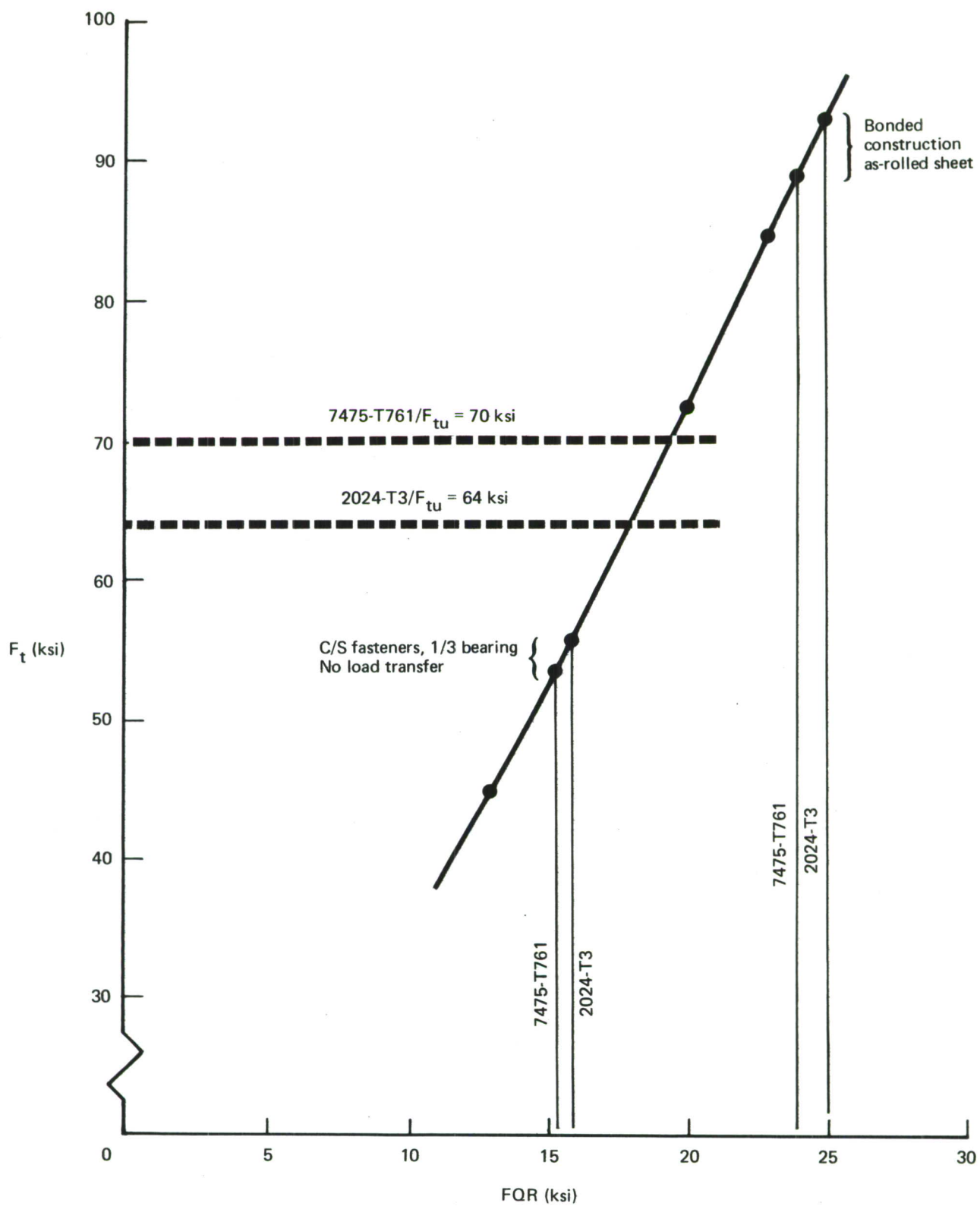


Figure 109 –Allowable Tension Stresses—Crown Structure

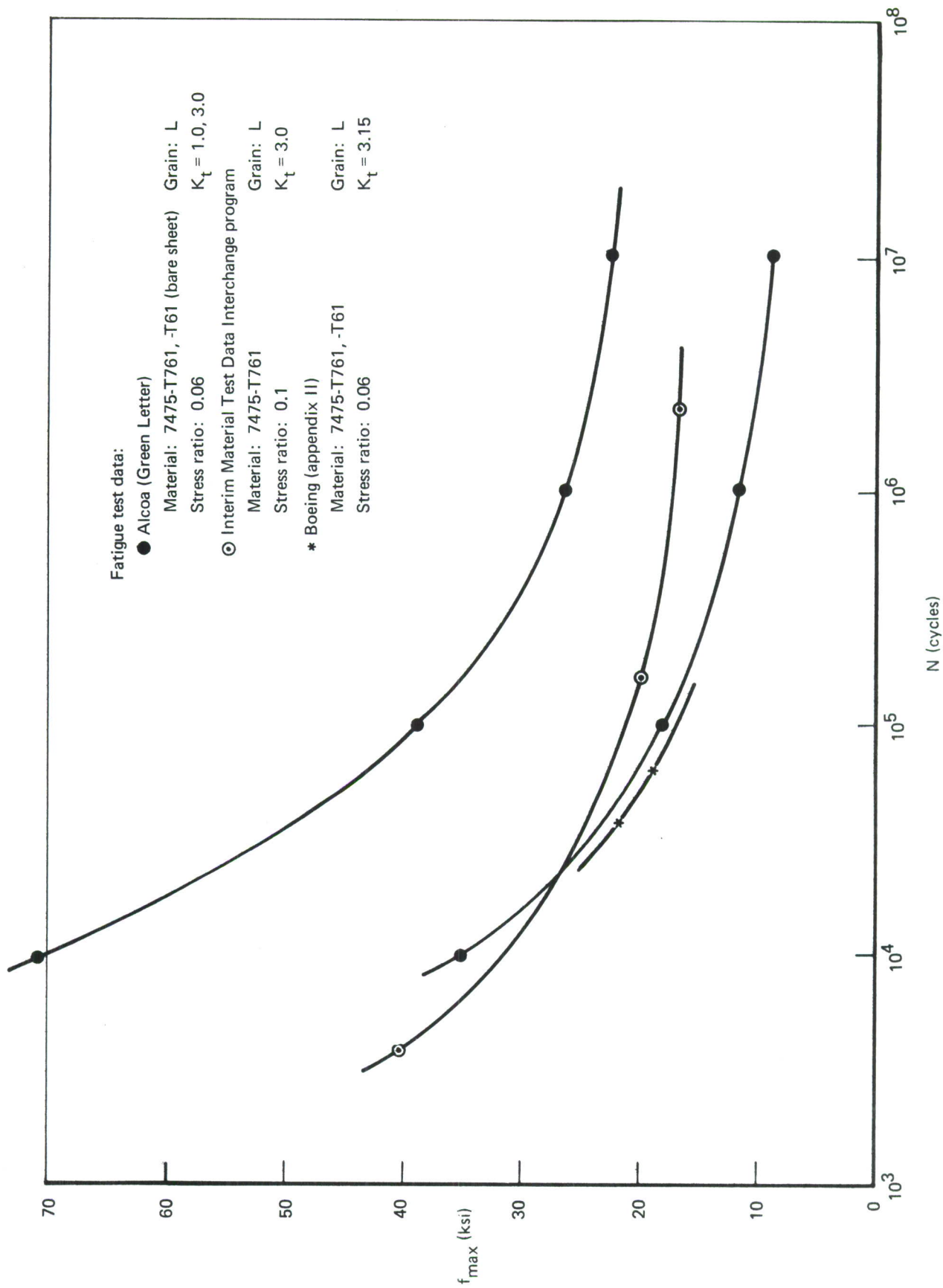


Figure 110.—Fatigue Test Data

c. Damage Tolerance

(1) Introduction

Damage tolerant design and analysis is required to ensure safety of the airframe structure throughout its service life. This requirement exists for aircraft certified for civil aviation use (FAR 25). The baseline airplane also exhibits sufficient damage tolerance to satisfy the requirements stated in MIL-STD-1530 (USAF) and the Air Force Damage Tolerance Criteria in appendix I. If the program goal of weight reduction is to be attained, more effective damage tolerant design concepts and materials must be utilized.

A cost- and weight-effective damage tolerant design requires careful attention to detail design and material selection. Damage tolerant design concept/material/weight trade studies were performed to identify those candidates which exhibit the greatest potential for weight savings.

The application of linear fracture mechanics techniques to fuselage shell structure to ensure satisfaction of damage tolerance requirements offers the opportunity to develop design details required by the unique conditions that prevail in pressurized fuselage structure:

- High biaxiality of stress field
- Curvature effects
- Pillowing effects of pressurization

The effects of these conditions have been considered in the selection of shell materials, structural details, and allowable stress levels.

Full-scale fail-safe testing conducted on the baseline substantiates the analysis and design techniques used on that airframe. Data from these tests were used to further extend the principles of fracture mechanics to the structural design and analysis of the advanced fuselage component.

(2) Damage Tolerance Criteria

The damage tolerance criteria adopted for use on the advanced cargo fuselage component are shown in table XXIII. The requirements of appendix I were adopted in toto for the cargo fuselage component. In the absence of a specific requirement for foreign-body penetration or battle damage, the Boeing criterion for residual strength capability after impact by a 12-inch turbine blade at an energy level of 2900 foot-pounds, in defined areas, was adopted with the concurrence of the Air Force. The defined areas of potential blade impact are shown in figure 111. The damage resulting from blade impact is assumed to be in-flight evident; therefore, the residual strength load requirement for the intact structure will be the load that would be exceeded once during a period of 100 flights.

Table XXIII.—Criteria for Damage Tolerance

Requirement	Baseline	USAF Damage Tolerance Criteria Revision D, Aug. 18, 1972 (ref. app. I)	ADP advanced cargo fuselage
Period of unrepaired service use	Stable crack growth between D checks (20% of fleet at 9000 hr)	USAF damage tolerance criteria: structure must satisfy at least one of the periods of unrepaired service usage specified in section 2 or 3	USAF Damage Tolerance Criteria, Revision D
Residual strength load condition	FAR 25: 0.92 x limit load ARB: limit load	USAF damage tolerance criteria: $P_{XX} = \text{one occurrence}/100 \times F_{XX}$ or $P_{YY} = 1.15 \times P_{XX}$ (at instant of load-path failure)	USAF Damage Tolerance Criteria, Revision D
Damage assumption for residual strength condition	FAR 25: Obvious partial failure of a principal load element	USAF damage tolerance criteria: the minimum assumed in-service damage specified in section 2 or 3 for the applicable degree of inspectability	USAF Damage Tolerance Criteria, Revision D
Foreign body penetration	Boeing: 12-in. turbine blade in defined areas	MIL-STD-1530 (USAF) Other crack-initiation mechanisms	USAF Damage Tolerance Criteria, Revision D, with concurrent supplement (Boeing criteria)

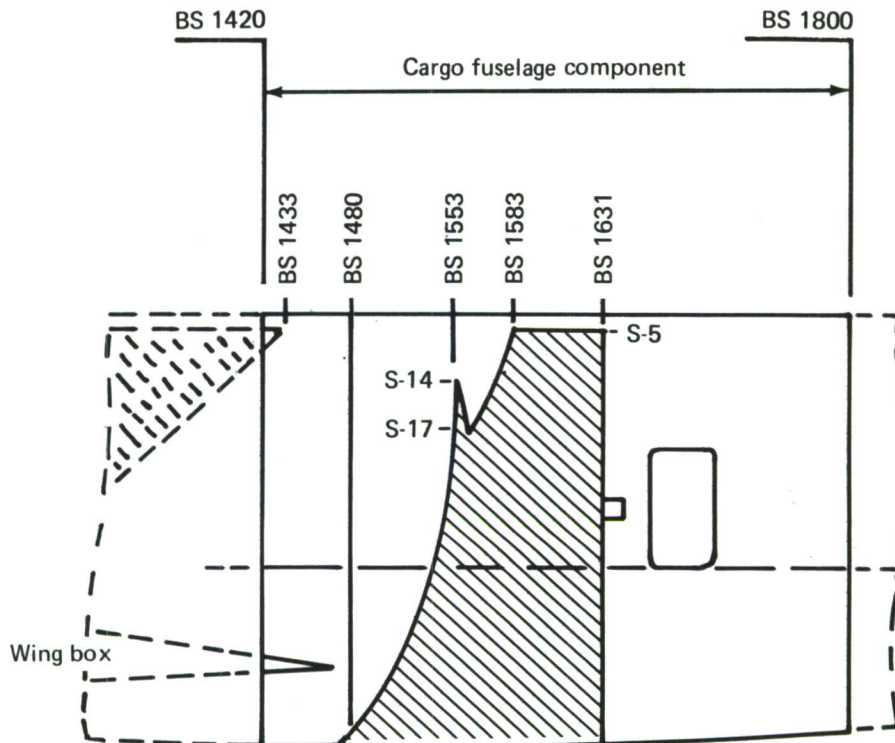


Figure 111.—Potential Blade Impact Areas

A criterion for the identification of fracture-critical parts, a key item of the fracture control plan specified in MIL-STD-1530 (USAF), was adopted for use on this program and is shown in table XXIV. All safety-of-flight structural elements have been analyzed and categorized as being either fracture-critical or non-fracture-critical parts per table XXIV.

(3) Damage Tolerance Analysis

The steps taken in conducting the damage tolerance analysis are:

- Establish stress spectra
- Assume initial damage
- Calculate stress intensity factor considering the effects of

Curvature

Load transfer

Stress distribution

Geometry

}

Linear fracture mechanics/
finite element analysis

Table XXIV.—Criteria for the Identification of Fracture-Critical Parts

Non-Fracture Critical Part	Fracture-Critical Part
<p>Satisfies any one of the following periods of unrepai red service usage specified for the following degrees of inspectability:</p> <ol style="list-style-type: none"> 1 In-service noninspectable 2 Depot or base level inspectable 3 Special visual inspectable <p>and minimum required residual strength (P_{XX}) using:</p> <ol style="list-style-type: none"> A Lowerbound values of K_C or K_{Ic} B Upperbound values of da/dn C Minimum initial damage assumptions specified in MIL-A-8866 <p>In addition:</p> <p>Parts in penetration areas must also satisfy the period of unrepai red usage specified for in-flight evident damage using (A) and (B) above.</p>	<p>Parts that fail to satisfy the requirements stated for non-fracture-critical parts shall be considered fracture critical. In addition, fracture-critical parts shall be categorized as:</p> <p>FC-I Parts: Satisfy the requirements for non-fracture-critical parts by virtue of revised initial damage assumptions.</p> <p>FC-II Parts: Satisfy the requirements for non-fracture-critical parts by virtue of revised lowerbound values of K_C or K_{Ic} or by virtue of revised upperbound values of da/dn.</p> <p>FC-III Parts: Satisfy the requirements for non-fracture-critical parts by virtue of revised in-service inspection requirements.</p>
Required Controls	Required Controls
<ol style="list-style-type: none"> 1 Complete inspection, process, corrosion, and quality control, as approved by the ADPO, will be established 2 Material procurement and manufacturing specifications, as approved by the ADPO, will be established. 3 Depot level and special field-service inspection procedures, as approved by the ADPO, will be established. 	<p>As shown for non-fracture-critical parts; however, additional specific controls shall be identified against the category of fracture criticality, i. e.,</p> <p>FC-I items require special quality control inspection techniques.</p> <p>FC-II items require special control on material procurement and processing.</p> <p>FC-III items require special control on in-service inspection and maintenance.</p> <p>The above listed controls will be established with the concurrence of the ADPO.</p>

- Compute crack growth considering the effects of

Environment	}	Computer program CRACKS
Stress ratio		
Retardation		

- Evaluate residual strength considering three possible modes of failure:

Skin failure	}	Modified Vlieger approach
Reinforcing element yielding		
Attachment failure		

These steps are analogous to those for fatigue analysis and are described below.

The stress spectra used are the same as those used on the baseline fuselage and are reported in section VI-1b1.

The stress intensity factors are calculated using either linear fracture mechanics principles or a finite element analysis computer program which reflects the elastoplastic behavior of structure prior to failure. Both methods are corrected to reflect the influence of:

- Curvature—The fuselage shell has a radius of 127.5 inches.
- Load Transfer—The effect of load transfer between severed and intact elements must be accommodated.
- Stress Distribution—Due to the existence of frames, the hoop tension stresses vary between midbay locations and over frames.
- Geometry—The effects of material placement and area ratios are taken into account.

Crack growth predictions are made by the use of the computer program CRACKS (ref. 13) with the Willenborg retardation model. The validity of the Willenborg retardation model for prediction of spectrum crack growth rates is considered to have been demonstrated for 2024-T3 and 7475-T61 by testing conducted during this program as reported in appendix II and section VI-1.

Residual strength capability is predicted by means of a modified Vlieger approach (ref. 14) that predicts three potential modes of failure:

- Sheet Dynamic Crack Growth—The condition of crack instability is reached when $K \geq K_c$.
- Reinforcing Element Yielding—For linear analysis the capability of reinforcing elements (stringers/frames) to participate in resisting cut ligament loads is truncated at yield stress.

- Attachment Failure—Dynamic failures may be precipitated when attachment elements (rivets or bond lines) fail.

(4) Analysis Locations

Damage tolerance analyses were conducted at the following locations to ascertain the adequacy under conditions of fatigue crack growth and to determine the allowable period of unrepaired service usage and residual strength capability.

- Crown—The crown was analyzed for the condition of transverse cracking under longitudinal stress. In this area, the stress field is predominantly uniaxial, with high longitudinal stress due to body bending and relatively low hoop tension stresses.
- Side of Body—The body side was analyzed for the condition of longitudinal cracking under the combined loading of hoop tension and body bending shears.
- Lower Lobe—The lower lobe was analyzed for the condition of longitudinal cracking under the combined loading of hoop tension and longitudinal compression.
- Keel Beam Web—The keel beam web was analyzed for the condition of web cracks under shear loading with a high degree of diagonal tension.

The analysis locations are shown in figure 112.

(5) Damage Tolerance Data Transfer

To ensure the satisfaction of all aspects of the damage tolerance criteria, all safety-of-flight items were analyzed to evaluate their performance under damage tolerance conditions. These analyses were conducted for the various candidate structural configurations developed by the Design unit for each safety-of-flight item on the component. Stress limitations to ensure attainment of the required period of unrepaired service usage and residual strengths were determined for each configuration and incorporated into structural sizing.

The requirements of appendix I specify that two damage tolerance requirements be satisfied. Safety-of-flight elements must be shown to possess an adequate period of unrepaired service usage and residual load strength capability.

Period of Unrepaired Service Usage: Fatigue crack growth studies were made on the 7475-T761 skin panels selected for use on the advanced cargo fuselage component. These studies were conducted to determine the limitation required on the allowable hoop tension stress to ensure an adequate period of unrepaired service usage (table XXIV). The structure is considered to be a multiple load path independent structure; therefore, the minimum assumed in-service damage for depot or base level inspectable and special visual inspectable structure was assumed.

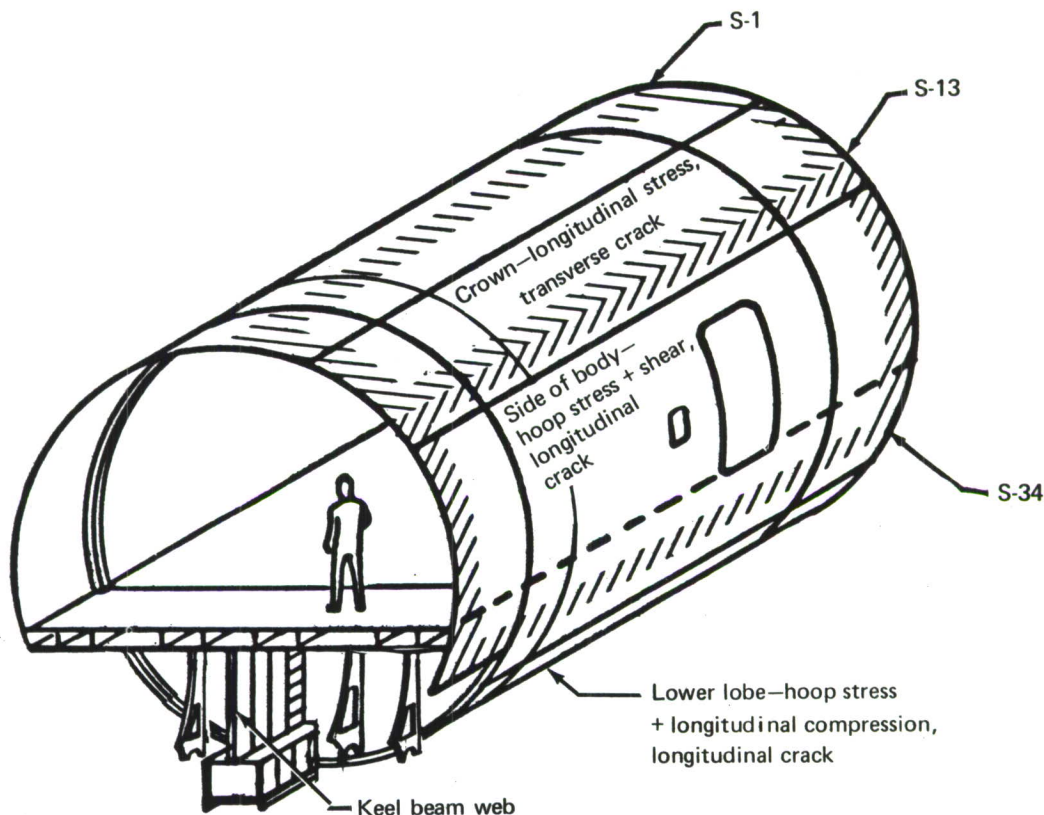


Figure 112.—Damage Tolerance Analysis Locations

Upper-bound fatigue crack growth rates as determined from material test data reported in appendix II were used. The environmental exposure was considered to consist of 80% of total service time in moist air ($RH \geq 90\%$) and the remaining 20% of service in a salt environment (3.5% NaCl). This environmental exposure is considered to be extreme in view of total fleet experience reported in section VI-2; however, it is considered to be possible for airplane utilization in the tropics.

The results of this analysis are shown in figure 113 in terms of the fatigue crack growth life as a function of nominal hoop stress. These curves are typical of those transmitted to the stress and design elements of the program team.

Residual Load Strength Capability: The fuselage skins were analyzed for residual load strength capability under the in-service damage assumption of a full-frame bay skin crack. This assumed damage is conservative for bonded construction in penetration areas with 20-inch tear strap (frame) spacing, as it is in excess of the 12-inch foreign body penetration requirement. However, negligible weight penalty could be identified as associated with this assumption.

Blade penetration testing conducted at Boeing indicates that blade penetration results in a slight amount of sheet tearing about the penetration site. Calculations indicate that the penetration condition results in a stress intensity approximately 8% less

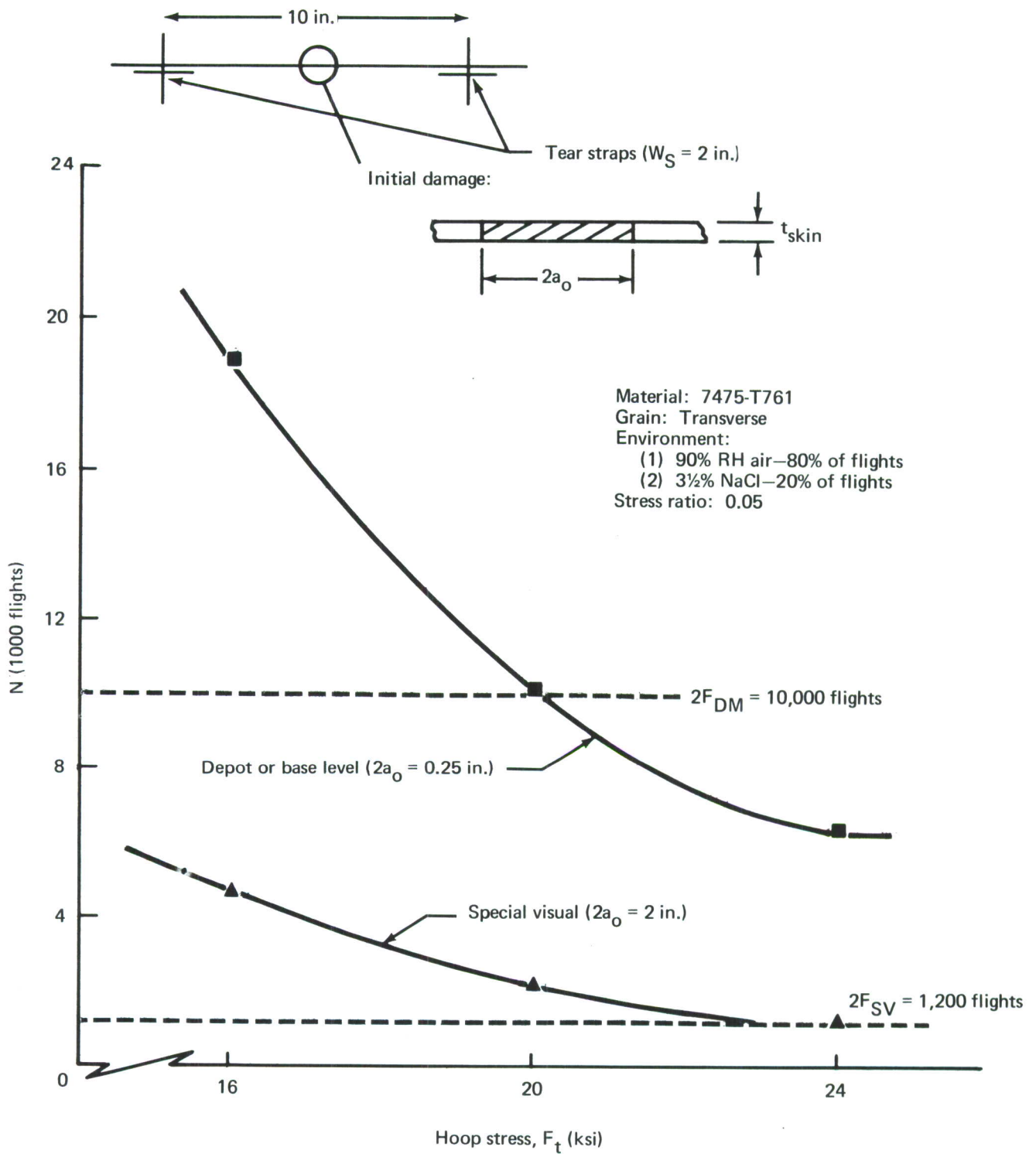


Figure 113.—Fatigue Crack Growth Life—Hoop Loading

than the lower-bound critical stress intensity determined for the 7475-T761 sheet material at the allowable hoop tension stress levels for full-bay (20-inch) skin cracks. For these reasons the full-bay skin crack is believed to be realistic.

Figure 114 shows the results of this analysis. This particular example provides allowable gross stress, F_t , values (hoop direction) as a function of tear strap and/or effective frame area ratios for the residual strength condition of a full-bay skin crack. Since the damage assumption of a full-bay skin crack was considered as critical, a dynamic magnification factor of 1.15 was assumed for the determination of P_{YY} .

The data shown in figures 113 and 114 permit rapid determination of side-of-body skin sizing to satisfy damage tolerance conditions.

(6) Damage Tolerance Trade Studies

Damage tolerance trade studies were conducted to identify those structural parameters which exhibit the greatest potential for lightweight, cost-effective structure. An example of a few of the damage tolerance trade studies which were conducted are:

- Process (joining technique) trades
- Material trades
- Geometry trades

Process (Joining Technique) Trades: Studies were made to compare the relative damage tolerance of bonded and riveted construction. This was done to evaluate any benefits that might be derived by changing from the conventional joining technique (riveting).

The comparison was made by evaluating the crack growth in each type of construction for appropriate initial damage. As shown in figure 115, the bonded construction demonstrates significantly slower crack growth. This is as expected since the dependent nature of the hole drilling and finishing operation for mechanically fastened structure requires an initial assumption of a 0.02-inch through-the-thickness flaw emanating from fastener holes. (For this example, a pair of through-the-thickness flaws was assumed.) This assumption results in much higher stress intensities than those resulting from the surface flaws assumed for the bonded construction. The superior fatigue crack growth behavior of bonded construction, in addition to its improved static strength and fatigue performance, led to its selection as the primary joining technique to be used on all advanced concepts.

Fatigue crack growth behavior for bonded honeycomb construction is considered as a special case of the bonded construction shown in figure 115. For honeycomb sandwich panels with one face skin cracked, tests conducted at Boeing (ref. 3) indicate that even slower fatigue crack growth results, due to load transfer through the core to the intact skin (fig. 116). The honeycomb sandwich thus exhibits potential for even higher allowable working stresses than those shown in figure 115; however, additional testing will be required before this potential may be realized.

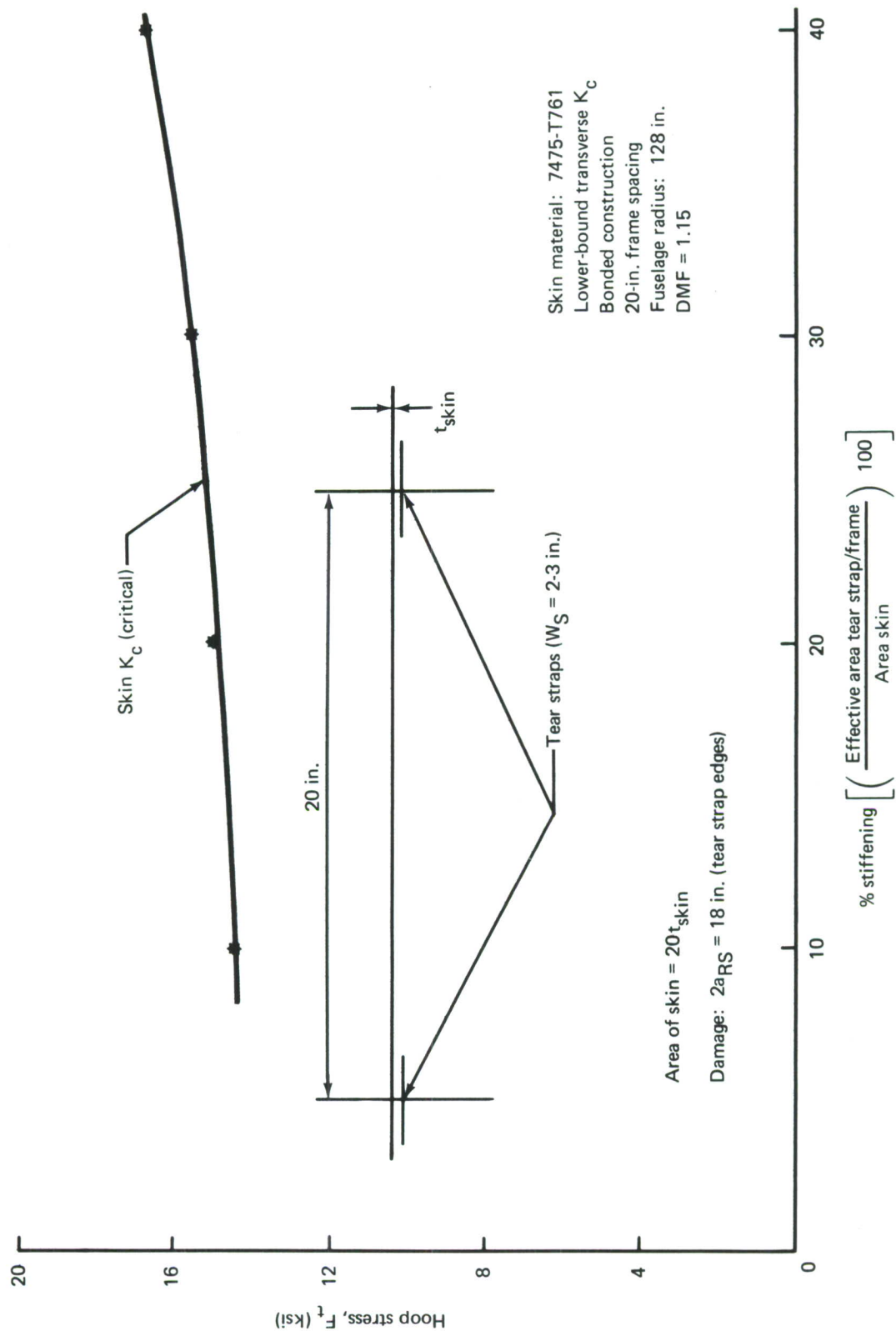


Figure 114. —Residual Strength—Hoop Loading

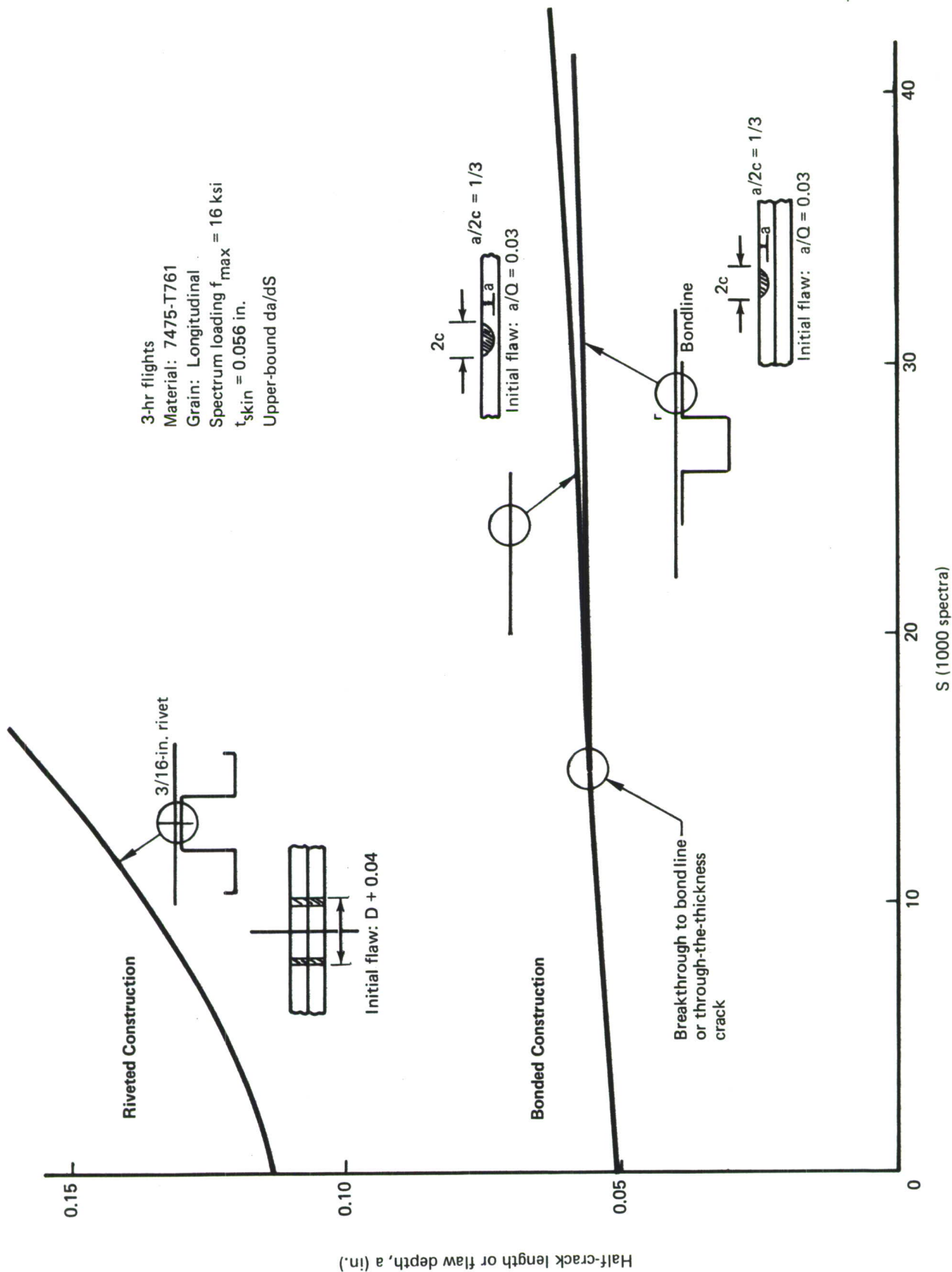


Figure 115.—Crack Growth From Initial Flaw—Bonded/Riveted Structure, Crown Location

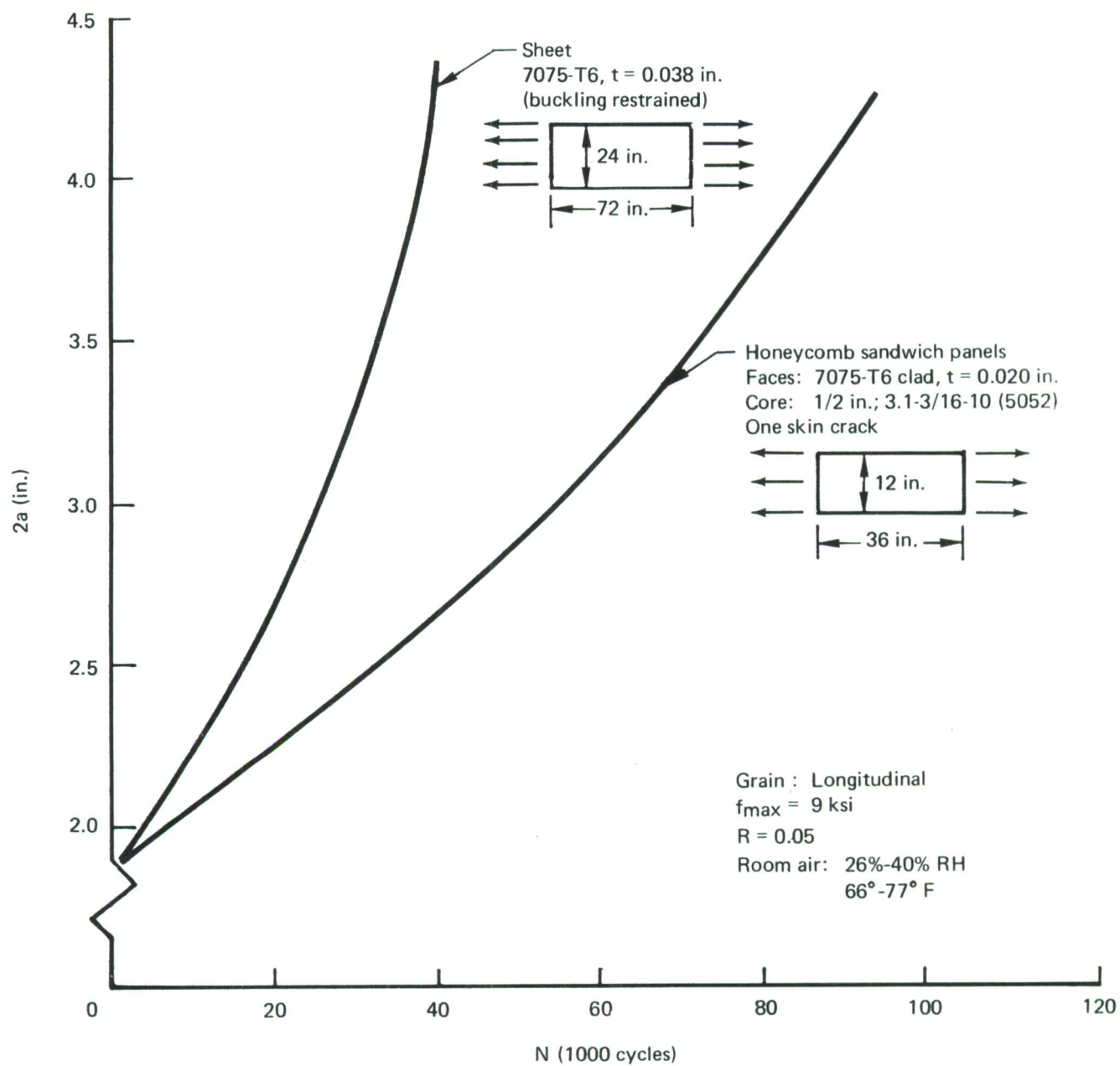


Figure 116.—Fatigue Crack Growth Rates: Sheet versus Honeycomb Sandwich

It is also to be noted from figure 115 that the surface flaw assumed as initial damage in bonded structure is more critical at midbay than at a stiffener. Therefore, all subsequent analyses involving flaw crack growth in bonded structure consider the flaw to be located at midbay.

Material Trades: Material trade studies were conducted to assess the potential improvement in structural efficiency (weight) to be obtained by changing the shell covering material from 2024-T3 (baseline) to 7475-T761. An examination of the material properties indicates the superiority in static properties of 7475-T761 over the baseline material. These higher static properties would in themselves lead to lighter structure under ultimate design conditions; however, the damage tolerance of structure fabricated from this material must be evaluated.

Material testing conducted on this program (app. II) demonstrated that the 7475-T761 exhibits much slower fatigue crack growth rates for loading in the transverse grain direction than the baseline 2024-T3, with essentially equivalent fracture toughness, K_{IC} , in this direction.

The damage tolerance condition of fore and aft cracking (longitudinal grain direction on the skin sheet material) typically dictates the size of a major portion of fuselage skins on pressurized fuselages. Thus, a material trade study was conducted to assess the possible improvement in damage tolerance to be obtained through the use of 7475-T761 skin material. Figure 117 shows that 7475-T761 exhibits significantly slower crack growth than the baseline skin. It was thus decided to use 7475-T761 material for the fuselage skins to take advantage of its greater damage tolerance capability.

The use of 7075-T6 skins in the lower quadrant of the stiffened shell concepts, in place of the 2024-T351 plate used on the baseline, was studied. Due to its rapid fatigue crack growth rates and low critical stress intensity in the transverse grain direction, the fatigue crack growth life obtained through the use of this material for lower lobe skins would result in fracture-critical skins. The high costs associated with the controls required for fracture-critical elements (sec. VI-4) make the use of this material less cost effective for lower lobe skins than 2024-T351.

The use of 7475-T761 and T61 skins was also studied for this application, and it was found that the use of either temper results in non-fracture-critical skins. Use of either material offers a potential for weight savings over the baseline due to the higher yield strength of these materials. However, since the column buckling allowable of the lower lobe stringers is equal to the yield strength of the 7475-T761, no further weight savings could be identified as attainable with the use of the 7475-T61. Moreover, the T761 temper offers increased damage tolerance capability over that offered by T61.

For these reasons, it was decided that 7475-T761 sheet would be used for all fuselage skins on the stiffened shell concepts. This use of 7475-T761 sheet results in a weight savings for all the advanced, stiffened shell concepts (ref. sec. IV-5).

The honeycomb shell concept uses 7475-T61 skins in the upper and lower panels. The 2024-T3 and 7073-T6 basic honeycomb shell design uses 7075-T6 as face sheet

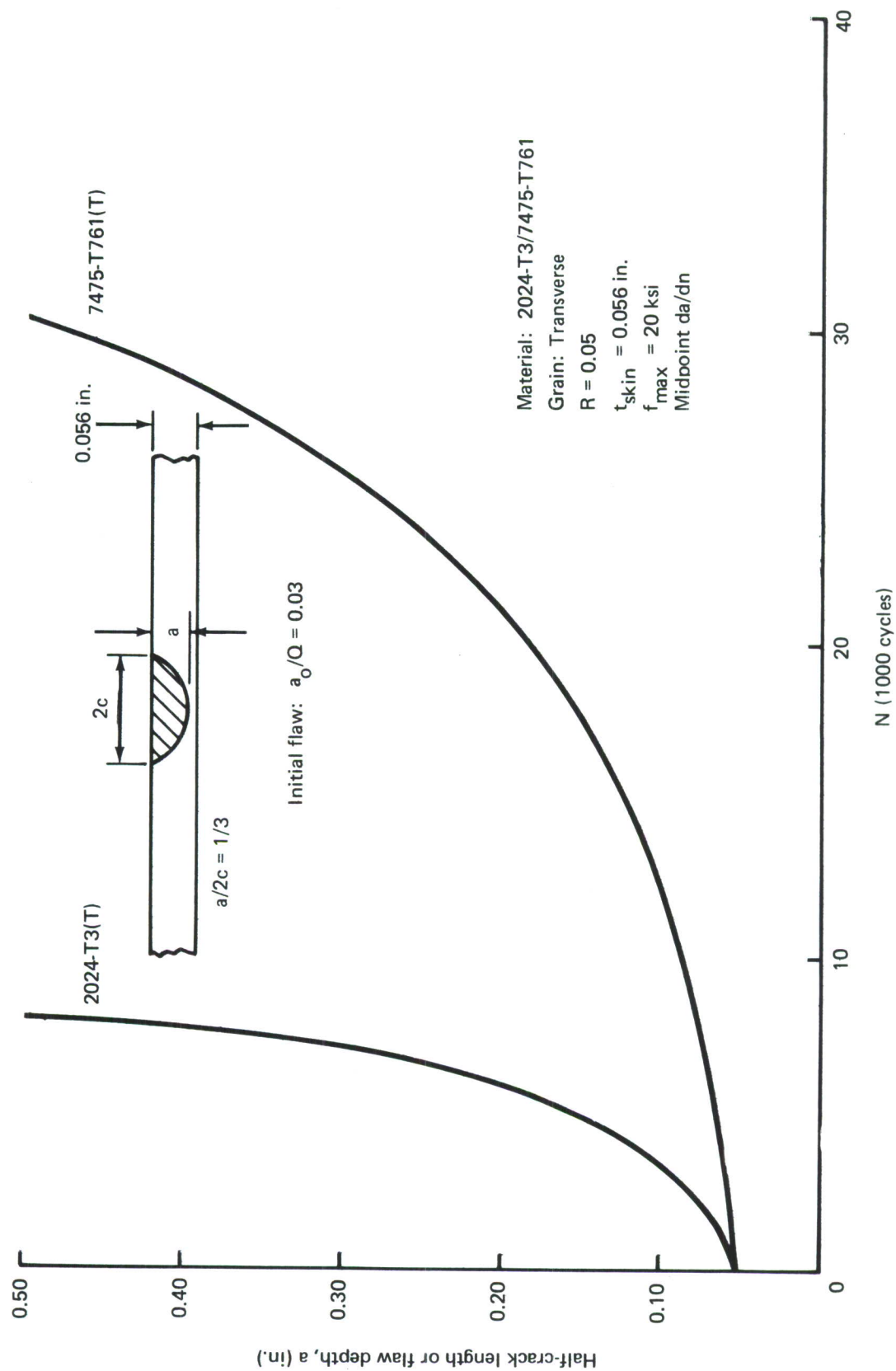


Figure 117.—Crack Growth From Initial Flaw—2024-T3/7475-T761, Side-of-Body Location

material in these locations, and the 7475-T61 in this application offers enhanced damage tolerance capability.

Geometry Trades: Stringer or tear strap spacing has a significant influence on the residual strength of multiple-load-path structure. The influence of tear strap spacing on allowable nominal hoop tension stress was evaluated by determining the residual strength of configurations with 10- or 20-inch strap spacings.

Figure 118 shows the residual strength (hoop direction) of bonded structure with 10-inch strap spacing in nonpenetration areas for the one-bay-crack damage condition. Figure 114 shows the same for 20-inch strap (frame) spacing. A 35% increase in allowable stress is possible by halving the baseline tear strap spacing (20 inches) where the skin gage is "sized" by residual-strength considerations. Therefore, all fuselage skins in nonpenetration areas, with the exception of honeycomb sandwich skins, were designed with 10-inch tear strap spacing.

(7) Material Testing

The material test plan adopted for this program emphasized fracture mechanics testing to further develop the fracture mechanics properties of the advanced materials which exhibited potential for use on this program. The material test program and results are shown in appendix II.

The results of material testing conducted at Boeing, data obtained through the interim material test data interchange program described under "Aluminum" in section IV-2a1, and data extracted from the literature were considered.

Of particular interest are the fatigue crack growth rate test results obtained for both tempers of the 7475 alloy sheet. Fatigue crack growth rates for loading in the longitudinal direction confirmed data presented in reference 9. However, those for loading in the transverse direction demonstrate the orthotropic nature of this material under conditions of crack growth. This material exhibits a fatigue crack growth rate in the longitudinal grain direction (T-L) an order of magnitude slower than that of the baseline 2024 (table VIII). This fracture characteristic makes 7475 alloy particularly attractive for use on pressurized fuselage shells where a high biaxial stress prevails.

The test results obtained for the 7050-T736 and the 7075-T76511 verify the data available in the literature and that obtained through the interim material test data interchange program described under "Aluminum" in section IV-2a1.

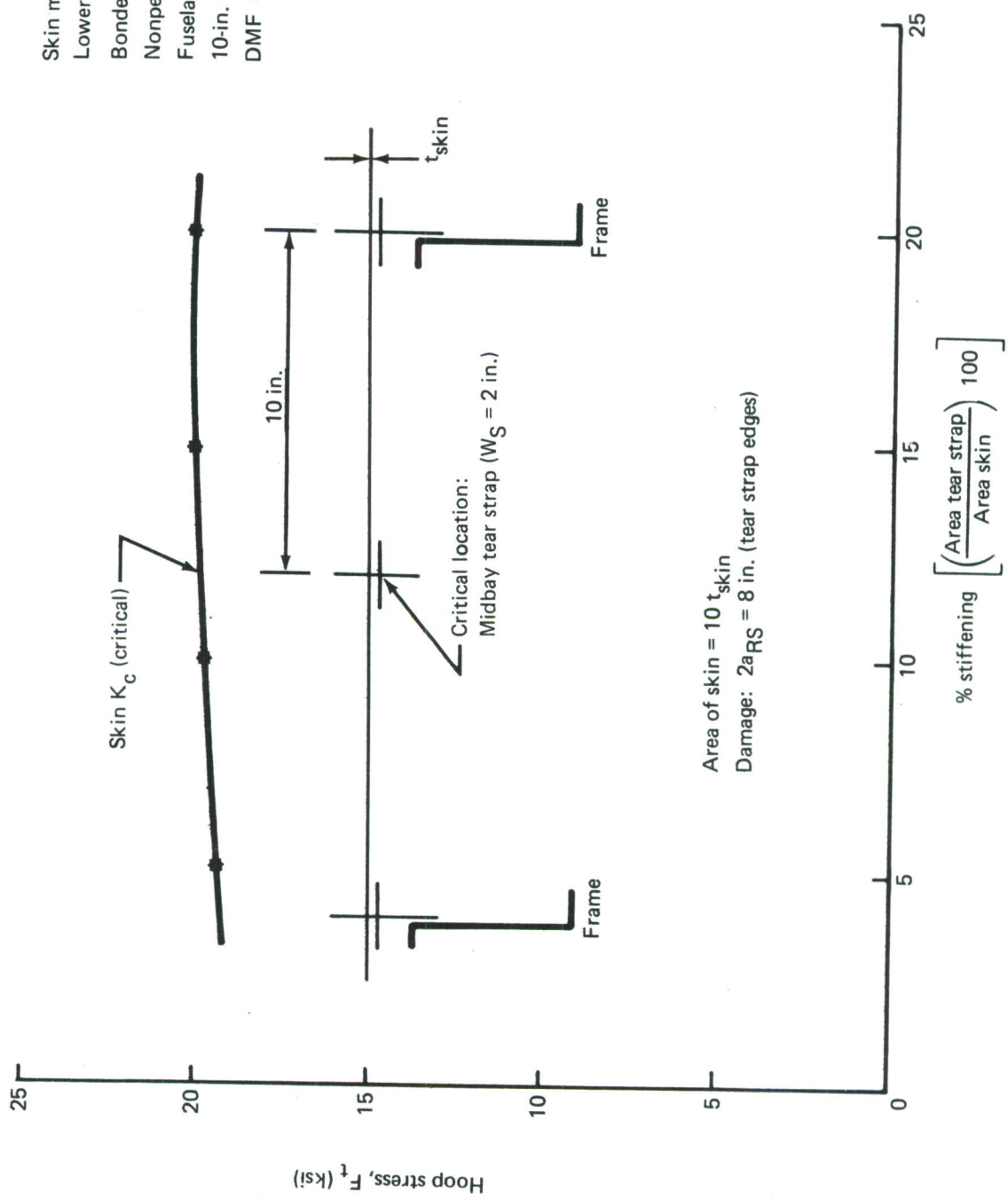


Figure 118. – Residual Strength—Hoop Loading

Skin material: 7475-T761
 Lower-bound K_c
 Bonded construction
 Nonpenetration area
 Fuselage radius: 128 in.
 10-in. tear strap spacing
 DMF = 1.15

5. WEIGHT ESTIMATING

The level of structural concept design definition for weight estimation in this study is much more detailed than that for typical preliminary design studies. Details of skin and pad-ups, splices, straps, and fastener concepts have been defined. The comparison baseline weights are taken from very detailed actual and calculated data. Weight analysis accuracy has a direct effect on the validity of weight and cost study results. The weight results reported here are based on a thorough preliminary design definition and are considered to be as accurate as that definition.

Weights for each selected shell concept in the level 2 and level 3 analyses were calculated and compared to the baseline weights. A description of the baseline structures and advanced concept weight analysis methods follows.

a. Data Base

(1) Study Section

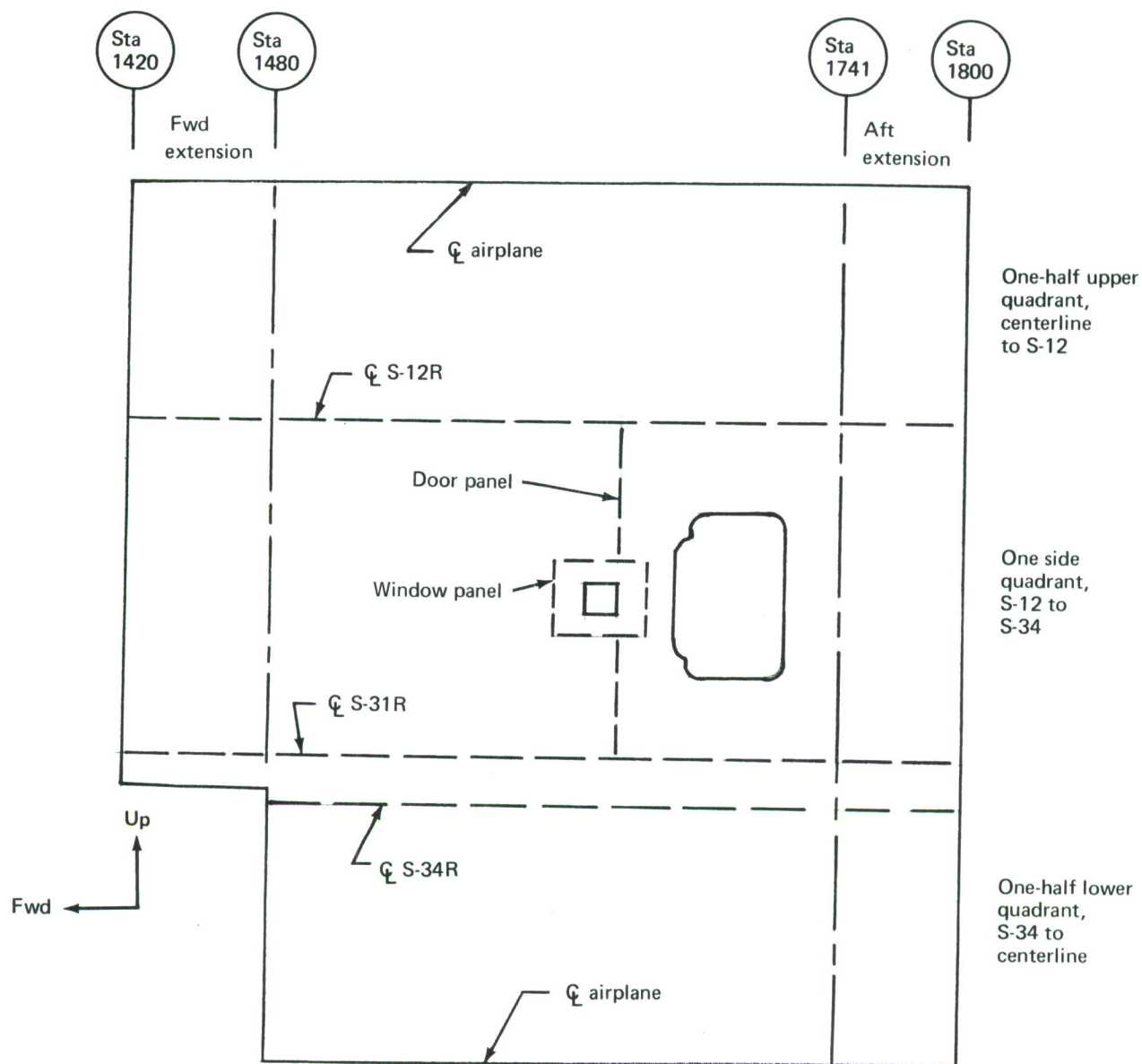
The study section consists of the following items located between body stations 1420 and 1800 on the 747-100 aircraft:

- Skin and stringers
- Frames
- Fail-safe straps
- Body station 1480 bulkhead
- Door and window cutout redistribution structure
- Landing gear fittings
- Keel beam
- Floor beams
- Pressure deck

Figure 119 shows the left side of the study section skin in flat pattern. The upper, side, and lower quadrants are identified.

(2) Baseline Weights

The baseline 747-100 weight statement was prepared by first identifying the structural items to be included. Calculated weight and sizing were next obtained from weight and structures records. Exact actual or calculated weights were obtained for all structure between body stations 1480 and 1741. Exact calculated weights could be obtained



Study Section

Proportioned weights

1. Skin and stringers
2. Frames
3. Fail-safe straps
4. Press deck
5. Floor beams
6. Keel beam

Exact weights

1. Skin and stringers
2. Frames
3. Door and window stringers
4. Fail-safe straps
5. Station 1480 bulkhead
6. Landing gear fittings
7. Keel beam provisions
8. Floor beams

Proportioned weights

1. Skin and stringers

Exact weights

1. Frames
2. Fail-safe straps
3. Floor beams

Figure 119.—Baseline Study Section

for some of the structure in the aft 60-inch extension (stations 1741 to 1800), but it was necessary to proportion the structural weight of other items that are continuous to the next production break. It was also necessary to proportion the structural weight of the forward 60-inch extension. Refer to figure 119 for a list of exact and proportioned weights.

Since the advanced concepts study is concentrated on the investigation of shell structure in the sized section between stations 1480 and 1741, the items in this section were itemized and the upper, side, and lower quadrants were separated. The forward and aft shell extensions and other items, e.g., floor beams, keel beam, etc., were also listed, as shown in figure 119.

b. Estimating Method

The method of weight analysis described here for the level 3 phase of the study is typical for level 2 also. The differences in calculated weights between level 2 and level 3 are the result of more extensive structural analysis and design detail provided in level 3.

(1) Skin/Stringer Concepts

Weights for the three stiffened shell concepts (internal stringer, continuous bead, and external stringer) were obtained as follows:

- 1) The skin gage, stringer area, and stringer spacing required to satisfy the design loads and criteria were determined by the Stress and Design groups at 12 circumferential locations per side at four body stations, as shown in figure 120. These sizings were converted into an average skin thickness (\bar{t}) at each analysis location and transmitted to the Weights unit.

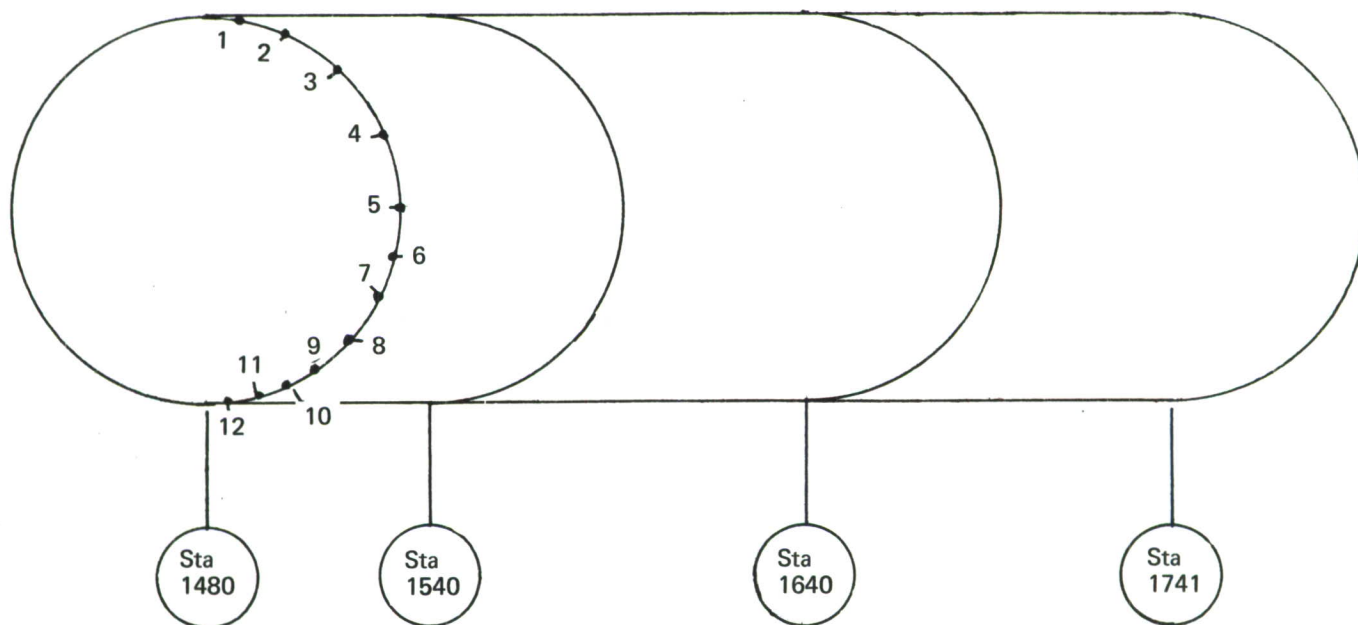
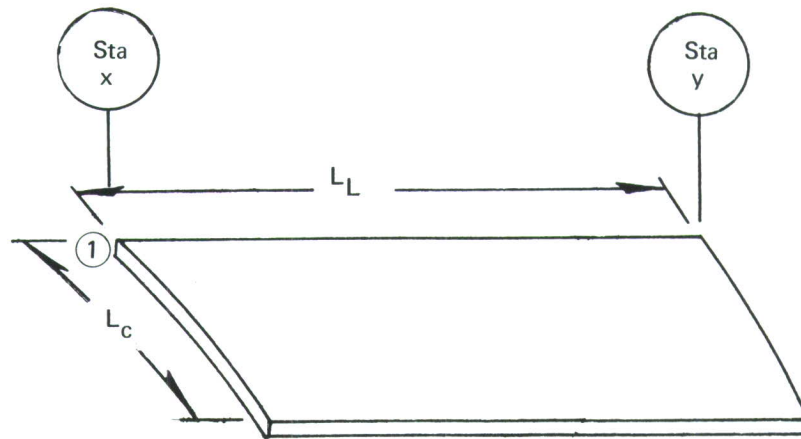


Figure 120.— \bar{t} Locations

- 2) The \bar{t} values were assumed to vary linearly between analysis points, both circumferentially and longitudinally. This assumption is consistent with the structural distribution on the baseline airplane.
- 3) The theoretical weight of the skin and stringers, which is represented by \bar{t} , was found by determining the volume of material required and multiplying it by the specific weight of aluminum. The volume of material was obtained by averaging \bar{t} between circumferential locations and body stations, and multiplying by the longitudinal distance between stations. The procedure is illustrated in figure 121.



1.
$$\frac{\bar{t}_1 + \bar{t}_2}{2} = \bar{t}_{1-2}$$
2.
$$(\bar{t}_{1-2} L_c)_x = (A_{1-2})_x$$
3. Repeat steps 1 and 2 for station y
4.
$$\left[\frac{(A_{1-2})_x + (A_{1-2})_y}{2} \right] (L_L) = \text{panel volume}$$
5.
$$(\text{Vol}) (\text{Wt/cu in.}) = \text{panel weight}$$
6.
$$\Sigma \text{ Panel weights} = \text{shell weight}$$

Figure 121.—Typical Panel Weight Calculation

- 4) Weights obtained in step 3 were multiplied by an actual-to-theoretical factor to account for local pad-ups. Baseline quadrant detail weights were compared to weights derived from theoretical sizing originally provided by the Stress group to obtain the actual-to-theoretical factors. A summary of the factors by quadrant is as follows:

<u>Quadrant</u>	<u>Actual-to-Theoretical Factor</u>
Upper	1.024
Side	1.026
Lower	1.020

There were no significant differences between the preceding factors and those used in the in-house bonding development study, and they are considered to be within the accuracy required for a preliminary design effort.

- 5) Actual aircraft structure also contains other non-optimum features such as splices, fasteners, bonding, etc., which must be included in the weight estimate. The weights of bonded splices were calculated from layouts provided by the Design group. Mechanical splice and fastener weights were taken from the 747 baseline. A unit weight of 0.065 pound per square foot was used to determine the adhesive weight of the bonded concepts. The unit weights of fairing and insulation materials selected by the Boeing Materials Technology group for the external stringer concept are shown below.

<u>Material</u>	<u>Unit Weight</u>
Fiberglass skin	0.15 pound per square foot
Molded batting	2.5-3.0 pounds per cubic foot
Inside insulation	0.075 pound per square foot

- 6) The frame weights for each shell concept were based on modifications to the baseline frames as defined by Stress and Design groups. Fail-safe chords and straps were added where required.
- 7) The forward and aft shell extensions (stations 1420 to 1480 and 1741 to 1800) were weighed by extrapolating the structural arrangement of each concept into the extensions on a pounds-per-square-foot basis.

(2) Honeycomb Concept

The honeycomb concept weights are based on the in-house IR&D structural bonding development program data which were updated to agree with the study configuration and material revisions. These weights were calculated from the detail drawings of this program and reflect weight savings of high confidence level in the study section.

c. Weight Summary—Level 2 Concepts

The level 2 weight analysis results are shown in table XXV.

Table XXV.—Level 2 Weight Analysis Results, 2024 and 7075 Material

Item	Baseline	Internal stringer	Continuous bead	Stiffened honeycomb	Honeycomb	External stringer
Upper quadrant						
Skin and stringers/core	753	650	656	711	560	762
Frames	157	157	157	239	101	101
Splices, fasteners, and edges	49	49	49	156	263	49
Straps	28	30	—	—	—	—
Total	987	886	953	1,106	924	912
Side quadrant						
Skin and stringers/core	1,362	1,153	1,204	1,273	976	1,336
Frames	371	371	462	409	173	173
Splices, fasteners, and edges	84	84	84	352	522	84
Straps	24	60	—	—	—	—
Total	1,841	1,668	1,750	2,034	1,671	1,593
Lower quadrant						
Skin and stringers/core	1,372	1,330	1,280	1,213	837	1,457
Frames	484	484	484	484	252	252
Splices, fasteners, and edges	64	64	64	165	185	64
Total	1,920	1,878	1,828	1,862	1,274	1,773
Weight of sized section (1480 to 1741)	4,748	4,432	4,531	5,002	3,869	4,278
Percent change from baseline	0	-6.7%	-4.6%	+5.3%	-18.6%	-9.9%
Weight of shell extensions (1420-1480, 1741-1800)	2,149	1,888	1,968	2,165	1,858	1,837
Total weight of items studied	6,897	6,320	6,499	7,167	5,727	6,115
Percent change from baseline	0	-8.4%	-5.8%	+3.9%	-16.9%	-11.3%
Weight of baseline items held constant during study	3,645	3,645	3,645	3,645	3,645	3,645
Total section weight	10,542	9,965	10,144	10,812	9,372	9,760
Percent change from baseline	0	-5.5%	-3.8%	+2.6%	-11.1%	-7.4%

d. Final Concept Weights

Weights for the level 3 portion of this study are summarized in tables XXVI and XXVII. Level 3 considered the use of the aluminum alloy 7475-T761 for each concept. Significant weight savings were obtained by substituting this material in place of the baseline 2024/7075 combination except in the case of honeycomb, where the effect of its application was limited.

It should be noted that the level 2 and level 3 baseline weights differ by 74 pounds. This weight increment represents an additional piece of lower segment structure identified in the detailed weight listing to be a part of the baseline structure. Weight was also

Table XXVI.—Level 3 Weight Analysis Results, 2024 and 7075 Material

Item	Baseline	Internal stringer	Continuous bead	Honeycomb	External stringer
Upper quadrant					
Skin and stringers/core	753	658	654	560	614
Frames	142	138	158	101	130
Splices, fasteners, and edges	49	45	58	263	45
Straps	28	14	—	—	4
Foam and insulation (Δ wt)	—	—	—	—	13
Total	972	855	870	924	806
Side quadrant					
Skin and stringers/core	1,748	1,730	1,686	1,369	1,646
Frames	336	291	340	173	269
Splices, fasteners, and edges	84	81	104	522	81
Straps	24	23	—	—	6
Foam and insulation (Δ wt)	—	—	—	—	24
Total	2,192	2,125	2,130	2,064	2,026
Lower quadrant					
Skin and stringers/core	1,721	1,344	1,420	1,111	1,305
Frames	484	443	443	252	443
Splices, fasteners, and edges	64	50	39	185	50
Foam and insulation (Δ wt)	—	—	—	—	12
Total	2,269	1,837	1,902	1,548	1,810
Weight of sized section (1480 to 1741)	5,433	4,817	4,902	4,536	4,642
Percent change from baseline	0	-11.3%	-9.8%	-16.5%	-14.6%
Weight of shell extensions (1420-1480, 1741-1800)	2,199	1,953	1,918	1,858	1,855
Total weight of items studied	7,632	6,770	6,820	6,394	6,497
Percent change from baseline	0	-11.3%	-10.6%	-16.2%	-14.9%
Weight of baseline items held constant during study	2,984	2,984	2,984	2,984	2,984
Total section weight	10,616	9,754	9,804	9,378	9,481
Percent change from baseline	0	-8.1%	-7.6%	-11.7%	-10.7%

Table XXVII.—Level 3 Weight Analysis Results, 7475 Material

Item	Baseline	Internal stringer	Continuous bead	Honeycomb	External stringer
Upper quadrant					
Skin and stringers/core	753	614	636	545	582
Frames	142	138	158	101	130
Splices, fasteners, and edges	49	45	58	263	45
Straps	28	14	—	—	4
Foam and insulation (Δ wt)	—	—	—	—	13
Total	972	811	852	909	774
Side quadrant					
Skin and stringers/core	1,748	1,643	1,676	1,356	1,584
Frames	336	291	340	173	269
Splices, fasteners, and edges	84	81	104	522	81
Straps	24	23	—	—	6
Foam and insulation (Δ wt)	—	—	—	—	24
Total	2,192	2,038	2,120	2,051	1,964
Lower quadrant					
Skin and stringers/core	1,721	1,185	1,339	1,111	1,184
Frames	484	443	443	252	443
Splices, fasteners, and edges	64	50	39	185	50
Foam and insulation (Δ wt)	—	—	—	—	12
Total	2,269	1,678	1,821	1,548	1,689
Weight of sized section (1480 to 1741)	5,433	4,527	4,793	4,508	4,427
Percent change from baseline	0	-16.7%	-11.8%	-17.0%	-18.5%
Weight of shell extensions (1420-1480, 1741-1800)	2,199	1,829	1,881	1,858	1,765
Total weight of items studied	7,632	6,356	6,674	6,366	6,192
Percent change from baseline	0	-16.7%	-12.6%	-16.6%	-18.9%
Weight of baseline items held constant during study	2,984	2,984	2,984	2,984	2,984
Total section weight	10,616	9,340	9,658	9,350	9,176
Percent change from baseline	0	-12.0%	-9.0%	-11.9%	-13.6%

redistributed in the level 3 baseline because some of the items held constant in level 2 (lower quadrant keel beam fittings and door framing) were grouped with the appropriate quadrant.

The externally stiffened concept summary contains a delta weight for fairing and insulation. This delta weight is the difference between the existing insulation, which is removed in this concept, and the external fairing and insulation added to replace it. The baseline total insulation weight is 487 pounds and the concept fairing/insulation weight is 536 pounds. The items held constant during the shell study are listed in table XXVIII.

Table XXVIII.—Component Weights Considered Constant for Level 3 Shell Studies

Component	Weight (lb)
1480 bulkhead	1195
Keel beam	299
Landing gear fittings	785
Floor beams	433
Windows	26
Pressure deck	246
Total	2984

(1) Geometry and Material Change Effects

The final four shell concepts were sized and weighed using the baseline materials 2024-T3 and 7075-T6. The results of this study show the weight saving due to improved geometry and the use of bonding instead of riveting. The concepts were also sized and weighed using 7475-T761 instead of 2024-T3 for the skin material. Table XXIX shows the weight deltas for each, the final total weight saving, and the percent weight saving for the participating structure.

Table XXIX.—Source of Weight Saving, Level 3 Shell Studies (Body Stations 1420 to 1800)

Concept	Δ weight due to geometry and bonding baseline material (lb)	Δ weight baseline material replaced with 7475 aluminum (lb)	Final concept weight (lb)	Weight change (% of participating structure)
Internal stringer	- 862	-414	-1276	-17
Continuous bead	- 812	-141	- 958	-13
Honeycomb	-1238	- 28	-1266	-17
External stringer	-1135	-305	-1440	-19

The honeycomb design using 2024-T3 and 7075-T6 had 2024-T3 on the side panels and 7075-T6 on the crown and lower panels. The final 7475 design uses 7475-T761 on the side panels and 7475-T61 on the crown and lower panels. Since only the side panels were 2024-T3 and much of it was minimum gage, there is only a small weight improvement for this concept using 7475 material.

e. Weight Savings—Results

The study weight results and percentage weight savings are tabulated in tables XXVI and XXVII.

(1) Weight Reduction—Study Section

In the study section, only the shell portion (skins, stringers, frames, and straps) showed a significant weight reduction. Refer to section III-4 for a discussion of other structural items.

(2) Weight Reduction—Total Fuselage

Extending the design concepts to the total fuselage results in a preliminary estimated weight saving as summarized in table XXX.

Table XXX.—Weight Savings as a Percent of Total Body Structure

	Internal stringer		Continuous bead		Honeycomb		External stringer	
	2024/7075	7475	2024/7075	7475	2024/7075	7475	2024/7075	7475
Percent weight saving	6.3	7.7	5.5	6.0	7.0	7.1	7.3	8.3

6. MANUFACTURING

Manufacturing participation in phase IA has been to provide guidance towards a manufacturable design—a design that is not only achievable but one that also minimizes manufacturing costs. Additionally, consideration has been given to the processing and tooling (both that available and that to be developed) required for each of the designs considered. The facilities that would be required were reviewed, and their availability was noted. Identified new facility requirements were not considered in costing the three shell design concepts. Where new processes or revisions to existing processes are required, the need for training personnel was noted.

Final assembly operations have been reviewed to provide a complete picture of the costs associated with a design. The scope of the manufacturing tasks necessary to fabricate a design has been developed, and preliminary flow charts have been prepared.

a. Manufacturing Requirements

Common to all three body shell concepts is adhesive bonding. The facility and process requirements to fabricate adhesive-bonded primary structure are discussed in this section.

Besides the means to form or machine the pieces that make up a bonded assembly, facilities required for uniform bonding quality include a metal surface preparation line that prepares a bondable surface and applies corrosion-inhibiting adhesive primer, and an environmentally controlled area (dust- and fume-free air) where the details are laid up. Curing the adhesive (the next step) requires a source of heat and pressure; an autoclave is preferred. Nondestructive testing equipment is required to verify the bonding process.

The large size of bonded body quadrants creates problems in bonding assembly jig (BAJ) -and handling tool designs. These problems were solved on a previous in-house program that fabricated bonded primary structure of 747 size. There had been no experience with adhesive bonding tools of this size, and so several approaches were tried. Initially, it was believed that quadrants should be laid up and bonded full size. Not recognized in this first plan was the difficulty of people-access to the part, caused by the sheer size of the tool. A vertical tool was next tried, which gave essentially no better access. Next, it was decided to go back to a horizontal tool, but instead of fabricating the whole quadrant in one piece, panels were made which later would be bonded into the quadrant. This has been proven to be the most efficient bonding approach.

Many handling problems were anticipated because of the large panel/quadrant size. Heretofore, bonded assemblies could be positioned by hand so that a crane might be attached to further move them. It was recognized that these simple methods would not work, and so a full-size demonstrator was built and various handling tools were designed and tried out. Criteria are available to fully support the design of handling equipment (overhead and on wheels) for large adhesive-bonded aircraft structure.

Process and facility requirements are called out in the fabrication sequences, which are detailed in the following subsections. In a production program, the requirement

for high reliability in adhesive-bonded primary aircraft structure can best be met if the metal surface preparation and application of corrosion-inhibiting primer are done in an environmentally controlled, continuous process line. Such a facility provides protection from airborne contamination, ensures proper sequence of process steps, and facilitates the control of processing parameters, e.g., time, temperature, and solution strength. Facility management by computer can be accomplished after operating parameters have been established.

b. Manufacturing Planning

The proposed manufacturing sequences for each of the three selected body shell concepts are shown in figures 122 through 127. The plan is arranged to show, first, those beginning process steps that are common to all concepts. Next, the processing that is individual to each concept is shown, and finally, those steps again common to the completion of processing and assembly are grouped into one sequence.

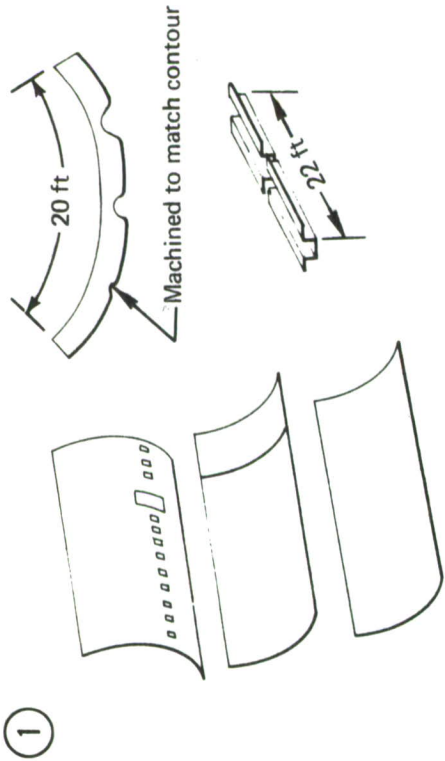
The processing entitled "Primary Fabrication of Details for Any Concept" (fig. 122) starts with receiving the raw materials and includes forming, machining, cleaning, priming, and storing of the details. The plan for machining simple contour, stretch-formed skins or doublers makes use of the technique of pulling the part flat on a vacuum chuck and machining the required contours like any other flat part. Parts machined in this manner assume their formed contour upon release from the vacuum chuck.

The waffle doubler for concept 3 (internal stringer) would be bonded to the skin in the flat, and the skin/doubler would be stretch-formed as one assembly.

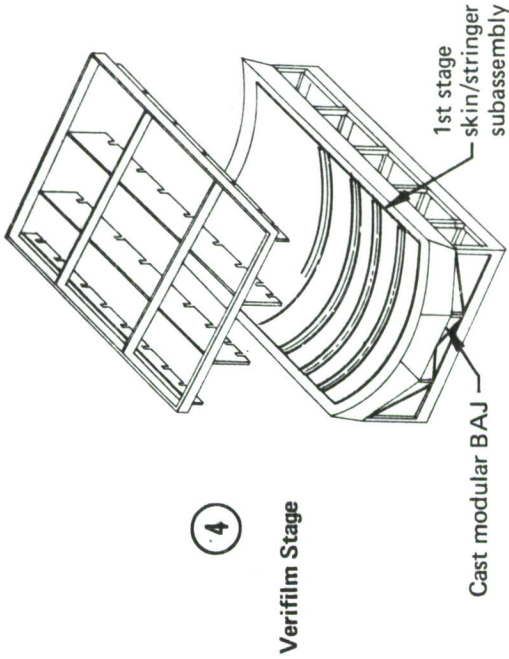
The next three sequences (figs. 123, 124, and 125) show that processing is individualized for the three body shell concepts. All critical stages of bonding will be Verifilmed to confirm part fit-up. Fit-up factors include the ability of tooling to hold parts in correct alignment and to exert the pressure required to develop specified bond line thicknesses and the capability of shop personnel for following specified bagging procedures and determining that parts have been formed to acceptable bonding tolerances. Included in figures 123, 124, and 125 are sketches of proposed tooling for use, along with some tooling details and handling equipment.

Concept 1, honeycomb (fig. 123), will have three stages of bonding to make a quadrant assembly. The core blanket lengths and widths will be stabilized by bonding on a nylon peel ply. Following roll forming, they will be machined to fit skin contours. In the first bonding stage, the exterior skins, their machined doublers, tear straps, door and window frames, and core blankets will be bonded. In the second stage, the inner skins and splice doublers will be bonded to the previously bonded subassembly. The frame tees are bonded in the final stage.

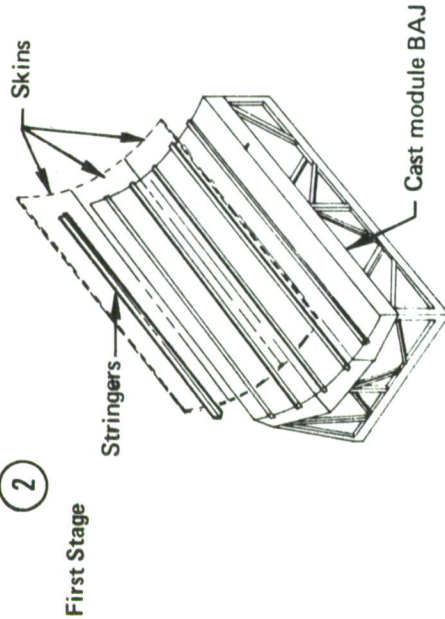
Concept 2, external stringer quadrants (fig. 124), requires two stages of bonding. In the first stage, the skins, splice doublers, and stringers are bonded together in a cast module bonding assembly jig. The frame tees are then joined to this first assembly in the second stage.



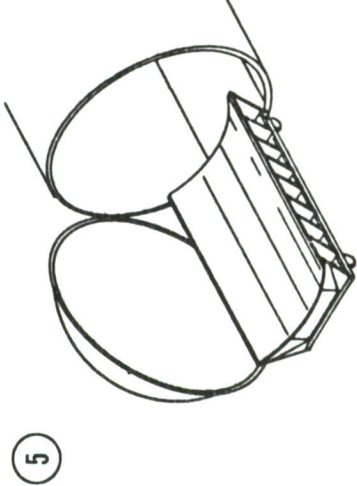
Draw prefabricated details from stock



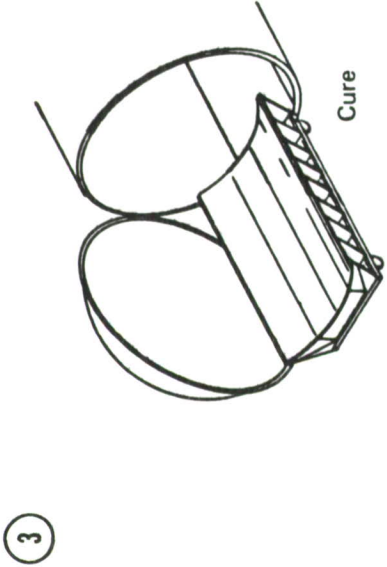
Reclean BAJ
Apply release film
Reload and locate skin/stringer subassembly in BAJ
Cut tape for verifilm cycle of frame tees
Sandwich tape between two plies of release film
Locate film sandwich on subassembly at each frame tee
Load and locate each frame tee by pins and frame tee locating fixture (MIT)
Tape frame tees in place
Remove MIT
Bag per standard shop procedures
Check locations with MIT
Vacuum leak check
Move to autoclave area



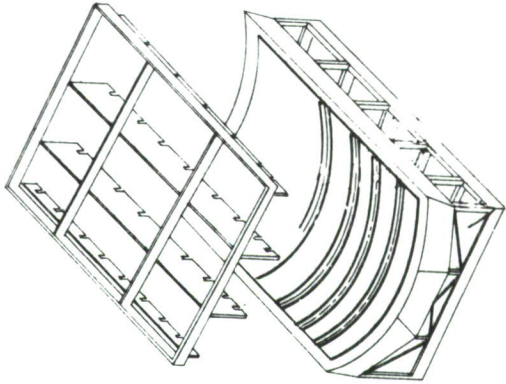
Clean BAJ with MEK
Apply release film to BAJ surface
Cut and apply adhesive to stringer flanges and associated doublers
Load stringers, flange up, in recess of BAJ, pin each end
Load and locate each skin and associated splice doublers
Load caul plate over skin surface
Check location of details
Bag per standard shop procedures
Vacuum leak check
Move to autoclave area



Autoclave cure
Remove from autoclave
Return to layup area
Debag verifilm cycle
Inspect and evaluate verifilm-cured adhesive
Make adjustment to film for bond cycle



Autoclave cure
Remove from autoclave
Return to layup area
Debag subassembly
NDT



Inspect BAJ and subassembly for cleanliness
MEK wipe bond surface for frame tees
MEK wipe all frame tee bond surfaces
Cut and apply film adhesive for each frame tee (modified bondline per verifilm)
Load and locate frame tees on assembly
Use MIT for location on station lines
Tape in place
Remove MIT
Bag per standard shop procedures
Recheck locations with MIT
Vacuum leak check
Move to autoclave
Note:
It may be profitable to leave the MIT on the assembly during the cure cycle.

Figure 124. –Skin/Stringer Concept—External

Concept 3, internal stringer quadrants (fig. 125), also requires two stages of bonding. In the first stage, the skin/doubler assembly and stringers are bonded. The frame tees are bonded to the skin/doubler/stringer assembly in the second stage. The bonding steps described above could conceivably change for a production program as a result of learning from the proposed development work.

Figure 126 shows the processing to complete a quadrant, including attachment of body frame J-sections, the ultrasonic NDT of bonded areas, and the handling and transportation equipment used to deliver the quadrant to the assembly area.

In a normal manufacturing sequence, the body J-frames would be riveted to the webs of the bonded tees right after the NDT of the bonded quadrant. Assembly work on the top quadrant would deviate from this as it is the “keystone” piece, being the last to be joined to the other quadrants. The other three joined quadrants constitute a very rigid assembly, so there is a requirement for the top quadrant to have some flexibility to permit making the mechanical longitudinal joints. Consequently, the top section J-frames may be installed after the longitudinal joints are made.

Specialized handling equipment is used to remove the large assembly from the bonding assembly jig and place it on the shipping fixture for transport to the body assembly area.

Body assembly operations are shown in figure 127. As a cost savings, the test jig will be used in the follow-on program as the assembly fixture for the test section. The assembly sequence shown in figure 127 is generally representative of a production assembly sequence, the main difference being the joining sequence across the production break in the fuselage shell. Assembly operations begin with loading of the bottom quadrant. Next, the station 1480 bulkhead chord and web are installed, landing gear trunnions are installed and the lower panel is positioned, the keel beam chord is located and attached, followed by the complete installation of the keel beam box. The keel beam web installation follows, and the station 1480 bulkhead, side forgings, and upper segments are temporarily positioned while the pressure deck at station 1420 is jig located and installed.

Aft section side quadrants are installed next, followed by the aft section upper quadrant. Forward section side and upper quadrants follow, and the 1480 bulkhead installation is completed. Mechanical splices (circumferential at station 1480 and the longitudinal splices on both aft and forward sections) are made. Installation of floor beams and plywood floor; completion of the pressure deck, keel beam installations, and frame splices; and installation of the dummy door and window finish the test section assembly.

c. Tooling Requirements

The design of adhesive bonding tools has evolved from the plaster master model to the more economical and accurate standard from which part and tool dimensions are now taken—the concept of master dimensions information (MDI). Surfaces of the aircraft are described mathematically by the design engineer, and these data are fed into a computer that produces a tape that controls a numerically controlled milling machine. The mill will accurately reproduce the contour information generated by the design engineer.

The design of large bonding assembly jigs (BAJs) for the type of assemblies required for the three fuselage concepts presents new and unique problems. The BAJs must provide convenient worker access, be able to be heated at the maximum rate allowed by the process, resist bonding process forces, and be airtight. BAJ construction will depend on the contour of the part to be bonded. Thus, tools for single-contoured parts (figs. 128 and 129) lend themselves to machined headers and a laminated aluminum bonding surface. Compound contoured parts are best bonded on cast aluminum tools (figs. 130 and 131). Considerable tooling information for large BAJs has been developed through in-house funded efforts and is directly applicable to fabrication of bonded primary fuselage structure.

d. Assembly Requirements

Final assembly of adhesive-bonded primary structure will be accomplished with fewer labor hours than are needed for the baseline designs. This savings comes from two major sources. First, there will be fewer parts to install at final assembly. Second, each of the quadrants constitutes a stiffer structure than the several bits and pieces that make up the details joined in the baseline final assembly. This much stiffer structure will fit both the final assembly tool and its mating parts with little need for adjustment. Of course, detail parts for bonding into the quadrants will have to be made to closer tolerances than details for the baseline because of the limited pressure available to force parts, both to contour and together, to meet bond line thickness tolerances during the bond cycle.

To provide the small amount of circumferential adjustment likely to be needed, both ends of each frame web on each quadrant will arrive at the final assembly jig unfastened. Each quadrant will be trimmed to net length before final assembly. Fore and aft adjustment is provided by the circumferential joint.

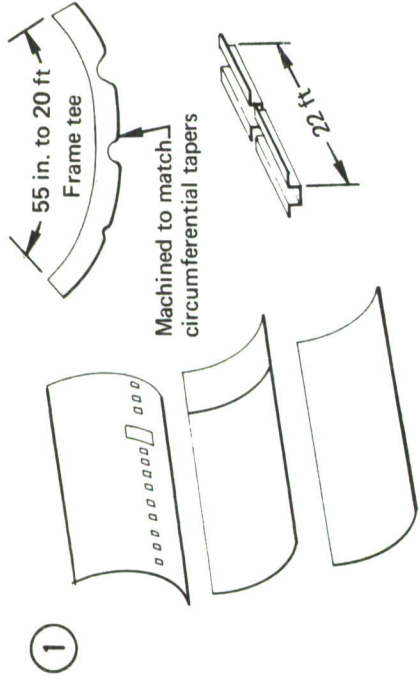
e. Manufacturing Considerations

Adhesive bonding and the mechanical fastenings specified for use in the three body shell design concepts are discussed below.

(1) Adhesive Bonding

Adhesive bonding provides real benefits to the manufacturing of primary aircraft structure. First, fabrication costs of all the bonded body shell concepts are less than those of the baseline (riveted skin/stringer). There are fewer parts; more of the assembly of the quadrants is done in subassembly (bonding) stages; and a stiffer, closer tolerance subassembly is offered to the final assembly area where the operations of joining the quadrants will be faster. Inventory costs are reduced by the lessened number of details. Major assembly tools for bonded structure are less costly than those for the conventional baseline structure.

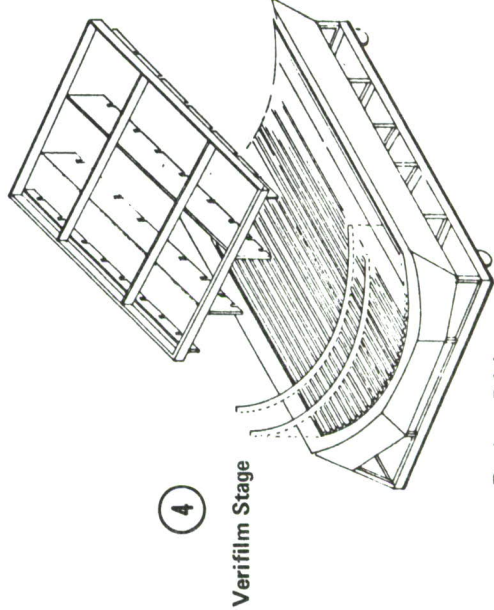
Although manufacturing is successfully working with present adhesive systems, these systems impose a time limit on assembly curing. Extra effort is required to schedule and plan operations to achieve optimum factory flow.



Draw prefabricated details from stock

Note:

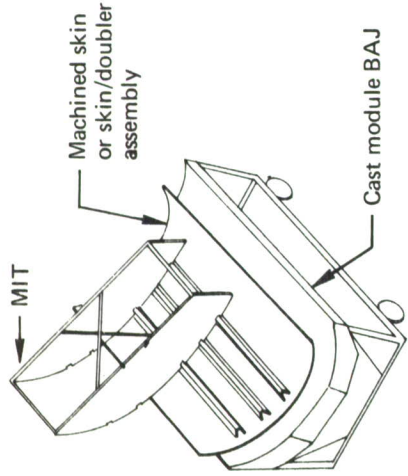
- One-piece skins will be stretch formed, pulled flat on vacuum chuck, machined by NC tapes, cleaned, primed, baked, and stored
- Bonded skin/doubler subassemblies can be bonded in flat, stretch formed, chem-milled or pulled flat and machined, cleaned, primed, baked, and stored.



- Reclean BAJ
- Apply release film
- Reload and locate skin/stringer subassembly in BAJ
- Cut tape for verifilm cycle of frame tees
- Sandwich tape between two plies of release film
- Locate film sandwich on subassembly at each frame tee
- Load and locate each frame tee by pins and frame tee locating fixture (MIT)
- Tape frame tees in place
- Remove MIT
- Bag per standard shop procedures
- Check locations with MIT
- Vacuum leak check
- Move to autoclave area

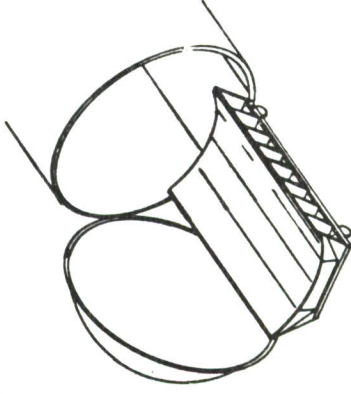
2

First Stage



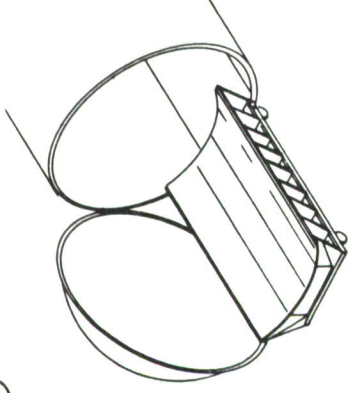
- Clean BAJ with MEK
- Apply release film
- Load, locate, and pin skins to BAJ
- MEK wipe primed stringers to activate primer
- Cut and apply film adhesive film to stringer flanges
- MEK wipe skin surfaces
- Load stringers on skins, pin at each end. Tape along edges. Use Stringer locating fixture for center location
- Bag per standard shop procedures
- Vacuum leak check
- Move to autoclave area

5



- Autoclave cure
- Remove from autoclave
- Return to layout area
- Debag verifilm cycle
- Inspect and evaluate verifilm-cured adhesive
- Make adjustment to film for bond cycle

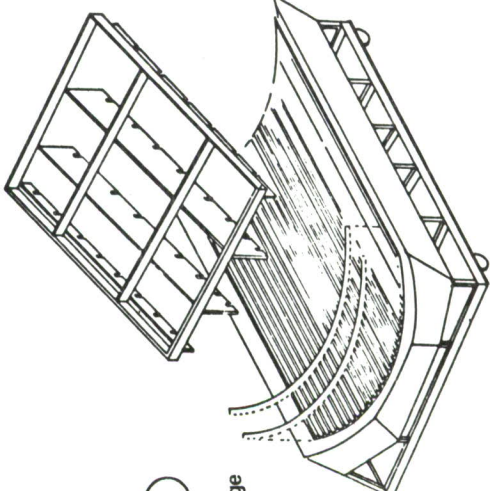
3



- Autoclave cure
- Remove from autoclave
- Return to layout area
- Debag subassembly
- NDT

6

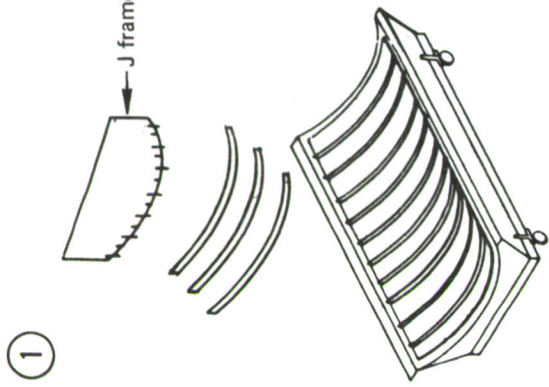
Second Stage



- Inspect BAJ and subassembly for cleanliness
- MEK wipe bond surface for frame tees
- MEK wipe all frame tee bond surfaces
- Cut and apply film adhesive for each frame tee (modified bondline per verifilm)
- Load and locate frame tees on assembly
- Use MIT for location on station lines
- Tape in place
- Remove MIT
- Bag per standard shop procedures
- Recheck locations with MIT
- Vacuum leak check
- Move to autoclave

Note: It may be profitable to leave the MIT on the assembly during the cure cycle.

Figure 125.—Internal Shell Stringer Concept



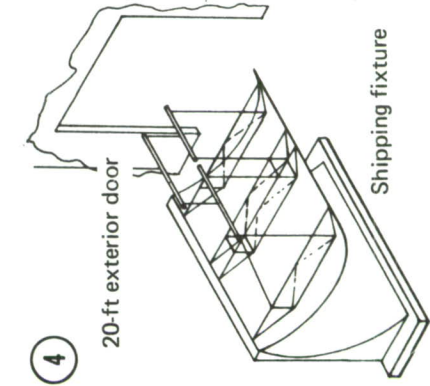
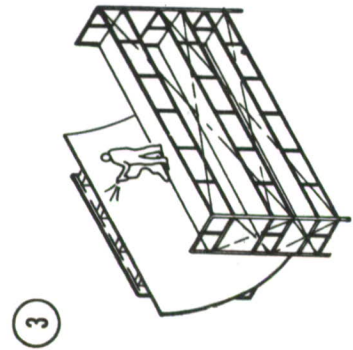
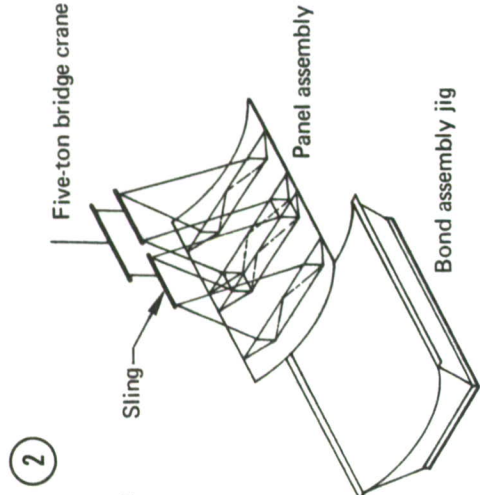
Inspect J frames for trim and pilot holes
 Locate in position on each frame tee
 Back drill Cleco holes from pilot holes
 Insert Cleco fasteners
 Back drill all holes in each J frame to frame tee
 Remove J frame and deburr
 Replace J frame—hold with Cleco's
 Install rivets and set with portable hand squeezer
 Apply seal material
 Inspect per drawing
 Move to final assembly area

Remove from BAJ with overhead crane
 Set up in NDT fixture for QC inspection

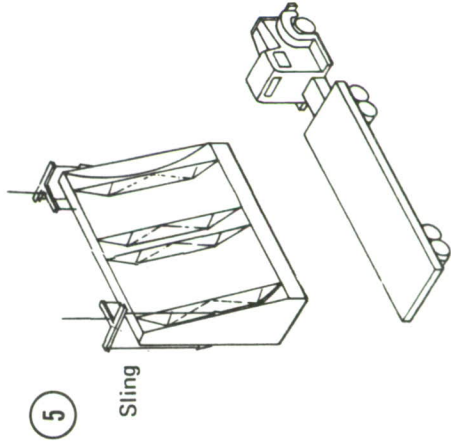
Perform TTU* operation and record information on colored printout
 Clean, Alodine, and apply protective coatings.

*Through-transmission ultrasonic (NDT inspection)

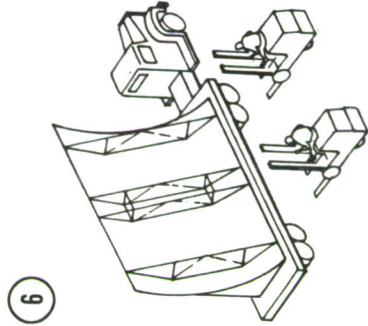
Noïdestructive test, clean, and apply protective coating



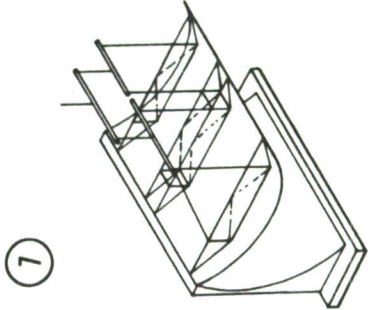
Move to shipping fixture
 Load and secure for transport



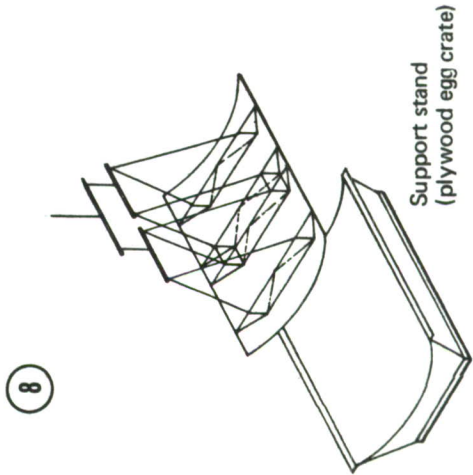
Load on truck and transport to final assembly area



Unload at final assembly area



Remove from transportation dolly



Nest in support stand until ready for jig loading

Figure 126. –Quadrant Assembly, Inspection, and Shipping

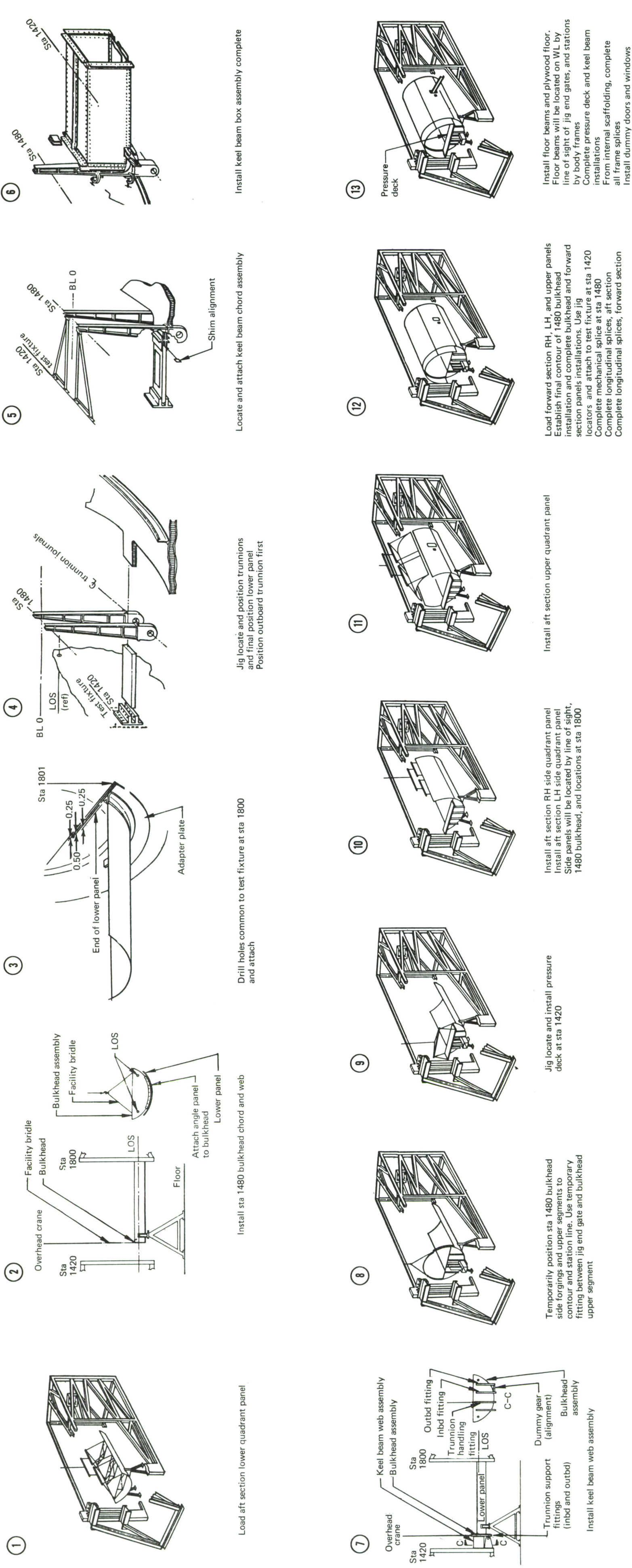


Figure 127. — Test Section Assembly

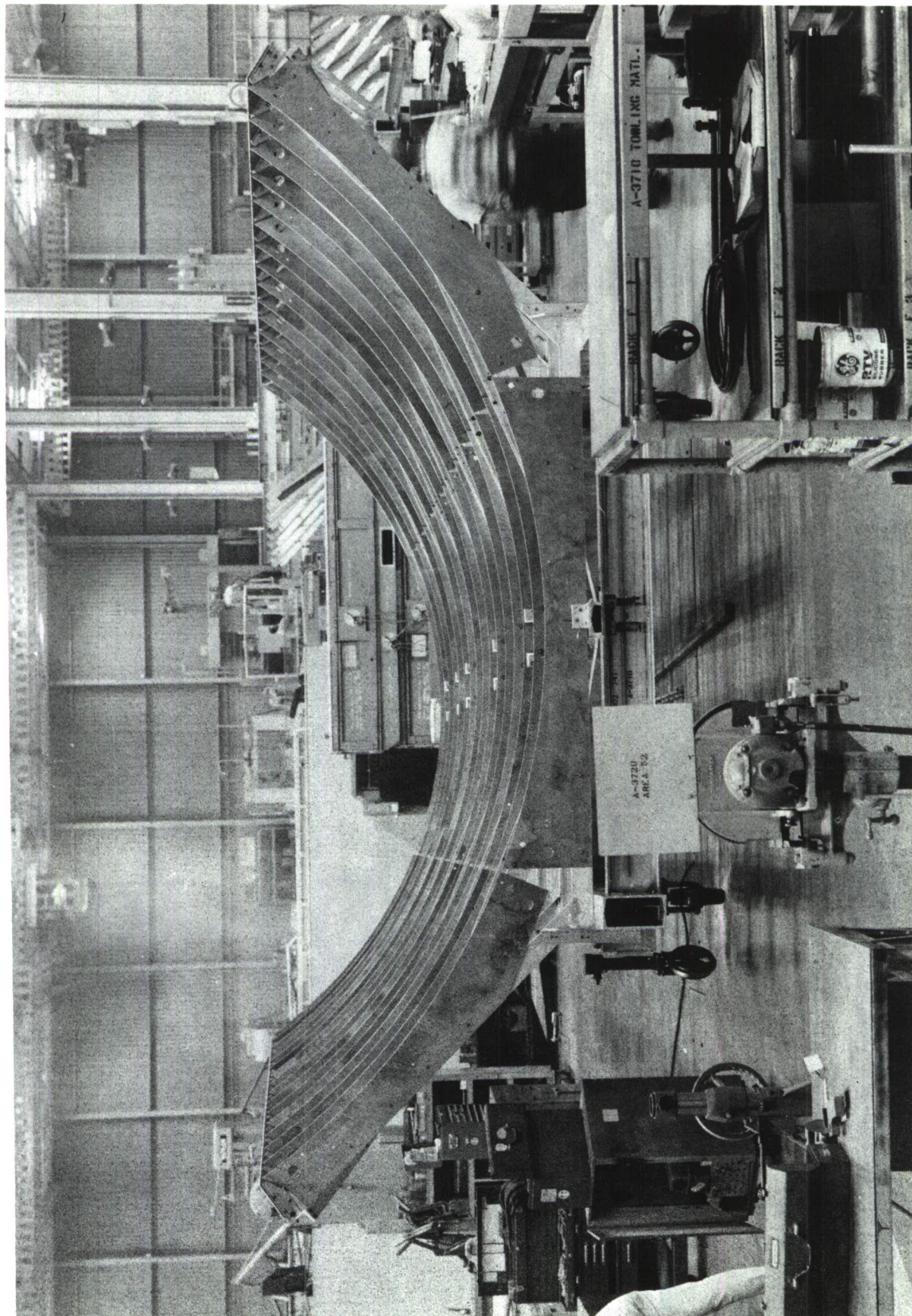


Figure 128.—Header-and-Skin-Type Bonding Assembly Jig for Simple Contours (Headers Ready for Application of Jig Skins)



Figure 129.—Header-and-Skin-Type Bonding Assembly Jig Skins Being Installed

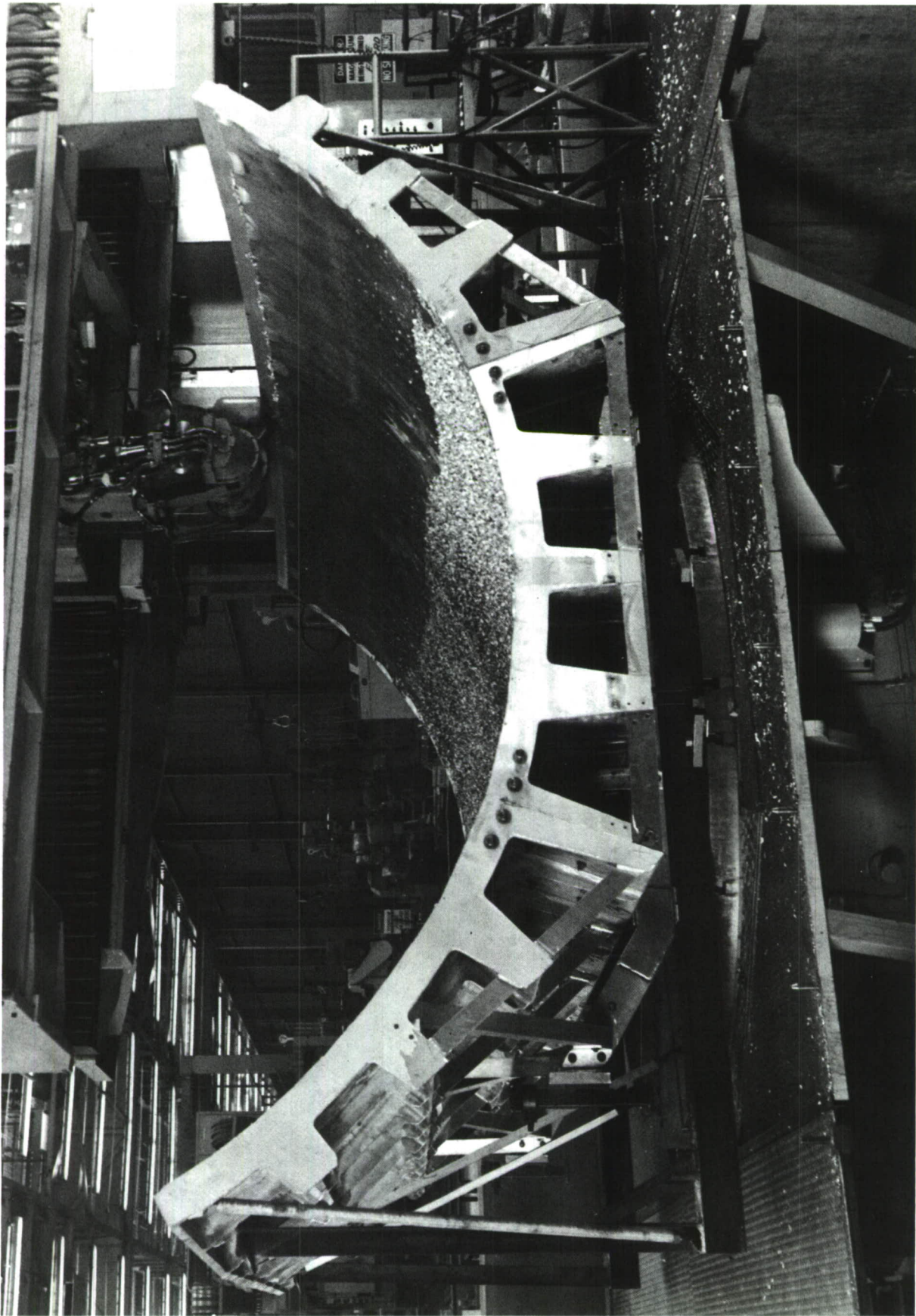


Figure 130. – Three-Piece Cast Aluminum, Compound Contoured Bonding Assembly Jig (Machined on Five-Axis Mill)

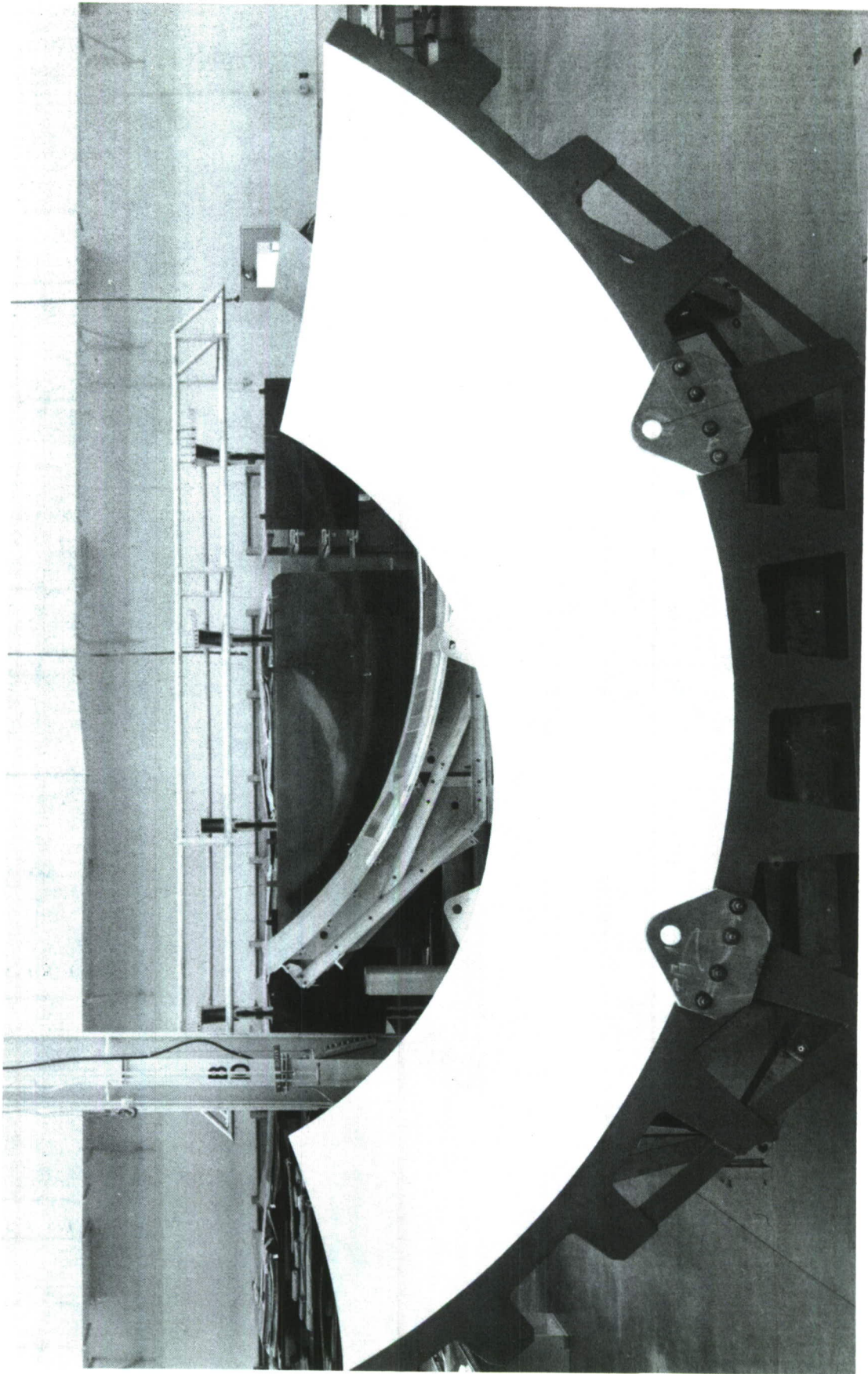


Figure 131.—Completed Cast Aluminum, Compound Contoured Bonding Assembly Jig

Adhesive bonding requires continuous process control to achieve high reliability; thus, it will benefit from a high degree of automation in both fabrication and NDT. However, the continuous process needs to be developed, followed by the design, fabrication, test, and implementation of a production facility.

A method for production verification of bonded assembly strength requires development to add more confidence to adhesive-bonded primary structure.

Although Manufacturing has learned how to cope with the change in shape, caused by adhesive shrinkage, that occurs during cure of large bonded panels, an adhesive system that does not shrink on curing, or one that minimizes shrinkage, will improve manufacturing costs.

(2) Mechanical Fastening

At the request of Manufacturing, to avoid the use of high-cost taper-shank fasteners (Taper-Loks), Engineering has chosen either screw thread or collar and annular-grooved pin, straight-shank fasteners in high-interference, cold-worked holes for the fatigue-critical splice areas. The interference fit of these fasteners in their holes will vary from a minimum of 0.001 inch to a maximum of 0.0025 inch. Although Manufacturing is capable of making these installations, there is a need to verify their equivalence to the tapered shank fastener joint in bonded honeycomb construction.

Straight-shank, overdriven rivets will be used in reduced fatigue severity areas of the quadrant splices.

(3) Summary

Manufacturing cost for the three shell designs will be less than for the baseline. Final assembly will take less labor because the quadrants will arrive at the assembly areas as much more accurate fabrications and with a minimum of parts to be added at final assembly. State-of-the-art fasteners will be specified.

f. Technology Development Required

Materials and processes which are needed or which need improvement for adhesive-bonded primary structure are discussed below.

Adhesive systems impose restrictions on manufacturing processes and part/assembly flow. For example, present adhesive systems impose a time limit within which assemblies must be cured and require careful phasing to fit into shop work schedules. More flexible time limits would benefit Manufacturing.

In bonding composites to metals, differential thermal expansion greatly complicates the process. An adhesive system is needed that can be cured at reduced or room temperature.

The close fit/tolerance requirements for parts to be bonded are a constraint on reducing parts cost. An adhesive system that can work with gaps up to 0.030 inch maximum between mating parts would improve the part fit and tolerance requirement and thus reduce cost.

Finally, adhesive shrinkage distorts large panels when they are cured. An adhesive system that does not shrink on curing or one that minimizes shrinkage would improve manufacturing costs.

The application of adhesives by curtain coating offers the advantages of thinner adhesive film (than that prepackaged in roll form as a sheet) and therefore lower adhesive weight in bonded assembly, and a process that is fully adaptable to automation and is very rapid (compared to hand application of film adhesive). For these reasons, a curtain coating formulation should be available for every adhesive system.

Manufacturing processes for a new reticulating adhesive need to be developed (see sec. III-5d2). This adhesive offers the design engineer the advantages of thinner bond lines with attendant adhesive weight savings of 60% and an increase of 20% in tensile strength.

Manufacturing operations would benefit from refinement of existing or development of new processes. Processes for bonded repairs to adhesive-bonded primary structure need refinement. The need for repairs occurs both during fabrication and while the structure is in service. Repair techniques for both small and large damaged areas must be determined and the efficiency of the repairs measured.

One repair scheme that should be investigated is that of bonding up joints (where repairs can be expected) from thin sandwiched sheet. When a repair in this area is required, the joint would be opened by peeling the layers of metal.

A highly reliable production process for verifying joint strength in adhesive-bonded primary structure is needed. The quality of bonded joints in subassemblies and major assemblies could thus be ensured. Moreover, this process, if adaptable to customer use, could attest to continued joint integrity.

The operations essential to obtaining reliable and durable adhesive-bonded joints are metal preparation and adhesive primer application. An environmentally controlled continuous process line appears to be a very desirable facility that would accomplish these two operations. Automating this facility would improve both process costs and reliability.

In summary, opportunities exist in process development and refinement that will promote greatly the acceptance of adhesive-bonded primary aircraft structure.

g. Manufacturing Cost Assessments

Each design concept was compared with the baseline 747 body section in terms of relative manufacturing complexity. Estimating ground rules included optimum tooling and facilities, and a minimum production of 201 identical study sections. The rationale is as follows.

(1) Standard Hours

Each concept, including the baseline, was estimated using standard labor hours to minimize the estimator's subjective evaluation. Individual shop variables were not included. Attempts were made to maintain the degree of completeness of the work statement and to draw comparable information for each of the concepts, including the baseline, to prevent unequal emphasis of any one concept.

(2) Complexity Factors

Manufacturing complexity factors were derived by establishing the baseline design as 100% and relating the other concepts to it in percentage terms.

(3) Learning Curves

The bonded shell concepts are expected to follow a 77% composite curve similar to that of the baseline concept for the study section.

While current, small, secondary bonded structures usually have an 85% curve, the larger, more complex primary structure assemblies tend to steepen the curve. A new major production program would justify optimum tooling, facilities, and techniques that, when subjected to the general factory environment, will generate many new ideas and procedures to sustain the steeper curve.

The initial production unit hours will be quite high with a very steep primary curve, leveling off to a flat projection. How flat and how soon is difficult to forecast for the reasons stated, but it appears conservative to expect as good a composite curve as we now have with the conventional construction.

7. QUALITY ASSURANCE/NONDESTRUCTIVE INSPECTION (NDI)

a. Quality Assurance Tasks

Quality Assurance participates in all phases of Boeing developmental programs, from basic raw materials receiving through consolidation and fabrication of finished structure. Quality assurance support provided during this first iteration preliminary design phase was directed at identifying the present and advanced methods for maintaining and improving the inspection and process controls required. The design concepts were evaluated, compared against each other, and rated for inspectability and process control requirements from raw material to finished product.

Maximum allowable defect sizes were compared with available NDI sensitivity limits, and the need for NDI development and/or a demonstration program was determined. Currently available NDI techniques (table XXXI) are sufficient to support the cargo fuselage program development within the scope of the fracture control plan requirements. A study was made anticipating the quality assurance needs to comply with the fracture control requirements, and an NDI demonstration program (sec. VI-3) was planned to determine the practical flaw detection sensitivity limits.

b. Concept Review Tasks

Each concept was reviewed to identify the material control, fabrication process control, and inspectability of the finished hardware to ensure that required quality level was attained. In-service inspection requirements, such as accessibility and portability of NDT instruments, were also evaluated. Manufacturing plans were reviewed to identify and compare inspection and process control requirements for each new design. During the reviews, consideration was given to inspection costs, facility requirements, and operator skills.

c. Quality Assurance—Concept Tasks

Outlined below is a quality assurance program plan that ensures attainment of the required quality level in the design, development, manufacturing, modification, repair, and maintenance of the delivered product. This quality assurance plan identifies the quality requirements at each manufacturing step. This plan includes, but is not limited to, design and development controls, procurement controls, fabrication and assembly controls, and process controls.

A schematic diagram of the quality assurance plan is shown in figure 132. All the key controls during a manufacturing process are emphasized. A typical example of quality control responsibilities during the adhesive bonding process is outlined in figure 133.

(1) Design and Development Controls

Quality Control personnel participate in specification review, design reviews, and technical interchanges to determine product inspectability, functional and inspection test requirements, material and process controls, and environmental controls.

Table XXXI.—Boeing Current NDI Status

Methods		Materials					Adhesive bonded structure defects	Brazed honeycomb structure defects	Processes					Field inspection					Dynamic testing												
		Wrought metals		Cast metals		Composites	Nonmetals	Single laminate defects	Multilaminate defects	Core defects	Fillet size	Fillet unbond	Node unbond	Crushed core	Welding		Forming		Surface cleaning	Metal structure		Composites	Fastener holes	Fire damage (aluminum)	Adhesive bonded structure	Brazed honeycomb structure	Crack growth	Structural behavior	Fatigue		
		Magnetic	Nonmagnetic	Magnetic	Nonmagnetic										Magnetic	Nonmagnetic	Magnetic	Nonmagnetic		Magnetic	Nonmagnetic									Heat treating	Magnetic
Acoustic	Acoustic emission														○	○													○	○	○
	Ultrasonic thru transmission					●		●	●	●	▼			○											▼						
	Ultrasonic pulse echo	●	●	▼	▼	○		▼			●	●	▼	●	●	●					●	●	○	●	●	●	●				
	Ultrasonic resonant					○		▼				○		▼								○			●	○					
	Ultrasonic delta scan														○	○															
	Ultrasonic surface	▼	▼																		●	●									
	Acoustic impact							▼	▼	▼				▼											▼						
Electromagnetic	Eddy current	▼	●	▼	▼													▼	●		▼	▼		●	●						
	Magnetic particle	●		●											●			●			●			▼							
	Micro wave (nonmetals)					○	○																○								
	Magnetic rubber	▼		▼											○			▼			○			▼							
	Magnetic perturbation	▼		▼											○			○			○										
	Electric current injection		○		○																○										
	Magnetic property meas	○		○											○			○													
Radiation	X-radiography	▼	▼	●	●	▼	●			●	▼	▼	●	●	●	●	▼				●	●	▼	▼	●	▼					
	In-motion radiography					○							○	○	▼	▼					○	○									
	Pulsed radiography												○	○	○																
	Scintillation scanning														○	○															
	Gamma radiography			●	●										○	○					○	○									
	Neutron					○	○	○	○		○																				
	X-ray vidicon					○							○	○	○	○															
Other	Liquid penetrant	▼	●	▼	●		●							▼	●	○	▼	●			▼	●	▼								
	Optical holography							○																	○	○	○	○			
	Thermography					●	○				○	○	○	○											○	○					
	Evaporative rate analysis																			○											
	Interferometry																													○	
	Visual	●	●	●	●	●	●	●	●	●	●	●	●	●	●	●	●	●	●	●	●	●	●	●	●	●	●	●	●	●	●
	Fatigue life gage																														○

- Preferred current practice
- ▼ Alternative
- Under development

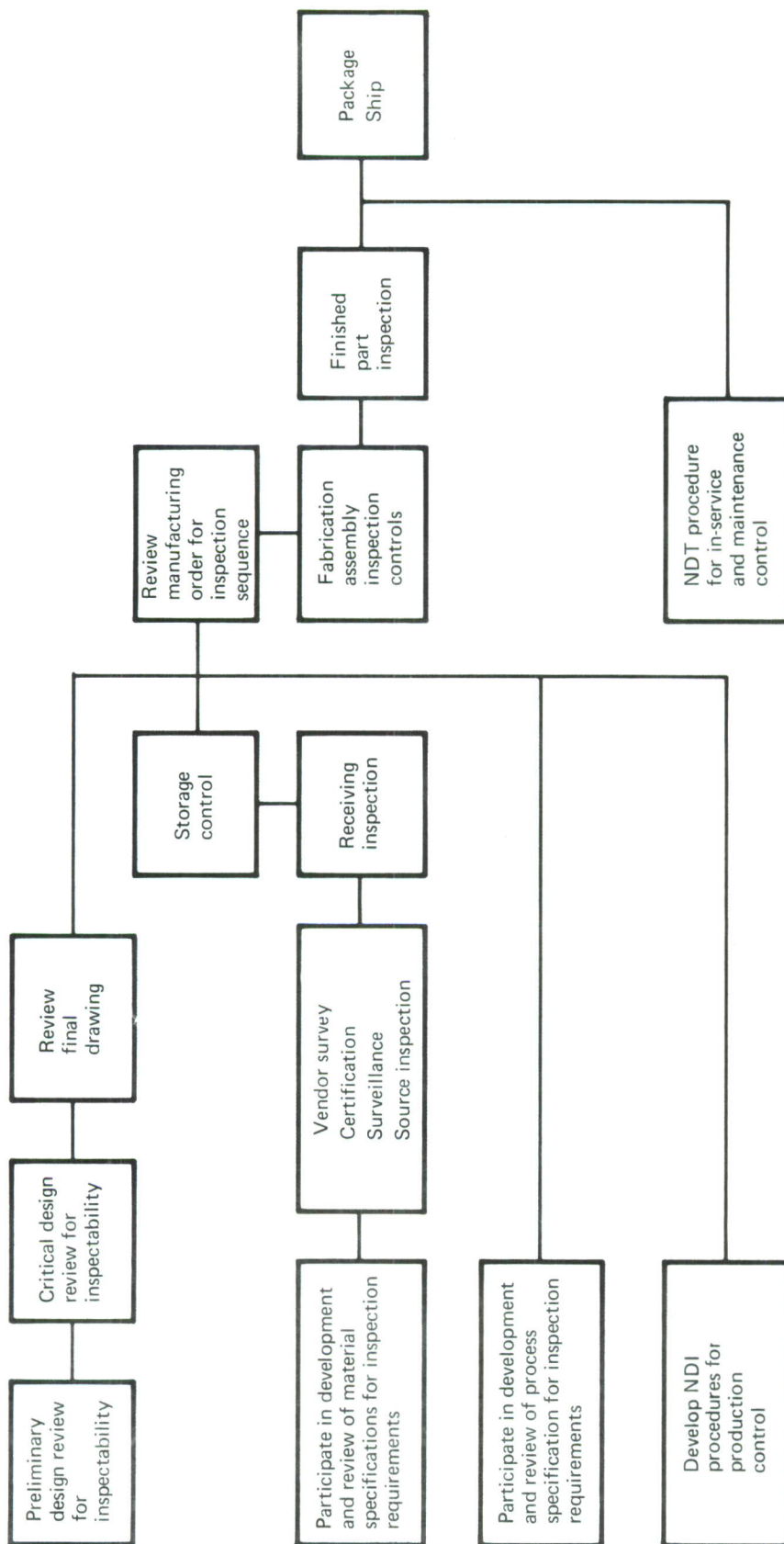


Figure 132.—AMS/ADP Cargo Fuselage—Quality Assurance Plan

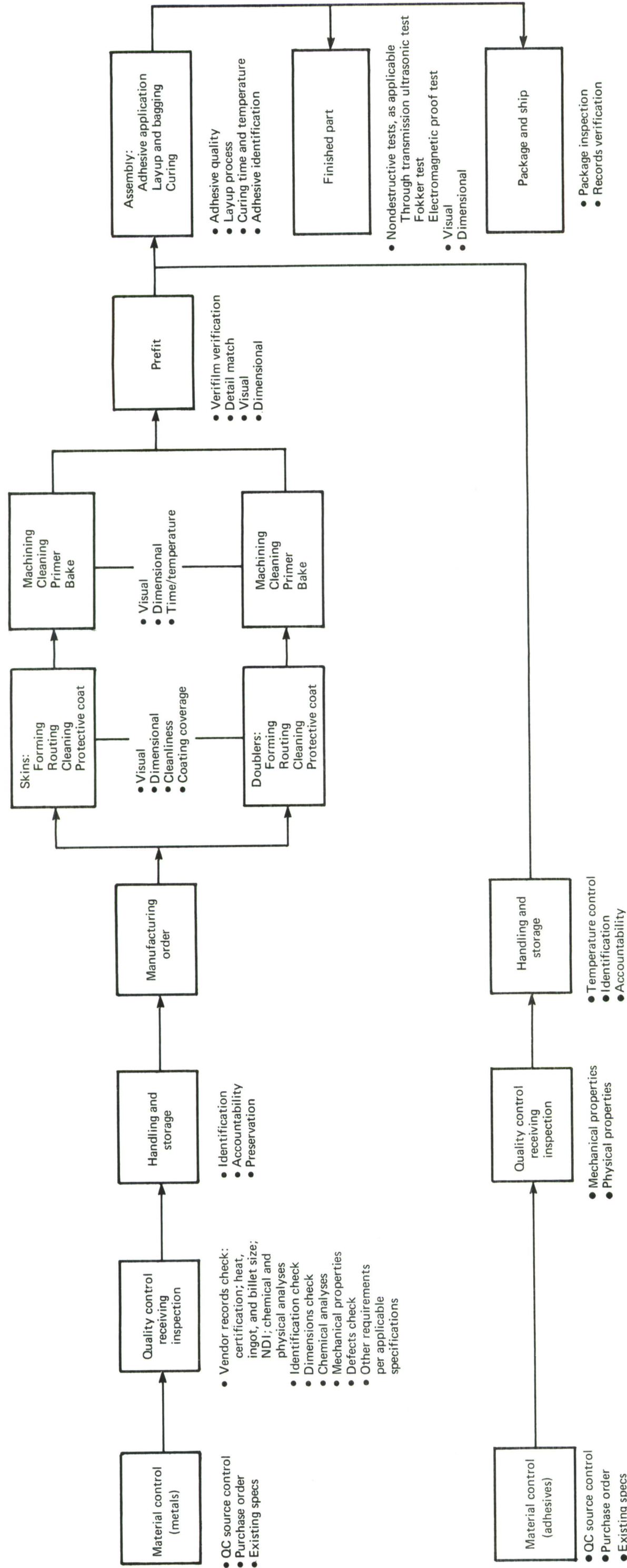


Figure 133. – Quality Control-NDI Flow Chart for Adhesive Bonding Process and Assembly

A central inspection record system facilitates the retrieval and tracing of data on request. Traceability cross referenced to part number, and particularly to fracture/fatigue-critical designated parts, is required for accurate test data and service experience correlation.

(2) Procurement Control

Quality control requirements are imposed on suppliers through the material and process specification on purchase orders. In addition, suppliers are required to maintain a quality system in accordance with an established quality control plan. The use of qualified supplies supported by surveillance and source inspection is essential. Materials and parts for fracture/fatigue-critical parts are to be designated with special notations throughout the procurement cycle. Receiving inspection and testing is required to ensure that the quality level of procured materials and parts conforms to the requirements of engineering drawings, documents, specifications, and the purchase order. Handling, storage, and preservation of procured items must meet the purchase order requirements and all procurement specifications. Special attention is given to materials for fracture/fatigue-critical parts, characterized as FC-I, FC-II, or FC-III parts as defined in section IV-4c.

(3) Fabrication and Assembly Control

Quality Control responsibility during fabrication and assembly is to verify that materials and workmanship conform to all engineering criteria. Included in these responsibilities are the monitoring of process facilities, materials control, operating sequences, and process control, and the certification of manufacturing and inspection personnel and equipment. For example, quality control checks during an adhesive bonding process are identified in figure 133. Inspection records are maintained by using inspection symbols and stamps, recording critical dimensions and process requirements, and verifying configuration data. Nonconformances are recorded for corrective action as well as for test data/service experience correlation. Particular attention to fracture/fatigue-critical parts is required to satisfy the fracture control program requirements of MIL-STD-1530 (USAF).

(4) Process Control

The quality assurance program ensures that all processes used in the fabrication, assembly, and installation of parts are controlled in accordance with documented specifications. Training and certification of inspection and manufacturing personnel are provided wherever critical processes and special skills are required. Recording of results and discrepancies provides data required for critical process review.

d. NDI Requirements

Latest NDI technology as well as routine NDI methods are applied to all manufactured products. Penetrant inspection is used extensively for detecting surface flaws. Eddy current inspection is used for thickness measurements, conductivity measurements, and crack detection in drilled holes. Ultrasonic inspection and X-ray techniques detect internal flaws. Under an AFML contract (F33615-72-C-1205), an ultrasonic technique is

being developed for detecting cracks under installed fasteners. Progress has been made in ultrasonic fastener hole-scanning techniques, display of test results, and identification of transducer requirements.

A wide range of inspection capabilities is applied to adhesive-bonded structures. It is planned that all adhesive-bonded assemblies for the cargo fuselage program will be evaluated by means of the NDT technique of ultrasonic through-transmission scanning with the multilevel recording system, shown in figure 134. Portable instruments, such as the Fokker bond tester, the Sondicator, the harmonic bond tester, and the ultrasonic contact inspection are used as an adjunct to the through-transmission technique. These NDI techniques are capable of detecting voids in single or multiple bond line structures.

There is no production instrument to determine the strength of a bonded assembly. A prototype unit of an electromagnetic proof tester that can verify the strength of a bonded assembly to a specified level was developed in a Boeing in-house IR&D program. Further in-house funded development of this technique and construction of a production model is planned.

(1) Facility Requirements

Extensive quality assurance facilities are available, as shown in table XXXI. The following facilities are identified to support the NDI requirements of section IV-7d.

- Penetrant
- Eddy current
- Ultrasonics
- X-ray
- Adhesive bond inspection
 - Ultrasonic through-transmission
 - Portable instruments (Fokker, Sondicator, harmonic, etc.)
 - Electromagnetic proof tester (prototype)

(2) Capability Requirements

The sensitivities of presently available NDI techniques under normal conditions are listed in table XXXII.

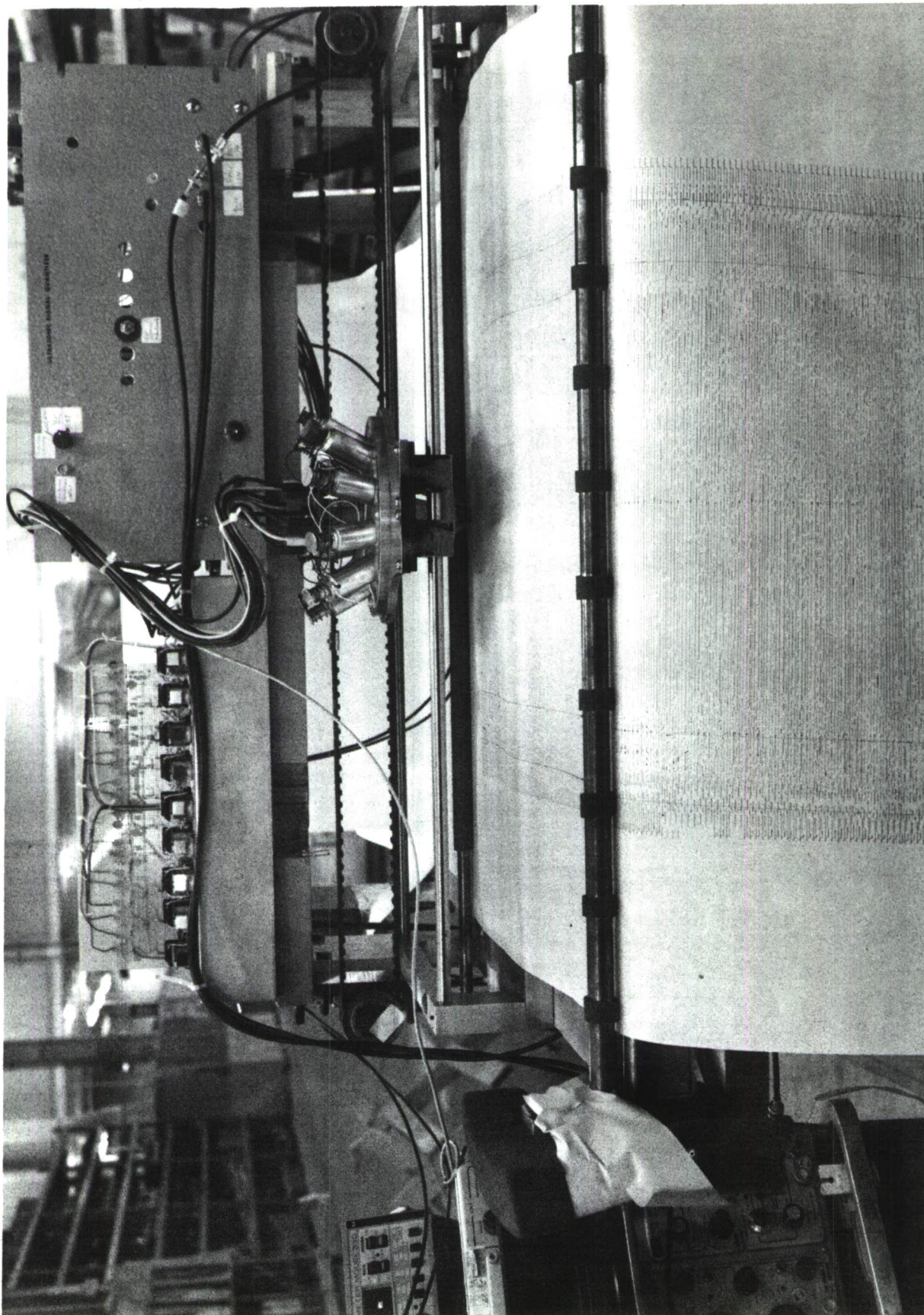


Figure 1 34. —Prototype Multilevel Recorder

Table XXXII.—Sensitivity of NDI Techniques

Technique	Defect type	Sensitivity limit
Penetrant	Surface cracks	0.020 in. or larger
Eddy current	Cracks inside holes	0.030 in. or larger
Ultrasonics	Cracks under fasteners	0.050 in. or larger
Ultrasonics	Internal flaws	0.030 in. or larger
Ultrasonics	Bonding voids	0.5 in. x 0.5 in. or larger
Electromagnetic	Bond strength	Verify to a specified level

e. Fracture Control Plan—Quality Control Requirements

The criteria for the identification of fracture-critical parts (sec. IV-4c) provide for special controls on those parts determined to be fracture critical. The quality control plan identifies the specific quality control procedures required for the three categories of fracture criticality and provides for implementation.

(1) Fabrication Control

Parts identified as category FC-I fracture critical will be subjected to stringent fabrication control to ensure that flaws larger than those assumed in damage tolerance analysis will be detected and that appropriate action will be taken. Subsequent to final assembly, penetrant inspection to detect surface flaws will be conducted on all FC-I parts or in those local areas of components designated as FC-I areas.

Eddy current inspection to detect the existence of flaws emanating from holes will be conducted on all FC-I parts or in those local areas of components designated as FC-I areas. This inspection will be made subsequent to the final step in hole preparation preceding fastener preparation.

Eddy current inspection by manual means requires about 2 minutes per hole, which is considered prohibitively slow. An automated eddy current inspection probe, sequenced between the hole reaming and rivet installation step on the numerically controlled riveter, is planned for development.

(2) Material Control

Parts identified as category FC-II fracture critical will be subjected to further source/process/finish controls in addition to the normal receiving inspection (sec. IV-7c2). Material exhibiting properties inferior to those assumed in the damage tolerance analysis will

be eliminated. Tests will be conducted on all billets, forgings, extrusions, plates, or other forms (from which final parts are to be finished) to evaluate the material fatigue crack growth rates. A slice will be cut from items, or integral projections thereof at receiving inspections, so that specimens from each slice may be tested. These specimens will be processed simultaneously with the same material from which they were cut.

(3) In-Service Inspection

Parts identified as category FC-III fracture critical will be subjected to intensified in-service inspection and maintenance requirements. It is presently intended that all FC-III parts be subjected to a complete penetrant inspection during the depot level maintenance inspection to detect surface flaws and flaws propagating from under fastener heads.

(4) NDI Demonstration

Boeing has the NDI capability of detecting flaws equal to the minimum initial flaw size of USAF Damage Tolerance Criteria (app. I). However, when designs are based on initial flaw size assumptions less than those specified in appendix I, an NDI demonstration program is performed to verify that all flaws equal to or greater than the design flaw size are detected to the reliability and confidence level specified in appendix I.

(5) Traceability of Material

Records for traceability of material must be maintained per MIL-STD-1530 (USAF). All acceptable materials will be stamped with a serial number, which is transferred to the records of parts fabricated from this material. After final installation of parts, the records are stored in a special storage area and are retrievable on demand.

f. Technology Development

Void detection capability has been successfully developed and implemented on adhesive-bonded structures. However, there is a need to determine the bond strength of the bonded parts. Boeing, with an in-house IR&D program, has developed an electromagnetic proof testing technique; a prototype unit currently under evaluation is shown in figure 135. Further development of this test method is planned from which the design and construction of a production model will result (fig. 136).

Ultrasonic through-transmission is fully implemented by Boeing on current production programs. However, some additional development work is needed to design and build a scanning unit (see fig. 137) for inspecting a full-scale fuselage section.

Eddy current inspection, when used manually, is successful in detecting cracks in drilled holes prior to fastener installation. There is a need to investigate and develop an automated eddy current inspection system to be used on the numerically controlled riveter.

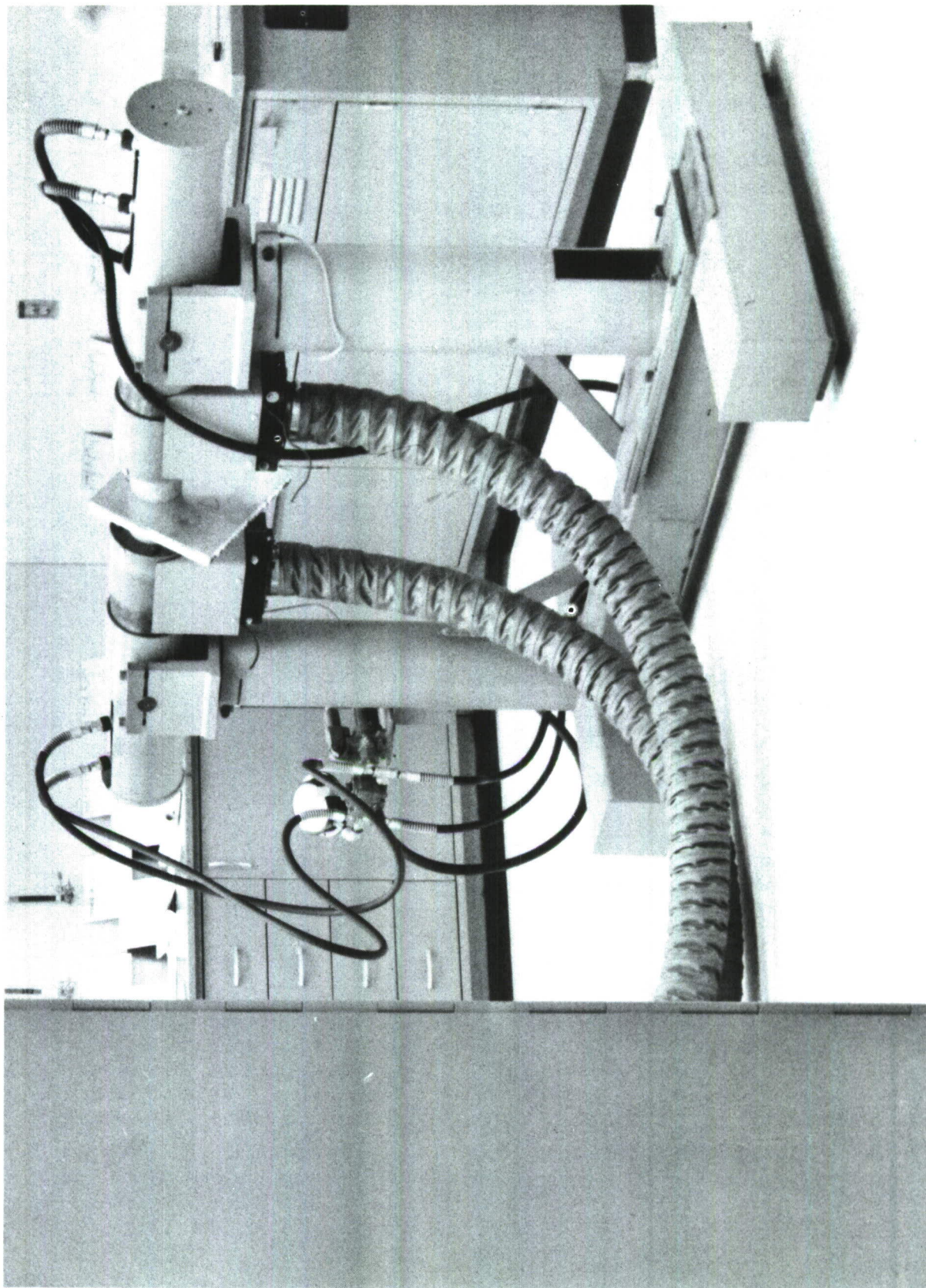


Figure 135. –Prototype –Electromagnetic Proof Testing Facility

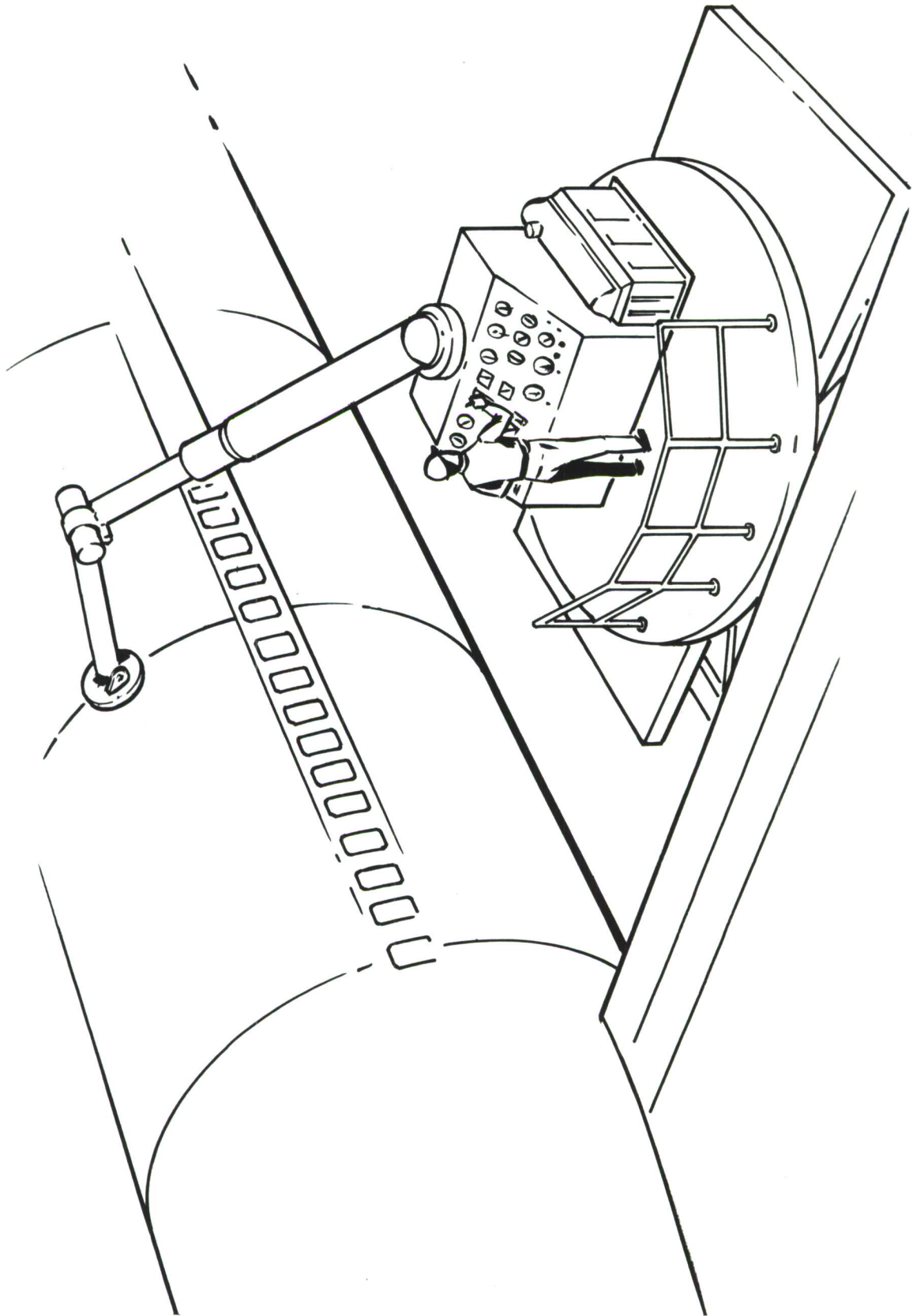


Figure 136 —Production Model of Bond Proof Testing Unit

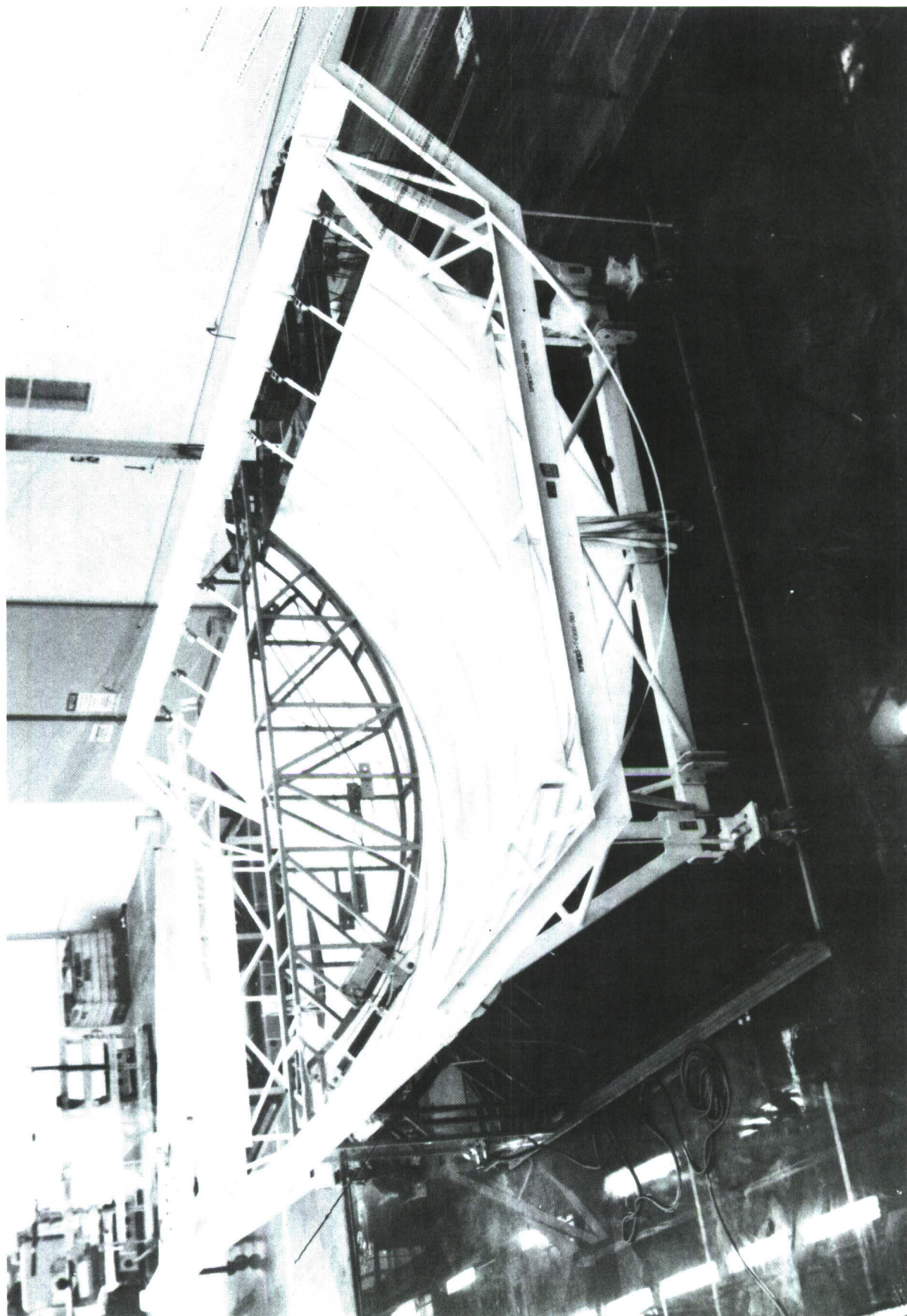


Figure 137.—Ultrasonic Through-Transmission Inspection Facility

8. COST ESTIMATING

a. Introduction

The 747-100 airplane, from which the baseline study section is derived, is part of the latest generation of transport aircraft that incorporates today's technology in terms of engineering design and economical production practices. These two interrelated elements have contributed to the production of an airplane with one of the lowest costs per pound of airframe structure. Solid baseline cost data were available for use in comparing cost estimates of the new structural concepts evaluated during this study. Because of the extremely low cost of the baseline structure, a unique challenge is presented in seeking lower cost alternates.

b. Background

The cost estimating baseline data for this study is based on the average cost of 201 shipsets of model 747-100 airframe production. Basic elements include:

- A detailed and confirmed weight statement
- A dollar-per-pound rate of finished production material
- A detailed direct labor estimate of the selected fuselage section (stations 1480 to 1741)
- A support labor factor defining the relations of such support functions as Industrial Engineering, Materiel, Production Engineering, and Quality Control to direct production effort. The rate for this study has been established at 30% of direct production effort for the body area.
- A dollar-per-hour rate for nonrecurring effort
- A dollar-per-hour rate for recurring effort

c. Cost Estimating Method

The sections of fuselage under study are produced for Boeing by Norair. Actual production cost records of this manufacturer were used as comparison checks against the detail baseline labor estimate developed by Boeing to attain the required level of comparison between the baseline and the several concepts.

The recurring costs were developed as follows: Production labor hours for airplane 1 were developed by a detailed estimate of effort for the study area. Cumulative hours for 201 shipsets were obtained using a 77% experience curve. Results of these computations were compared to actual production costs of the subcontractor. Because the difference was less than 0.5%, no adjustments were made to the estimate.

Support labor was applied at the rate of 30% of production labor and added to production labor to obtain total manufacturing labor hours. The current representative production wraparound labor rate was applied to the recurring labor hours.

The detail estimate proportioned the labor hours for the analysis section as follows:

- 9% for the upper quadrant
- 36% for the side quadrant
- 23% for the lower quadrant
- 32% for the fore and aft body extensions, stations 1420 to 1480 and 1741 to 1800

Production material cost per airplane for the study area was derived from the cost of 201 shipsets of material purchased for the mid and aft body areas. From this, a dollar-per-pound rate for finished materials was developed. This rate was applied to material weights to develop material cost for all components of the study.

d. Concept Cost Estimates

Concept cost estimates were developed by applying complexity factors to the baseline direct labor and nonrecurring costs. Complexity factors were developed for each concept by Manufacturing. Tables XXXIII through XXXVII show the cost estimate elements and totals for the baseline and the four shell concepts. The complexity percentages of both nonrecurring and recurring elements changed as design details and technical considerations became more visible. Quadrants and major components within quadrants do not follow the complexity factor of a concept, but vary depending upon component location, weight, design, material and fabrication, and assembly techniques. The baseline dollars-per-pound rate (1971 dollars) has been escalated by 4% for the 1973 computations. The material utilization factor for all concepts and product design iterations in this study has been assumed to be the same as that for the baseline. The baseline experience curve of 77% was used for all concepts. All costs shown are in 1973 dollars.

The sum of all component recurring and nonrecurring costs and a percentage of their sum as profit give the total average study section out-the-door cost for each concept. Table XXXVIII presents the relative cost of the baseline and the four concepts.

*Table XXXIII.—Level 3 Weight and Cost Summary by Quadrant
(Average of 201 Airplanes)
Station 1420-1800—Baseline*

Item	Weight (lb)	Material (1973 \$)	Labor (hr)	Labor (1973 \$)	Total (1973 \$)
Upper quadrant					
Skin and stringers	753	6,491	625	17,500	23,991
Frames	142	1,224	278	7,784	9,008
Splices, fasteners, and edges	49	422	28	784	1,206
Straps	28	241	30	840	1,081
Total	972	8,378	961	26,908	35,286
Side quadrant					
Skin and stringers	1,748	15,068	2,184	61,152	76,220
Frames	336	2,896	962	26,936	29,832
Splices, fasteners, and edges	84	724	518	14,504	15,228
Straps	24	207	37	1,036	1,243
Total	2,192	18,895	3,701	103,628	122,523
Lower quadrant					
Skin and stringers	1,721	14,835	1,496	41,888	56,723
Frames	484	4,172	724	20,272	24,444
Splices, fasteners, and edges	64	552	154	4,312	4,864
Total	2,269	19,559	2,374	66,472	86,031
Sized section 1480-1741 total	5,433	48,832	7,036	197,008	243,840
Shell extensions (Sta 1420-1480 and 1741-1800)	2,199	18,955	3,180	89,040	107,995
Total of items studied	7,632	65,787	10,216	286,048	351,835
Constant items					
Section 44 lower lobe					
Sta 1480 bulkhead	1,195				47,800
Aft keel beam	299				9,568
Landing gear fittings	785				39,250
Windows	26				212
Pressure deck and floor beams	679				22,830
Total	2,984				119,660
Total recurring cost					471,495
Total nonrecurring cost					193,726
Total cost					665,221
Profit					79,826
Unit total	10,616				745,047

*Table XXXIV.—Level 3 Weight and Cost Summary by Quadrant
(Average of 201 Airplanes)
Station 1420-1800—Internal Stringer Concept*

Item	7475 weight (lb)	Material (1973 \$)	Labor (hr)	Labor (1973 \$)	Total (1973 \$)
Upper quadrant					
Skin and stringers	614	5,293	672	18,816	24,109
Frames	138	1,190	278	7,784	8,974
Splices, fasteners, and edges	45	388	29	812	1,200
Straps	14	121	30	840	961
Total	811	6,992	1,009	28,252	35,244
Side quadrant					
Skin and stringers	1,643	14,164	1,900	53,200	67,364
Frames	291	2,508	920	25,760	28,268
Splices, fasteners, and edges	81	698	561	15,708	16,406
Straps	23	198	37	1,036	1,234
Total	2,038	17,568	3,418	95,704	113,272
Lower quadrant					
Skin and stringers	1,185	10,214	901	25,228	35,442
Frames	443	3,819	710	19,880	23,699
Splices, fasteners, and edges	50	431	133	3,724	4,155
Total	1,678	14,464	1,744	48,832	63,296
Sized section 1480-1741 total	4,527	39,024	6,171	172,788	211,812
Shell extensions (Sta 1420-1480 and 1741-1800)	1,829	15,766	2,767	77,476	93,242
Total of items studied	6,356	54,790	8,938	250,264	305,054
Constant items					
Section 44 lower lobe					
Sta 1480 bulkhead	1,195				47,800
Aft keel beam	299				9,568
Landing gear fittings	785				39,250
Windows	26				212
Pressure deck and floor beams	679				22,830
Total	2,984				119,660
Total recurring cost					424,714
Total nonrecurring cost					213,070
Total cost					637,784
Profit					76,534
Unit total	9,340				714,318

*Table XXXV.—Level 3 Weight and Cost Summary by Quadrant
(Average of 201 Airplanes)
Station 1420-1800—Continuous-Bead Concept*

Item	7475 weight (lb)	Material (1973 \$)	Labor (hr)	Labor (1973 \$)	Total (1973 \$)
Upper quadrant					
Skin and beads	636	5,482	637	17,836	23,318
Frames	158	1,362	278	7,784	9,146
Splices, fasteners, and edges	58	500	29	812	1,312
Straps	0	0	0	0	0
Total	852	7,344	944	26,432	33,776
Side quadrant					
Skin and beads	1,676	14,447	1,922	53,816	68,263
Frames	340	2,620	940	26,320	28,940
Splices, fasteners, and edges	104	896	504	14,112	15,008
Straps	0	0	0	0	0
Total	2,120	17,963	3,366	94,248	112,211
Lower quadrant					
Skin and beads	1,339	11,542	974	27,272	38,814
Frames	443	3,819	720	20,160	23,979
Splices, fasteners, and edges	39	336	187	5,236	5,572
Total	1,821	15,697	1,881	52,668	68,365
Sized section 1480-1741 total	4,793	41,004	6,191	173,348	214,352
Shell extensions (Sta 1420-1480 and 1741-1800)	1,881	16,214	2,798	78,344	94,558
Total of items studied	6,674	57,218	8,989	251,692	308,910
Constant items					
Section 44 lower lobe					
Sta 1480 bulkhead	1,195				47,800
Aft keel beam	299				9,568
Landing gear fittings	785				39,250
Windows	26				212
Pressure deck and floor beams	679				22,830
Total	2,984				119,660
Total recurring cost					428,570
Total nonrecurring cost					222,768
Total cost					651,338
Profit					78,160
Unit total	9,658				729,498

*Table XXXVI.—Level 3 Weight and Cost Summary by Quadrant
(Average of 201 Airplanes)
Station 1420-1800—Honeycomb Concept*

Item	7475 weight (lb)	Material (1973 \$)	Labor (hr)	Labor (1973 \$)	Total (1973 \$)
Upper quadrant					
Skin and core	5.5	4,698	625	17,500	22,198
Frames	101	871	278	7,784	8,655
Splices, fasteners, and edges	203	2,267	28	784	3,051
Straps	0	0	0	0	0
Total	909	7,836	931	26,068	33,904
Side quadrant					
Skin and core	1,306	11,689	2,246	62,888	74,577
Frames	173	1,491	900	25,200	26,691
Splices, fasteners, and edges	52	4,500	518	14,504	19,004
Straps	0	0	0	0	0
Total	2,031	17,680	3,664	102,592	120,272
Lower quadrant					
Skin and core	1,111	9,577	1,520	42,560	52,137
Frames	232	2,172	700	19,600	21,772
Splices, fasteners, and edges	135	1,595	154	4,312	5,907
Total	1,518	13,344	2,374	66,472	79,816
Sized section 1480-1741 total	4,538	38,860	6,969	195,132	233,992
Shell extensions (Sta 1420-1480 and 1741-1800)	1,838	16,016	3,180	89,040	105,056
Total of items studied	6,336	54,876	10,149	284,172	339,048
Constant items					
Section 44 lower lobe					
Sta 1480 bulkhead	1,135				47,800
Aft keel beam	239				9,568
Landing gear fittings	735				39,250
Windows	26				212
Pressure deck and floor beams	679				22,830
Total	2,934				119,660
Total recurring cost					458,708
Total nonrecurring cost					193,726
Total cost					652,434
Profit					78,292
Unit total	9,350				730,726

*Table XXXVII.—Level 3 Weight and Cost Summary by Quadrant
(Average of 201 Airplanes)
Station 1420-1800—External Stringer Concept*

Item	7475 weight (lb)	Material (1973 \$)	Labor (hr)	Labor (1973 \$)	Total (1973 \$)
Upper quadrant					
Skin and stringers	582	5,017	444	12,432	17,449
Frames	130	1,121	278	7,784	8,905
Splices, fasteners, and edges	45	388	29	812	1,200
Straps	4	34	30	840	874
External insulation (Delta)	13	1,680	0	0	1,680
Total	774	8,240	781	21,868	30,108
Side quadrant					
Skin and stringers	1,584	13,654	1,500	42,000	55,654
Frames	269	2,319	900	25,200	27,519
Splices, fasteners, and edges	81	698	471	13,188	13,886
Straps	6	52	37	1,036	1,088
External insulation (Delta)	24	3,049	0	0	3,049
Total	1,964	19,772	2,908	81,424	101,196
Lower quadrant					
Skin and stringers	1,184	10,206	914	25,592	35,798
Frames	443	3,819	700	19,600	23,419
Splices, fasteners, and edges	50	431	185	5,180	5,611
External insulation (Delta)	12	1,493			1,493
Total	1,689	15,949	1,799	50,372	66,321
Sized section 1480-1741 total	4,427	43,961	5,488	153,664	197,625
Shell extension (Sta 1420-1480 and 1741-1800)	1,765	15,214	2,480	69,440	84,654
Total of items studied	6,192	59,175	7,968	223,104	282,279
Constant items					
Section 44 lower lobe					
Sta 1480 bulkhead	1,195				47,800
Aft keel beam	299				9,568
Landing gear fittings	785				39,250
Windows	26				212
Pressure deck and floor beams	679				22,830
Total	2,984				119,660
Total recurring cost					401,939
Total nonrecurring cost					222,768
Total cost					624,707
Profit					74,965
Unit total	9,176				699,672

Table XXXVIII.—Relative Concept Cost Estimates

	Total study section			Four quadrants and shell extensions	
Concept	Total	Total recurring	Total nonrecurring	Material	Recurring labor
Baseline	1.00	1.00	1.00	1.00	1.00
Internal stringer	0.96	0.90	1.10	0.83	0.87
Continuous bead	0.98	0.91	1.15	0.87	0.88
Honeycomb	0.98	0.97	1.00	0.83	0.99
External stringer	0.94	0.85	1.15	0.90	0.78

SECTION V

RECOMMENDED FOLLOW-ON PROGRAM

1. INTRODUCTION

In planning the follow-on phases of the cargo fuselage program, the essential planning guidelines must be identified. These guidelines are:

- Establish a firm base for the payoff and cost effectiveness of advanced metallic fuselage structure.
- Validate both the static, fatigue, and damage tolerance reliability and the fabrication, inspection, and maintenance feasibility by fabrication and test of a critical fuselage advanced structural component.
- Provide the information transfer required to allow the incorporation of advanced metallic structure in future Air Force aircraft systems.

The success of the planned program in meeting these guidelines is dependent on full technology coverage throughout the program. This requires a closely coordinated team of Engineering, Manufacturing, and Quality Control personnel. Each element of the team will contribute significantly to establishing a high confidence in the information generated by the program. Boeing has applied the total team coverage to phase 1A and will continue the coverage throughout the follow-on program.

Major program direction and the highlights of the recommended follow-on program are depicted in the flow chart of figure 138. The program schedule and milestones are shown in figure 139. The following sections deal with specific tasks recommended for each phase.

2. PHASE 1B—PRELIMINARY DESIGN

Phase 1B is a second iteration of the phase 1A preliminary design and analysis on the final three USAF-approved concepts. The design emphasis will be placed on refining details and identifying the critical components of each concept. Analysis will be performed in greater depth in order to determine the weights to a higher confidence level and to ensure the structural integrity. Computerized analysis techniques, including optimization and finite element analysis programs, will be used. These programs will establish better detail in the vicinity of high concentrated load introduction and major cutouts.

Design innovation will not be constrained except within the limits defined by the basic structural concepts selected, since increased depth of design exploration frequently exposes problem areas that invite innovations.

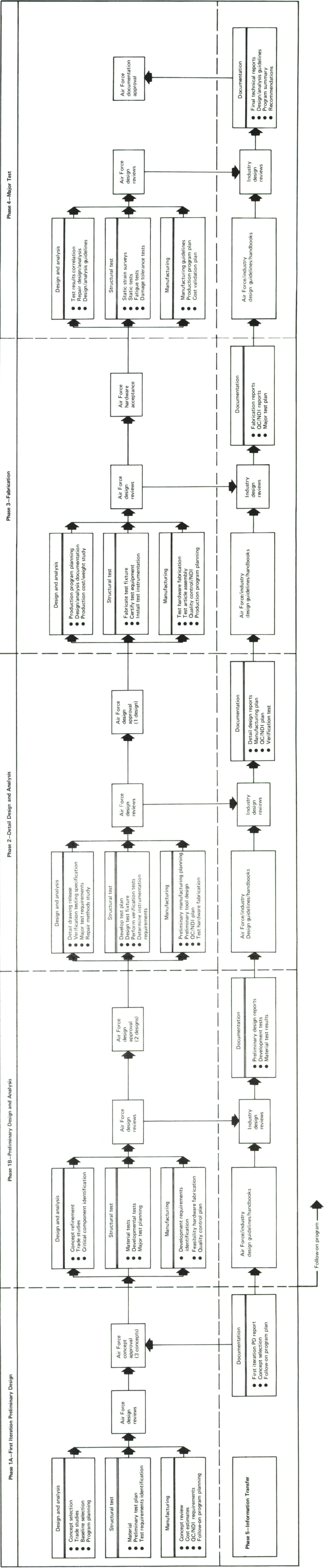


Figure 1.38—Follow-On Program Flow Chart

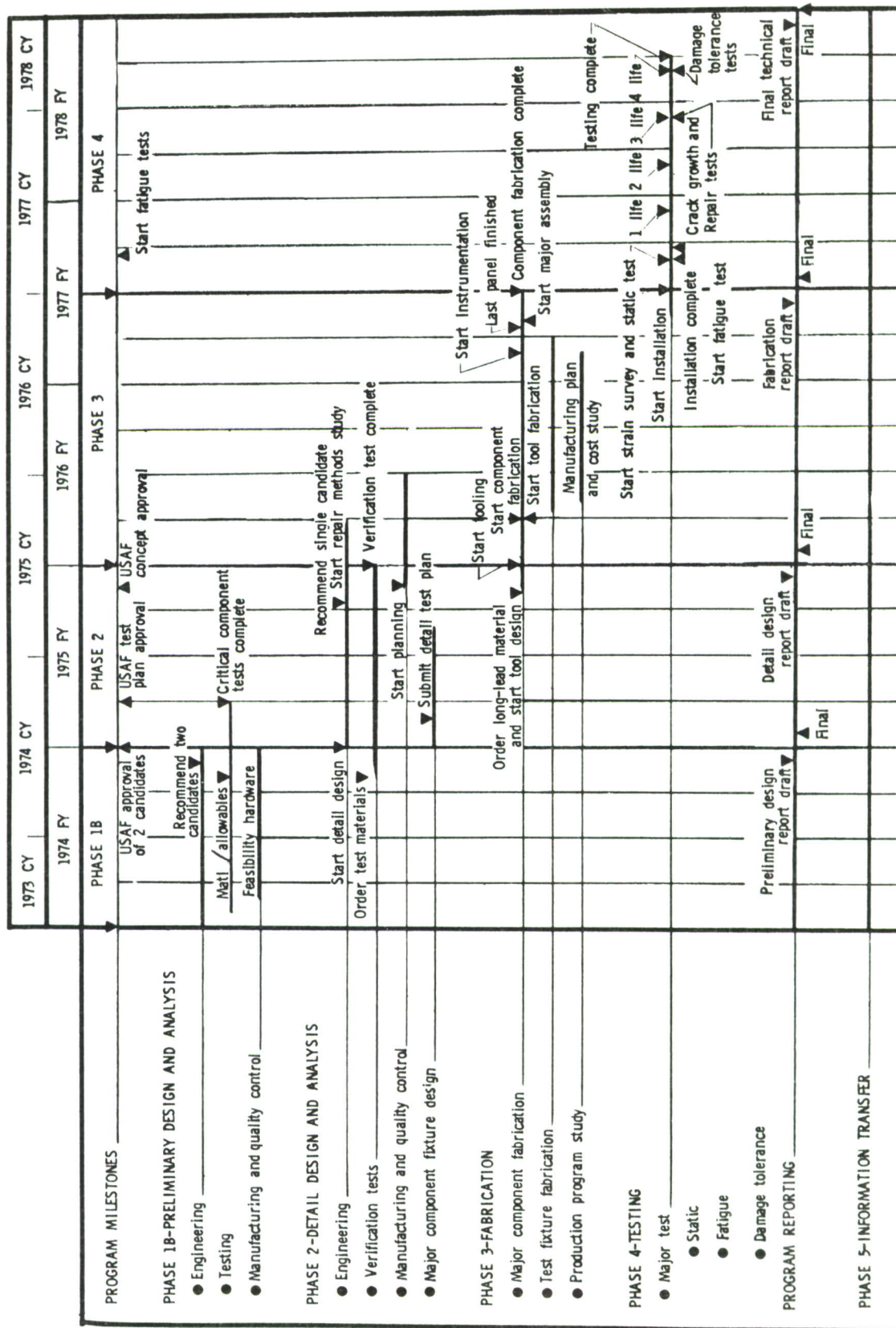


Figure 139.-Follow-On Program Schedule

Critical design details must be identified and tested in a development program sequence such that the test data will permit selection of the best details for the designs in phase 2. An orderly test program will allow isolation of the parameters influencing the quality of the design and incorporation of the best details into the final design.

Structural testing will be conducted to the extent necessary to support the preliminary design, detail design, and manufacturing development program. Phase 1B tests will include material and structural allowables, specific design details, and selected components. Material and structural allowable tests will be performed to the extent necessary to define the material characteristics and parameters. Specific details and components will be tested to verify basic concept acceptability. Static, fatigue, and residual strength tests will be integrated into a test sequence planned to provide for orderly structural development.

New structural concepts may require that new tooling and assembly methods be devised. In order to determine and understand the design compromises that will be encountered, manufacturing feasibility hardware must be fabricated. This procedure will lend confidence to the selection of the manufacturing option for the final design concept selected in phase 2.

Since new materials and processes will be used, work will be initiated in this phase to establish the basic material properties and characteristics. This requires that new process control parameters be established and validated so that adequate control can be assured prior to major component fabrication.

Preliminary planning for phases 2 through 4 will be conducted to identify the manufacturing and quality control development required and to establish the basic philosophy for the major structural test program.

3. PHASE 2—DETAIL DESIGN AND ANALYSIS

Two recommended and USAF-approved concepts will be subjected to detail design and analysis during this phase. Engineering drawings of details similar to those required for a production airframe will be prepared for both concepts. Finite element computer analyses will be refined to establish the final detail load distribution and stiffness. Design details exhibiting the highest fatigue quality during developmental testing will be incorporated in the selected configurations.

Verification tests will be performed to ensure that the desired design quality has been achieved. These will consist of static, fatigue, and residual strength component tests. Testing may also be performed to define the limits on manufacturing processes and inspection capabilities.

Structural repair methods will be developed and evaluated. These methods will consider the potential of inadvertent damage occurring during fabrication, assembly, or test. Consideration will be given to establishing these techniques to repair of damage that may occur in service requiring repair at remote sites.

Major test program plans and the instrumentation requirements will be established. The test fixture for the major test program will be designed and fabrication and assembly drawings prepared. Schedules and critical long-lead material requirements for the fixture will be determined. Aircraft systems interface requirements need to be identified and validation testing defined.

Manufacturing plans will be initiated and the preliminary tools designed in order to meet the required schedules for phase 3 fabrication. Facilities that may be required for cost-effective production and are unusual to the industry will be identified. Manufacturing feasibility for final designs may be established by fabricating panels to be used in verification tests.

4. PHASE 3—FABRICATION

The fabrication of the major test article, the test fixture, and the required tooling will be completed in this phase. Since reliable cost data are required for production program planning, the basic design of the components and the tooling should be representative of a production airplane approach; however, quality will be tailored to that required for the test article. Problems encountered in component fabrication that may have a significant impact on a production application will be identified.

Application of the selected design concept to an entire fuselage structure can be studied during this phase to allow realistic cost and weight estimating procedures to be developed for new structural concepts. Work in phases 1B and 2 will provide the necessary design and weight prediction information for the selected concept. Practical experience in tooling, manufacturing, and quality control of full-size components will be obtained during this phase and will provide a starting basis for production aircraft planning.

Structural test personnel will coordinate the fabrication of the test fixture and ensure the availability of the required test and monitoring equipment. Major test article assembly will be initiated and the article prepared for transfer to the test site.

5. PHASE 4—TEST

The major test article will be installed in the test fixture and prepared for structural test. Figure 140 illustrates the major test article and fixture. Instrumentation will be completed and all data monitoring and recording equipment will be verified. Test data reduction and reporting will be done in accordance with the established plan.

After the test systems are verified, a static strain survey will be conducted to provide a baseline for comparison with the stresses and deformations predicted by analysis. The test results will be correlated with the stress analysis and any significant variations evaluated.

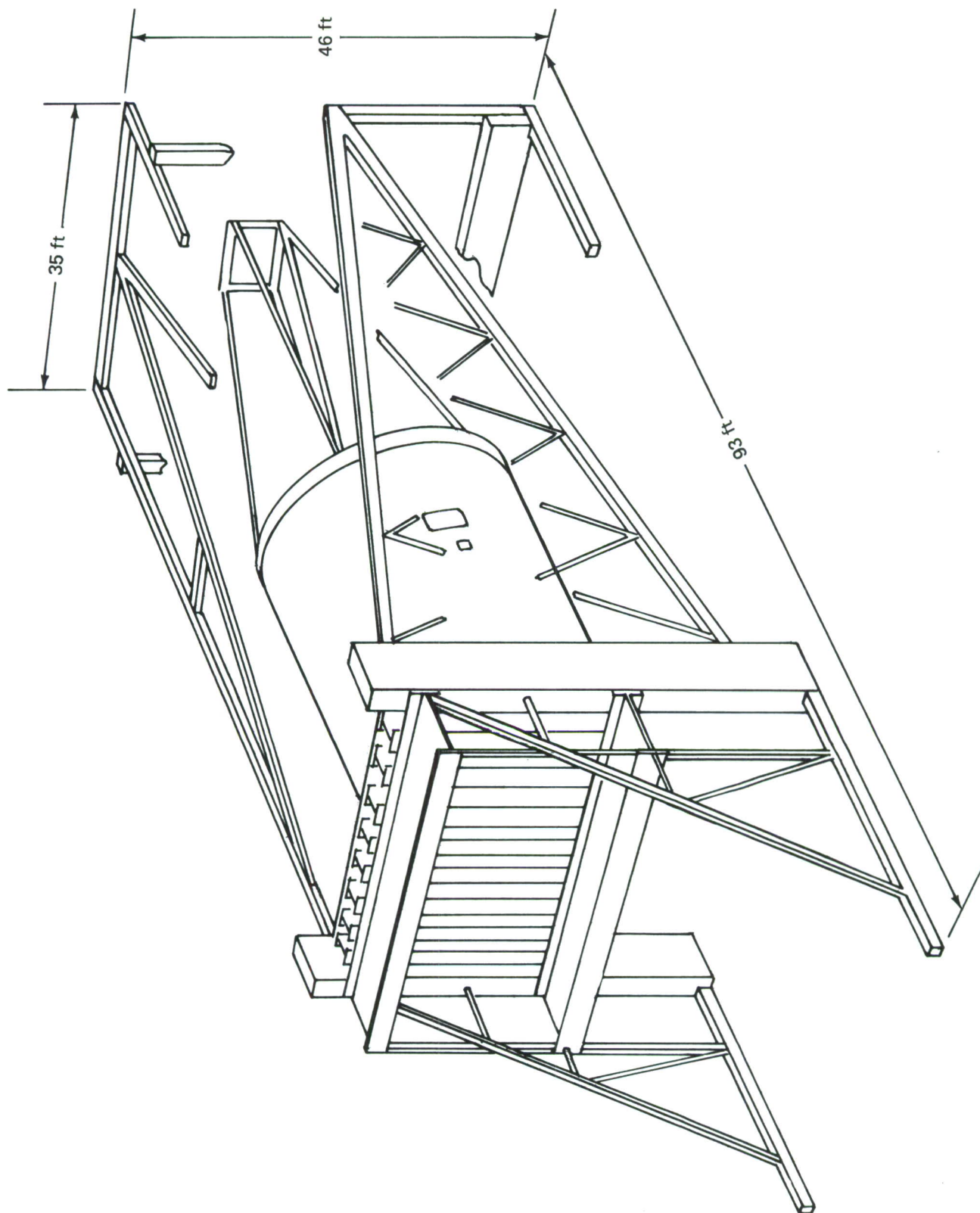


Figure 140.—Major Test Article and Fixture

Simulated flight-by-flight spectrum fatigue testing to four lifetimes will be conducted. The loading sequence will include the concentrated loads from the landing gear and the keel beam as well as the usual bending moments, shears, torsion, and internal pressure. After three lifetimes, the structure can have cracks introduced at previously selected fatigue-critical locations and crack growth rate studies performed. After adequate data have been obtained on crack growth rates, the structure can be repaired and the stress distribution determined. Following repair, the fatigue cycling would be completed.

After fatigue testing is complete, the structure will be subjected to damage tolerance testing. Damage will be introduced at selected locations and the structure loaded to the critical damage tolerance levels. This testing will verify the damage tolerant design concepts and parameters.

The sequence of testing can also include an ultimate load test that would follow the fatigue test and precede the damage tolerance test. The testing can be controlled to avoid loss of the test article and still demonstrate the ability of the design to meet ultimate load requirements. However, the testing sequence outline provides for the maximum return of information required to adequately demonstrate the integrity of the structural concept.

Four aircraft lifetimes will be demonstrated on the basic structure, structural repairs will be verified to one lifetime, and the damage tolerance of the structure will be demonstrated.

6. PHASE 5—INFORMATION TRANSFER

This phase consists of a continuing interchange of information within government and industry concerning the results, trends, and conclusions of this program. It is essential that this information be presented in such a manner that it can be used by personnel with a wide range of interests, objectives, and backgrounds.

Efficient information transfer on a program of this magnitude will involve reassessment of the normal channels of communication. Among the methods to be considered to accomplish the dissemination of information on this program will be the following:

- Organization of seminars at WPAFB and/or Boeing, with invitations to industry and government, at appropriate points in the program. Variations could include tours by Boeing and Air Force personnel to specific locations near major aircraft companies. This could reduce the cost to the participating companies and increase the exposure of the program to the industry.
- Location and participation at Boeing by Air Force engineers in the complete follow-on program. Daily contact between USAF and Boeing engineers will provide the highest possible understanding of the program status and results.
- Publication of monthly one-page bulletins by Boeing, containing abstracts highlighting significant work and results, with wide distribution to governmental agencies and industrial organizations specified by the Air Force.

- Participation of Boeing personnel, including preparation and presentation of papers, in technical committee meetings and symposia (e.g., MIL-HDBK-5 and -23 Committees, ASTM Committees, SAMPE, AIAA, etc.).

It is anticipated that these methods can be used to increase the awareness of the technical community concerning the progress and status of the program. Focal points of information transfer will be established in order to provide rapid access to written data. Personal contact will be used to permit a free interchange of design philosophy and offer the opportunity to critique and discuss program results.

Basically, two types of formal reporting are involved:

- Regularly scheduled contract summary reports per Air Force specifications
- Supplemental reporting designed to provide program data for presentation to both technical and management personnel

These reports will consist of monthly reports, interim technical phase summaries, and final technical reports. In addition, slides, viewgraphs, video tapes, and motion pictures suitable for use by either government or Boeing personnel will be prepared for use at oral reviews, briefings, contract status report meetings, or technical seminars.

Information transfer is an extremely important phase of the AMS-ADP. It is imperative that personnel with a role in future Air Force systems selection receive maximum exposure to the program. Significant results are often buried in reports and never affect the decision process. Personal contact is the best way to obtain maximum leverage from the program and to ensure timely, effective use of the information generated.

SECTION VI

RELATED STUDIES, CONTRACT ADDITION

Studies were conducted to acquire the background information and the recorded actual service experience accumulated on the baseline airplane and to assess the impact, in terms of structural weight and cost, of the application of the requirements of Damage Tolerance Criteria, Revision D (app. I) and MIL-STD-1530 (USAF) to an existing airframe structure.

1. INVESTIGATION OF IMPACT OF VARIATIONS IN DAMAGE TOLERANCE REQUIREMENTS ON STRUCTURAL WEIGHT OR CRACK GROWTH LIFE

a. Introduction

The objective of this study was to assess the impact of variations in damage tolerance requirements or material properties on the structural weight or fatigue crack growth life of the baseline component. The baseline component selected for this study is the aft fuselage section of the Boeing 747-100 as described in section II.

The study was conducted on the fuselage shell material. Crown and side-of-body locations were selected because their loading and damage tolerance conditions are completely different. The crown location chosen is representative of the fuselage crown structure throughout section 46; the side-of-body location selected is representative of the fuselage side-of-body structure throughout section 46. Therefore, application of the damage tolerance requirements at these two locations results in conclusions that are applicable only to those corresponding areas.

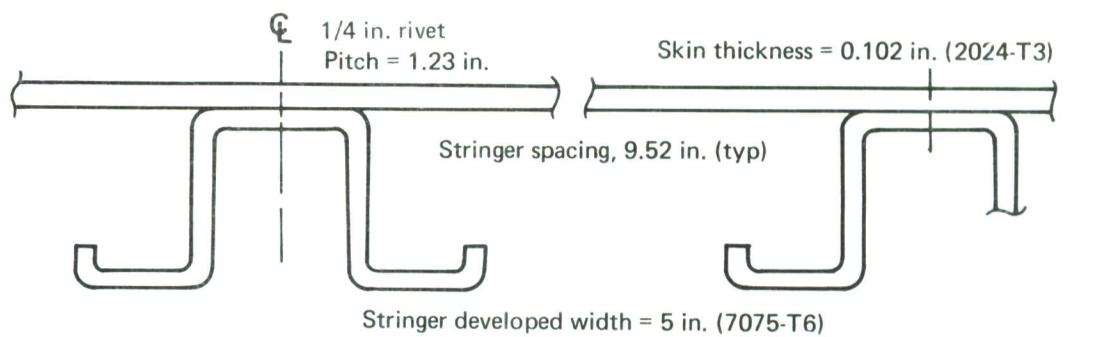
The locations selected for analysis (see fig. 105) are:

- Crown (S-1) station 1580
- Side-of-body (S-23) station 1580

The crown is critical for conditions of transverse cracking under longitudinal axial loading caused by body bending and pressure conditions. The fuselage crown is of conventional skin/stringer construction with hat stringers spaced at 9.52 inches on centers (fig. 141a). Since fuselage general instability requirements dictate a stiff frame at crown locations, all frames in this quadrant are of shear-tied construction (fig. 141b).

The side-of-body is critical for the condition of longitudinal cracking due to the combined effects of hoop and longitudinal tension caused by internal pressurization and shear and longitudinal tension caused by body-bending conditions.

The baseline structural arrangement at the side-of-body location selected for this study consists of a shear-tied frame with a fail-safe chord (fig. 141b). An alternate means of



a. Crown Structure

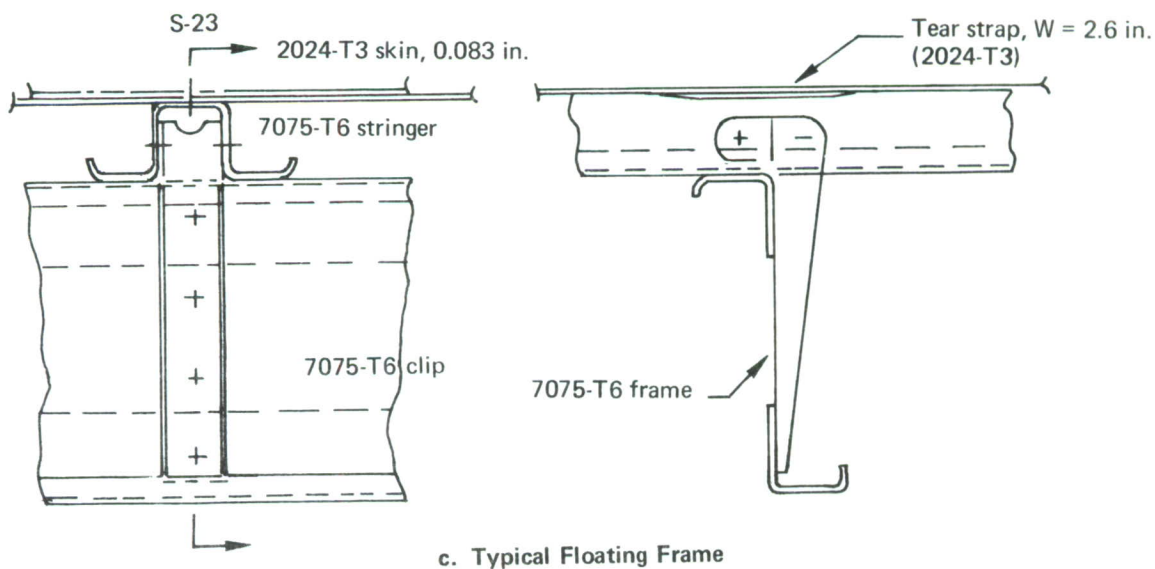
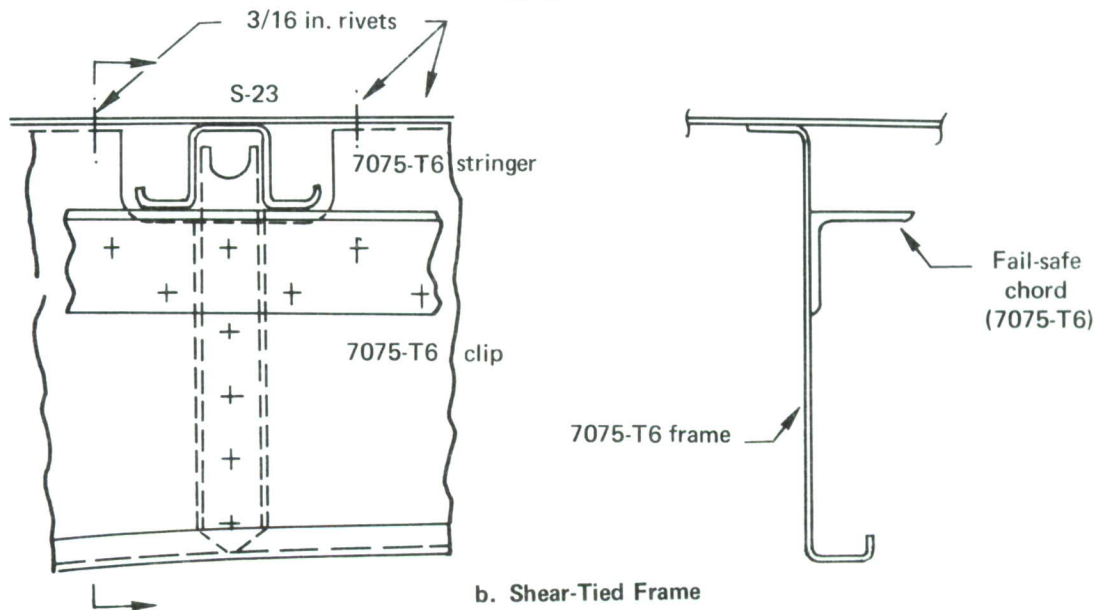


Figure I41.—Frame Construction

construction which is used at many side-of-body panels of the baseline component consists of the floating-frame configuration with tear straps (fig. 141c). These two types of construction are interchangeable within the baseline component and possess equal damage tolerance capability under civil aviation fail-safe requirements. Under the damage tolerance requirement of a specified period of unrepaired service usage (app. I), they exhibit different capabilities; therefore, analysis will be conducted on both types of construction.

Only those types of damage, either “initial” or “in-service,” defined for multiple-load path fail-safe structure in appendix I will be used for these studies.

No analysis was conducted on lower lobe locations since they are not normally critical under damage tolerance conditions due to predominantly compressive loading.

b. Basic Data

(1) Loads

The loads used for these studies are those used in the design of the baseline. The stress spectra at the S-1 crown location resulting from these loads are shown in:

- Figure 142, 1-hour flight stress exceedance curve
- Figure 143, 3-hour flight stress exceedance curve
- Figure 144, 7-hour flight stress exceedance curve

The stress spectra at the S-23 side-of-body location resulting from these loads are shown in:

- Figure 145, 1-hour flight stress exceedance curve
- Figure 146, 3-hour flight stress exceedance curve
- Figure 147, 7-hour flight stress exceedance curve

These stress spectra, in conjunction with computer program CRACKS (ref. 13), are used to determine spectrum fatigue crack growth rate (da/dS) as a function of number of flights.

The maximum stress encountered once in an airplane operational interval (number of flights) is shown for both study locations in figure 148. These stresses are used to determine residual strength requirements.

(2) Material Data

A literature search was initiated to define the limits of variability of the critical stress intensity factor (K_{IC}) of 2024-T3 and 7075-T6 sheet. These materials are extensively used for skin material (2024) and for formed stringers (7075). The results are

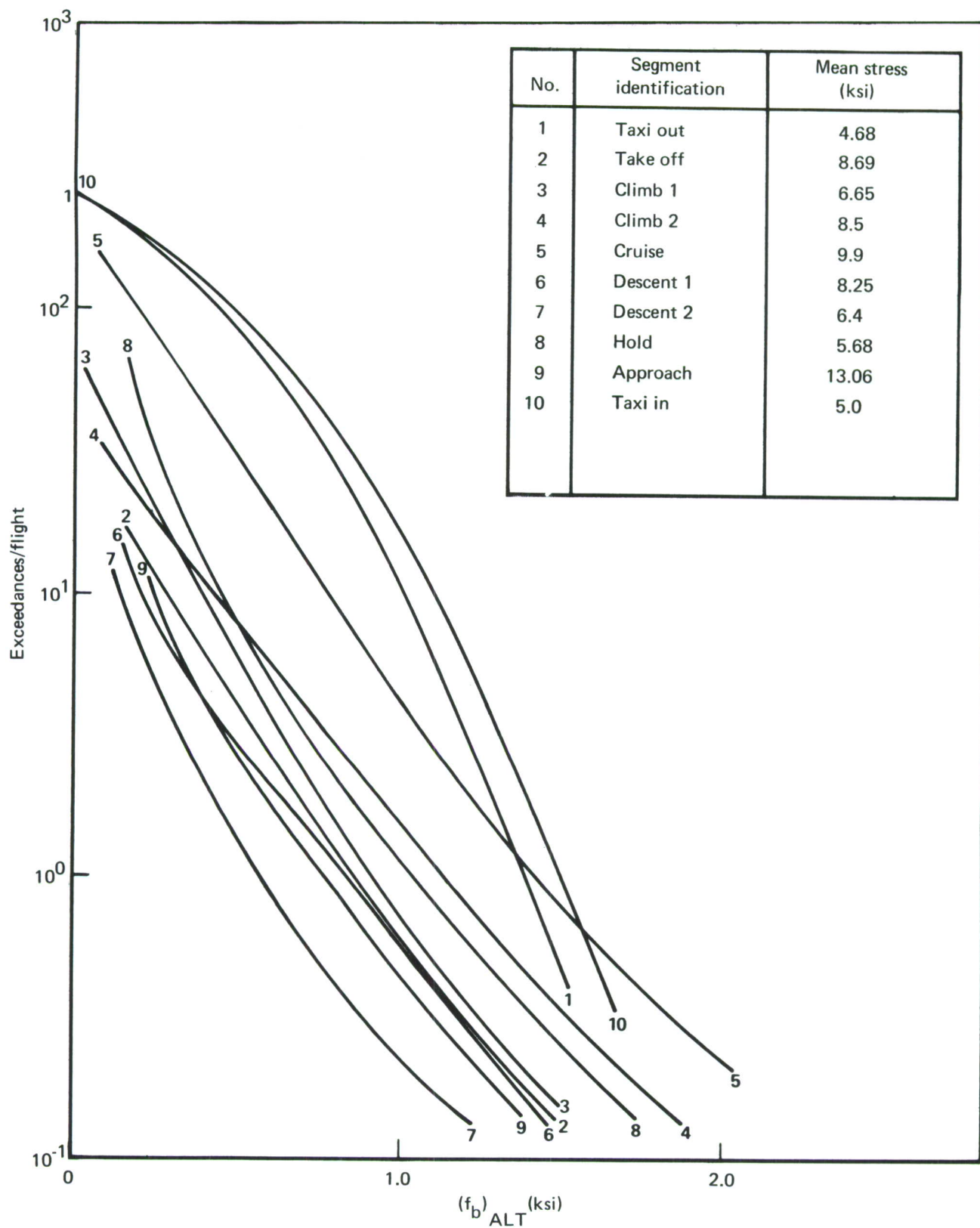


Figure 142.—Crown Stress Exceedances (1-Hr Flight)

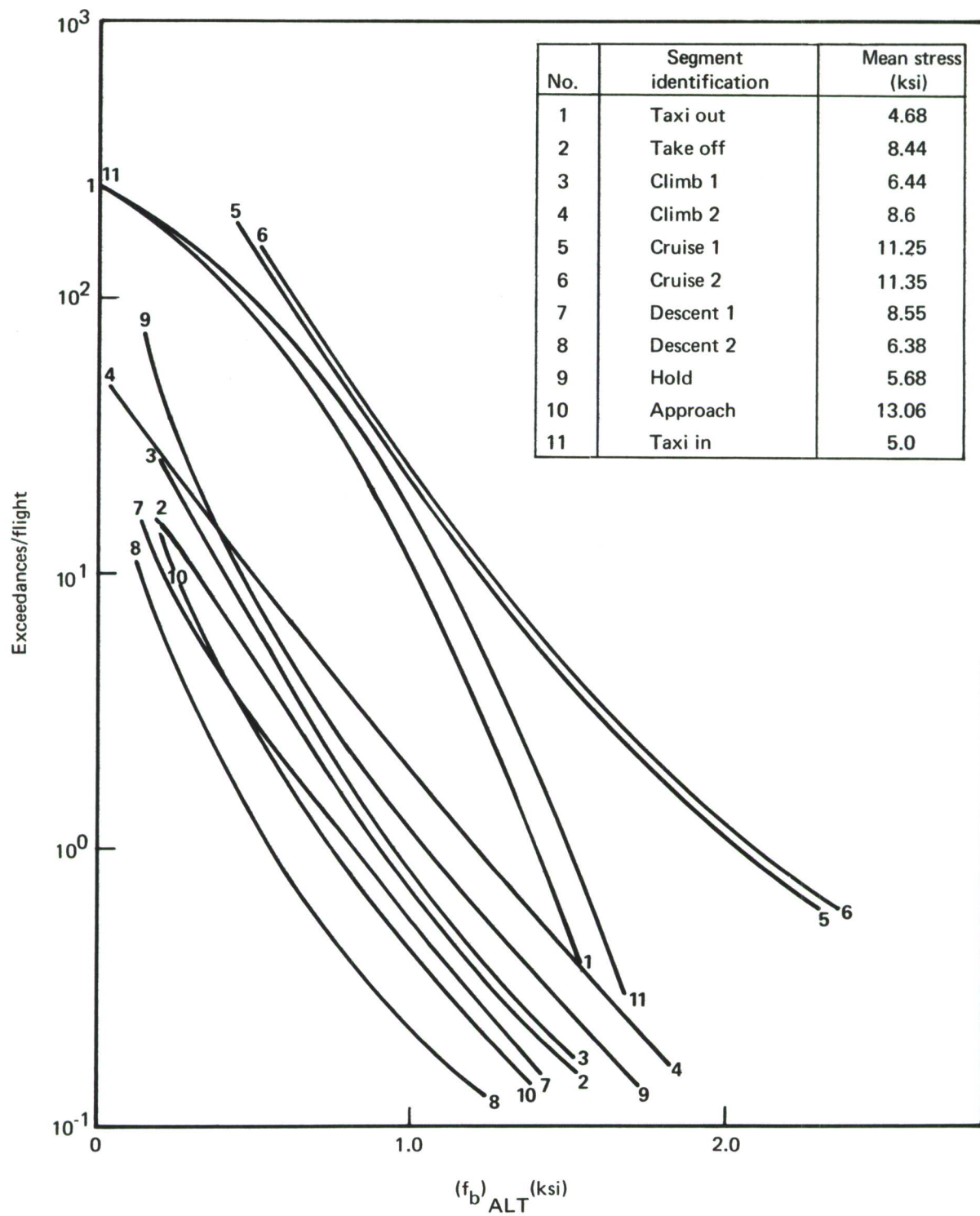


Figure 143.—Crown Stress Exceedances (3-Hr Flight)

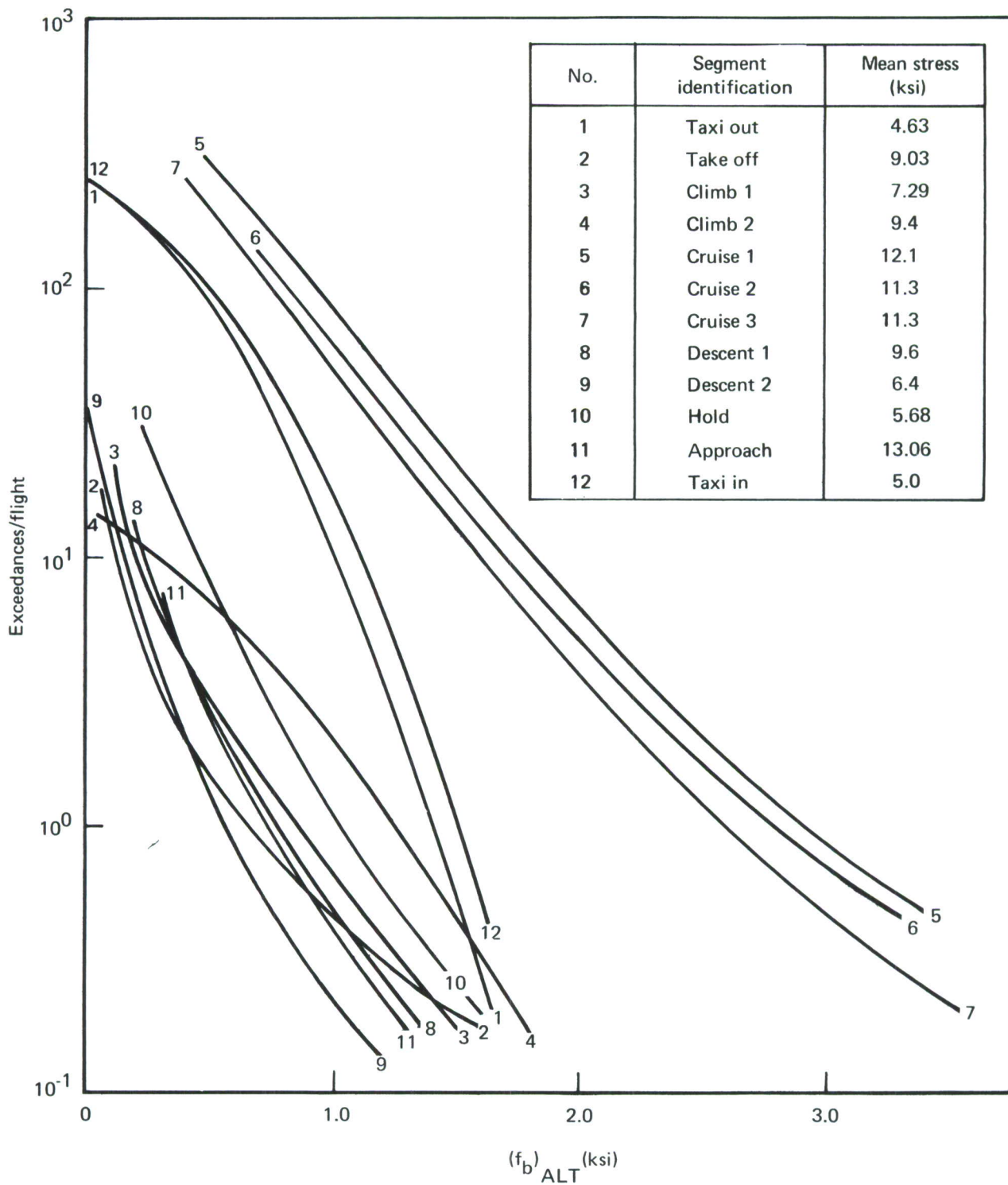


Figure 144.—Crown Stress Exceedances (7-Hr Flight)

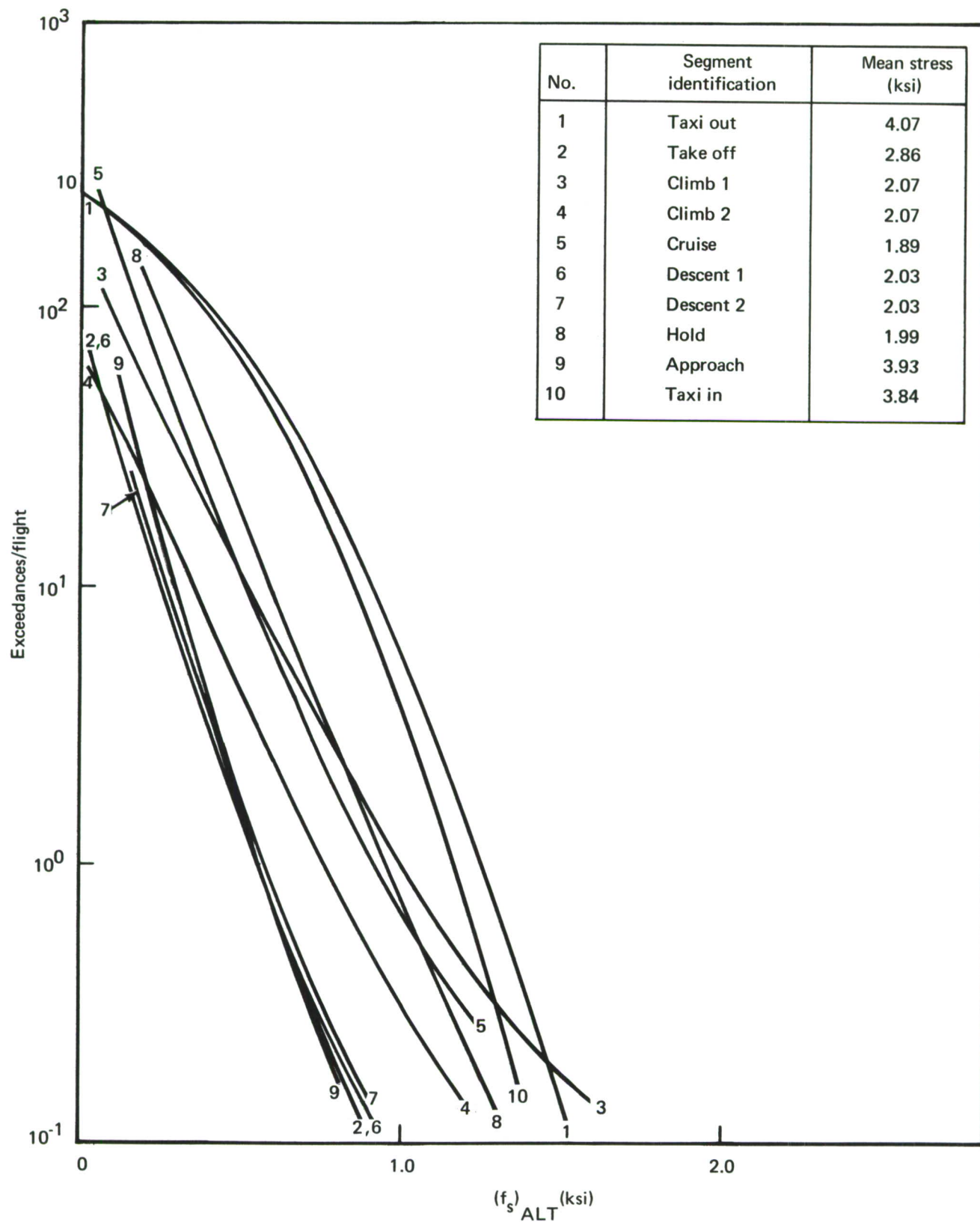


Figure 145.—Side-of-Body Stress Exceedances (1-Hr Flight)

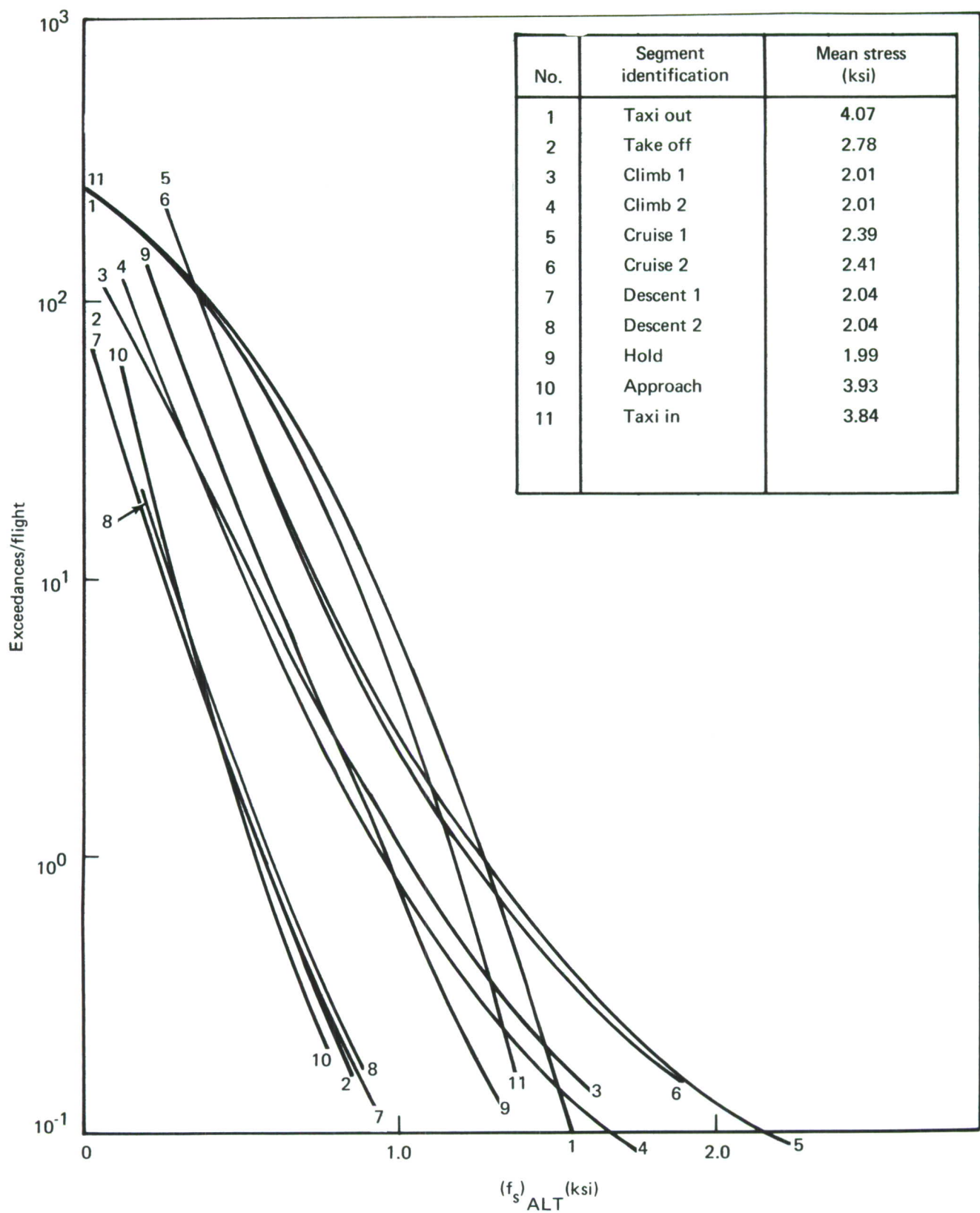


Figure 146.—Side-of-Body Stress Exceedances (3-Hr Flight)

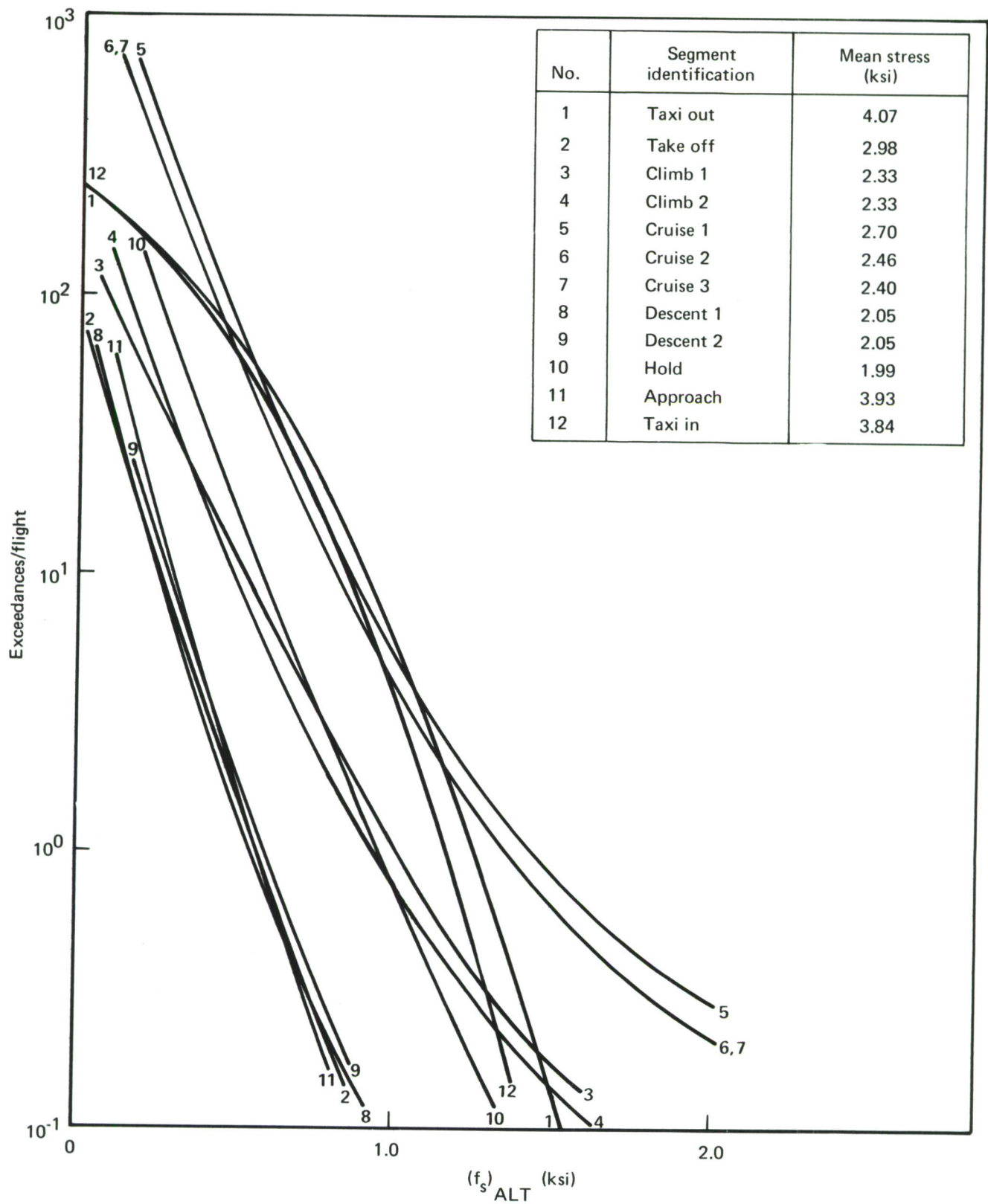


Figure 147.—Side-of-Body Stress Exceedances (7-Hr Flight)

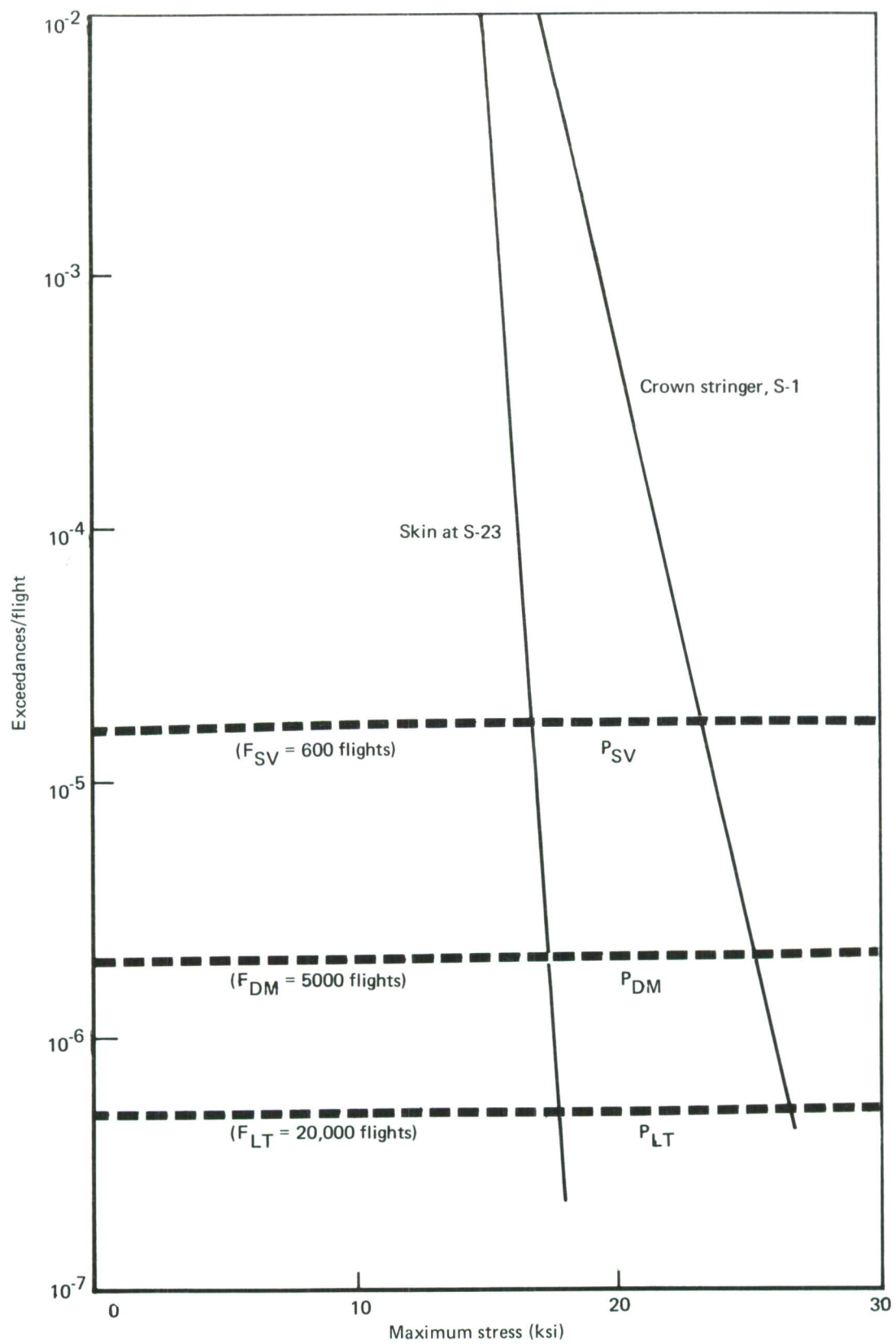


Figure 148 —Maximum Stress Exceedances (3-Hr Flight)

shown in figures 149, 150, and 151. The relatively uniform range of observed values of K_C for these materials implies that the predicted values of residual-strength capability will remain essentially constant whether K_C is chosen from the upper, midrange, or lower bound of the data. Thus, the choice of such value has relatively little impact on structural weight.

Another literature search was initiated to define the limits of variability in observed fatigue crack growth rate data of 2024-T3 and 7075-T6 sheet. The results are shown in figures 152, 153, and 154. The fatigue crack growth rate data (da/dn) for these materials exhibit considerable scatter between the upper, midpoint, and lower bounds of the data. Such wide variations will result in a direct impact on the allowable period of unrepaired service usage at constant stress or a reduced impact on allowable stress to maintain a constant period of unrepaired service usage (due to the exponential nature of the crack growth rate law).

A spectrum fatigue crack growth rate test was conducted to verify the analytical crack growth model proposed for use on this study. A single specimen of 2024-T3 sheet, baseline skin material, was tested for fatigue crack growth rate under the stress spectrum shown in figure 155. This spectrum represents crown stresses which are exceeded once per flight segment during a 3-hour flight (medium-range mission). The decision to test to this spectrum is based on analysis which shows that fatigue damage accumulated during 20,000 three-hour flights (60,000 flight-hours total life) is very nearly equal to that accumulated under the design mission mix. Cyclic stresses shown are those stresses occurring once per flight segment.

The correlation of analyses, using computer program CRACKS (ref. 13), which incorporates the Willenborg crack retardation model, with the observed test results is shown in figure 156. The best fit of analytical results to those observed in test is achieved by use of the upper-bound values of the fatigue crack growth rate, da/dn .

The fact that the best fit of predicted growth rates and the observed results is achieved by using upper-bound fatigue crack growth rates was unexpected, since the material was taken from stock and had passed normal quality control procedures (material procurement per QQ-A-250/5). Comparison of these results with those obtained from a single 7475-T61 panel under the same loading spectrum yields the following observations (see fig. II-22):

- Growth rates are in good agreement at midrange levels of K_{max} .
- 2024-T3 growth rates are faster at low K_{max} values than those observed for the 7475-T61.

Since constant amplitude testing shows 7475-T61 crack growth rates 1.3 to 2 times faster than 2024-T3 (see table VIII), the above limited observations are only an indication that the 2024-T3 specimen is best characterized by upper-bound crack growth data.

A study was made to determine the effects of stress spectra truncation on predicted crack growth rates, with the results shown in figure 157. The following cases were analyzed at the S-1 location with the stress spectra shown in figures 142 through 144:

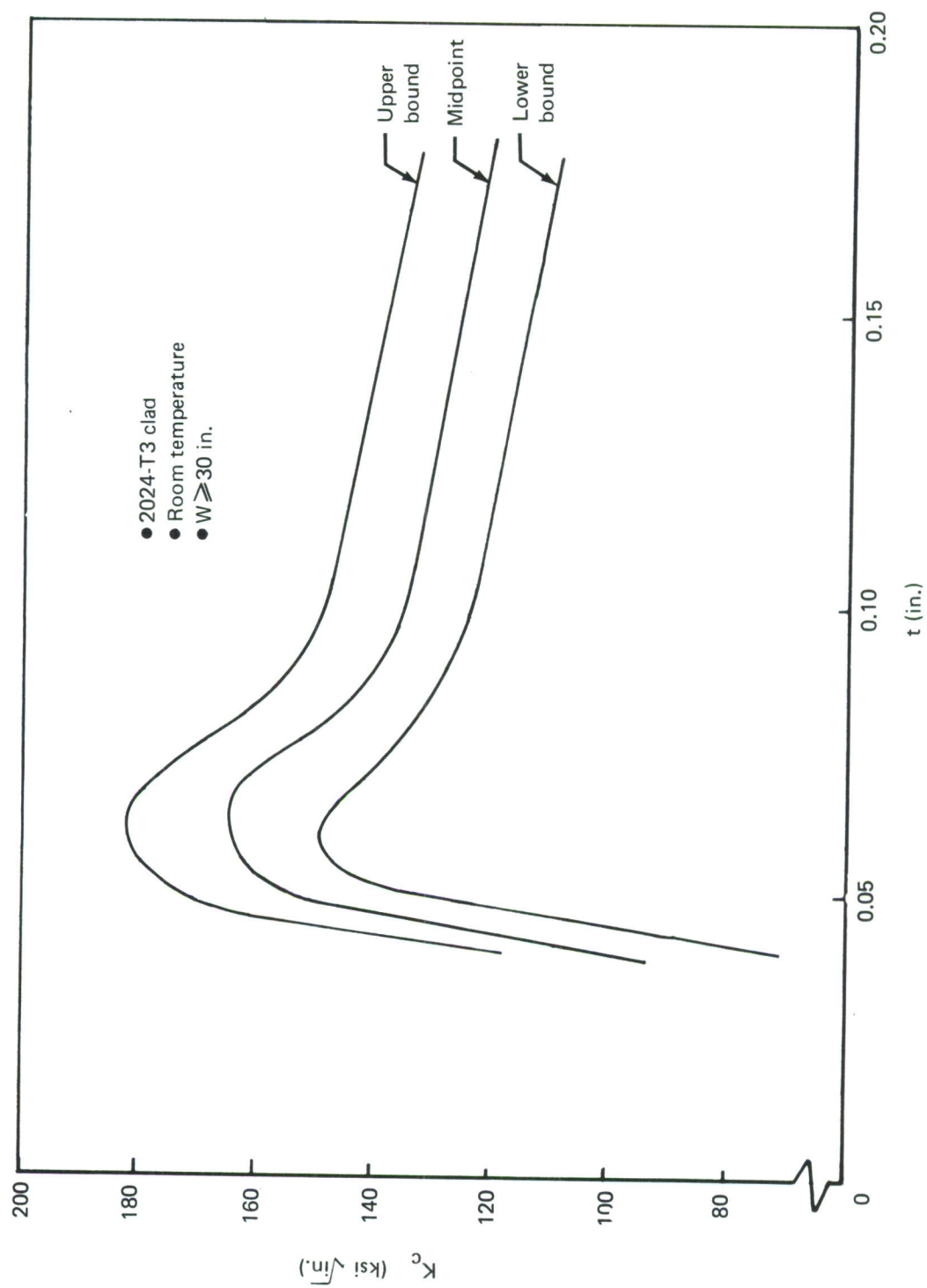


Figure 149.—Critical Stress Intensity Factor (2024-T3, L-T)

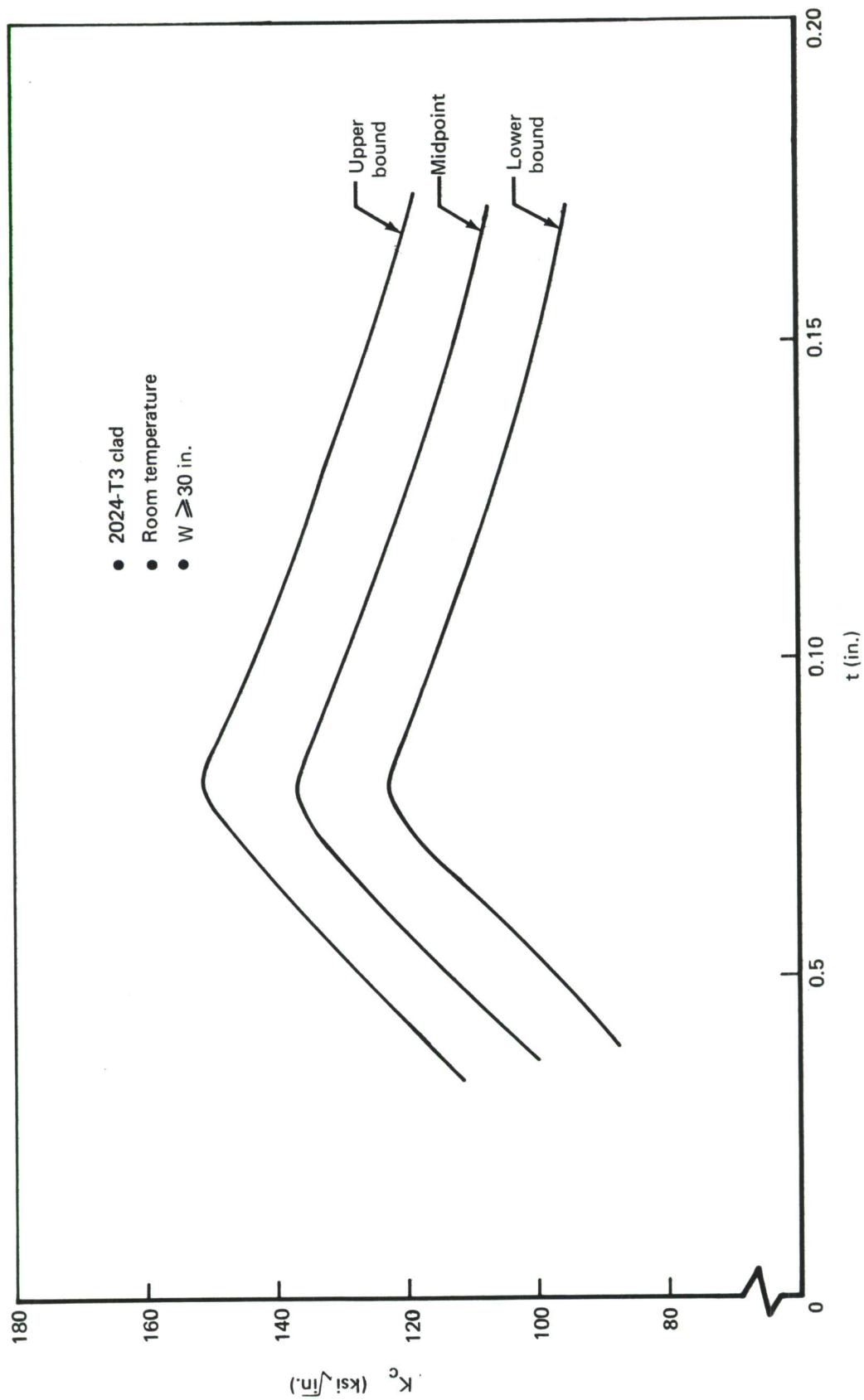


Figure 150.—Critical Stress Intensity Factor (2024-T3, T-L)

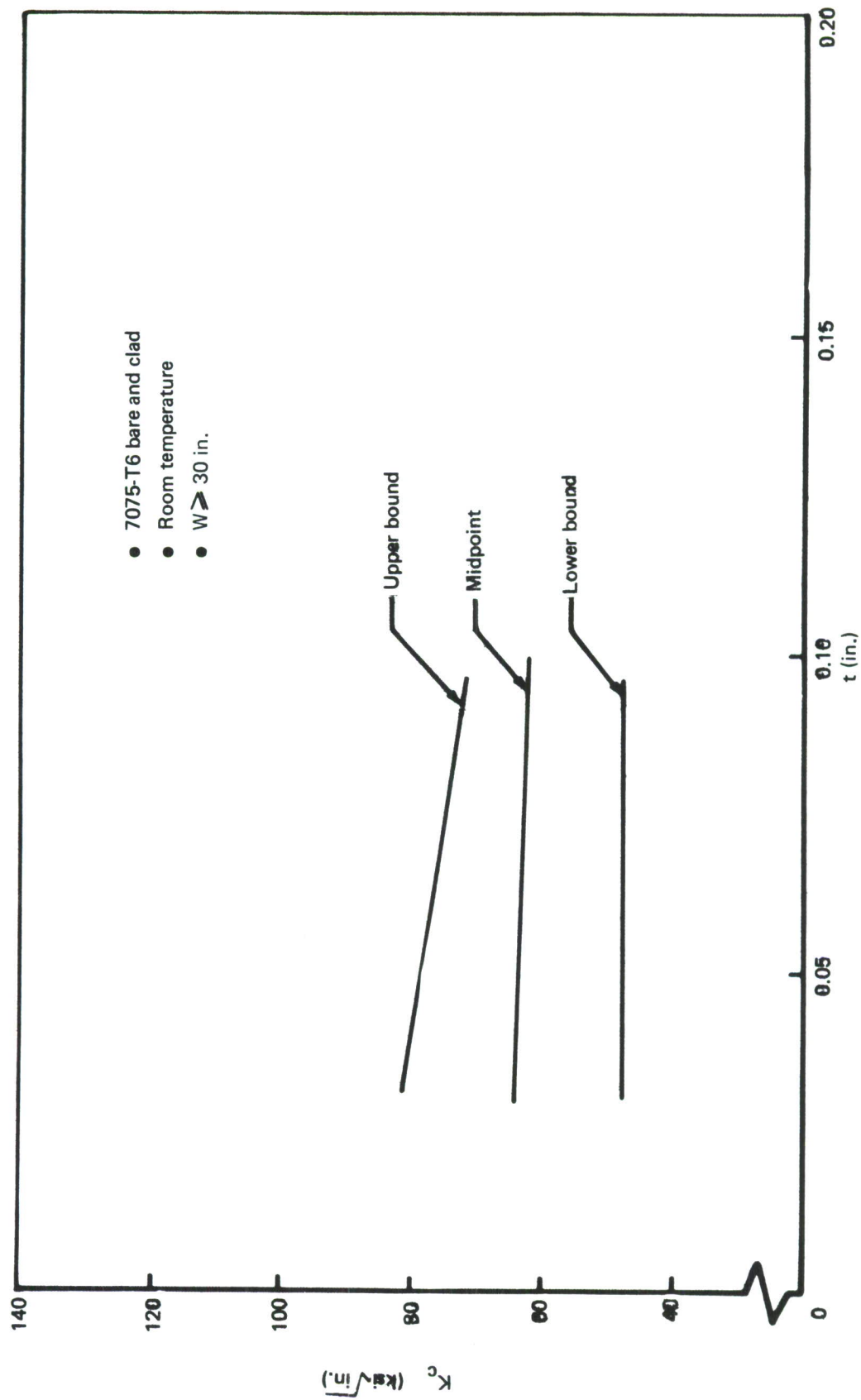


Figure 151.—Critical Stress Intensity Factor (7075-T6, L-T)

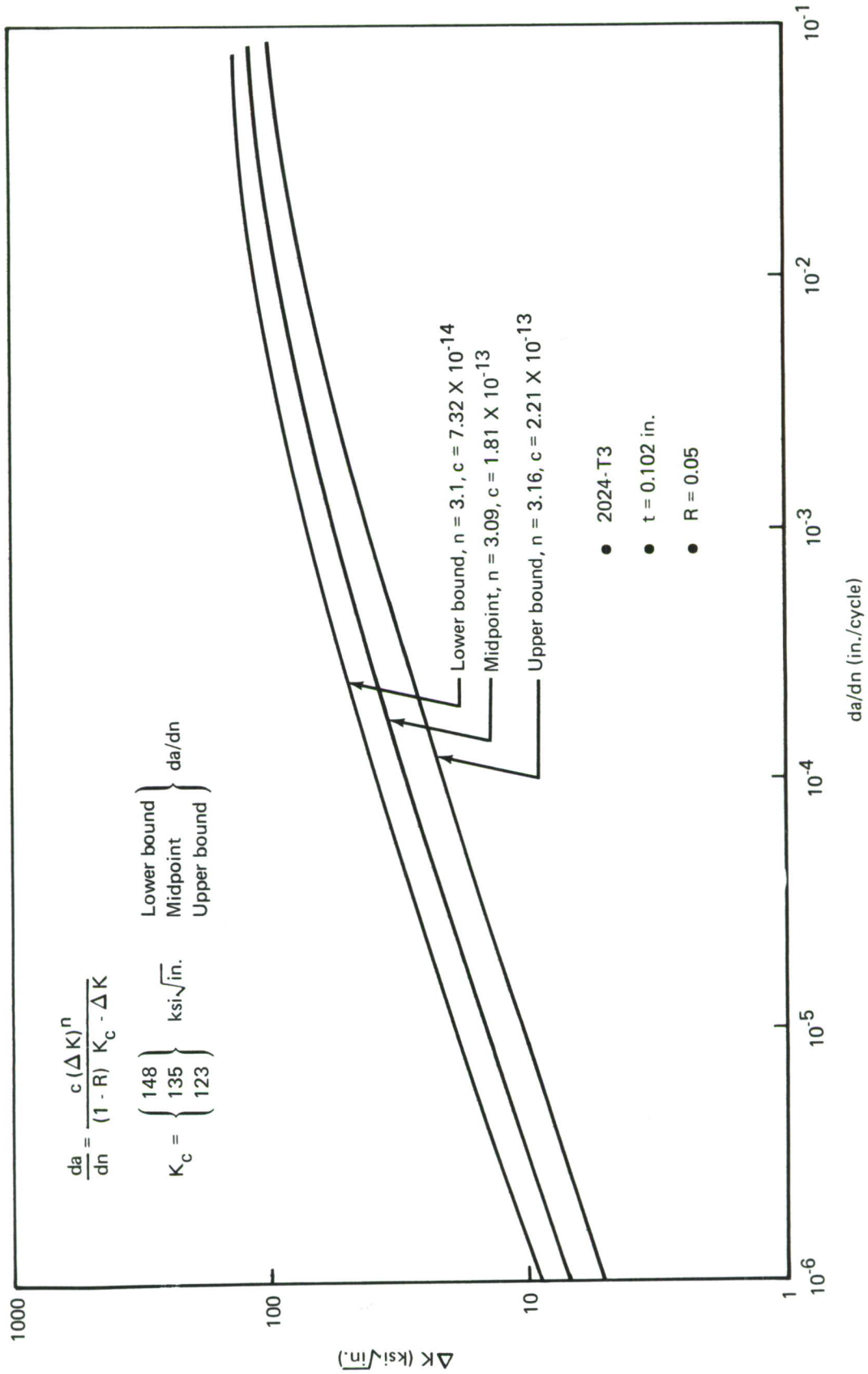


Figure 152. — Fatigue Crack Growth Rates (2024-T3, L-T)

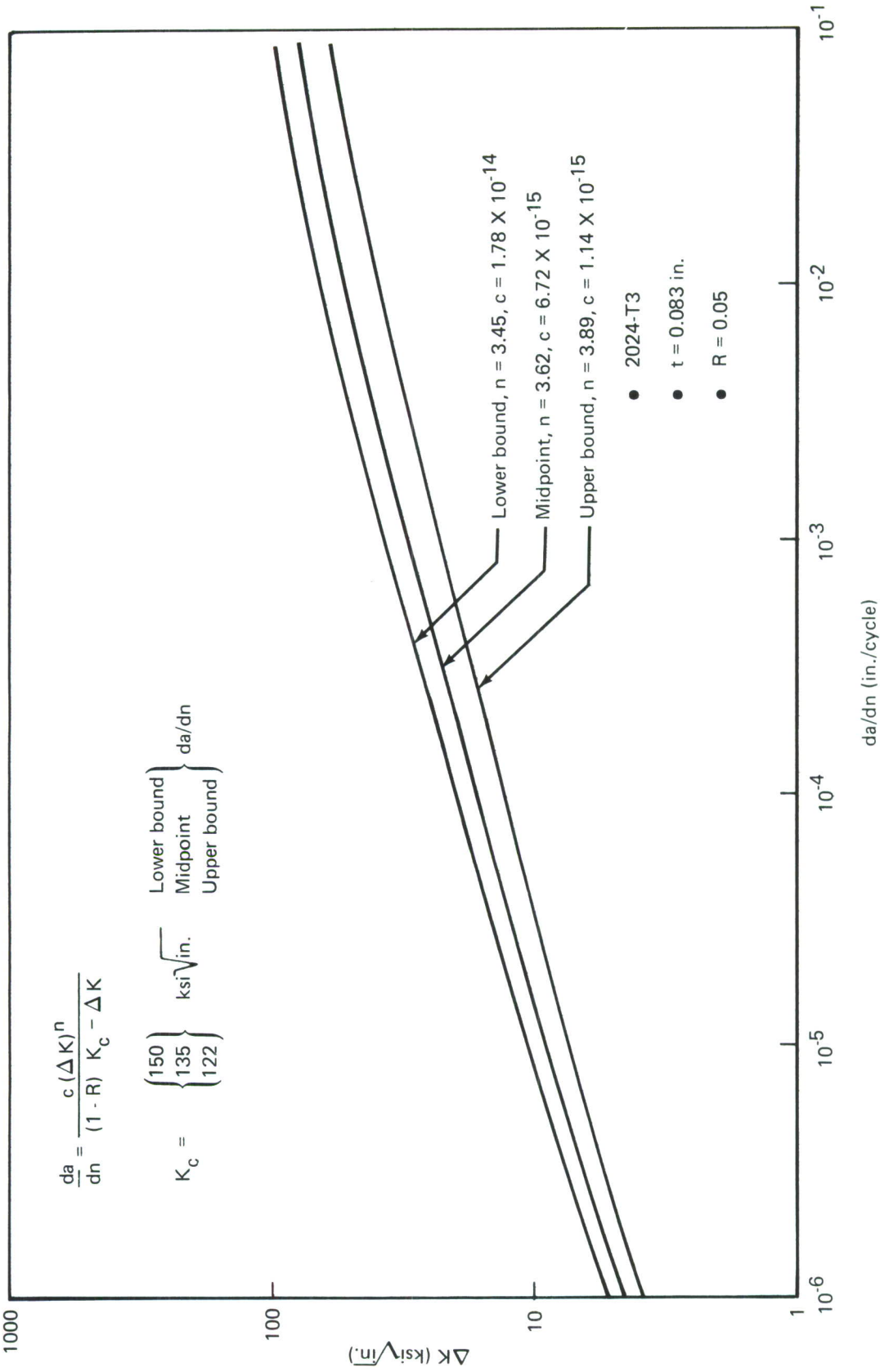


Figure 153. – Fatigue Crack Growth Rates (2024-T3, T-L)

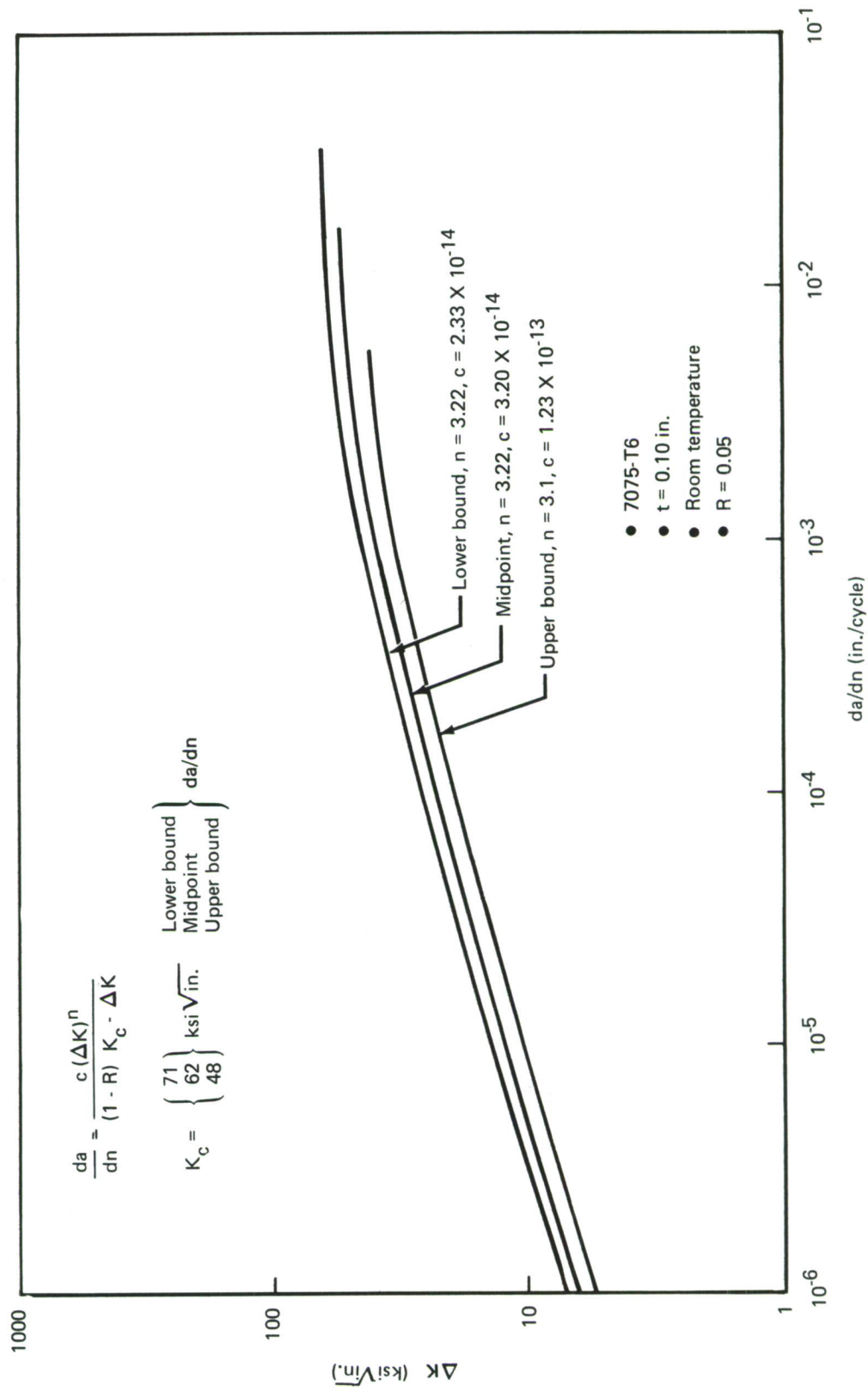


Figure 154.—Fatigue Crack Growth Rates (7075-T6, L-T)

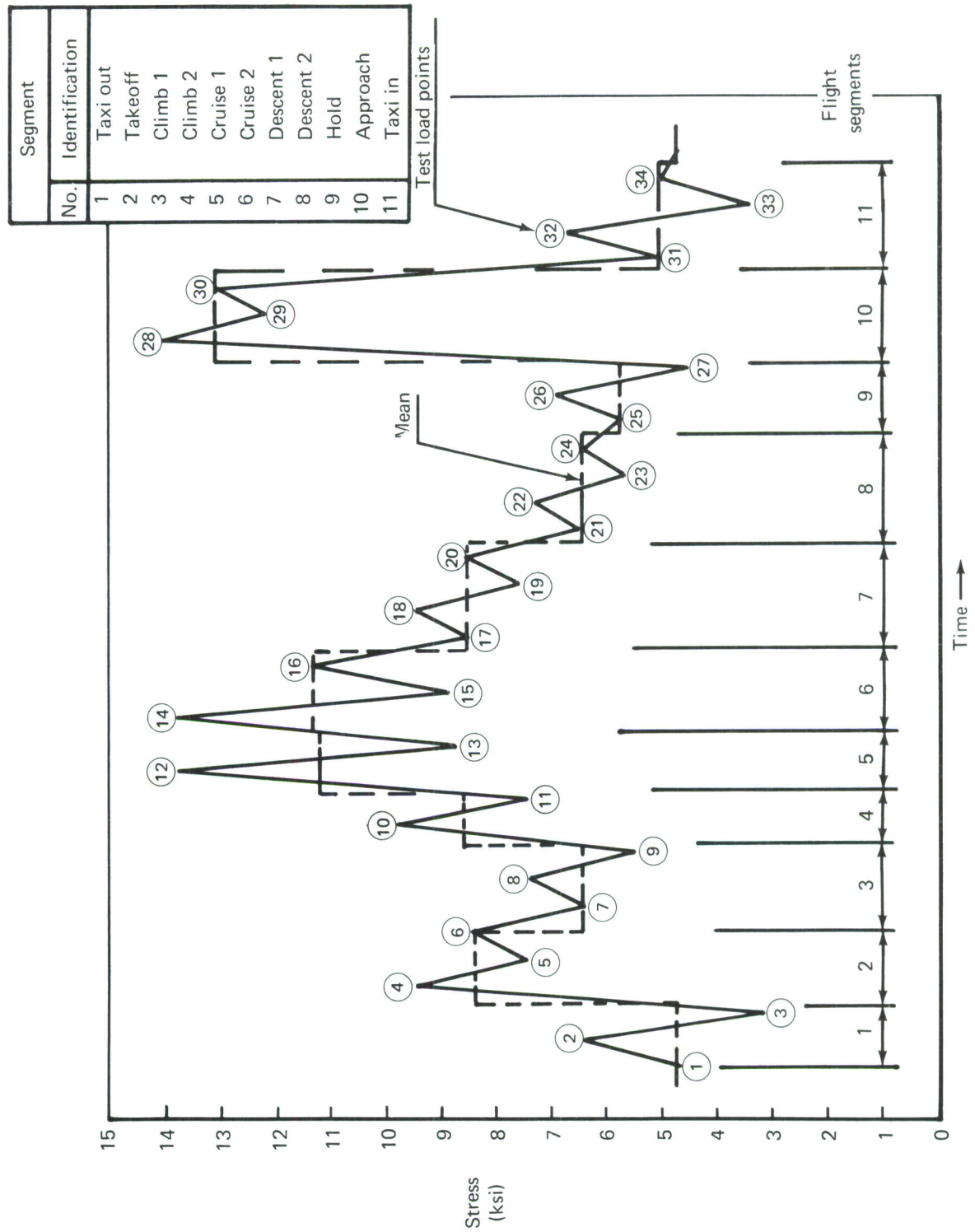


Figure 155.—Panel Test Spectrum

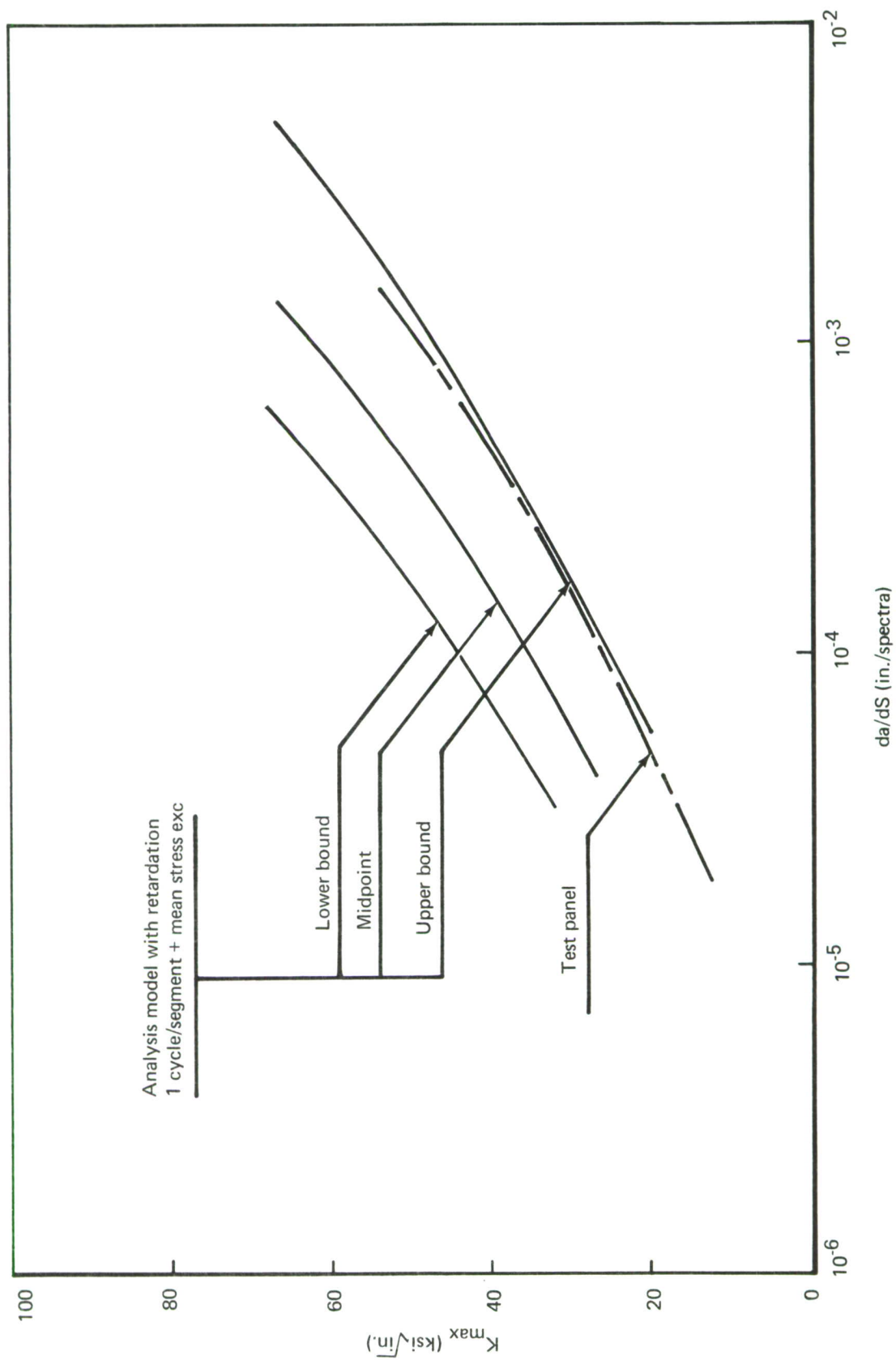


Figure 156. — Test Versus Analysis

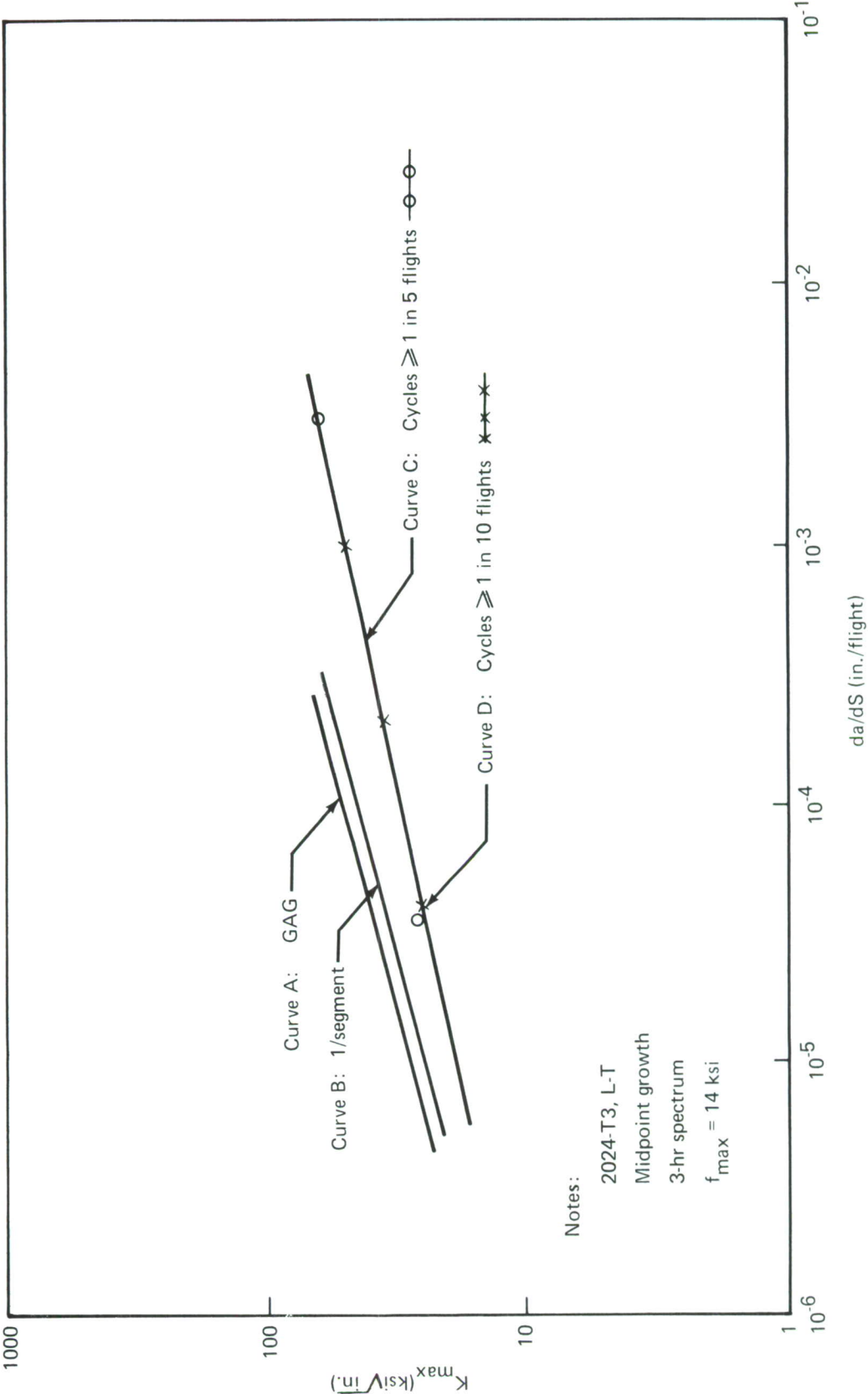


Figure 157.—Effect of Stress Spectra Truncation—Crown

- Growth rates for ground-air-ground stresses only (curve A)
- Growth rates retaining only those cyclic stresses which are exceeded once per flight segment (curve B)
- Growth rates retaining all cyclic stresses which occur with a frequency equal to or greater than once every five flights (curve C)
- Growth rates retaining all cyclic stresses which occur with a frequency equal to or greater than once every 10 flights (curve D)

The results of this study indicate that growth rates must be calculated retaining all cyclic stresses which occur with a frequency equal to or greater than once every five flights. Growth rates calculated for this condition are approximately five times those due to a spectrum composed of once-per-segment stresses, and the use of once-per-segment stresses only would be grossly unconservative. Growth rates calculated retaining those cyclic stresses occurring with a frequency equal to or greater than once every 10 flights are very nearly equal to those of curve C. This implies that the inclusion of higher infrequently applied stresses is canceled by the retardation effects of the overloads; thus, the high stress occurrence may be ignored without undue effect on the results.

As a result, it was decided to calculate crack growth rates using a stress spectrum which retained all cyclic stresses which occur with a frequency equal to or greater than once every five flights.

Using computer program CRACKS (ref. 13) and the stress spectrum described above, crack growth rates per flight (da/dS) have been calculated for the various materials at both study locations and are shown in figures 158 through 165. An index to these figures is contained in table XXXIX.

The midpoint da/dS values shown for the side-of-body skins under the 1-, 3-, and 7-hour stress spectra are equal due to the predominating effects of the hoop tension stress due to internal pressure, which has a frequency of once per flight. These curves are translated to the right of those shown in figure 153 for the 2024 material due to the influence of body-bending shears; however, the differences in the cyclic stress spectra for the 1-, 3-, and 7-hour missions are overridden by the effects of internal pressurization. The da/dS values shown for the 2024-T3 tear straps and 7075-T6 frames are the same as those shown in figures 153 and 154, with the ordinate changed from ΔK to K_{max} . These elements are loaded by pressure stresses only, which experience one cycle per flight, making da/dS equal to da/dn .

These crack growth rate curves (da/dS) are used to calculate fatigue crack growth.

(3) Analysis Methodology

The monocoque covering is of riveted skin/stringer (frame) construction. Damage tolerance analysis must reflect the interaction and load transfer between damaged

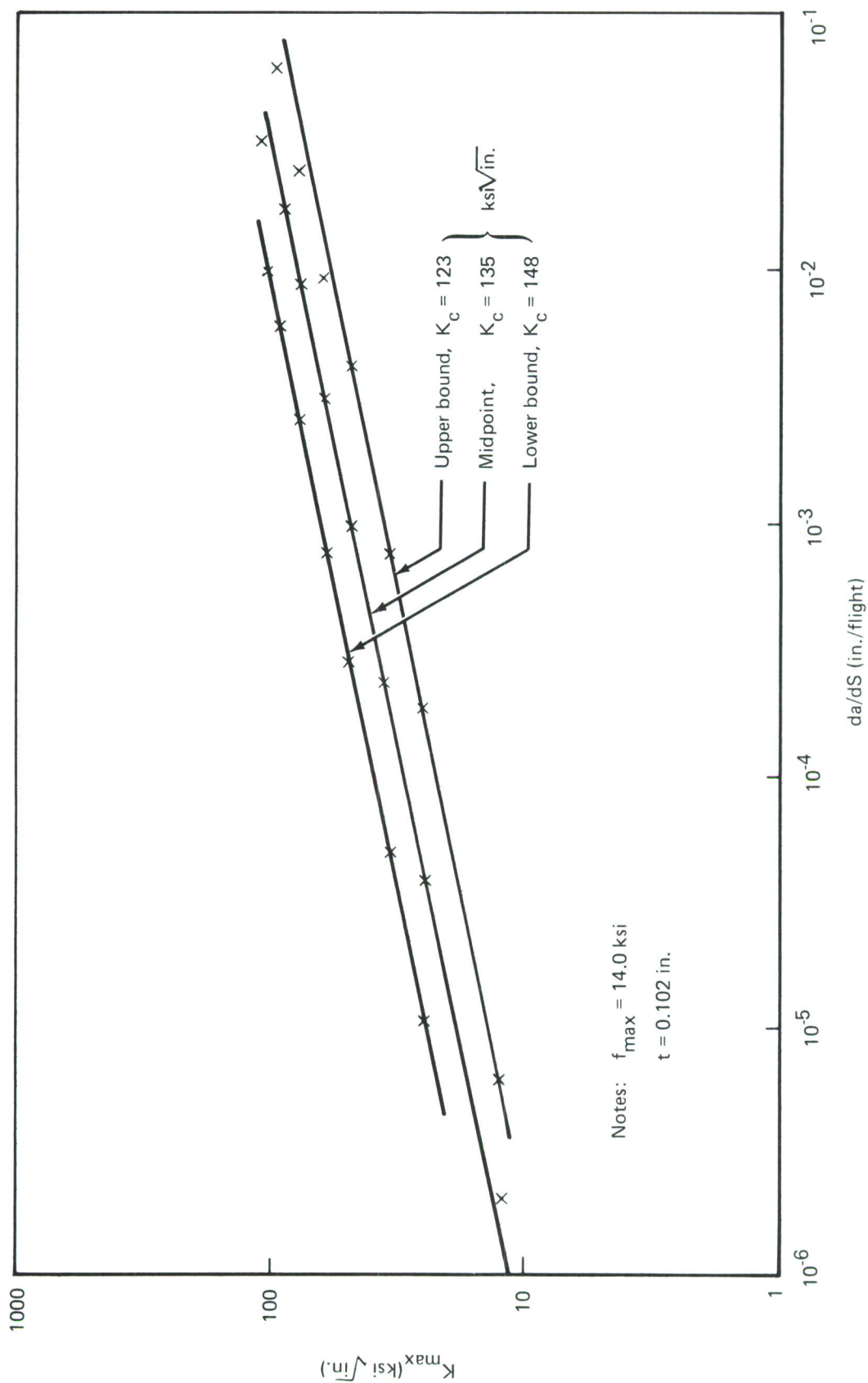


Figure 158. — 3-Hr Spectrum Crack Growth Rates—Crown (2024-T3, L-T)

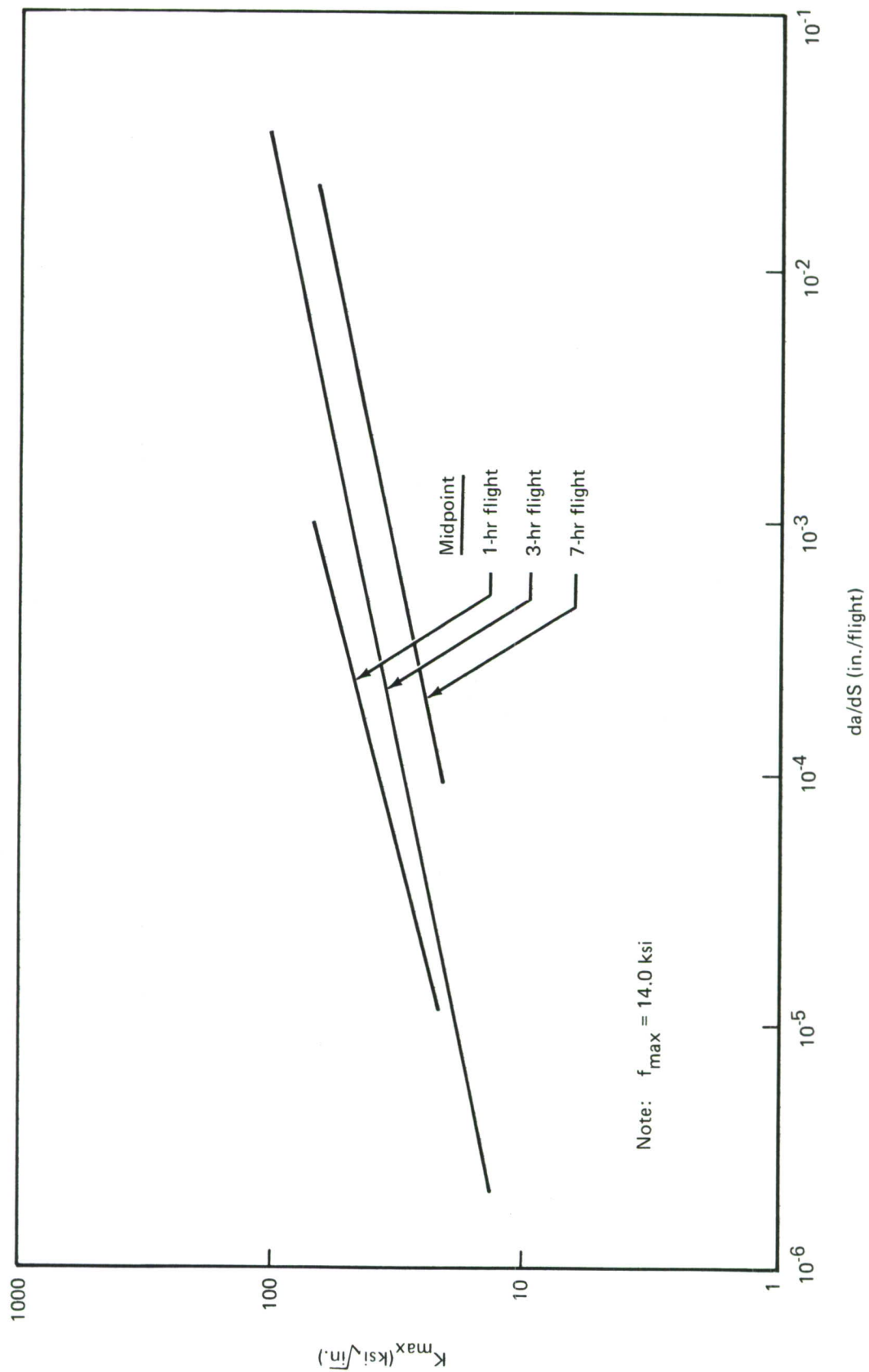


Figure 159.—Spectrum Crack Growth Rates—Crown (2024-T3, L-T)

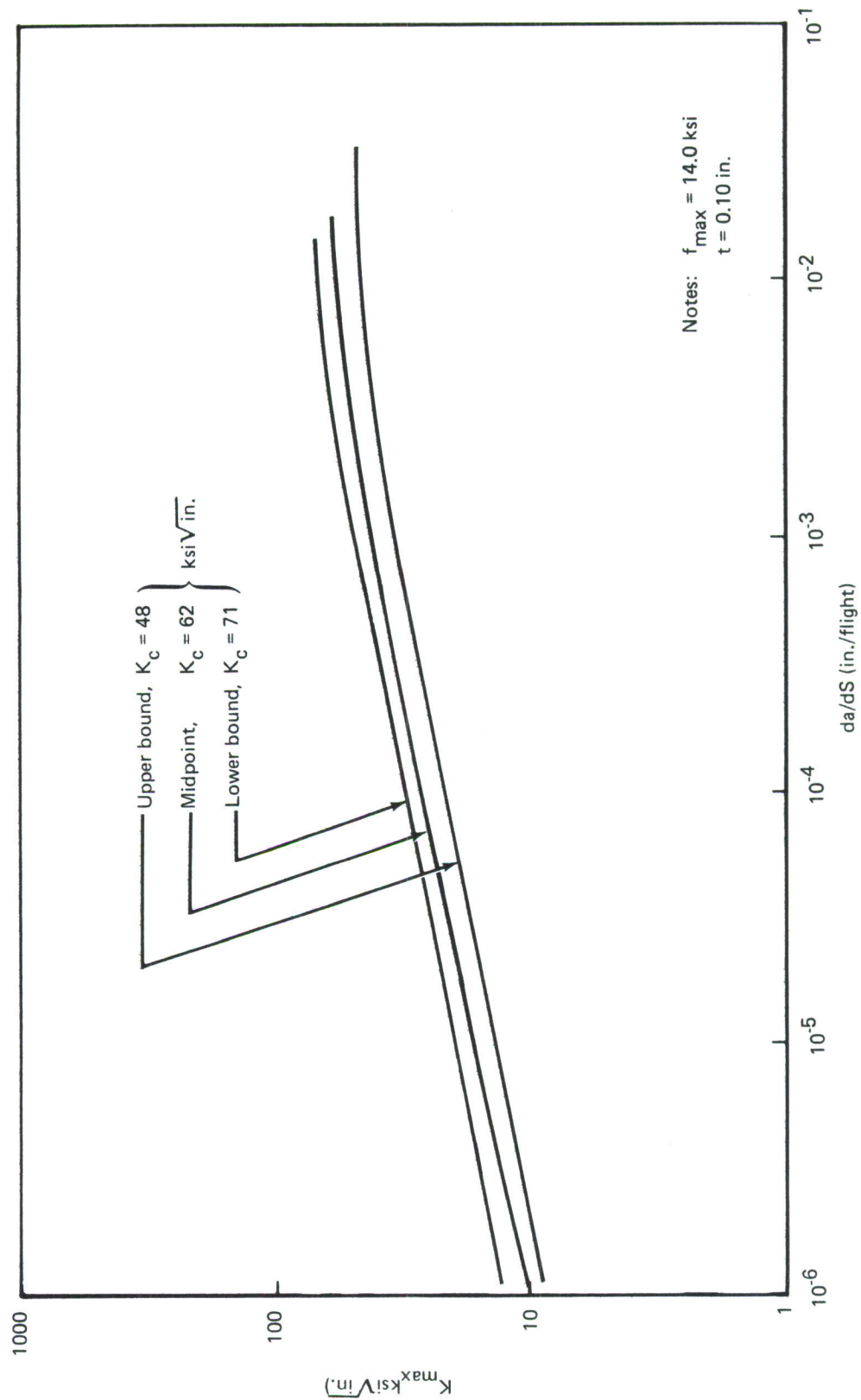


Figure 160.—3-Hr Spectrum Crack Growth Rates—Crown (7075-T6, L-T)

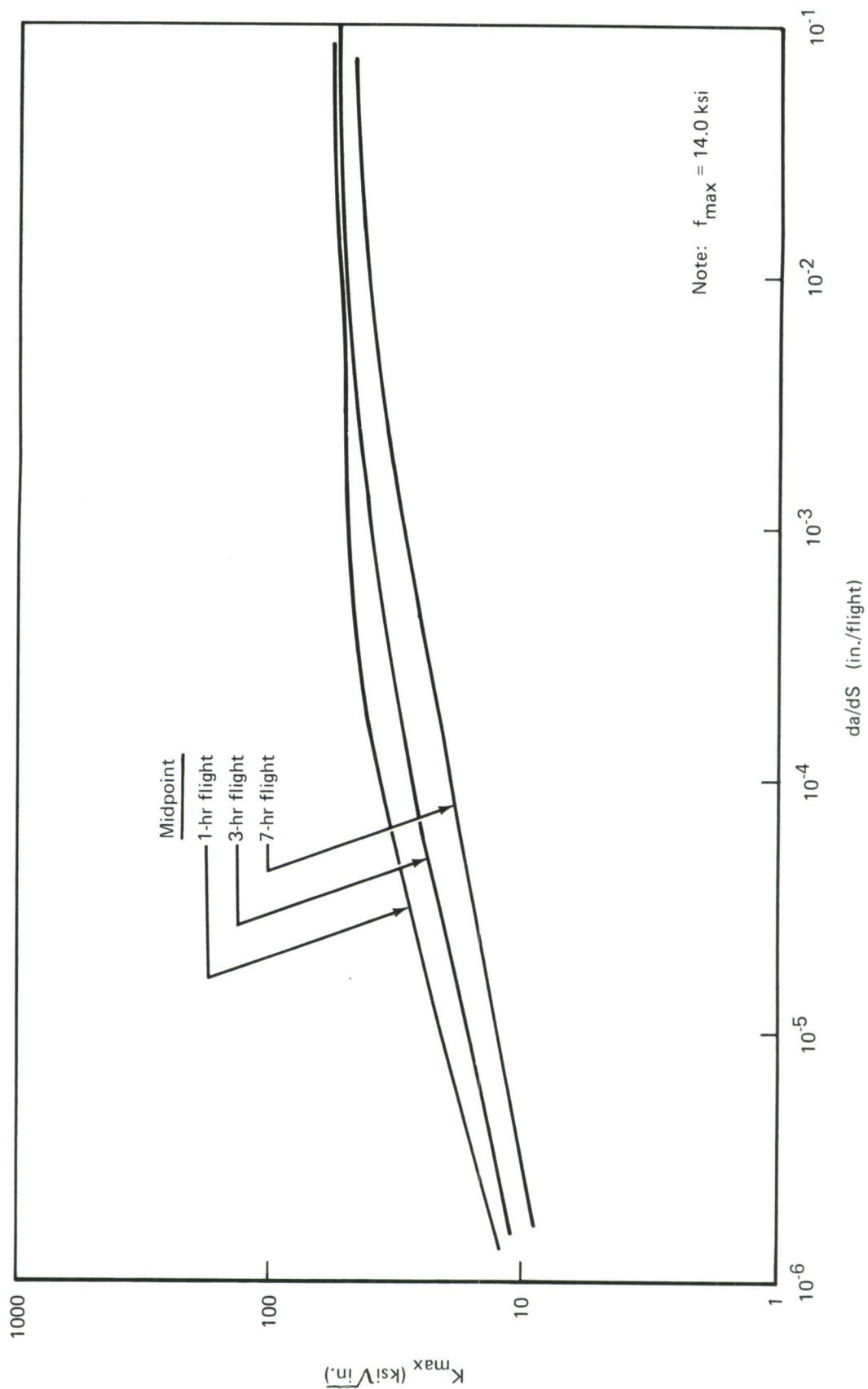


Figure 161.—Spectrum Crack Growth Rates—Crown (7075-T6, L-T)

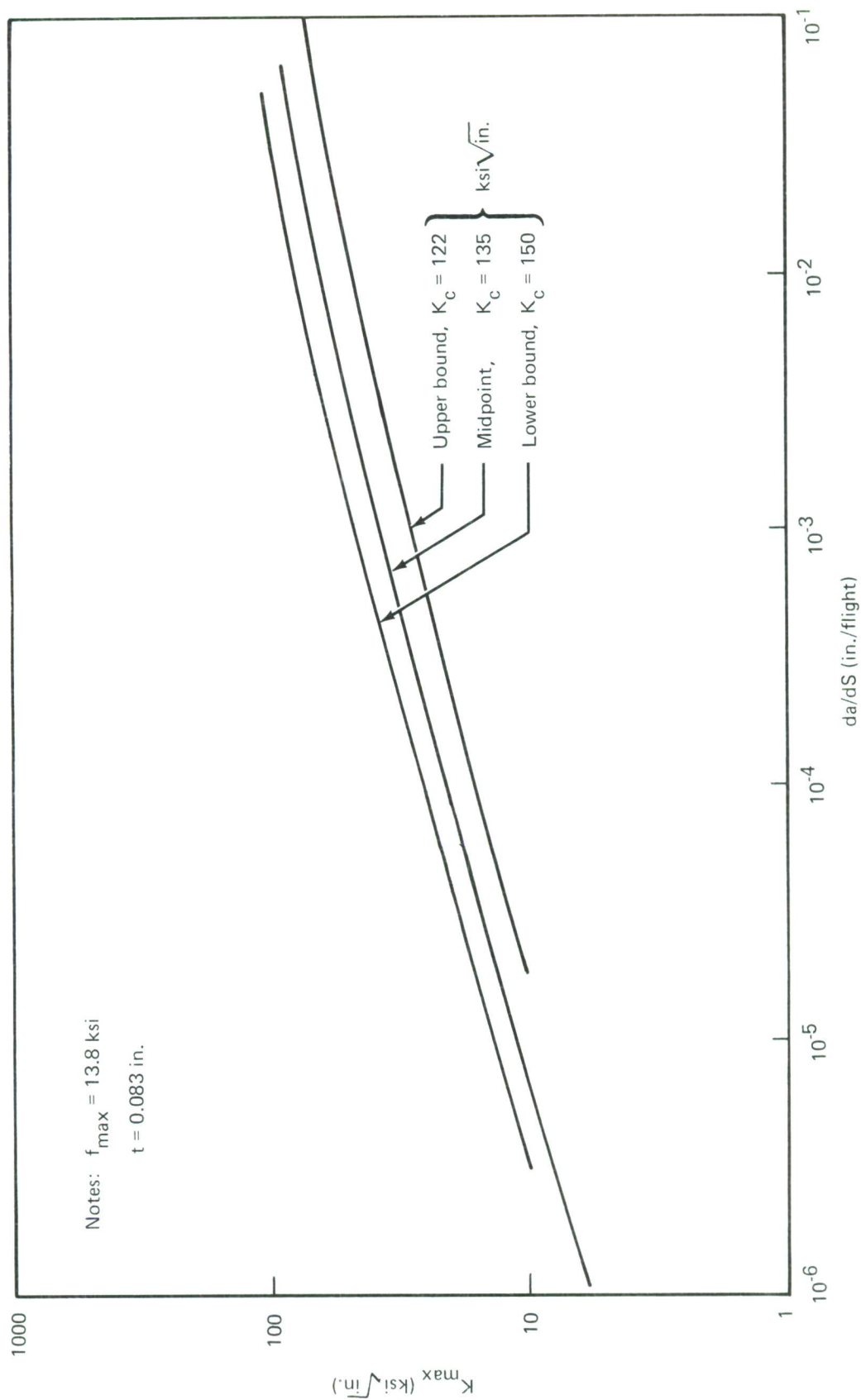


Figure 162. — 3-Hr Spectrum Crack Growth Rates—Side of Body (2024-T3, T-L)

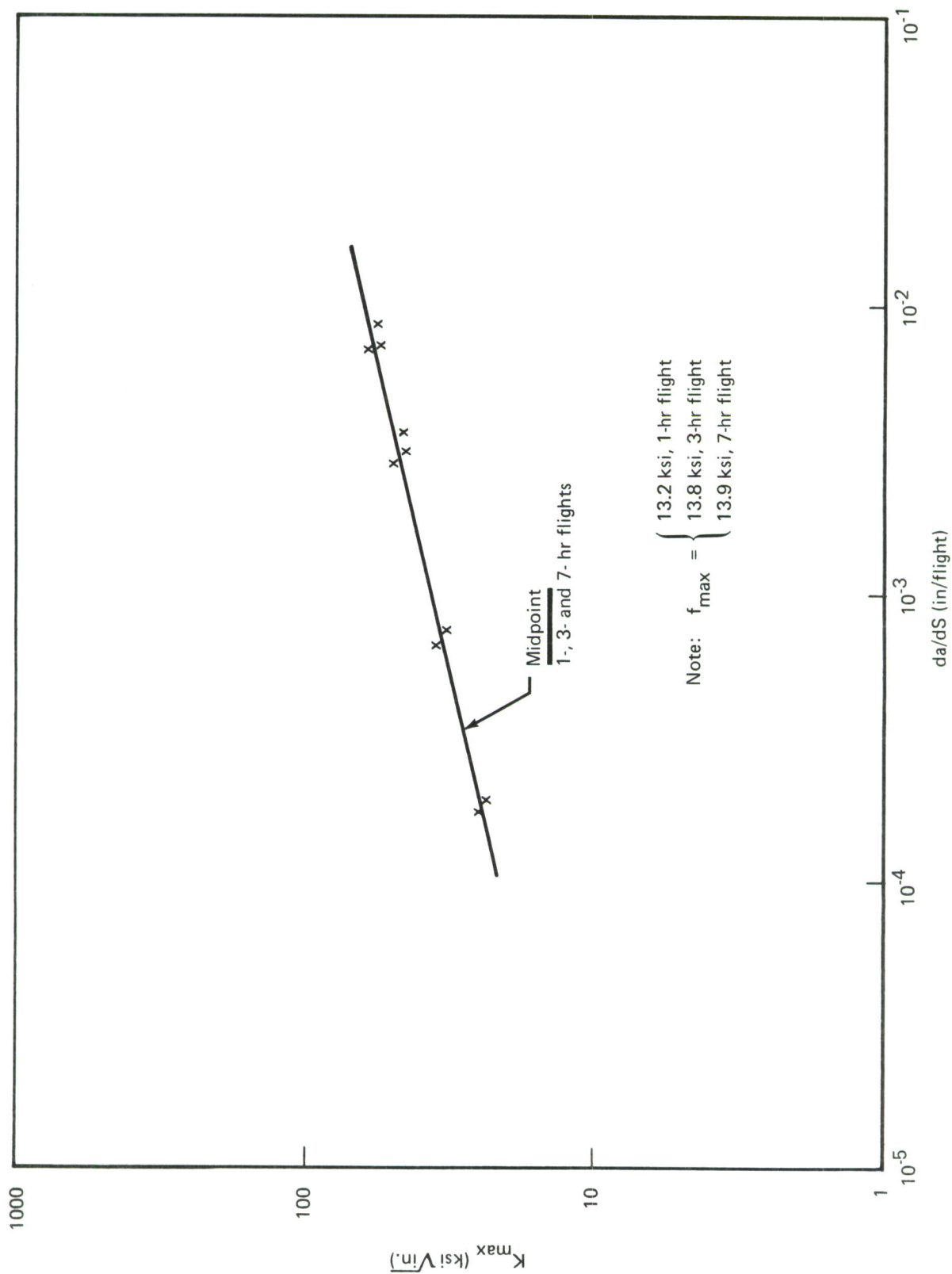


Figure 163.—Spectrum Crack Growth Rates—Side of Body (2024-T3, T-L)

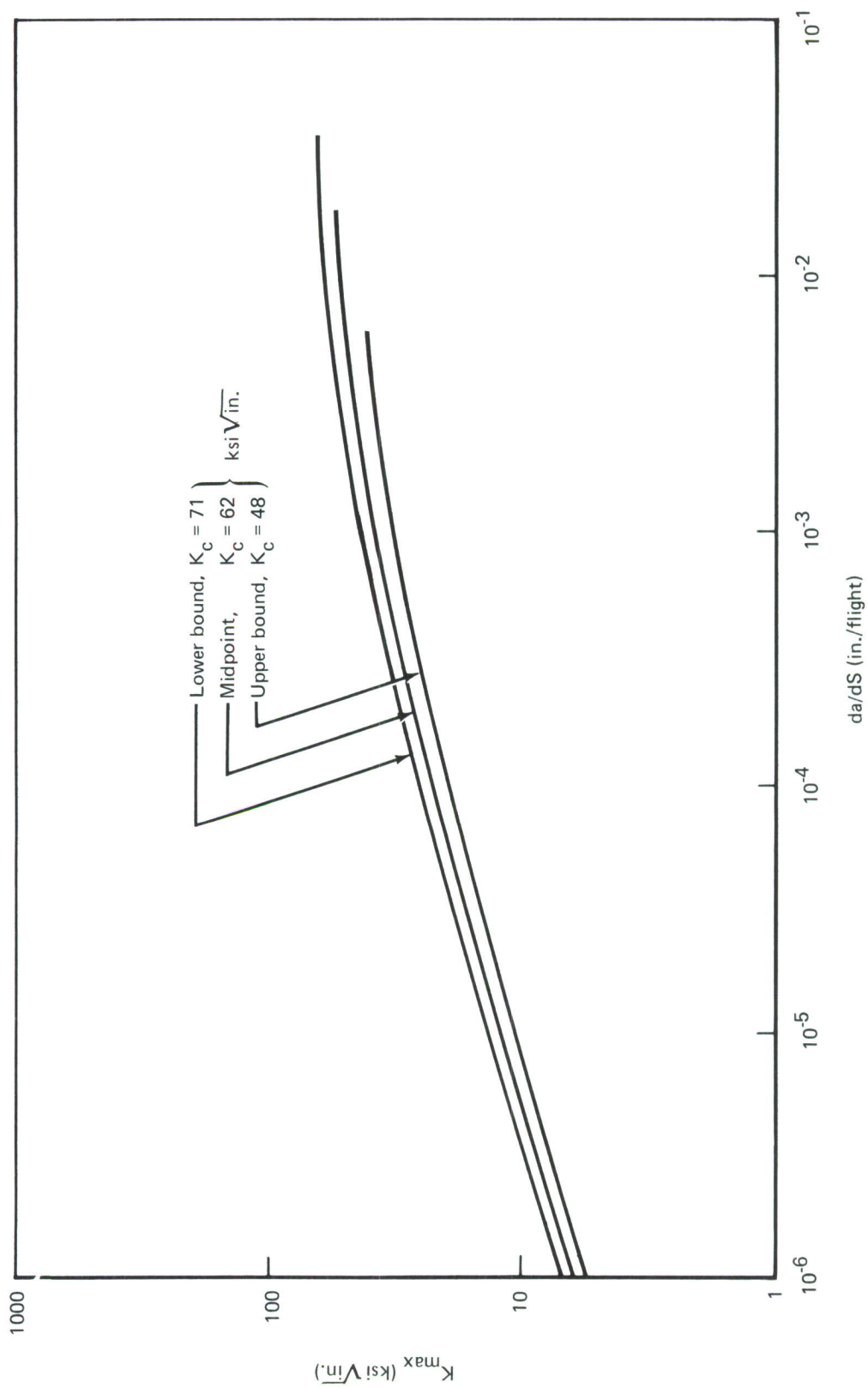


Figure 164.—Fatigue Crack Growth Rates (7075-T6, L-T)

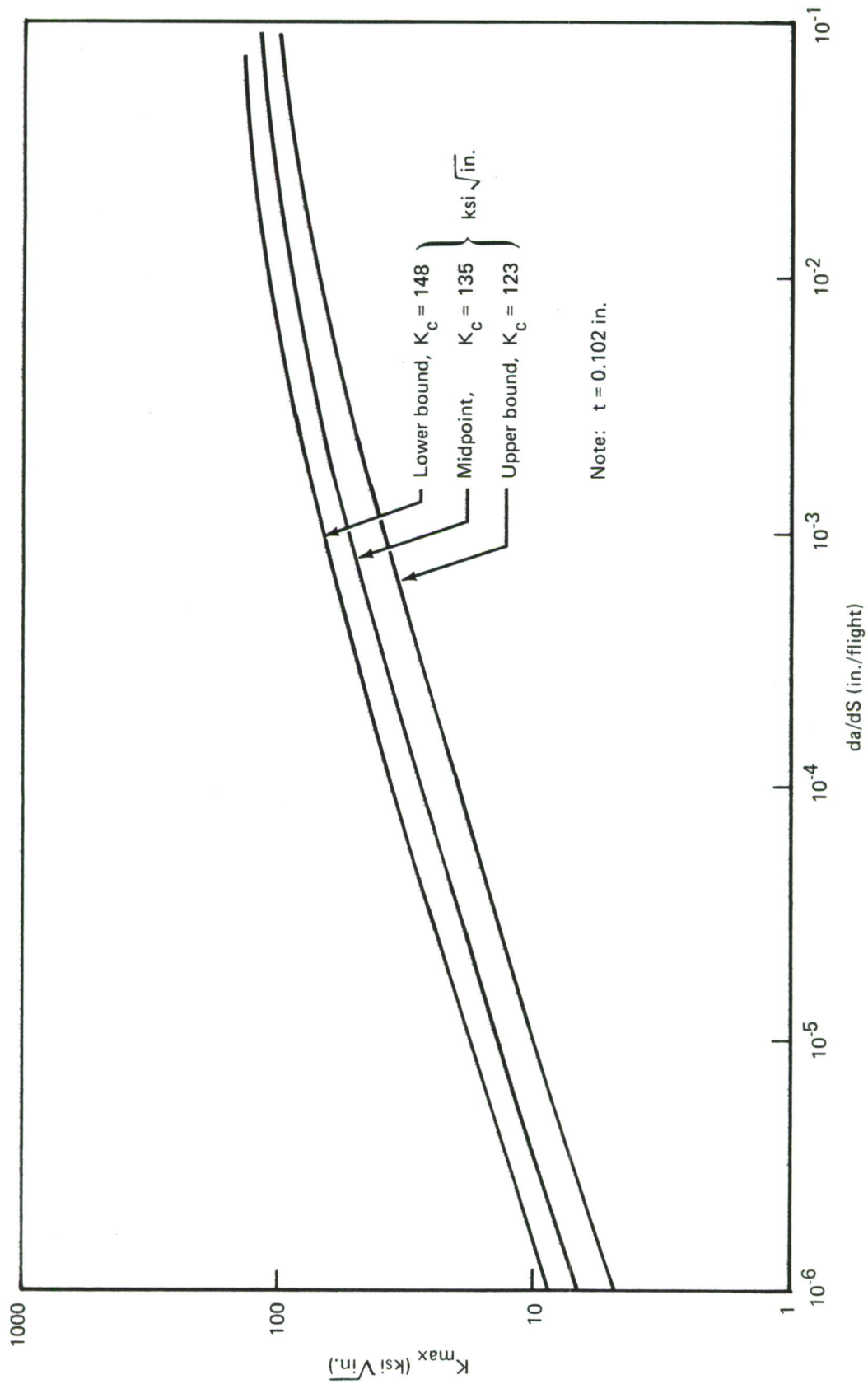


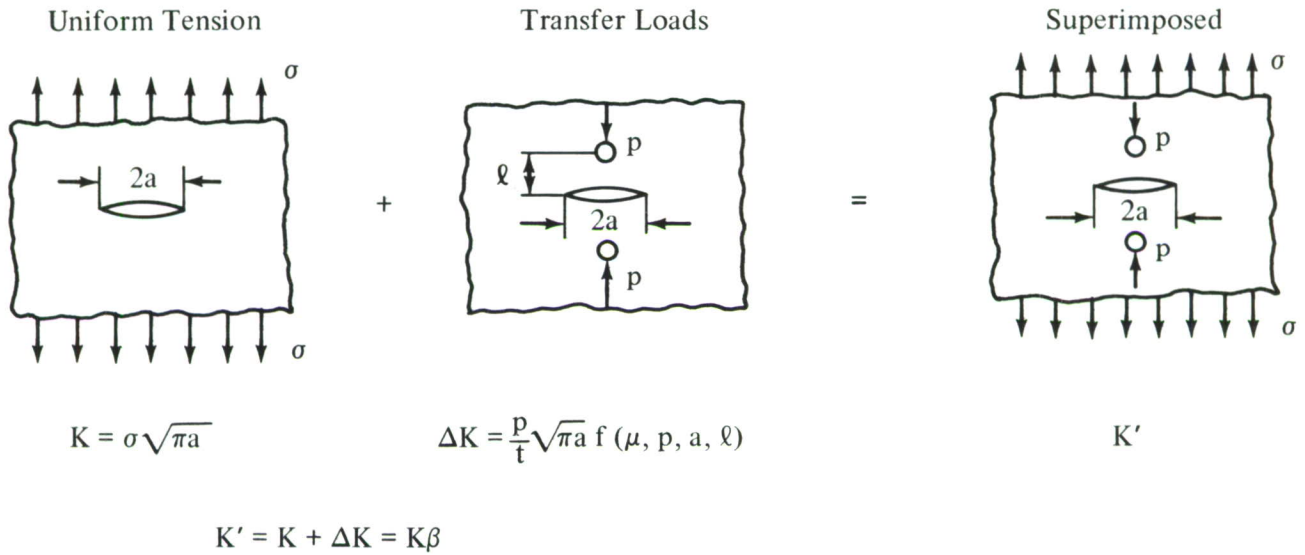
Figure 165.—Fatigue Crack Growth Rates (2024-T3, L-T)

Table XXXIX. —Spectrum Crack Growth Rate Data

Location	Material	Flight duration				
		1 hr	3 hr			7 hr
		Midpoint	Lower bound	Midpoint	Upper bound	Midpoint
Crown	2024-T3 skin	Fig. 159	Fig. 158	Fig. 158 Fig. 159	Fig. 158	Fig. 159
	7075-T6 stringer	Fig. 161	Fig. 160	Fig. 160 Fig. 161	Fig. 160	Fig. 161
Side of body	2024-T3 skin	Fig. 163	Fig. 162	Fig. 162 Fig. 163	Fig. 162	Fig. 163
	7075-T6 frame	Fig. 164	Fig. 164	Fig. 164	Fig. 164	Fig. 164
	2024-T3 tear strap	Fig. 165	Fig. 165	Fig. 165	Fig. 165	Fig. 165

and intact elements under damage tolerance conditions. The load transfer effect is accommodated by the following analysis.

A classical continuum analysis is conducted enforcing strain compatibility at skin-to-reinforcing-element attachment points. This analysis reflects the elastic behavior of skin reinforcing element and attachments (rivets). It is used to determine the magnification factors, β , to be applied to the classical infinite sheet crack stress intensity factor to reflect load transfer. β factors are defined as follows:



where $\beta = 1 + f(\mu, p, a, l)$

These β factors are used to determine crack stress intensity factors under conditions of fatigue crack growth since fatigue crack growth occurs in the elastic behavior range.

The β factors at the crown location for the condition of a transverse skin crack centered over a broken stringer are shown in figure 166.

The β factors at the side-of-body location for the condition of a longitudinal skin crack centered over a broken or partially intact tear strap or frame are shown in figure 167.

The classical continuum analysis described above is also used, with appropriate plasticity corrections, to determine the allowable gross area failure stress under damage tolerance residual strength conditions. The failure stresses are plotted against the skin crack length for the crown (fig. 168) and side-of-body (fig. 169) locations.

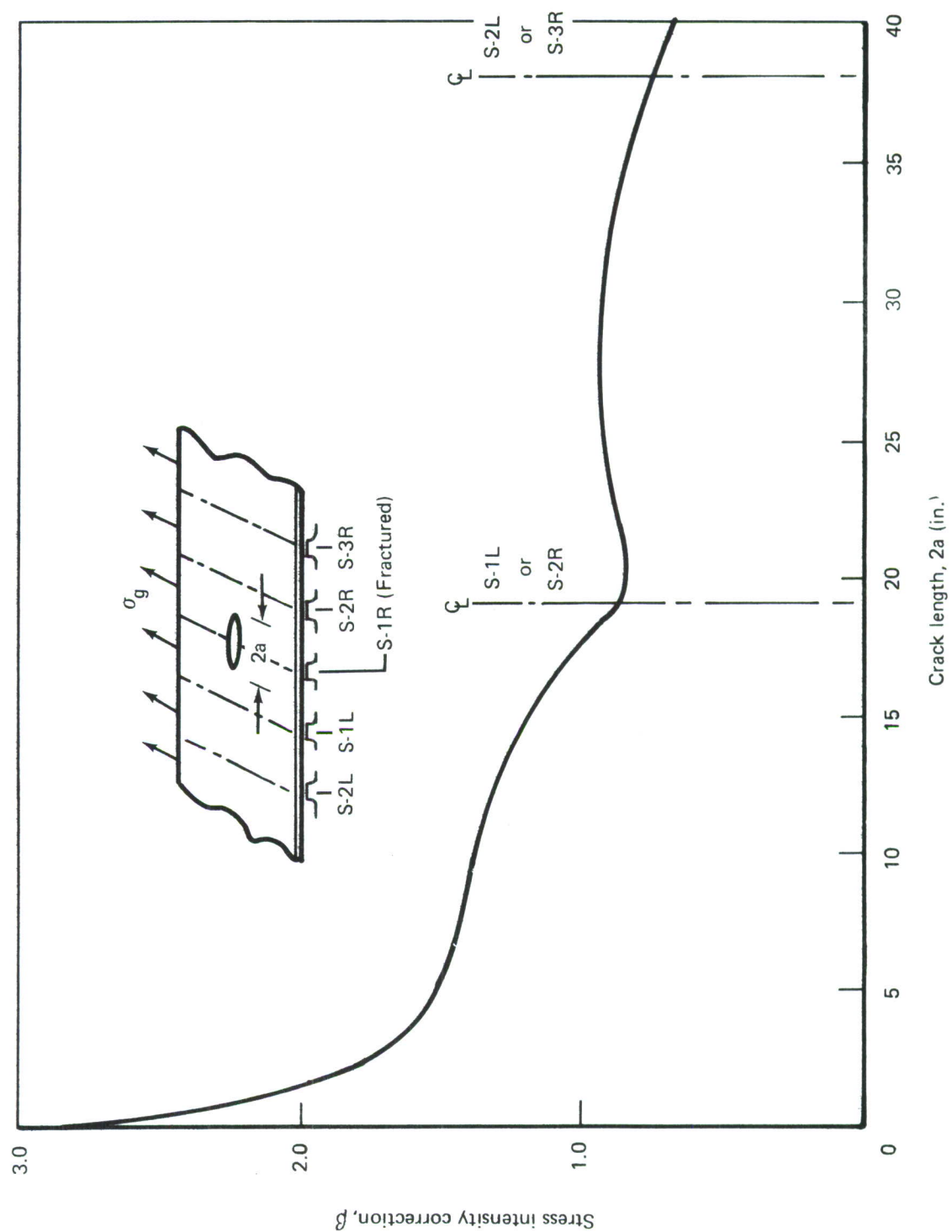


Figure 166. —Stress Intensity Correction, Crown

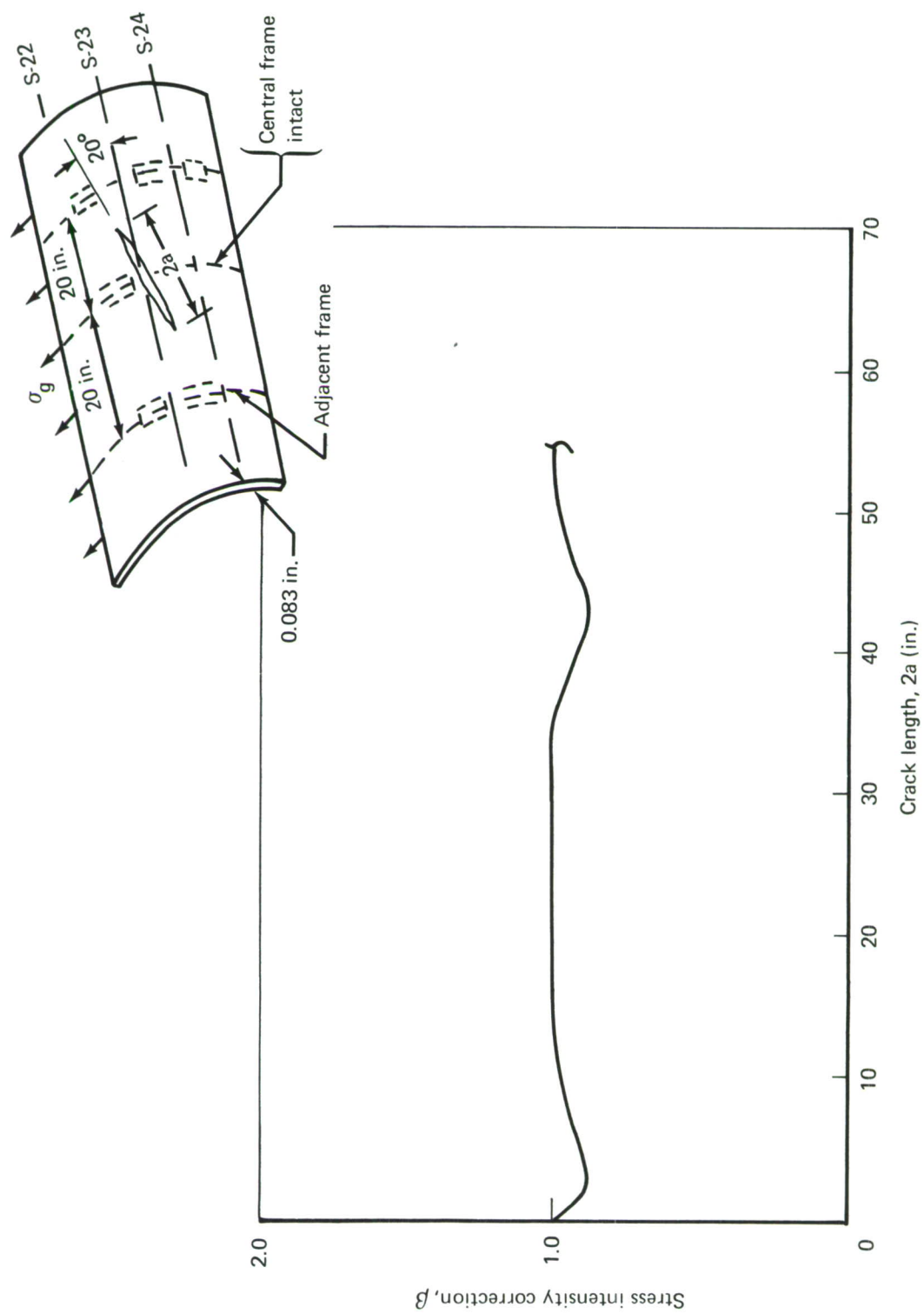


Figure 167.—Stress Intensity Correction, Side of Body

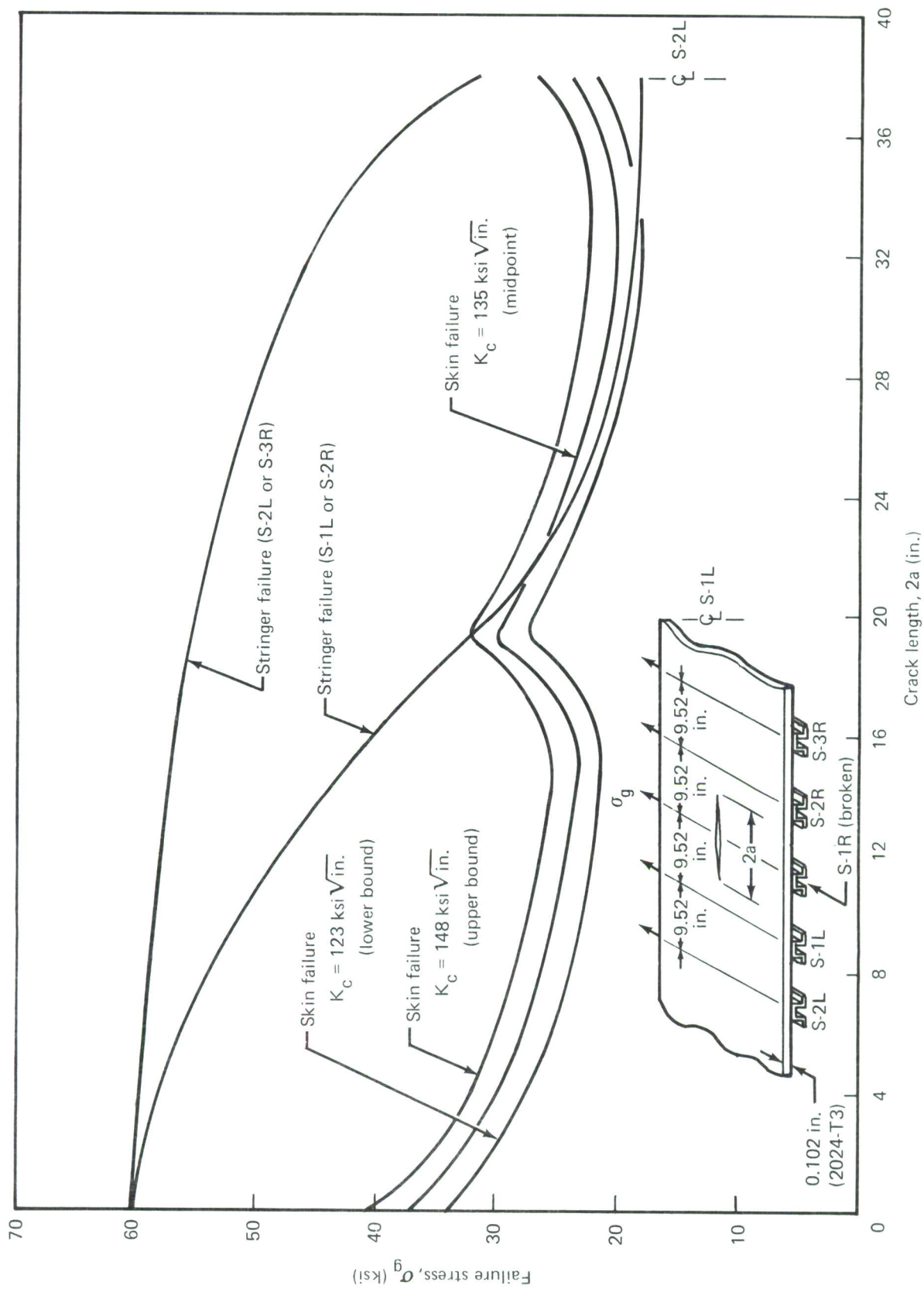


Figure 168.—Residual Strength Capability, C_{res} vs $2a$

c. Analytical Results

(1) Baseline Period of Unrepaired Usage

The baseline capability in terms of period of unrepaired usage was determined under the condition of a 0.020-inch through-the-thickness crack emanating from one edge of a dependent fastener hole and growing to a crack length equal to a $2a_{cr}$ with any of the following:

- A broken central stringer (crown location)
- A partially cracked central frame (side-of-body location, baseline construction)
- A partially cracked central tear strap (side-of-body location, alternate construction)

The rationale for the assumption of a partially cracked frame or tear strap is expanded on later in this section.

The following conditions were used to calculate the baseline period of unrepaired usage capability:

- Spectrum stresses and midpoint crack growth rates (da/dS) resulting from a medium range (3 hours) mission (figs. 158, 160, 162, 164, and 166)
- A residual strength load, P_{LT} , of that which would be experienced once in 20×10^5 flights (fig. 148)
- A critical crack length as determined from figures 168 or 169 using static “B” allowables and midpoint fracture (K_C) values.

The initial damage assumption results in stress intensity factors below the fatigue crack threshold; under these conditions life is a multiple of the required goal. Due to the following considerations the assumption of dependent cracks emanating from one edge of a fastener hole will be dropped.

- Any manufacturing operation which introduces defects, potential sources of crack initiation, into the bore of a fastener hole would in all probability produce a multiple of such defects, of which two could be diametrically opposed.
- Investigation of the reports of observed fatigue failures accumulated during fatigue testing of the full-scale baseline airplane indicates that the overwhelming majority of cracks observed at fastener holes propagated from both sides of those holes. While such cracks were not always of equal length when first observed, implying that the initial defects were not exactly equal, analysis of such cracks indicates that they did indeed propagate from defects with very nearly equal initial stress intensity factors.

- The assumption of single cracks emanating from holes is unconservative and as such does little to ensure safety of flight under damage tolerance considerations.

As a result of these observations, this study was reiterated using an initial damage assumption of a pair of diametrically opposed 0.020-inch through-the-thickness cracks emanating from fastener holes.

The cracking assumptions made in conducting this and following studies are described as follows:

- **Crown Location—Cracks growing out of initial flaws in both the skin and stringer.** At some point in time (determined from growth rates) the stringer fails and the skin crack (of length equal to the initial flaw plus growth in time required to fracture the stringer) is grown to the appropriate critical length.
- **Side-of-Body Location (Shear-Tied Frames)—Cracks growing out of initial flaws in both the skin and frame at common fasteners.** Since there are no common fasteners connecting the skin, frame, and fail-safe chords the fail-safe chord is assumed to remain intact. The skin crack is then grown to $2a_{cr}$ with the appropriate frame crack growth and with the fail-safe chord intact.
- **Side-of-Body Location (Floating Frame Configuration)—Cracks growing out of initial flaws in both the skin and tear straps at common fasteners.** Here the frame is assumed to remain intact while the skin crack propagates to $2a_{cr}$, with the appropriate tear strap crack growth.

In all cases considered, when the skin critical intensity factor is reached, unrepaired service usage capability is assumed to be exhausted. For example, at the crown location at a stress of 26.4 ksi (residual strength load requirement, P_{LT}), the skin crack becomes dynamic at a length of 8.0 inches (using the midpoint K_c value of 135 ksi $\sqrt{\text{in.}}$ (see fig. 168). The crack will arrest at the stringers, assuming 15% dynamic magnification factor; however, at this point in time the unrepaired service usage capability is assumed to be exhausted. For the side-of-body location crack growth is stable until the crack tip passes the adjacent frames.

Due to the slow crack growth rate of the 2024-T3 tear straps and the mild stress environment experienced by these elements ($f_{max} = 10.3$ ksi) the stress intensity factor resulting from initial flaws is less than threshold values. Since the tear strap does not fracture, the behavior of the floating-frame configuration under crack growth conditions is the same as that of the baseline configuration (shear-tied frame). As a result, the floating-frame configuration will be dropped from further consideration in the sensitivity studies.

The results of this study, in terms of baseline unrepaired service usage capability, are shown in figure 170 (crown location) and figure 171 (side-of-body location).

It is noted that in the crown location the stringer fractures before the skin crack has propagated to its critical length. The crown skin and stringer are stressed equally

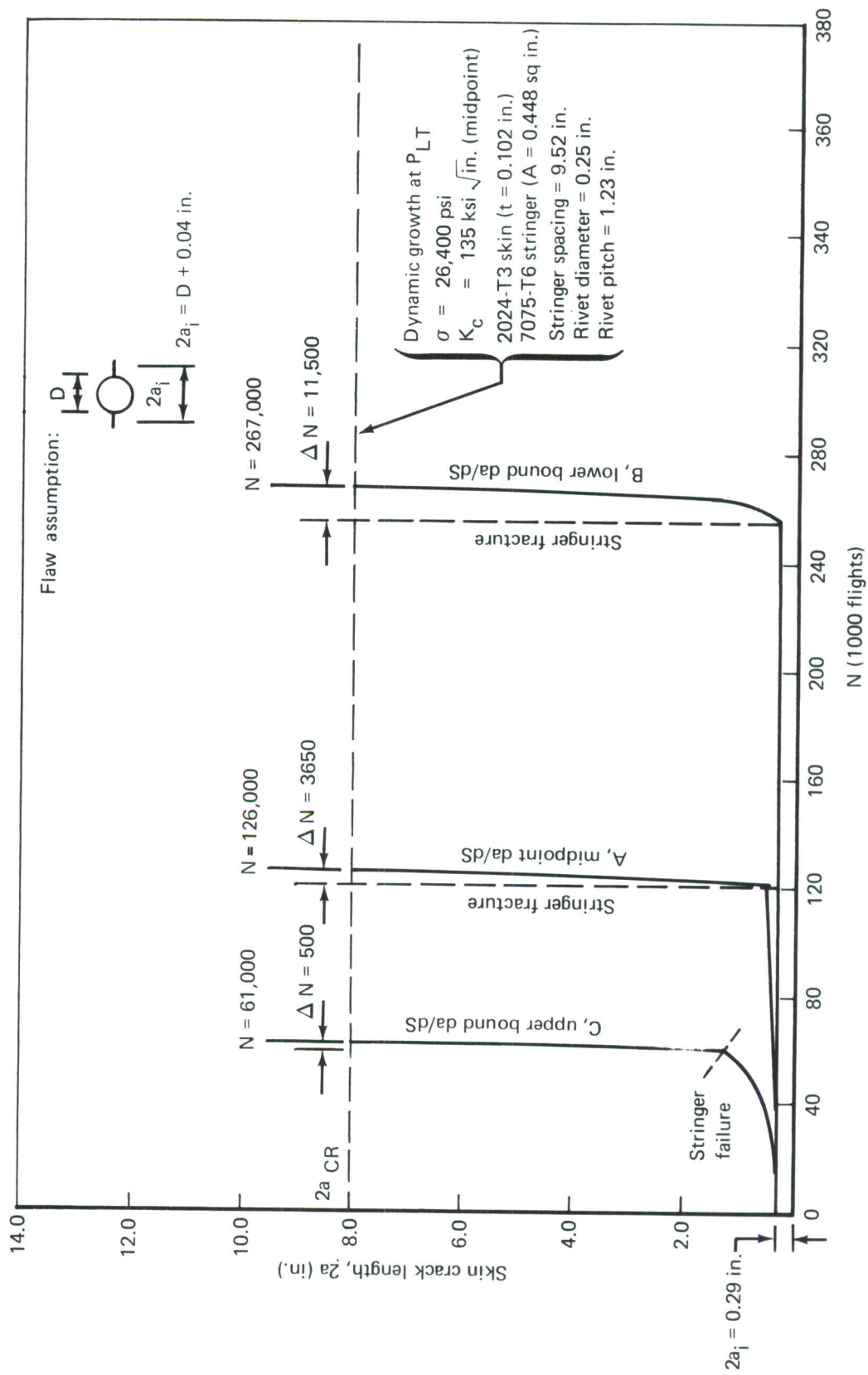


Figure 170.—Crown Location, Crack Growth From Initial Flaw (3-Hr Flight)

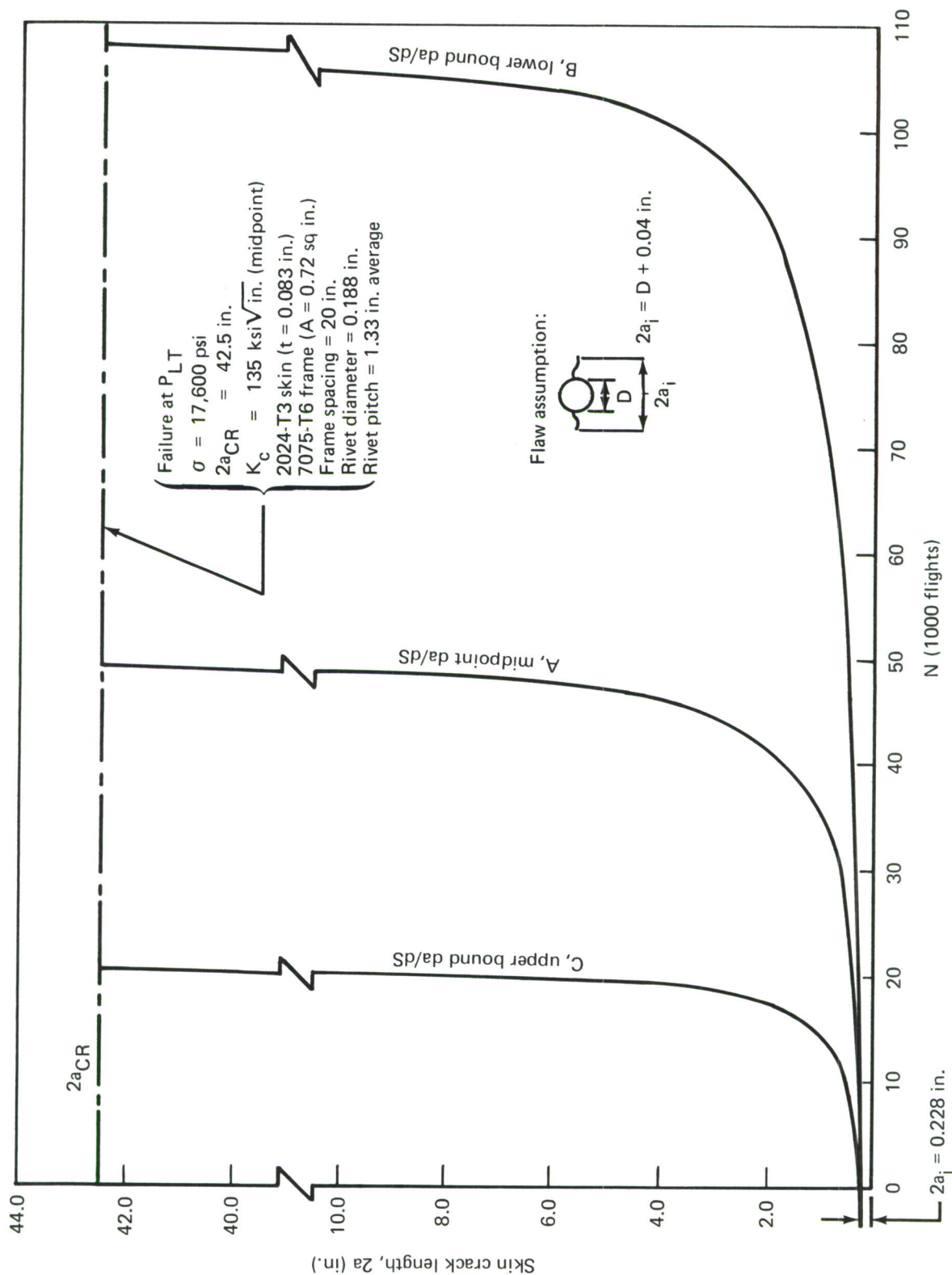


Figure 171.—Side-of-Body Location, Crack Growth From Initial Flaw

for body-bending conditions, and the rapid crack growth rate associated with the 7075 stringers and finite width of the stringer cause it to fracture before the skin crack has attained critical length.

For the side-of-body locations a completely different condition exists. The skin is under a combined loading caused by internal pressure (hoop stress) and body-bending shears. This effect causes the skin to experience a maximum principal stress of 13.8 ksi during the 3-hour mission. The frames (or tear straps) are loaded uniaxially, by body pressurization only, with a maximum stress of 10.3 ksi during the 3-hour mission. Since the skin is loaded in the transverse grain direction by the complete spectrum stresses while the frames are loaded by pressure (one cycle per flight), spectrum crack growth rates for the frame are much slower than those of the skin. This slow crack growth, combined with the reduced stresses in the frame, results in the frame remaining partially intact when the skin crack has attained critical length.

The assumed mode of failure shown for the side-of-body location, skin crack plus partially intact reinforcing element, results in an unrepaired service usage capability for the baseline construction which is a multiple of the baseline design goals.

This study was reiterated using K_{IC} data taken from the lower bound and the upper bound of the data (figs. 149 and 150). These K_{IC} values were used to determine revised critical crack lengths ($2a_{cr}$) using figures 168 or 169. The impact on life in terms of a revised number of cycles is shown in table XL. The impact on stress and weight to achieve life equal to that of the baseline was determined and is shown in table XL.

Those cases shown in table XL which indicate a possible increase in allowable stress, hence decrease in weight or cost, are meaningless since other static design considerations will govern.

(2) Effects of Varying Material Crack Growth Rates

The studies outlined in section VI-1c1 were reiterated using midpoint K_{IC} data and crack growth rate data (da/dS) as taken from figures 158, 162, 164, and 165 for both upper and lower bounds.

The results are shown in figure 170 and in figure 171, curves B and C. Curve B shows the effects of crack growth rates taken from the lower bound da/dS values, while curve C shows the effects on life of crack growth rates taken from the upper bound (da/dS) values.

The effects on life and stress due to variations in the crack growth rates (da/dS) are shown in table XL. In all cases studied, the unrepaired service usage capability under the damage tolerance condition of cracks propagating from initial flaws is a multiple of the baseline airplane design goals.

Table XL. –Impact of Material Property and Usage Spectra Variability
for Lifetime Period of Unrepaired Service Usage

Constant	Variable	Baseline structure capability		Impact on stress and weight to maintain capability equal to baseline			
		Crown (flights)	Side of body (flights)	Crown ^a		Side of body ^b	
				Allowable stress GAG (psi)	Weight increment (lb)	Allowable stress GAG (psi)	Weight increment (lb)
Midpoint K_C , (average usage)	da/dS (lower bound)	267,000	107,100	16,400	-111	16,900	-251
	da/dS (midpoint)	126,000	48,700	14,000	0	13,800	0
	da/dS (upper bound)	61,000	19,700	12,000	126	10,900	361
Midpoint da/dS (average usage)	K_C (lower bound)	125,700	48,700	14,000	0	13,800	0
	K_C (midpoint)	126,000	48,700	14,000	0	13,800	0
	K_C (upper bound)	127,000	48,700	14,000	0	13,800	0
Midpoint da/dS (midpoint K_C)	Mild usage	222,000	48,700	15,800	-86	13,800	0
	Average usage	126,000	48,700	14,000	0	13,800	0
	Severe usage	38,000	48,700	10,900	214	13,800	0

^aBaseline: Crown—Allowable stress, GAG = 14,000 psi
—Panel weight (skin str) = 753 lb

^bBaseline: Side of body—Allowable stress, GAG = 13,800 psi
—Panel weight (skin str) = 1362 lb

(3) Effects of Varying Usage

Studies outlined in section VI-1c1 were reiterated to determine the effects of mild and severe usage spectra on:

- Period of unrepaired service usage capability, maintaining baseline stress levels as a constant
- Allowable stresses, maintaining baseline life capability as a constant
- Change in structural weight for the case of revised allowable stress to maintain baseline period of unrepaired usage capability

For the purpose of this study, mild or severe usage is defined as that resulting from differences in airplane operational use. The environmental effects encountered in operation are not significant, for the baseline materials, when compared with the stress spectrum effects resulting from differences in mission mix. Determination of mild or severe usage is based on number of flights as opposed to total operational life.

- Mild usage is defined as that resulting from flight blocks composed of short-range flights (1-hour duration) only.
- Severe usage is defined as that resulting from flight blocks composed of long-range flights (7-hour duration) only.

Spectrum crack growth rates, da/dS , for mild and severe usage are shown in figures 159, 161, 163, 164, and 165.

The results of this study in terms of unrepaired service usage capability are shown in figure 172 for the crown location only. Since there is no discernible difference in the spectrum crack growth rates for the 1-, 3-, and 7-hour missions for the side-of-body locations (fig. 163), the unrepaired service usage capability at this location (in terms of number of flights) is independent of mission length.

The effects of the assumed usage spectra on the unrepaired service usage allowable stress and structural weight for the crown location are shown in table XL. Upon investigation of figure 172 it may be readily observed that, although the unrepaired service usage capability in terms of flights under the severe usage spectra is shorter than that under the mild or average spectra, for constant total operational time (flight-hours) a mission mix consisting entirely of 1-hour flights is most severe. This is due to the predominating influence of the ground-air-ground portion of the stress spectra.

(4) Effects of Varying Initial Damage Size

As was done for varying usage, studies outlined in section VI-1c1 were also reiterated to determine the effects of variation in initial damage size assumptions on:

- Period of unrepaired service usage capability, maintaining baseline stress levels as a constant

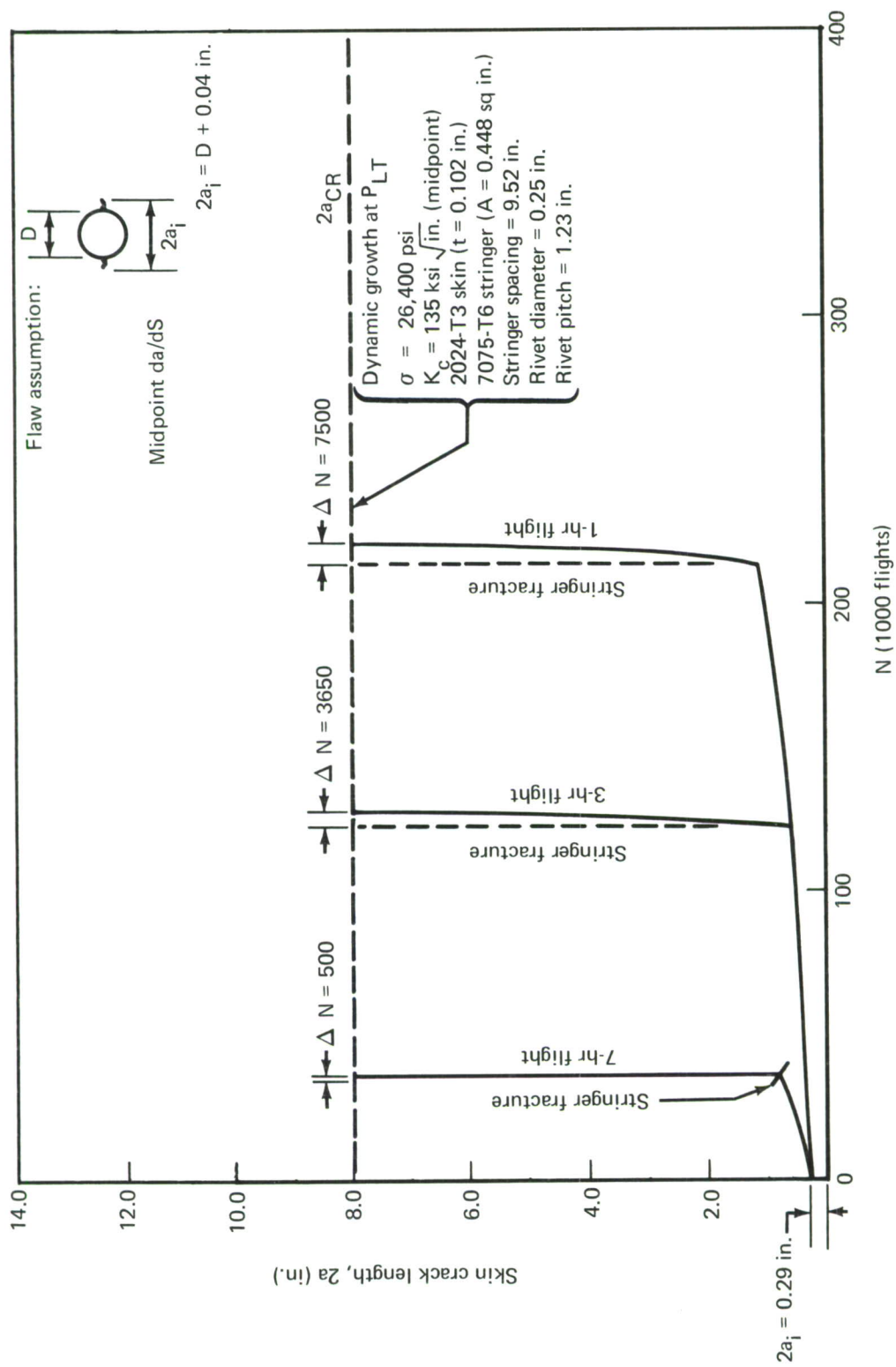


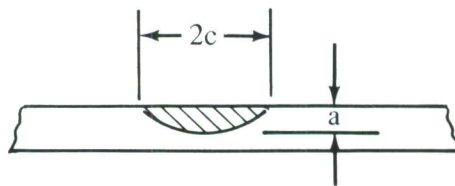
Figure 172.—Crown Location, Crack Growth From Initial Flaw (1-, 3-, and 7-Hr Flights)

- Allowable stresses, maintaining baseline life capability as a constant
- Change in structural weight for the case of revised allowable stresses.

These studies were conducted using typical midpoint fracture data and the 3-hour stress spectrum. The following initial damages were assumed:

- Surface flaws with $a/Q = 0.020, 0.030, \text{ and } 0.040$ inch
- Through-the-thickness cracks emanating from fastener holes of $a = 0.025, 0.050, \text{ and } 0.075$ inch

For cracks from holes, a total crack length of $D + 2a$ was assumed. For surface flaws, a crack shape parameter of $a/2c = 0.33$ inch was assumed.



Surface Crack Shape

Surface flaws were assumed to occur at midbay, between stringers for the crown location and between frames for the side-of-body location. These are assumed to be the critical locations since the relieving influence of transfer loads from the reinforcing elements is negligible. The stress intensities resulting from these initial damage assumptions are below threshold values for fatigue crack growth; therefore, the period of unrepaired service capability under these conditions is undefined.

It is concluded that surface flaws of these sizes (a/Q) are not as severe as through-the-thickness flaws at fastener holes; therefore, they were dropped from further consideration in this study.

The results of varying the length of the through-the-thickness cracks at fastener holes used for initial damage assumptions are shown in figures 173 and 174, in terms of life capability, for the crown and side-of-body locations, respectively. The impact of this variation in initial damage assumption on unrepaired service usage, stress, and structural weight are shown in table XLI and figure 175.

(5) Effects of Varying Inspection Intervals

Studies were conducted to determine the impact of in-service inspection considerations on the Damage Tolerance Criteria, appendix I, and its application to the baseline. This was accomplished by performing the following parametric analyses (for these studies, average (midpoint) material properties and usage were assumed).

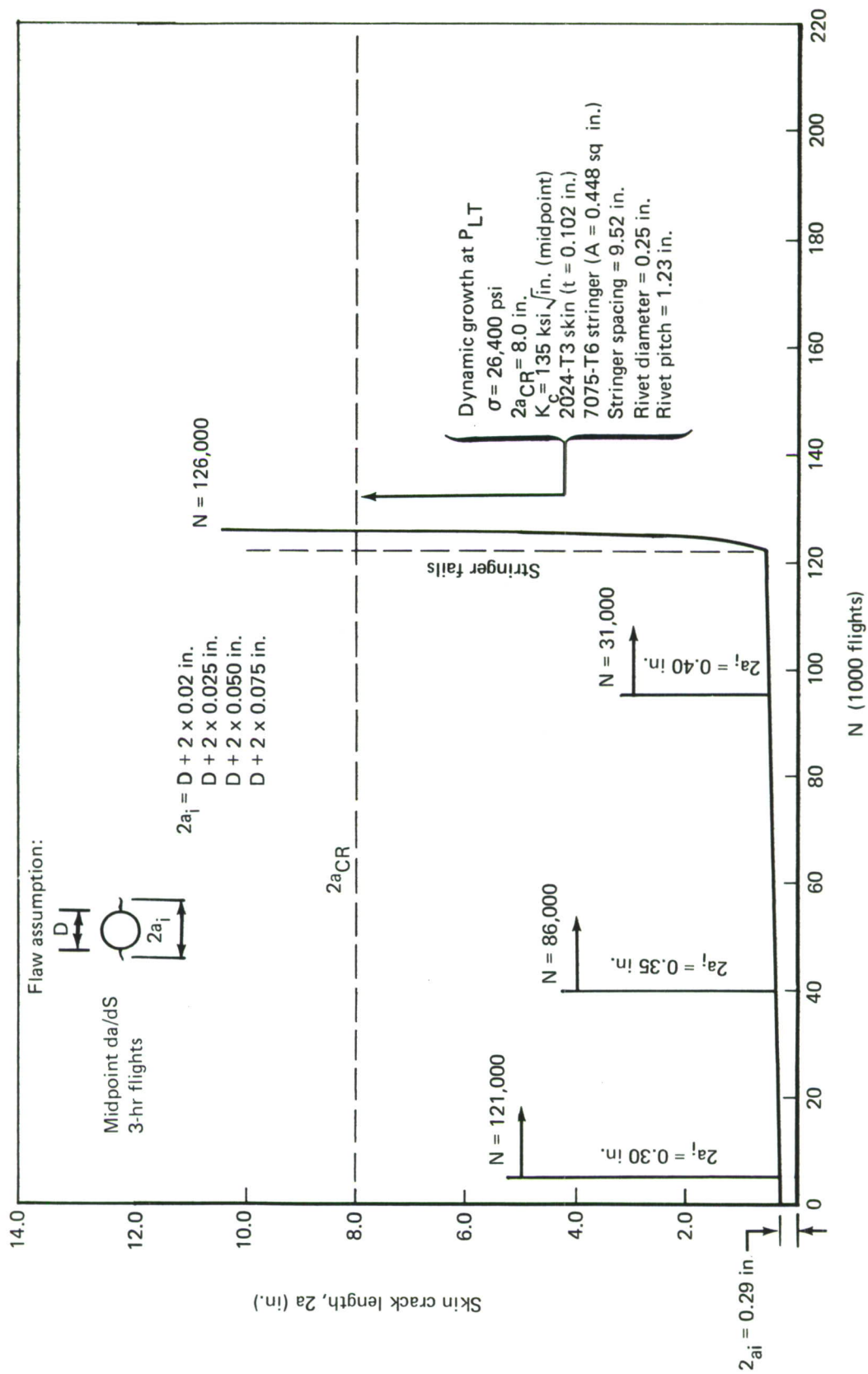


Figure 173.—Crown Location, Crack Growth From Initial Flaw

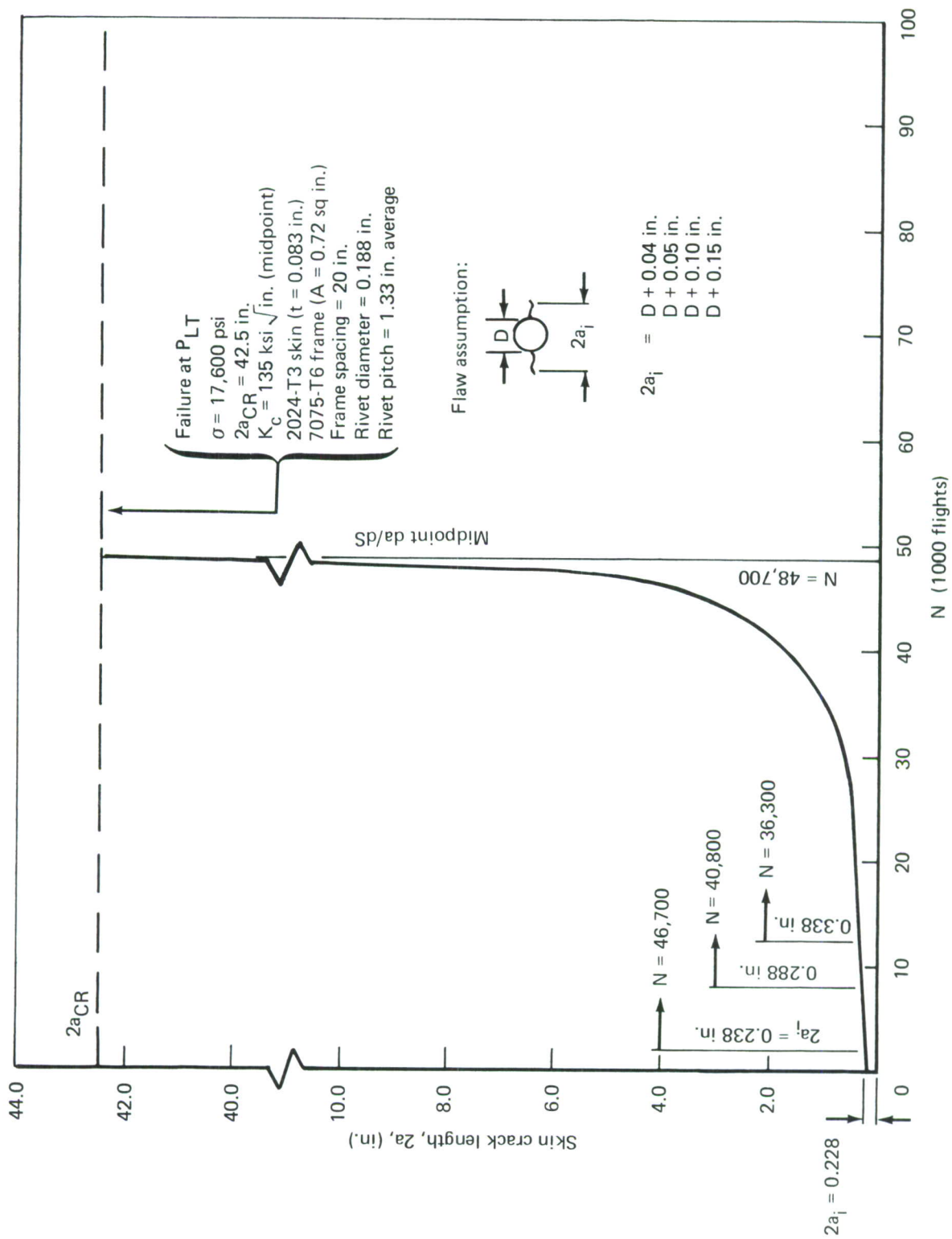


Figure 174.—Side-of-Body Location, Crack Growth From Initial Flaw

Table XLI.—Impact of Variability in Initial Damage Assumption and Period of Unrepaired Service Usage on Stress and Weight

Variable	Inspection interval	Baseline structure capability		Impact on stress and weight to maintain capability equal to baseline			Refer to figure
		Crown (flights)	Side of body (flights)	Crown ^a		Side of body ^b	
				Allowable stress GAG (psi)	Weight increment (lb)	Allowable stress GAG (psi)	Weight increment (lb)
Variation in initial flaw size assumption							
$a_i = 0.020$ in.	F_{LT}	126,000	48,700	14,000	0	13,800	0
$a_i = 0.025$ in.	F_{LT}	121,000	46,700	14,000	0	13,800	0
$a_i = 0.075$ in.	F_{LT}	31,000	36,300	10,400	261	12,900	95
Variation in depot level inspection interval							
Baseline F_{DM}	F_{DM}	9,950	9,175	14,000	0	13,800	0
0.5 x baseline F_{DM}	F_{DM}	4,975	4,600	16,200	-102	16,500	-224
2 x baseline F_{DM}	F_{DM}	19,900	18,350	12,100	119	11,520	272
Variation in special visual inspection interval							
Baseline F_{SV}	F_{SV}	750	1,300	14,000	0	13,800	0
0.5 x baseline F_{SV}	F_{SV}	375	650	16,200	-102	16,500	-224
2 x baseline F_{SV}	F_{SV}	1,500	2,600	12,100	119	11,520	272

^aBaseline: Crown—Allowable stress, GAG = 14,000 psi
Panel weight (skin str) = 753 lb

^bBaseline: Side of body—Allowable stress, GAG = 13,800 psi
Panel weight (skin str) = 1,362 lb

Degree of inspectability—in-service noninspectable

Baseline initial flaw size assumption— $2a_i = 0.04$ in.

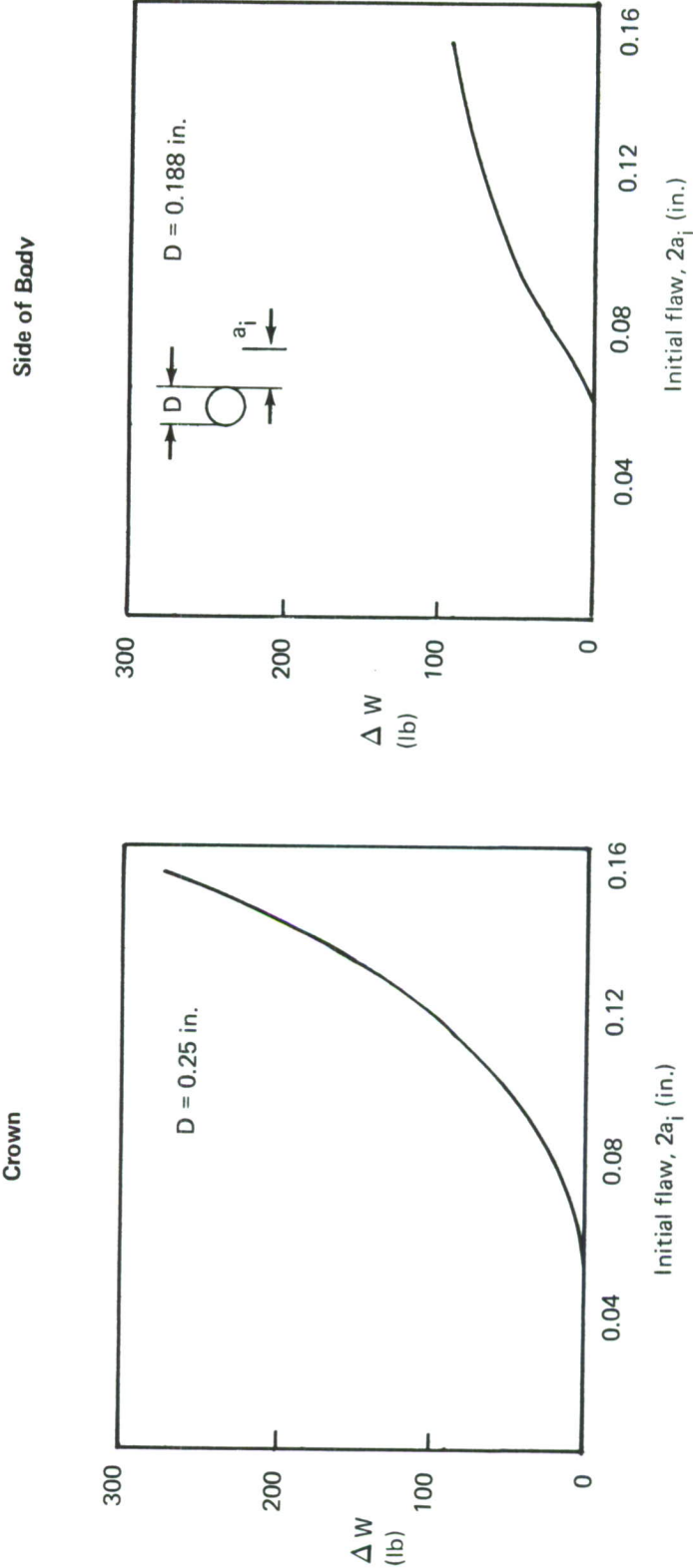
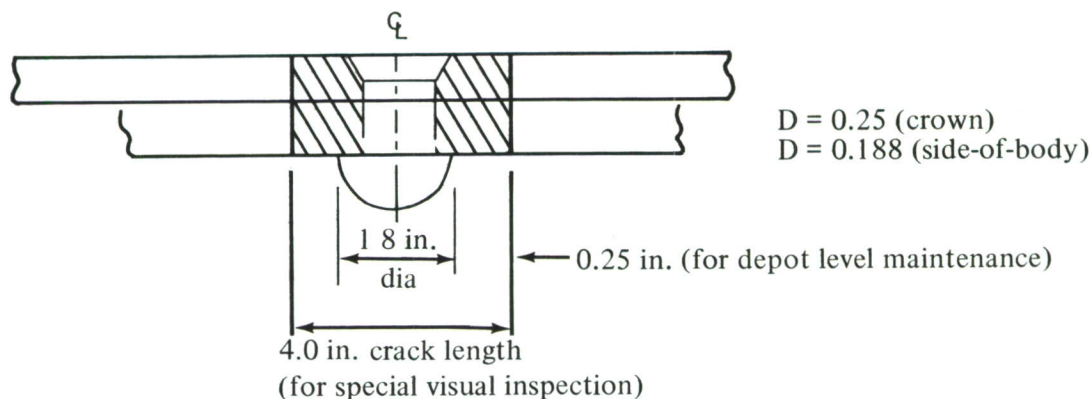


Figure 175. —Weight Increment to Maintain Baseline F_{LT} Capability—Variation in Initial Flaw Size Assumption

The impact on design stress of variations in the inspection intervals was determined for the following classes of inspectability as defined in appendix I:

- 1) The impact of varying the depot level inspection interval was investigated. The baseline depot level inspection interval, F_{DM} , is defined as one-half the time required to grow a pair of diametrically opposed through-the-thickness cracks, emanating from fastener holes, having 0.25 inch of uncovered length to either:
 - a) $2a_{cr}$ skin crack with a broken central stringer (crown location)
 - b) $2a_{cr}$ skin crack with a partially broken central frame (side-of-body location)
- 2) The impact of varying the special visual inspection interval was investigated. The baseline special visual inspection interval, F_{SV} , is defined as one-half that time required to grow a 4-inch-long skin crack to either of a or b above.

The determination of the “uncovered” crack length specified in appendix I is as shown below:



Uncovered Crack Length Determination

The inspectable cracks are assumed to exist in the critical element with a crack in the adjacent element of length equal to the initial flaw, plus that growth in the adjacent element crack which occurs during the period required to grow the critical element crack to inspectable length.

The definition of special visual inspection requirements contained in appendix I precludes the possibility of detecting fuselage-reinforcing-element cracks; therefore, only skin cracks are assumed to be special visual inspectable.

Appendix I, paragraph 3.4.5, specifies that “an uncovered, open 2-inch, through-the-thickness crack” is special visual inspectable. Analysis of the fatigue damage reports accumulated during fatigue testing of the baseline component indicates that several uncovered cracks of length greater than 2 inches were overlooked during visual inspection. These inspections were conducted by trained personnel, in close proximity to the structure, and on firm scaffolding; however, they were not instructed to scrutinize localized areas for cracking. In view of the fact that the “in-service special visual inspection” is assumed to be

conducted under conditions similar to those for the fatigue test component, it is felt that a minimum detectability limit of 4 inches is more meaningful.

The inspection intervals determined for the baseline construction in 1 and 2 above are shown in figures 176 and 177, for the crown and side-of-body locations, respectively.

A study was conducted on the impact on allowable stress and structural weight of changing the inspection intervals, F_{SV} and F_{DM} , to 50% and 200% of the baseline intervals. The results of this study are shown in table XLI and figures 178 and 179, in terms of the impact on allowable stress and structural weight of the baseline.

Since the baseline component was not designed to the damage tolerance criteria of appendix I, the assumption is made that inspection intervals will be defined by the capability of the baseline structure under that standard. The applicable inspection intervals are considered to be:

- Depot level maintenance—crown and side of body
- Special visual—crown and side of body
- Walkaround visual—side of body
- In-flight evident—side of body

The crown location is not assumed to be “walkaround visual” or “in-flight evident” inspectable. The side-of-body location is assumed to be inspectable under those conditions with a crack detectability limit of a two-bay skin crack (approximately 40 inches long); however, investigation of figures 173 and 174 indicates that the inherent capability of the baseline structure is a large multiple of that required by appendix I.

(6) Effects of Varying Initial In-Service Damage Size

A study was conducted of the impact on allowable stress and structural weight of varying the assumed initial damage present at the beginning of the inspection intervals, F_{DM} and F_{SV} . The method used to define the inspection interval assumes initial damage present at the beginning of that inspection interval equal to a defined inspectable length. The initial damage will be varied by changing the minimum inspectable cracks specified in section VI-1c5 to:

- 1) Depot level inspectable crack: a through-the-thickness pair of diametrically opposed cracks emanating from a fastener hole having 0.50 and 0.75 inch of uncovered length.
- 2) Special visual inspectable crack: from the present minimum of 4 inches to, first, a 3-inch-long, then a 2-inch-long skin crack.

Detectable flaw assumption:

Depot level (stringer)

Special visual (skin)

$2a_i = 2.0$ in.

$2a_i = 3.0$ in.

$2a_i = 4.0$ in.

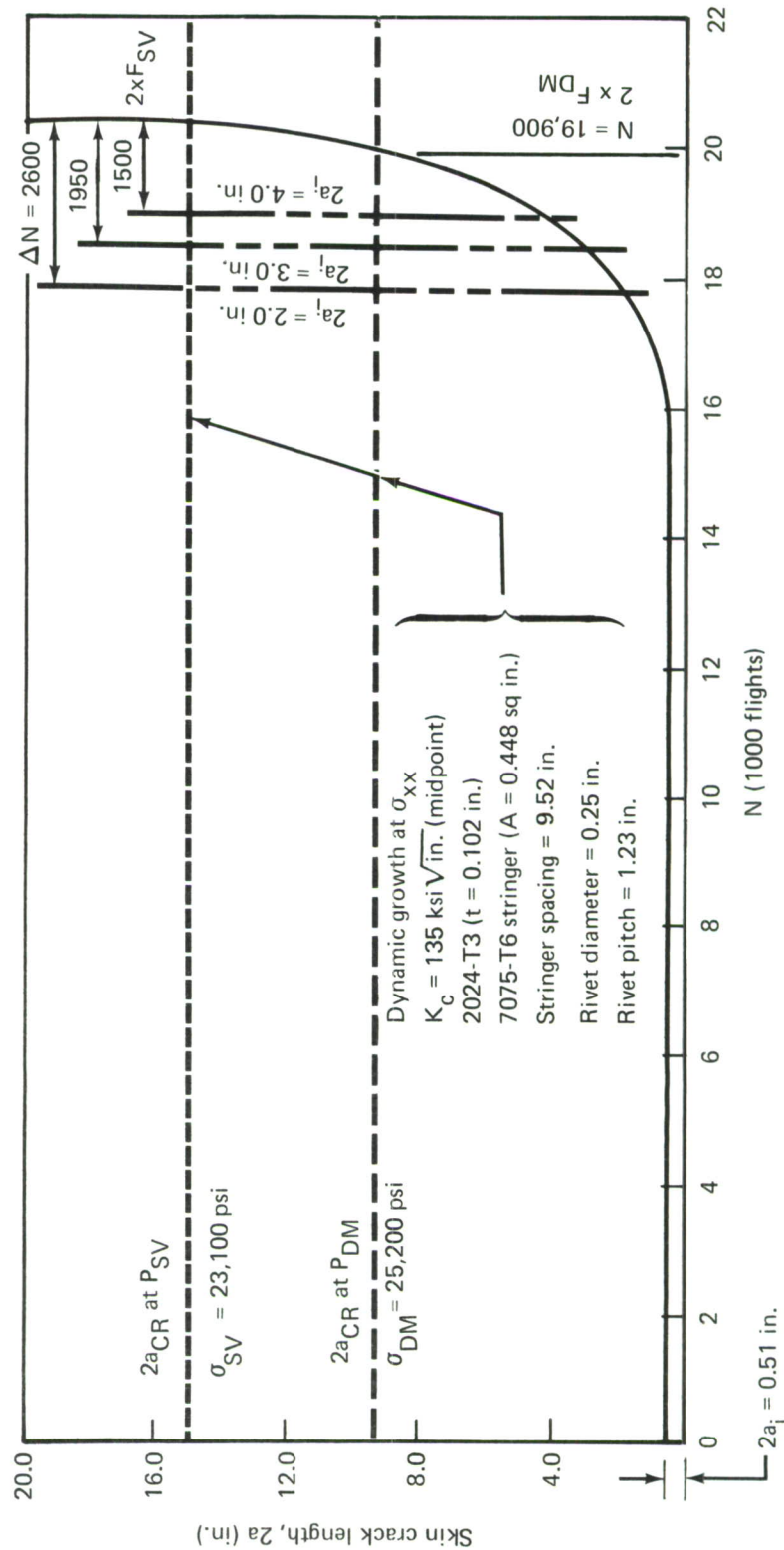
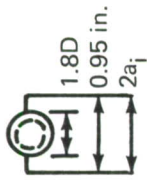


Figure 176.—Crown Location, Crack Growth From Detectable Flaw

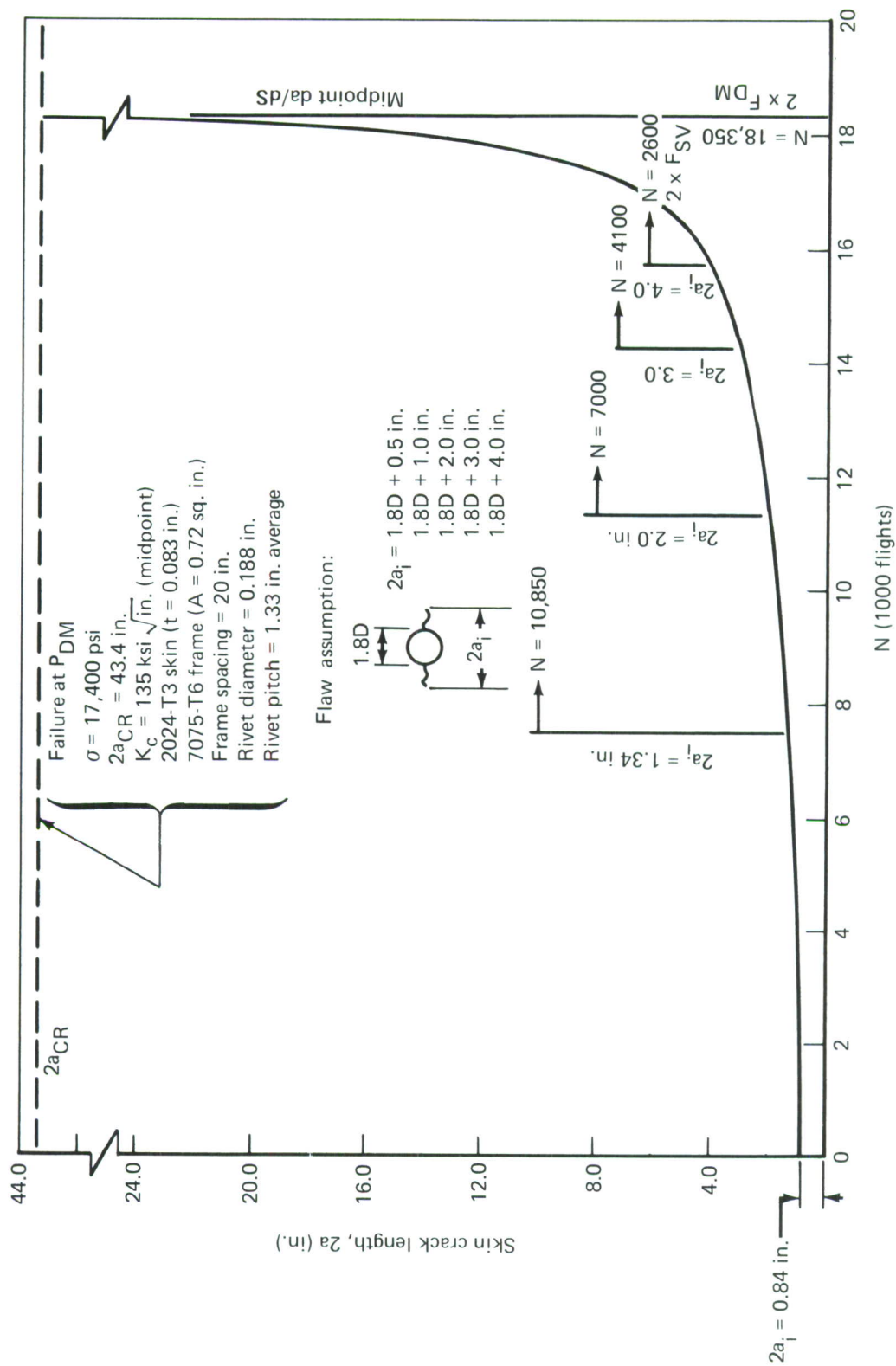


Figure 177. —Side-of-Body Location, Crack Growth From Detectable Flaw

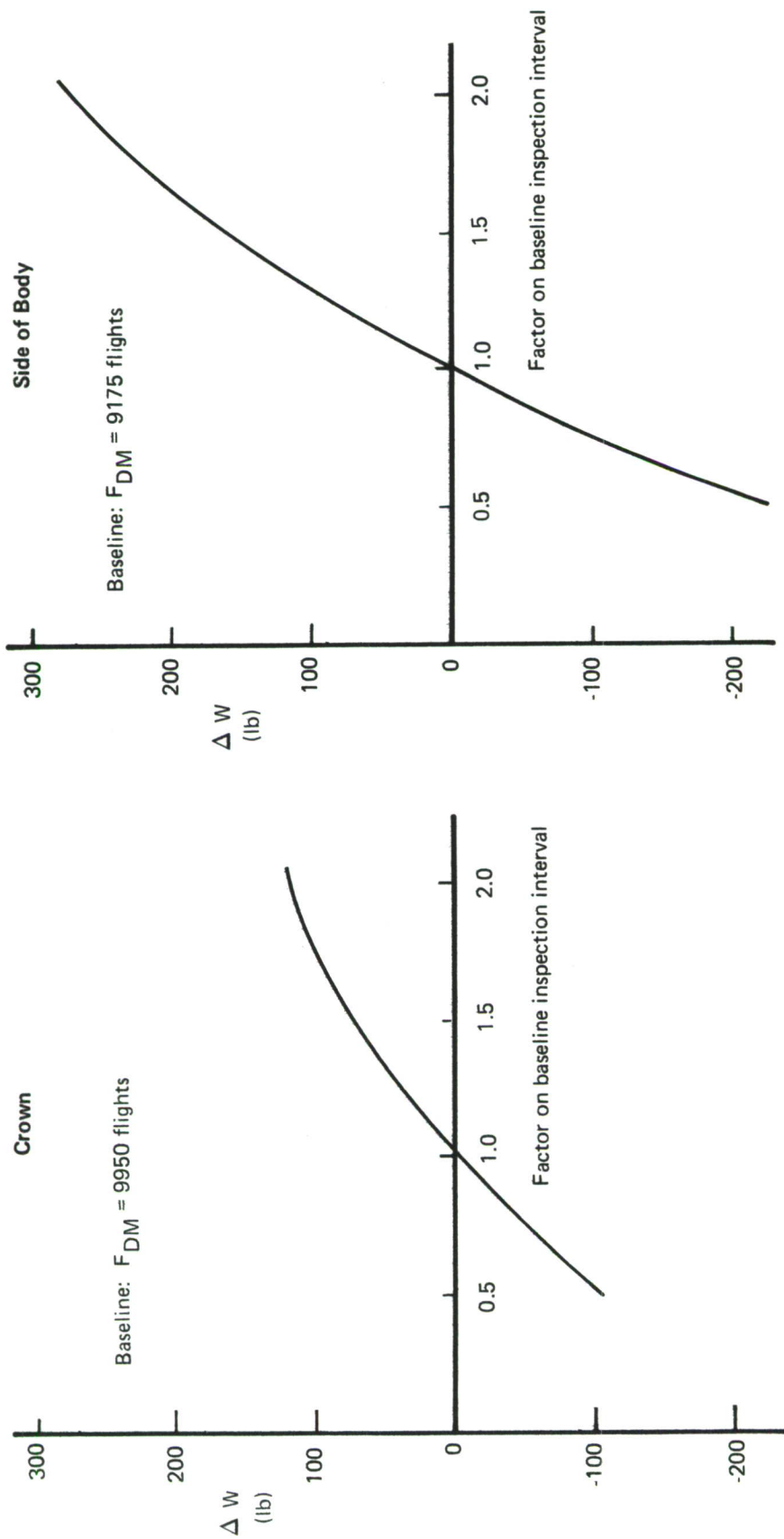


Figure 178. -Weight Increment Due to Variation in Depot Level Inspection Interval

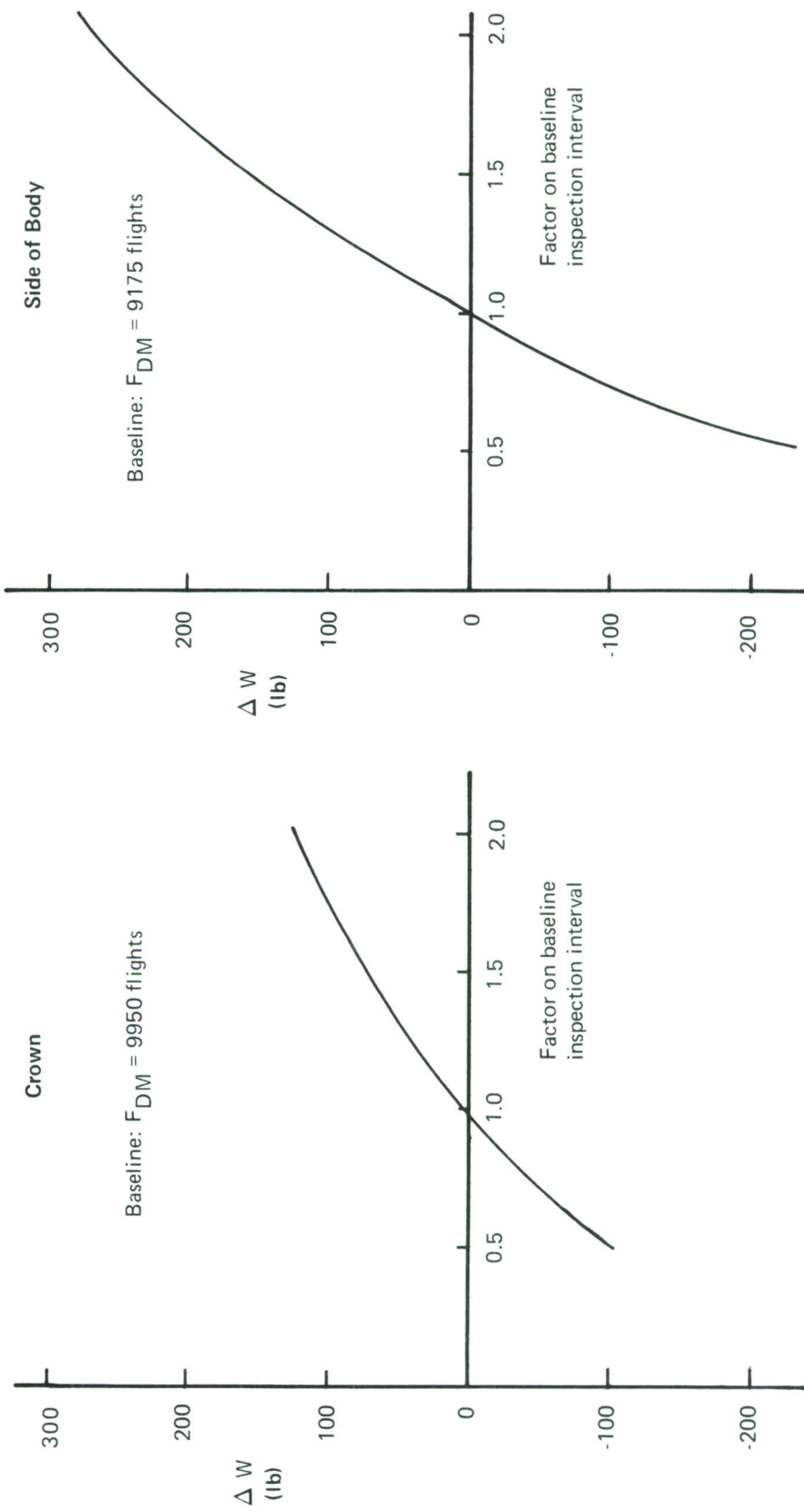


Figure 179. — Weight Increment Due to Variation in Special Visual Inspection Interval

The results of this study are shown in figures 176 and 177 for the crown and side-of-body locations, respectively. The impact on allowable stress and weight of the baseline component is shown in table XLII and figures 180 and 181.

(7) Effects of Varying Period of Safe Crack Growth After Failure of a Single Principal Element

A study was conducted to determine the impact of variation in the period of safe crack growth after the failure of a single principal element in multiple load path structure on allowable stress and structural weight.

This study was conducted for the crown location in the course of performing the study outlined in section VI-1c1. That study indicated that the crown skin failure occurs after stringer failure.

For the purpose of this study only, the minimum limit of detectability for depot level maintenance is assumed to be a failed stringer. It is felt that only under conditions corresponding to those called out in appendix I as depot or base level conditions, i.e., X-ray, etc., will there be a possibility of detecting failed stringers (lining, insulation, plumbing, or wire bundles are not normally considered as removable).

Assuming a stringer failure, inspection of figure 170 indicates that the crack growth life remaining in the skin after stringer failure is 3650 flights (midpoint values). Under the requirements of appendix I, depot level maintenance period, F_{DM} , is defined as once every 1825 flights. The impact of varying F_{DM} to

$$F_{DM} = \text{once every 3650 flights (2 x baseline)}$$

$$F_{DM} = \text{once every 5475 flights (3 x baseline)}$$

has been studied. The results of this study in terms of the impact on allowable stress and structural weight are shown in table XLII and figure 182.

This study was not conducted for the side-of-body location since the probability of a frame failure, given the baseline construction and materials, is virtually nonexistent. The requirement for consideration of a failed element should be based on a rational analysis, recognizing all parameters which affect crack growth; consequently, this requirement while reasonable for the crown is totally unrealistic for the side-of-body location.

(8) Effects of Multiple Defects

A study of service experience and fatigue damage reports accumulated on the commercial fleet (707, 727, 737, and 747) was conducted to determine the occurrence of multiple cracking. The initial flaw assumption of a pair of cracks emanating from fastener holes adopted for this entire study is in itself a multiple cracking assumption based on service experience.

Table XLII.—Impact of Variability of Damage Detectability Limits and Inspection Interval

Variable	Inspection interval	Baseline structure capability		Impact on stress and weight to maintain capability equal to baseline				Refer to figure
		Crown (flights)	Side of body (flights)	Crown ^a		Side of body ^b		
				Allowable stress GAG (psi)	Weight increment (lb)	Allowable stress GAG (psi)	Weight increment (lb)	
Variation in depot level inspectability limit								
$a_i = 0.25$ in.	F_{DM}	19,900	18,350	14,000	0	13,800	0	180 ↓
$a_i = 0.50$ in.	F_{DM}	11,400	10,850	12,500	90	12,000	204	
$a_i = 0.75$ in.	F_{DM}	8,500	7,800	11,700	151	11,000	347	
Variation in special visual inspectability limit								
$2a_i = 4$ in.	F_{SV}	1,500	2,600	14,000	0	13,800	0	181 ↓
$2a_i = 3$ in.	F_{SV}	1,950	4,100	14,800	-41	15,500	-150	
$2a_i = 2$ in.	F_{SV}	2,600	7,000	15,700	-83	17,900	-311	
Variation in depot level inspection interval								
Broken stringer Baseline F_{DM}^c	F_{DM}	—	—	14,000	0	Crown study only		182 ↓
Broken stringer 2x baseline F_{DM}	F_{DM}	—	—	12,100	119	Crown study only		
Broken stringer 3x baseline F_{DM}	F_{DM}	—	—	11,100	197	Crown study only		

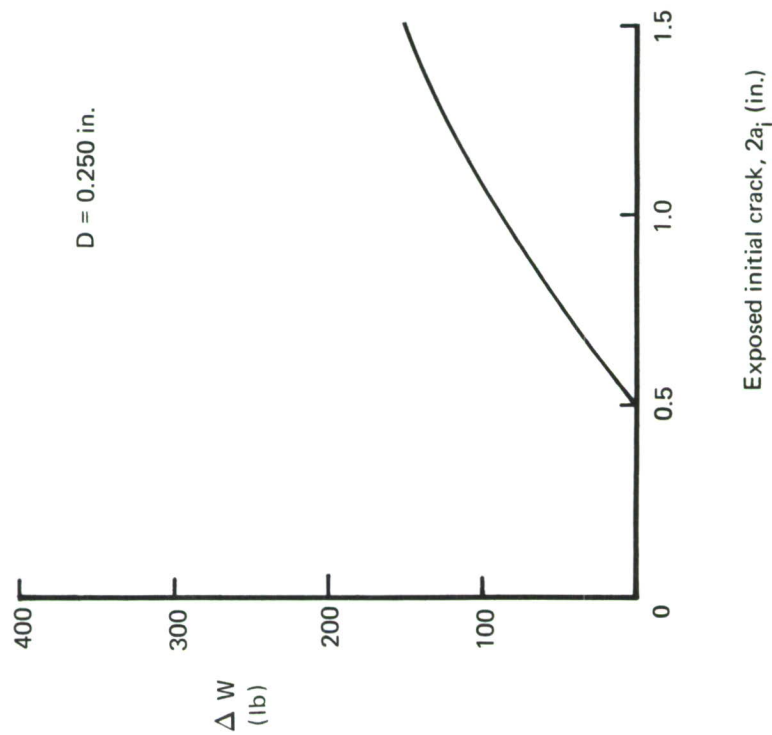
^aBaseline: Crown—Allowable stress, GAG = 14,000 psi

Panel weight (skin str) = 753 lb

^bBaseline: Side of body—Allowable stress, GAG = 13,800 psi
Panel weight (skin str) = 1,362 lb^cBaseline F_{DM} = 1,825 flights

- Baseline inspectability limit— $2a_i = 0.50$ in.

Crown



Side of Body

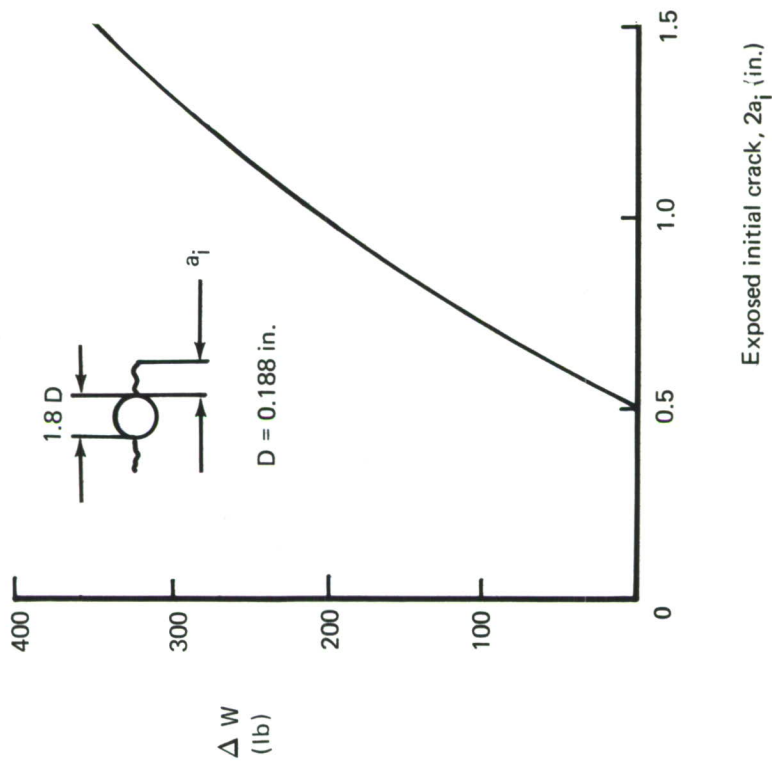


Figure 180.—Weight Increment to Maintain Baseline F_{DM} Capability—Variation in Depot Level Inspectability Limit

- Baseline inspectability limit $-2a_i = 4.0$ in.

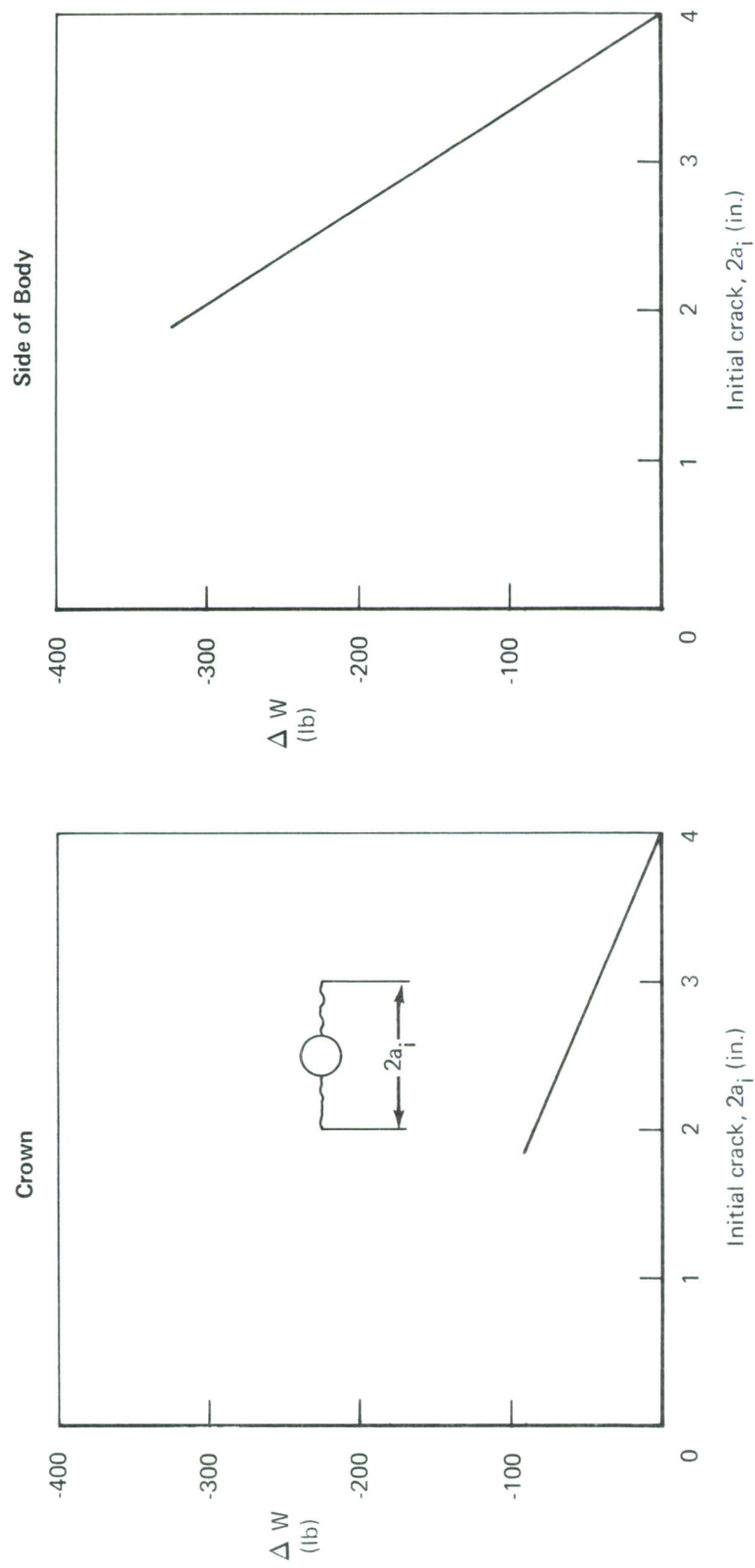


Figure 181.—Weight Increment to Maintain Baseline F_{SV} Capability—Variation in Special Visual Inspectability Limit

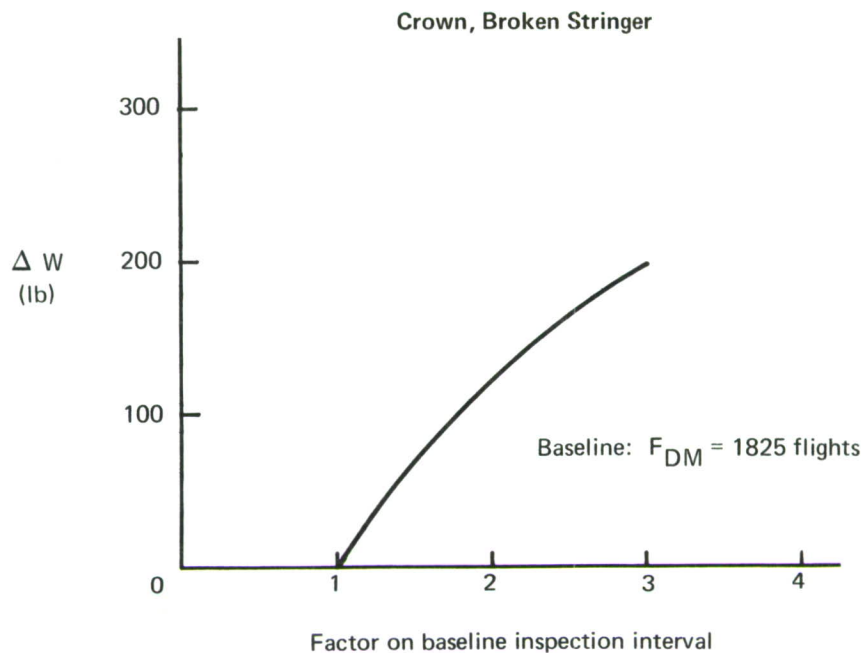


Figure 182.—Weight Increment Due to Variation in Depot Level Inspection Interval

The survey has identified isolated incidents of fatigue cracking at these locations (707 and 727 fleet); however, no incidents of multiple cracking have been observed at locations similar to those selected for this study. As a result, the assumption of multiple cracking is unwarranted at these locations; however, the sensitivity of period of unrepaired service usage predictions to an assumption of multiple cracking was studied at the following locations:

- Crown Location—The initial flaw defined in section VI-1c1 was assumed to exist at each skin-to-frame attachment point at body station 1580, in conjunction with an initial flaw in the skin/stringer attachment at that point. The crack growth life was then determined as the crack growth period to failure.
- Side-of-Body Location—The initial flaw defined in section VI-1c1 was assumed to exist at each skin/stringer attachment along S-23.

The results of this study are shown in figure 183. The impact of the multiple cracking assumption is noted when figure 183 is compared with figures 170 or 171. The period of unrepaired service usage capability, 123,000 flights at the crown location and 25,600 flights at the side-of-body location, is still greater than the total required operational life of the baseline.

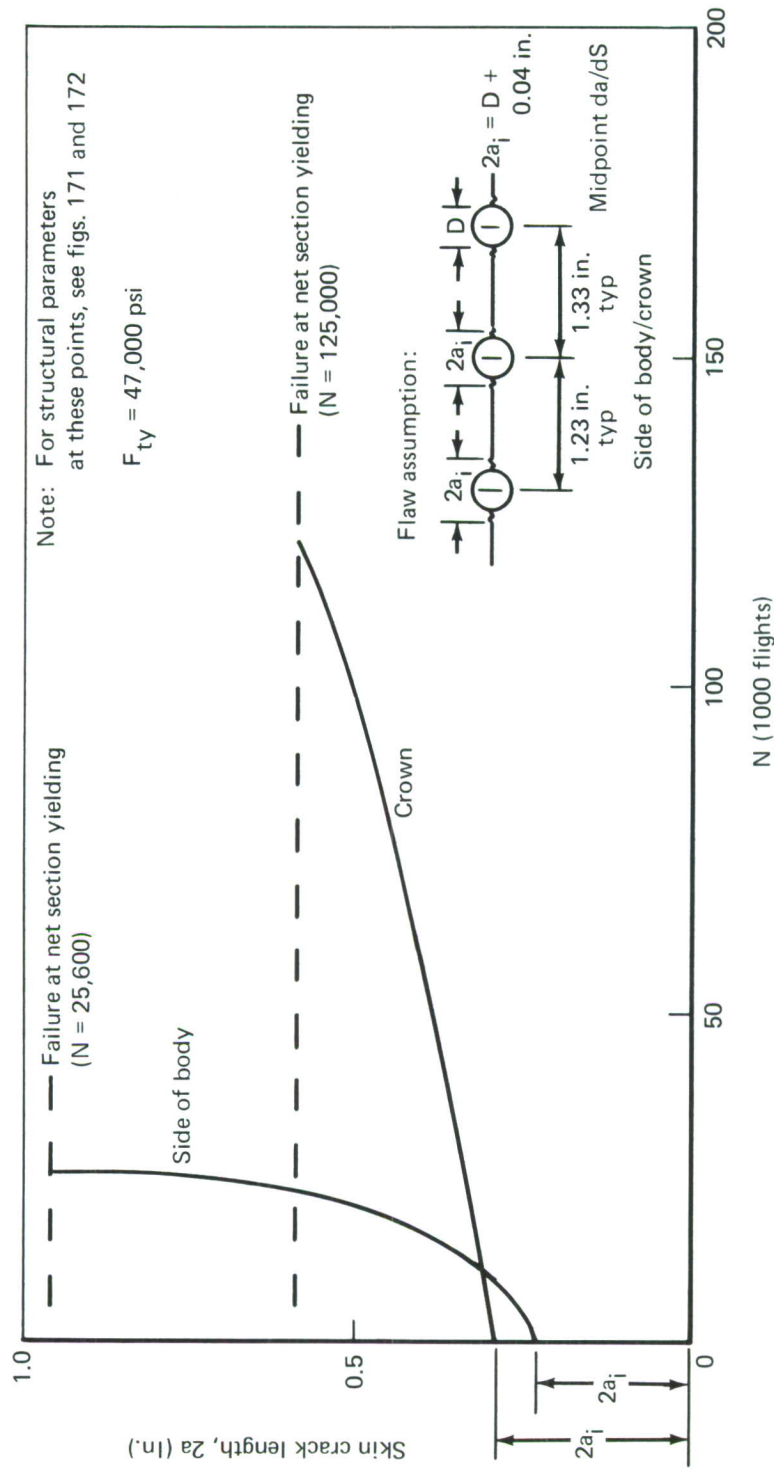


Figure 183. —Crown and Side-of-Body Locations, Crack Growth From Multiple Defects

(9) Effects of Varying Residual Load Requirement

Studies were conducted to determine the impact on stress levels, structural weight, and period of unrepairs service usage capability of varying the residual load requirement from that load which could occur in 100 inspection intervals, to that which could occur in 10 and 1 inspection intervals. The effects of varying the residual load strength requirements were analyzed for the following inspection intervals:

- Lifetime, P_{LT}
- Depot level maintenance, P_{DM}

This study was limited to the crown location (transverse cracking) since the stress exceedance curve (fig. 148) is virtually vertical at the side-of-body location. The residual load stress requirements are shown in table XLIII, as determined from figure 148. The results of this study in terms of the impact of allowable stress and structural weight on the baseline are shown in table XLIV.

It is noted that at this location the limit load stress is 29,000 psi, which is actually greater than that determined at 100 inspection intervals. The stress exceedance curve (fig. 148) was derived from the same data as were used to determine figure 184; however, the airplane response when flying the fatigue mission, representative of actual operation, is quite different from that used to determine civil fail-safe load levels. Civil regulations require that the fail-safe load requirement be obtained by "searching" the entire airplane operational envelope and determining the most critical flight condition which may occur. As a result, the 747 fail-safe condition under civil regulations was determined from a flaps-down maneuver condition at an altitude where full cabin pressurization exists. The fail-safe load stress levels presented in table XLIII result from flaps-down maneuver during the approach segment of the fatigue mission. The insensitivity of life predictions, with resulting structural changes due to the variation in residual strength load requirement, is due to the extremely long critical crack lengths and the rapid crack growth as critical length is approached, i.e., the crack growth curve is nearly vertical at this time.

d. Concluding Remarks

Due to the low operating stresses on the baseline structure, the allowable periods of unrepairs service usage are a multiple of those called out as typical in the attachments to appendix I. The typical values specified in the attachment to appendix I and those determined in these studies are summarized in table XLV for a 60,000-hour transport airplane.

The low stress levels imposed on the baseline airplane due to the use of the low static strength 2024 skin material and reduced fatigue capability of riveted construction results in a high degree of damage tolerance. The application of the increased working stress levels to the baseline component to enhance structural efficiency and reduce cost and weight will in itself tend to reduce damage tolerance capability. However, it is felt that with proper attention to damage tolerant design details, and the application of advanced concepts and materials, damage tolerance capability will be maintained.

Table XLIII.—Residual Load Requirement for Crown Location

Type of inspection	Inspection interval F_{xx} (flights)	f_{xx} at $100 F_{xx}$ (psi)	f_{xx} at $10 F_{xx}$ (psi)	f_{xx} at F_{xx} (psi)
Lifetime	20,000	26,400	24,500	22,200
Depot level	5,000	25,200	23,200	21,000
Special visual	500	23,100	21,000	18,900

Table XLIV.—Effect of Varying Residual Load Requirements

Inspection interval F_{xx}	Factor on F_{xx} (N)	Impact on baseline structure capability F_{xx} (flights)	Impact on stress and weight to maintain baseline capability	
			Allowable stress GAG (psi)	Weight increment (lb)
Lifetime	100	126,000	14,000	0
	10	126,000	14,000	0
	1	131,000	14,000	0
Depot level	100	10,000	14,000	0
	10	10,500	14,000	0
	1	11,600	14,450	-22
Special visual	100	750	14,000	0
	10	2,750	18,400	-178
	1	3,750	19,600	-218

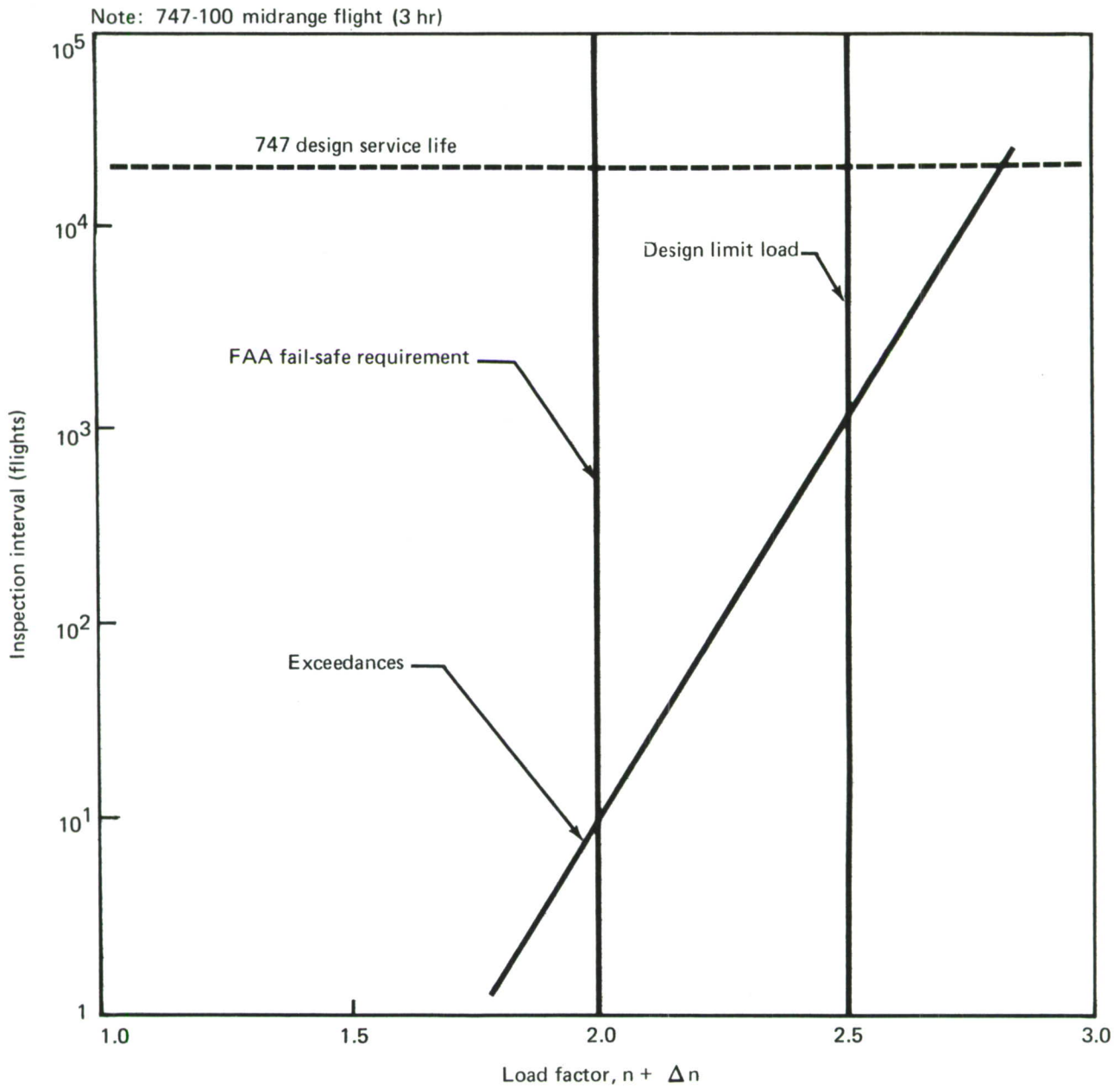


Figure 184.—Load Factor Exceedances for 100X Inspection Interval

Table XLV.—Baseline Capability Compared to Typical Requirements

Type of inspection	Inspection interval	Period of unrepaired service use (flights)		
		Typical (app. I)	Baseline capability	
			Side	Crown
Lifetime	None	20,000	48,700	126,000
Depot level	1/4 lifetime	10,000	18,350	19,900
Special visual	1 year	^a 1,200	2,600	1,500

^a The special visual inspection interval is determined at an annual average utilization rate of 1800 hours per year at the 3-hour average mission. MIL-STD-1530 (USAF), table II, specifies that for medium and heavy cargo aircraft, 15,000 fuselage pressurizations are required over the 25-year service period. This results in an average utilization rate of 600 flights per year.

2. SURVEY OF 747-100 SERVICE EXPERIENCE

a. Introduction

Service experience accumulated on the baseline structure was assessed to identify the thermal and chemical environment spectra applicable to the baseline. The results and conclusions made on the basis of this study follow.

b. Exterior Environment

To define the typical 747-100 service environment, the route structure has been reviewed for specific weeks in 1971 and 1972. These data are believed to be typical for the 747 fleet usage during the entire operational life of the 747 because the 747 is normally bought for specific routes, and economical operation of the aircraft does not allow a large degree of flexibility in route selection.

The commercial 747-100 airplane contains a flight recorder, which records time, heading, and altitude of the airplane in addition to load factors for the center of gravity. The data contain no environmental information such as temperature and humidity. The data are analyzed by DOT and NASA Langley but are not yet available for the 747-100.

Since actual flight experience of individual airplanes is not available for analysis, the environment must be assessed from the route structure and the frequencies of flights. The routes were characterized as:

- Polar
- North Atlantic
- North Pacific
- South Pacific
- Continental North America
- Continental Europe
- Eurasia
- Tropical

The flights scheduled for the first weeks of September 1971 and May 1972 (ref. 15) are shown in table XLVI. The table gives the flight hours involved and the distribution of geographical locations in percentage of total flight hours. The differences between the two weeks of September 1971 and May 1972 are small and as a consequence the most recent data (May 72) are used in the following discussion.

Table XLVI.—Scheduled 747 Flights

Routes	September 1971 flight hours		May 1972 flight hours	
	Hr	%	Hr	%
Subarctic	56	0.5	380	3.3
North Atlantic	4,812	45.3	3,500	29.8
North Pacific	1,607	14.8	1,494	12.8
Continental North America	2,286	23.4	3,300	28.2
Continental Europe	127	1.2	260	2.2
Eurasia	1,407	13.1	1,456	12.4
Tropical	159	1.7	1,330	11.3
Total	10,627	100	11,720	100

During this period approximately 150 airplanes were in service; thus, the average utilization is 11.1 flight-hours per day and 12.9 parking hours. It is assumed that parking occurs in the same locality as flights, so that for each 11.1 flight-hours in a certain environment the plane is subject to 12.9 hours of parking at sea level in that environment. This assumption probably overestimates the amount of parking time in Subarctic regions, where the only airport used is Fairbanks. Accordingly the hours were cut and added to parking time in midlatitude airports. Table XLVII shows the climates and hours spent in each environment (data taken from ref. 16).

Data on actual exterior environment are inadequate for refined analysis as well as characterization of different operational areas. The data gathered are mean values typical of zones around the world, and do not reflect local specific conditions or the large variability of weather for the same latitude. Some general conclusions may, however, be drawn from the data:

- Because an airplane is on the ground most of the time, this phase of operations requires further study. This comment is further reinforced by observing the small variability of the flight environment.
- Except for the tropical flights (Tropic, South Pacific) all flights during the year are conducted in air between -53° and -69°F at a relative humidity of approximately 30%. This is an extremely small variation even if the tropical flights are included (-16°F and 20% relative humidity).

Table XLVII.—Exposure Hours Per Week For Various Routes (January and July)

Area	Month	Environment ^a	Temperature (°F)	Humidity (%)	Hours exposure
Subarctic	January	F	-67	30	380
		P	3	80	200
	July	F	-53	30	380
		P	57	75	200
North Atlantic	January	F	-69	30	3500
		P	3	80	4060
	July	F	-54	30	3500
		P	57	75	4060
North Pacific	January	F	-67	30	2600
		P	30	77	3000
	July	F	-72	30	2600
		P	70	75	3000
Continental North America	January	F	-67	30	3300
		P	30	77	3900
	July	F	-72	30	3300
		P	70	75	3900
South Pacific	January	F	-16	20	180
		P	78	75	210
	July	F	-16	20	180
		P	78	75	210
Continental Europe	January	F	-67	30	260
		P	30	77	400
	July	F	-72	30	260
		P	70	75	400
Eurasia	January	F	-67	30	350
		P	57	80	400
	July	F	-64	30	350
		P	82	80	400
Tropic	January	F	-16	20	1150
		P	78	75	1340
	July	F	-16	20	1150
		P	78	75	1340

^aF denotes flight environment

P denotes park environment

c. Interior Environment

Airplane interior environment is much more complicated to characterize than the exterior environment. When the airplane systems are working, air is delivered to the cabin interior from the air-conditioning units; this air has very uniform temperature and is generally very dry: relative humidity is less than 10%.

During flight operations air to the interior is delivered from the compressor stage of any engine. The air is cooled, compressed, and dehumidified before entering the cabin. This way the air on entering the cabin has equal or less moisture than the ambient air, which typically has 20%-30% relative humidity at -50°F. The structure in the shell and the air next to it experience ambient temperature (-50°F) and somewhat less than 20%-30% relative humidity.

Interior structure insulated from the fuselage shell is subject to 60°-70° F air at a relative humidity of 10%.

No actual data exist on the structural environment in the interior of the 747-100, so the only indications come from service reports and structural inspection records.

d. Maintenance Requirements and Observed Structural Deficiencies

In the Boeing Maintenance Manual for the 747, maintenance and inspection are categorized in A, B, C, and D checks in addition to structural inspection after 4500 and 9000 flight-hours. The required maintenance operations and the intervals between A, B, C, and D checks, as well as the structural inspection, are determined by the FAA 747 Maintenance Review Board (MRB), which updates the operations and the schedule as required by the experience of the operators and reports from inspections.

Mechanical problems found at unscheduled times are reported by the FAA in Mechanical Reliability Reports (MRRs) which are sent to all 747 operators by Boeing in monthly letter reports, which also include the findings of the structural inspections at 4500 and 9000 hours.

No structural inspection is scheduled for body section 46 at 4500 hours. The first scheduled structural inspection is conducted after 9000 hours of operation; however, investigation of MRRs indicates that structural damage is detected at nonscheduled inspections during the normal course of servicing.

No serious or potentially serious structural problems have developed in section 46 of the 747-100 airplane.

3. ASSESSMENT OF NDI DEMONSTRATION PROGRAM

a. Introduction

Structure qualified to the minimum periods of unrepaired service usage specified in appendix I, using the initial flaw assumptions defined in that specification, are classified as "non-fracture-critical" and as such are subject to normal procedural quality control. Structure analyzed to initial flaw assumptions smaller than those defined in appendix I are considered, by Boeing definition, to be "fracture critical," category FC-I (sec. IV-4c2), and are subject to special quality control inspection techniques which are intended to ensure the detection and elimination of flaws larger than those assumed in the analysis. Appendix I requires that the intended special quality control inspection procedure be demonstrated to be capable under production conditions of detecting those assumed smaller flaws to specified confidence and reliability levels.

The baseline 747 fuselage shell structure has been determined to be non-fracture-critical; consequently, no NDI demonstration program would be required. However, to assess the production impact of an NDI program, a demonstration program has been prepared.

A study has been made to determine the method of conducting an NDI demonstration program to demonstrate the capability of various NDT techniques to detect initial flaws smaller than those specified in appendix I. This program has been established for the baseline monocoque structure as if that structure were fracture critical, category FC-I.

The demonstration program is planned to develop statistically meaningful data defining the capability of nondestructive inspection methods to detect surface and hole flaws in a production environment. Detection capabilities will be assessed for penetrant and eddy current nondestructive inspection methods. These methods are considered the most practical for this investigation.

Laboratory data have often been used in the past to imply production inspection capability of a particular NDT technique without taking into consideration the actual inspection conditions which may significantly influence the capability of that NDT technique. Every effort has been made to accurately represent actual production conditions when conducting the demonstration program.

b. General Approach

This program is organized in a manner to provide a statistically valid evaluation of the flaw detection capability of the penetrant and eddy current methods when applied to specimens containing manufacturing defects closely representative of those which may be expected in a production part. It is intended that the penetrant inspection be demonstrated to exhibit the required sensitivity to detect surface flaws. It is also intended that the eddy current inspection technique be validated for use in the detection of flaws emanating from holes. These methods were selected on the basis of their known capabilities under laboratory conditions and their practicality under production conditions.

The specimen configuration to be tested, and the manner by which it is introduced into the normal inspection system, is of fundamental importance to the goals of this program. The specimen configuration is to be small and is to resemble production parts. The size criterion is to facilitate cleaning of the specimens in an ultrasonic cleaning tank. This will involve fabrication of many specimens with a selected percentage of specimens having flaws.

The final specimen configuration selected will be similar to production parts typical of airplane sections, to minimize awareness of the operator that he is being evaluated, a key consideration in this program. This will also involve issuance of normal paperwork through Planning. The types of flaws to be fabricated have been selected as highly representative of the production flaw geometries.

A method of fabricating flaws is planned which has a number of advantages for a program of this kind. The compressed notch lends itself to predetermining precisely the shape, dimensions, and location of the flaw within the finished machined test specimen. It provides a discontinuity better suited to NDI methods than unmodified EDM notches and at much less cost per flaw than fatigue cracks.

The Boeing Commercial Airplane Company has received a contract from AFCS (contract F33615-72-2202), in which the use of the compressed EDM notch was proposed for the representation of manufacturing-type defects. Deliberately created fatigue cracks have been broadly accepted as approximating natural flaws in NDT sensitivity studies, as NDT standard flaws, and in linear elastic fracture mechanics investigations. However, the compressed EDM notch was adopted by the Air Force in this contract as more closely simulating production processing flaw characteristics important to NDT detection capabilities. The majority of naturally occurring production flaws occur during processing involving permanent deformation (rolling, forging, extruding, forming), and the more difficult flaws to detect reliably are those that originated during, or were later subjected to, plastic compressive straining. Fatigue cracks, by contrast, usually are created below the elastic stress limit and develop fewer of the characteristics of production flaws.

Work is presently in progress to identify the critical flaw fabrication parameters (EDM notch size, compressive strains, etc.) and to completely define the capability of the proposed procedure. In the event that this procedure proves incapable of producing satisfactory flaw characteristics for purposes of this program, it is intended that the test flaws be fabricated by means of cyclically loading EDM notches to initiate and propagate a fatigue crack with subsequent machining of the item to produce the desired results. This alternate method of flaw fabrication will result in an increase in the cost of this program; however, since the major cost items are the required NDT inspections and paperwork, the increment in total program costs is considered minor.

c. Specimen Fabrication

The material selected represents the skin and stringer material used in the 747 cargo crown fuselage section—2024-T3 aluminum for the skin and 7075-T6 for the stringer. Thickness will range between 0.062 and 0.310 inch.

The fabrication of flaws by compressing sawcuts and EDM notches is a straightforward method that has been previously used at Boeing. It is easily controlled, but has not been documented to fully account for such things as change in flaw size and width as a function of compressive strain. Manufacturing shop operations will be recorded and results assessed in sufficient detail to permit duplication.

Artificially flawed inspection test specimens will be fabricated in configurations shown in figures 185 through 189.

Specimen E-1 will contain a small compressed EDM slot as shown in figure 185. The specimen is cut to the final shape required with the grain direction shown. The sheet is bent on a standard bending fixture, with the bend greater than 90°. A small EDM notch is placed on the bend radius as shown. The sheet is then bent back to 90°, which results in the required notch compression.

Specimen E-2 will be similar to E-1. However, the small, compressed EDM slot will be on the inside radius as shown in figure 186. The EDM notch is placed in a preformed part which is then bent as shown to produce the required notch compression.

Specimen E-3 will contain a small, compressed EDM notch emanating from the hole as shown in figure 187. A flat sheet with a grain flow as shown is bent and notched on the convex surface. The sheet is then flattened by reversed bending to result in closure of the notch. High-intensity shot peening will be used as necessary on the lower surface to eliminate the elastic recovery (springback) which would otherwise cause a partial reopening of the notches. A sheet for the top panel with matching drilled holes is bolted together with the bottom panel to cover the EDM notch.

Specimen E-4 will contain a small, compressed EDM notch as shown in figure 188. An EDM notch is placed in a strain-concentrating groove as shown and compressed to close the notch. After compression, the groove is machined off to leave a compressed notch on the surface.

Specimen E-5 will contain a small, compressed EDM notch as shown in figure 189. Holes are drilled and EDM notches placed as shown. The specimen is compressed as shown. The holes are redrilled or reamed to the size of flaw required. Additional holes are drilled in locations shown.

d. Inspection Procedures

Repeated inspections of the specimens will be made to acquire a statistically significant number of observations. These will be conducted in such a manner as to ensure that each inspection is independent of the others. Inspections will be performed with different personnel, equipment, and equipment standardizations, and at times and locations sufficiently varied to obtain unique observations. All inspection and test instruments will have current approval of the Boeing Calibration/Certification Laboratory to ensure proper and accurate functioning.

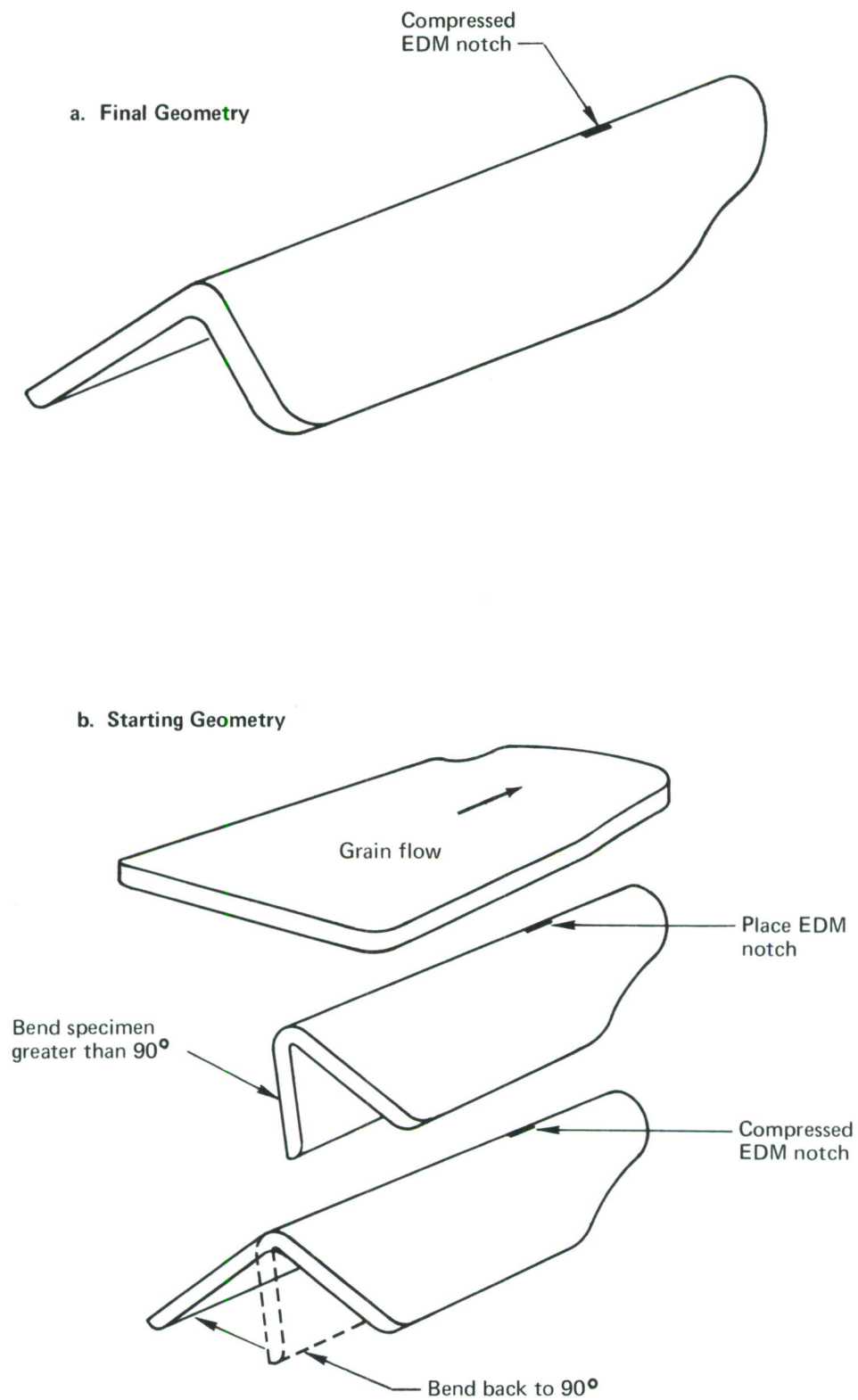
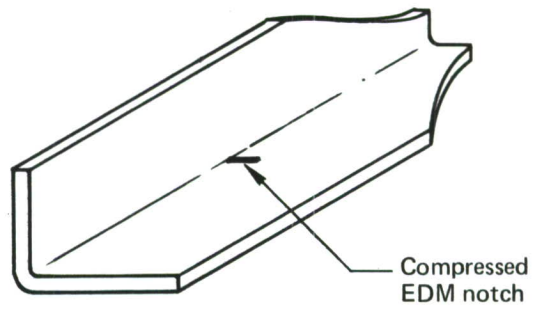


Figure 185.—Surface Flaw Specimen E-1

a. Final Geometry



b. Starting Geometry

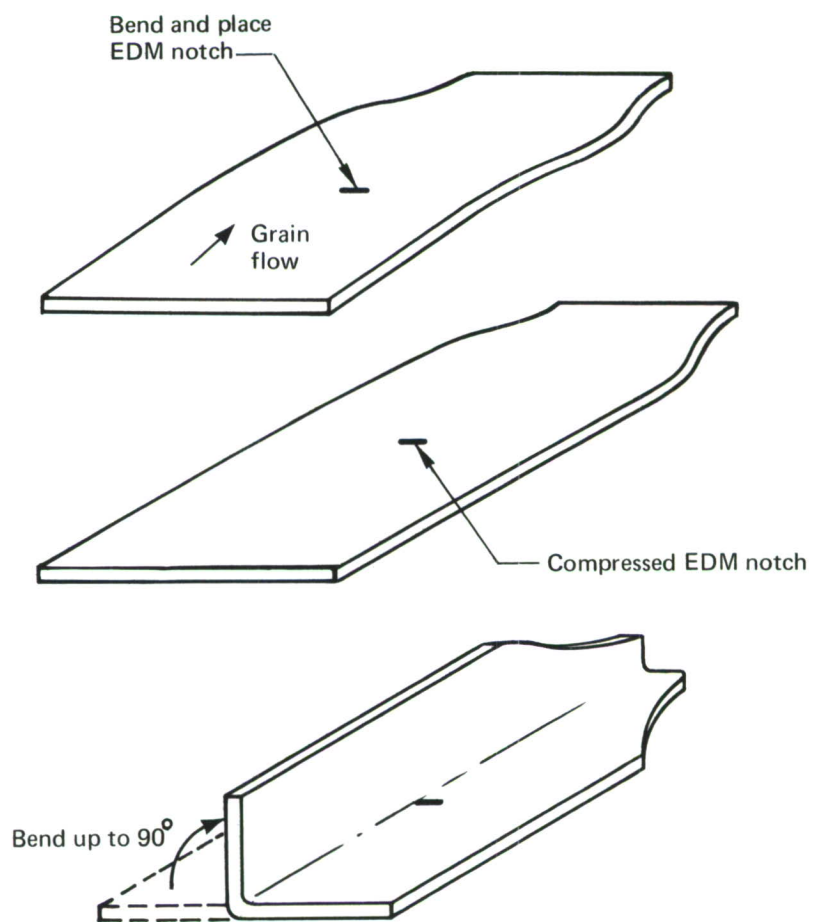


Figure 186.—Surface Flaw Specimen E-2

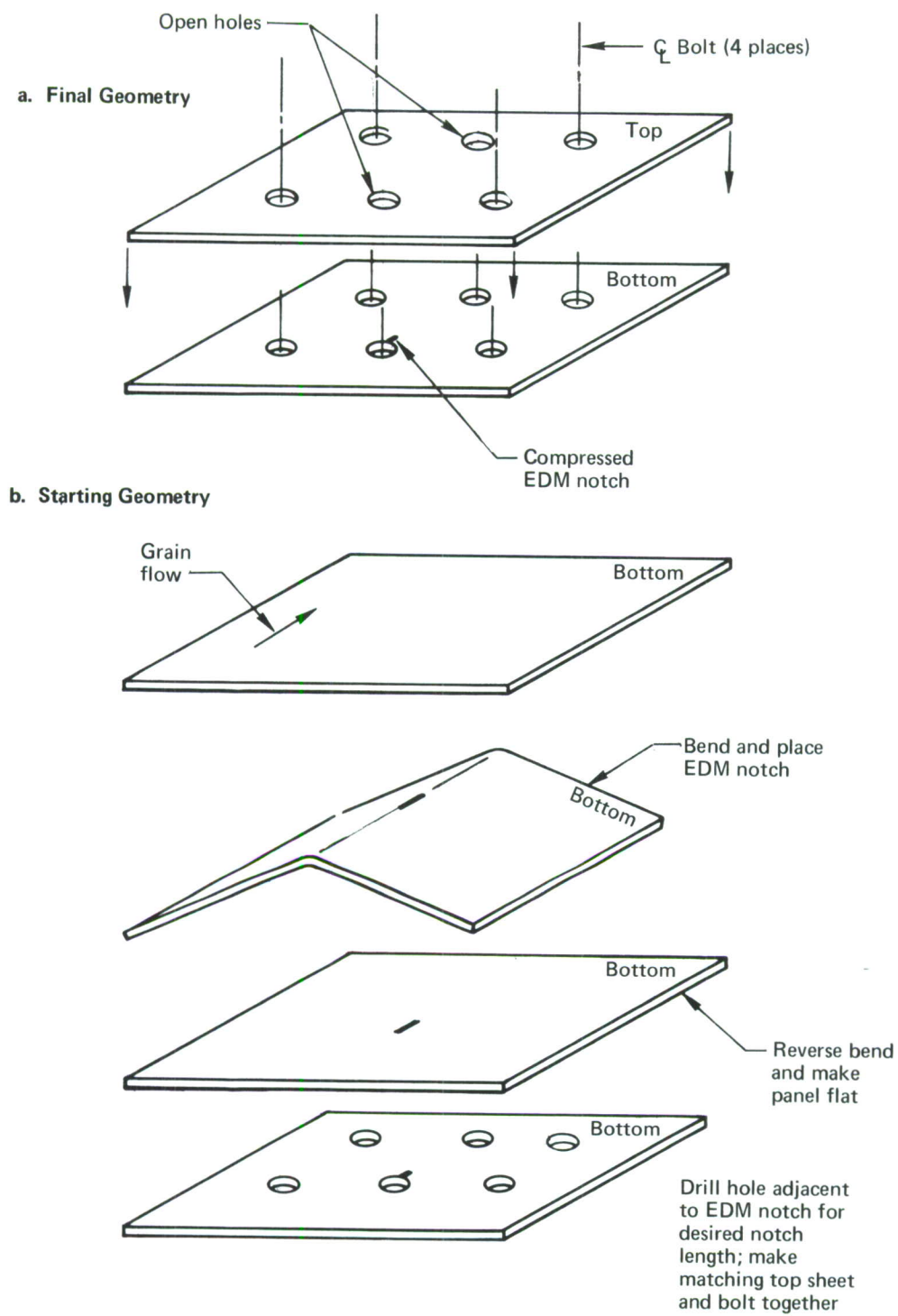
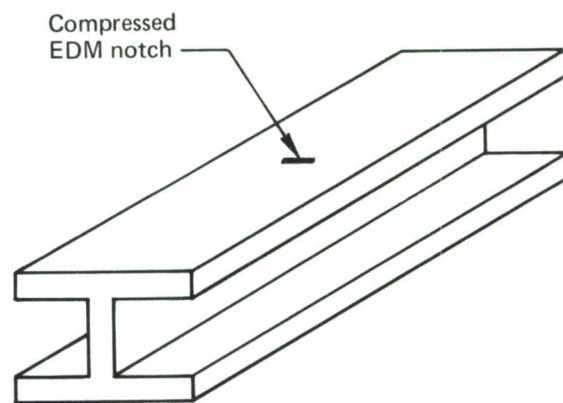


Figure 187.—Hole Plan Specimen E-3

a. Final Geometry



b. Starting Geometry

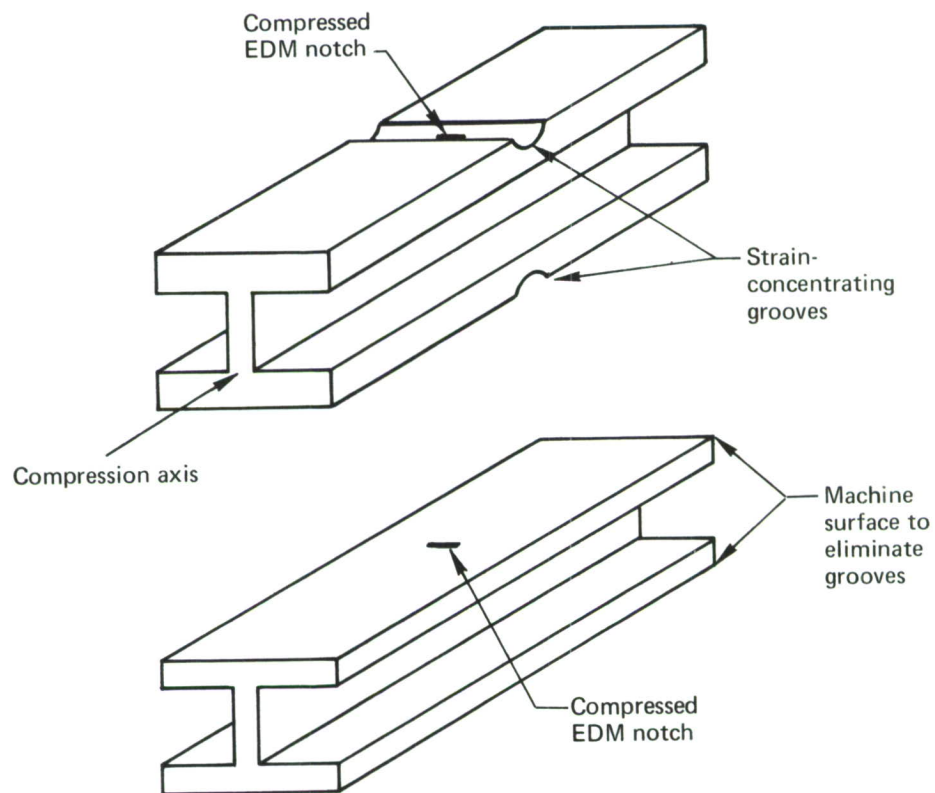
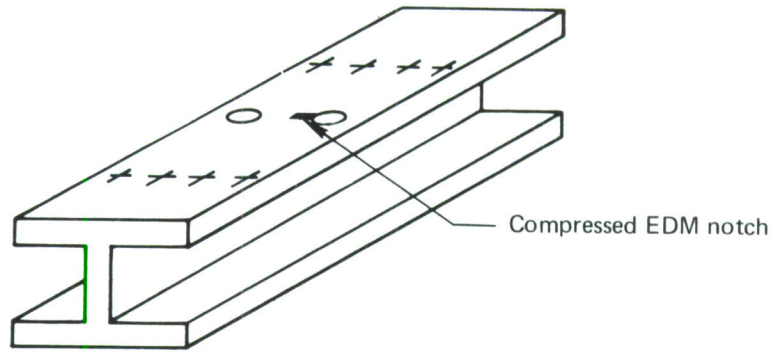


Figure 188.—Surface Flaw Specimen E-4

a. Final Geometry



b. Starting Geometry

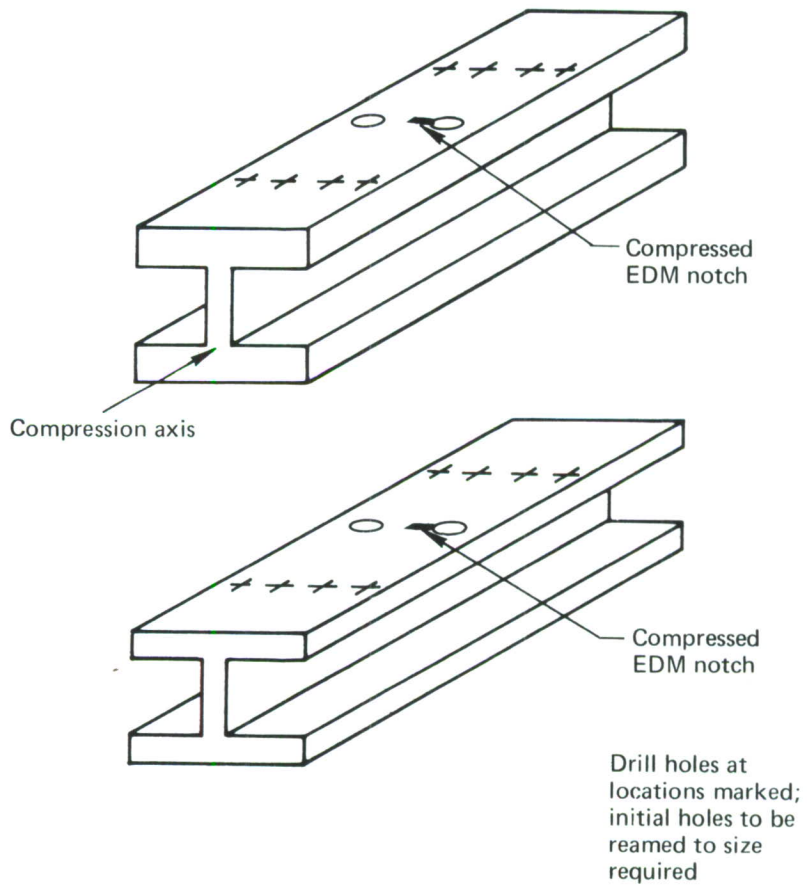


Figure 189.—Hole Flaw Specimen E-5

The sequence of inspection will be controlled through normal manufacturing planning procedures. These procedures will be written to minimize operator awareness that a special NDT demonstration program is in effect. To eliminate the human element from this evaluation, it is intended that the knowledge that a demonstration program is in progress be restricted to the manufacturing planner and program engineer.

(1) Penetrant Inspection

The penetrant inspection procedure for surface flaw inspection will be performed according to a Boeing process specification which meets the requirements of government specifications MIL-I-6866 and will represent the current state of the art.

The post-emulsification, fluorescent penetrant system will be used with a wet developer for the laboratory test. The Magnaflux Corporation product ZL-30A, a high-sensitivity system, will be used. Six production inspection facilities will be used for the demonstration of penetrant inspection capabilities in a shop environment. Two levels of sensitivity, high and medium, will be represented in the production environment utilizing both post-emulsifiable and water-washable penetrant. Table XLVIII outlines the type of operation, penetrant, and sensitivity level.

Table XLVIII.—Penetrant Facilities

Type	Penetrant	Sensitivity
Electrostatic	P-133 P-134 D-499C	Medium
Dip operation	ZP-2A ZP-5	Medium
Dip operation	P-133 D-499B	Medium
Dip operation	ZL-2A ZL-4B ZP-4A	High
Dip operation	HM-407 ZP-13	Medium
Dip operation	P-133 D-499B	Medium

The most critical problem of post-inspection cleaning relates to repeated inspections by the penetrant method. It is necessary that each inspection be followed by a thorough cleaning so that the specimen presented for each successive inspection has been restored to its original, contamination-free condition. The problem has long been recognized in penetrant inspection studies of comparative evaluations of inspection materials, manufacturing processes, and relative capabilities of facilities or personnel. Cleaning procedures have been developed which, while seemingly satisfactory, have not been thoroughly tested nor defined in a process specification. Current Boeing practice for

cleaning fatigue cracks has been a prolonged (30 minutes) immersion in acetone while exposed to a 6.11 watts per centimeter ultrasonic cleaner. This practice will be the takeoff point for the investigation of optimum reproducible cleaning procedures. Other approaches using vapor degreasing, cyclic solvent, and thermal exposures will be examined.

This portion of the program will be dependent upon the demonstration of wholly effective cleaning between inspections, as described in section VI-3a1. Development of the cleaning procedures must precede the penetrant inspection evaluation.

(2) Eddy Current Inspection

Eddy current inspection procedures for the detection of cracks emanating from holes will be defined in a Boeing process specification. This is required as this inspection is not normally performed in the production environment after the shop has fabricated holes in parts.

The eddy current hole inspection will be conducted with commercially available hole probes and the Magnaflux ED-520 eddy current instrument. The instruments will be calibrated on crack standards and procedures outlined in the Boeing process specification.

Three inspection facilities will be used for demonstration of eddy current capabilities in a shop environment.

e. Flaw Characterizations

Optical methods will be used to determine the flaw length and width at the surface of specimens for use in penetrant evaluation. Depth measurements will be taken for the flaws emanating from fastener holes. Fracture examination will be used on selected flaws to establish actual flaw dimensions in the plan view. Flaw opening width, as a dimension significant to penetrant sensitivity, will be determined by optical and electron microscopy of specimen surfaces after the conclusion of NDI tests.

f. Records

Detailed records will be obtained and kept for each inspection operation. All operational functions pertinent to performance will be recorded, as well as the inspection results obtained. Operational records will confirm that specified procedures were uniformly followed and may aid in interpreting any anomalies revealed by statistical analysis of the data.

g. Statistical Evaluation

Statistics for each flaw size, specimen configuration, and NDI method will be converted to sensitivity ratio ($SR = \text{number of successes} / \text{total opportunities for success or failure to detect flaw}$). Confidence limits will be calculated for SR assuming a binomial distribution and 95% confidence level. For sample sizes above 30, the normal approximation for the binomial and binomial probability plotting paper, based on the normal

approximation (such as Bradley binomial plotting paper produced by T.E.A.M., Inc.), will be used to simplify confidence limit calculations. For sample sizes less than 30, reference to "Tables of the Binomial Probability Distribution" (National Bureau of Standards, Applied Mathematics Series 6, 1950) will be made. A sample of 30 observations with no failures is needed to verify that SR exceeds 0.90 with 95% confidence; however, considering lack of a prior information and difficulty of exact sizing of flaws, SR as a function of flaw geometry will be estimated by interpolation from an appropriate plot such as figure 190. A sample of 10 observations with no failures is needed to verify that SR exceeds 0.90 with 50% confidence (assuming one-sided confidence limits and binomial distribution).

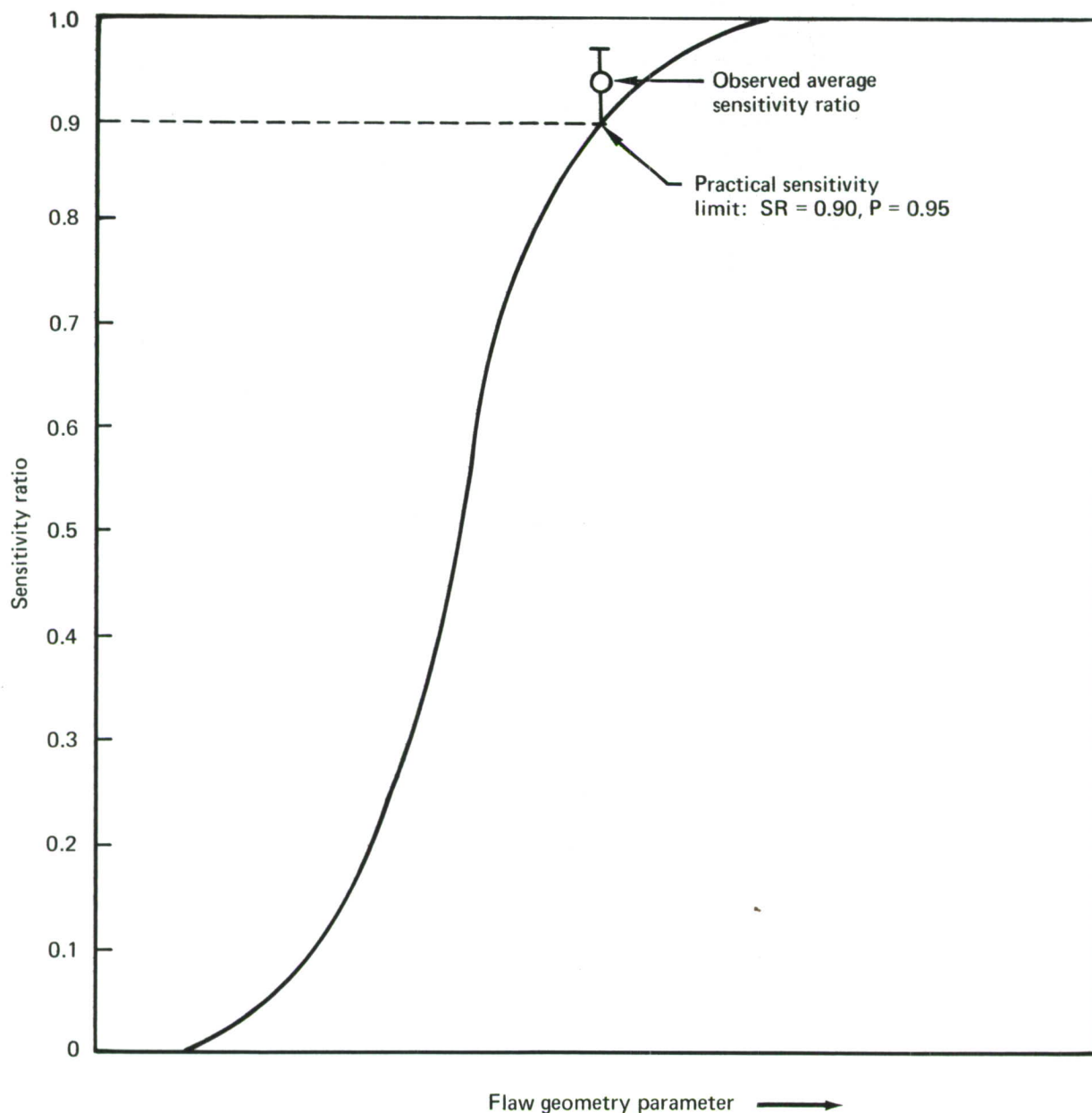


Figure 190.—Generalized Sensitivity Ratio

Figure 190 represents the expected generalized form of this plot with the SR = 0.90 point located exactly.

No interactions are expected between NDI tests, flaw size, and test facilities; however, there may be an interaction between flaw geometry and specimen configuration. For evaluating the significance of possible effects, contingency tables based on the chi-square distribution with observed vs expected numbers of successes and failures as the statistical parameters will be used whenever appropriate. Any statistical significance will be considered at the 95% confidence level.

Flaw quantities required will become exactly known only during the program. Initially, five sizes of flaws and five specimen configurations have been planned as shown in table XLIX as the likely minimum to ensure bracketing the 95% confidence interval that 90% of the flaws would be detected in a safe-life structure. In a fail-safe structure where a 50% confidence interval of 90% detection is required, fewer observations would be needed.

Table XLIX.—Specimen Requirements

Configuration	Alloy	Initial test	Flaw size range	Additional specimens	Applicable NDI	Total specimens
E-1	2024-T3	5	5	40	Penetrant	50
E-2	2024-T3	5	5	40	Penetrant	50
E-3	7075-T6	5	5	90	Eddy current	100
E-4	7075-T6	5	5	90	Penetrant	100
E-5	7075-T6	5	5	90	Eddy current	100

h. Estimated Man-Hours for Demonstration Programs

It is estimated that 9000 man-hours of engineering, planning, fabrication of test specimens, testing, data reduction, reporting, and coordination with AFML are required to implement the NDT demonstration program.

This estimate is based on demonstrating NDI capability of the 95/90 (reliability/confidence) level.

Since the demonstration of NDI capability to a 90/50 reliability and confidence level involves only a reduction in the required number of observations tested, it is estimated that the cost would remain essentially constant (9000 man-hours).

4. STUDY OF FRACTURE CONTROL PROGRAM IMPLEMENTATION— INCREMENTAL COST

All aspects of the application of the fracture control program required by MIL-STD-1530 were reviewed and analyzed. The estimated cost of applying the fracture control program to the baseline was determined along with potential modifications that would effect a cost reduction.

The salient distinction between the requirements of the fatigue and fracture control program as described in section 5.1.3 of MIL-STD-1530 and normal civil practice is in the additional controls imposed on parts considered to be fracture critical. A criterion for the identification of fracture-critical parts has been established in the course of conducting the damage tolerance analysis of the advanced cargo fuselage structural concepts (sec. IV-4c2, table XXIV).

This study is restricted to the baseline fuselage shell (skin and stringers), since this element represents a major portion of the structural weight of the baseline component and conclusions derived from this study may be considered to be applicable to the entire component. It has been determined that under the criteria adopted for the identification of fracture-critical parts, the entire baseline must be considered as non-fracture-critical; however, the impact of the application of all aspects of the fracture control plan to the crown and side panels has been analyzed as though these items were indeed fracture critical. The results of this study are shown in figure 191.

It is apparent that the common costs associated with the application of the fracture control program are insignificant when compared with those costs associated with the special controls required for fracture-critical parts. These incremental control costs for the side-of-body and crown panels (total shell weight = 3477 pounds) are:

FC-I parts: \$4.10 per pound

FC-II parts: \$21.50 per pound

FC-III parts: \$11.40 per pound

An adequate damage tolerance trade study conducted during the early design phases of a program will identify and minimize those items which must be designated as fracture-critical parts. No modifications to the requirements of the fracture control program are recommended.

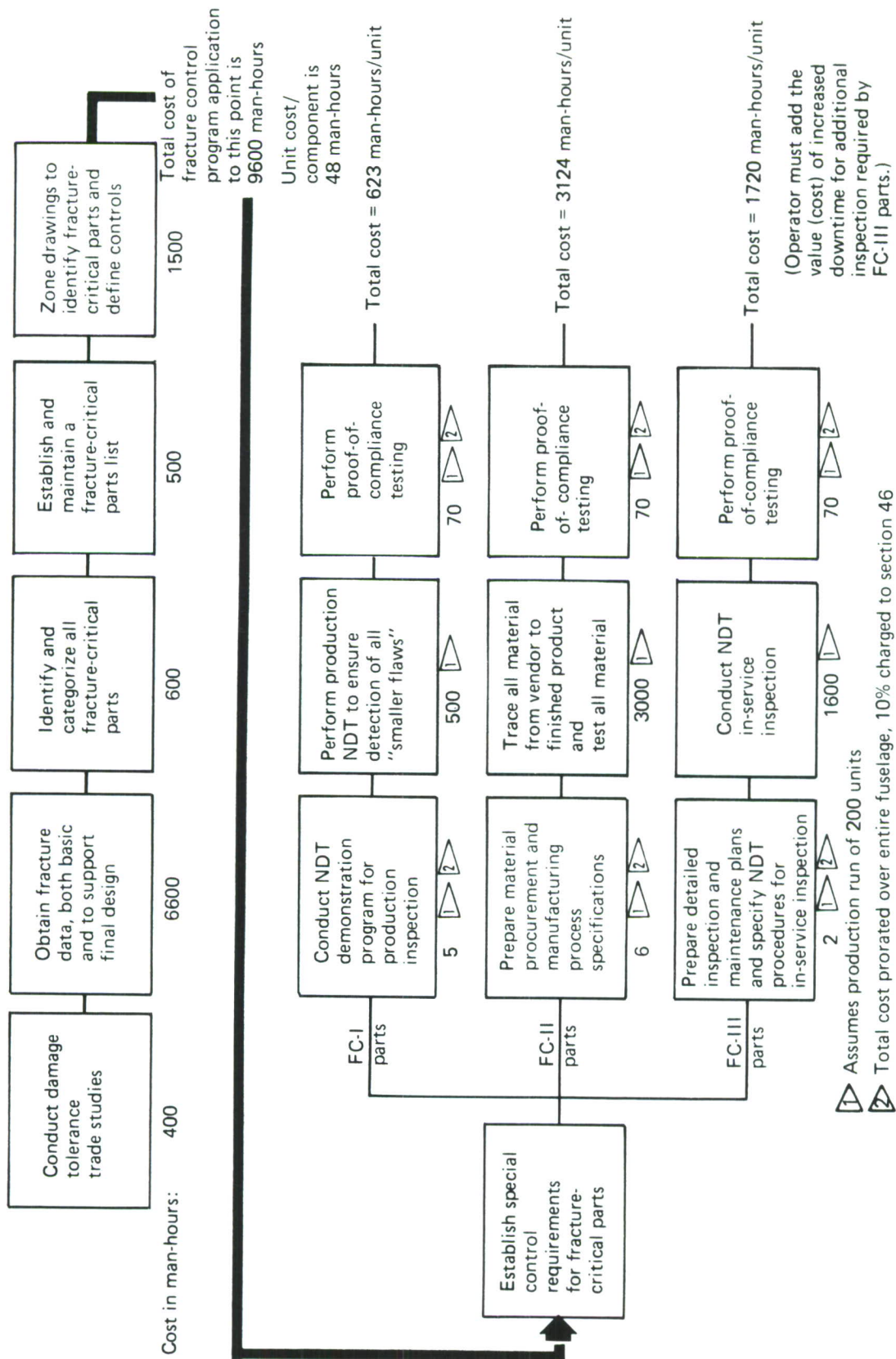


Figure 191.—Costs Associated With Application of Fracture Control Plan

5. STUDY OF ADVISABILITY OF PROOF TESTING IN LIEU OF NDT

Proof load testing has proved a valuable and important addition to conventional NDT evaluation for types of structure characterized by extremely small critical flaw sizes, e.g., pressure vessels, heavy fittings, and thick wing planks. This study assesses the role of proof testing as a supplement to or substitute for conventional NDT evaluation of the baseline fuselage shell. The feasibility of proof testing of the following was investigated:

- Panels
- Critical joints
- Large components (fuselage sections)
- Complete fuselage

The application of proof testing in lieu of or as an addition to conventional NDT techniques must be considered within the scope of the flaw sizes which the proof load is intended to expose and those manufacturing processes which may be reasonably expected to produce such flaws. A brief description of the manufacturing processes and assembly sequences involved in the fabrication of the study section follows.

The fabricated skin panels (fig. 192), side, bottom, and upper quadrant, are shipped to Boeing with frames, stringers, window reinforcing, etc., attached. These skin panels are then joined in an assembly jig together with the floor and floor support structure. The section is then removed from the assembly jig and mated to the adjacent fuselage sections at the section breaks. All joining is done by mechanical fastening in holes that are drilled in place. Damage tolerance criteria and related studies and service experience of section VI indicate that the primary source of flaws, which may degrade the period of unrepaired usage or residual strength capability of the structure, occurs at improperly drilled or reamed holes.

The use of mechanical fastening as the primary means of structural joining precludes the detection of potential failure sites by proof testing prior to the assembly of a complete fuselage. Individual elements could be proof tested prior to assembly; however, such proof testing could not expose potential problems at assembly splices. Since these assembly splices are critical fracture details, it is felt that proof testing of components is unwarranted. The practical aspects of applying sufficient loading to the assembled component to effect a proof test are formidable; however, this is not in itself sufficient reason to reject proof testing (as demonstrated by static load testing to failure of a complete airplane).

The primary limitation of linear-elastic fracture mechanics in the determination of proof load stress levels is that, at stress levels above the yield strength of the material, fracture cannot be described by the critical stress intensity parameter K_{IC} , and subcritical flaw growth cannot be described as a function of the crack-tip stress intensity factor, K . Empirical methods may be resorted to in order to overcome this limitation; however, other considerations, the discussion of which follows, militate against a proof loading program for the study component. As a result, the generation of empirically derived nonlinear fracture mechanics data, and the attendant cost of the test program required to generate such data,

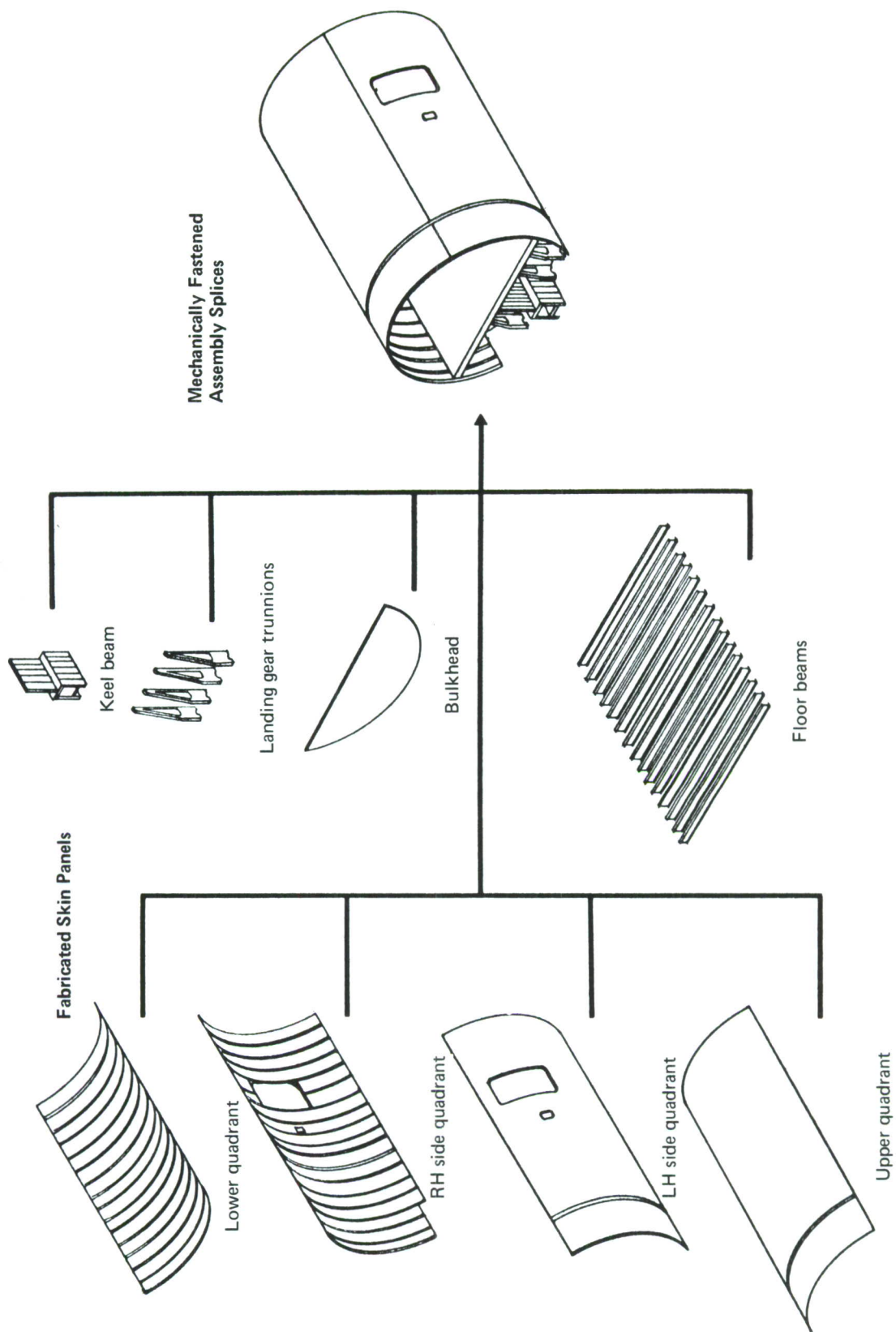


Figure 192. – Fuselage Assembly Sequence

will not be assessed. In the following discussion the consideration of proof testing will be confined to applications wherein the required stress levels are less than those which result in net section yielding. For typical fuselage structure, net area through a line of fasteners (skin-to-frame or skin-to-stringer) averages 85% of the gross area; therefore, proof load stresses will be limited to $0.85 F_{ty}$:

$$\begin{array}{rcl} \text{Crown } F_{ty} & = & 39 \text{ ksi (longitudinal)} \\ & \text{or} & \\ \text{Side-of-body } F_{ty} & = & 35 \text{ ksi (transverse)} \end{array}$$

To prevent service failures due to insufficient residual load capability, three basic parameters which have to be considered are (1) initial flaw size, (2) critical flaw size, and (3) subcritical flaw growth characteristics. For the baseline structure, items (2) and (3) are determined as a result of studies described in sections IV-1c1, and VI-1c5. Item (1) is as specified in appendix I. In the case of the crown and side-of-body study locations, the critical flaw sizes at the specified minimum residual strength, as determined for various inspection frequencies, are shown in figure 193, along with the anticipated subcritical flaw growth characteristics as determined for these various inspection frequencies. Also indicated in figure 193 as cutoff lines are those flaws which may be expected to exhibit dynamic crack growth at a gross section stress equal to $0.85 F_{ty}$ with K_C data as taken from the upper bound of the material K_C data (app. I).

It may be observed that for the side-of-body location the minimum size of through-the-thickness flaws which may be detected by proof testing to a stress equal to $0.85 F_{ty}$ is larger than that specified as detectable by conventional NDT techniques (ref. app. I), for in-service noninspectable, depot level inspectable, or special visual inspectable structure. The smallest flaw that may be detected by proof loading to $0.85 F_{ty}$ is 10 inches, whereas appendix I specifies that 2-inch-long skin cracks are special visual inspectable. As a result of these observations it is concluded that proof load testing offers no improvement in subcritical flaw detection over that associated with conventional NDT techniques; therefore, as an inspection technique, proof load testing has no merit for the side-of-body location of the baseline component.

It is further observed that, for crown locations, proof load testing to a stress equal to $0.85 F_{ty}$ can reveal flaws smaller only than those specified as detectable by conventional NDT techniques (see app. I) for special visual inspectable structure. The smallest flaw that may be detected, at the crown location, by proof loading to $0.85 F_{ty}$ is 1.9 inches with the central stringer intact. This is smaller than the 2-inch crack specified in appendix I as special visual inspectable; therefore, such cracks may be detected by proof loading techniques. It may be noted that the proof load stress levels require a load level of 75% of that required for an ultimate load test, and that the loading fixtures required to achieve such stresses are not normally considered to be available at facilities at which special visual inspection is conducted.

In view of the above considerations, it is concluded that proof load testing has no merit as either a supplement to or substitute for conventional NDT evaluation of the baseline fuselage shell component.

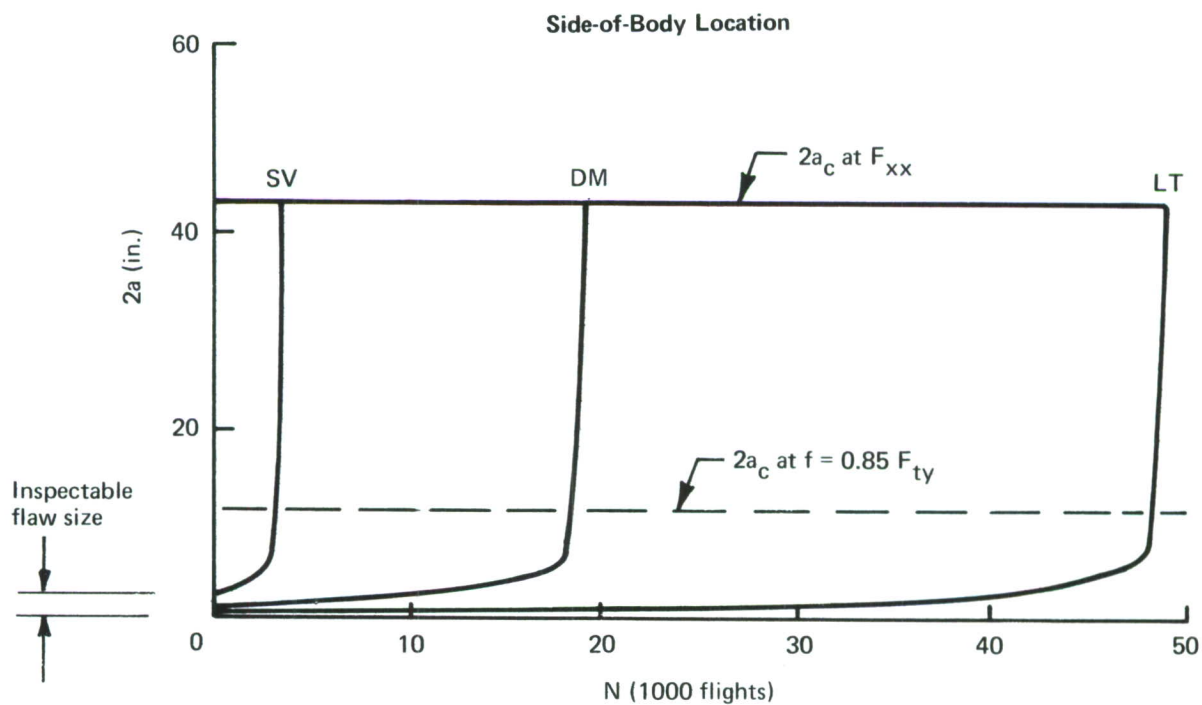
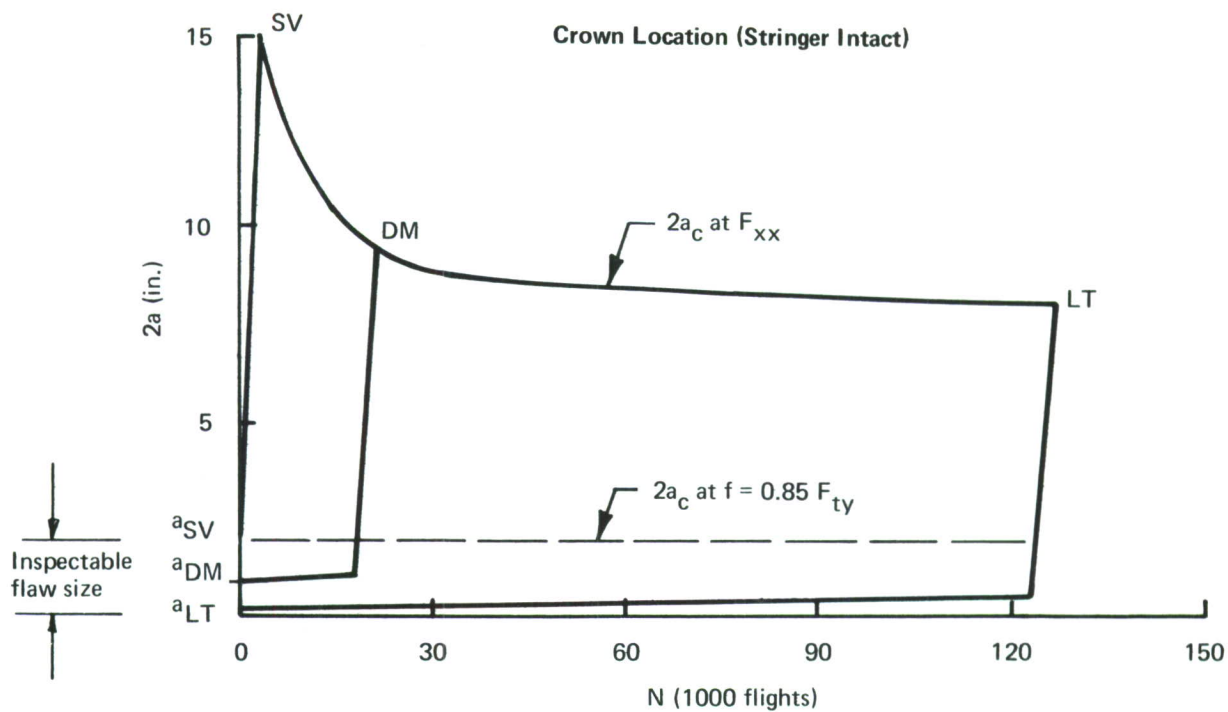


Figure 193.—Proof Load Detection Capability

USAF DAMAGE TOLERANCE CRITERIA

1.0 Definitions and General Requirements

1.1 Definitions

1.1.1 Degree of Inspectability. The degree of inspectability of each element of safety of flight structure shall be established in accordance with the following definitions.

1.1.1.1 In-Flight Evident Inspectable - Structure is in-flight evident inspectable if the nature and extent of damage occurring in flight will result directly in characteristics which make the flight crew immediately and unmistakably aware that significant damage has occurred and that the mission should not be continued.

1.1.1.2 Ground Evident Inspectable - Structure is ground evident inspectable if the nature and extent of damage being considered will be readily and unmistakably obvious to ground personnel without specifically inspecting the structure for damage.

1.1.1.3 Walkaround Inspectable - Structure is walkaround inspectable if the nature and extent of damage being considered is unlikely to be overlooked by personnel conducting a visual inspection of the structure. This inspection normally shall be a visual look at the exterior of the structure from ground level without removal of access panels or doors and without special inspection aids.

1.1.1.4 Special Visual Inspectable - Structure is special visual inspectable if the nature and extent of damage being considered is unlikely

to be overlooked by personnel conducting a detailed visual inspection of the aircraft for the purpose of finding damaged structure. The procedure may include removal of access panels and doors, and may permit simple visual aids such as mirrors and magnifying glasses. Removal of paint, sealant, etc. and use of NDI techniques such as penetrant, x-ray, etc. are not part of a special visual inspection.

1.1.1.5 Depot or Base Level Inspectable - Structure is depot or base level inspectable if the nature and extent of damage being considered will be detected with a 90% probability at 95% confidence level for slow crack growth structure and with 90% probability at 50% confidence level for fail safe structure. The inspection procedures may include NDI techniques such as penetrant, x-ray, ultrasonic, etc. Accessibility considerations may include removal of those components designed for removal.

1.1.1.6 In-Service Non-Inspectable Structure - Structure is in-service non-inspectable if either damage size or accessibility preclude detection during one or more of the above inspections.

1.1.2 Frequency of Inspection - Frequency of inspection is the number of times that a particular type of inspection is to be conducted during the service life of the aircraft.

1.1.3 Minimum Period of Unrepaired Service Usage - Minimum period of unrepaired service usage is that period of time during which the appropriate level of damage (assumed initial or in-service) is presumed to remain unrepaired and allowed to grow within the structure.

- 1.1.4 Minimum Required Residual Strength (P_{XX}) - The minimum required residual strength shall be as specified in Paragraph 1.2.2.
- 1.1.5 Minimum Assumed Initial Damage Size - The minimum assumed initial damage size is the smallest crack-like defect which shall be used as a starting point for analyzing residual strength and crack growth characteristics of the structure.
- 1.1.6 Minimum Assumed In-Service Damage Size - The minimum assumed in-service damage size is the smallest damage which shall be assumed to exist in the structure after completion of an in-service inspection.
- 1.1.7 Damage Growth Limit - Damage growth limit is the maximum amount of damage growth allowed within a specified interval so as not to degrade the residual strength below a specified minimum level.
- 1.1.8 Slow Crack Growth Structure - Slow crack growth structure consists of those design concepts where flaws or defects are not allowed to attain the critical size required for unstable rapid propagation.
- 1.1.9 Crack Arrest Fail Safe Structure - This is structure which is designed and fabricated such that unstable rapid propagation will be stopped within a continuous area of the structure prior to complete failure and the strength and safety of the remaining undamaged structure will not be degraded below a specified level for a specified period of unrepaired service usage.
- 1.1.10 Multiple Load Path-Fail Safe Structure - This is structure which is designed and fabricated in segments (with each segment consisting of one or more individual elements) such that failure of any single segment

(i.e. load path) will not degrade the strength and safety below a specified level for a specified period of unrepaired service usage.

1.1.10.1 Multiple Load Path-Dependent Structure - Multiple load path structure is classified as dependent if, by design, a common source of cracking exists in adjacent load paths at one location due to the nature of the assembly or manufacturing procedures. An example of multiple load path-dependent structure is planked tension skin where individual members are spliced in the spanwise direction by common fasteners with common drilling and assembly operations.

1.1.10.2 Multiple Load Path-Independent Structure - Multiple load path structure is classified as independent if by design, it is unlikely that a common source of cracking exists in more than a single load path at one location due to the nature of assembly or manufacturing procedures.

1.2 General Requirements

1.2.1 Analysis Requirements - It shall be a requirement to classify all safety of flight structure with regard to type of damage tolerance approach and degree of inspectability and perform the required analytical work necessary to demonstrate compliance with specific requirements in this specification. The analysis shall assume the presence of crack-like defects, placed in the most unfavorable orientation with respect to the applied stress and the material properties, and shall predict the growth behavior in the chemical, thermal, and sustained and cyclic stress environment to which that portion of the component shall be subjected. In addition, the interaction effects of variable loading shall be considered. Regardless of

the damage tolerance concept single initial flaws of the specified size shall be assumed to exist in each separate element of the structure. For structural elements where it is likely due to the fabrication and assembly operations that the flaws in two or more elements exist at the same location in the structure this shall be assumed.

1.2.2 Residual Strength Requirements - The minimum required residual strength is the minimum load which must be sustained by the aircraft with damage present without endangering safety of flight or degrading the performance of the aircraft for the specified minimum period of unrepaired service usage. This includes loss of strength, loss of stiffness, excessive permanent deformation, loss of control, or by reduction of the flutter speed below V_L . The minimum residual strength requirements are specified in Sections 2.0 through 4.0 in terms of the minimum load P_{XX} that the structure must be able to sustain at any time during the specified minimum period of unrepaired service usage with the specified damage present. The magnitude of P_{XX} varies with the overall degree of inspectability of the structure (e.g. P_{FE} applies to flight evident, P_{SV} applies to special visual inspectable, etc). The P_{XX} load shall be determined from average load exceedance data and shall be that load that could occur once in 100 times the applicable inspection interval (e.g. P_{DM} is the load that could occur once in 100 depot or base level inspection intervals). For fail safe structure there is a requirement to sustain a minimum load, P_{YY} , at the instant

of load path failure (or crack arrest) in addition to being able to sustain the load, P_{XX} , subsequent to load path failure (or crack arrest) at any time during the specified interval. The single load path failure (or crack arrest) load, P_{YY} , shall include a dynamic factor (D.F.). In lieu of test or analytical data to the contrary a dynamic factor of 1.15 shall be used. The magnitude of P_{YY} shall depend upon the overall inspectability and the specific inspectability of the intact structure for subcritical damage (i.e. damage less than failed load paths or arrested cracks). P_{YY} shall be determined per the following table:

<u>OVERALL DEGREE OF INSPECTABILITY</u>	<u>INSPECTABILITY FOR MIN. ASSUMED IN-SERVICE SUB- CRITICAL DAMAGE SIZES</u>	<u>P_{YY}</u>
In-Flight Evident	Walkaround Visual	D.F. X P _{WV}
	Special Visual	D.F. X P _{SV}
	Depot or Base Level	D.F. X P _{DM}
	Non-Inspectable	D.F. X P _{LT}
Ground Evident	Walkaround Visual	D.F. X P _{WV}
	Special Visual	D.F. X P _{SV}
	Depot or Base Level	D.F. X P _{DM}
	Non-Inspectable	D.F. X P _{LT}
Walkaround Visual	Walkaround Visual	D.F. X P _{WV}
	Special Visual	D.F. X P _{SV}
	Depot or Base Level	D.F. X P _{DM}
	Non-Inspectable	D.F. X P _{LT}
Special Visual	Special Visual	D.F. X P _{SV}
	Depot or Base Level	D.F. X P _{DM}
	Non-Inspectable	D.F. X P _{LT}
Depot or Base Level	Depot or Base Level	D.F. X P _{DM}
	Non-Inspectable	D.F. X P _{LT}
Non-Inspectable	Non-Inspectable	D.F. X P _{LT}

1.2.3 Test Requirements

1.2.3.1 Specimen Testing - Valid data shall be determined in accordance with the procedures set forth in the 1970 ASTM Standards Test Method E3999-70T, or as described in AFFDL-TR-69-111 or by alternate methods approved by the procuring agency. The materials from which the structure identified in Paragraph 1.2.1 are to be fabricated shall be controlled by a system of procedures and/or specifications which are sufficient to preclude the utilization in fracture critical areas of materials possessing K_{IC} (or K_C) values inferior to those assumed in design. Tests will be conducted on all billets, forgings, extrusions, plates, or other forms (from which final parts are to be finished) to evaluate the fracture toughness. A slice will be cut from these items, or integral projections thereof, at receiving inspections, so that specimens from each slice may be tested. These specimens shall have been heat treated with the same material from which they were cut. When sufficient data are available, sampling procedures may be instituted on approval of the Air Force.

1.2.3.2 Component Testing - Fail safe tests will be conducted on that structure which is considered to be fail safe to verify that the failure of a load path or rapid propagation of a crack will not result in loss of the entire structure. Tests will be performed during the preproduction design verification component test program and the full scale qualification test program. These tests will be conducted by pre-cracking a particular member to the critical crack length and applying the load P_{yy} . Tests will be conducted on selected critical structure, particularly slow crack growth components, to verify the

analytical crack propagation rates. Initial flaws of the specified size will be initiated at the critical point(s) and propagation rates measured. These tests will be performed during the preproduction design verification test program and during the full scale qualification test program. Wherever possible, the structural components used for static test and fatigue test will be used to perform these tests. If in certain cases, this is not possible, then additional components will be fabricated for testing.

1.2.4 Fracture Control Plan. General guidelines for the fracture control plan are provided in 5.1.3 of MIL-STD-XXX.

2.0 Slow Crack Growth Structure

2.1 Walkaround Inspectable

2.1.1 The Frequency of Inspection and inspection interval shall be specified in the system RFP, Prime Item Development Specification or other contract documents as applicable.

2.1.2 The Minimum Period of Unrepaired Service Usage shall be five (5) times the inspection interval specified in 2.1.1.

2.1.3 The Minimum Required Residual Strength shall be P_{WV} .

2.1.4 Minimum Assumed Initial Damage. The damage assumed to exist in new structure as a result of fabrication operations shall be an .050" long through the thickness crack emanating from one side of a hole. At locations other than holes the assumed initial damage size shall be $(a/Q) = .100$ where a is measured in the principal direction of crack growth and Q is the flaw shape parameter. A smaller initial flaw size may be assumed subsequent to a demonstration that all flaws larger than this assumed size have at least a 90% probability of detection with a 95% confidence using the selected production inspection procedure, equipment and personnel. This demonstration shall be subject to USAF approval. A smaller initial size may be assumed if proof test inspection is used. In this case the minimum assumed initial size shall be the calculated critical size at the proof test stress levels and temperature using the upper bound of the material K_{IC} data.

2.1.5 Minimum Assumed in-Service Damage Size - The smallest damage which can be presumed to exist in fuel tank structure after completion of a walk-around inspection shall be an uncovered open 2" through the thickness crack. A smaller through the thickness crack may be assumed only after it is shown (analytically or experimentally) that fuel leakage will occur and can be detected during the inspection. Other slow crack growth structure shall be assumed to be walkaround uninspectable.

2.1.6 Damage Growth Limits.

2.1.6.1 Fabrication Damage - Initial damage as specified in Paragraph 2.1.4 shall not grow to critical size and cause failure of the structure due to the application of P_{DM} in the minimum period of unrepaired service usage specified in Paragraph 2.3.2.

2.1.6.2 In-Service Damage - In-service damage size specified in Paragraph 2.1.5 shall not grow to critical size and cause failure of the structure due to the application of P_{WV} in the minimum period of unrepaired service usage specified in Paragraph 2.1.2.

2.2 Special Visual Inspectable

2.2.1 The Frequency of Inspection and inspection intervals shall be specified in the system RFP, PIDS or other contract documents as applicable.

2.2.2 The Minimum Period of Unrepaired Service Usage shall be two (2) times the inspection interval specified in 2.2.1.

2.2.3 The Minimum Required Residual Strength shall be P_{SV} .

2.2.4 The Minimum Assumed Initial Damage shall be as specified in 2.1.4.

2.2.5 Minimum Assumed In-Service Damage Size - The smallest damage which can be presumed to exist in the structure after completion of special visual inspection shall be an uncovered open 2" through the thickness crack. A smaller through the thickness crack may be assumed only in those special cases where inspection statistics on similar structure or unique design features clearly indicate that smaller cracks can and will be found.

2.2.6 Damage Growth Limits.

2.2.6.1 Fabrication Damage - 2.1.6.1 applies.

2.2.6.2 In-Service Damage - In-service damage size specified in Paragraph 2.2.5 shall not grow to critical size and cause failure of the structure due to the application of P_{SV} in the minimum period of unrepaired service usage specified in Paragraph 2.2.2

2.3 Depot or Base Level Inspectable

2.3.1 The Frequency of Inspection and inspection intervals shall be specified in the system RFP, PIDS or other contract documents as applicable.

2.3.2 The Minimum Period of Unrepaired Service Usage shall be two (2) times the inspection interval specified in 2.3.1.

2.3.3 The Minimum Required Residual Strength shall be P_{DM} .

2.3.4 The Minimum Assumed Initial Damage shall be as specified in 2.1.4.

2.3.5 The Minimum Assumed In Service Damage Size - The smallest damage which can be presumed to exist in the structure after completion of a depot or base level inspection shall be as follows:

2.3.5.1 If The Component is to be removed from the aircraft and completely inspected with NDI procedures equivalent to those performed during fabrication, the minimum assumed damage size shall be that specified in 2.1.4.

2.3.5.2 Where NDI Techniques such as penetrant, magnetic particle or ultrasonics are applied to a component installed in the aircraft, the minimum assumed size shall be a through the thickness crack emanating from a fastener hole, having 0.250" of uncovered length. At other locations, the minimum assumed damage size shall be $a/Q = 0.20''$.

2.3.5.3 Where Visual Inspection is used, a 2" uncovered open through the thickness crack shall be the minimum size.

2.3.5.4 Smaller Flaw Sizes may be assumed under Paragraphs 2.3.5.2 and 2.3.5.3 subsequent to a demonstration that all flaws larger than the selected size have at least a 90% probability of detection with a 95% confidence using the specified in-service inspection procedures and equipment. This demonstration shall be subject to USAF approval.

2.3.5.5 Smaller Flaw Sizes may be assumed under 2.3.5.2 and 2.3.5.3 if deopt or base level proof test inspection is used. In this case the minimum assumed sizes shall be calculated critical sizes at the proof test stress levels and temperatures using the upper bound of the material K_{IC} data.

2.3.6 Damage Growth Limits.

2.3.6.1 Fabrication Damage - 2.1.6.1 applies.

2.3.6.2 In-Service Damage - In-service damage size specified in Paragraph 2.3.5 shall not grow to critical size and cause failure of the structure due to the application of P_{DN} in the minimum period of unrepaired service usage specified in Paragraph 2.3.2.

2.4 Non-Inspectable

2.4.1 The Frequency of Inspection is not applicable

2.4.2 The Minimum Period of Unrepaired Service Usage shall be two (2) design service lifetimes.

2.4.3 The Minimum Required Residual Strength shall be P_{LT} .

2.4.4 The Minimum Assumed Initial Damage shall be as specified in 2.1.4.

2.4.5 The Minimum Assumed In-Service Damage Size is not applicable.

2.4.6 Damage Growth Limits - Initial damage as specified in Paragraph 2.1.4 shall not grow to critical size and cause failure of the structure due to the application of P_{LT} in the minimum period of unrepaired service usage as specified in Paragraph 2.4.2.

3.0 Fail Safe - Multiple Load Path (MLP) Structure

3.1 In-Flight Evident

3.1.1 Frequency of Inspection is not applicable

3.1.2 The Minimum Period of Unrepaired Service Usage shall be that period of time between that when the damage becomes evident and the completion of an immediate return to base.

3.1.3 The Minimum Required Residual Strength shall be P_{FE} subsequent to load path failure and P_{YY} at time of load path failure.

3.1.4 Minimum Assumed Initial Damage

3.1.4.1 Intact New Structure - The damage assumed to exist in each load path of new structure as a result of fabrication operations shall be an .020" long through the thickness crack emanating from one side of a hole. At locations other than holes the assumed initial damage sizes shall be $(a/Q) = .030"$ where a is measured in the principal direction of crack growth and Q is the flaw shape parameter. A smaller initial flaw size may be assumed subsequent to a demonstration that all flaws larger than this assumed size have at least a 90% probability of detection with a 50% confidence level using the selected production inspection procedure, equipment, and personnel. This demonstration shall be subject to USAF approval.

3.1.4.2 Remaining Structure at Time of And Subsequent to Load Path Failure -

The damage assumed to exist adjacent to the primary failure in the remaining MLP dependent structure at time of and following the failure of a load path shall be equal to an .020" long through the thickness crack emanating from one side of a hole or damage level equal to $(a/Q) = .030"$ at locations other than holes, plus the amount of growth Δa which occurs

prior to load path failure. The damage assumed to exist adjacent to the primary failure in each load path of the remaining MLP independent structure at time of and following the failure of a load path shall be equal to an .010" radius semicircular corner crack emanating from one side of a hole or damage equal to $(a/Q) = 0.010$ " at locations other than holes, plus the amount of growth Δa which occurs prior to load path failure.

3.1.5 The Minimum Assumed In-Service Damage Size shall be a failed load path.

3.1.6 Damage Growth Limits

3.1.6.1 Intact New Structure - Initial damage as specified in Paragraph 3.1.4.1 shall not grow to critical size and cause failure of a load path due to the application of P_{DM} in the minimum period of unrepaired service usage specified in Paragraph 3.5.2. If the structure is not inspectable for subcritical cracks, the initial damage specified in 3.1.4.1 shall not grow to critical size and cause failure of a load path due to the application of P_{LT} in one lifetime.

3.1.6.2 In Remaining Structure Subsequent to Load Path Failure - Damage as specified in Paragraph 3.1.4.2 shall not grow to critical size and cause failure of the remaining structure due to the application of P_{FE} in the minimum period of unrepaired service usage specified in Paragraph 3.1.2.

3.2 Ground Evident

3.2.1 Frequency of Inspection shall be once per flight.

3.2.2 The Minimum Period of Unrepaired Service Usage shall be one complete flight.

3.2.3 The Minimum Residual Strength shall be P_{GE} subsequent to load path failure and P_{YY} at time of load path failure.

3.2.4 Minimum Assumed Initial Damage

3.2.4.1 The Damage in Intact New Structure shall be as specified in 3.1.4.1.

3.2.4.2 The Damage in Remaining Structure at Time of And Subsequent to Load Path Failure - shall be as specified in 3.1.4.2.

3.2.5 The Minimum Assumed In-Service Damage Size shall be a failed load path.

3.2.6 Damage Growth Limits

3.2.6.1 Intact New Structure - 3.1.6.1 applies.

3.2.6.2 In Remaining Structure Subsequent to Load Path Failure - Damage as specified in Paragraph 3.1.4.2 shall not grow to critical size and cause failure of the remaining structure due to the application of P_{GE} in the minimum period of unrepaired service usage specified in Paragraph 3.2.2.

3.3 Walkaround Visual Inspectable

3.3.1 Frequency of Inspection and inspection interval shall be specified in the system RFP, PIDS or other contract document as applicable.

3.3.2 The Minimum Period of Unrepaired Service Usage shall be five (5) times the walkaround inspection interval specified in 3.3.1.

3.3.3 The Minimum Residual Strength shall be P_{WV} subsequent to in-service inspection, and P_{YY} at time of load path failure.

3.3.4 Minimum Assumed Initial Damage

3.3.4.1 The Damage in Intact New Structure shall be as specified in 3.1.4.1.

3.3.4.2 Remaining Structure Subsequent to Load Path Failure and Intact Structure Subsequent to In-Service Inspection - The damage assumed to exist adjacent to the primary failure in the remaining MLP dependent structure at time of and following the failure of a load path (or significant damage to the load path) shall be equal to an .020" long through the thickness crack emanating from one side of a hole or damage equal to $a/Q = .030''$ at locations other than holes, plus the amount of growth Δa which occurs prior to load path failure or prior to in-service inspection. The damage assumed to exist adjacent to the primary failure in each load path of the remaining MLP independent structure at time of and following failure of a load path (or significant damage to the load path) shall be equal to an .010" radius semicircular corner crack emanating from one side of a hole or damage equal to $a/Q = 0.010''$ at locations other than holes, plus the amount of growth Δa which occurs prior to a load path failure or prior to in-service inspection.

3.3.5 The Minimum Assumed In-Service Damage shall be as specified in Paragraph 2.1.5 or a failed member, whichever is applicable.

3.3.6 Damage Growth Limits

3.3.6.1 Intact New Structure - 3.1.6.1 applies.

3.3.6.2 Intact Structure - Subsequent to In-Service Inspection - If the detectable damage is less than a failed load path then the minimum assumed damage in one load path shall be as specified in Paragraph 2.1.5. This damage plus the damage assumed to exist in the remaining structure at the time of inspection as defined in Paragraph 3.3.4.2, shall not grow

to critical size and cause failure of the structure due to the application of P_{WV} in the minimum period of unrepaired service usage specified in Paragraph 3.3.2.

3.3.6.3 Remaining Structure - Subsequent to Load Path Failure - If the in-service detectable damage size is a failed load path then the damage in the remaining structure as defined in Paragraph 3.3.4.2 shall not grow to critical size and cause failure of the remaining structure due to the application of P_{WV} in the minimum period of unrepaired service usage specified in Paragraph 3.3.2.

3.4 Special Visual Inspectable

3.4.1 Frequency of Inspection and inspection intervals shall be specified in the systems RFP, PIDS or other contract document as applicable.

3.4.2 The Minimum Period of Unrepaired Service Usage shall be two (2) times the special visual inspection interval specified in 3.4.1.

3.4.3 The Minimum Required Residual Strength shall be P_{SV} subsequent to in-service inspection, and P_{YY} at time of load path failure.

3.4.4 The Minimum Assumed Initial Damage shall be as specified in Paragraph 3.3.4.

3.4.5 The Minimum Assumed In-Service Damage shall be as specified in 2.2.5 or a failed member, whichever is applicable.

3.4.6 Damage Growth Limits

3.4.6.1 Intact New Structure - 3.1.6.1 applies.

3.4.6.2 Intact Structure - Subsequent to In-Service Inspection - If the in-service detectable damage size is less than a failed load path then the

minimum assumed damage in one load path shall be as specified in Paragraph 2.2.4. This damage plus the damage assumed to exist in the remaining structure at the time of inspection as defined in Paragraph 3.3.4.2 shall not grow to critical size and cause failure of the structure due to the application of P_{SV} in the minimum period of unrepaired service usage as specified in Paragraph 3.4.2.

3.4.6.3 Remaining Structure - Subsequent to Load Path Failure - If the in-service detectable damage is a failed load path, then the damage in the remaining structure as defined in Paragraph 3.3.4.2 shall not grow to critical size and cause failure of the structure due to the application of P_{SV} in the minimum period of unrepaired service usage as specified in Paragraph 3.4.2.

3.5 Depot or Base Level Inspectable

3.5.1 The Frequency of Inspection and inspection interval shall be specified in the system RFP, PIDS, or other contract documents as applicable.

3.5.2 The Minimum Period of Unrepaired Service Usage shall be two (2) times the depot or base level inspection interval specified in 3.5.1.

3.5.3 The Minimum Residual Strength shall be P_{DM} subsequent to in-service inspection, and P_{YY} at time of load path failure.

3.5.4 Minimum Assumed Initial Damage shall be as specified in Paragraph 3.3.4.

3.5.5 The Minimum Assumed In-Service Damage shall be as specified in Paragraph 2.3.5 or a failed member whichever is applicable.

3.5.6 Damage Growth Limits

3.5.6.1 Intact New Structure - 3.1.6.1 applies.

3.5.6.2 Intact Structure - Subsequent to In-Service Inspection - If the in-service detectable damage is less than a failed load path, then the minimum assumed damage in one load path shall be as specified in 2.3.5. This damage plus the damage assumed to exist in the remaining structure at the time of inspection as defined in Paragraph 3.3.4.2 shall not grow to critical size and cause failure of the structure due to the application of P_{DM} in the minimum period of unrepaired service usage as specified in 3.5.2.

3.5.6.3 Remaining Structure - Subsequent to Load Path Failure - If the in-service detectable damage is a failed load path, then the damage in the remaining structure as defined in Paragraph 3.3.4.2 shall not grow to critical size and cause failure of the remaining structure due to the application of P_{DM} in the minimum period of unrepaired service usage specified in Paragraph 3.5.2.

3.6 In-Service Non-Inspectable

3.6.1 The Frequency of Inspection is not applicable.

3.6.2 The Minimum Period of Unrepaired Service Usage shall be one design service lifetime.

3.6.3 The Minimum Residual Strength shall be P_{LT} subsequent to load path failure, and P_{YY} at time of load path failure.

3.6.4 Minimum Assumed Initial Damage shall be as specified in Paragraph 3.3.4.

3.6.5 The Minimum Assumed In-Service Damage is not applicable.

3.6.6 Damage Growth Limits

3.6.6.1 Intact New Structure - Initial damage as specified in Paragraph 3.3.4.1 shall not grow to critical size and cause failure of a load path due to the application of P_{LT} in the minimum period of unrepaired service usage specified in Paragraph 3.6.2.

3.6.6.2 Remaining Structure - Subsequent to Load Path Failure - Subsequent to load path failure, initial damage in the remaining structure as specified in Paragraph 3.3.4.2 shall not grow to critical size and cause failure of the remaining structure due to the application of P_{LT} in the minimum period of unrepaired service usage specified in Paragraph 3.6.2.

4.0 Fail Safe - Crack Arrest Structure

4.1 In-Flight Evident

4.1.1 Frequency of Inspection is not applicable.

4.1.2 The Minimum Period of Unrepaired Service Usage shall be that period of time between that when the damage becomes evident and completion of an immediate return to base.

4.1.3 The Minimum Required Residual Strength shall be P_{yy} at time of crack arrest and P_{FE} subsequent to crack arrest.

4.1.4 Minimum Assumed Initial Damage.

4.1.4.1 The Damage in Intact New Structure shall be as specified in 3.1.4.1.

4.1.4.2 Remaining Structure At Time of and Subsequent to Crack Arrest.

The damage assumed to exist in the remaining structure following arrest of a rapidly propagating crack shall depend upon the particular geometry.

In conventional skin stringer (or frame) construction this shall be assumed as two panels (bays) of cracked skin plus the broken central stringer (or frame). Where tear straps are provided between stringers (or frames), this damage shall be assumed as cracked skin between tear straps plus the broken central stringer (or frame). Other configurations shall assume equivalent damage as mutually agreed upon by the contractor and the AF.

4.1.5 The Minimum Assumed In-Service Damage shall be as specified in Paragraph 4.1.4.2.

4.1.6 Damage Growth Limits

4.1.6.1 Intact New Structure - Initial damage as specified in Paragraph 3.1.4.1 shall not grow to the size which would cause an initial rapid propagation due to the application of P_{DM} in the minimum period of unrepaired service usage specified in Paragraph 4.5.2. If the structure is not inspectable for subcritical cracks, the initial damage specified in 3.1.4.1 shall not grow to the size which would cause an initial rapid crack propagation due to the application of P_{LT} in one lifetime.

4.1.6.2 Remaining Structure Subsequent to Crack Arrest - Damage as specified in Paragraph 4.1.4.2 shall not grow to the size required to cause complete structural failure due to the application of P_{FE} in the minimum period of unrepaired service usage specified in Paragraph 4.1.2.

4.2 Ground Evident

4.2.1 Frequency of Inspection shall be once per flight.

4.2.2 The Minimum Period of Unrepaired Service Usage shall be one complete flight.

4.2.3 The Minimum Required Residual Strength shall be P_{GE} subsequent to crack arrest and P_{YY} at time of crack arrest.

4.2.4 Minimum Assumed Initial Damage.

4.2.4.1 The Damage In Intact New Structure shall be as specified in 3.1.4.1.

4.2.4.2 The Damage In Remaining Structure at Time of And Subsequent to Crack Arrest shall be as specified in 4.1.4.2.

4.2.5 The Minimum Assumed In-Service Damage shall be as specified in Paragraph 4.1.4.2.

4.2.6 Damage Growth Limits.

4.2.6.1 Intact New Structure - 4.1.6.1 applies.

4.2.6.2 Remaining Structure Subsequent to Crack Arrest - Damage as specified in Paragraph 4.1.4.2 shall not grow to the size required to cause complete structural failure due to the application of P_{GE} in the minimum period of unrepaired service usage specified in Paragraph 4.2.2.

4.3 Walkaround Visual Inspectable

4.3.1 Frequency of Inspection shall be as specified in the system RFP, PIDS, or other contract documents as applicable.

4.3.2 The Minimum Period of Unrepaired Service Usage shall be five (5) times the walkaround inspection interval specified 4.3.1.

4.3.3 The Minimum Required Residual Strength shall be P_{WV} subsequent to in-service inspection, and P_{YY} at time of crack arrest.

4.3.4 Minimum Assumed Initial Damage

4.3.4.1 The Damage In Intact New Structure shall be as specified in 3.1.4.1.

4.3.4.2 The Damage In Remaining Structure at Time of And Subsequent to Crack Arrest shall be as specified in 4.1.4.2.

4.3.5 The Minimum Assumed In-Service Damage shall be as specified in Paragraph 2.1.5 (assumed to be located at an inaccessible, failed stringer or frame), or specified in Paragraph 4.1.4.2, whichever is applicable.

4.3.6 Damage Growth Limits

4.3.6.1 Intact New Structure - 4.1.6.2 applies.

4.3.6.2 Intact Structure - Subsequent to In-Service Inspection - If the in-service detectable damage is less than an arrested crack as described in

Paragraph 4.1.4.2, then the minimum assumed damage as specified in Paragraph 4.3.5 shall not grow to the size required to cause complete structural failure due to the application of P_{WV} in the minimum period of unrepaired service usage specified in Paragraph 4.3.2.

4.3.6.3 Remaining Structure Subsequent to Crack Arrest - Damage as specified in Paragraph 4.3.5 shall not grow to the size required to cause complete structural failure due to the application of P_{WV} in the specified period of unrepaired usage specified in Paragraph 4.3.2.

4.4 Special Visual Inspectable

4.4.1 Frequency of Inspection shall be as specified in the system RFP, PIDS or other contract documents as applicable.

4.4.2 The Minimum Period of Unrepaired Service Usage shall be two (2) times the special visual inspection interval specified in 4.4.1.

4.4.3 The Minimum Required Residual Strength shall be P_{SV} subsequent to in-service inspection, and P_{YY} at time of crack arrest.

4.4.4 Minimum Assumed Initial Damage

4.4.4.1 The Damage In Intact New Structure shall be as specified in 3.1.4.1.

4.4.4.2 The Damage in Remaining Structure at Time of And Subsequent to Crack Arrest shall be as specified in 4.1.4.2.

4.4.5 The Minimum Assumed In-Service Damage shall be as specified in Paragraph 2.2.5 (assumed to be located at an inaccessible, failed stringer or frame), or as specified in Paragraph 4.1.4.2, whichever is applicable.

4.4.6 Damage Growth Limits

4.4.6.1 Intact New Structure - 4.1.6.2 applies.

4.4.6.2 Intact Structure - Subsequent to In-Service Inspection - If the in-service detectable damage is less than an arrested crack as described in Paragraph 4.1.4.2, then the minimum assumed damage as specified in Paragraph 4.4.5 shall not grow to the size required to cause complete structural failure due to the application of P_{SV} in the minimum period of unrepaired service usage specified in Paragraph 4.4.2.

4.4.6.3 Remaining Structure Subsequent to Crack Arrest - Damage as specified in Paragraph 4.1.4.2 shall not grow to the size required to cause complete structural failure due to the application of P_{SV} in the minimum period of unrepaired service usage specified in Paragraph 4.4.2.

4.5 Depot or Base Level Inspectable

4.5.1 Frequency of Inspection shall be specified in the system RFP, PIDS or other contract documents, as applicable.

4.5.2 The Minimum Period of Unrepaired Service Usage shall be two (2) times the depot or base level inspection interval specified in 4.5.1.

4.5.3 The Minimum Required Residual Strength shall be P_{DM} subsequent to in-service inspection and P_{YY} at time of crack arrest.

4.5.4 Minimum Assumed Initial Damage

4.5.4.1 The Damage In Intact New Structure shall be as specified in 3.1.4.1.

4.5.4.2 The Damage In Remaining Structure at Time of And Subsequent to Crack Arrest shall be as specified in 4.1.4.2.

4.5.5 The Minimum Assumed In-Service Damage shall be as specified in Paragraph 2.3.5 (assumed to be located at an inaccessible failed stringer or frame), or as specified in Paragraph 4.1.4.2, whichever is applicable.

4.5.6 Damage Growth Limits

4.5.6.1 Intact New Structure - 4.1.6.2 applies.

4.5.6.2 Intact Structure - Subsequent to In-Service Inspection - If the in-service detectable damage is less than an arrested crack as described in Paragraph 4.1.4.2, then the minimum assumed damage as specified in Paragraph 4.5.5 shall not grow to the size required to cause complete structural failure due to the application of P_{DM} in the minimum period of unrepaired service usage specified in Paragraph 4.5.2.

4.5.6.3 Remaining Structure Subsequent to Crack Arrest - Damage as specified in Paragraph 4.5.5 shall not grow to the size required to cause complete structural failure due to the application of P_{DM} in the minimum period of unrepaired service usage specified in Paragraph 4.5.2.

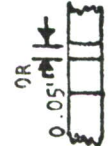
4.6 In-Service Non-Inspectable Crack Arrest Structure shall not be allowed.

SLOW CRACK GROWTH STRUCTURE


DEGREE OF INSPECTABILITY	FREQUENCY OF INSPECTION	MIN. PERIOD OF UNREPAIRED SERVICE USAGE (F _{XX})	MIN. REQ'D RESIDUAL STRENGTH (P _{XX})	MIN. ASSUMED INITIAL DAMAGE SIZES (a)	MIN. ASSUMED IN-SERVICE DAMAGE SIZES (l)	DAMAGE GROWTH LIMITS
--------------------------	-------------------------	------------------------------------------------------------	-------------------------------------------------	---------------------------------------	------------------------------------------	----------------------

IN FLIGHT EVIDENT \longleftrightarrow N/A




GROUND EVIDENT \longleftrightarrow N/A

WALK AROUND VISUAL	SPECIFIED IN CONTRACT DOCUMENTS (10 FLTS. TYPICAL)	5 X FREQ (F _{WV})	P _{WV}	a/Q = 0.10  OR SMALLER IF DEMONSTRATED	2" Open Thru Crack Unless Detection Of Smaller Size Demonstrated	<p>1 Shall not grow to critical @ P_{WV} in F_{WV}</p> <p>a Shall not grow to critical @ P_{DM} in F_{DM}</p>
SPECIAL VISUAL	SPECIFIED IN CONTRACT DOCUMENTS (1 YR. TYP)	2 X FREQ (F _{SV})	P _{SV}			<p>1 Shall not grow to critical @ P_{SV} in F_{SV}</p> <p>a Shall not grow to critical @ P_{DM} in F_{DM}</p>
DEPOT OR BASE LEVEL	SPECIFIED IN CONTRACT DOCUMENTS (1/4 LIFE-TIME TYP.)	2 X FREQ (F _{DM})	P _{DM}		(a/Q)DM	<p>1 Shall not grow to critical @ P_{DM} in F_{DM}</p> <p>a Shall not grow to critical @ P_{DM} in F_{DM}</p>
NON INSPECTABLE	N/A	² LIFETIMES (F _{LT})	P _{LT}		N/A	a Shall not grow to critical @ P _{LT} in F _{LT}

FAIL SAFE - CRACK ARREST STRUCTURE

DEGREE OF INSPECTABILITY	FREQUENCY OF INSPECTION	MIN. PERIOD OF UNREPAIRED SERVICE USAGE (F _{XX})	MIN. REQUIRED RESIDUAL STRENGTH (P _{XX})	MIN ASSUMED INITIAL DAMAGE SIZE		MIN. ASSUMED IN-SERVICE DAMAGE SIZE (1)	DAMAGE GROWTH LIMITS
				INTACT NEW STRUCTURE a ₁	IN REMAINING STRUCTURE a ₂		
IN FLIGHT EVIDENT	N/A	RETURN TO BASE (F _{FE})	P _{FE}	↑	↑	2 Cracked Skin Panels Plus Failed Central Stringer (Or Equivalent)	a ₁ Shall not cause initial rapid propagation @ P _{DM} in F _{DM} 1 Shall not cause complete failure @ P _{FE} in F _{FE}
GROUND EVIDENT	EVERY FLIGHT	ONE FLIGHT (F _{GE})	P _{GE}	 a/Q = 0.03 0.02"	2 Cracked Skin Panels Plus Failed Central stringer (or equivalent)	a ₁ Shall not cause initial rapid propagation at P _{DM} in F _{DM} 1 Shall not cause complete failure @ P _{GE} in F _{GE}	
WALK AROUND VISUAL	SPECIFIED IN CONTRACT DOCUMENTS (10 FLIGHTS TYPICAL)	5 X FREQ (F _{WV})	P _{WV}	Or Smaller if Demonstrated	↑	a ₂ or 2" or Greater through crack in skin at failed stringer whichever is applicable	a ₁ Shall not cause initial rapid propagation @ P _{DM} in F _{DM} 1 Shall not cause complete failure @ P _{WV} in F _{WV}
SPECIAL VISUAL	SPECIFIED IN CONTRACT DOCUMENTS (ONE YEAR TYPICAL)	2 X FREQ (F _{SV})	P _{SV}	↑	↑	Smaller crack if demonstrated	a ₁ Shall not cause initial rapid propagation @ P _{DM} in F _{DM} 1 Shall not cause complete failure @ P _{SV} in F _{SV}
DEPOT OR BASE LEVEL	SPECIFIED IN CONTRACT DOCUMENTS (1/4 LIFE-TIME TYPICAL)	2 X FREQ (F _{DM})	P _{DM}	↑	↑	(a/Q) DM As specified in 2.3.5 or a ₂	a ₁ Shall not cause initial rapid propagation @ P _{DM} in F _{DM} 1 Shall not cause complete failure @ P _{DM} in F _{DM}

FAIL SAFE - MULTIPLE LOAD PATH STRUCTURE

DEGREE OF INSPECTABILITY	FREQUENCY OF INSPECTION	MIN PERIOD OF UNREPAIRED SERVICE USAGE (F _{XX})	MIN REQ'D RESIDUAL STRENGTH (P _{XX})	MIN ASSUMED INITIAL DAMAGE SIZE			MIN ASSUMED IN-SERVICE DAMAGE SIZE	DAMAGE GROWTH LIMITS
				INTACT NEW STRUCTURE (a ₁)	REMAINING STRUCTURE DEPENDENT LOAD PATH (a ₂)	INDEPENDENT LOAD PATH (a ₃)		
IN FLIGHT EVIDENT	N/A	RETURN TO BASE (F _{FE})	P _{FE}	a/Q = .03 	Failed Load Path Plus a ₁ + Δ a in adjacent load paths	Failed load path plus a/Q = .01 or 	a ₂ or a ₃	a ₁ Shall not grow to critical @ P _{DM} in F _{DM} a ₂ or a ₃ Shall not grow to critical @ P _{FE} in F _{FE} a ₁ Shall not grow to critical @ P _{DM} in F _{DM} a ₂ or a ₃ Shall not grow to critical @ P _{GE} in F _{GE} a ₁ Shall not grow to critical @ P _{DM} in F _{DM} a ₂ or a ₃ Shall not grow to critical @ P _{WV} in F _{WV} a ₁ Shall not grow to critical @ P _{DM} in F _{DM} a ₂ or a ₃ Shall not grow to critical @ P _{SV} in F _{SV}
GROUND EVIDENT	EVERY FLIGHT	ONE FLIGHT (F _{GE})	P _{GE}	or Smaller if Demographic	2" crack Plus a ₁ + Δ a in adjacent load paths	2" crack plus a/Q = .01 or 		
WALK AROUND VISUAL	SPECIFIED IN CONTRACT DOCUMENTS (10 FLTS TYPICAL)	5 X FREQ (F _{WV})	P _{WV}					
SPECIAL VISUAL	SPECIFIED IN CONTRACT DOCUMENTS (ONE YEAR TYPICAL)	2 X FREQ (F _{SV})	P _{SV}					
DEPOT OR BASE LEVEL	SPECIFIED IN CONTRACT DOCUMENTS (1/4 LIFE-TIME TYPICAL)	2 X FREQ (F _{DM})	P _{DM}				(a/Q)DM as specified in 2.3.5	a ₁ Shall not grow to critical @ P _{DM} in F _{DM} a ₂ or a ₃ Shall not grow to critical @ P _{DM} in F _{DM} (a/Q)DM Shall not grow to critical @ P _{DM} in F _{DM}
NON INSPECTABLE	N/A	ONE LIFETIME (F _{LT})	P _{LT}			Δ a in adjacent load paths	N/A	a ₁ Shall not grow to critical @ P _{LT} in F _{LT} a ₂ or a ₃ Shall not grow to critical @ P _{LT} in F _{LT}

APPENDIX II

MATERIAL TESTING

INTRODUCTION

Material testing conducted in this phase of the program was held to a minimum level commensurate with a first iteration preliminary design effort. All testing was conducted to the provisions of reference 17 with a limited amount of additional testing as approved by the Air Force. Test guidelines are summarized as follows:

- Testing was conducted on materials that exhibited high potential for use on this program.
- Testing was limited to those candidate materials for which available static, fatigue, and fracture data were inadequate for preliminary design.
- The testing, data reduction, and validity checks were performed for fracture toughness in accordance with procedures given in references 7 and 18. Testing for K_{Isc} and da/dt values for forgings and extrusions was conducted with the procedures outlined in reference 19.
- The data are presented in such form as to be suitable for merging with other AFML data to secure a sample of sufficient size for statistical evaluation.

Testing was completed according to a schedule that allowed incorporation of test results in material selection and design concept evaluation.

The aluminum alloys investigated in this testing are shown in table II-I; also indicated is the type of testing to which they were subjected.

FATIGUE TESTS (FQR)

Twelve fatigue specimens were fabricated and cycled to failure. Refer to table II-II for panel definition and figure II-1 for panel geometry and test results. The FQR for 7475-T761 and 7475-T61, as determined from these data, is just slightly under 12 ksi, whereas the FQR for 2024-T3 is 12 ksi for the same geometric K_t .

FATIGUE CRACK GROWTH (da/dn) AND PLANE STRESS FRACTURE TOUGHNESS (K_{Ic})

Thirty-four center-crack tension (CCT) specimens were tested to obtain fatigue crack growth rate data.

Table II-III lists the panel configurations tested in humid air. Figures II-2 through II-5 show the test conditions and the results. Table II-IV lists the panel configurations tested in a salt solution, and figures II-6 through II-9 show the test conditions and test results.

To obtain higher ΔK (greater than 40 ksi $\sqrt{\text{in.}}$) versus crack growth rate (da/dn) data, the 12-inch-wide sustained load panels were fatigue cycled after da/dt crack growth testing. Refer to table II-V for panel definition and figures II-10 and II-11 for test results.

Two additional panels were subjected to fatigue crack growth rate testing. The specimen configuration is defined in table II-VI, with test results shown in figure II-12.

PLANE STRESS FRACTURE TOUGHNESS (K_{Ic})

All 34 crack growth panels were fractured at a loading rate of 1000 psi per second; high-speed movies (1000 frames per second) were taken of all fractures to assess test validity according to reference 7 (see table II-VII).

Figure II-13 shows all 24-inch-wide panel K_{Ic} values plotted as a function of gage for 7475-T761 (L,T) and 7475-T61 (L,T); 36-inch-wide panel data are shown in figure II-14. Figure II-15 shows the K_{Ic} results as a function of panel width for all 0.040-inch-gage 7475-T761 (L,T) and 7475-T61 (L,T) panels. Figure II-16 shows the data for 0.112-inch-gage material.

FATIGUE CRACK GROWTH AND PLANE STRAIN FRACTURE TOUGHNESS (K_{Ic})

Twelve compact tension (CT) specimens were tested to obtain cyclic crack growth data for extrusion and forging material. Table II-VIII defines the specimens tested, and figures II-17 through II-19 present the results as determined in three environments. Table II-IX compares the crack growth rates as a function of environment.

All specimens were pulled to failure, and table II-X identifies the calculated values and interpretation of fracture results (K_{Ic} determination) according to reference 18.

STRESS CORROSION CRACK GROWTH (da/dt) AND THRESHOLD STRESS INTENSITY (K_{Isc}) FOR SHEET

Eight center crack tension (CCT) panels were sustain loaded to determine the susceptibility of 7475 sheet to stress corrosion cracking. The panels and test results are described in table II-XI, and a representative crack-length-versus-time plot is shown in figure II-20.

STRESS CORROSION CRACK GROWTH AND THRESHOLD STRESS INTENSITY (K_{Isc}) FOR THICK SECTIONS

Six double cantilever beam (DCB) specimens were loaded to obtain stress corrosion crack growth rates and K_{Isc} for thick sections. Table II-XII summarizes the test conditions.

Figure II-21 shows the test results in the form of K_I versus crack length a for a given displacement δ . Initial and final values are indicated for all specimens tested; contours of constant K_I representing the equation in figure II-21 are shown for reference.

Table II-XIII lists the crack growth for a specific time interval and the resulting average velocity for each specimen. It should be noted that all specimens with grain orientation x-w fractured in the x direction before precracking was complete, thus invalidating all testing for stress corrosion cracking in the transverse grain direction.

SPECTRUM LOADED CRACK GROWTH (da/dS)

Two panels were spectrum loaded to obtain crack growth rate data. The load spectrum is shown in figure 161 of section VI. Panel data are given in table II-XIV. Figure II-22 shows the crack growth rate in inches per spectrum plotted as a function of the maximum spectrum stress intensity, K_{max} .

STATIC PROPERTIES (F_{ty} , F_{tu} , E)

Thirteen tensile specimens were loaded to obtain yield, ultimate strength, and elastic modulus values for the materials listed in table II-XV. Figure II-23 is a representative load-deformation plot with the pertinent data values indicated.

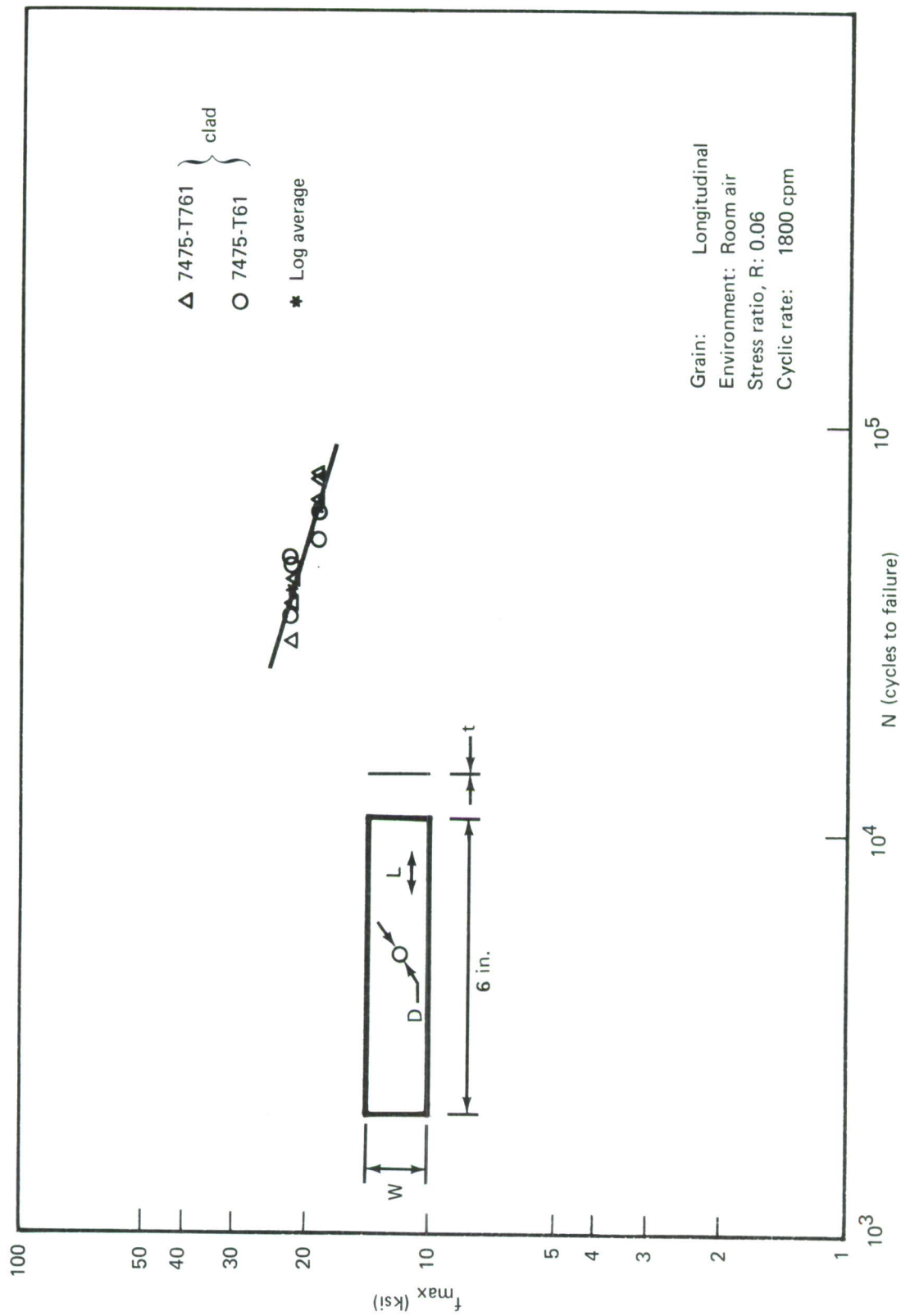


Figure II-1. - Fatigue Characterization Data ($K_t = 3.15$)

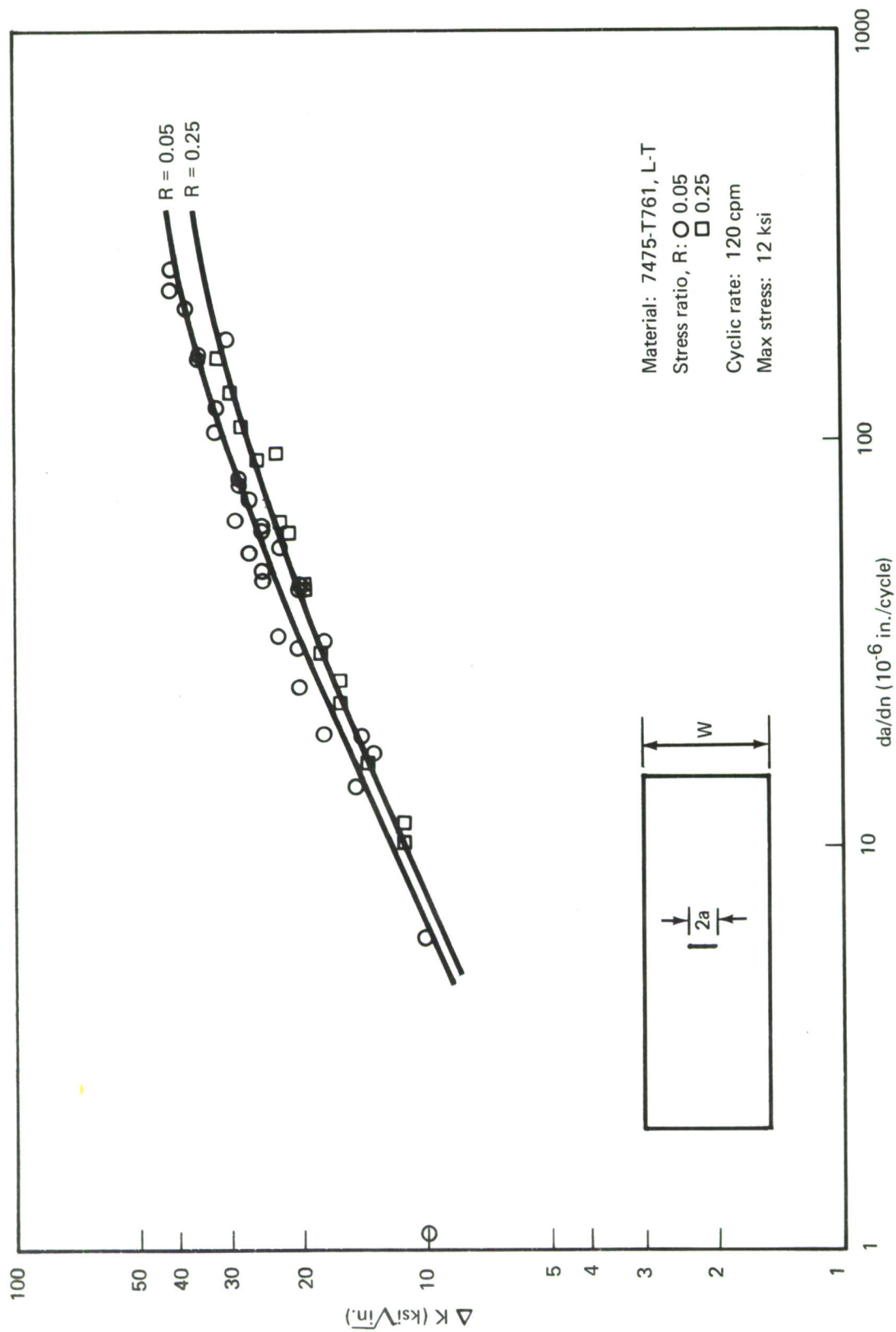


Figure II-2.—Fatigue Crack Propagation Data (7475-T761, L-T, 90% RH Air)

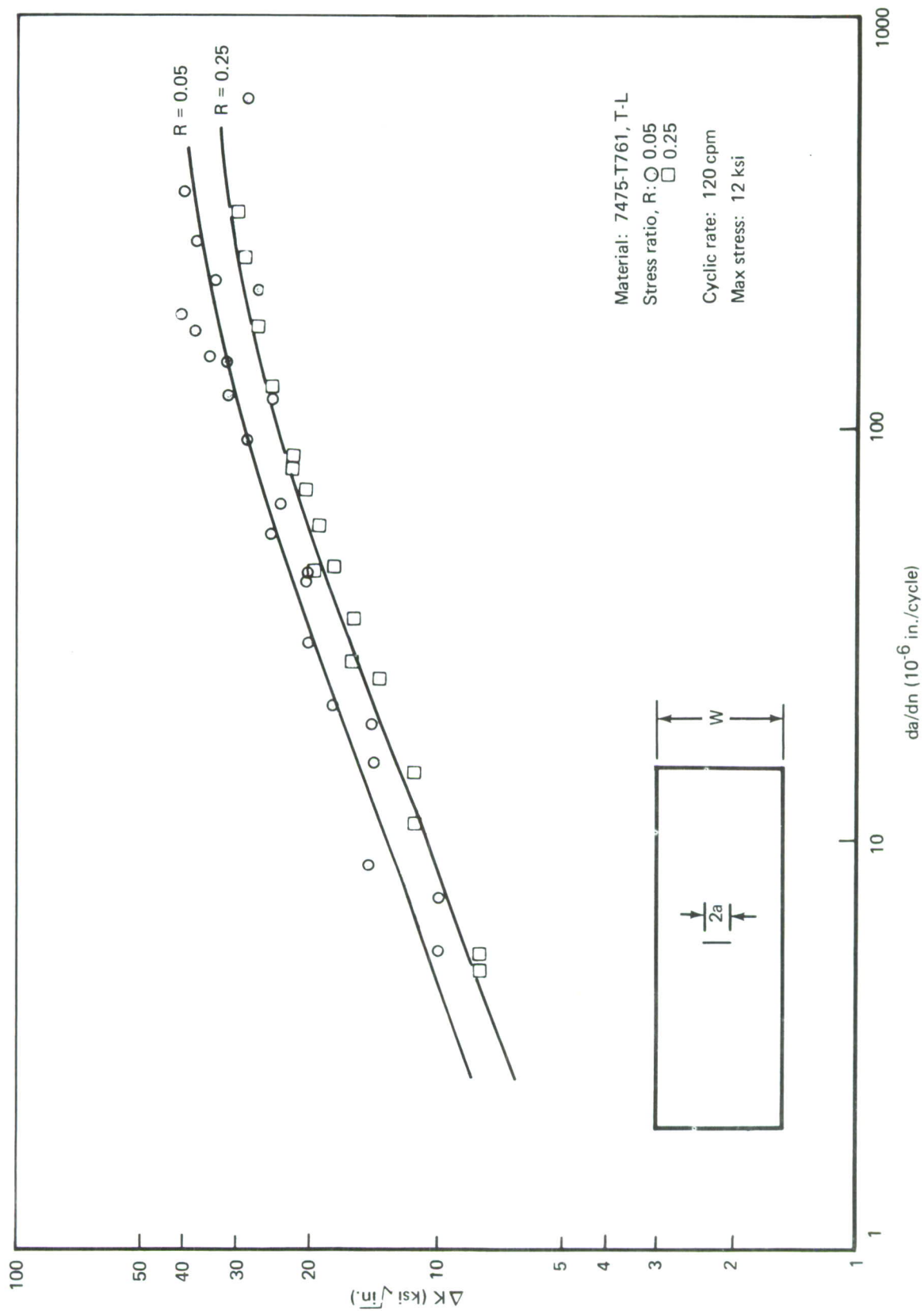


Figure II-3. —Fatigue Crack Propagation Data (7475-T761, T-L, 90% RH Air)

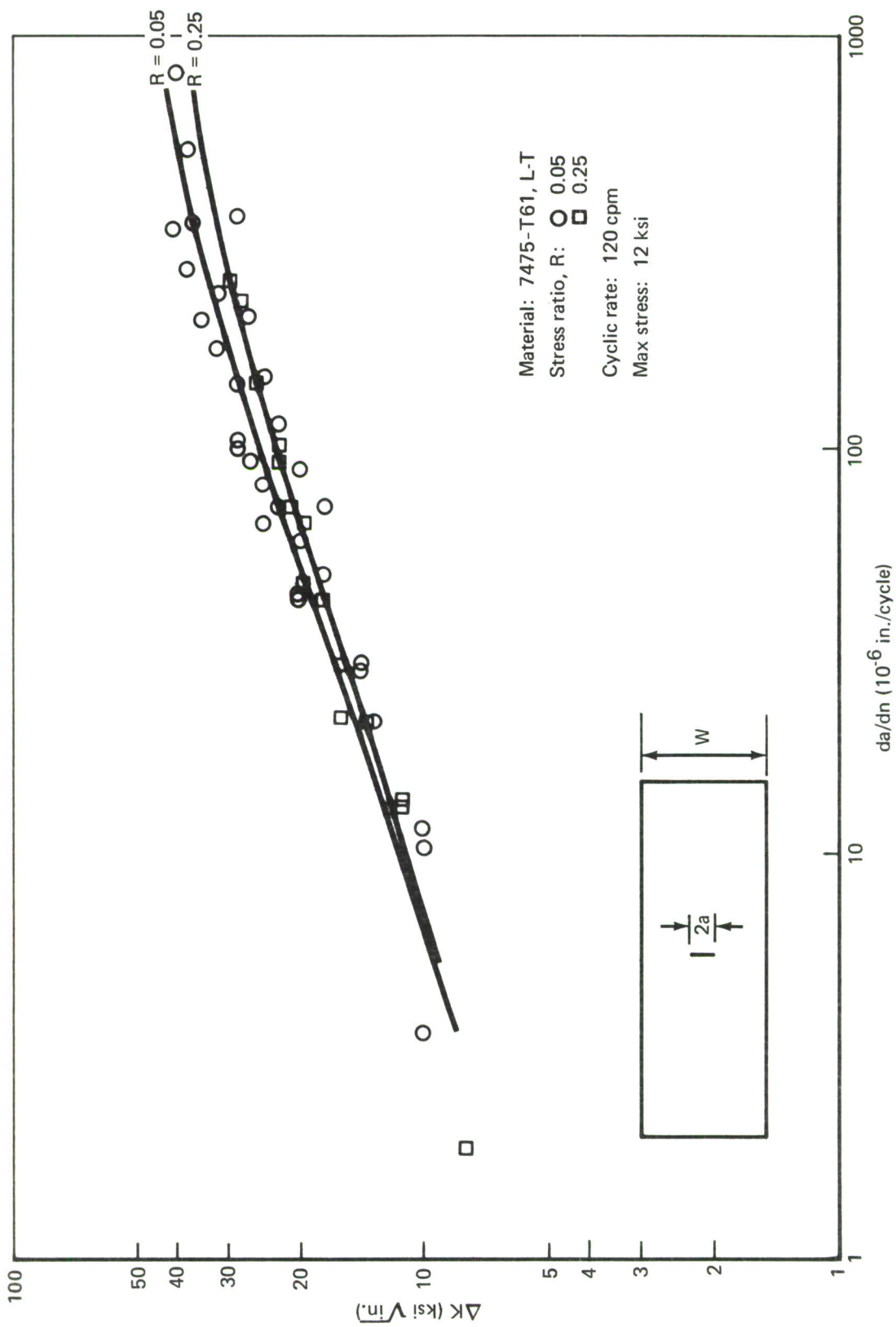


Figure II-4. —Fatigue Crack Propagation Data (7475-T61, L-T, 90% RH Air)

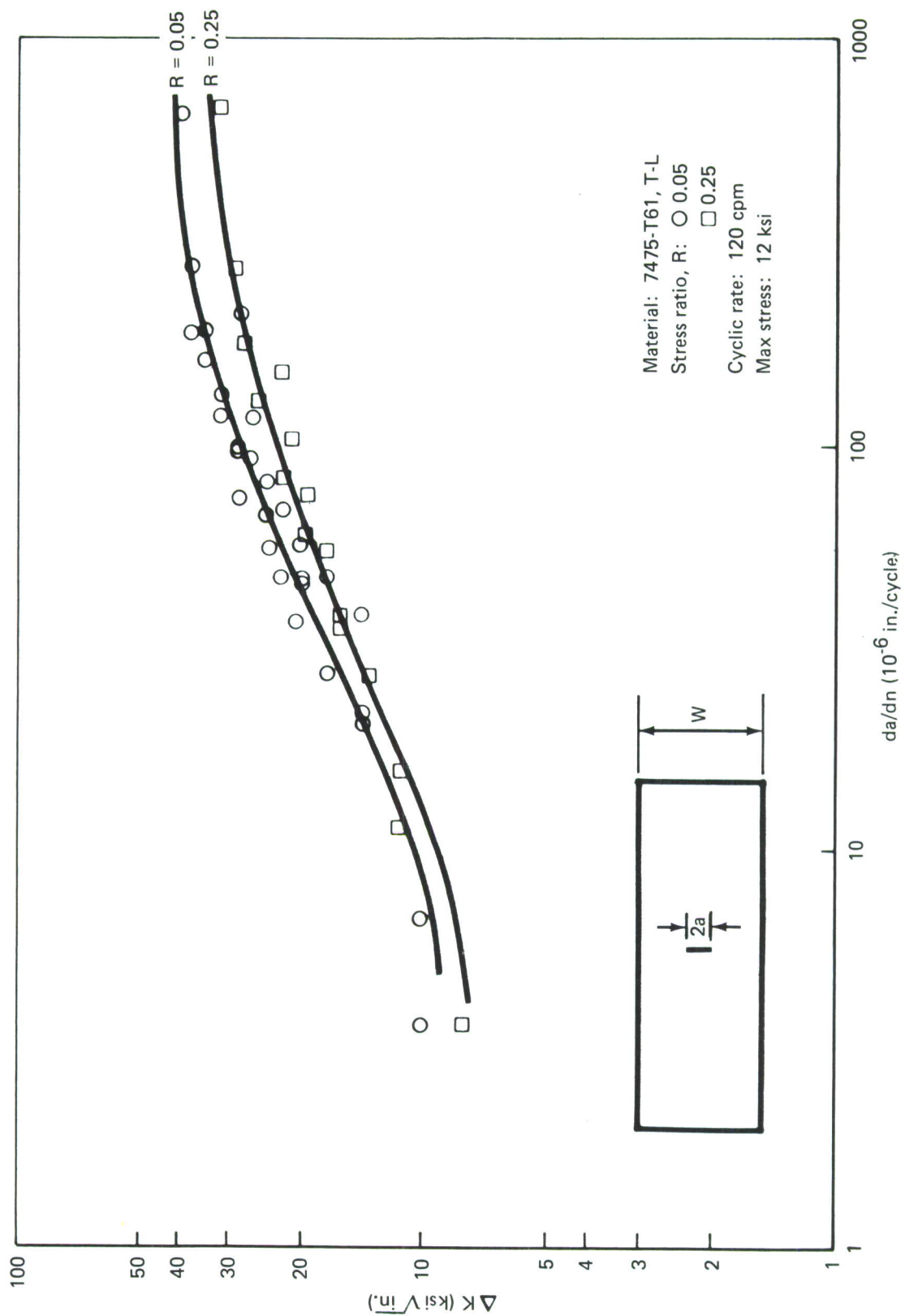


Figure II-5. —Fatigue Crack Propagation Data (7475-T61, T-L, 90% RH Air)

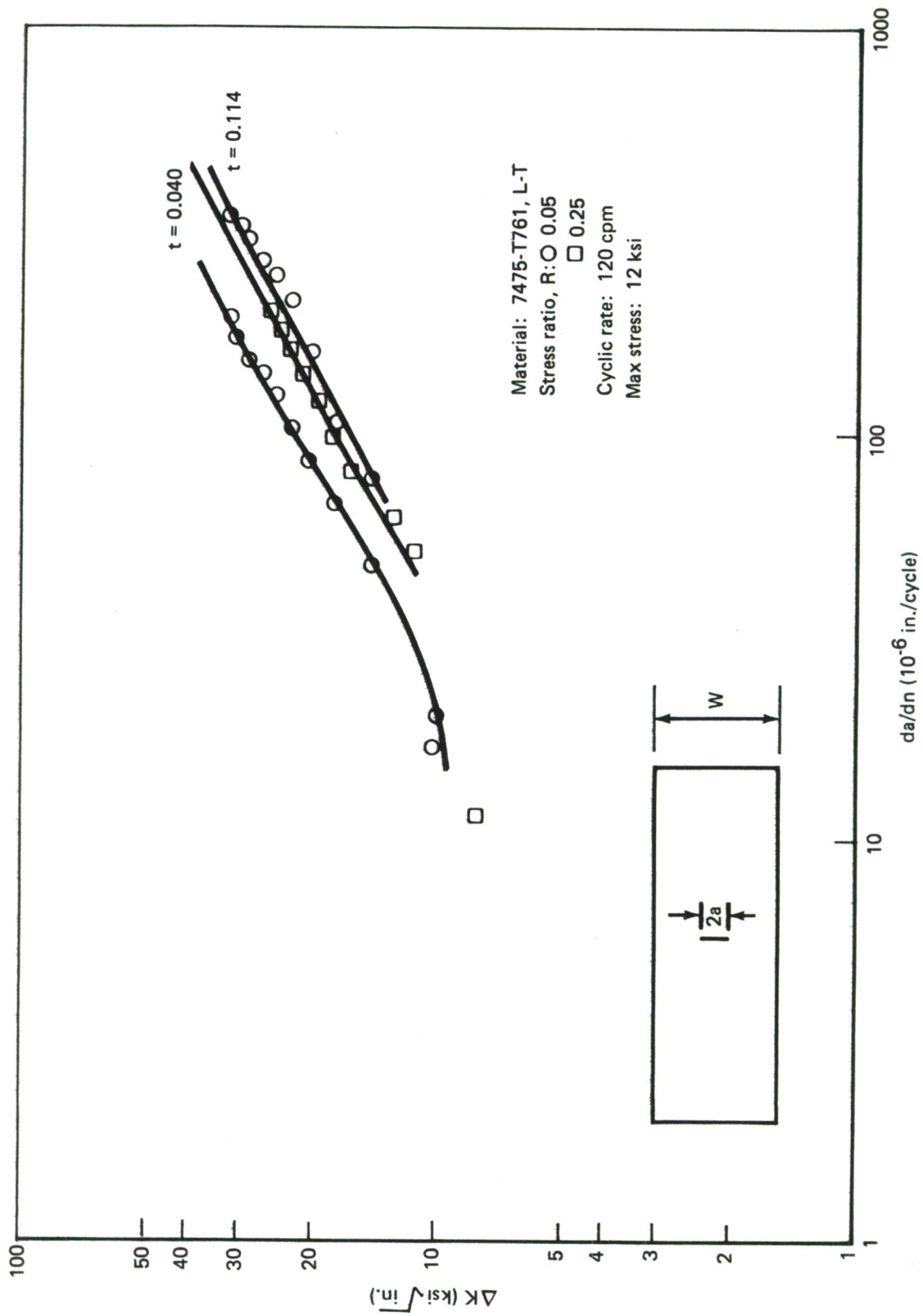


Figure II-6. — Fatigue Crack Propagation Data (7475-T761, L-T, 3½% NaCl Solution)

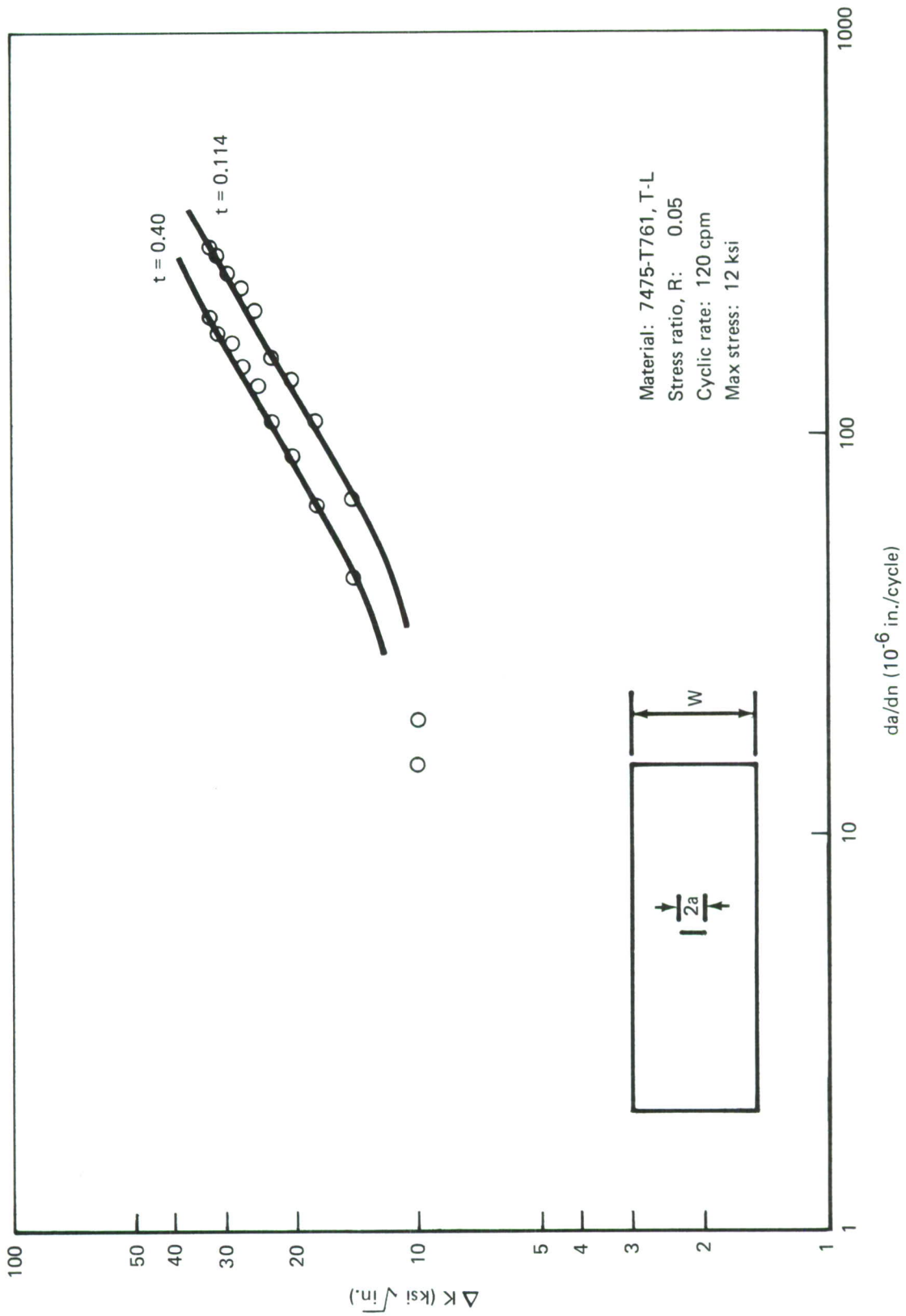


Figure II-7. —Fatigue Crack Propagation Data (7475-T761, T-L, 3½% NaCl Solution)

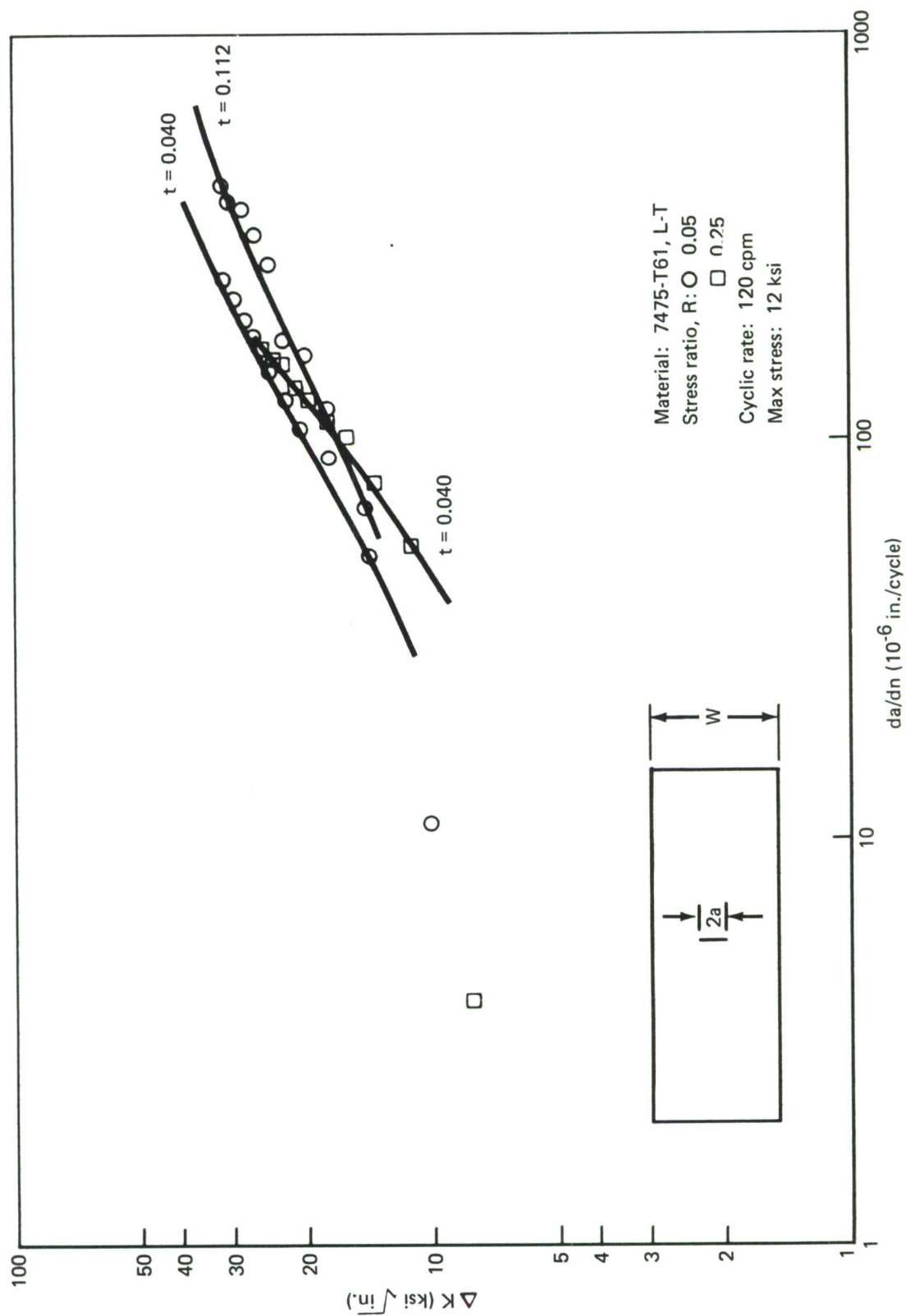


Figure II-8. —Fatigue Crack Propagation Data (7475-T61, L-T, 3½% NaCl Solution)

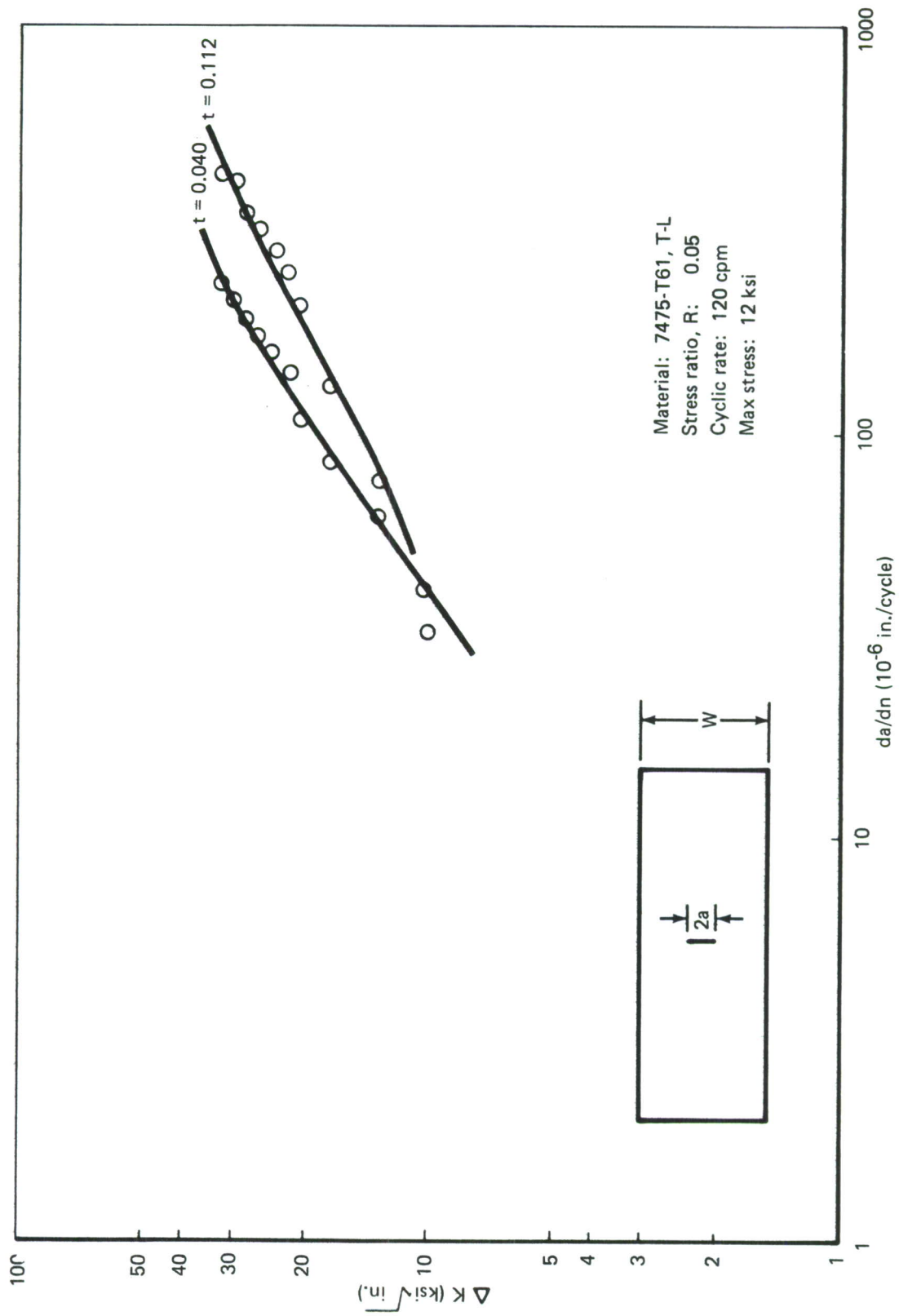


Figure II-9. — Fatigue Crack Propagation Data (7475-T61, T-L, 3½% NaCl Solution)

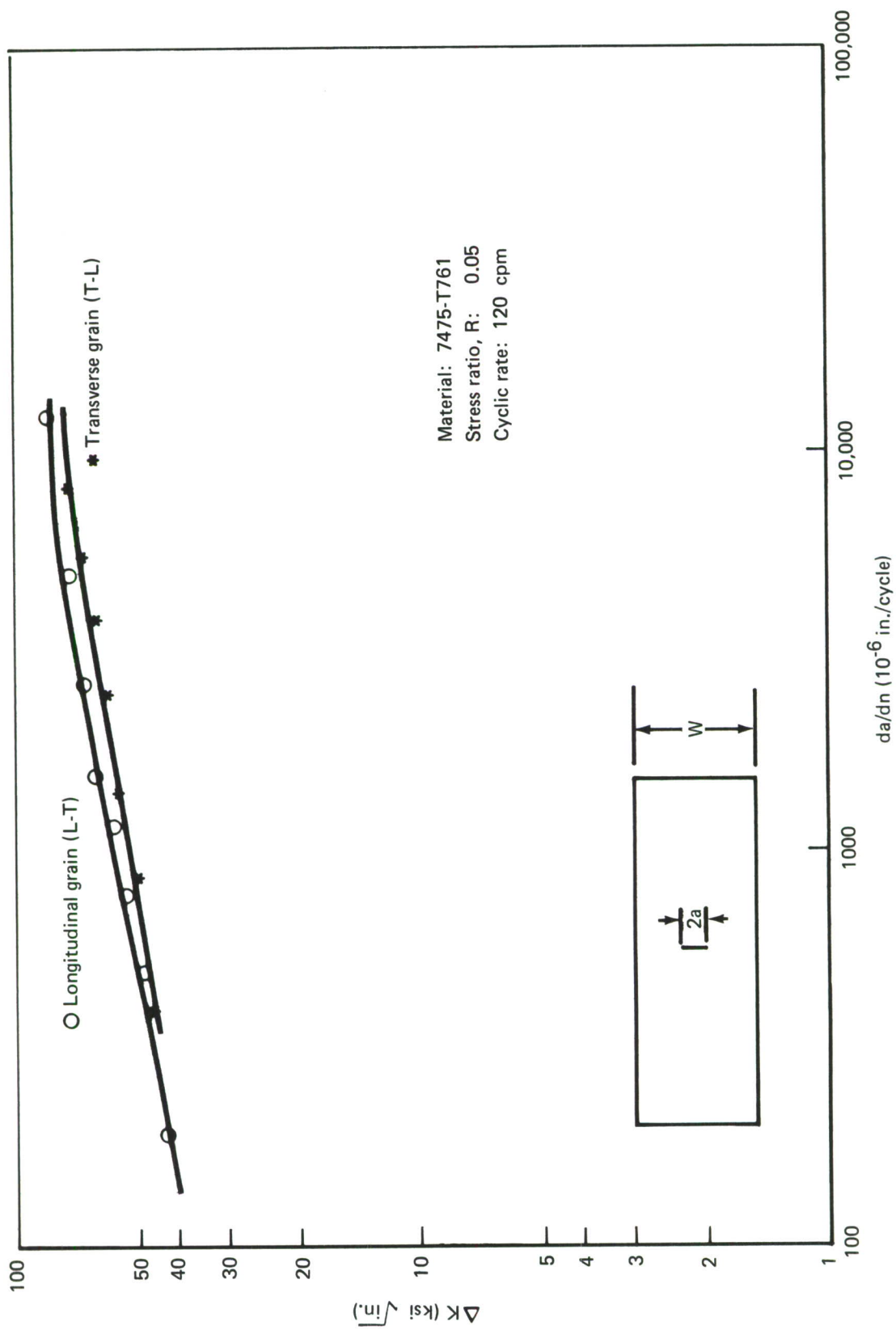


Figure II-10.—Fatigue Crack Propagation Data (7475-T761, 90% RH Air)

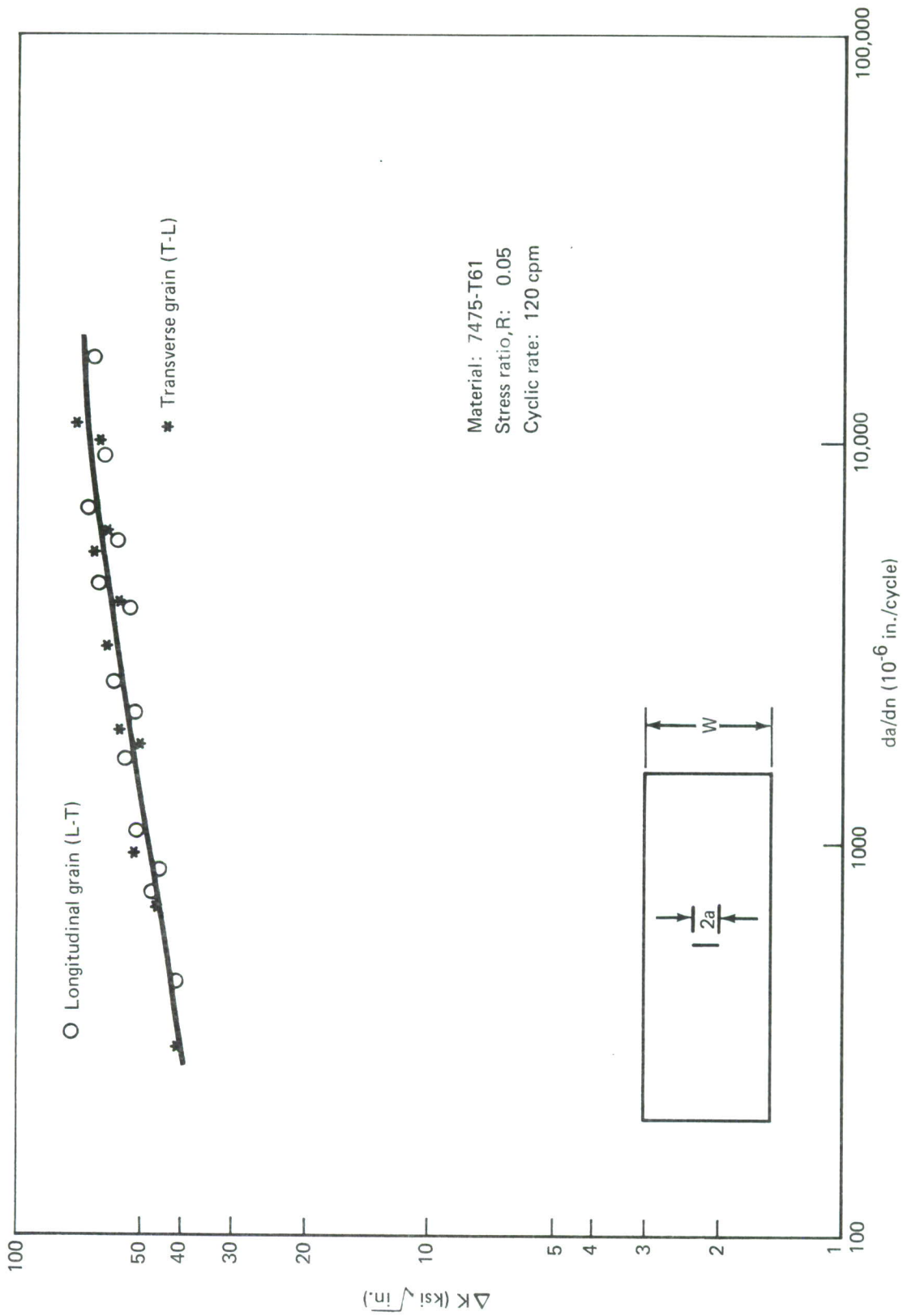


Figure II-11.—Fatigue Crack Propagation Data (7475-T61, 90% RH Air)

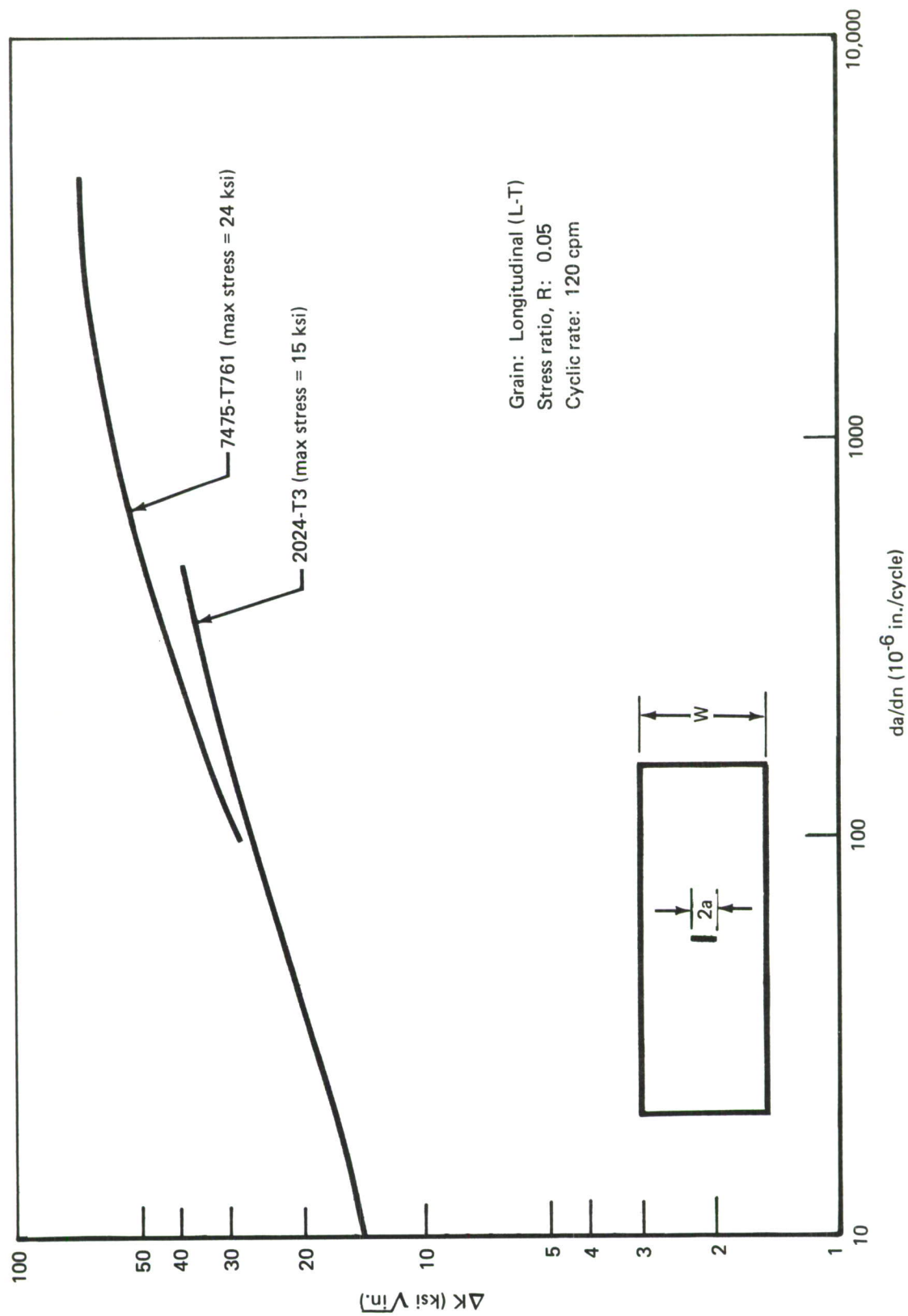


Figure II-12. —Fatigue Crack Propagation Data (7475-T761 and 2024-T3, 90% RH Air)

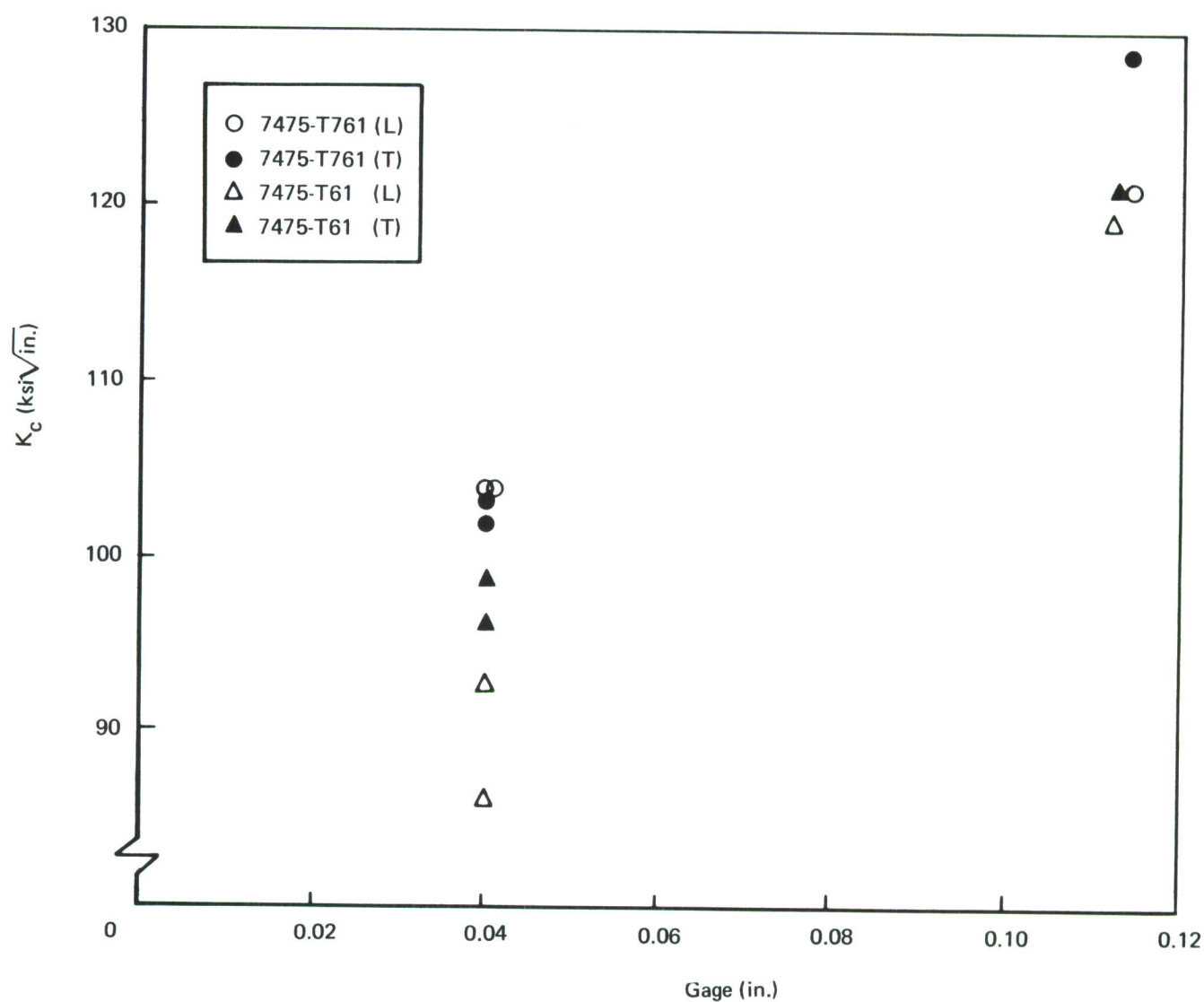


Figure II-13.—Plane Stress Fracture Toughness ($W = 24$ In.)

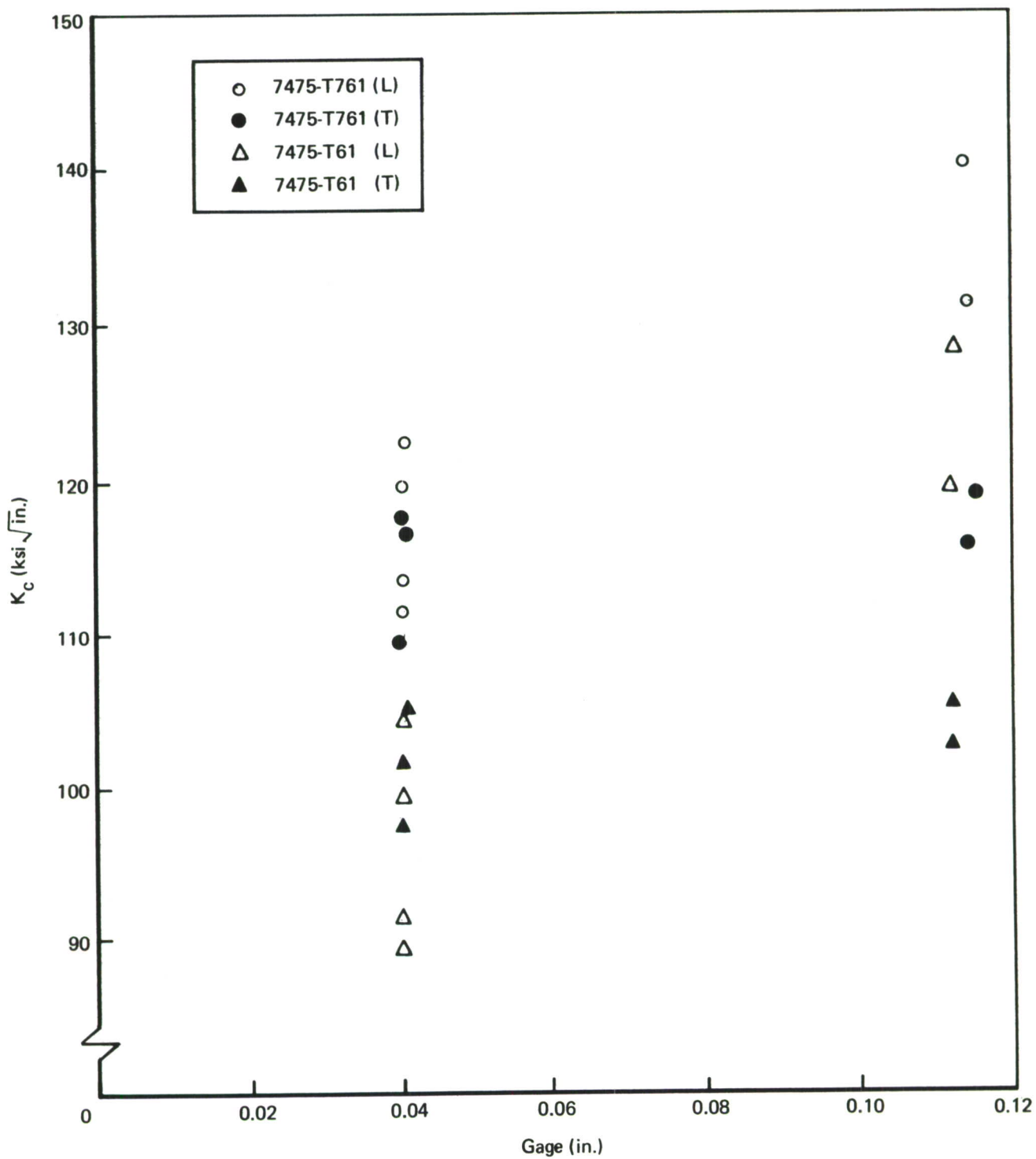


Figure II-14.—Plane Stress Fracture Toughness ($W = 36$ In.)

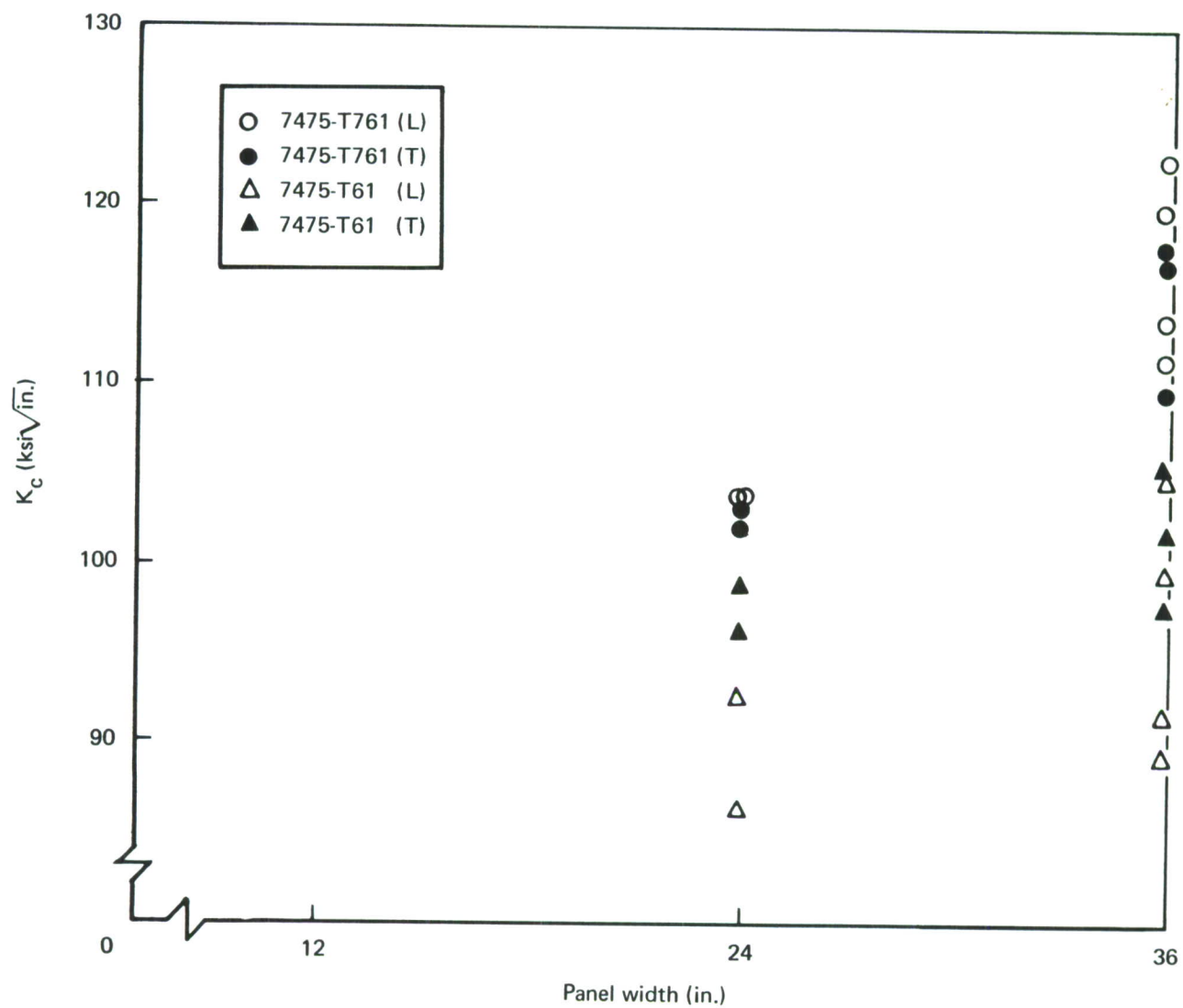


Figure II-15.—Plane Stress Fracture Toughness ($t = 0.040$ in.)

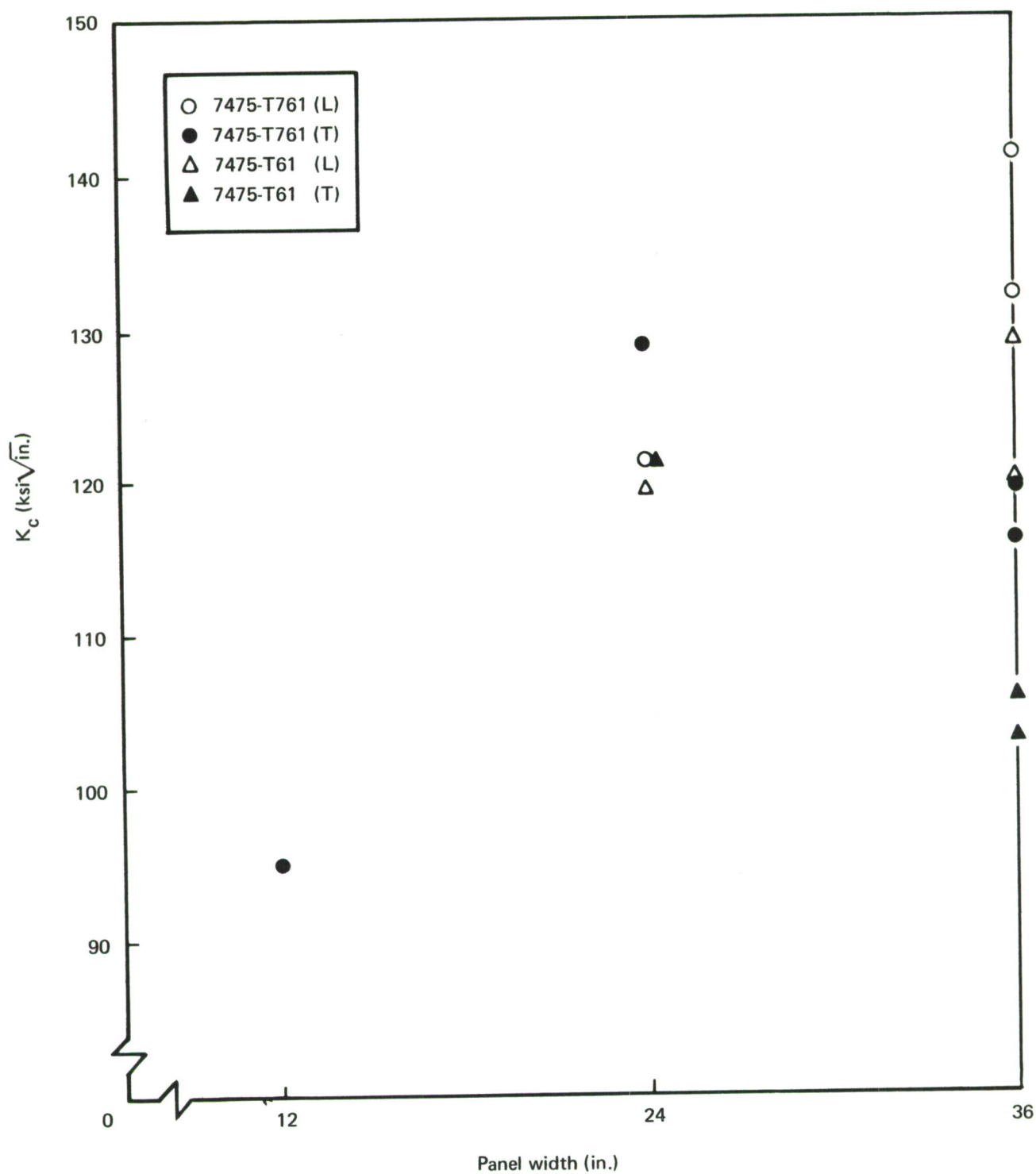


Figure II-16.—Plane Stress Fracture Toughness ($t = 0.112$ In.)

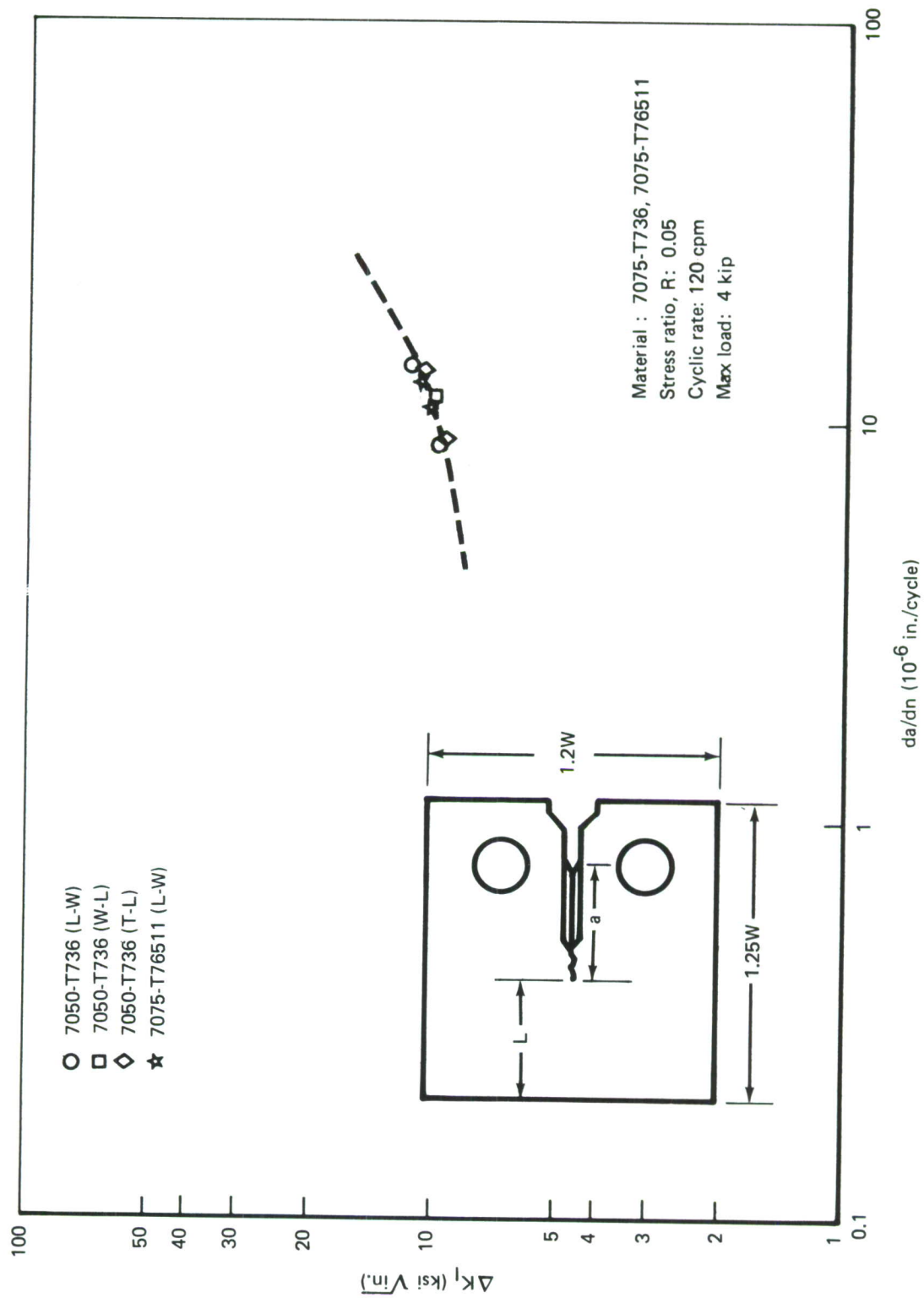


Figure II-17.—Fatigue Crack Propagation Data (7050-T736 and 7075-T76511, 90% RH Air)

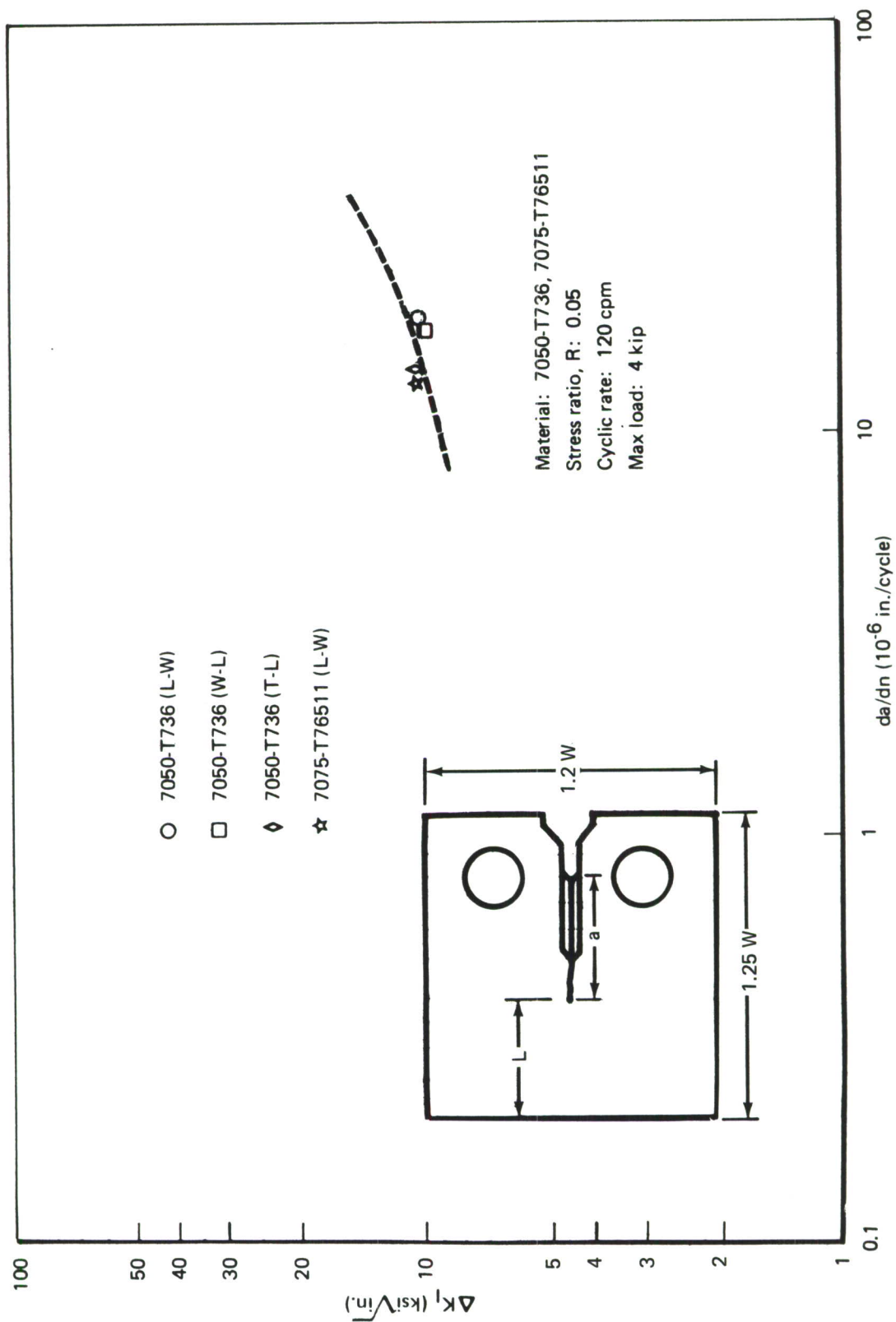


Figure II-18.—Fatigue Crack Propagation Data (7050-T736 and 7075-T76511, Water)

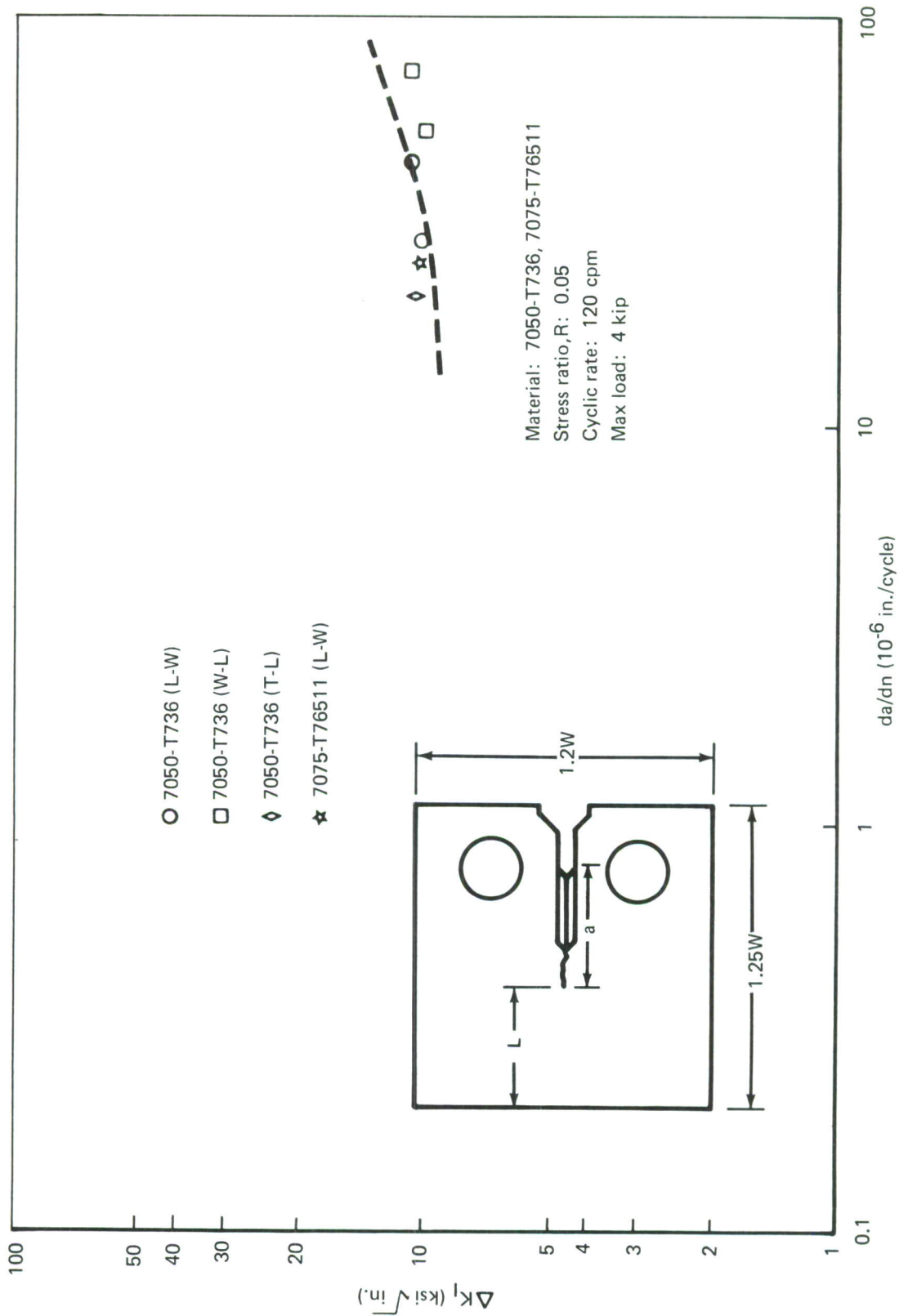


Figure II-19. — Fatigue Crack Propagation Data (7050-T736 and 7075-T76511, 3½% NaCl Solution)

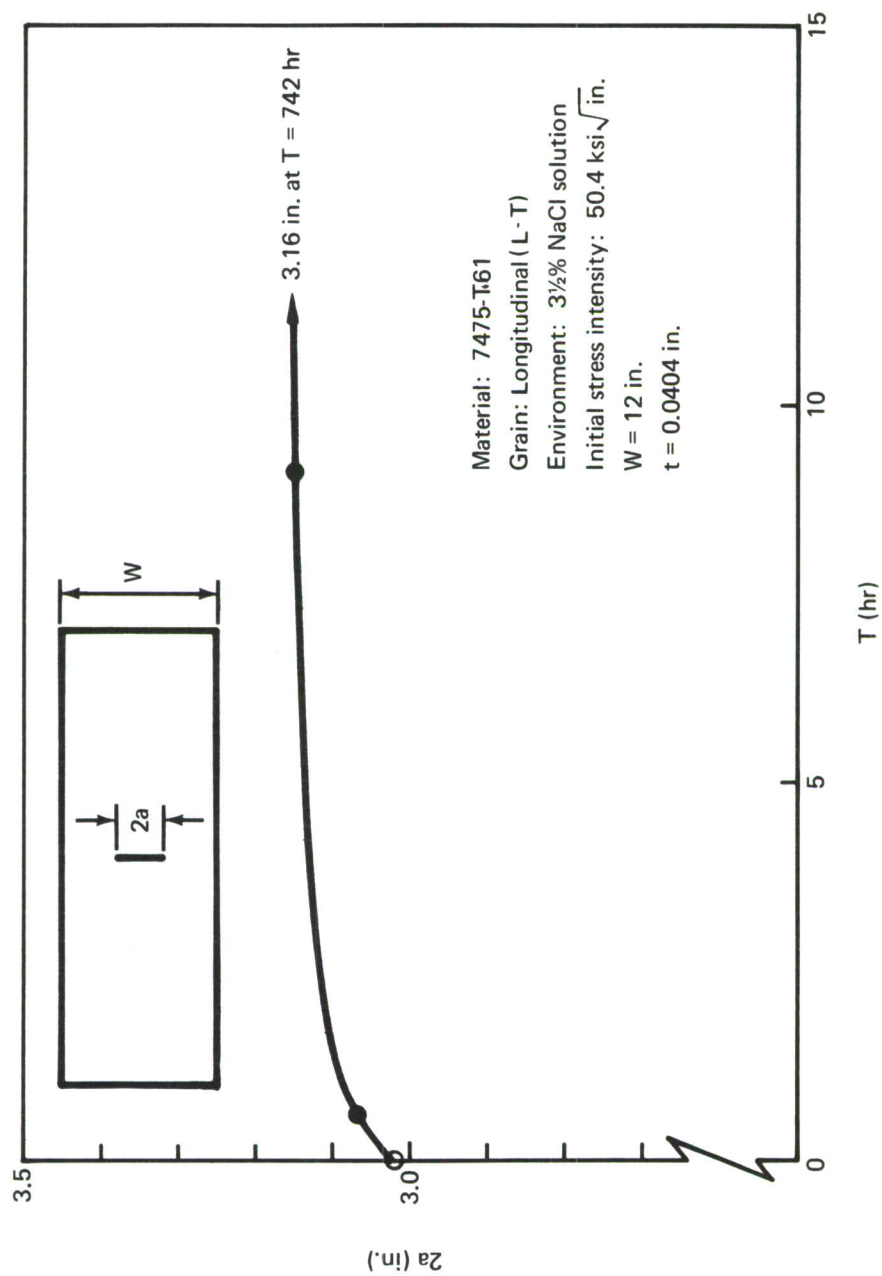


Figure II-20.—Stress Corrosion Crack Growth

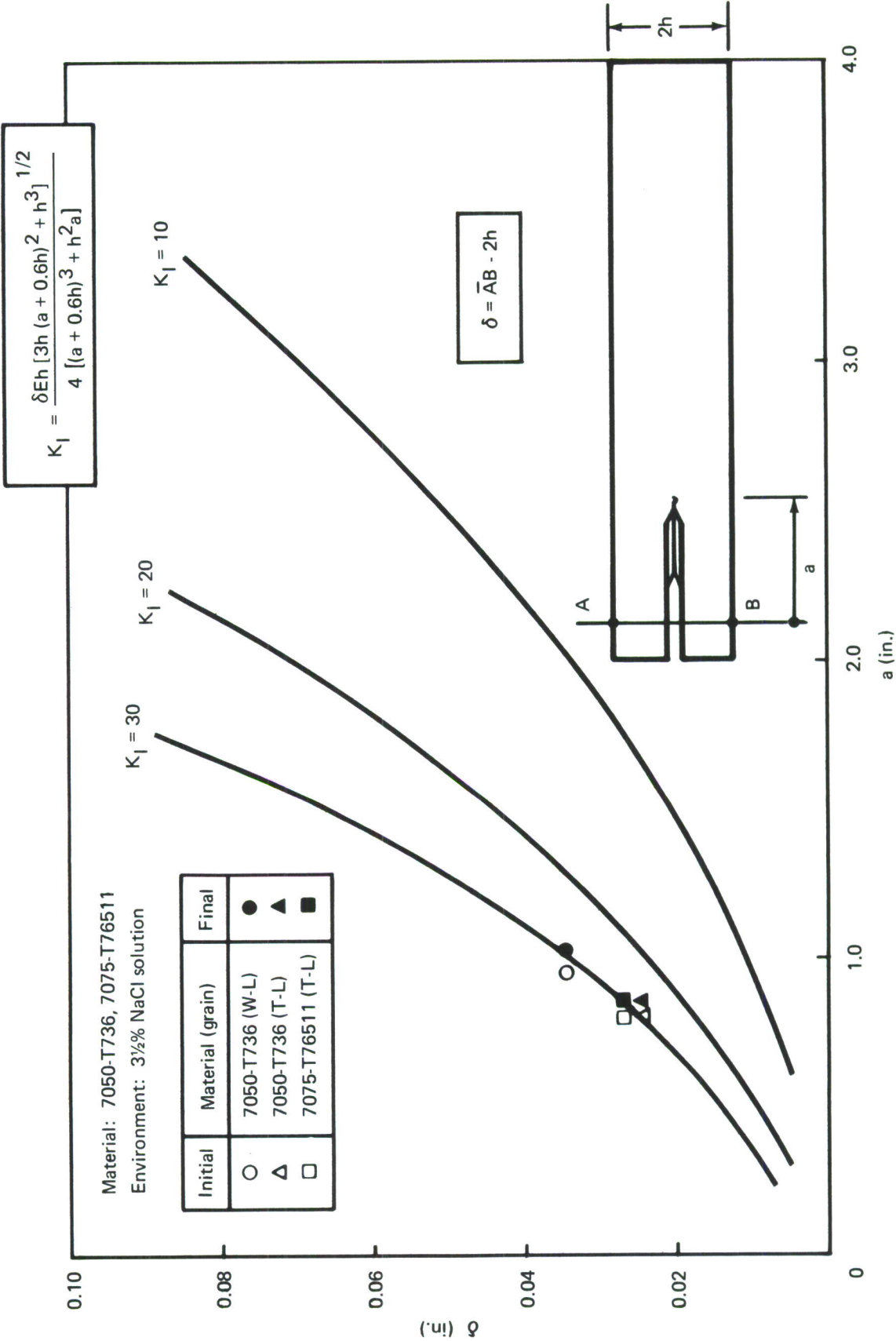


Figure II-21. –Stress Corrosion Crack Growth and K_{Isc}

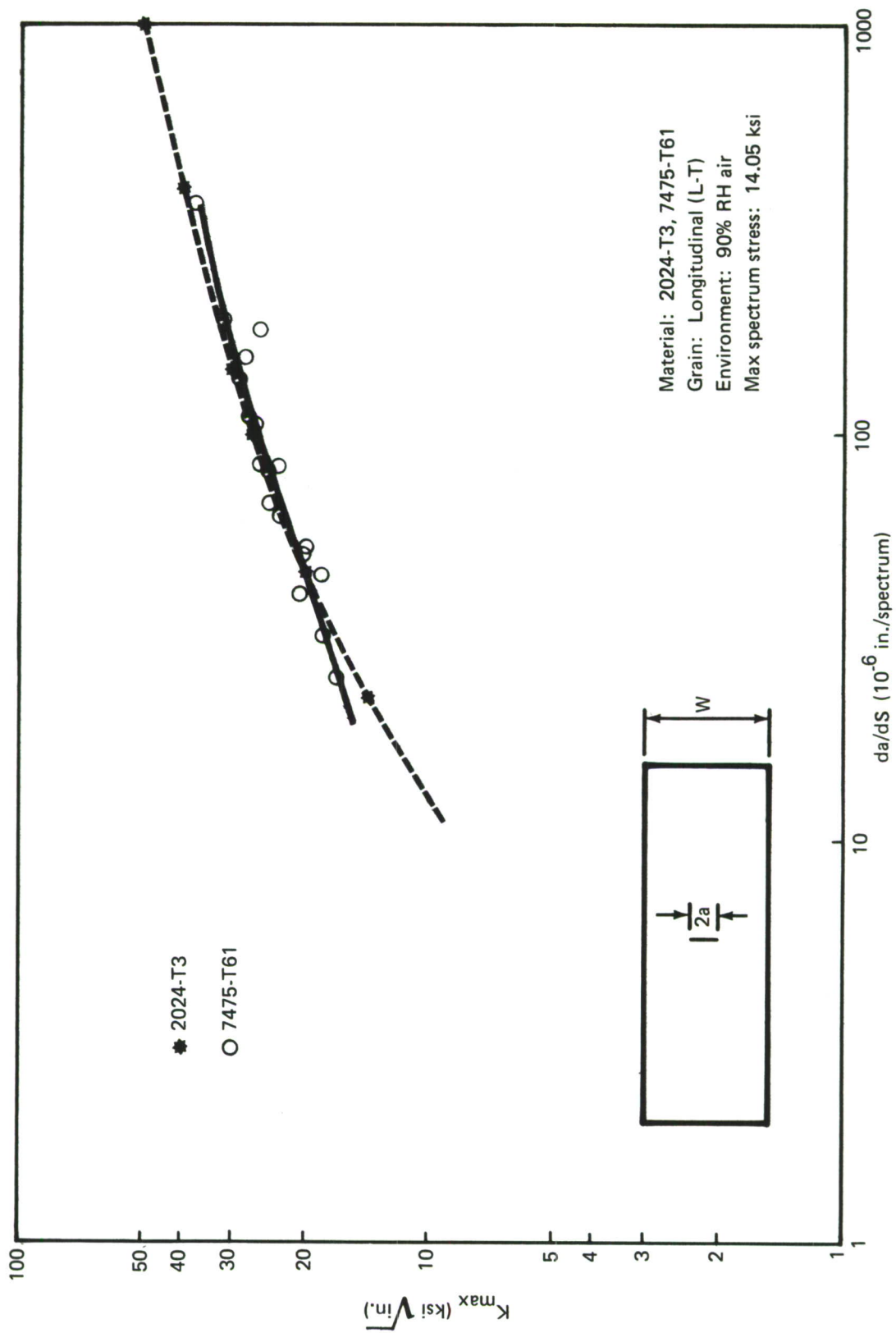


Figure II-22. — Fatigue Crack Propagation Data (2024-T3 and 7475-T61)

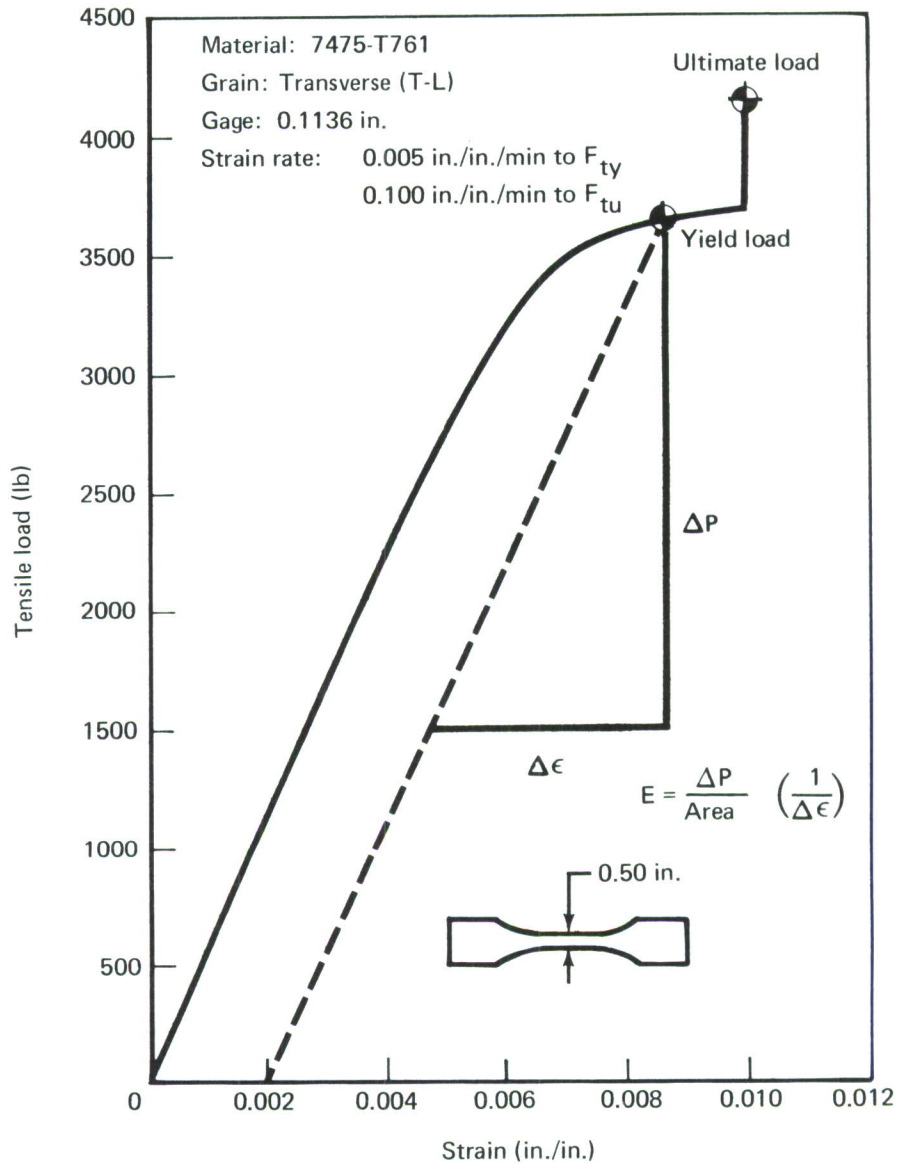


Figure II-23. — Tension Test

Table II-I.—Material Characterization Test Specimens

Material (form)	F Q R	da/dn			K _c	K _{Ic}	da/dt (3½% NaCl)	K _{scc}	K _{Isc}	da/dS	F _{ty} , F _{tu} , E
		90% RH air	Water	3½% NaCl							
7475-T761 (sheet)	6	17		5	18		4	4			4
7475-T61 (sheet)	6	16		5	17		4	4		1	4
7050-T736 (forg)		3	3	3		9	5		5		3
7075-T76511 (extrus)		1	1	1		3	1		1		2
2024-T3 (sheet)		1								1	

Table II-II.—Fatigue Specimen Definition

Material	No. of specimens	Grain	t (in.)	W (in.)	D (in.)
7475-T761	6	L	0.0404	0.997	0.182
			0.0404	0.996	0.182
			0.0404	0.996	0.182
			0.0403	0.995	0.183
			0.0403	0.995	0.183
			0.0403	0.996	0.183
7475-T61	6	L	0.0399	0.995	0.182
			0.0399	0.995	0.182
			0.0399	0.994	0.182
			0.040	0.995	0.182
			0.040	0.996	0.183
			0.040	0.996	0.182

Table II-III.—Center Crack Tension Specimens (da/dn in 90% RH Air)

Material	No.	Grain	W (in.)	t (in.)	$2a_F$ (in.)
7475-T761	2	L	24	0.0401	4.03
				0.0403	3.99
	2	T	24	0.0398	4.0
				0.040	4.0
	1	L	24	0.114	4.01
	1	T	24	0.115	4.01
7475-T61	2	L	24	0.040	4.0
				0.040	4.01
	2	T	24	0.0398	4.09
				0.0401	4.01
	1	L	24	0.1122	4.0
	1	T	24	0.1132	4.14
7475-T761	2	L	36	0.0397	8.06
				0.0398	8.0
	2	T	36	0.0406	8.05
				0.0409	8.0
	1	L	36	0.1138	8.01
	1	T	36	0.1153	8.0
7475-T61	2	L	36	0.0401	8.0
				0.0403	8.0
	2	T	36	0.0401	8.02
				0.0401	8.0
	1	L	36	0.1124	7.99
	1	T	36	0.1125	8.01

Table II-IV.—Center Crack Tension Specimens (da/dn in 3½% NaCl Solution)

Material	No.	Grain	W (in.)	t (in.)	$2a_F$ (in.)
7475-T761	2	L	36	0.0399	5.33
				0.0397	5.33
	1	T	36	0.0395	5.33
	1	L	36	0.1140	5.33
	1	T	36	0.1140	5.37
7475-T61	2	L	36	0.0398	5.33
				0.040	5.34
	1	T	36	0.0401	5.34
	1	L	36	0.1125	5.33
	1	T	36	0.1124	5.35

Table II-V.—“High” ΔK Crack Growth Tests (da/dn in 90% RH Air)

Material	Grain	t (in.)	Maximum stress (ksi)
7475-T761	L	0.040	35
7475-T761	T	0.040	22
7475-T761	L	0.114	25
7475-T761	T	0.114	35
7475-T61	L	0.0404	20
7475-T61	T	0.040	22
7475-T61	L	0.111	22
7475-T61	T	0.112	24

Table II-VI—Additional Crack Growth Panels (da/dn in 90% RH Air)

Material	Grain	W (in.)	t (in.)	$2a_o$ (in.)	$2a_F$ (in.)
7475-T761	L	12	0.1153	0.81	6.93
2024-T3	L	12	0.1278	0.50	0.73
				2.48	3.995
				0.99	1.83

Table II-VII.—Fracture Toughness (K_{IC}) Test Validity

Material	Grain	Gage (in.)	Width (in.)	K_{IC} (ksi $\sqrt{\text{in.}}$)	2a at DCG ^a	f_{max} (ksi)	Validity ^b
7475-T761	L	0.0401	24	103.9	8.50	40.77	NV
↓	L	0.0403	↓	103.9	11.75	40.89	NV
↓	T	0.0398	↓	101.9	13.25	40.10	NV
↓	T	0.0400	↓	103.1	7.75	40.58	V
7475-T761	L	0.1140	↓	121.1	6.75	47.57	NV
↓	T	0.1150	↓	128.6	6.50	50.50	NV
7475-T61	L	0.0400	↓	86.2	9.25	33.94	NV
↓	L	0.0400	↓	92.8	18.	36.45	NV
↓	T	0.0398	↓	98.7	12.	38.48	NV
↓	T	0.0401	↓	96.1	7.75	37.74	V
↓	L	0.1122	↓	119.2	12.	46.91	NV
7475-T61	T	0.1132	24	121.2	8.25	46.88	NV
7475-T761	L	0.0397	36	122.4	23.0	33.63	NV
↓	L	0.0398	↓	119.8	17.75	33.08	NV
↓	T	0.0406	↓	117.4	17.50	32.18	NV
↓	T	0.0409	↓	116.5	18.25	32.17	NV
↓	L	0.1138	↓	141.0	12.	38.92	V
7475-T761	T	0.1153	↓	118.9	14.0	32.84	NV
7475-T61	L	0.0401	↓	99.4	16.25	27.45	NV
↓	L	0.0403	↓	104.4	14.0	28.83	NV
↓	T	0.0401	↓	97.4	18.25	26.89	NV
↓	T	0.0401	↓	105.2	12.	29.04	V
↓	L	0.1124	↓	128.6	13.75	35.51	NV
7475-T61	T	0.1125	↓	105.4	11.75	29.11	V
7475-T761	L	0.0399	↓	113.7	10.25	39.00	V
↓	L	0.0397	↓	111.6	11.25	38.30	V
↓	T	0.0395	↓	109.7	14.0	37.65	NV
↓	L	0.1140	↓	131.7	9.75	45.18	NV
7475-T761	T	0.1140	↓	115.8	17.25	39.45	NV
7475-T61	L	0.0398	↓	91.8	9.5	31.51	V
↓	L	0.0400	↓	89.2	20.25	30.61	NV
↓	T	0.0401	↓	101.7	22.0	34.86	NV
↓	L	0.1125	↓	119.7	—	41.08	—
7475-T61	T	0.1124	36	102.6	12.0	35.06	V

^aDCG = Dynamic crack growth

^bV = Valid test; NV = Invalid test

Table II-VIII.—Compact Tension Specimens (da/dn in 90% RH Air, H_2O , and 3½% NaCl)

Material (form)	No.	Grain	W (in.)	B (in.)	L_F avg value (in.)
7050-T736 (forg)	3	L-W	4.0	1.5004 1.5069 1.5075	2.08 2.11 2.13
7050-T736 (forg)	3	W-L	4.0	1.5008 1.5066 1.5086	2.18 2.11 2.09
7050-T736 (forg)	3	T-L	4.0	1.5092 1.5089 1.5086	2.09 2.12 2.13
7075-T76511 (extrus)	3	L-W	4.0	1.5004 1.5010 1.5015	2.12 2.11 2.12

Table II-IX.—Plane Strain Crack Growth/Environment ($R = 0.05$)

Material (grain)	da/dn at $\Delta K_I = 10 \text{ ksi} \sqrt{\text{in.}}$ (in./cycle)		
	90% RH air	Water	3½% NaCl solution
7050-T736 (L-W)	$9.5 (10^{-6})$	$1.85 (10^{-5})$	$2.5 (10^{-5})$
7050-T736 (W-L)	$1.12 (10^{-5})$	$1.85 (10^{-5})$	$5 (10^{-5})$
7050-T736 (T-L)	10^{-5}	$1.4 (10^{-5})$	$1.6 (10^{-5})$
7075-T76511 (L-W)	10^{-5}	$1.25 (10^{-5})$	$2 (10^{-5})$

Table II-X.—Plane Strain Fracture Toughness

Material	No.	Grain	P_{\max} (lb)	P_S (lb)	P_Q (lb)	a_{avg} (in.)	K_Q ($\text{ksi} \sqrt{\text{in.}}$)	K_{Ic} ($\text{ksi} \sqrt{\text{in.}}$)
7050-T736	3	L-W	12,650	12,400	12,430	1.97	47.7	NV ^a
			13,200	12,300	12,300	1.99	47.6	NV
			12,000	11,830	11,850	1.95	44.5	NV
7050-T736	3	W-L	7,300	7,300	7,300	1.96	27.8	NV
			6,050	6,050	6,050	1.96	22.9	22.9
			5,700	5,700	5,700	2.08	23.7	NV
7050-T736	3	T-L	6,400	6,400	6,400	1.98	24.6	24.6
			6,400	6,400	6,400	1.95	24.0	24.0
			6,800	6,800	6,800	1.93	25.3	25.3
7075-T76511	3	L-W	12,050	10,900	10,900	1.99	42.3	NV
			12,000	10,800	10,800	1.95	40.5	NV
			11,950	10,900	10,900	1.95	41.3	41.3

^aNV = Invalid test (ASTM E 399-70T)

Table II-XI.—Stress Corrosion Crack Growth Tests (da/dt in 3½% NaCl Solution)

Material (grain)	Gage (in.)	K_{initial} ($\text{ksi} \sqrt{\text{in.}}$)	$\Delta 2a_T$ (in.)	T (hr)	$(\Delta a/\Delta t)_{\text{avg}}$ (in./hr)
7475-T761 (L)	0.040	49.2	0.04	1060	$1.89 (10^{-5})$
7475-T761 (T)	0.040	50.3	0.01	862	$5.81 (10^{-6})$
7475-T761 (L)	0.114	49.8	0.02	840	$1.19 (10^{-5})$
7475-T761 (T)	0.114	49.7	0.01	556	$9. (10^{-6})$
^a 7475-T61 (L)	0.0404	50.4	0.14	742	$7.9 (10^{-5})$
7475-T61 (T)	0.040	50.2	0.06	887	$3.38 (10^{-5})$
7475-T61 (L)	0.111	49.2	0.055	1035	$2.6 (10^{-5})$
7475-T61 (T)	0.112	49.5	0.04	1008	$1.98 (10^{-5})$

^aSee figure II-20

Table II-XII. —Double Cantilever Beam (DCB) Specimens (Ref. 19)

Material	No.	Grain	2h	δ
7050-T736	2	L-W	(a)	(a)
7050-T736	1	W-L	1.0033	0.0338
7050-T736	1	T-L	1.003	0.0241
7050-T736	1	T-W	(a)	(a)
7050-T76511	1	T-L	1.0022	0.0264

^aSpecimen fractured during precracking

Table II-XIII. —Stress Corrosion Crack Growth and K_{Isc} Data (da/dt in 3½% NaCl Solution)

Material (grain)	\bar{a}_O (in.)	$K_O = K_{Ic}$ (ksi $\sqrt{\text{in.}}$)	\bar{a}_F (in.)	K_{IF} (ksi $\sqrt{\text{in.}}$)	$(\Delta a/\Delta t)$ avg (in./hr)	K_{Isc} (ksi $\sqrt{\text{in.}}$)
7050-T736 (W-L)	0.945	31.1	1.015	28.2	$9.4 (10^{-5})$	28.2
7050-T736 (T-L)	0.80	28.1	0.855	24.5	$7.4 (10^{-5})$	24.5
7075-T76511 (T-L)	0.79	31.8	0.845	29.1	$7.4 (10^{-5})$	29.1

Table II-XIV. —Spectrum Loaded Panels (da/dS in 90% RH Air)

Material	Grain	W (in.)	t (in.)	$2a_O$ (in.)
2024-T3	L	36	0.125	0.75 2.5 1.5
7475-T61	L	12	0.040	0.80 1.00 1.35 1.76

Table II-XV.—Static Properties (F_{ty} , F_{tu} , E)

Material (form)	Grain	Gage (in.)	F_{ty} (ksi)	F_{tu} (ksi)	E^a (ksi)
7475-T761 (sheet)	L	0.0404	59.8	68.7	$8.72 (10^3)$
	T	0.0404	59.9	67.25	$8.69 (10^3)$
	L	0.114	66.5	73.7	$9.37 (10^3)$
	(b) T	0.1136	65.3	74.5	$9.81 (10^3)$
7475-T61 (sheet)	L	0.0404	68.6	74.5	$8.41 (10^3)$
	T	0.0403	65.7	73.6	$8.79 (10^3)$
	L	0.1136	75.3	80.1	$9.7 (10^3)$
	T	0.1136	73.1	80.6	$9.98 (10^3)$
7075-T76511 (extrus)	L	0.2482 ϕ	73.5	81.5	$10.36 (10^3)$
	T	0.2486 ϕ	64.5	74.2	$11.01 (10^3)$
7050-T736 (forg)	L-W	0.2487 ϕ	72.25	79.7	$10.0 (10^3)$
	W-L	0.2489 ϕ	61.4	70.7	$10.46 (10^3)$
	T-L	0.2483 ϕ	62.4	70.5	$10.2 (10^3)$

^aIndicated values from load-deformation plots

^bSee figure II-23

REFERENCES

1. P. C. Paris, G. R. Irwin, and R. Hertzberg, *Investigation and Analysis Development of Early Life Aircraft Structural Failures*, AFFDL-TR-70-199, March 1971.
2. L. L. Bryson and J. E. McCarty, *Design Criteria and Loads Document—ADP Cargo/Tanker Fuselage Component*, D6-55039, Boeing Commercial Airplane Company, March 1973.
3. S. H. Smith, T. R. Porter, and W. L. Engstrom, *Fatigue Crack Propagation Behavior and Residual Strength of Bonded Strap Reinforced, Lamellated and Sandwich Panels*, AFFDL-TR-70-144, September 1970.
4. Dean Davis, *Advanced Metallic Structure: Air Superiority Fighter Wing Design for Improved Cost, Weight, and Integrity*, AFFDL-TR-73-50 (to be released).
5. Carroll Bigham, et al., *Advanced Metallic Structure: Cargo Wing Design for Improved Cost, Weight, and Integrity*, AFFDL-TR-73-51 (to be released).
6. Fred Figge, *Advanced Metallic Structure: Air Superiority Fighter Wing Design for Improved Cost, Weight, and Integrity*, AFFDL-TR-73-52 (to be released).
7. *Summary Report of the Fifth MIL-HDBK-5 Residual Strength Task Group Meeting, Item 67-15b*, Battelle, Columbus Laboratories, April 14-15, 1971.
8. D. Y. Wang, "Plane Stress Fracture Toughness and Fatigue Crack Propagation of Aluminum Alloy Wide Panels," Douglas paper 6054, presented to Sixth National Symposium on Fracture Mechanics, ASTM, August 1972.
9. J. A. Dickson, "Alcoa 467 Process X7475 Alloy," Alcoa Green Letter, May 1970.
10. *Material Properties of Hexcel Honeycomb Materials*, TSB 120, Hexcel Aerospace, August 15, 1972.
11. *Advanced Composites Design Guide*, vol. 1, third edition, Advanced Composites Division, AFML-AFSC, Wright-Patterson Air Force Base, November 1971.
12. C. F. Tiffany, R. P. Stewart, and Capt. T. K. Moore, *Fatigue and Stress-Corrosion Test of Selected Fasteners/Hole Processes*, ASD-TR-72-111, January 1973.
13. R. J. Engle, Jr., *CRACKS, A Fortran IV Digital Computer Program for Crack Propagation Analysis*, AFFDL-TR-70-107, October 1970.
14. H. Vlieger, *Residual Strength of Cracked Stiffened Panels*, NLR-TR71004U (National Aerospace Laboratory NLR), Amsterdam, Netherlands, December 1970.

15. *Quick Reference Edition of Official Airline Guide*, no. 103, published by Ruben H. Donnelley, May 1972.
16. S. L. Valley, *Handbook of Geophysics and Space Environment*, McGraw Hill, 1965.
17. Material Test Plan enclosed with Boeing correspondence 6-8733-AFC-21, J. E. McCarty (The Boeing Company) to Dr. Lynn Rogers (Air Force Flight Dynamics Laboratory), November 7, 1972.
18. *Tentative Method of Test for Plane Strain Fracture Toughness of Metallic Materials*, ASTM E 399-70T, March 19, 1970.
19. M. O. Speidel and M. V. Hyatt, "Stress Corrosion Cracking of High Strength Aluminum Alloys," *Advances in Corrosion Science and Technology*, vol. II, edited by M. G. Fontana and R. W. Staehle, Plenum Press, New York, 1972, pp. 115-335.

Unclassified

Security Classification

DOCUMENT CONTROL DATA -R & D

(Security classification of title, body of abstract and indexing annotation must be entered when the overall report is classified)

1. ORIGINATING ACTIVITY (Corporate author) Boeing Commercial Airplane Company P. O. Box 3707 Seattle, Washington 98124		2a. REPORT SECURITY CLASSIFICATION Unclassified	
		2b. GROUP NA	
3. REPORT TITLE Advanced Metallic Structure: Cargo Fuselage Design for Improved Cost, Weight, and Integrity			
4. DESCRIPTIVE NOTES (Type of report and inclusive dates) Final Report of work conducted 1 June 1972 to 1 April 1973			
5. AUTHOR(S) (First name, middle initial, last name) John E. McCarty, et al.			
6. REPORT DATE June 1973		7a. TOTAL NO. OF PAGES 442	7b. NO. OF REFS 19
8a. CONTRACT OR GRANT NO. F33615-72-C-1893		9a. ORIGINATOR'S REPORT NUMBER(S) AFFDL-TR-73-53	
b. PROJECT NO. 486U			
c.		9b. OTHER REPORT NO(S) (Any other numbers that may be assigned this report)	
d.		None	
10. DISTRIBUTION STATEMENT Distribution limited to U. S. Government agencies only; test and evaluation; statement applied June 1973. Other requests for this document must be referred to AF Flight Dynamics Laboratory (FBA), Wright-Patterson AFB, Ohio 45433.			
11. SUPPLEMENTARY NOTES		12. SPONSORING MILITARY ACTIVITY Advanced Development Program Air Force Flight Dynamics Laboratory Wright-Patterson Air Force Base, Ohio 45433	
13. ABSTRACT <p>This preliminary design study was conducted to identify, evaluate, and select advanced concepts for cargo aircraft fuselage structure. The goals were to reduce the structural weight, maintain the baseline fatigue life (60,000 flight-hours and 20,000 flights), and reduce the acquisition cost. All three selected fuselage shell concepts provide a reduction in both total unit cost (2% to 7%) and participating weight (17% to 19%). Fleet (50 to 89 aircraft) life cycle cost savings of \$120 to \$320 million over a 10-year period can be accrued from the projected aircraft weight savings. Screening of a broad base of structural concepts was conducted through three levels of design iteration. Three adhesive-bonded fuselage shell concepts are recommended for further study, development, and test evaluation. Adhesive-bonded construction was chosen as the primary assembly method to reduce structural weight because it allows a significant improvement in fatigue quality of the structure. The improved fatigue quality allowed effective utilization of the new aluminum alloys, which provide a combination of improved fracture toughness and strength. Fracture mechanics and fatigue life characteristics of new aluminum alloys were investigated in an exploratory testing program. Sensitivity studies were conducted to evaluate the impact of the application of the USAF Damage Tolerance Criteria, Revision D, on the baseline structure. The result of this study and the effect of implementing both a fracture control program and an NDI demonstration program are reported. A recommended follow-on program plan and schedule are included, with brief discussion of the key features of each follow-on program phase.</p>			

DD FORM 1 NOV 65 1473

Unclassified

Security Classification

Unclassified

Security Classification

14. KEY WORDS	LINK A		LINK B		LINK C	
	ROLE	WT	ROLE	WT	ROLE	WT
Design concepts Structure Fuselage shell Adhesive-bonded structure Material selection Fatigue Damage tolerance						

Unclassified

Security Classification